



University
of Glasgow

Lucas, Timothy David (1999) *Computational modelling of the golf stroke*. PhD thesis.

<http://theses.gla.ac.uk/5001/>

Copyright and moral rights for this thesis are retained by the author

A copy can be downloaded for personal non-commercial research or study, without prior permission or charge

This thesis cannot be reproduced or quoted extensively from without first obtaining permission in writing from the Author

The content must not be changed in any way or sold commercially in any format or medium without the formal permission of the Author

When referring to this work, full bibliographic details including the author, title, awarding institution and date of the thesis must be given

Computational modelling of the golf stroke

Timothy David Lucas

*Submitted for the degree
of
Doctor of Philosophy*

THE DEPARTMENT OF MECHANICAL ENGINEERING
THE UNIVERSITY OF GLASGOW

March 1999

© Timothy David Lucas, 1999.

This copy of the thesis has been supplied on condition that who consults it is understood to recognise that its copyright rests with its author and that no quotation from the thesis and no information derived from it may be published without the author's prior, written consent.

Abstract

The golf stroke was computationally modelled using finite element analysis. Results for the impact between the clubhead and the ball compared well with previous research, both practical and theoretical. The results imply that for thick face clubheads, such as irons, clubhead performance is independent of material stiffness but highly dependent on the friction of the interface and the clubhead geometry. The three ball flight predictors (speed, trajectory and spin rate) as a function of clubhead parameters are shown to be non-trivial. Acceptable models of impact could be achieved using rigid faces for thick face clubheads with the centre of mass and clubhead inertia accurately described. Results on ball construction effects imply that both the stiffness and mass distribution throughout the ball affect performance. The large deformations of the ball mean that classic rigid body mechanics cannot suffice in golf impact predictions.

A model of the golf swing based on a double pendulum was constructed and shaft performance examined for various styles of golf swing. Shaft parameters thought to affect performance were quantitatively evaluated and results compared well with previous research. Increased clubhead speeds at impact were achieved with shafts of lighter weight or reduced bending stiffness for all styles of golf swing examined. The cause of bending forward of the shaft at impact was identified to occur from the large centrifugal forces acting on the head and the increased bending stiffness of the shaft also due to centrifugal force. On a detailed level shaft behaviour was affected by vibrations which appeared chaotic due to the changing stiffness of the system. This is expected to be less of an effect in an actual golf shot due to the damping provided by the human participant.

Key words: golf, clubhead, shaft, swing, impact, sports engineering, finite element analysis

List of contents

<i>Abstract</i>	2
<i>List of contents</i>	3
<i>List of figures</i>	8
<i>List of tables</i>	15
<i>Preface</i>	16
<i>Acknowledgments</i>	17
<i>Bobby Jones quotation</i>	18
1.0 Introduction	19
1.1. Scope of work.....	20
1.2 The rules of golf.....	21
1.3 Clubs.....	23
1.3.1 Wood clubheads	23
1.3.2 Iron clubheads	25
1.3.3 Shafts	26
1.3.3.1 Wooden	27
1.3.3.2 Steel.....	27
1.3.3.3 Composite.....	27
1.3.3.4 Other materials.....	29
1.3.4 Grips.....	29
1.4 Balls.....	30
1.5 Golf research - a historical perspective.....	31
1.6 Golf research - the state of the art.....	34
1.6.1 Clubheads	35
1.6.1.1 Material.....	35
1.6.1.2 Geometry	39
1.6.1.3 Dynamics	46
1.6.2 Golf swing and shafts.....	47
1.6.2.1 Shaft properties.....	48
1.6.2.2 Club matching	51

1.6.2.3 Double pendulum	52
1.6.2.4 Experimental tests	55
1.6.2.5 Modelling the swing and shafts	61
1.6.2.6 Further advances in modelling shafts	64
1.6.3 Balls	65
1.6.3.1 Aerodynamics	66
1.6.3.2 Experimental tests	66
1.6.3.3 Impact studies	67
1.6.3.4 Temperature	67
2.0 Computational stress analysis	86
2.1 Basic concepts	86
2.2 Stress and Strain	87
2.3 Multiaxial stress and strain states	89
2.4 Tensors	91
2.5 Finite element analysis	93
2.5.1 Computational analysis	95
3.0 Reverse engineering of a golf clubhead	101
3.1 Manual method	101
3.1.1 Model evaluation	102
3.2 Stereo Photography	102
3.2.1 Procedure	103
3.2.2 File formats	103
3.2.3 Model evaluation	104
3.3 Discussion of results	104
4.0 The finite element impact model	114
4.1 Construction of model	114
4.1.1 The clubhead	114
4.1.2 The ball	115
4.1.3 Computing facilities	118
4.1.4 Additional input data	119

4.2 Impact results	120
4.2.1 Deformed plots	120
4.2.2 Stress and strain plots	121
4.2.3 Variable - variable graphs.....	122
4.2.4 Post processing of numerical output.....	122
4.2.5 Derivation of ball flight predictors.....	123
4.2.5.1 Speed	123
4.2.5.2 Direction	124
4.2.5.3 Spin rate.....	125
4.3 Clubhead properties, straight hit	126
4.3.1 Material	127
4.3.1.1 Stiffness	127
4.3.1.2 Friction	131
4.3.1.3 Density.....	136
4.3.1.4 Hardness	137
4.3.1.5 Stress waves.....	137
4.3.2 Geometry.....	139
4.3.2.1 Mass	139
4.3.2.2 Loft.....	141
4.3.2.3 Mass distribution.....	146
4.3.2.4 Grooves	146
4.3.2.5 Curvature.....	147
4.3.2.6 Geometrical stiffness	148
4.3.2.7 Open/closed	148
4.3.3 Dynamics.....	149
4.3.3.1 Speed	149
4.3.3.2 Trajectory	150
4.4 Mishits	151
4.4.1 Off-sweet-spot impacts.....	151
4.4.2 Clubhead rotation due to loft.....	155
4.5 Ball properties.....	159
4.5.1 Compression tests.....	160
4.5.2 Cover stiffness	161

4.5.3 Core stiffness for a two-piece ball	162
4.5.4 Stiffness distribution.....	164
4.5.5 Mass distribution.....	165
5.0 Reverse engineering of a golf shaft _____	286
5.1 Existing shafts	286
5.1.2 Knife edge tests	286
5.2 Shaft model.....	287
5.3 Discussion.....	288
6.0 Reverse engineering a golf swing _____	291
6.1 Mechanical golfer	291
6.1.1 Practical tests.....	291
6.1.2 Discussion	292
6.2 Human golfers.....	293
6.3 High speed video.....	293
6.3.1 Mechanical golfer.....	293
6.3.2 Human golfers	294
6.4 Discussion of results.....	294
7.0 The finite element swing and shaft model _____	303
7.1 Construction of model.....	303
7.1.1 The swing.....	303
7.1.1.2 Force-time profiles	304
7.1.1.3 The wrist.....	305
7.1.1.4 Topswing positions	306
7.1.2 The shaft model.....	307
7.1.2.1 Clubhead mass	307
7.1.2.2 Frequency verification	307
7.1.3 Analysis procedure.....	309
7.2 Swing results.....	309
7.2.1 Deformed plots	309
7.2.2 Stress and strain plots	311

7.2.3 Variable-variable graphs.....	311
7.2.4 Derivation of shaft performance predictors.....	312
7.2.4.1 Speed.....	312
7.2.4.2 Elevation.....	313
7.2.4.3 Loft.....	313
7.2.5 Mesh density convergence.....	313
7.3 Shaft properties.....	314
7.3.1 Flex.....	314
7.3.1.1 Frequency analysis.....	315
7.3.1.2 Swing analyses.....	316
7.3.1.3 Offset mass.....	318
7.3.2 Torque.....	320
7.3.3 Bend point.....	320
7.3.4 Damping.....	321
7.3.5 Weight.....	321
7.4 Wrist modelling.....	322
8.0 Conclusions and recommendations	352
8.1 Impact modelling.....	352
8.2 Swing modelling.....	354
References	356
Appendices	368

List of figures

- Figure 1.1 A modern metal 'wood'.
- Figure 1.2 A cut through of a modern metal 'wood', showing foam.
- Figure 1.3 A cut through of a modern metal 'wood', showing reinforcement ribs.
- Figure 1.4 A modern metal 'wood', with insert of hard material.
- Figure 1.5 Rear of a 5-iron cavity back clubhead.
- Figure 1.6 Two-piece ball construction.
- Figure 1.7 The golf equipment system.
- Figure 1.8 Possible effects of varying initial ball flight parameters.
- Figure 1.9 Tangential (V_t) and normal (V_n) velocity components of clubhead.
- Figure 1.10 Tangential and normal force on clubhead, Gobush (1990).
- Figure 1.11 Onion layer model of golf ball, Gobush (1995).
- Figure 1.12 Improved performance for increased inertia clubhead. Cavity back design - top, blade design - bottom.
- Figure 1.13 Reduced 'gear effect' for curved clubfaces.
- Figure 1.14 Bend point measurement techniques.
- Figure 1.15 Bend point, why it may make a difference.
- Figure 1.16 Cochran and Stobbs (1968) double pendulum model.
- Figure 1.17 'Iron Byron' courtesy of True Temper, USA.
- Figure 2.1 Uniaxial testing machine.
- Figure 2.2 Force/Extension for a mild steel specimen up to failure (Shames 1989).
- Figure 2.3 Three types of stress.
- Figure 2.4 Examples of commonly used Finite Elements.
- Figure 3.1 Ceramic clubhead, sliced into nine sections.
- Figure 3.2 Catia CAD solid model of clubhead.
- Figure 3.3 Catia CAD solid model of clubhead.
- Figure 3.4 Complete C3D processing chain.
- Figure 3.5 Metal driver used in C3D stereo photography process.
- Figure 3.6 Flow chart of routes investigated.
- Figure 3.7 AutoCAD representation of crown and sole surfaces.
- Figure 3.8 Microstation representation of crown surface.

- Figure 4.1 Solid model of clubhead.
- Figure 4.2 Drawing of solid model clubhead (dimensions in mm). Rotational inertias about centre of mass (density = 7800 kgm^{-3}).
- Figure 4.3 Rigid element model of clubhead, rotated to show reference node behind hitting face.
- Figure 4.4 Mesh of ball model, with cut away to show inner elements of core and cover.
- Figure 4.5 Stress/Strain relationship of a hyperelastic material (vulcanised rubber).
- Figure 4.6 Clubhead and ball initial positions, illustrating the coordinate system.
- Figure 4.7 Deformed plot of the model, at 0.150 ms.
- Figure 4.8 Deformed plot of the model, at 0.270 ms.
- Figure 4.9 Deformed plot of the model, at 0.470 ms.
- Figure 4.10 Snapshots of clubhead/ball impact.
- Figure 4.11 ϵ_{33} contour plot for a section of ball, 0.150 ms after impact.
- Figure 4.12 ϵ_{33} contour plot for a section of ball, 5.0 ms after impact.
- Figure 4.13 σ_{33} contour plot for clubhead face, 0.150 ms after impact.
- Figure 4.14 Ball and clubhead speed over the period of a 1 ms analysis.
- Figure 4.15 Effect of friction on ball speed, averaged over various integrating periods.
- Figure 4.16 Two exaggerated ball trajectories for varying impact conditions.
- Figure 4.17 Approximating the position vector to the origin vector.
- Figure 4.18 Effect of friction on launch angle. Calculated at various instants.
- Figure 4.19 3-dimensional mesh of ball showing node numbers.
- Figure 4.20 2-dimensional mapping of ball showing node numbers.
- Figure 4.21 Effect of friction on ball spin, averaged over various integrating periods.
- Figure 4.22 Effect of modulus on ball dispersion.
- Figure 4.23 Effect of modulus on ball speed.
- Figure 4.24 Effect of modulus on ball launch.
- Figure 4.25 Effect of modulus on ball spin.
- Figure 4.26 Effect of friction on ball launch.
- Figure 4.27 Effect of friction on ball speed.
- Figure 4.28 Effect of friction on ball spin.

- Figure 4.29 Sliding of ball on clubhead.
- Figure 4.30 Turning moment arm about centre of mass.
- Figure 4.31 Positive tangential (F_t) and normal (F_n) force components on clubhead.
- Figure 4.32 Calculation of F_t/F_n from Gobush (1990) results.
- Figure 4.33 Effect of modulus on ball spin, zero friction.
- Figure 4.34 Effect of friction on ball speed, rigid and solid.
- Figure 4.35 Effect of friction on ball launch, rigid and solid.
- Figure 4.36 Effect of friction on ball dispersion, rigid and solid.
- Figure 4.37 Effect of friction on ball spin, rigid and solid.
- Figure 4.38 Effect of stress wave velocity on ball speed.
- Figure 4.39 σ_{33} contour plot of underneath of solid clubhead, at 0.210 ms.
- Figure 4.40 Clubhead back design, A-flat.
- Figure 4.41 Clubhead back design, B-raised cross.
- Figure 4.42 Clubhead back design, C-indented cross.
- Figure 4.43 Effect of clubhead mass on ball speed.
- Figure 4.44 Effect of clubhead mass on ball launch.
- Figure 4.45 Effect of clubhead mass on ball normalised velocity. Abaqus and analytical.
- Figure 4.46 Effect of clubhead mass on effective coefficient of restitution for Abaqus.
- Figure 4.47 Effect of friction on ball speed, 00° loft.
- Figure 4.48 Effect of friction on ball launch, 00° loft.
- Figure 4.49 Effect of friction on ball spin, 00° loft.
- Figure 4.50 Effect of friction on ball speed, 10° loft.
- Figure 4.51 Effect of friction on ball launch, 10° loft.
- Figure 4.52 Effect of friction on ball spin, 10° loft.
- Figure 4.53 Effect of friction on ball speed, 20° loft.
- Figure 4.54 Effect of friction on ball launch, 20° loft.
- Figure 4.55 Effect of friction on ball spin, 20° loft.
- Figure 4.56 Effect of friction on ball speed, 30° loft.
- Figure 4.57 Effect of friction on ball launch, 30° loft.
- Figure 4.58 Effect of friction on ball spin, 30° loft.

- Figure 4.59 Effect of friction on ball speed, 40° loft.
- Figure 4.60 Effect of friction on ball launch, 40° loft.
- Figure 4.61 Effect of friction on ball spin, 40° loft.
- Figure 4.62 Effect of friction on ball speed, 50, 60, 70 and 80° loft.
- Figure 4.63 Effect of friction on ball launch, 50, 60, 70 and 80° loft.
- Figure 4.64 Effect of friction on ball spin, 50, 60, 70 and 80° loft.
- Figure 4.65 Effect of loft on ball speed.
- Figure 4.66 Effect of loft on ball launch.
- Figure 4.67 Effect of loft on ball spin.
- Figure 4.68 Error in spin prediction for low friction.
- Figure 4.69 Curved clubface, 30° tangent at initial point of contact.
- Figure 4.70 Ball speed from curved surface, tangent = 30°.
- Figure 4.71 Ball launch from curved surface, tangent = 30°.
- Figure 4.72 Ball spin from curved surface, tangent = 30°.
- Figure 4.73 Sidespin generated by open clubface.
- Figure 4.74 Effect of clubhead velocity on ball speed.
- Figure 4.75 Effect of clubhead velocity on ball launch.
- Figure 4.76 Effect of clubhead velocity on ball spin.
- Figure 4.77 Effect of clubhead velocity on effective coefficient of restitution for Abaqus.
- Figure 4.78 Clubhead trajectory 10° below horizontal.
- Figure 4.79 Effect of mishit on speed, centre of mass 0 mm behind face.
- Figure 4.80 Effect of mishit on launch, centre of mass 0 mm behind face.
- Figure 4.81 Effect of mishit on spin, centre of mass 0 mm behind face.
- Figure 4.82 Effect of mishit on speed, centre of mass 5 mm behind face.
- Figure 4.83 Effect of mishit on launch, centre of mass 5 mm behind face.
- Figure 4.84 Effect of mishit on spin, centre of mass 5 mm behind face.
- Figure 4.85 Effect of mishit on speed, centre of mass 30 mm behind face.
- Figure 4.86 Effect of mishit on launch, centre of mass 30 mm behind face.
- Figure 4.87 Effect of mishit on spin, centre of mass 30 mm behind face.
- Figure 4.88 Effect of mishit on speed.
- Figure 4.89 Effect of mishit on launch.

- Figure 4.90 Effect of mishit on spin.
- Figure 4.91 Average reaction force vectors (not to scale).
- Figure 4.92 Rotational displacement of clubhead during impact, centre of mass 0 mm behind face.
- Figure 4.93 Rotational displacement of clubhead during impact, centre of mass at various distance behind face.
- Figure 4.94 Shaft tip velocity, centre of mass at various distance behind face.
- Figure 4.95 Rotational displacement for shots off the sweet-spot, above and below 1 mm.
- Figure 4.96 Shaft tip velocity for shots off the sweet-spot, above and below 5 mm.
- Figure 4.97 Half ball model used in compression tests.
- Figure 4.98 10 mm compression of model and existing golf balls (Mather and Immohr 1996).
- Figure 4.99 10 mm compression of varying cover stiffness models.
- Figure 4.100 Effect of cover stiffness on ball speed.
- Figure 4.101 Effect of cover stiffness on ball launch.
- Figure 4.102 Effect of cover stiffness on ball spin.
- Figure 4.103 Stress/strain behaviour of various hyperelastic core stiffness.
- Figure 4.104 10 mm compression of varying core stiffness models.
- Figure 4.105 Effect of core stiffness on ball speed.
- Figure 4.106 Effect of core stiffness on ball launch.
- Figure 4.107 Effect of core stiffness on ball spin.
- Figure 4.108 Ball constructions used to analyse dual stiffness effects.
- Figure 4.109 10 mm compression of varying dual core stiffness models.
- Figure 4.110 Effect of dual core stiffness on ball speed.
- Figure 4.111 Effect of dual core stiffness on ball launch.
- Figure 4.112 Effect of dual core stiffness on ball spin.
- Figure 4.113 Ball constructions used to analyse inertia effects.
- Figure 4.114 Effect of ball inertia on ball speed.
- Figure 4.115 Effect of ball inertia on ball launch.
- Figure 4.116 Effect of ball inertia on ball spin.
- Figure 5.1 Knife edge shaft test.
- Figure 6.1 University of Glasgow's mechanical golfer, 'Dai Laughing'.

- Figure 6.2 Position of target and tee in mechanical golfer tests.
- Figure 6.3 Target, thick black line shows limit of damage.
- Figure 6.4 Snapshot from high speed recording of 'Dai Laughing'.
- Figure 6.5 Velocity of wrist hinge of 'Dai Laughing'.
- Figure 6.6 Snapshot from high speed recording of an amateur golfer.
- Figure 6.7 Velocity of wrist hinge of an amateur golfer.
- Figure 7.1 Swing model dimensions and 8 element shaft model.
- Figure 7.2 Force-time profiles (FTP).
- Figure 7.3 Wrist spring 'force - displacement' characteristics.
- Figure 7.4 Transformation from address to 90°-135° topswing.
- Figure 7.5 Finite element model of 90°-135° topswing.
- Figure 7.6 Snapshots of model downswing.
- Figure 7.7 Shaft shape at impact, X-Y plot.
- Figure 7.8 Shaft shape at impact, radius of curvature.
- Figure 7.9 Curvature contour plot for swing model at impact.
- Figure 7.10 Wrist and clubhead speed during downswing analysis.
- Figure 7.11 Bending moments in shaft during downswing analysis.
- Figure 7.12 Curvature in shaft during downswing analysis.
- Figure 7.13 Effect of shaft stiffness on mode 1 frequency.
- Figure 7.14 Wrist and clubhead speed during downswing, 40 and 60-flex.
- Figure 7.15 Curvature change in shaft during downswing 40 and 60-flex.
- Figure 7.16 Effect of shaft stiffness on clubhead speed.
- Figure 7.17 Effect of shaft stiffness on change in dynamic loft.
- Figure 7.18 Effect of shaft stiffness on clubhead elevation.
- Figure 7.19 Effect of offset mass on clubhead speed.
- Figure 7.20 Effect of offset mass on clubhead elevation.
- Figure 7.21 Effect of offset mass on change in dynamic loft.
- Figure 7.22 Radius of curvature near the clubhead for various offset models.
- Figure 7.23 Shaft deflection plots showing bend profiles.
- Figure 7.24 Wrist and clubhead speed during downswing, 50 and 150 g.
- Figure 7.25 Effect of shaft weight on clubhead speed.
- Figure 7.26 Effect of shaft weight on change in dynamic loft.
- Figure 7.27 Effect of shaft weight on clubhead elevation.

- Figure 7.28 Swing impact positions for 50 and 150 g shafts (not to scale).
- Figure A-1(1) Calibration plate used for C3D process.
- Figure A-3(1) Original design of mount for clubhead, not constructed due to limitations of C3D process, sheet 1.
- Figure A-3(2) Original design of mount for clubhead, not constructed due to limitations of C3D process, sheet 2.
- Figure B-4(1) Effect of clubhead modulus on ball speed, zero friction.
- Figure B-4(2) Effect of clubhead modulus on ball launch, zero friction.
- Figure B-4(3) Effect of clubhead modulus on ball dispersion, zero friction.
- Figure D-2(1) Bending moments in shaft during downswing, zero offset mass.
- Figure D-2(2) Curvature in shaft during downswing, zero offset mass.

List of tables

Table 1.1	Typical loft angles of golf clubheads (Dorling Kindersley 1998).
Table 1.2	Golf swing times, various golfing ability (McTeigue and Lamb 1995).
Table 4.1	Hyperelastic material coefficients calculated for test data by Abaqus/Explicit.
Table 4.2	Initial centres of mass and inertias of the clubhead and the ball.
Table 4.3	Behaviour of different clubhead designs.
Table 4.4	Effects of trajectory on ball flight predictors.
Table 4.5	Coordinates for minimal clubhead rotation.
Table 4.6	Ball flight predictors for mishits ± 5 mm from sweet-spot, 30° loft clubhead.
Table 4.7	Static compression values based on 200 lbf compression test (Sullivan and Melvin 1990).
Table 5.1	Knife edge experimental and model results.
Table 7.1	Forces and times for FAPs and topswings.
Table 7.2	Results of frequency verification, offset mass 40mm.
Table 7.3	Radius of curvature in each element at impact, offset 40mm.
Table 7.4	Shaft performance indicators for varying mesh densities.
Table 7.5	Effect of shaft stiffness on modal frequencies.
Table 7.6	Graded shaft frequencies for a typical driver (Tutleman 1998).
Table 7.7	Radius of curvature for shaft tip for various flex.
Table 7.8	Dynamic impact parameters for bend point swing analysis.
Table A-2(1)	Dimensions and coordinates of posts. Tolerances on posts ± 0.001 mm.
Table B-3(1)	Rotation and translation for rigid lofted clubheads.
Table C-1(1)	Measured properties of selection of graphite composite shafts.
Table C-2(1)	Finite element shaft model data, used in knife edge tests.
Table D-3(1)	Element stiffness values for bend point analysis.

Preface

The current work encompasses research carried out between 1995 and 1999 in the Ballistics and Impact Group, Department of Mechanical Engineering, The University of Glasgow.

The work begins in **chapter 1** with a necessarily extensive review of relevant previous work on golf science. The large amount of published literature available has, I hope, been identified. This base of knowledge continues to grow, almost exponentially. Conferences planned for 2000 include the 3rd Sports Engineering Conference in Sydney 10th - 12th June, and no less than three separate conferences on golf research. Updating the work to include all relevant material threatened to make the research a never ending task. It was necessary to draw a line somewhere and all published proceedings have been included up to the date of submission with the exception of the 3rd International World Scientific Congress on Golf.

An introduction to the stress analysis techniques used is given in **chapter 2** before the analysis of the golf stroke continues using a two track approach;

- modelling of the impact between the clubhead and ball (**chapters 3 and 4**)
- modelling of the golf swing and shaft behaviour (**chapters 5, 6 and 7**)

Final discussions on how the work can be continued is given in **chapter 8** before a full list of references is given. A bibliography of all published golf information sourced is not included as it would have required numerous additional volumes. Requests are welcome from those interested in golf science who require directions to additional publications beyond those given in the references.

Tim Lucas

25th March 1999

Acknowledgments

Especially to Dr. Ron Thomson for academic as well as personal support and development.

Faculty of Engineering, University of Glasgow for a scholarship to undertake the research.

Professor John Hancock, Alan Birkbeck, Jesper Ankersen, Jin Siong Soh and all others who passed through the Ballistics and Impact Group near the end of the 20th century.

To the late Al Adam, former Managing Director of John Letters and Sons, a close friend and part-time golf guru. If it were not for Al, the work may have been finished sooner but my life much less enriched.

This thesis is dedicated to Jenny Dewar for every type of support. To attempt to list them would only do her an injustice. Thank you.

“Anyone who hopes to reduce putting or any other department of golf to an exact science is in for serious disappointment and will only suffer from the attempt.”

Bobby Jones *



Courtesy of GolfWeb Sportsline USA.

*** Bobby Jones (1902-1971) B.Sc. (Mech. Eng., Georgia Tech.)
1930 - Still as an amateur golfer retired after winning
all four majors of that year.
Co-built the Masters course; Augusta National.**

1.0 Introduction

In the late 20th century, sport has seen massive growth both in terms of participation and in economic worth. Taylor (1998) reports that the General Household Survey shows the number of UK adults 'regularly' taking part in sport (ie any sport played within the four weeks prior to the survey) increasing from 39% in 1977 to 65% by 1990. The figures also suggest that the level of participation has now plateaued with all active adults wishing to take part in sport doing so. Sport however continues to grow, over the last decade major increases have been seen in the participants frequency of activity and a shift is observed to less-competitive, individual, 'leisure sports' such as swimming, walking and cycling (Taylor 1998), possibly as a result of changing employment patterns. This growth has led to an expansion not only in the more obvious sports and leisure industries such as equipment and clothing manufacture but also in facilities provision and in less obvious areas such as media coverage. This growth is expected to continue well into the next century, as people work fewer hours and so have more leisure time, and as increased life expectancy allows more time in retirement, often with greater disposable income (Easterling 1993). Sport and exercise are also seen as an issue of private lifestyle and of public health, to be encouraged in a world which is increasingly hazardous in many other respects.

The sports equipment industry is currently estimated to be worth £3,282 million in the UK alone, accounting for 32% of the total consumer spending on sports (Taylor 1998). While manufacturers design equipment with profit in mind, they must meet the demands of the buyers. These are two fold: improved performance and improved safety. To fulfil this demand, the production of modern sports equipment relies on a multidisciplinary approach drawing on conceptual product design, mechanical engineering, materials engineering, biomechanics and medicine amongst others. It must be noted here that the purchasers requirements of improved performance are not necessarily provided by the equipment suppliers in a tangible form, successful sales of equipment can be achieved on the basis of hype alone. Frank Thomas (1994), Technical Director of the United States Golf Association (USGA) explained how hype can lead to improved player performance perceived from better performing equipment by an alteration and relaxation of the players mind. The study of such effects is beyond the

current work, mention is made as an acceptance of the role human behaviour plays in the perception and evaluation of sports equipment, reinforcing the need for a thorough scientific understanding of the performance of sports equipment systems. The current work focuses on the mechanical engineering aspect, modelling the forces and deformations generated in one example of an equipment 'system', that of golf.

1.1 Scope of work

Golf is an ancient game. It was first recorded in 1457 (Lewis 1995) but little is known about it prior to 1554. The time over which the game has been played has allowed the equipment to evolve. Clubs were originally made from the cheapest and most abundant material of the time, wood. Lewis even reports admittedly flimsy evidence from the 17th century that balls were also constructed from wood. There is however stronger evidence that balls of that time were manufactured from leather. Over the years other materials have been used and presently, with the demand for higher performance equipment, participants can choose from what is almost an overabundance of equipment specifications. Each is reputed to offer advantages to the golfer; softer feel, harder feel, higher or lower trajectory of flight, straighter shots and increased initial ball speed, the latter often portrayed as most important to golfers insofar as it increases 'carry'. Each claim (and often its opposite) is used in the marketing of clubs with golfers, often with higher than average disposable income, being amongst the most enthusiastic sportsmen to adopt the 'latest' equipment. Many claims of improved performance are based on the mechanics of impact but these are often just suggestions with little supporting evidence, whether experimental or theoretical.

The complexity of a thorough and rigorous test programme for clubs has led to largely unsubstantiated claims and counter-claims being made about club and ball properties. The variables that influence a shot are numerous and many of these, eg air humidity, temperature and windspeed, cannot be directly controlled in the open. Experimental research is then expensive. In addition, properties may be interconnected in a way that makes isolating individual properties not possible. Furthermore, repeating the initial impact conditions exactly is not possible for a human golfer and expensive, often complex machines are required to give reproducible impact conditions. Practical

research is thus problematic and costly. It is the aim of the current work to utilise modern computational methods of engineering analysis to model aspects of the golf shot, with a view to quantifying club and ball properties in a way which may not even be possible in practical testing.

1.2 The rules of golf

The rules of golf were formally drawn up in 1774 with equipment rules appearing for the first time in an appendix in the 1920's, only little changes have been necessary over the last 220 years (Thomas 1994). Prior to the 1920's the only reference to clubs was the clause "*clubs shall be of the traditional and customary form and make and shall contain no contrivances such as springs.*" The rules are a joint publication of the Royal and Ancient (R&A 1997) and the USGA coming in a surprisingly small booklet that is updated every four years. Few public libraries (and probably few golfers) have a copy but they often own much larger books that try to interpret the rules for golfers. The rules include restrictions on equipment and its design which are simply laid out and stated in a way that designers would find difficult to misunderstand or deliberately flaunt. Specific rules on design are discussed in subsequent sections, along with current trends in equipment.

The rules of golf exist to protect the integrity of the game and there is much popular discussion on how equipment may be altering the sport. The current work may be seen as posing a threat to this traditional nature, and it is therefore worth considering the evidence. Thomas (1994) concluded that driving distances between 1968 to 1993 increased no more than 12 yards while the average winning score in professional tournaments improved at the rate of one stroke per 21 years, lower down the field this improvement was greater, one stroke per 14.5 years for the 25th place man. This indicates a narrowing of the field commensurate with other spectator sports (see below). More recent figures presented by Uihlein (1998) gave the average driving figures for the top ten longest hitters on the USPGA tour in 1997 as 286 yards, a 15 yard increase over the yardage for 1980. While this average figure was raised by the likes of long hitters such as John Daly and Tiger Woods, the average driving distance of all players on the tour increased by only 10 yards during the last 17 years. Hale (1995) demonstrated how

the use of such statistics can be misleading in predicting performance increases but these figures readily address the woes of the critics who believe the modern equipment to allow the ball to be hit too far. Such percentage increases in the players drives and scores is comparable to that seen in other sports during a similar time period, for example in throwing events in the Olympics performance increases between 3½% and 6% per ten years are seen depending on the event (Cochran 1990). With the increase in financial incentives in golf attracting sportspersons from other activities much credit must be attributed to improved fitness, diet, training and mental attitude. In the amateur game advances in equipment have undoubtedly made the game easier to play for higher-handicappers who find game improvement clubs easier to hit. For these players the game has become more enjoyable and this can only have helped in the growth of golf, however over the period between 1981 and 1998 the US national average handicap has dropped from only 16.8 to 16.6 (Associated Press 1998). For the professional player the ability to endorse new equipment (fees can greatly exceed likely winnings) leads to less requirement to perform well in competition and less stress in what is for them often a profession of luck. Changing equipment for a professional who has just won a major tournament would not seem a sensible decision, Johnson (1997) however gives examples of players who chose the endorsement route with a subsequent deterioration of their game. Such players under contract are unable to blame their equipment, and concoct excuses that are not confirmed by the statisticians examining their play.

Lockwood (1992) described how sports that attract big audiences are those where the winning margin is small and the victor not necessarily the better player. He considered the exciting finish to the 1989 Tour de France which after 3,284 km was won by only 8 seconds and the Oxbridge boat race, which ends in the better boat winning. These examples might be considered alongside a major golf tournament result where the winning margin is typically one shot. Equipment improvements that would increase the results margin would probably be to the expense of the game as a spectator sport. Readers must draw their own conclusions on whether improving the chances of the better player/team winning would be to the detriment of their chosen sport but the rules of golf, particularly on equipment design, are such as to preserve the nature of the game for participants and spectators while allowing enough scope not to inhibit the golf

equipment industry. The rules are biannually discussed by a joint committee of the USGA and R&A and are redrafted every four years to meet these ends.

1.3 Clubs

Clubs come in a variety of shapes, weights and materials and a golfer's bag can contain a maximum of 14 different clubs (Rules - Section 4-4), each with the intended purpose of effecting a different ball flight. Each club consists of a grip, a shaft and a clubhead. The head is the most obvious difference between clubs and this leads to the general division of clubs into 'woods' and 'irons' (and a 'putter', used for shots on the green).

1.3.1 Wood clubheads

Woods are 'drivers', used by golfers to achieve long distances and are typically played 'off the tee'. They are characterised by having a larger volume of head than 'irons', with the centre of gravity further behind the clubface, and typically have a longer shaft. Woods traditionally had a head which was actually made of a wood such as persimmon or laminated maple but now, confusingly, they are predominately made of metal. The advantage of wood in the traditional, solid-headed driver was the use of a lower density material which allowed a larger volume of clubhead for a given mass and hence a higher rotational inertia. This led to a more forgiving clubhead which the player needed to be less precise in hitting, which in turn allows for a longer shaft length leading to higher clubhead speeds during the golf swing. Metal 'woods' are made from denser material (eg steel) but modern manufacturing processes allow the production of structurally stiff, hollow heads with even greater volume and rotational inertia than traditional wooden drivers. The current trend is to use exotic metals such as titanium to produce larger heads for a given mass and retain structural rigidity.

A modern wood is shown in figure 1.1. This has a volume of 250 cm^3 and a mass of 198 g. The oversized head is perceived as being even more forgiving on off-centre shots as the rotational inertia is increased. The face of a wood is slightly curved to reduce what is known as the 'gear effect'. In this, if the ball is hit off-centre to the left or right, spin is imparted about a vertical axis and the resultant aerodynamic forces tend to bring

the mishit shot back towards the intended target. The curved face is chosen so that the ball does not overcorrect and the radius of curvature across the face is known as the 'bulge'. Curvature is also applied vertically, from top to bottom on the face which, in golf phraseology, is 'roll'. The gear effect occurs in all clubs but is more noticeable in woods, as the centre of mass is further behind the hitting face. This is discussed further in section 1.6.1.2.

Hollow metal woods were originally filled with a structural foam the sole purpose of which was to reduce 'ringing' and give a pleasant 'solid' sound on impact. As acceptance of metal designs has increased, a unique metal sound is now desired by golfers and foam is not included. The metal shell is usually constructed from two castings of the same material. The face is strengthened internally with a number of vertical ribs cast behind the clubface. Figure 1.2 shows a sectioned half of a metal 'wood', clearly indicating the foam. Figure 1.3 shows the other half with the foam removed to display the strengthening ribs. A second type of wood is shown in figure 1.4. This incorporates an insert in the clubface which is reputed to affect ball flight. The insert is generally made of a very hard material and the score mark shown in the figure is the result of a failed attempt to cut through the insert. This, incidentally, ended in breakage of the sawblade.

Modern casting and fabrication methods admit mechanisation and the use of semi-skilled labour in the manufacture of metal woods. In contrast, traditional wooden heads are created by craftsmen in a labour intensive process, described by Wood and Wood (1995). The hitting area in these traditional clubs must also be covered with a polymer to protect the clubface while the sole is reinforced with a wear-resistant metal plate which also lowers the centre of mass. Each of these processes adds to the cost.

Traditional heads can be given an increased, ie 'improved', moment of inertia by creating a hollow area within the head and filling with a low density material such as cork. A similar method was used unsuccessfully and illegally by the baseball player Billy Hatcher, whose bat broke, spraying the infield with cork, in 1987 (Bahill and Karnavas 1991).

The use of wood as a material of construction is diminishing as more modern and exotic materials such as titanium alloys, ceramics and fibre-reinforced composites become increasingly popular.

Woods are usually used for long shots and as such have low angles of loft (a definition of loft is given later in section 1.6.1.2). Table 1.1 gives typical values for a set of clubs and shows the woods having lofts between 10° and 21°, although a current resurgence in the use of fairway woods is increasing this loft range (Achenbach 1997). The hitting area is grooved, usually with horizontal lines and punch marks although alternative patterns have been used. The rules of golf (Rules - Appendix II, Section 4-1e) specify the geometry and dimensions acceptable for both the head and face markings.

Club	Loft
Driver	10°
3 wood	15°
5 wood	21°
3	22°
4	26°
5	30°
6	34°
7	38°
8	42°
9	46°
Pitching wedge	50°
Sand wedge	56°

Table 1.1 Typical loft angles of golf clubheads (Dorling Kindersley 1998).

1.3.2 Iron clubheads

‘Irons’ make up the majority of clubs within a golfer’s bag. They are used for shots varying from long (220 yds) to short chips and so come in a variety of lofts, as given in table 1.1, and a variety of shaft lengths to create different clubhead speeds at impact. Although there have been some attempts to use other materials, eg woven carbon fibre, ‘iron’ heads tend to be made of metal.

The rules of golf (Rules - Appendix II, 4-1e) restrict the geometry of iron heads and include the caveat for all clubs that the “*face shall not have the effect at impact of a spring*” Iron heads are normally constructed from one homogenous material but changes introduced in 1992 allow them to be constructed from more than one material. However “*the impact area must be of a single material*” This has led to the use of

inserts placed in the hitting area to reputedly affect the ball's flight. Modern casting techniques also admit the design of cavity backed irons which have a void in the back directly behind the hitting face, as shown in figure 1.5. As with woods this leads to increased rotational inertia for a given mass and so makes the club more forgiving on off-centre hits. The emergence of such cavity backed 'game-improvement' clubs has led to the original, usually forged, clubs becoming known as 'blades'. Irons also have grooves upon their faces and the design of these is also governed by the rules of golf (Rules - Appendix II, 4-1e). It is worth mentioning here the incident of the 1980's when a club manufacturer, Karsten Manufacturing, took the USGA and the PGA tour of America to court over a ruling on grooves which caused their clubs to be deemed non-conforming and illegal with the respective authorities. It is the experience of the author that while many people are aware of the ruling there is wide confusion over the exact issues. An excellent reference article (Tutleman 1994) is available for those seeking more information.

1.3.3 Shafts

Shafts, like clubheads, were traditionally also made of wood but these were eventually replaced by steel. This remained the norm until the 1980's when, after a decline in the defence industry, new materials and manufacturing processes were declassified. Nowadays shafts come in a variety of materials and geometric shapes, with formerly exotic materials such as carbon fibre composites being used to lower the mass of the shaft while retaining other, desirable, characteristics such as stiffness. Lighter shafts lead to various benefits: either a decrease in the overall club mass leading to a higher swing speed for the same applied force or, if the whole club mass remains constant, increased head weighting leading to faster initial ball speed for the same clubhead velocity and a possible greater moment of inertia for the clubhead. Changing the mass of the shaft also affects the swing weight, a measure of the turning moment of the club about a position 14 inches from the butt of the shaft, (see section 1.6.2.2)

From 1980 to 1994 the number of companies worldwide producing golf shafts increased from fewer than five to more than a hundred (Wishon 1995). This led to an overabundance of golf shafts available, each with unique properties. However although

there is widespread awareness of the essential role played by the shaft, a lack of understanding of the effect of different shaft characteristics has led to mystery and indeed some mystique surrounding the effects of different shafts.

1.3.3.1 Wooden

During the early stages of the game of golf, shafts were constructed of hickory but these wooden shafts were very flexible and weathered quickly. Their consistency and durability was therefore questionable, with frequent breakage on the course, often with a loss of the clubhead along with the shaft. This led to other materials being investigated and at present the use of wooden shafts in golf clubs is limited to a few traditionalists.

1.3.3.2 Steel

By far the majority of shafts have been constructed from tapered steel tubing. Original steel shafts were made from welded tubular steel which was extruded in a step wise fashion to produce a stepped taper (a more modern development is the smooth tapered shaft). The properties of the shaft are inherently dependent on the material used and the geometric shape. Shafts with elliptical cross sections have been used to reduce out of swing-plane bending but these are now prohibited under the rules of golf (Rules - Appendix II, 4-1b) which states that the shaft shall "*bend in such a way that the deflection is the same regardless of how the shaft is rotated about its longitudinal axis*" and shall "*twist the same amount in both directions*". There must obviously be a tolerance in such a rule but this is unstated and it is, for example, unknown to what extent the weld affects the axisymmetry.

1.3.3.3 Composite

Composite shafts have the benefit of being able to retain some of the desirable properties of steel, such as high stiffness, but with reduced mass. The material is usually in the form of an epoxy resin matrix with reinforcing fibres such as glass, boron or carbon. Carbon-fibre is usually known by the American term 'graphite' in golf and this has been the most successful of the modern composite materials.

Graphite shafts are made from a variety of processes including the laminated sheet process, filament winding and resin transfer moulding (RTM). The laminated sheet process is the most widely used and, perhaps surprisingly, produces shafts of the best quality. This is because the process most readily lends itself to the production of an anisotropic material in which longitudinal fibres are used to give the shaft the correct bending stiffness while fibres laid at other angles, typically $\pm 45^\circ$ to the shaft axis give the shaft the desired torsional properties. Other than anisotropy, the main advantage of composites is a reduction in mass, with shafts of 50 g being possible, a saving of up to 90 g over traditional steel shafts. High modulus fibres are also used to give increased stiffness for less mass, albeit at increased cost.

The introduction of composite shafts was not a smooth one. Early shafts had the reinforcement fibres running only parallel to the axis of the shaft and this led to poor torsional stiffness. This was important as the centre of gravity of the head is offset from the shaft axis and during the swing inertial forces can lead to the head becoming misaligned at impact. This was corrected for by the $\pm 45^\circ$ fibres, however poor manufacturing quality led to the need to sort shafts into categories of bending stiffness and torsional stiffness (discussed in section 1.6.2) and allowed for the marketing of shafts to golfers based on these properties. The need to grade the shafts led to each manufacturer constructing unique test methods and no standard test procedure is available. This has led to the abnormality that shafts labeled a specific 'flex' by one manufacturer can be designated a different flex by another (Horwood 1995). These issues along with the variability from shaft to shaft in a post-sorted batch compared to steel reduced the uptake of graphite shafts by professional players who need to depend on consistency. Amateur players more readily took to graphite for the benefits of reduced mass and increased damping which reduces harmful vibrations from mishit shots (Proctor 1995). As the quality of graphite shaft production has increased professional players have moved to graphite in their 'woods' where less accuracy is needed while retaining steel shafts for their more precision shots played with 'irons' (Proctor 1995). While the trend is for graphite to make its way into the irons of professional players as quality improves, the current work has revealed no hard scientific evidence to justify this trend. The effects of hype and marketing and business strategy of the equipment manufacturers should not be discounted.

1.3.3.4 Other materials

Materials other than steel have been used for shafts, with aluminum and titanium being the most successful in terms of sales. However these suffer from some of the drawbacks of steel, being (almost) isotropic and having similar specific stiffnesses (ie stiffness to mass) and yet are more expensive. This makes them less marketable than either steel or composite shafts.

1.3.4 Grips

The sole purpose of the grip is to provide a secure, non-slip connection between the golfer and the club, especially during the stages just prior to impact when the centripetal forces are about 320 N, (Daish 1972). The biomechanics of the human wrist is such that its movement is more restricted the tighter the hand grips, a statement the reader can confirm easily. High friction between club and hands is thus essential in promoting wrist flexibility. Cochran (1995) stated that the grip may be the most important part of the club to get right and yet is the part most taken for granted. This view is supported by the lack of published research into the effect of the grip and by the large number of different grips available to players. Aldridge (1995) accepted that this was due to individual club manufacturers requiring uniquely patterned grips for their products, a purely cosmetic requirement. Lancaster (1995) categorised grips by material: buffed and un-buffed rubber, plastic or cord composites, and by design features that owe more to road vehicle tyre technology than to golf. He concluded that the variance in performance from different grips was attributable to an effect on the golfer both in terms of confidence and control. However, one of the aims of the current work is to remove the subjectivity of the golfer and so the role of the grip is beyond the scope of the current work. It's pivotal role and the possibilities for future research are however accepted.

1.4 Balls

There are numerous designs of golf ball available. All are and must be spherical (in contrast to, say, rugby balls). They have an exterior pattern of dimples to roughen the face and shift the transition to turbulent air flow, to reduce drag and create lift when the ball backspins. The science of the effects of dimples is an area of current interest, with researchers using such sophisticated techniques as computational fluid dynamics (CFD) to model these aerodynamic effects (Shaw 1995). The balls' specification is governed by the rules of golf (Rules - Appendix III) which, to allow for variations in design, stipulate:

- Weight (maximum - 45.93 g)
- Diameter (minimum - 42.67 mm)
- Spherical symmetry
- Initial velocity (maximum - 76.2 ms^{-1} , under a 'standard hit'*)
- Overall distance (maximum - 256 m, under a 'standard hit'*)

Some evidence (Lewis 1995) suggests that balls were originally manufactured from hard wood, with inevitable damage to the hitting face (a pleasing idea for modern manufacturers of golf equipment). However even if these existed, they were soon replaced by softer balls such as the 'feathery'. This had a leather casing stuffed full of goose feathers. It was expensive and not noted for its durability, especially on mishit shots. At a time of greatest growth in the game of golf, around 1700, a ball called the 'guttie' began to be played (Golf Museum, St. Andrews 1998). These were manufactured from a natural rubber compound, gutta percha, obtained from South America. They were cheaper than the feathery and this, along with the growth in public and private transport and other social changes, helped in the growth of the game. The relatively poor performance of the then existing balls became the subject of research and the coefficient of restitution was improved by Haskey who used strands of rubber,

* **Footnote**

Details of the standard hits involve hitting the ball with a rotating fly wheel for the initial velocity test and a mechanical golfer for the overall distance standard. Both these test are due to be replaced by 'virtual flight testing' in 1999 (USGA 1998).

wound under tension around a dense core and covered with balata, a natural rubber which was again not very durable (Lewis 1995). Such balls are still in use today, more so by tour professionals, with current 'club' golfers tending to prefer a more modern durable two-piece ball which retains many of the properties of the wound ball but is easier to manufacture and is therefore cheaper. A typical two-piece ball construction is shown in figure 1.6. This ball consists of a solid rubber core covered by a thermoplastic synthetic cover. It is the most popular ball in the present market (Proctor 1995) and different combinations of core and cover stiffness are available, each of which is claimed to give different playing characteristics. At the bottom end of the market there is the one-piece ball, which is even easier to manufacture and has found use as a practice ball and on driving ranges.

1.5 Golf research - a historical perspective

The history of golf and golfing science have their own fascination and might be the subject of an academic or popular publication in their own right. Here a brief review is appropriate before the current state of the art is examined.

Some of the first published scientific work on golf and other ball sports was conducted by Peter Guthrie Tait, Professor of Natural Philosophy at the University of Edinburgh from 1860 to 1901 (McKirdy 1990). Tait's first written comment on golf was in 1887 in a letter to Lord Kelvin in Glasgow and to James Maxwell. Subsequent letters between the physicists discussed the merits of the spin imparted to the ball and Tait is to be credited with establishing its significance. His experiments on golf impact at the time were rudimentary by the scientific standards of today and relied on ingenuity to study the complexity of the shot. McKirdy (1990) describes in detail his apparatus for measuring contact times of shot. However, many of his predictions on the limits of golfing performance were often broken by his son Freddie Tait, a professional golfer and, perhaps, his chief assistant. Tait himself was an avid golfer and his biography (Knott 1911) gives a humorous account of an attempt at night-time golf using phosphorescent balls, played along with Crum-Brown, the Professor of Chemistry at Edinburgh. Their play was abruptly halted when Crum-Brown set his glove on fire and burnt his hand.

Early work on golf and ball sports was often conducted by world-renowned scientists and Daish (1972) uses these examples to dismiss those critics who believe the application of science to such matters to be frivolous and, at worst, a prostitution of their subject. Such work includes Gaspard Gustave de Coriolis's 1835 paper on the mathematical theories of billiards. Nobel prize winners are represented by Lord Ralyeigh who published an 1870 paper on '*The irregular flight of a tennis ball*' and Sir J.J. Thomson who published '*The dynamics of a golf ball*' in 1910. More recently contributions to the subject include a paper by the aircraft designer Barnes Wallis on the flight of a golf ball and by R.A. Lyttleton on the swing of sports balls.

Many of these early works relied on the application of new mathematical theories to ball behaviour but the first real systematic practical examination of the golf shot was conducted by The Scientific Golf Society of Great Britain (S.G.S.G.B) whose findings are recorded in '*A search for the perfect swing*' (Cochran and Stobbs 1968). This documents what was then known about the golf swing as a dynamic event and how a double pendulum model of the swing could be used to represent the human effort. The publication also included tests on the impact of clubs with the ball, a summary of the then current knowledge of ballistics as applied to golf and comparisons with practical tests. A more lengthy treatise on the impact between clubhead and ball, giving both theory and practical results, was also published by a member of the S.G.S.G.B. in his book '*The physics of ball games*' (Daish 1972). Both of these modelled the head as a free body impacting the ball, also regarded as a free body. The simplification inherent in this model was recognised but the relative flexibility of the shaft compared to the head means that it is a reasonable approximation and practical tests with a head that could disconnect from the shaft on impact confirmed its validity. It continues to be used in much of the current work.

A follow-on research programme based on the 1968 work of the S.G.S.G.B. summarised in '*A search for the perfect swing*', was intended but never executed. Research on the science of golf was then continued mainly by commercial companies with financial resources but with a sales-driven agenda. However, towards the end of the eighties and with the changing social patterns already discussed, scientific papers on sports technologies again started appearing and 1990 saw the 1st World Scientific Congress on

Golf in St. Andrews. This was organised by the successor to the S.G.S.G.B. and brought together an international audience of industrial researchers, academics and others interested in the science of golf. The conference was an unexpected success with the call for papers being greatly oversubscribed (Farrally 1990). 59 papers were published, in four main areas:

- human factors
- performance statistics
- technology and equipment
- golf course management and the environment

The 2nd World Scientific Congress on Golf was held in 1994 with 92 papers in three main areas:

- the golfer
- the equipment
- the course and the game

The success of the 2nd congress led to a spin off scientific publication '*Golf the scientific way*' (Cochran 1995). This contained rewrites from the congress and additional material on golf research, 48 papers in total, together with the inevitable advertisements. Seven main areas are covered in the publication:

- clubs
- shafts
- golf balls
- equipment & golf wear
- the human element
- statistics and performance
- the golf course

The 3rd World Scientific Congress was held in July 1998.

In addition to the World Congresses on Golf, a more general forum for sports research, the International Sports Engineering Association (ISEA) was created in 1995. This held its inaugural conference in Sheffield in 1996 and the proceedings list 6 papers on golf. The second conference was held in July 1998 and the ISEA Sports Engineering Journal was launched in September 1998.

Other relevant publications include *'The physics of golf'*, (Jorgensen 1994), which uses practical experiments and theories to examine the game. Also available are number of journal papers, numerous popular monthly magazines and thousands of patent applications on golf equipment now partly available through the Internet, and general golf science discussed through other media.

1.6 Golf research - the state of the art

A full simulation of the golf stroke must include the player, their equipment, their environment and the interactions between all of these. However the current work focuses on engineering design aspects of the equipment and so the psychology of the player and of the uncontrollable environment must be regarded as secondary. In this spirit, as shown in figure 1.7, the player is replaced by boundary conditions at the grip on the shaft and a two-track approach is adopted to modelling the equipment subsystem:

- analysis of the clubhead, regarded as an extended body detached from the shaft and with an initial velocity, impacting the ball, also an extended body, in a time scale of the order of milliseconds
- analysis of the shaft during the downswing with the clubhead modelled as a point mass.

To reduce the influence of random factors, experimental work on clubheads is often carried out using mechanical golfers. Based on the double pendulum design, these are capable of producing more consistent hitting conditions than human golfers. The complexity of the machines varies enormously from the pneumatic but expensive **Iron Byron** (USGA 1998) to the University of Glasgow's Sports Engineering Group's spring-driven **Dai Laughing**, described later in chapter 6.

To provide a starting point for this work, it is then appropriate to summarise the results from the existing scientific literature in a structured way looking first at the clubhead, then the shaft and finally the ball.

1.6.1 Clubheads

As noted in section 1.5, the Cochran and Stobbs (1968) model in which the clubhead is considered as a free body impacting a free-body ball has been the basis of much of the subsequent research into those properties of clubheads that affect ball flight, whether material properties, geometric shape or dynamic parameters at impact. It is then appropriate to initially adopt such a model and to review the known engineering factors which influence the results.

1.6.1.1 Material

Golf equipment is often marketed by begging the question of whether clubhead material properties have an influence on the shot produced (Pedler 1997). However the engineering properties which might influence a shot are relatively few and include stiffness, friction coefficient, density and hardness. Unfortunately these strictly-defined engineering terms are used in the popular golf literature in a manner not always in accord with their scientific meaning. Golf writers, for example (Pedler 1997), will attest to the different shot-making ability of soft and hard faces but, for reasons outlined in subsequent sections, the property of influence is more likely to be stiffness. Practical tests on the influence of individual material properties are however inherently difficult since a change of material, to effect a change in one property, will usually lead to a change in another property. Computational analysis is of benefit here in allowing for direct control over each property in isolation.

Stiffness

Stiffness is often regarded as affecting the ball velocity after impact. The popular view, albeit marketing led (see, for example advertisements in *Golf World*, (Various 1997)), is that a more rigid clubhead allows for more energy transfer to the ball. This is predicated on the idea that stiffer materials strain less for a given stress, that the work done is

smaller and so less energy is used up in club deformation. Such is the justification on which ceramic clubheads and stiff, ceramic inserts are currently marketed. However practical tests on the effect of the stiffness of clubheads are rare. Wood and Wood (1995) described a statistical survey in the 1980s by Yamaha, using drivers made of wood, graphite and metal. No effect on distance or accuracy was recorded and in fact, participants could only identify the different clubs by their sound on impact. Wood (the material) was, incidentally, the preferred choice, producing a note near middle C, a pleasant sound similar to that of a human voice.

Take (1995) reports on tests carried out by Daiwa, in which a ball impacted a static plate containing steel and carbon fibre reinforced plastic (CFRP) inserts. They concluded that CFRP can reduce spin rates at higher loft angles but their results are confused by the different impact speeds at different lofts and their inability to isolate the varying mechanical properties of friction and density

Stiffer materials or, more accurately, materials with a higher stiffness to mass ratio, do allow club designers to produce clubheads of greater volume for a given mass. This is the main basis on which titanium headed drivers are sold. There is however current concern from the regulatory bodies that such thin faced metal woods can create a 'spring back effect' also sometimes known as 'trampolining' which may enhance initial ball velocity off the clubface. November 1998, saw the Executive committee of the USGA approve a controversial new test for *Enhanced Rebound Velocity* (Rules - Appendix II, 4-1e). This is discussed in more detail in section 4.3 along with test results from the current work.

Finally, the stiffness of the material also affects the velocity of the stress waves travelling through the clubhead. This does not appear to have been addressed at all in the literature and is discussed in more detail below.

Friction

The effects of clubface friction on the ball flight have been reported to a greater extent than stiffness, probably due to widespread recognition of the importance of backspin* in the flight of the ball. Contrary to many reports in the popular sporting press, including some by professional golfers (Anon, *New Scientist* 1989), all well-hit golf strokes impart backspin to the ball (Jorgenson 1994). The effect of this is to induce lift on the ball and the possible consequences are shown in figure 1.8 for two different types of golf shot. In the low launch-angle shot with a high translational velocity, typically a drive, spin-induced lift prolongs the flight path significantly. Cochran and Stobbs (1968) estimated the spin to increase carry by '100 yards' on a well-hit shot. At the higher launch-angles played with a more lofted club, backspin still induces lift but its main effect on the shot is to reduce the forward velocity of the ball, which appears to hang back in the air and land more vertically, often with sufficient backspin to cause it to return some distance back towards the striker after bouncing (Haake 1989).

Initial efforts to understand the role of friction in generating backspin were carried out by Cochran and Stobbs (1968) in a series of tests using two 5-irons with differing coefficients of friction. The results were not conclusive, as the friction coefficients were not known quantitatively, but they did tend to imply that backspin was independent of friction coefficient. Daish (1972) used the elementary dynamics of rigid bodies to hypothesise how spin might be imparted to a golf ball in a manner not dissimilar to that of a snooker ball, ie sliding followed by rolling. Jorgensen (1994) also used the sliding-rolling theory to explain the spin imparted to a ball and included a simple home experiment for readers to perform. In all these sources, different spin rates are mentioned for different lofts of club but there is little theoretical basis on which to predict actual values. The generalised rigid body mechanics of the shot is shown in figure 1.9, where the velocity of the clubhead is considered as two perpendicular vectors, V_n - normal to the clubface and V_t - tangential to the face. This diagram is used in much literature to explain how as the loft of the club increases the tangential velocity increases causing more backspin on the ball. Gobush (1990) described an experiment using force

* Footnote

Spin may also be applied about any other axis and cause corresponding deviations in flight. For conciseness only backspin is referred to.

transducers to measure the normal and tangential forces caused by an impacting ball on a static plate and calculated the spin from the tangential force and the initial radius of the ball. The results were in accord with values measured by stroboscopic photography. A recreation of Gobush's results are given in figure 1.10 for a wound ball traveling at 29 ms^{-1} striking the plate at 20° and an impact contact time of approximately 450 microseconds. The steps in the normal force curve are common to balls with air spaces such as a wound ball. It is to be noted that the tangential force measured from the plate force transducers changes direction $2/3$ through impact. Liebermann (1990) also reported the effects of the frictional conditions at impact on spin-rate, again using the experimental procedure of firing a ball at an oblique static block. He reproduced the unusual finding from a USGA 1987 (Lieberman 1990) study, that impacts in damp, grassy conditions likely to result in reduced friction, can produce increased spin rates at certain loft angles. More recently, Gobush (1995), using the same experimental procedure, reported spin rates generated from different loft angles under various unknown friction coefficients. He then used a rigid-body/spring theory to explain the spins generated. In this, the ball is regarded as having layers, like an onion, linked by springs which store strain energy due to tangential forces (figure 1.11). This energy is released after impact, causing backspin. Gobush (1996) also used Maw's equation for elastic oblique impact (Maw 1975) to infer friction coefficients from measuring pre- and post- impact ball trajectories and compared these with values obtained from force transducers on the clubhead.

In summary the current view is that spin is generated by sliding of the ball up the clubface followed by a friction-induced rolling action which may be calculated by measuring the tangential forces present during impact. However such calculations are based on rigid body mechanics and take no account of the finite deformation of the ball.

Density

The effect of clubhead material density on the total mass of the clubhead is discussed in section 1.6.1.2. A second effect of density is to alter the velocity of the stress waves traveling through the material. This is considered in more detail below.

Hardness

In engineering, 'hardness' is measured by a test such as the *Vickers Hardness Test* in which a material such as diamond makes a permanent indentation in the specimen (Ashby 1996). The size of this indentation is then (inversely) expressed as the 'hardness' of the test-piece. Hardness is thus a composite measure of the evolution of the yield stress in a material, from its initial value, as plastic deformation occurs. Hardness has been mentioned in the golf literature (Cochran 1995) as being an important material property in the performance of both the ball and the clubhead but if engineering hardness is important, it can only be indirectly. It is most likely that such reports have confused hardness with stiffness.

Stress Wave Velocity

The stress wave velocity (v) is a function (Macaulay 1987) of both stiffness (E) and density (ρ), thus:

$$v = \sqrt{\frac{E}{\rho}}$$

The effect of stress wave velocity on golf club performance does not appear to have been researched but, if stress waves could be reflected back towards the impact area at a precise time, they might have a beneficial effect on the ball in terms of increasing initial ball velocity. The computational approach used in the current work may be useful in this respect.

1.6.1.2 Geometry

The geometry of a clubhead is widely accepted to affect the shot played and so is strictly governed by the rules of golf (Rules - Appendix II). Cochran (1995) regarded the work of Chou et al (1995) as being perhaps the most comprehensive series of club tests ever reported. This included the results of several years of testing into the effect of head geometry in five different areas: head size, mass distribution, loft, offset and mishits. Their results were mainly from robot hitting tests and were subject to the limitations of practical experimentation. For example in investigating the effect of '*clubhead face*

size' using different designs of clubhead, they claim there is a natural shift in the position of the centre of gravity of the head up and away from the shaft. If the ball impact position remains the same this will affect rotation of the clubhead during impact. Also, in using robot testing the effect of the new position of the centre of gravity of the head is such as to change the bending of the shaft during the swing such that the clubhead position and velocity pre impact are varied. This demonstrates the many problems associated with practical testing. Their results from attempting to isolate a property such as *clubhead face size* are unique to the designs they used, the shaft properties and the robot hitter's specific golf swing.

Mass

Theoretically the mass of the clubhead can be shown to have a direct effect on the flight of the ball through both the conservation of momentum and the coefficient of restitution (e) equations. The latter is assumed to be independent of clubhead mass. Considering mass (M) and velocity (V), conservation of momentum gives

$$M_c V_c^0 + M_b V_b^0 = M_c V_c^1 + M_b V_b^1$$

where subscript **b** refers to the ball and **c** to the clubhead and superscript **0** pre-impact velocity and **1** post-impact. The coefficient of restitution (e) is defined as the ratio of the incident and separation relative velocities, thus:

$$e = \frac{\text{velocity of separation}}{\text{velocity of approach}} = \frac{V_b^1 - V_c^1}{V_c^0 - V_b^0}$$

Macaulay (1987) stated that while 'e' was originally thought to be a constant property, it can vary significantly with velocity, mass and other impact conditions. However over the range of speeds found in golf, it is acceptable to assume a constant value. In the particular instance where the ball is initially stationary these equations can be combined to give.

$$V_b^1 = \frac{M_c V_c^0 (1 + e)}{M_c + M_b}$$

For a constant initial clubhead velocity, the initial velocity of the ball is directly proportional to the mass fraction,

$$\frac{M_c}{M_c + M_b}$$

This increases towards unity as the club head mass increases, but higher masses are more difficult for human muscles to accelerate during the downswing and an optimum mass of clubhead is chosen, typically about 225 g. Cochran and Stobbs (1968) have shown experimental evidence using real players that small deviations from the ‘typical’ mass have little effect on distance. In terms of energy transfer the maximum efficiency of delivery of kinetic energy from club to ball occurs when the two have the same mass but to generate the maximum kinetic energy during the swing a golfer requires a clubhead which is much heavier than the ball. Again the ideal lies between the two extremes. Bahill and Karnavas (1991) observed baseball players swinging bats of various masses and determined the mass to give the maximum ball speed. Their results showed that the batted ball speed was constant for bats above a certain mass and the *ideal bat weight* was chosen to give 1% less than this maximum speed (definition *ideal bat weight* = the lightest bat possible that gives 99% of maximum batted ball speed). Their results highlighted the difference between the *ideal bat weight* and that used by most players, especially juniors. On their recommendations the San Francisco Giants adopted new bats and subsequently finished top of their league.

There appears to be only limited similar practical work (Daish 1972) on the optimum club mass for a golfer but then the golfswing is complicated by the relative flexibility of the shaft during the downswing, by centrifugal stiffening (Mather and Jowett 1998) and by the changing inertia of the club due to these effects. Even though a redistribution of mass is the justification for lightweight composite shafts, a reduction in total club mass

may be less advantageous in golf than in baseball, in which bat maneuverability is also a factor.

Loft

Loft is often defined as the angle the clubface makes to the shaft (Chou et al 1995) yet this simple definition is clearly not sufficient for curved clubfaces such as in a 'wood'.

Other definitions are available, yet there is no industry standard and rather than refer to loft angles equipment manufacturers prefer to use a non proportional numeric system, with an increase in the numerical scale representing a weakening loft (increasing loft angle). Typical loft angles and their numeric scale equivalent were given in table 1.1.

A term commonly used is 'dynamic loft' which refers to the loft the clubface makes to the vertical at the instant before impact. This is controlled largely by the individual golfers swing technique and the bending behaviour of the shaft (see section 1.6.2).

Winfield and Tan (1994) used a numerical optimisation algorithm to calculate clubhead loft and clubhead elevation at impact to maximise the flight distance from a drive. Their model was based on rigid body impact and utilised an aerodynamic algorithm to calculate flight distances. Their results gave the ideal loft as 2.74° at a swing elevation of 27.44° and, while they stated that this loft was not supplied by equipment manufacturers, they admitted such an elevation angle would require a 10 inch tee ! Reducing the optimisation to a single parameter problem, they calculated tables of ideal loft for given swing elevation angles and vice-versa. It is to be noted that their results are specific to the aerodynamic model used, which would vary for other ball constructions. Other than Winfield and Tan (1994) there is little published information relating to loft as a parameter. However it is often varied as a matter of course in other investigations and for example, Gobush (1990) used force transducers in a ball/rigid plate experiment with plate angles of 20° and 40° .

Mass distribution

This refers not only to the moments of inertia of golf clubheads but also the positioning of the centre of gravity within the head. The wide understanding is that peripherally weighted heads with larger inertia are more forgiving on off-centre-hits (Cochran 1990). Cochran mentioned this as one of the advances in golf equipment to come from theory rather than evolution and is the basis upon which Ping putters became so successful in

the 1970's (Karsten 1998). Figure 1.12 shows the plan view situation of a 10 mm mishit towards the toe of the club. Values are guessed for demonstration purposes and show the cavity back design maintaining better direction towards the target, with less reduction in velocity and less sidespin. Although the hypothesis of improved performance has been confirmed by many experimenters including Olsavsky (1994) and Chou et al (1995) using robot and human hitting tests, their results are complicated by the use of curved clubfaces in the drivers tested (see below) and the positioning of the centre of gravity, which undoubtedly varies between clubhead designs. In this respect computational methods will be advantageous in examining the effect of moment of inertia while holding other parameters constant. Such a procedure was attempted by Iwatsubo et al (1998) using a 3-D finite element model of a clubhead and ball. The material properties are linear elastic and a coulomb friction model of coefficient 0.05 is used for contact. Nine clubhead models with geometric alterations were investigated, but direct control over the centre of mass and moments of inertia was not possible, although absolute values were known. Their results confirmed the relationship between moment of inertia and improved performance and they also claimed indications that lowering the centre of mass of the clubhead has a similar effect, but this latter correlation is not clear from their results. Their means of measuring post impact ball velocity and spin was similar to the method used in the current work and is discussed in more detail in section 4.2.5. In both the experimental cases mentioned above, Olsavsky and Chou et al, the moments of inertia of the clubhead are only given relatively. An experimental procedure for measuring the inertia matrix for an irregular ellipsoidal rigid body such as a golf club head has been proposed by Johnson (1994). However knowledge of existing clubhead inertias is scant, and current methods of production utilising CAD could be of benefit here. Whittaker et al (1990) used idealised clubhead shapes approximate to a five iron to investigate increases in moments of inertia for a cavity backed head compared to a blade. They reported increases of 70%, 29.7% and 16.3% for the moments of inertia about three orthogonal axis. Hartzell and Nesbit (1996) described a method for calculating possible geometries of a clubhead given the desired inertia matrix and basic initial shape parameters such as face profile. An adaptive random search optimisation algorithm is used to calculate the back weighting, while an operator may also apply geometric influence.

The effect of the positioning of the centre of mass of the clubhead was also addressed in the experiments of Chou et al (1995). Their results agree with accepted theory that lowering the position of the centre of gravity within the head promotes increased backspin and higher initial trajectory. This is due to rotation of the head during impact in a similar manner to that shown in figure 1.12, higher inertia clubheads being less affected by the positioning of the centre of mass. Chou et al results are again complicated by the curvature of the clubface in the drivers used (in this instance roll rather than bulge) and the position of the centre of mass of the head affecting the bending of the shaft and therefore the dynamic loft and swing elevation at impact.

Grooves

There is currently little published research work on the effect of grooves other than the Cochran and Stobbs (1968) finding that there was no significant difference between a 5-iron smooth or grooved clubface. It is not known under what conditions the experiment took place, or if lubricating the face was investigated. Woods and Mase (1990) reported an experiment using fibre optics to measure the deformation of balata and Surlyn covered balls into a grooved plate under static loading. The intensity of light traveling along the groove was reduced as the ball was compressed. They confirmed that the more compliant material, balata, deformed to a greater extent into the grooves and stated that the material build up in the grooves occurred in a non-linear relationship with load applied. Their experiment was not calibrated and results are only qualitative.

Grooves are present on nearly all clubs with the exception of a driver by Cubic Balance (Cubic Balance 1998). Incidentally this manufacturer claims that the absence of grooves will reduce backspin and therefore promote a longer straighter drive. The origin of the existence of grooves is not known and if they have any added benefit it has been found only be evolution rather than theory. The importance (and indeed mystique) of grooves was convinced upon golfers from the high profile case of Karsten versus USGA and PGA of America in the 1980's (Tutleman 1998). It is important to note that while the USGA deemed the clubs non-conforming on the basis of a measurement of distance between grooves, the PGA of America conspicuously never presented any evidence showing that grooves affected ball flight.

Clubface curvature

Curving the face has been used for a long time in clubhead design and no individual has been attributed with the invention. Even clubs from the 17th Century in the Golf Museum, St. Andrews clearly show degrees of curvature, or 'bulge' and 'roll' in golf terminology. Roll is the vertical curvature and bulge the horizontal. Shaping of the face is carried out to reduce the 'gear effect', which is so known as it resembles the meshing of two gears. (Mahaffey and Melvin 1995). Figure 1.12 showed how for a mishit shot off the toe of the club, the club rotates during impact and the opening out of the clubhead leads to clockwise (slice) spin and an error in trajectory away from the intended target line. When the centre of mass of the clubhead is significantly behind the clubface, as in figure 1.13, rotation of the head also applies a tangential force to the ball creating anti-clockwise (hook) spin, this is the gear effect. The ball's resultant spin after impact comes from the summation of the two opposing elements. For a wood with a flat face the centre of mass is sufficiently behind the clubface that the gear effect is predominant and the ball would set off right of the target but during flight the spin will bring the ball back across the target line to land on the left. As is shown for the flat surface in figure 1.13. Creating a curved face reduces the gear effect element and attempts to lessen the ball flight's over correction. It is to be noted that all clubs create a gear effect, it is only when the centre of mass of the head is sufficiently behind the face that the gear effect becomes predominant and over correction can occur, in iron clubs where the centre of mass is close to the face the gear effect is less and helps reduce side spin generated by a mishit. It is clear from the above explanation that obtaining the correct bulge and roll for any clubhead design is a difficult task. Traditionally it has been determined by the eye of the craftsperson and with simple tools. Such a traditional clubmaker, Maltbie (1986), states that the bulge should have a circular radius of 8-11 inches and the roll 11 inches. Current methods of production most likely use an empirical design and test approach, as there is little research into clubface curvature with the exception of Winfield and Tan (1996) and Iwatsubo et al (1998). Iwatsubo (in the same experiment as mentioned above under the heading mass distribution) merely confirmed that as mishits move away from the point of no clubhead rotation, spin increased and then decreased due to the curvature of their finite element clubhead face, which was not specified. Winfield and Tan carried out an optimisation algorithm, similar to the procedure they used above in optimising loft. They optimised the clubhead

curvature radius to provide minimum dispersion from the intended target line but again their model was based on rigid body impact and utilised an aerodynamic algorithm to predict ball landing positions. They calculated optimum values of bulge and roll as 17 and 24 inches respectively. These values are specific to the ball properties used in the aerodynamic calculation, the velocity of the clubhead (110 mph) and loft angle. Their model did not include additional factors such as clubhead trajectory, friction of impact materials, ball material properties, etc. The significant difference between their result and that which has been found by evolution is to be noted.

1.6.1.3 Dynamics

As the golf stroke is a dynamic event it is necessary to consider appropriate velocity components of the clubhead which may affect the subsequent ball flight. As the impact time is of short duration, typically $\frac{1}{2}$ millisecond (Scheie 1990) the current work considers the clubhead approaching the ball with a constant velocity. This is an approximation but the change in elevation and acceleration of the clubhead caused by the golfer during the final moments of the downswing is negligible compared to that caused by impact. The size of this approximation error can be shown to be negligible by a simple example. Consider a clubhead approaching a ball traveling at 44.69 ms^{-1} (100 mph) and rotating about a fixed pivot 1.0 metre (40 inches) away. This radius is shorter than a standard driver and the 'fixed pivot' is not strictly the case as the hands continue to move during the swing. However both approximations lead to an over estimation of the error. The difference in swing elevation angle or the clubhead trajectory vector during 0.0005 seconds is calculated as 1.28° . In addition it is possible to calculate any likely change in speed due to clubhead acceleration. If an average acceleration of 223.5 ms^{-2} is taken, based on accelerating the clubhead from stationary to 44.69 ms^{-1} in 0.2 second, (the downswing of an amateur golfer is typically 0.38 seconds, senior PGA tour - 0.28 and US PGA tour - 0.29 (McTeigue and Lamb 1995), so this is a safe overestimation), the change in speed during 0.0005 seconds is 0.11 ms^{-1} and change in velocity, both elevation and speed, is thus minimal compared to any that occurs due to contact with the ball. The calculations also demonstrate the error in the commonly held idea that accelerating the clubhead through impact will benefit ball flight. Any acceleration of the clubhead occurring through impact is negligible and could have been

more usefully used pre-impact. This is not to deny that the intention of accelerating the clubhead through the ball is not a good one for the golfer or that during acceleration the clubhead is less likely to be moved off line. Indeed a survey of 9 professional golfers showed that they all accelerated their putter head through impact with the ball. (Daish 1972).

Velocity

The velocity of the clubhead at impact is a vector describing the speed at which it is traveling and the elevation. With the exception of Winfield and Tan's (1994) loft optimisation results for specified clubhead elevations, most golf literature only makes use of the conservation of momentum and coefficient of restitution (e) definition (see section 1.6.1.2) to predict a linear relationship between clubhead velocity and initial ball speed. Although it is to be expected that e will reduce at high velocities due to the damping of the materials, specifically the ball, the range of possible clubhead velocities suggests that any change in e is negligible. The clubhead speed at impact is often measured for golfers of all abilities, in an effort to match the shaft stiffness to the power of the swing, while clubhead speeds also vary as the club length changes. One of the current long hitters on the professional tour, Tiger Woods has been recorded as having a clubhead speed of 130 mph. This must be considered near the upper limit and in the current work a velocity of 50 ms^{-1} (112 mph) is used in most analyses to simplify presentation of the results.

1.6.2 Golf swing and shafts

The current work aims to predict the performance of the golf club under the forces generated during the golf swing. Unfortunately and obvious as it may appear to the reader the golf swing is carried out by human beings. So not only does the equipment deform and react to the human's output but, conversely, the human reacts to the equipment's behaviour. The current work then approaches the task on two tracks: modelling of existing shafts and modelling of the golf swing. In its broadest sense, the second approach is a very large area of study and has been addressed by numerous researchers, each expert in their own field. It includes, for example, psychological studies. However, no attempt is made to review such a wide body of knowledge and

only those issues relating to the modelling of the swing within the current context are included. Interested readers are directed to the sources given in section 1.5 for further information on the mechanics of the swing.

Investigations into the performance of shafts followed on from successes that the equipment industry achieved with its research into clubhead designs. Many of these studies aimed to identify shaft properties that effect the swing performance of the club but care must be taken interpreting the published studies as they are often from industry related sources and highlight properties or results more in accordance with a marketing strategy than with objective science. The parameters affecting performance of the shaft must relate to the engineering properties of the material and the geometric design. However the terms used in golf research derive from measurements taken from the finished product and it is appropriate in the current work to relate shaft performance within these terms. It is believed (Horwood 1995), (Butler and Winfield 1995), (Wishon 1995) that five key properties determine the shaft's behavior during the swing: flex, torque, bend point, damping and weight. These golf terms must be defined in unambiguous engineering terminology before any attempt to review the state of the art in golf shaft research.

1.6.2.1 Shaft properties

Flex

Flex perhaps best exemplifies the problem in specifying shaft properties. It is measured as the bending deflection of the shaft under an applied load. However neither the boundary conditions of the shaft, nor the load position nor its magnitude are standardised. One common industry procedure is to clamp the butt and apply 2.72 kg (6 lbs) at the tip (Horwood 1995). The tip deflection is measured from a 'tip deflection board' and shafts are then graded, typically into the letter-coded categories **l**, **a**, **r**, **s**, **x**, corresponding to a decrease in the tip deflection and referring respectively to **ladies**, **amateurs**, **regular**, **stiff** and **extra stiff**. The engineering property of the shaft being investigated in such a test is the bending stiffness but flex will be used in the current text in accordance with other golf literature. The lack of a test standard can lead to any specific shaft appearing under different grades from different manufacturers. Indeed,

Wishon (1995) carried out tests on over 1000 shafts and showed the difference in flex between shafts of the same letter code was often greater than the mean flex difference between grades.

Frequency measurement is also used in the assessment of flex. The shaft is clamped at the butt and the tip deflected by hand and released to oscillate freely. The frequency is then recorded and expressed in cycles per minute (cpm). This natural frequency is related to the system stiffness, and hence to the flex, by the cantilever vibration equation:

$$f_n = \frac{1}{2\pi} \sqrt{\frac{K}{m}}$$

where	f_n	=	natural frequency of vibration
	K	=	system stiffness
	m	=	system mass

The boundary conditions of the shaft are not specified. Nor is the presence or absence of a grip or clubhead. However, like the tip deflection method, frequency measurement allows quantitative grading of shafts into categories. The system may be used on raw shafts with a standard mass applied at the tip or on constructed clubs in an effort to 'frequency match' a set (see section 1.6.2.2).

Torque

Torque is used to describe the angle by which the shaft twists about its longitudinal axis when a turning moment is applied axially. It is measured in degrees but again neither the boundary conditions, nor the load position nor its magnitude are specified. One common industry procedure is to clamp the butt and apply a 1.35 Nm moment arm at the tip (Horwood 1995). While the torque was fixed by the material and geometry in homogenous steel shafts, the advent of composites has allowed a greater variability and, whether a deliberate design feature or merely a by-product of manufacture, shafts are now marketed with varying torques. The engineering property of the shaft measured in this manner is the torsional stiffness and the golfing term 'torque' is a misnomer. It is however used in the current text.

Bend point

The bend point of the shaft is also known as the kick point or flex point but again an agreed definition does not currently exist. It is a single measure that makes an attempt to quantify the bending profile of a shaft. In the current work it will be used to refer to the position on the bent shaft furthest from a chord drawn from butt to tip. Shaft bending is created in various ways: by applying a bending force, compressive force or end bending moment (Horwood 1995) as in figure 1.14. The bend point is recorded as the distance from the tip to the point of maximum transverse deformation. Horwood (1995) gives a system in use in the Far East, where the ratio of the deflection in a standard flex test to one where the tip is constrained and the butt loaded is used to estimate the bend point. This system has the advantage of not requiring measurements from a curved surface. Horwood (1995) also states that if the bend point is within 25 mm of the geometric mid-point of the shaft it is labelled mid bend point. Outside this range it is classified as high or low. The theory behind the positioning of the bend point is shown in figure 1.15 and appears sound. Shafts with lower bend points lead to higher dynamic loft at impact, as the radius of curvature towards the tip is smaller, assuming the shaft is bent forward at impact. It is possible that this value was introduced due to criticism of the flex measurement that allows two shafts of identical flex to have different bending profiles and thus different performances.

Damping

Damping is a property of the shaft normally discussed in golf literature only qualitatively. It is claimed that the increased damping of composite shafts over steel leads to reduced 'feel' of the golf shot while also possibly reducing the incidence of ailments caused by post impact shaft vibration, especially after contact with the ground. A modern development in composite shafts is the use of thermoplastic epoxies rather than thermosets, the advantages claimed (in excess of the ubiquitous improved distance and accuracy) being increased damping (Jordan Golf 1998). No standard tests are available for measuring the damping of golf shafts and manufacturers make no quantitative claims.

Weight

Weight is (thankfully) a property over which there is no disagreement on measurement technique, even if the units still vary. The actual mass of the shaft is often quoted and in terms of performance the axiom is that lighter shafts lead to increased clubhead speeds at impact. Butler and Winfield (1995) state an expectation of increased clubhead speed of 1.3 ms^{-1} following a reduction in shaft mass from 120 g to 60 g as would typically derive from moving from a steel to a composite shaft. Frank Thomas (Tutleman 1998), Technical Director to the United States Golf Association, has stated that a shaft of reduced mass 56.7 g (2 oz) leads to increased velocity of 0.91 ms^{-1} (3 fps) and increased distances of 4.57 m (5 yds). Mass tolerances from manufacture can lead to variations in the other shaft properties previously mentioned and Horwood (1995) states tolerances of $\pm 7 \text{ g}$ and $\pm 2 \text{ g}$ for budget and high quality shafts respectively. Tighter tolerances may be achieved by sorting of shafts post production but this has limited value if the position of the centre of mass is not included. For high quality shafts a centre of mass tolerance of $\pm 3 \text{ mm}$ is typical.

1.6.2.2 Club matching

Attempts have been made to match the 'feel' of clubs across a set, to improve golfers' performance in their swing. The methods used do not relate directly to the performance of any individual shaft but mention is made here since they are important in the marketing of golf clubs.

Swing weight

In an attempt to match all clubs across a set each club may be designed to have the same swing weight. This is a value given to a completed golf club consisting of shaft, head and grip. The swing weight is measured as the turning moment of the club mass about a pivot 14 inches from the butt. The value in inch-ounces is converted to an alphanumeric scale in which each swing weight point represents a 2 inch-ounce difference. D0 is 240 inch-ounces, C9 is 238 inch-ounces and E1 is 262 inch-ounces. This 'lorythmic' scale dates back to its inventor, Robert Adams, who, in the 1920's, used it to match both Bobby Jones' and Frances Oimet's clubs (Tutleman 1998). While much debate has raged over its relevance (Cochran and Stobbs 1968), (Jorgensen 1994), (Cochran 1990),

it can be generally accepted that the method is an **attempt** to condense the heft factors of 1st and 2nd moments of inertia into a single numerical value. While neither of these is ever constant through a set of variable length clubs, matching of swing weight allows at least a reasonable match in 2nd moment of inertia. Various club manufacturers have at times produced clubs matched on 2nd moments of inertia but this method has not been widely accepted.

Frequency matching

In addition to the heft factors of the club, efforts have been made to match the flexibility across a set (Sato 1995), again to give each club a similar feel during swing. It is not possible to match the frequencies as the club length gets shorter and the system stiffness increases (even though the mass of the heads increases) and so a constant gradient of frequency against club length is used. This, like swing weight matching, attempts to provide a constant variation between clubs. A typical frequency gradient is given by Sato (1995), as a linear relationship between club length and frequency, from 255 cpm at 43 inches (a driver) up to 325 cpm at 35 inches (a pitching wedge).

1.6.2.3 Double pendulum

In any review of the behavior of the shaft during the swing one touches upon much wider research on the golf swing, the early work of which was carried out by the Golf Society of Great Britain (Cochran and Stobbs 1968). In this, a double pendulum model of the swing is built up from theory and with empirical results from photographic evidence of top golfers. Figure 1.16 shows the 'Cochran and Stobbs' double pendulum. The rigid top link represents the arms of a golfer and the rigid lower link represents the golf club. A torque can be applied to the model at the fixed pivot **O** to represent the major force input from the golfers legs and torso. Another torque can be applied at the variable pivot (or hinge) connecting the two links, to represent the wrists. A stop is included at the hinge to prevent closure of the wrist angle during the early part of the downswing, although in practice the human wrist does not allow radial deviation of the joint to more than approximately 100°. The forces can be varied to model various golfers' swings and the authors suggest that the golfer tries to follow the planar swing as simply as possible. However if the golfer's wrist is to perform as in the model, limb joints within the human

body necessitate rotation of the left arm about its longitudinal axis (with a corresponding rotation of the golf club). The bending behavior of the shaft in a real golf swing is thus much more complicated than in the two dimensional model. The limitations of the 2-D model were well-appreciated by Cochran and Stobbs (1968) but its use has been extended over the years and it is used in a modified form in the current work. Cochran and Stobbs (1968) used it to show that the effect of gravity in powering the swing is negligible and that wrist timing is essential in achieving a good golf swing. The wrist must apply a torque during the early stages of the swing to prevent closure of the wrist angle, an inherent property of the human wrist. In a well timed swing the wrist may also apply a restraining torque to prevent premature opening-out of the club, then an assisting torque once opening-out becomes desirable. Cochran and Stobbs included various 'time-lapse' double pendulum simulation diagrams to demonstrate the applications of wrist torque at different times during the swing. Such a diagram is included in figure 1.16 along with their original caption. Of course, they did not have the luxury of modern computing and little actual quantitative data is presented. For example, neither the masses nor the moments of inertia of the links nor the forces applied are given. They advised the continuing study of the pendulum model by other researchers with more resources and another member of the Golf Society of Great Britain (Daish 1972) derived the equations of motion for the double pendulum using a Lagrangian approach but again only gave qualitative results. In contrast, Lampsas (1975) used the equations and optimal control theory quantitatively to search for optimum torques to obtain maximum clubhead velocity at impact.

Mention must be given here to earlier work by Williams (1967) who matched a mathematical double pendulum to a classic stroboscopic photograph of Bobby Jones, showing clear similarities. Williams applied a constant torque to the upper lever, until opening out of the wrist angle, and then zero torque. No torque was applied at the wrist and only rigid links were used for the pendulum.

Jorgensen (1994) used a computer program to solve the differential equations of motion of the double pendulum and attempted, via iterative changes in the force inputs, to match the model swing to stroboscopic photographic evidence of a professional golfer. Little quantitative details of the model swing are given other than results from varying the

initial wrist cock angle. The force profiles, mass and moments of inertia of the model are not given. Only rigid links were used for the double pendulum model but an attempt was made to include shaft flexibility.

More recent quantitative work by Pickering (1998), using the double pendulum, has investigated the effect of the release angle. He used a mathematical two link rigid model in which the arms at the start of the downswing were rotated back 180° from the address position and the wrist cock was 90° . The release angle was then defined as the angle by which the upper link rotated during the downswing before the wrist was released. Solutions to the equations were obtained by a Runge-Kutta method and showed the effect of the release angle on the velocity, trajectory and position of the clubhead at the point of the swing when the head reaches maximum velocity, the hinge position was also noted. Results showed a minimum clubhead velocity at the release angle that occurs naturally if no constraint is applied to opening out of the lower lever. Maximum velocity occurred at a release angle of 90° , when the upper lever was horizontal, but results did not continue above a release angle of 90° . Computations were repeated for three types of club, viz 3, 6, and 9 iron which showed a vertical shift in the trend line. In each case, increasing the release angle beyond the natural opening point led to increased: velocity, displacement of the ball ahead of the swing axis and positive gradient of clubhead trajectory. Pickering also compared the behavior of the model to accepted golf swing practices. For example, the model predicted the position of the point of maximum clubhead velocity, for the same release angle, to move back towards the swing axis as the club length shortened. The corresponding view in golf practice is that the ball is moved back in the stance as the shorter clubs are used. He also repeated the computations to obtain the parameters of the swing when the ball impact was made directly below the swing axis. In all the simulations a constant torque was applied to the upper lever throughout the downswing, while the wrist torque was such as to maintain a 90° wrist cock until the release angle. Neither the mass of the upper lever nor the magnitude of the forces applied were given.

Golf machines

The need for manufacturers to carry out quantitative testing on the performance of clubs has led to a number of (often expensive) machines designed to carry out the golf swing in a more repeatable manner than with humans. Their use has been limited in published research and their utility in the design of equipment for players has been questioned (Mather 1995). However their continual use by the United States Golf Association in the testing of golf balls for conformance to the Overall Distance Standard (ODS) over the last 22 years warrants their inclusion in the current discussion, if only for historical interest since the machine is soon to be replaced by more sophisticated technology involving 'virtual flight testing' (USGA 1998). Levin (1998) reviewed the history of the most famous golf swing machine 'Iron Byron' as used by the USGA and shown in figure 1.17. Designed by engineers from True Temper in 1965 the swing machine is based on the swing of the 1940's golf professional Byron Nelson, who was observed using high speed photography at 10,000 frames/second. Iron Byron is powered by compressed air and in USGA ODS test achieves a clubhead speed of 109 mph. The machine incorporates a cam that matches Byron's (the golfer's) swing. This controls the rate of closure of the head to make it square at impact. Suzuki and Inooka (1998) point out the limitations of the machine, such as that the wrist angle is a function of the arm position and that the machine does not respond to changes in equipment. However there are currently thirty eight copies of the machine worldwide, in use by manufacturers for testing shafts, clubheads and balls.

1.6.2.4 Experimental tests

A general study of how the shaft properties affected the performance of the swing was done by Van Gheluwe et al (1990). They compared 51 male and female golfers playing with graphite fibre reinforced plastic (GFRP, or 'graphite') composite and metal shafts. The subjects hit balls in a golf simulator and were recorded with a high speed video camera to record swing attributes such as wrist cock angle and angular displacement of the arms. A statistical analysis showed no significant advantages of either type of shaft in terms of the ball flight as predicted by the simulator or significant differences in the swing kinematics measured using the camera. It is not stated whether the golfers or the

experimenters knew which shaft was being used (ie a double blind test), nor were any of the properties of the shafts given.

In a another practical examination Pelz (1990) carried out a 'blind' test on golfers performing with steel and graphite shafts, in the sense that the golfers were blinded as to where their shots had landed. Three USPGA Tour professionals hit at least thirty shots each with various clubs with different shafts but with the same head. While the results were not tested for statistical significance, the graphite shafts, which were 30 g lighter, hit longer. The stiffer shafts, both in steel and graphite, gave less dispersion, with the graphite having greater dispersion at all stiffnesses. The pre-shot routine of the golfers was not noted and it must be assumed that they were able to waggle and test the club before taking a shot.

Chou and Roberts (1994) tested the role that the bend point plays in altering the ball trajectory. Various bend point measurement methods, for both steel and graphite shafts, were compared to the results of actual testing. They expected that bend point values would have an effect on the initial trajectory of the ball, measured from the peak trajectory height. Both human and machine golfers were used but little correlation was noted. While accepting that their test was far from thorough, they gave indications that the balance point (centre of mass) and torque of the shaft may be more highly correlated with the ball flight trajectory than is the bend point.

Wrist torque

The influence of the wrist torque is clear from the research on the double pendulum. The swing is however successful if the wrist only hinders jackknifing, possibly offering resistance to premature opening-out but creating no torque to assist opening out. This was demonstrated by Cochran and Stobbs (1968) who showed photographic evidence of the swing of Alec Wilmot who was able to hit the ball 283 yards, a prodigious distance for that time, and by a one-armed golfer! The photographic evidence showed a late hit, indicating that the wrist hindered opening out of the wrist cock. Only minimal torque could be applied to assist opening out of the wrist due to the absence of a right hand push.

Much debate has continued into the behaviour of the wrist torques applied. Budney and Bellow (1990) used force transducers to measure the grip force under various locations of the two hands during a full golf swing, including takeaway, backswing, downswing and follow through. Results for golfers of various skill levels showed levels of grip were dangerously small at impact. This coincides with the fact that low levels of grip promote a free hinge action at the wrist (see section 1.3.4). The plots for the various golfers are comparable and indicate the right hand applying force just before impact. The transducers were however under the three fingers of the right hand and any force applied here would retard the club if supination of the left arm back to the clubhead being square to the swing line had not occurred. It is difficult to draw firm conclusions from their results as the grip force may not correlate with the forces applied to the wrist cock angle. Other research such as that by Robinson (1994) has indicated the importance of the kinematics of the wrist cock angle. These studies are discussed in more detail in the following section on motion analysis. A fuller review of other research into the behaviour of the wrist hinge in the golf swing was given by Dillman and Lange (1994).

Motion analysis

Much research on the golf swing has followed advances in motion analysis. Woods and Mase (1990) reviewed high speed analysis systems available for studying the motion of a downswing, less than 0.3 s for USPGA tour professionals (McTeigue and Lamb 1995). Other figures for amateurs and Senior tour players are given in table 1.2. These times mean that normal video cameras running at 25 frames/s are capable of capturing only 8 frames during the downswing. Incidentally the fact that the human eye sees such a frame rate as a continually moving image casts doubts on the observational claims made by non-technology-assisted analysers of the golf swing.

	backswing (seconds)	downswing (seconds)	whole swing (seconds)
U.S. PGA Tour	0.80	0.29	1.09
Senior PGA Tour	0.28	0.28	1.03
Amateur	0.38	0.38	1.29

Table 1.2 Golf swing times, various golfing ability (McTeigue and Lamb 1995).

Motion analysis systems vary in their complexity from the high speed video camera systems currently being employed to analyse the swing by the USGA in their ongoing 'Motion Analysis System' (Logan 1997) to the stroboscopic photographs of Bobby Jones used by Williams (1967). The USGA system uses 5 video cameras running at 240 frames/s while the golfer wears a special suit with markers attached at critical body positions. Logan (1997) states that the raw data is analysed by Nesbit who recreates the golfer's swing with the use of computer software of a robotic golfer. The forces and stresses are calculated and passed to the American Sports Medicine Institute in Birmingham, Alabama. Logan however quotes Frank Thomas, Technical Director to the USGA as saying he is 'not sure where the research is going or when any results will become available'. Nesbit et al (1994) discussed an android golfer developed with ADAMS/ANDROID software and driven by the data obtained from high speed video analysis of a human golfer. The static properties of the golf clubhead were obtained from finite element solid modelling. Problems with the android included making sure the feet remained in contact with the ground during the swing. They concluded with remarks to how the model could be used in conjunction with a systematic variation of club parameters to study the effect of equipment on the golfer. It was not made clear whether a flexible or rigid shaft was used.

Both Robinson (1994) and McLaughlin and Best (1994) carried out statistical analysis on the swings of golfers measured using the PEAK Three Dimensional Motion Analysis System, Version 5. Robinson carried out a multiple regression analysis technique to identify swing characteristics that best correlated with the clubhead velocity at impact and utilised force plates within the events measured. He listed, in order of significance, the events which lead to a high clubhead velocity. Top of the list was the wrist cock angle at the point in the downswing when the left arm was horizontal. The coefficient of significance was negative, indicating that smaller angles gave greater clubhead speed. This confirmed Cochran and Stobbs's work (1968) showing that the key to a powerful swing is the prevention of the premature opening out of the wrist cock angle in the downswing. However this may also indicate the need for an assistance shortly after opening out if correct timing of the swing is to be achieved. McLaughlin and Best used a one way analysis of variance to distinguish between the golfers of varying ability. They produced a list of events which showed a high degree of significance, amongst

these was the wrist cock angle at the position in the downswing when the left arm was horizontal. They noted that prevention of opening out of the wrist cock at this phase was a trait of the low-handicap golfer. Burden et al (1998) studied the golfer as distinct from the equipment, using two genlocked video recorders running at 50 fields per second. They were able to obtain shoulder and hip rotation angles during the swing and concluded that 75 % of their sample of eight golfers continued rotating the shoulders away from the target as the hips began turning back to initiate the downswing.

Cooper and Mather (1994) described a procedure using a stroboscope and a pair of normal photographic cameras to calculate the positions of the golf club during the swing of golfers of various ability. The spatial coordinates were calculated using an iterative linear transformation algorithm (ITL) and differentiated twice to obtain velocities and accelerations. This was necessarily followed by a smoothing procedure. They demonstrated how the velocity profiles of the club for different levels of golf expertise could be classified and made suggestions that the golfers of low skill levels would be better served by equipment that placed different forces upon their bodies. They also concluded that poor golfers had little ability to maintain the wrist cock angle for a sufficient time and that this allowed the club to swing out across the swing plane, with consequences for their shot quality. Mather and Cooper (1994) also made use of a finite element model to predict the forces involved in the swing and the bending behavior of the shaft. They stated that

“An important conclusion therefore is that the head deflection does not depend only on the speed of the clubhead but also on the time history of the input accelerations.”

The importance of maintaining the wrist cock angle under the increasing centrifugal force was discussed and they made a further suggestion that the poorer golfer could be helped in achieving the correct timing by the use of clubs of reduced head mass.

In similar work, Miura and Naruo (1998) recorded the clubhead and wrist velocity of various levels of golfers using synchronised CCD cameras and a video recorder. The 3-dimensional spatial coordinates were transformed into a best fit swing plane before differentiation was used to obtain the velocities and accelerations. Results were given

for various categories of golfer including professional, low-handicap amateur, mid-high handicap amateur, senior and lady. These showed quite distinct differences particularly in the wrist acceleration. Miura and Naruo attempted to model the swing using commercially available software, using rigid links for the pendulum and omitting a wrist stop. Forces were not applied but rather an acceleration profile was given to the upper lever. In the case of constant acceleration, severe jackknifing occurred and the model did not replicate a golf swing. A sinusoidal acceleration, actually specifying the negative acceleration of the wrist, gave a 'decent' golf swing. While their approach was contrary to the normal double pendulum model in which wrist deceleration occurs only due to momentum transfer, it does give rise to the concept that the golfer may deliberately decelerate the wrist hinge. Indeed in certain cases, where the equipment is poorly matched to the upper body inertia, a forced deceleration may be necessary to achieve an acceptable golf shot. Their wrist hinge velocity charts confirm the categorisation of golfer scheme taken by Mather (1995). The acceleration charts for the lady golfer showed a low constant level of acceleration, possibly because any higher acceleration would have prohibited the wrist uncocking as her upper body mass was lower than that matched to her clubs.

Strain gauging

Horwood (1994), in a review of the properties of the shaft that affect performance, gave results from strain gauging of the shaft during the swing. No technical details of the experiment were given such as the position of the gauges, the sampling frequency and whether the results are from a human or machine golfer. A bending moment versus time plot was shown and it was stated that it was for in-swing plane bending.

Butler and Winfield (1994) also gave results from strain gauging of the swing and claimed that after hundreds of tests trials most golfers were found to fit into one of three categories by the way the shaft was loaded. They gave the shaft deflection versus time plots for each category; deflection in the head toe up/down, head forward/back and torsional displacement. A strange anomaly of their results is the long downswing times of two of the categories, in excess of 0.5 seconds, much greater than those given by McTeigue and Lamb (1995) in table 1.2. This may have been due to the awkward nature of swinging an instrumented golf club but claims are made that the clubhead speed

at impact was 103 mph in each instance. They drew up a list of key attributes distinguishing each swing and advised that knowledge of these variables is important in the matching of specific shafts to individual swings. They included the important facts that it would be necessary to measure the variability between swings of the same golfer and include the mean and standard deviations in any matching and that a golfer's swing may be affected by the equipment being swung.

Strain gauging of the shaft was also carried out by Masuda and Kokima (1994) who noted the behaviour of the shaft under impact. Their work is referred to in more detail in Chapter 4, as an issue of impact.

1.6.2.5 Modelling the swing and shafts

Advancing upon the seminal work achieved with the double pendulum model of Cochran and Stobbs (1968), Milne and Davis (1992) used a mathematical approach to modelling the swing based on the double pendulum and using ramped forces at the shoulder and wrist pivots. The equations of motion were solved using a Runge-Kutta scheme. The 2-dimensional model incorporated shaft flexibility to predict the bending moments and deformed shape of the shaft during the swing, however an important essential feature of their model was that the stiffness of the shaft was inferred from a standard cantilever bending test. They admitted that this was erroneous due to the large centrifugal forces near impact which puts the shaft under considerable tension and affects its stiffness. They also state that the shaft bending frequency when held by the hands is not that of a clamped beam and is more appropriately modelled as pinned. They gave typical natural frequency values for a clamped shaft as 4.5 Hz whereas the pinned shaft was 25 - 30 Hz increasing to 35 - 40 Hz under the centrifugal force experienced near impact. Torques applied to the model were estimated from golfers swings where strain gauges were placed at three stations along the length of the shaft. Their results concluded that the bending properties of the shaft were not important in the dynamics of the swing and only altered the deformed state of the shaft near impact under the quasi-static situation of the offset mass of the clubhead and the large centrifugal force. Bending moment versus time plots from the strain gauges were displayed but the sampling rate was 200 Hz and multiple swings were needed to obtain complete data from all strain gauge stations. A

simple smoothing routine was also needed due to variations between swings and to minimise sampling errors. The results indicate that the shaft bends back during the first part of the downswing and then bends forwards just before impact. The largest bending moments occurred at the butt during the first half of the downswing. Milne and Davis (1992) also state that:

“(their model) could be used as a design tool to explore in detail the interaction between a range of shafts and ‘golfers’ as represented by their input torques. No attempt is made to do this here”

They concluded their research by testing a number of golfers in their ability to predict the flex of the shaft by taking shots without a pre-shot waggle. Neither the amateur nor professional golfers could do so, giving, if asked, a random selection of responses. The professionals had limited success with the woods.

Brylawski (1994) continued mathematical modelling of the shaft during the downswing using discretised elements to approximate the tapered shaft in three dimensions. The equations of motion were solved using a numerical integrator for each section along the shaft, however hardly any results were given. She drew the same conclusion of Milne and Davis (1992) that a quasi-static state leads to the deformation of the shaft at impact.

Mather (1995) claimed his own research also substantiated Milne and Davis's (1992) advice that, due to the lack of dynamic effect of shaft flex, the stiffest shafts possible should be used, with a compensation for a lack of increase in dynamic loft by bending being undertaken in the clubhead. Mather took the theory of centrifugal stiffening further by predicting the natural frequencies for static shafts clamped at the butt and graphically showing how shorter clubs have higher frequencies. He continued, showing how these frequencies would change under centrifugal stiffening. The higher velocities for the longer clubs leads to a sign change of the frequency gradient and the longer clubs now have a higher frequency than the shorter clubs and that therefore the stiffness of any individual shaft changes during the swing.

In later research Mather and Jowett (1998) examined the effect of centrifugal stiffening on the bend profiles of shafts. They compared the bend shapes in static and dynamic tests, using both a mechanical whirl rig and a human golfer for the dynamic tests. The shaft profiles were characterised with charts of radius of curvature against distance along the length of the shaft. Where necessary data was obtained from dynamic tests using stroboscopic photogrammetry. The theoretical prediction is made that, under centrifugal stiffening, the difference between the lowest natural frequencies of different shafts is reduced. In whirl rig tests two different shafts were clamped at their butt and rotated about an axis through the clamp. The rig was rotated up to and through first resonance to calculate the natural frequency and the bend profile of the shaft was recorded.

Unfortunately it was not possible to represent the clubhead with a mass offset from the shaft axis as oscillations created were beyond the space allowed by the machine. Instead, mass was placed symmetrically around the tip. Emphasis was also laid on the care needed due to the lack of damping in the shaft which could lead to large amplitude oscillations and shaft breakage. Results from the whirl rig showed minimum radius of curvature occurring at the butt for both shafts. While one shaft varied by less than 2 m radius of curvature over its length, the other shaft varied by 15 m. The results from the human tests compared the static bend profiles of the shafts to those obtained just pre-impact. While static tests had the bend point roughly in the middle of the shaft (between 450 and 550 from tip), the swing results indicate the bend point much close to the tip (less than 240 mm). The results also showed the shaft with the lower bend point in the static case having the higher bend point in the dynamic case. Mather and Jowett conclude that there is no simple transfer function between the bend profile of the shaft in the static tests and its shape during the swing.

In a further recent study Suzuki and Inooka (1998) included shaft elasticity in the double pendulum model. A mathematical approach was taken for the equations of motion by applying Hamilton's principle and solved using a Runge-Kutta method. Torque was applied to the upper lever while the wrist was either fixed at 90° or free. The club displacement (flexibility) is approximated from the eigenfunction equation of a cantilever that has a mass at the tip with no damping. They used the model driven by an initial shoulder torque of 100 Nm for 50 ms to investigate the effect of releasing the wrist at different times in the downswing. Plots showed the head velocity as a function of time,

with high frequency vibration occurring after the shaft boundary condition changed from fixed to free. No mention is made of the stiffness of the shaft changing due to centrifugal force, as discussed by Mather (1995) and Mather and Jowett (1998). In comparing clubhead velocity at impact a maximum was predicted for the instance when the wrist release coincided with the displacement of the shaft vibration crossing in the positive direction for the first time. Suzuki and Inooka (1998) continued, using the model to study the effect of shaft flexibility. A trapezoidal function (positive, zero, then negative gradient) for the upper lever torque was used to investigate the effect of changing the shaft stiffness. For three different stiffnesses the model was analysed, changing the magnitude and duration of the torque function, to satisfy a prescribed impact position of upper and lower lever. The method used to obtain the torque function is not described. The head velocity was plotted against the torque magnitude over a range possible for the specific shaft stiffness. Their results indicated higher stiffness shafts are required for higher clubhead speeds if the prescribed position of the model is to be met. They concluded that their model could be expanded to include torsional effects.

1.6.2.6 Further advances in modelling shafts

Advances in computational techniques has led to attempts to model the shaft flexibility during the swing. Swider and Ferraris (1994) proposed an experimental method for analysing the dynamic behavior, frequencies and mode shapes for a golf club using displacement sensors. They compared results with a finite element model, constructed from shell elements to cater for the anisotropy of composite shafts. Their results were comparable and they concluded that the model could be used in future studies involving the large displacements of the golf swing.

Whittaker (1996) used a number of approaches to investigate the difference between rigid, flexible and absent shafts in a simulated clubhead/ball impact. The flexible shaft is modelled as a uniform beam using lumped masses and in validating the model Whittaker stated that little difference between the first 10 mode frequencies is observed with a minimum of 6 elements for the shaft. Higher modes are to be expected to be important post-impact but these low order modes are predominant in the large dynamic

displacement of the golf swing. Whittaker (1996) used a double pendulum model for the downswing where the shoulder and wrist torques were obtained by trial and error to obtain a swing such that the upper pivot, wrists and clubhead were aligned at impact.

Friswell et al (1998) confirmed Whittaker's (1996) view that the low frequency modes dominate during the downswing. They modeled an existing golf club with finite elements and used a model updating procedure to improve the dynamics of the model as matched to Experimental Modal Analysis (EMA). Friswell et al chose beam elements for modelling, allowing for axial, bending and torsional strain. Shear strain was expected to be negligible. The clubhead was modelled as a point mass with an appropriate inertia matrix which was originally guessed. Model updating was carried out for the parameters describing the inertia matrix and the shaft stiffness. Discretisation errors were overcome by using a suitable number of elements (26 elements). They concluded that the model updating procedure was successful and that the validated model may be used to obtain more accurate estimates of the club response during the swing.

1.6.3 Balls

Current golf ball sales stand at \$1.1 billion (American dollars) per year worldwide (Johnson 1999). Sales take place within a fiercely competitive market that rewards innovation with market share (Sullivan and Melvin 1995). As with other types of golf equipment, a plethora of designs exists. The beginnings of 1999 saw two major golf equipment manufacturers join the ball market, Taylor Made (now part of the adidas-Salomon group) and Nike. Later in the year, Callaway Golf hope to launch their ball range (Yasuda 1999). Many of the new designs use exotic materials such as Titanium, that have seen success in clubheads and shafts. However Stutz' (1990) view, that little published data on the effect of ball construction on performance exists outside of patents, still remains. Incidentally the number of patents is not small, with 5000 between 1900 and 1995 (Sullivan and Melvin 1995). While the initial objectives of the current work were focused on the clubhead and shaft rather than the ball, the finite element model opened up further possibilities and some preliminary results on ball performance are included. It is therefore appropriate to briefly review previous work in this area.

1.6.3.1 Aerodynamics

Much of the work on golf ball performance is based on the flight aerodynamics well after impact and is beyond the scope of the current work. A study of the way in which ball improvements, of which there have been many, have changed the game is given by Aoyama (1995). He compared a modern wound ball, used by the majority of professional players, to its counterpart of 25 years previously. Using virtual flight testing, a computer simulation of the ball flight based on aerodynamic data, the playing differences between the two balls was identified. Neither ball gave a consistently longer and straighter shot under the full range of initial conditions of spin, launch angle and speed. However for 'typical' conditions, the modern ball was superior but only by a small amount, 10 yards at the most. Tomita and Chikaraishi (1995) discussed the effect of dimple patterns on golf ball performance and gave a frequency chart of the number of brands using different dimple numbers. An enlightening chart for those who doubt the competitiveness of the golf ball market, 46 different patterns appear for 935 brands! Shaw (1995) discussed the dimple arrangements further and demonstrated how computational fluid dynamics (CFD) and laser doppler anemometry may be used to study air flow around golf balls in flight. Many other publications are available on the aerodynamics of the golf ball and interested readers are directed to the sources given in section 1.5 for further information.

1.6.3.2 Experimental tests

Hale et al (1994) conducted rare tests on the playing performance of different ball designs. The work was 'rare' in the sense that it was not conducted by manufacturers with a marketing driven agenda, of which they give numerous examples. Eighteen golfers of three different playing abilities (low, medium and high handicap) were statistically analysed for both distance and accuracy playing six different ball designs. A significance difference between the balls was found for distance with the low handicap group. A specific 'unnamed' manufacturer's design gave more distance than its competitors. However, the results were reversed for the high handicap group. They concluded there was little significant difference between the ball performances they measured and the claims made by manufacturers.

1.6.3.3 Impact studies

Many of the impact studies discussed in section 1.6.1 were not primarily concerned with ball construction but with other impact parameters. However as a matter of course they often included results for different golf ball constructions. For example, Gobush (1995 and 1996) in examining the effect of friction, fired balls from an air cannon onto a static plate. He used wound and two-piece balls and claimed that the wound balls gave a higher spin rate. In another example Johnson and Liebermann (1996) constructed a mathematical model for normal (perpendicular) ball-barrier impact. They matched experimental results to their model for both two-piece and wound balls.

Sullivan and Melvin (1995) give the singularly relevant work on performance due to ball construction. They discuss the relationship between the ball cover hardness and overall ball compression and spin rate. They do not give details of the experiments conducted to obtain their results. This work is discussed further in section 4.5.

1.6.3.4 Temperature

The effect of ball temperature on behaviour is not to be underestimated. Cochran and Stobbs (1968) calculated values that distance improvements from a heated ball were significant implying an increase of 15 yards when warming the ball from 0 to 21°C. Indeed, this advantage may be greater than those obtainable from other equipment technologies and, of course, comes at less cost! Yamada (1995) carried out practical tests on the effect of temperature for a variety of designs and gave results for the ball dynamic parameters: speed, launch and spin. Results imply that each parameter is dependent on the temperature but in a different way. He concluded that, with better understanding, balls could be constructed to be less affected by temperature or even designed to perform well at specific temperatures.

For the golfer wishing to benefit from warmer balls, it must be remembered that rubber is a poor conductor of heat and several hours are necessary to warm the ball all the way through. It also loses heat slowly and the advice given by Cochran and Stobbs (1968) is

to warm the balls overnight and use an alternate ball for each hole, keeping the ball not in play in a warm pocket.

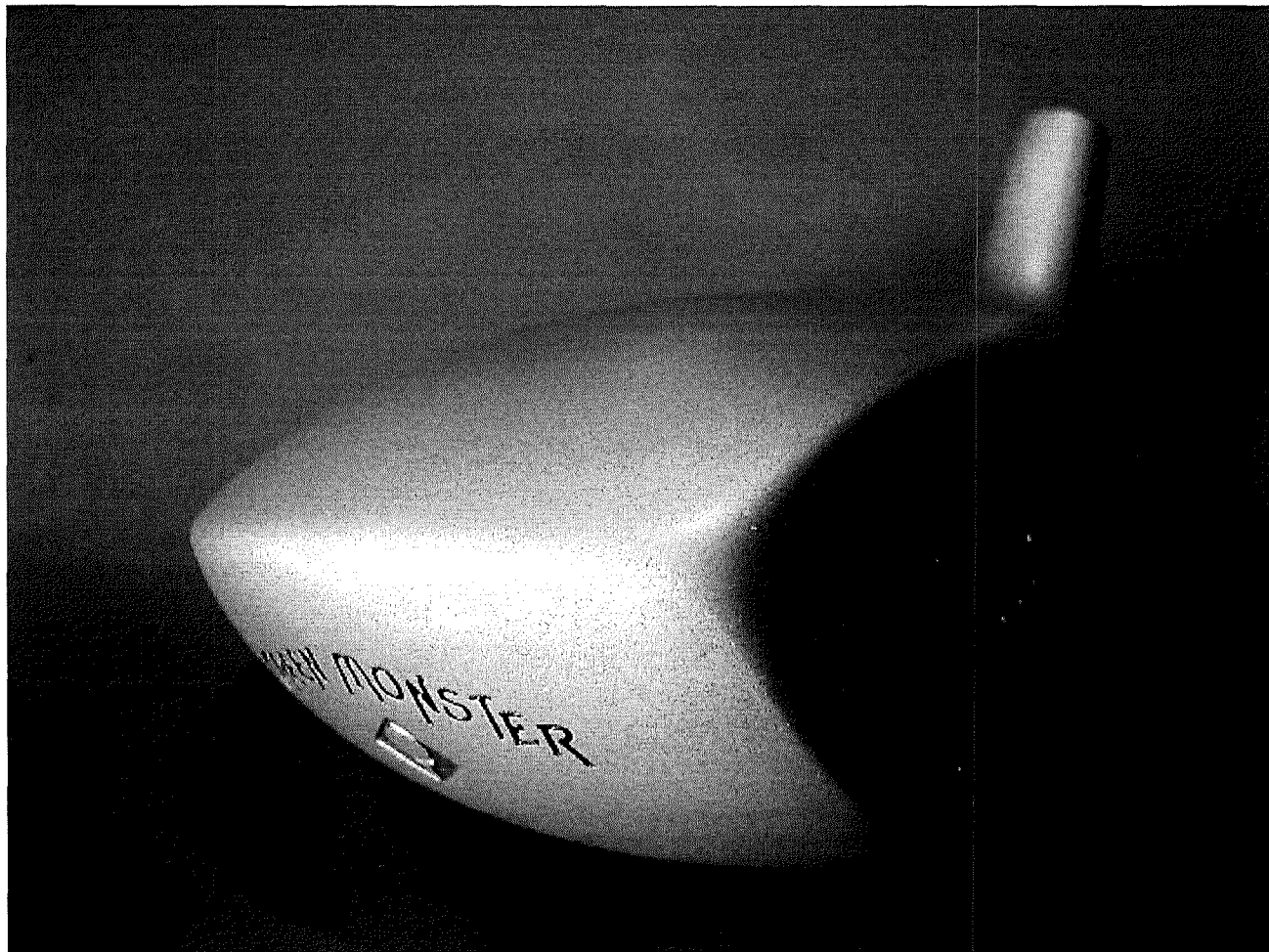


Figure 1.1 A modern metal 'wood'.

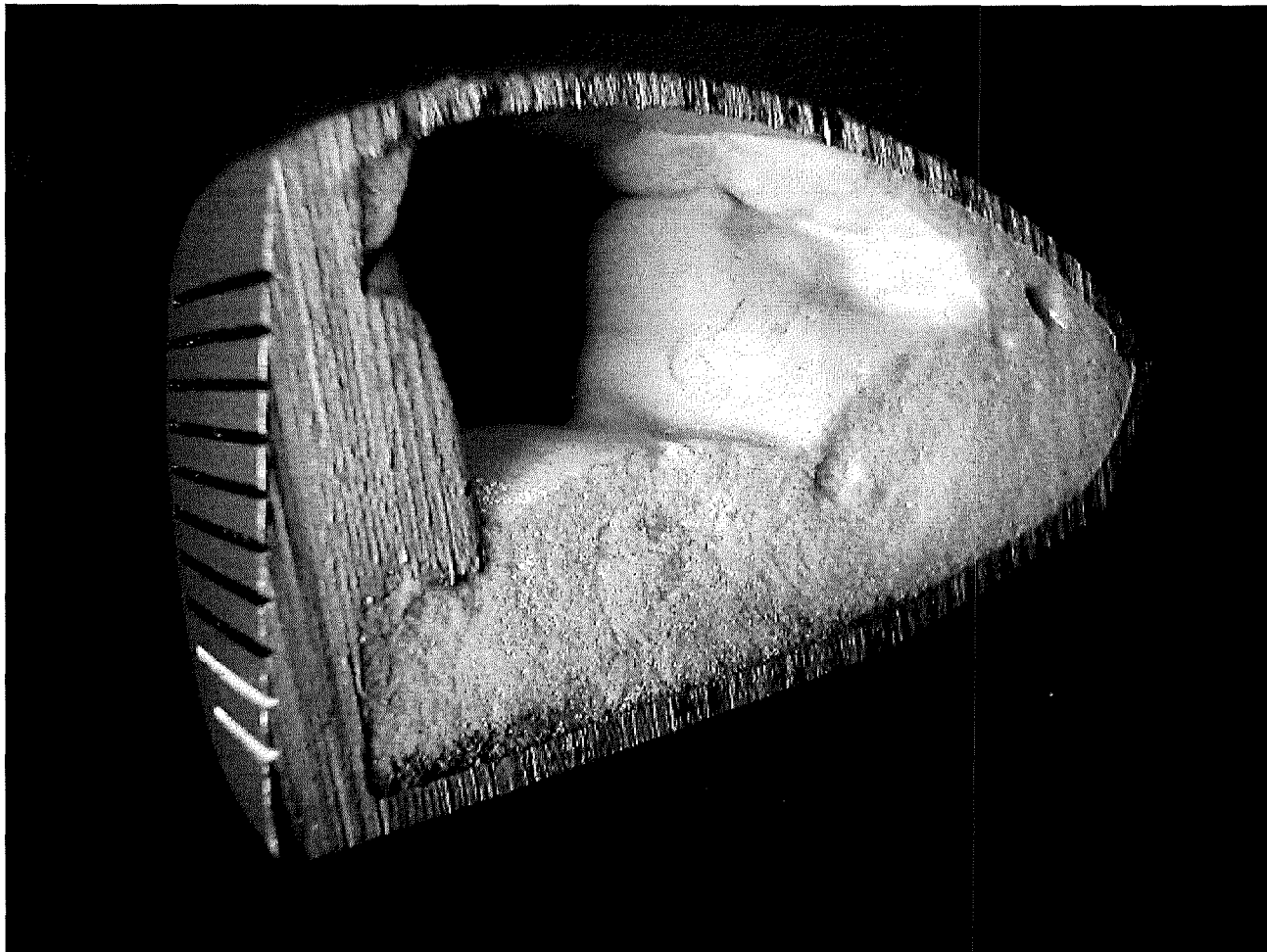


Figure 1.2 A cut through of a modern metal 'wood', showing foam.

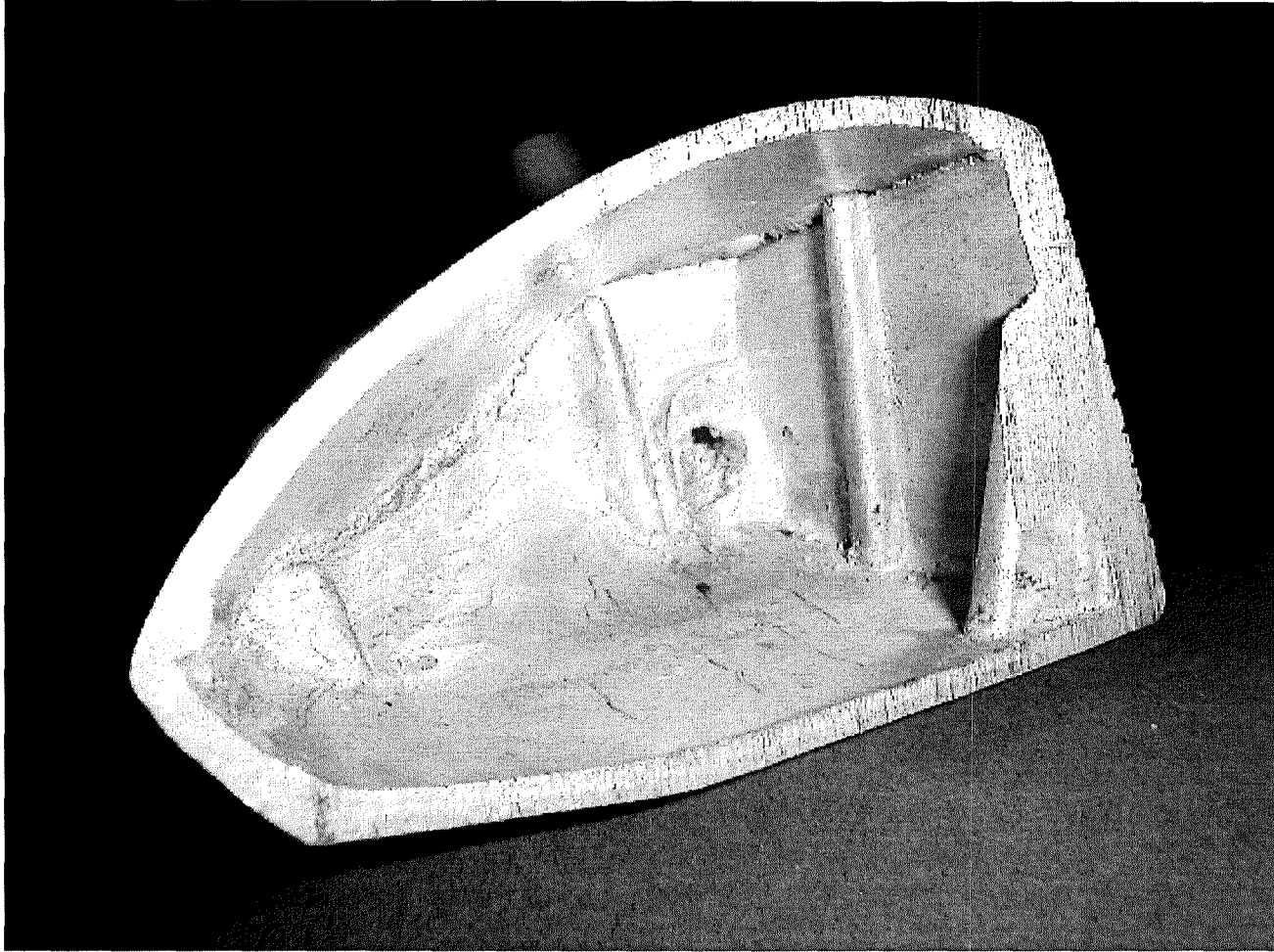


Figure 1.3 A cut through of a modern metal 'wood', showing reinforcement ribs.

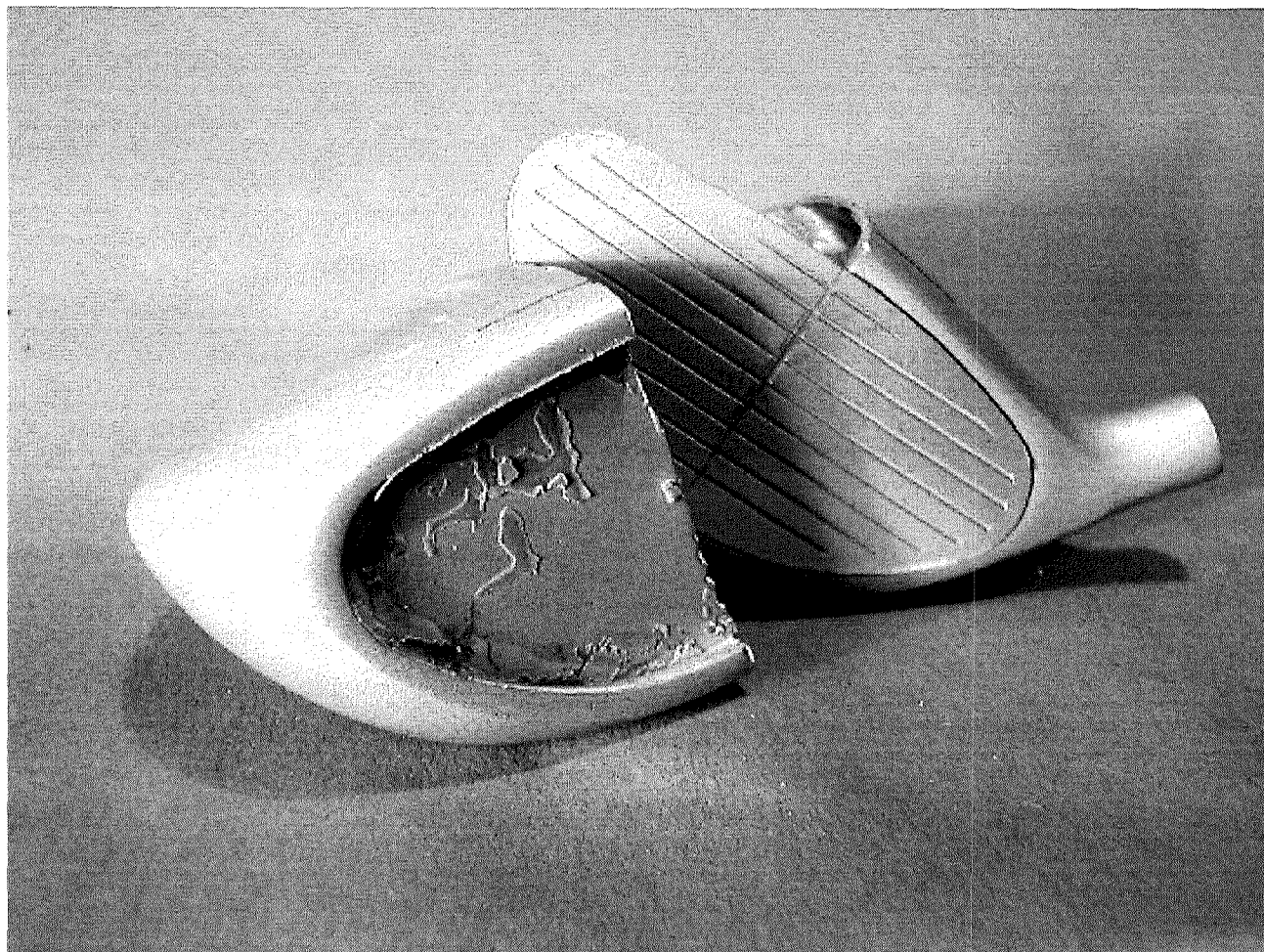


Figure 1.4 A modern metal 'wood', with insert of hard material.

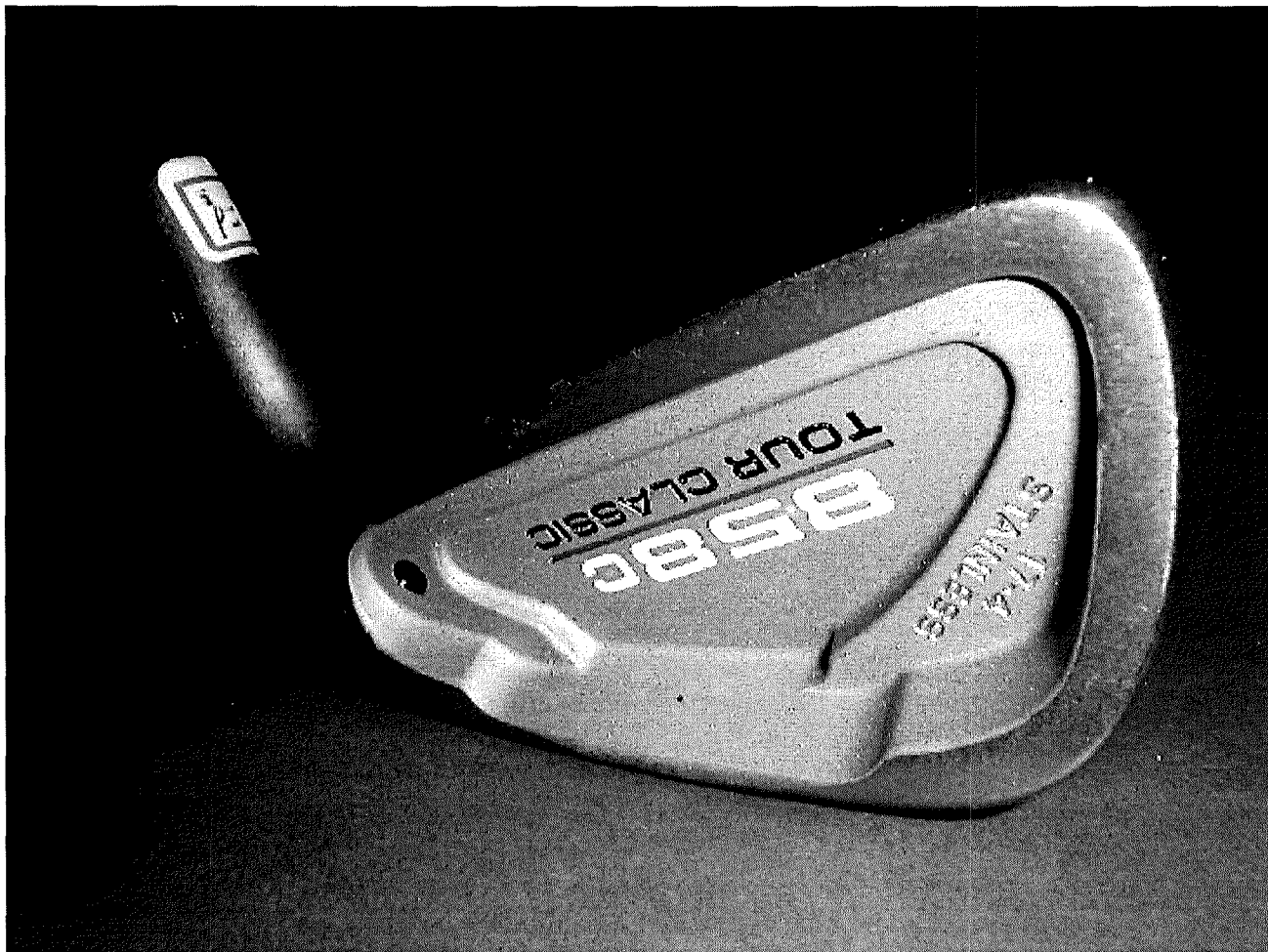


Figure 1.5 Rear of a 5-iron cavity back clubhead.

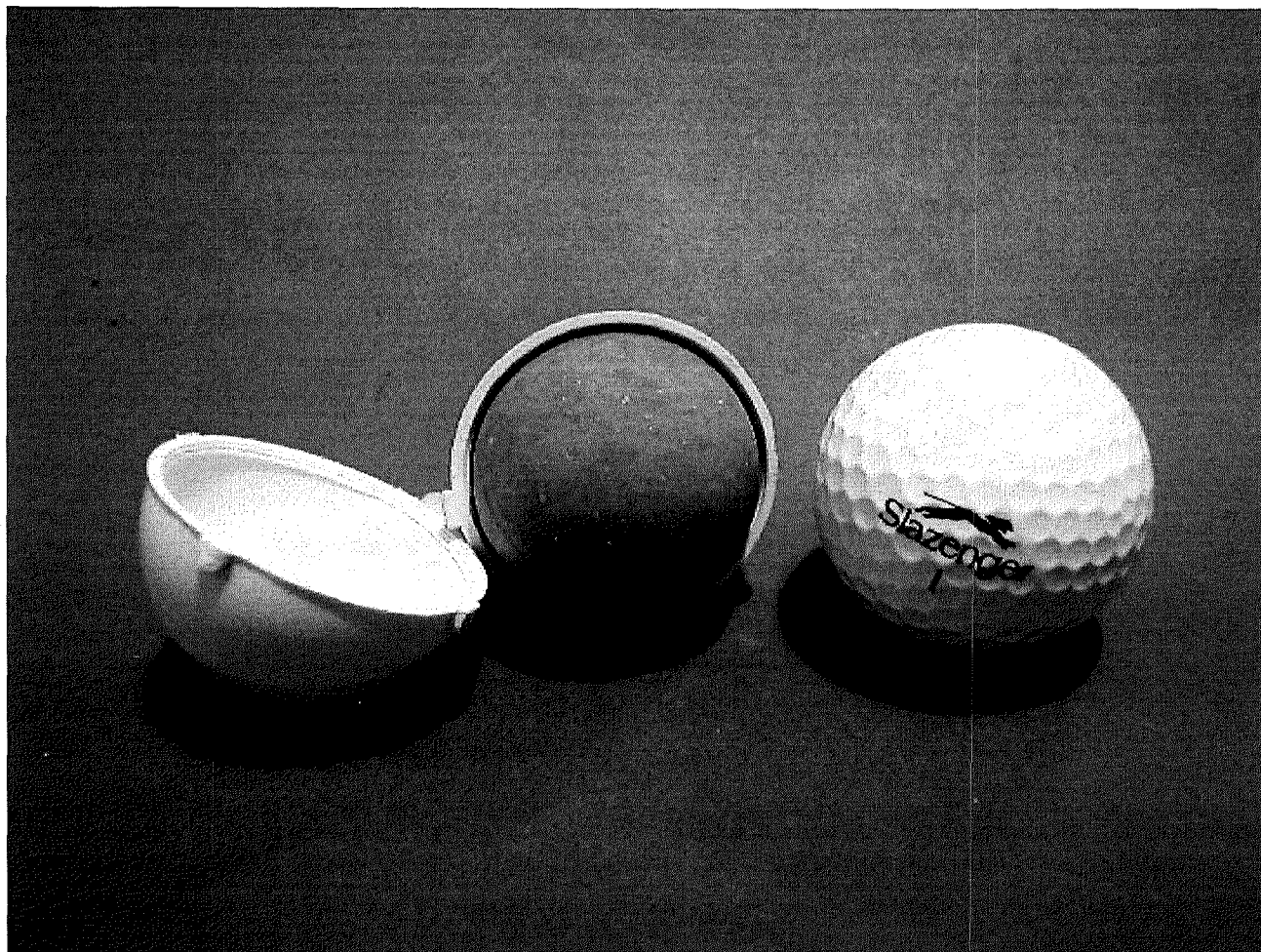


Figure 1.6 Two-piece ball construction.

Boundary conditions

Forces of time
dependent magnitude.

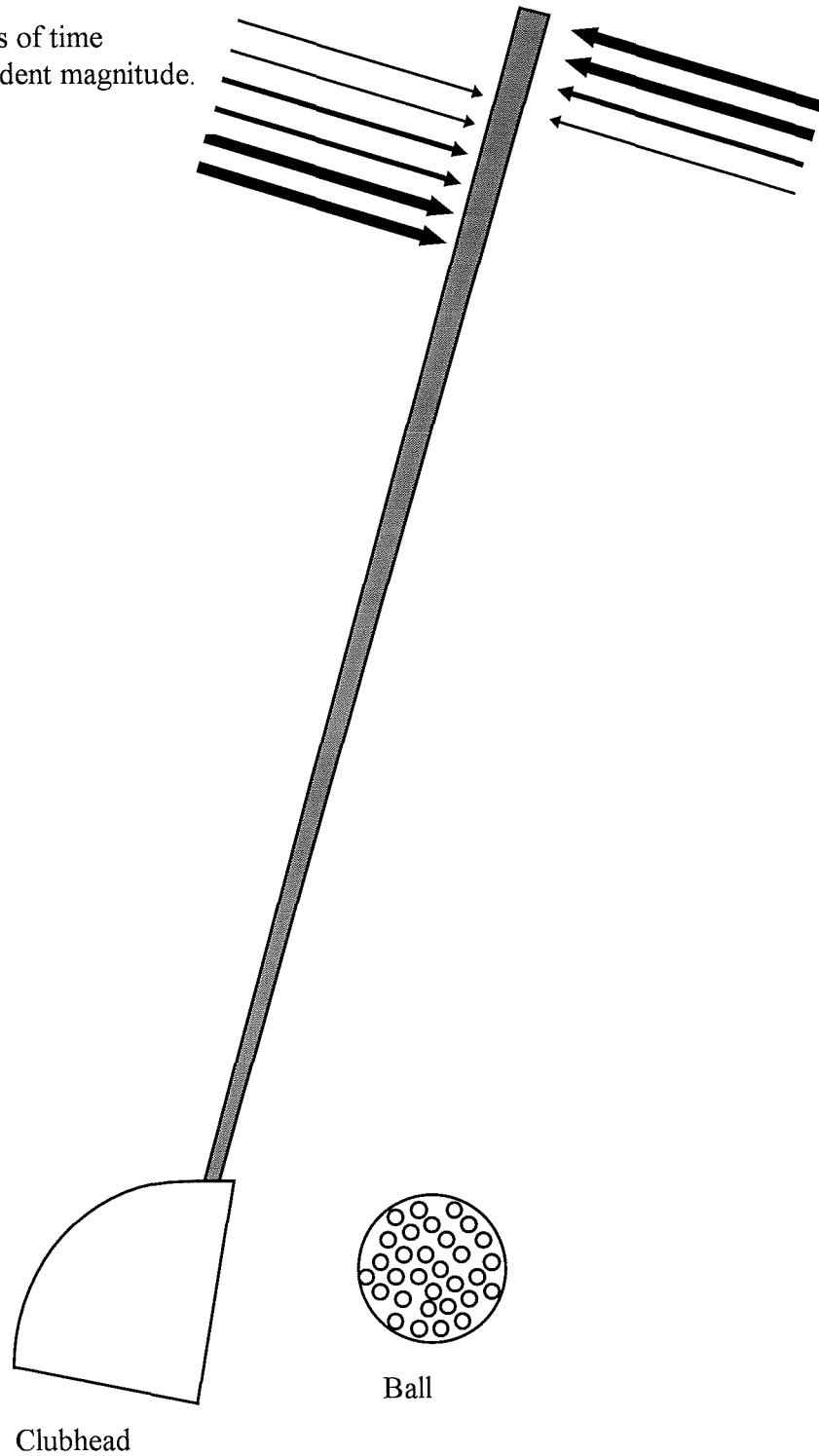


Figure 1.7 The golf equipment system.

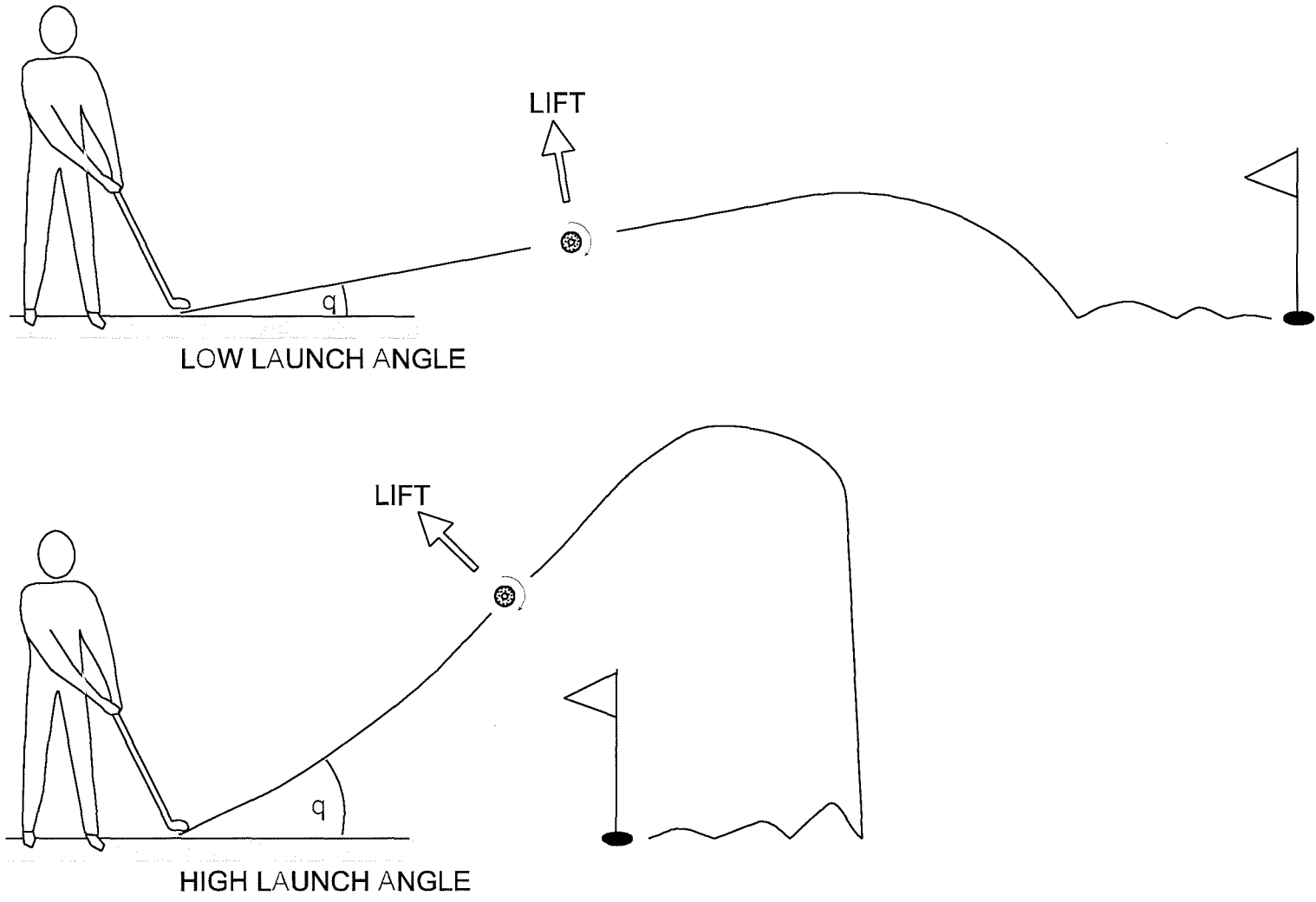
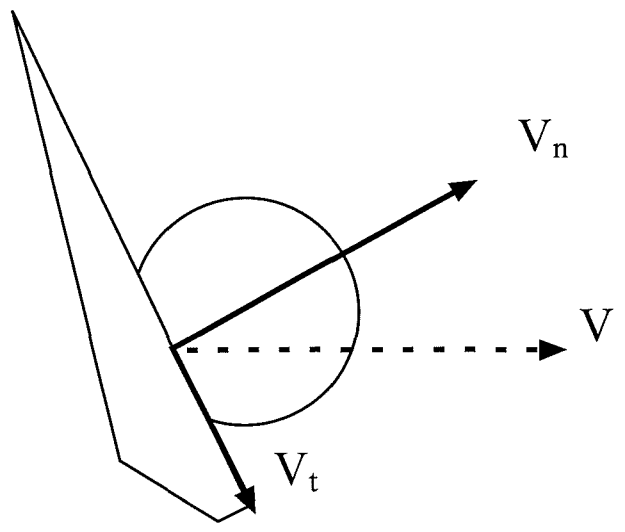
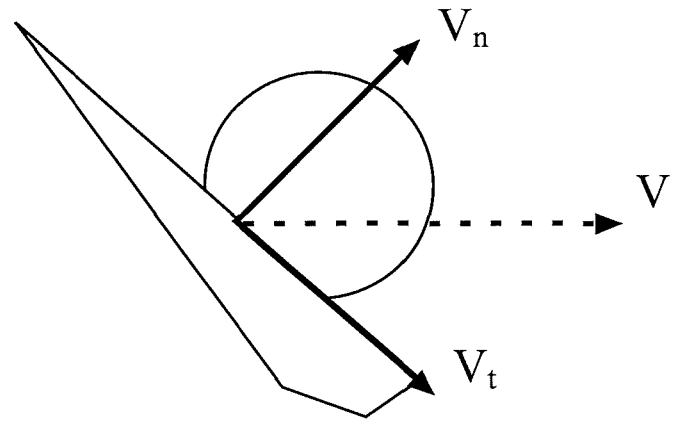


Figure 1.8 Possible effects of varying initial ball flight parameters.



loft angle $< 45^\circ$
 $V_n > V_t$



Loft angle $> 45^\circ$
 $V_n < V_t$

Figure 1.9 Tangential (V_t) and normal (V_n) velocity components of clubhead.

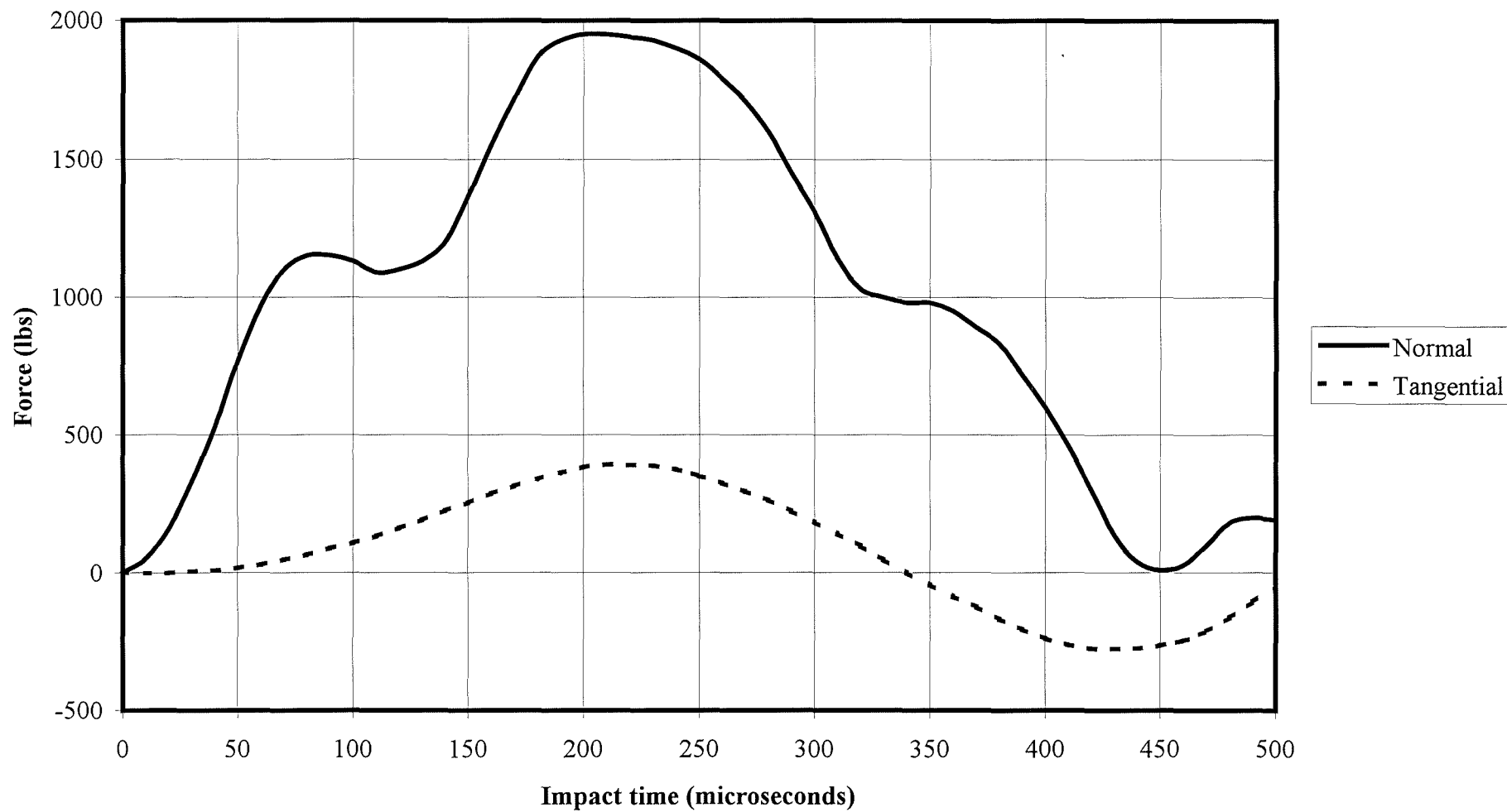


Figure 1.10 Tangential and normal force on clubhead, Gobush (1990).

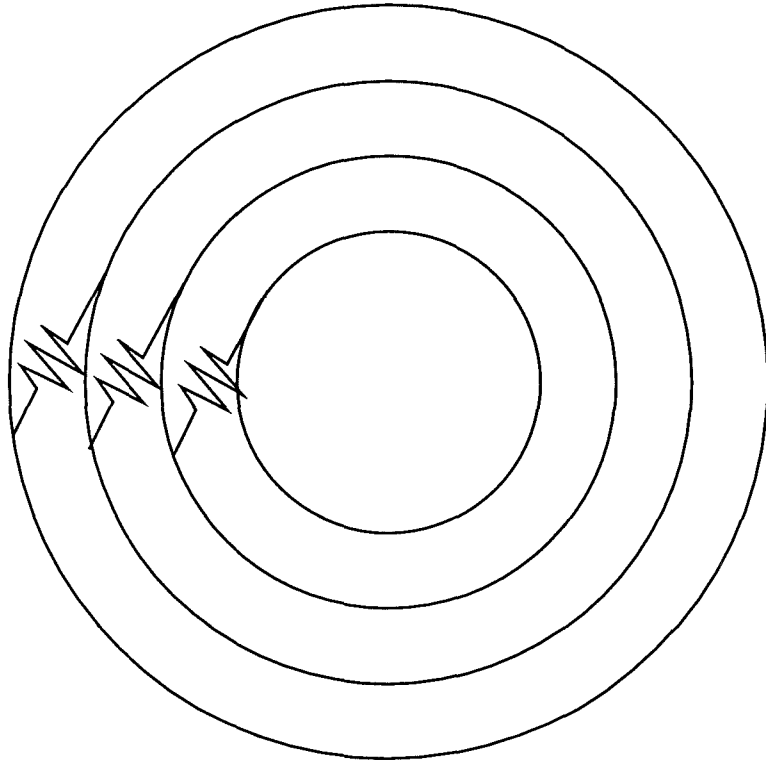


Figure 1.11 Onion layer model of golf ball, Gobush (1995).

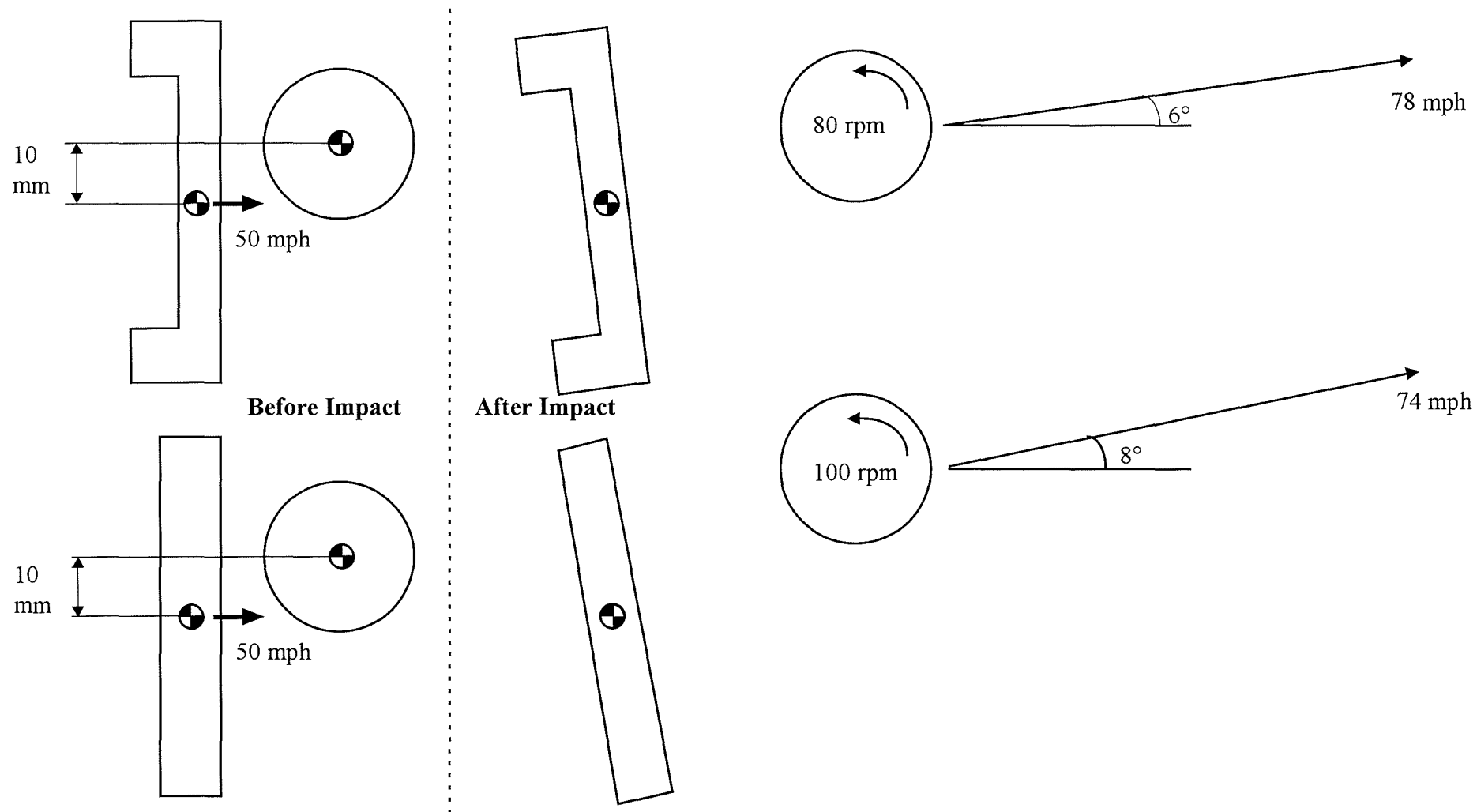


Figure 1.12 Improved performance for increased inertia clubhead. Cavity back design - top, blade design - bottom.

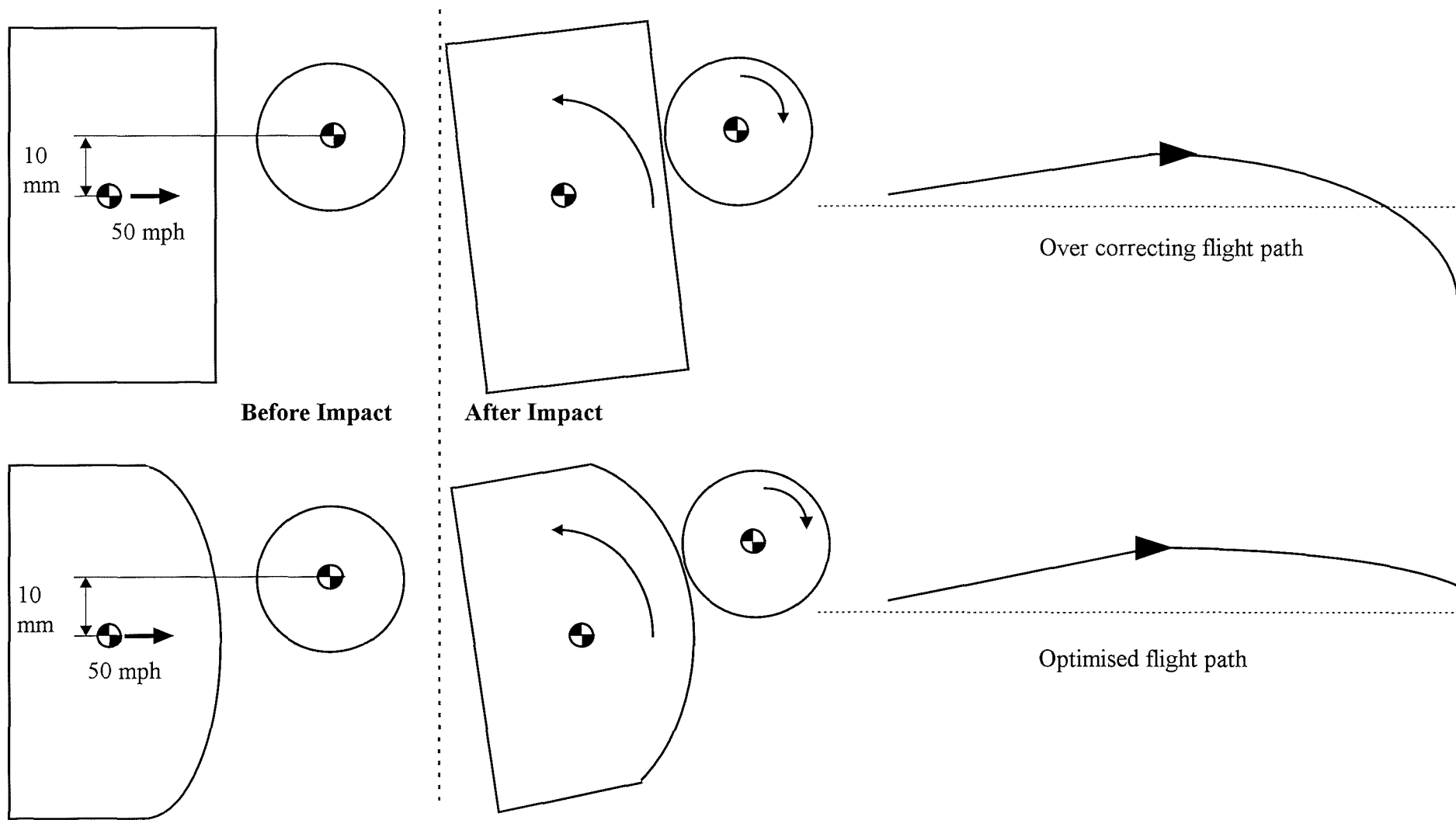


Figure 1.13 Reduced 'gear effect' for curved clubfaces.

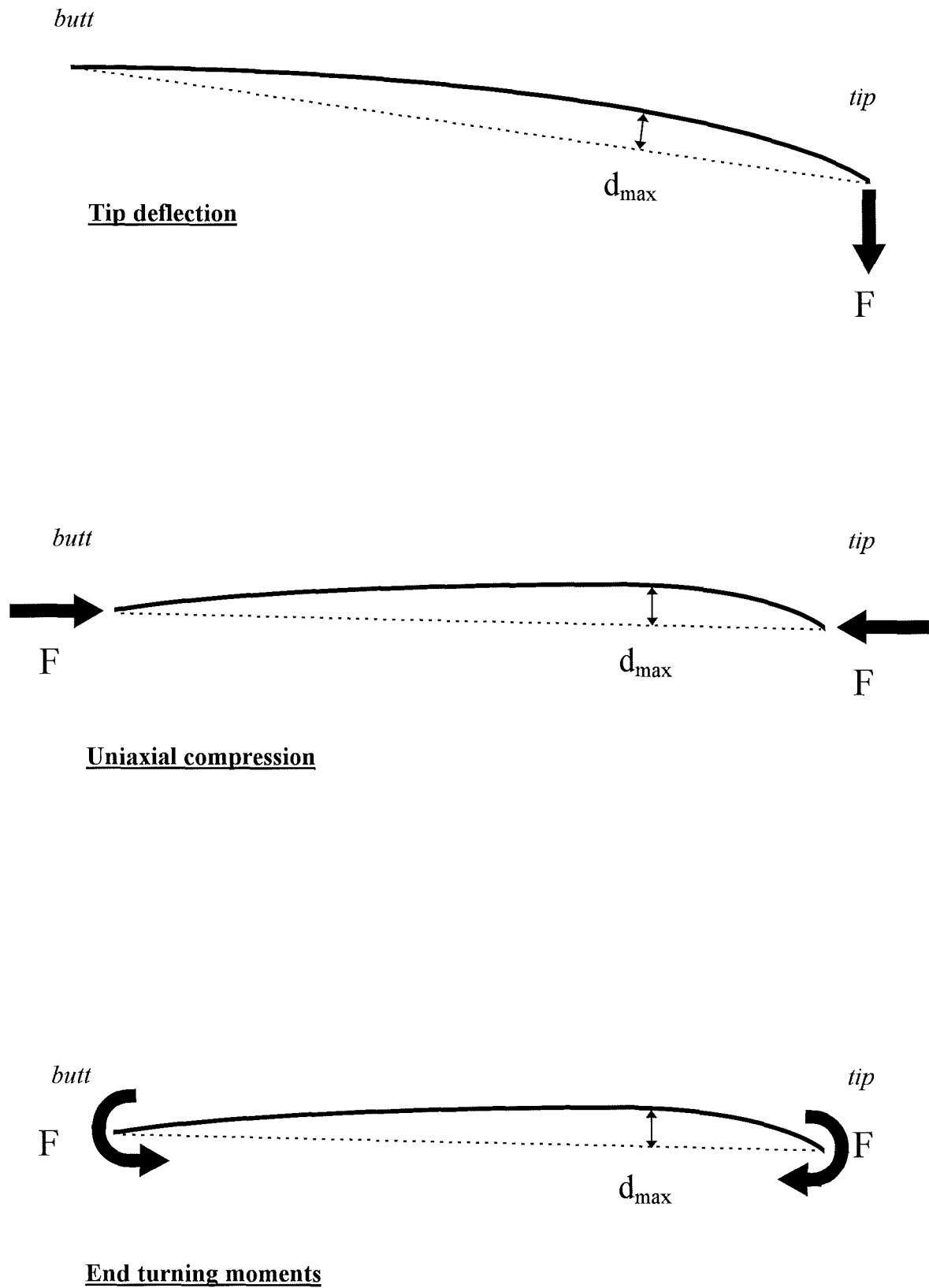
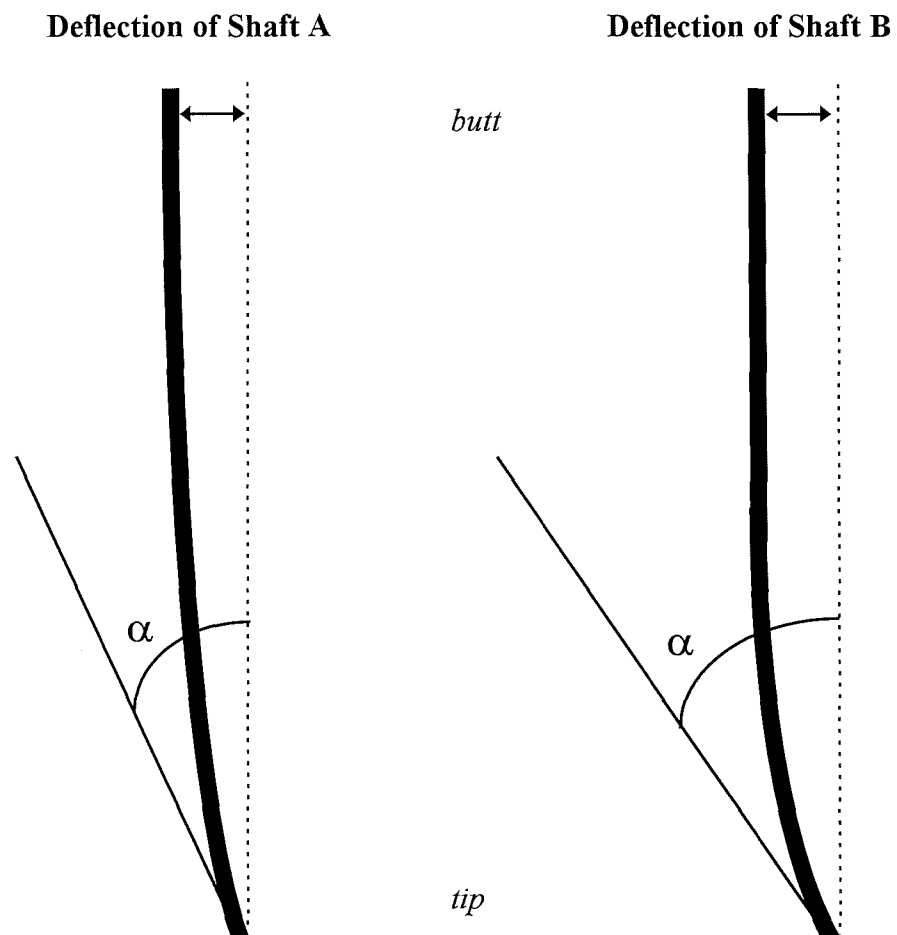


Figure 1.14 Bend point measurement techniques.



Bend Point, why it may make a difference.

While the deflection of shaft A and B are of equal magnitude, their bending profiles are different.

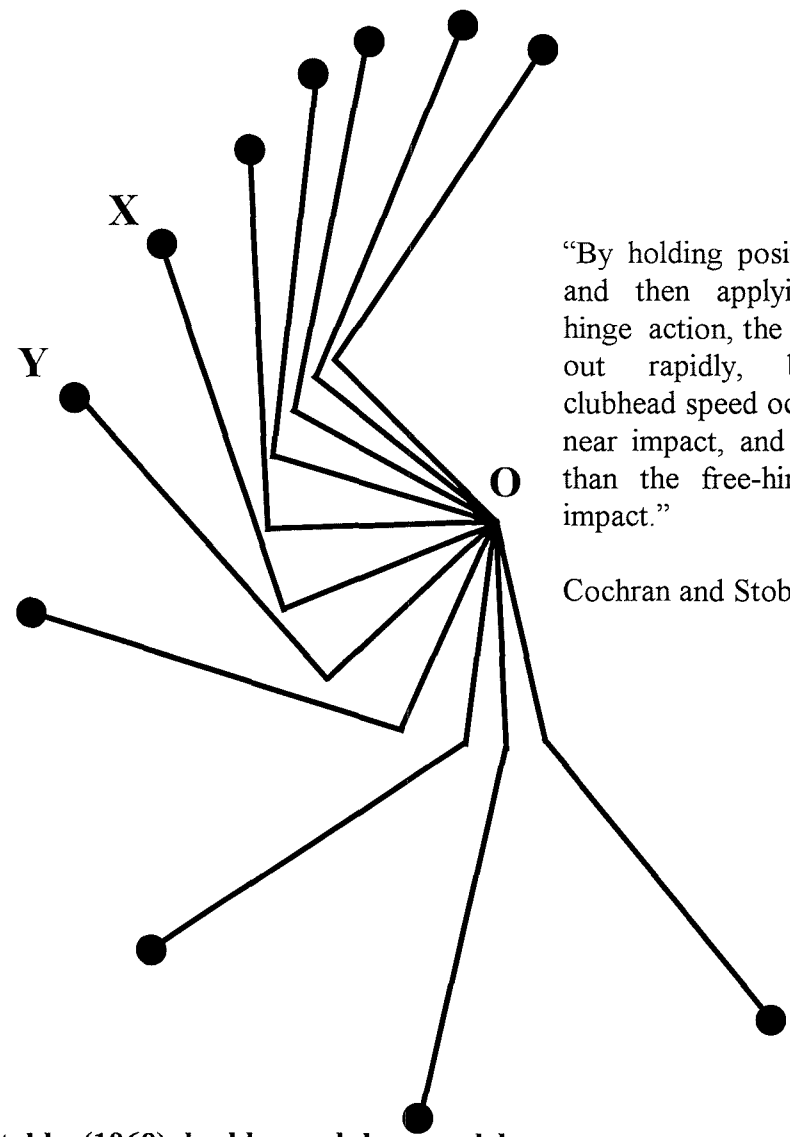
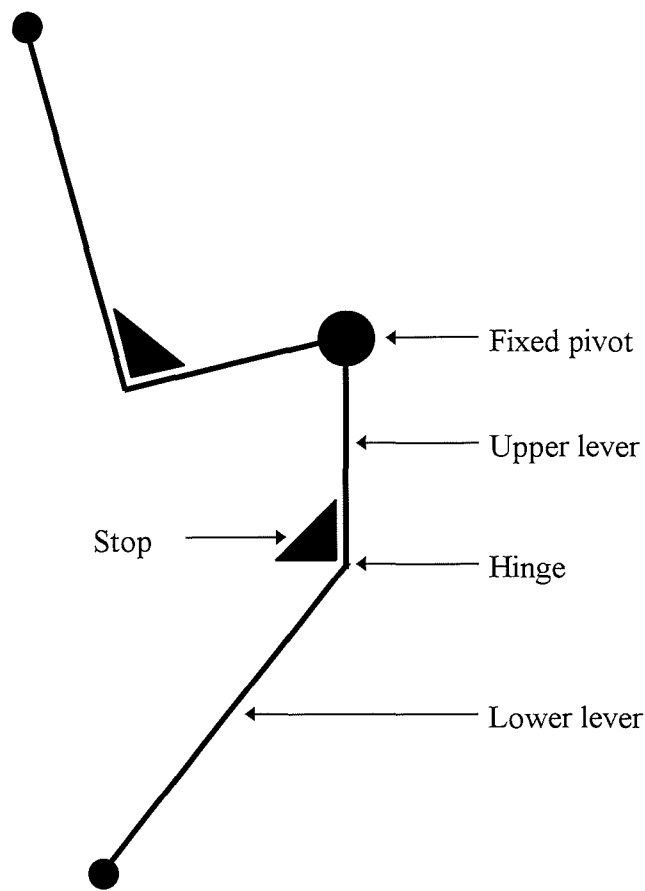
Shaft B is stiffer in the butt and more flexible in the tip, leading to a smaller radius of curvature at the shaft tip.

Tangents to the shafts at the tip show shaft B has a greater increase in dynamic loft due to bending.

Shaft B would be thought to have a lower bend point than shaft A.

(α = Increase in dynamic loft.)

Figure 1.15 Bend point, why it may make a difference.



“By holding position X until Y, and then applying the strong hinge action, the hinge still opens out rapidly, but maximum clubhead speed occurs once again near impact, and is even greater than the free-hinging speed at impact.”

Cochran and Stobbs (1968)

Figure 1.16 Cochran and Stobbs (1968) double pendulum model.

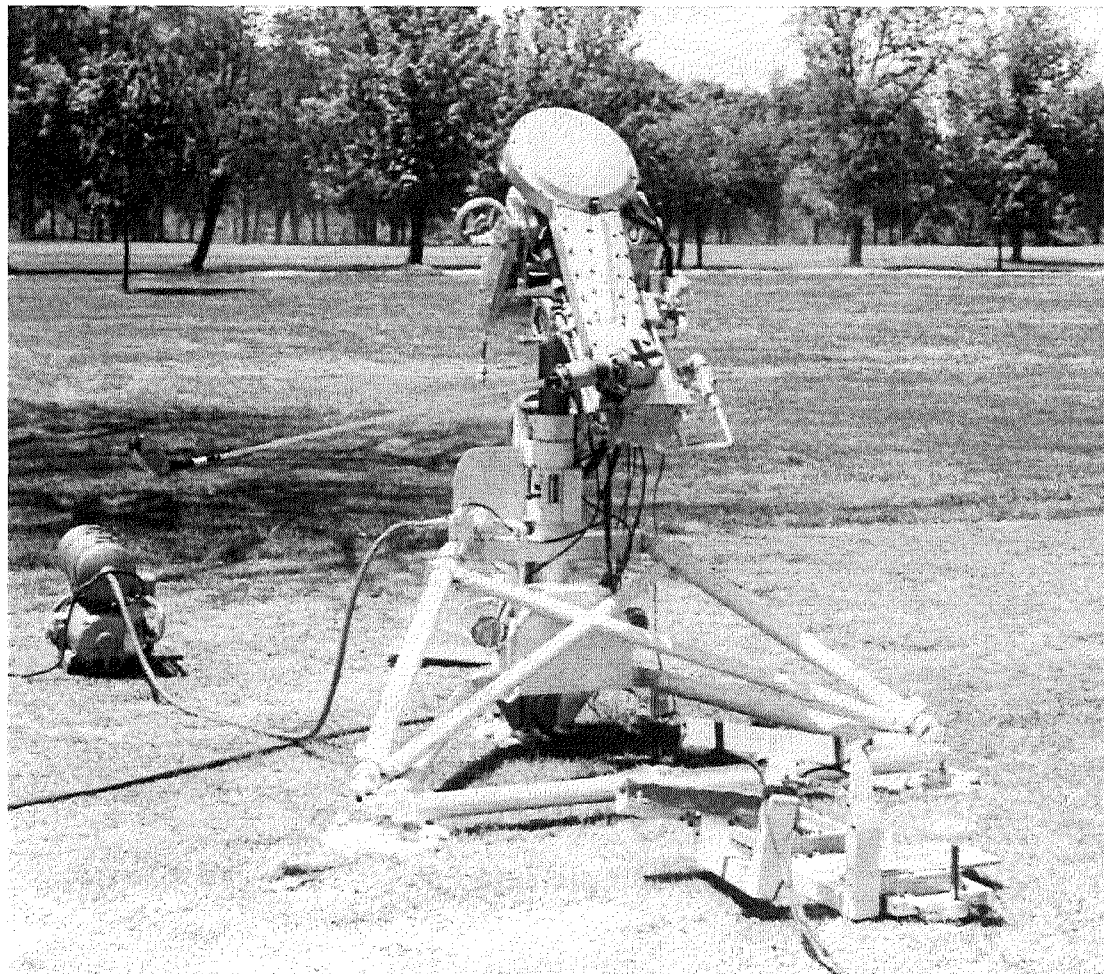


Figure 1.17 'Iron Byron' courtesy of True Temper, USA.

2.0 Computational stress analysis

One aim of the current work is to provide a scientific rationale for many of the well known features of golf club performance. The principal tool in this is engineering stress analysis and finite element analysis in particular. However these concepts may be unfamiliar to sports scientists far less sportspersons with a non-scientific background to whom the current work may be relevant. It is then appropriate to give a brief introduction to the subject.

2.1 Basic concepts

The strength and stiffness of a component are related through the constitutive equation. This cannot be determined purely theoretically but requires empirical results from a test such as a uniaxial tensile test used to determine the force-extension relation for a 1-dimensional component. In this test the component is clamped at one end and subjected to an increasing tensile force \mathbf{F} at the other end in a tensile testing machine such as that shown in figure 2.1.

\mathbf{F} is measured by a load cell, while the extension \mathbf{e} is measured by an extensometer. Results from the test allow the generation of a \mathbf{F}/\mathbf{e} graph, (force versus extension curve), shown in figure 2.2 for a mild steel specimen up to failure (Shames 1989).

For small displacements, where \mathbf{e} and \mathbf{F} are not too large, the \mathbf{F}/\mathbf{e} graph approaches a straight line. The relationship is known as linear and if the test specimen returns to its original shape when the load is removed the behaviour is known as linear elastic. Such behaviour can be described by the spring equation, where \mathbf{k} is known as the stiffness:

$$\mathbf{F} = \mathbf{k} * \mathbf{e}$$

Known as Hooke's Law, this equation can be applied to most engineering systems, provided \mathbf{F} and \mathbf{e} are not too large. In any system \mathbf{k} depends on the material and its shape and a separate test is required for each design modification. As an example in modeling the golf impact, deformations of the clubhead are small and the clubhead

returns to its original shape after impact. Such material behaviour can be thought of as linear elastic. In contrast, the golf ball, although returning to its original shape is elastic, cannot be assumed to be linear as the deformation of the ball is not small. Such behaviour is known as non-linear elastic and Hooke's Law does not hold.

2.2 Stress and strain

In comparing the strength of various materials it is necessary to compare specimens of the same dimensions. This is however not always practical, for example in measuring a wooden specimen a large component is required to average out the effect of individual grains, while a metal component of the same dimensions would be cumbersome.

From uniaxial tensile tests it is found that, provided the deformation which precedes fracture is small, the maximum force the specimen can withstand does not depend on its length L nor its shape or the cross-section but only on its cross-sectional area A . For different specimens of the same material:

$$F_{\text{MAX}} \propto A$$

$$F_{\text{MAX}} / A = \text{UTS}$$

where UTS is a constant called the ultimate tensile stress. UTS is a material constant, ie it is different for different materials and is a characteristic of the material.

Defining stress and the fracture stress as σ and σ_{MAX} respectively:

$$\sigma = F / A$$

$$\sigma_{\text{MAX}} = F_{\text{MAX}} / A$$

Stress thus has the same units as pressure and has SI units of Pascal (Pa), where:

$$1 \text{ Pa} = 1 \text{ Nm}^{-2}$$

typically stress values are many Pascals and it is more convenient to give engineering stresses as MPa or GPa.

Stresses may be tensile (pulling), compressive (pushing) or shearing (sliding) as in figure 2.3. Tensile or compressive stresses are known as normal or direct stresses. Shear stress, denoted τ , is also F/A , but care must be taken in choosing the correct area.

In mechanical engineering tensile stresses are taken as positive and compressive stresses as negative.

As with a simple spring a uniaxial specimen will extend from its initial length 0L to L under an applied load F but the stretch ratio $\lambda = L / {}^0L$ is not a good measure of deformation since, while elastomers can deform to values of 3 or 4, the limit for structural metals is about 1.001. All the actions then take place in the fourth significant figure. Strain denoted ϵ and defined as $\epsilon = 0$ in the undeformed state is thus used to measure the deformation of the material

The simplest strain measure is

$$\begin{aligned}\epsilon &= \lambda - 1 \\ &= L / {}^0L - 1 \\ &= (L - {}^0L) / {}^0L \\ &= e / {}^0L \\ &\cong e / L\end{aligned}$$

Provided the deformation is small, e for a linear elastic specimen is observed to depend not only on F but also A and L , such that:

$$e \propto (F * L) / A$$

hence

$$F/A \propto e / L$$

$$\sigma \propto \varepsilon$$

$$\sigma = \mathbf{E} * \varepsilon$$

where \mathbf{E} is a material constant called the elastic modulus or Young's modulus.

Shear stresses produce shear strains, denoted γ , and defined as the angle in radians by which the material is deformed, such that:

$$\tau \propto \gamma$$

$$\tau = \mathbf{G} * \gamma$$

where \mathbf{G} is also a material constant called the shear modulus.

2.3 Multiaxial stress and strain states

With most materials, extension in one direction leads to contraction in the other direction and a tensile stress in the 1-direction (x-direction), denoted σ_{11} , produces a tensile strain ε_{11} in the 1-direction and compressive strain ε_{22} and ε_{33} in the 2- and 3-directions respectively (the y- and z-directions). The ratio of these compressive strains to the tensile strain in the loaded direction is Poisson's ratio (ν), ie

$$\nu = -\varepsilon_{22} / \varepsilon_{11} = -\varepsilon_{33} / \varepsilon_{11}$$

where the negative sign is inserted to give a positive value for ν . This definition is for an isotropic material, defined as having the same properties in every direction, ν is the same no matter what two directions are chosen for its definition. Hence a stress σ_{11} produces three strains.

$$\varepsilon_{11} = \sigma_{11} / \mathbf{E}$$

$$\varepsilon_{22} = -\nu * \sigma_{11} / E$$

$$\varepsilon_{33} = -\nu * \sigma_{11} / E$$

If now the material is subjected to triaxial loading in which all three stresses are applied simultaneously, the three strains will be:

$$\varepsilon_{11} = \sigma_{11} / E - \nu * \sigma_{22} / E - \nu * \sigma_{33} / E$$

$$\varepsilon_{22} = \sigma_{22} / E - \nu * \sigma_{33} / E - \nu * \sigma_{11} / E$$

$$\varepsilon_{33} = \sigma_{33} / E - \nu * \sigma_{11} / E - \nu * \sigma_{22} / E$$

$$\Rightarrow \varepsilon_{11} = 1 / E * (\sigma_{11} - \nu * (\sigma_{22} + \sigma_{33}))$$

$$\Rightarrow \varepsilon_{22} = 1 / E * (\sigma_{22} - \nu * (\sigma_{33} + \sigma_{11}))$$

$$\Rightarrow \varepsilon_{33} = 1 / E * (\sigma_{33} - \nu * (\sigma_{11} + \sigma_{22}))$$

These three expressions and the corresponding three shear expressions may be conveniently written in matrix notation as:

$$\begin{bmatrix} \varepsilon_{11} \\ \varepsilon_{22} \\ \varepsilon_{33} \\ \varepsilon_{12} \\ \varepsilon_{13} \\ \varepsilon_{23} \end{bmatrix} = \begin{bmatrix} 1/E & -\nu/E & -\nu/E & 0 & 0 & 0 \\ -\nu/E & 1/E & -\nu/E & 0 & 0 & 0 \\ -\nu/E & -\nu/E & 1/E & 0 & 0 & 0 \\ 0 & 0 & 0 & 1/(2*G) & 0 & 0 \\ 0 & 0 & 0 & 0 & 1/(2*G) & 0 \\ 0 & 0 & 0 & 0 & 0 & 1/(2*G) \end{bmatrix} * \begin{bmatrix} \sigma_{11} \\ \sigma_{22} \\ \sigma_{33} \\ \sigma_{12} \\ \sigma_{13} \\ \sigma_{23} \end{bmatrix}$$

where the so called tensor shear strains ε_{ij} are defined as $1/2$ of the engineering strains.

This matrix is re-written more concisely as:

$$[\varepsilon] = [C] * [\sigma]$$

where $[\varepsilon]$ is the matrix of strains given fully above, $[\sigma]$ is the stress matrix and $[C]$ is the compliance matrix of the material.

E , ν and G are all elastic constants and for an isotropic material only two of these are independent and any one of them is expressible in terms of the other two via the relation:

$$\mathbf{E} = 2 * \mathbf{G} * (1 + \nu).$$

The 3-dimensional linear elastic constitutive equations may then be expressed in a number of alternative but equivalent forms. In particular they may be inverted to give:

$$[\boldsymbol{\sigma}] = [\mathbf{E}] * [\boldsymbol{\varepsilon}]$$

where $[\mathbf{E}] = [\mathbf{C}]^{-1}$

and is known as the stiffness matrix.

2.4 Tensors

In general, an engineering system comprises a 3-D body subject to external boundary conditions giving rise to an internal stress state in the body. Taking a small cube of the body it is apparent that the stress acting on each of the six faces will be a vector. For the cube to be held in equilibrium in 3 dimensions, only three of these six vectors are independent and so the stress state has three component vectors. A quantity that has a component vector in each (independent) direction is called a tensor. We may resolve the stress tensor into its three component vectors;

$$\underline{\underline{\sigma}} = \begin{bmatrix} \underline{\sigma}_{1\text{-direction}} \\ \underline{\sigma}_{2\text{-direction}} \\ \underline{\sigma}_{3\text{-direction}} \end{bmatrix}$$

However each vector has three 'scalar' components. So the stress tensor $\underline{\underline{\sigma}}$ has nine scalar components and may be written as:

$$[\sigma] = \begin{bmatrix} \sigma_{11} & \sigma_{12} & \sigma_{13} \\ \sigma_{21} & \sigma_{22} & \sigma_{23} \\ \sigma_{31} & \sigma_{32} & \sigma_{33} \end{bmatrix}$$

or

$$\underline{\underline{\sigma}} = [\sigma] = \sigma_{ij}$$

in symbolic, matrix, and subscript notations respectively. The off-diagonal terms are the shear stresses previously denoted τ .

Static equilibrium of the cube requires that:

$$\sigma_{ij} = \sigma_{ji}$$

This means that the stress tensor is symmetric, with only six independent components.

Indeed it is often convenient to write the stress tensor as a column matrix, thus:

$$[\sigma] = \begin{bmatrix} \sigma_{11} \\ \sigma_{22} \\ \sigma_{33} \\ \sigma_{12} \\ \sigma_{13} \\ \sigma_{23} \end{bmatrix}$$

It is possible to locate a 'principal basis' in which there are no shear components, ie a plane across which the vector has no shear component. Since there is no shear in the principal basis the principal stress tensor is:

$$[\sigma] = \begin{bmatrix} \sigma_1 & 0 & 0 \\ 0 & \sigma_2 & 0 \\ 0 & 0 & \sigma_3 \end{bmatrix}$$

By subtracting the rigid body translation and rotation from the displacement of a small line segment of material in 3-D, what is left is:

$$\begin{bmatrix} \partial u_1 / \partial x_1 & \frac{1}{2} * (\partial u_1 / \partial x_2 + \partial u_2 / \partial x_1) & \frac{1}{2} * (\partial u_1 / \partial x_3 + \partial u_3 / \partial x_1) \\ \frac{1}{2} * (\partial u_2 / \partial x_1 + \partial u_1 / \partial x_2) & \partial u_2 / \partial x_2 & \frac{1}{2} * (\partial u_2 / \partial x_3 + \partial u_3 / \partial x_2) \\ \frac{1}{2} * (\partial u_3 / \partial x_1 + \partial u_1 / \partial x_3) & \frac{1}{2} * (\partial u_3 / \partial x_2 + \partial u_2 / \partial x_3) & \partial u_3 / \partial x_3 \end{bmatrix}$$

This is the part of the total displacement that is responsible for the stress in the body. It is then the **strain tensor** and is also symmetric. The shear strain terms are off the diagonal. Apart from the $\frac{1}{2}$, these components are the same as the elementary definition of engineering shear strain γ . Furthermore on the leading diagonal the terms reduce to:

$$\varepsilon_{ii} = \partial u_i / \partial x_i$$

which in 1 dimension reduces further, to:

$$\varepsilon = du / dx$$

ie the familiar strain-displacement equation.

2.5 Finite element analysis

Finite element analysis (FEA) is a well known - almost ubiquitous - computational stress analysis technique and is the principal analysis technique used in the current work. In stress analysis, the aim is to calculate the stresses in the component and hence determine how it will deform or break. Stress is defined as the force acting on a component divided by the area over which the force acts but this simple calculation is not always possible. However stress can also be obtained, via strain, from displacement u . This can be done by integrating a differential equation, such as:

$$\mathbf{E} * \mathbf{A} * (d^2u/dx^2) = 0$$

for a uniaxial component. This particular equation is easy to integrate analytically but this is not generally so and we must use a computer-aided numerical method such as FEA.

FEA has been called the most powerful analysis technique ever made available to engineers. Fundamentally it is a technique for solving partial differential equations whose domains are geometrically too complicated to admit analytical solutions. The domain is divided into subdomains small enough for the field variable to be approximated by a simple function of position. In this way a component is regarded as an assembly ('mesh') of small building bricks ('finite elements') connected at the corners ('nodes') and in each of which the field variable (eg displacement u) varies in a much simpler way than it does through the whole component. This principle is illustrated by the development of a uniaxial finite element.

At each end of the bar (1) and (2) there are forces F_1 and F_2 and displacements u_1 and u_2 , two of which will be known while two are unknown. We assume that u can be linearly interpolated between the nodal values. Algebraically this means that:

$$u = u_{(1)} + (x-x_{(1)})/(x_{(2)} - x_{(1)}) * (u_{(2)}-u_{(1)})$$

where x is a coordinate whose origin is not necessarily at the left end of the bar. In fact what is important in determining u_x is not the absolute value of x rather the relative position of the point within the bar, eg halfway along. This is better indicated by a normalised or parametric coordinate basis ξ in which

$$\xi_1 = -1 \quad \text{and}$$

$$\xi_2 = +1$$

and so the middle of the bar is always at $\xi = 0$.

The coordinates x and ξ of any point can be related by;

$$x = \frac{1}{2} * (1 - \xi) * x_1 + \frac{1}{2} * (1 + \xi) * x_2$$

and in matrix form

$$\begin{aligned} x &= \left[\frac{1}{2} * (1-\xi) \quad \frac{1}{2} * (1+\xi) \right] * [x_1 \quad x_2]^T \\ &= [N_1 \quad N_2] * [x_1 \quad x_2]^T \\ &= [N]^T * [X_{(i)}] \end{aligned}$$

Where the vectors are assumed to be columns. Replacing x by ξ , the displacement interpolation can be rewritten as:

$$\begin{aligned} u &= \frac{1}{2} * (1-\xi) * u_{(1)} + \frac{1}{2} * (1+\xi) * u_{(2)} \\ &\equiv [N]^T * [u_{(i)}] \end{aligned}$$

and this can be put into the differential equation. The equation can be then integrated, eg using the Principle of Virtual Displacements, and the boundary conditions inserted to get the constants of integration. When this is done the result is;

$$\begin{bmatrix} F_{(1)} \\ F_{(2)} \end{bmatrix} = \frac{E * A}{L} \begin{bmatrix} 1 & -1 \\ -1 & 1 \end{bmatrix} * \begin{bmatrix} u_{(1)} \\ u_{(2)} \end{bmatrix}$$

$$\begin{bmatrix} F_{(i)} \end{bmatrix} = [k] * \begin{bmatrix} u_{(i)} \end{bmatrix}$$

where $[k]$ is the stiffness matrix. Once the stiffness matrix has been calculated for an element it is only necessary to insert the boundary conditions to determine its response.

2.5.1 Computational Analysis

In building a finite element model it is necessary to divide the complex geometry to be studied into simpler smaller individual domains, the elements. Such a process is known as meshing and the resulting computer file describes the domains by specifying nodal positions, infinitesimal points within a coordinate system. These **nodes** are then connected to make up individual **elements**. In 1 dimension only one coordinate is necessary to position a node, while in fully 3 dimensions an orthogonal, spherical or

cylindrical coordinate system must be used. The process of meshing may be carried out semi-automatically by a pre-processor package or manually. The type of element chosen is the analysts prerogative and is one of the most critical steps in an analysis, both in terms of performance and cost.

The 2 noded uniaxial **bar** described in the previous section is the simplest finite element to conceive. Figure 2.4 shows the bar diagrammatically along with other elements. The 3-dimensional equivalent of the bar is called a **truss** and while a truss element can move in 3-D, it can only sustain tensile or compressive forces. If transverse forces which cause bending are required, eg as in a golf shaft, it is possible to use a **beam** element.

For full 2-D and 3-D continuum analysis, the equivalent of the bar is the **plane** element. There are 3-noded triangular plane elements but these can be unreliable and 4-noded quad elements are more robust. Plane elements contain only the in-plane degrees of freedom and do not admit bending. The continuum equivalent of a beam is a **plate** element and to include stretching as well there are **shell** elements.

In analysing more complex solid 3-D geometric entities, such as the golf clubhead, it is necessary to use full 3-D **solid** elements. There are 4-noded tetrahedral elements but as with triangles these are not reliable and a better choice is a hexahedral such as an 8-noded brick. This allows displacement in all three directions at each corner node. Solid elements do not generally include rotational degrees of freedom and so the calculation of rotational velocities is a problem. This is addressed later.

Finally, there are special purpose elements which do specific tasks. For example, a rigid element might be used to represent a stiff connection between parts of a structure.

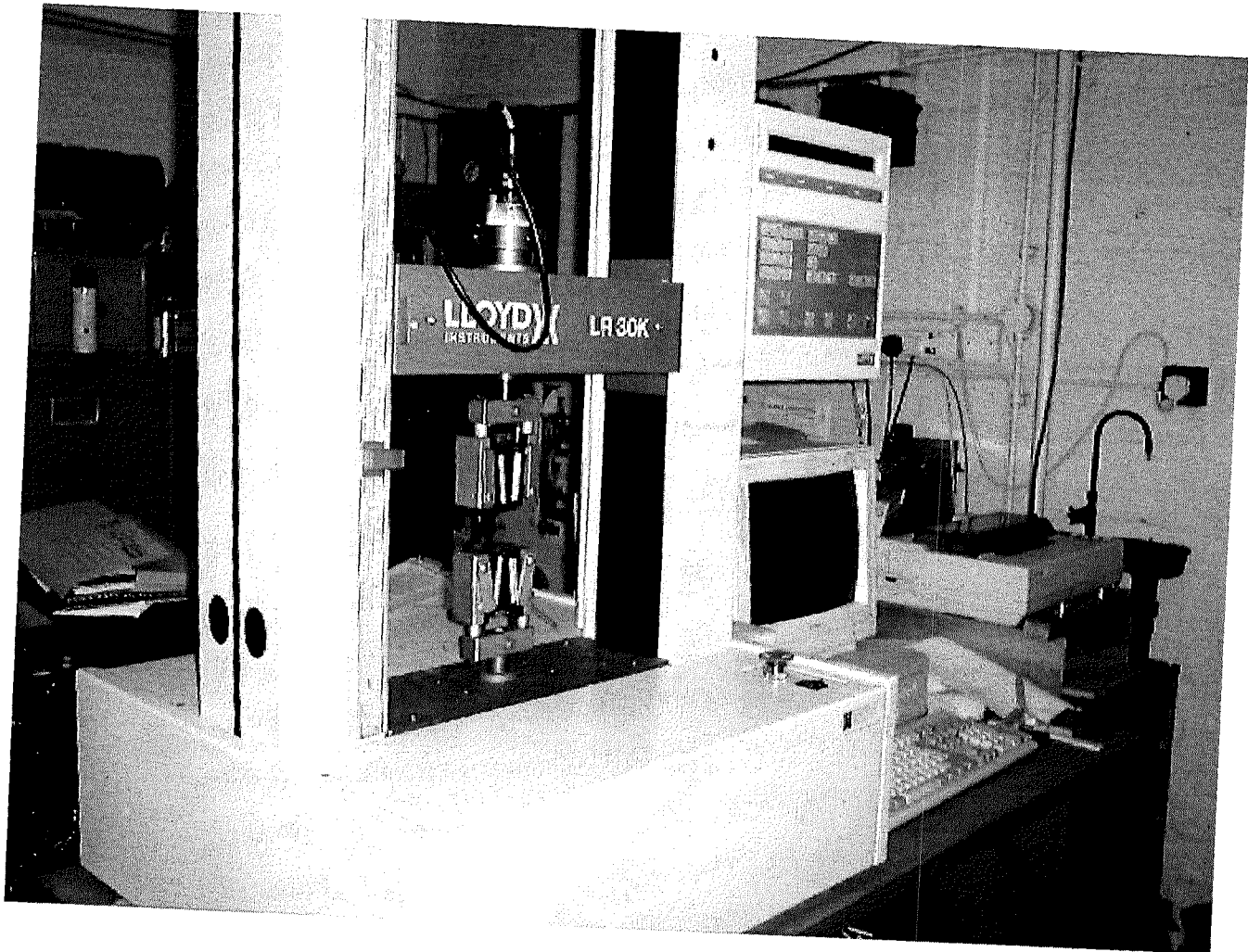


Figure 2.1 Uniaxial testing machine.

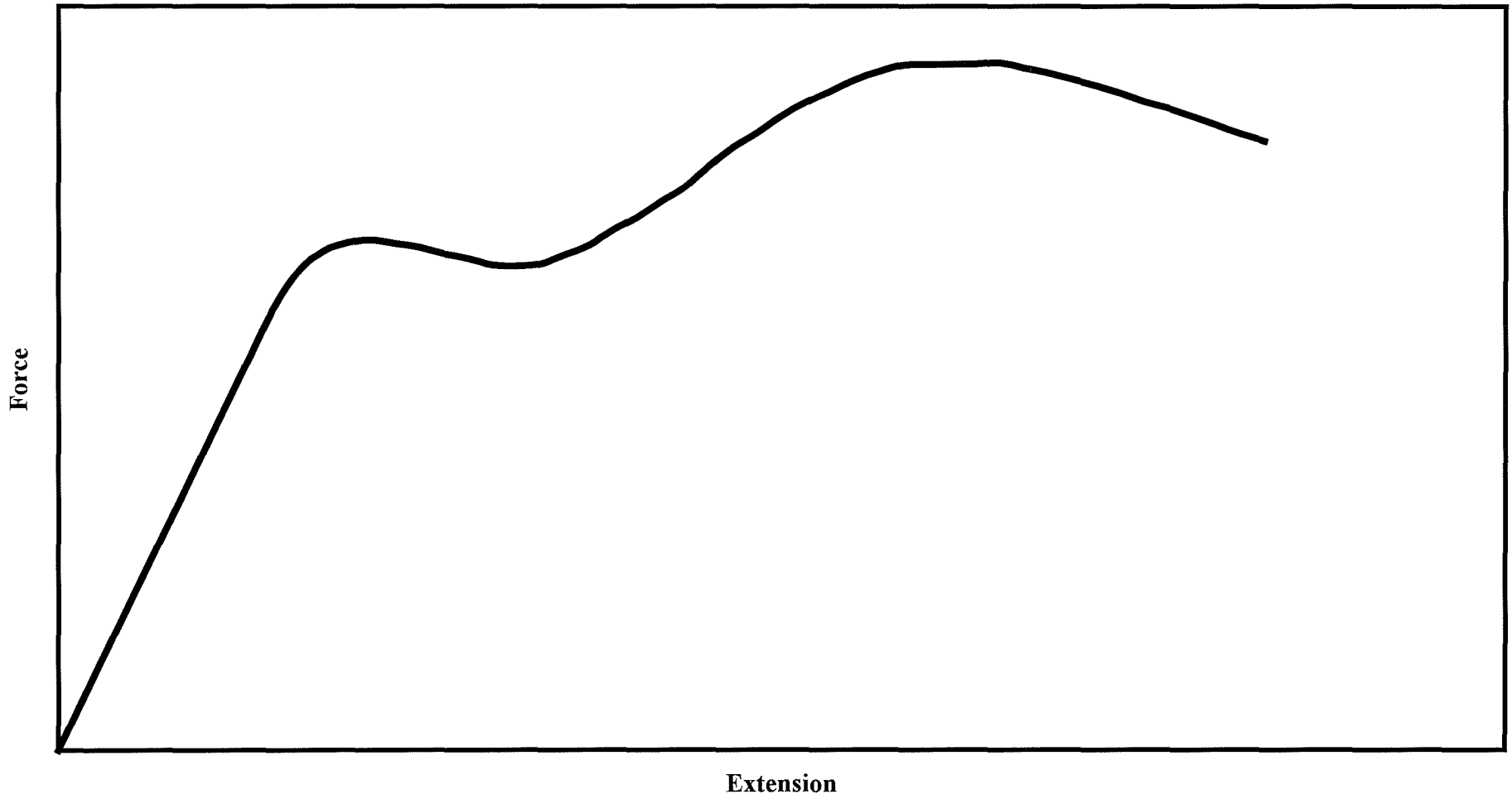
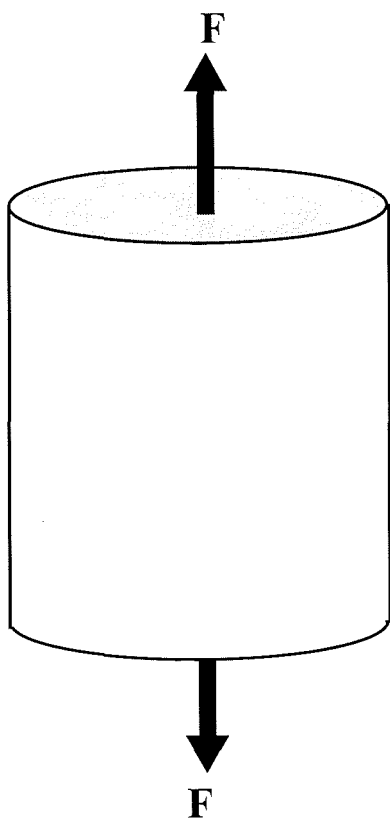
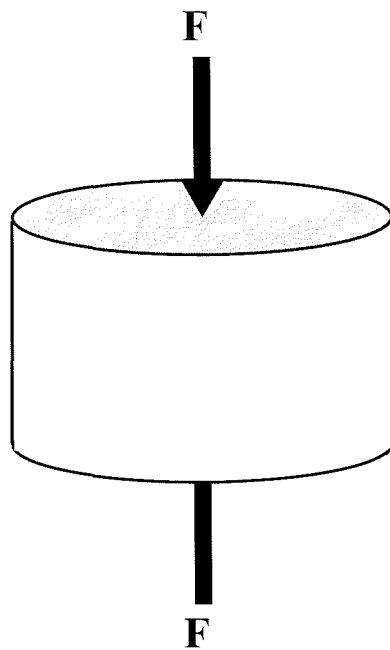


Figure 2.2 Force/Extension for a mild steel specimen up to failure (Shames 1989).



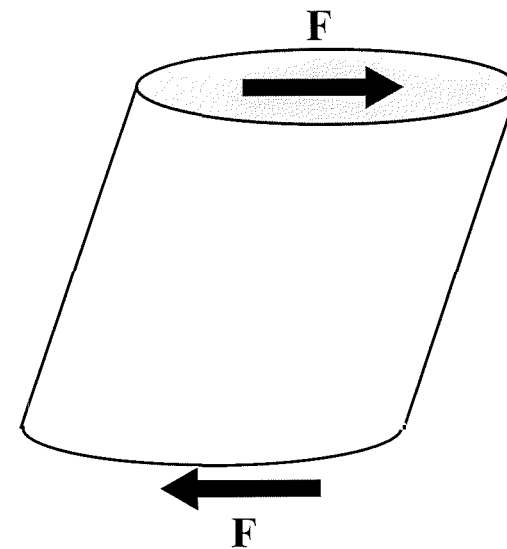
Tension

Stress = force/area



Compression

Stress = force/area



Shear

Stress = force/area

Figure 2.3 Three types of stress.

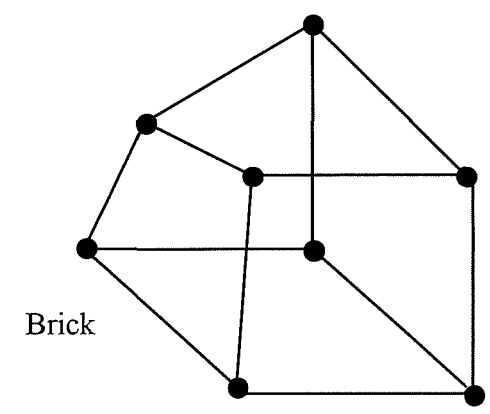
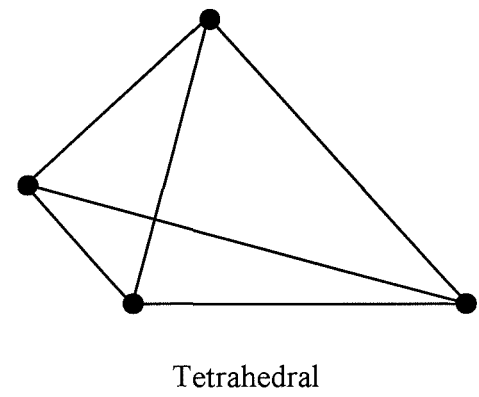
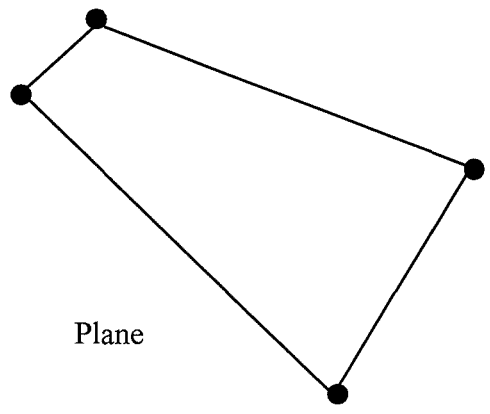
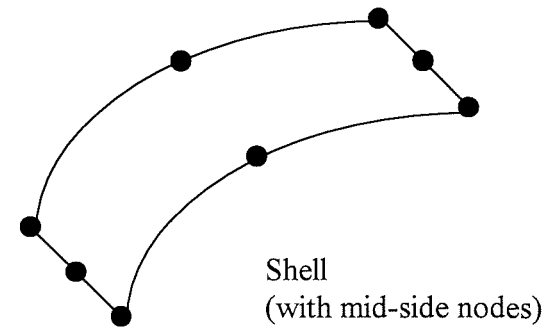
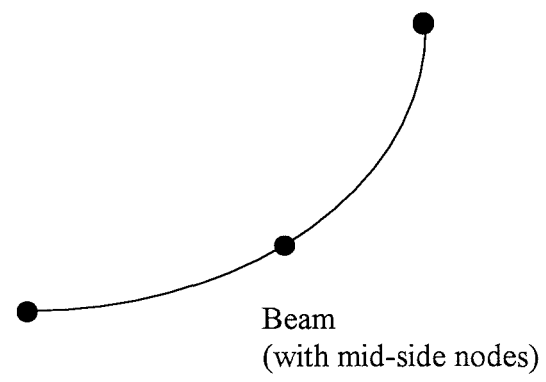
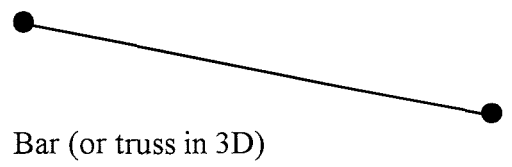


Figure 2.4 Examples of commonly used Finite Elements.

3.0 Reverse engineering of a golf clubhead

Clubhead designs, are normally created by craftspersons working for golf club manufacturers. Their original sculptured designs are carved in wax and then sent to a production facility, normally in an overseas country, which produce moulds and prototypes for testing. This process leads to a lack of engineering information on the geometric shape of the clubhead, and a subsequent difficulty in building computer models for existing designs. To successfully model present clubhead designs and evaluate their performance there is need for a reverse engineering process, which is able to analyse clubheads and describe their shape. For a Finite Element model to be created it is necessary to have suitable information about the geometry, such that a CAD model can be created. Mitchell (1996) described such a feature based approach for golf clubheads. Such procedures are also becoming increasingly important for other pre-CAD existing objects, which require to be modeled to allow for design upgrades.

3.1 Manual method

A manual slicing method was used to find the geometry of an existing clubhead, and to subsequently build a model in the solid geometry CAD package, Catia (Dassault Systèmes, version 4). Complicated shapes may be built up in CAD by specifying the cross-sectional profiles, at various planes through the object. To achieve these profiles the clubhead was sliced into nine segments, and is shown in figure 3.1. Before slicing, a hole was drilled along the heel/toe axis, (a line from the toe to the heel of the club), to provide a reference for each segment relative to each other. Individual segments yielded a cross-sectional profile which was recorded using graph paper. The coordinates of points lying on the circumference of each profile were used to build up the model in Catia. The points were selected approximately every five millimetres, forty points being needed for the biggest cross-section. The thickness of the cutting blade was used to give each profile the correct volume, before a solid model incorporating all the profiles was generated, shown in figures 3.2 and 3.3. A finite element mesh was created for the solid and analysed using Abaqus (Hibbert, Karlsson & Sorensen Inc. version 5.5).

3.1.1 Model evaluation

The finite element model of the clubhead was achieved, validating the route taken to model the clubhead. However the model is lacking in a number of ways which prohibited its practical use in any further studies. On close inspection, the hitting surface of the head was heavily undulated, due to the nodes not being present in a consistent smooth surface, this is a common occurrence when using automatic and semi automatic meshing techniques within CAD packages. The uneven surface would lead to spurious results if the head was used for clubhead-ball impact analysis as the resultant flight of the ball is largely dependent upon the normal of the striking surface relevant to the motion of the club. It is possible to move the nodes into a single plane, by a transformation, but this would only be relevant for clubfaces with a flat surface, such as the iron clubs. Drivers have a degree of curvature on the hitting surface and this affects the flight of the ball. In mishit shots the curvature causes side spin which corrects for the ball's initial error in flight trajectory away from the target. To increase the accuracy of the model it may be possible to take more slices leading to more cross-sectional profiles, but due to the hardness of the clubhead material, and the thickness of the blade needed to slice it, a limit is placed on the number of segments possible. Other areas by which the correctness of the model may be improved are to take more points on the circumference of the individual segment profiles. However this was already at a high level and it was felt the accuracy was limited more by the number of slices possible. Due to the above factors, the destructiveness of the test, and the labour intensity of the procedure, along with the proneness of human errors that could occur, another method of analysing the clubhead was investigated.

3.2 Stereo Photography

This method uses a pair of cameras to generate two slightly differing images of a single object, a software package is then used to construct a 3-D model of the objects surface. This route is currently being investigated by the Turing Institute, Glasgow, who in 1997 released a version of their software C3D, to be used by police forces in analyzing 3-D surfaces of human faces. The process and the C3D software, pre-release, were used to obtain a surface description of a golf clubhead, from which a finite element model was

created. The C3D software is a GUI-based computer program that converts the implicit 3-D information contained within the stereo image pairs into an explicit 3-D surface model in a standard CAD file format. Figure 3.4 outlines the complete C3D processing chain.

3.2.1 Procedure

The C3D processing chain ends with the production of a standard CAD file format, DXF file. The file contains the coordinates of each triangulation point contained on the surface and the order of their connectivity. For the clubhead two files are produced giving the lower and upper (sole and crown) surfaces. A certain amount of overlap occurs, such that parts of the clubhead appear in both surfaces. To capture the images of the clubhead and calibrate the object space, it was necessary to provide a calibration device of a similar object volume, and a turntable and mounting with which to hold the clubhead. Appendix A, gives the technical drawings of the devices designed and constructed. Figure 3.5 shows the metal driver that was examined using the C3D process. Holes drilled through the clubhead were used to securely attach the clubhead to the turntable mountings.

3.2.2 File formats

The two files from the C3D process chain, are written in DXF (AutoCAD Drawing Exchange Format). This may be imported into Microstation (Bentley Systems, version 5) or AutoCAD (Autodesk, version 12), the latter allowing for image adjustment and for the two halves to be joined together in a single file. In moving forward from this file format towards a finite element model it is necessary to export the file in the IGES (International Graphics Exchange Specification) format. This file is readable by Patran (MacNeal-Schwendler Corporation, version 7.0), from which a solid model can be generated. It is important to note that the size of the files increases along the chain, from the 2KB disk space needed for the DXF file, to 2MB when in IGES format and increasing thereafter. Other software packages were investigated to find a suitable and efficient path. A flow chart is given in figure 3.6 showing all routes investigated.

3.2.3 Model evaluation

Because of the complexity of the surfaces, it was not possible to join the two halves of the clubhead together and form a single surface, some areas on the clubhead had been neglected, while others were mapped twice. The two surfaces are shown in figures 3.7, as they were seen when imported into AutoCAD, and figures 3.8 shows the crown surface in Microstation with rendering having been applied. The smoothness of the object surface is of a much higher degree than that generated by the manual method and this is clearly seen, even though analysis of the clubhead was carried out using the minimum of triangulation points possible to keep the file size small and to ease in understanding the process. The C3D process is capable of a much higher degree of resolution, but this was not felt necessary at this investigative stage. It was possible to create finite element models from Patran of the clubhead surfaces, so confirming the path taken. However problems occurred when matching the two surfaces together. This could possibly be avoided using small notches in the areas where the clubhead appears in both images, but first the obstacle of obtaining a full object surface mapping needs to be cleared. Taking more images of the clubhead in different orientations could be of benefit, but a new turntable, able to hold the clubhead in a variety of positions, would need to be manufactured. The lighting necessary for the C3D process to work would also restrict the orientations possible.

3.3 Discussion of results

Both methods were capable of producing finite element models of the clubhead. The manual method relies largely on the time available and the accuracy required, it is of limited value in attempting to precisely model complex curved surfaces. The stereo photography method allowed curved surfaces to be modeled more accurately, but is still at a prototype stage when trying to model full object surfaces. However, uncertainties still occur over how to model hollow clubheads, as the centre of mass, and moments of inertia rely firmly on the thickness of material used to form the clubhead. Examination of existing clubheads shows there to be thicker material at the hitting surface than elsewhere on the club. Uniformity of thickness elsewhere is not a certainty, and left to the manufacture to decide. The inclusion of stiffening bars and welds adds to the

problem of producing a finite element model of a hollow clubhead, even when the surface geometry is known. A combination of the two processes may result in a method at present to model existing clubhead designs. However while reverse engineering would have enabled interesting comparisons of actual products, and does appear to be possible, it was regarded as a secondary objective compared to the need to understand the mechanics of the golf stroke. Further development of the reverse engineering route was therefore abandoned and attention focused on simplified models of solid iron clubheads.

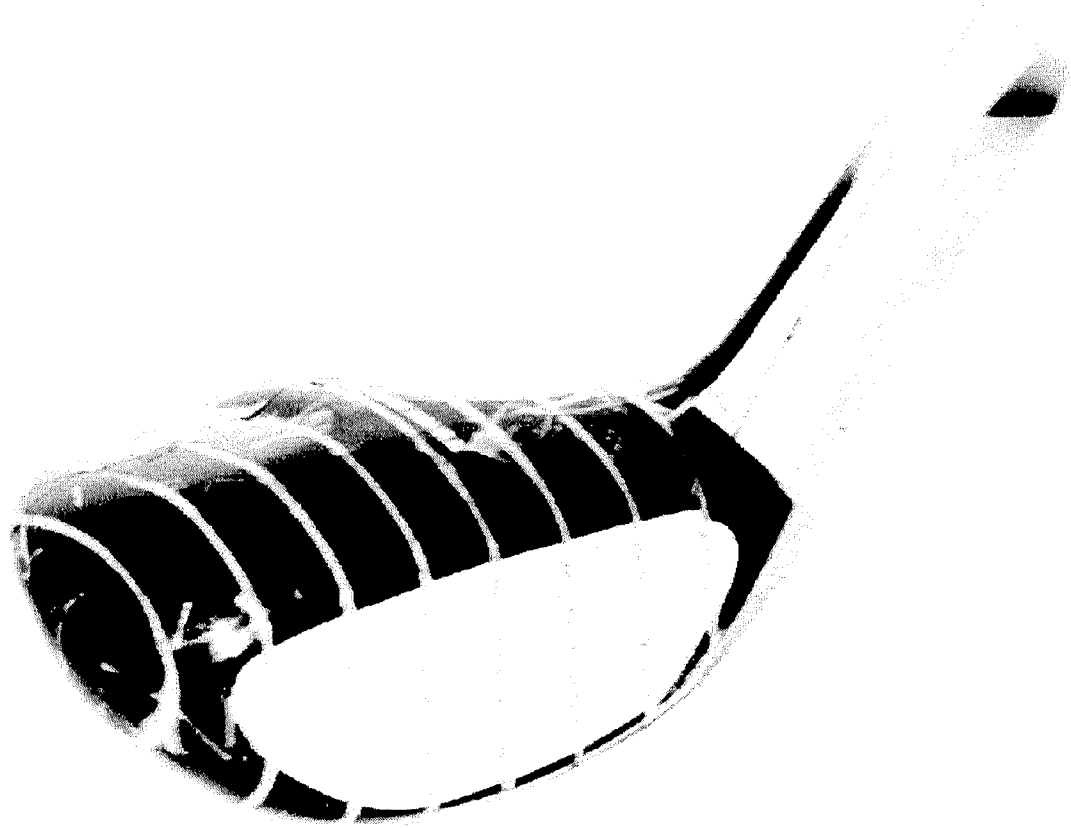


Figure 3.1 Ceramic clubhead, sliced into nine sections.

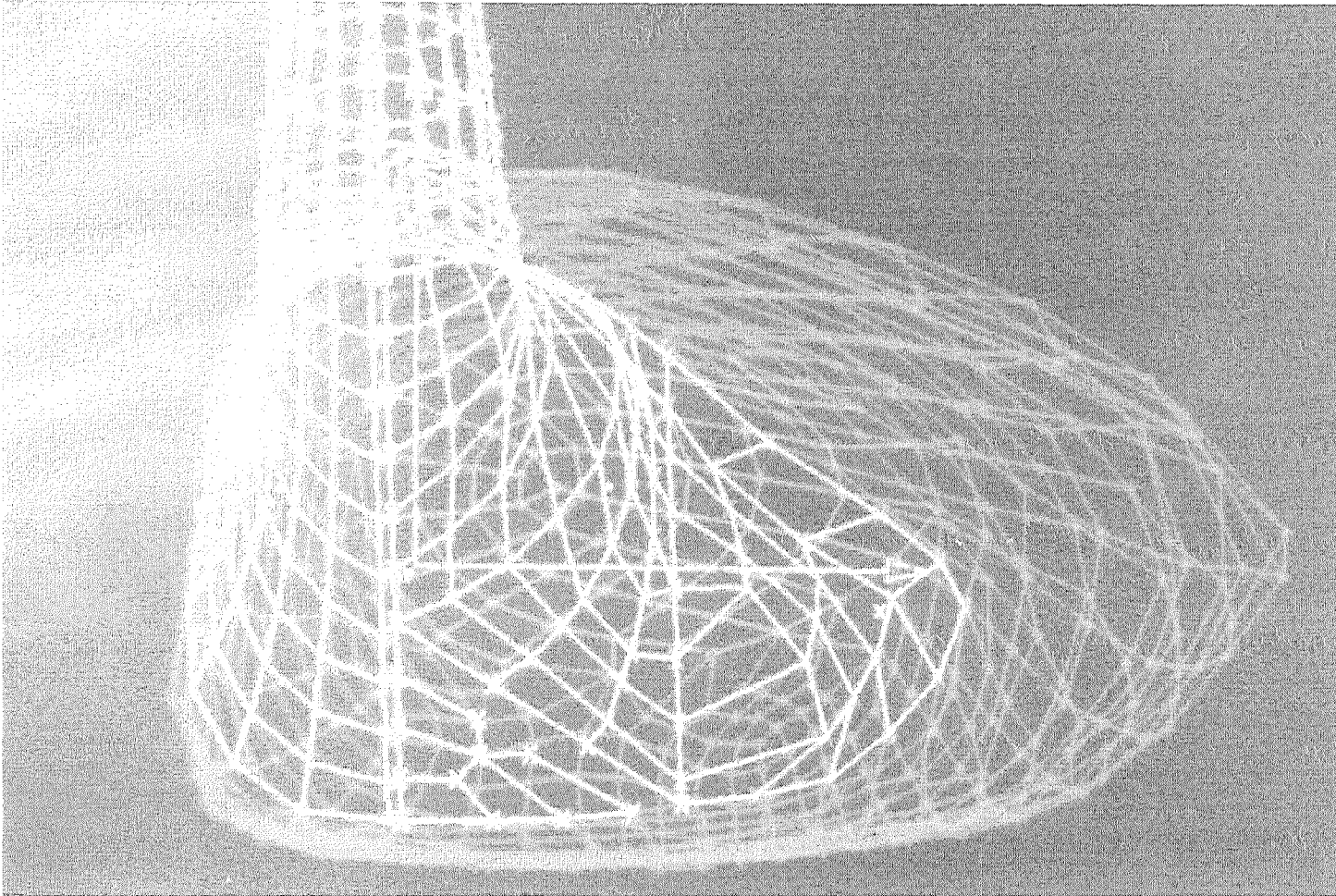


Figure 3.2 Catia CAD solid model of clubhead.

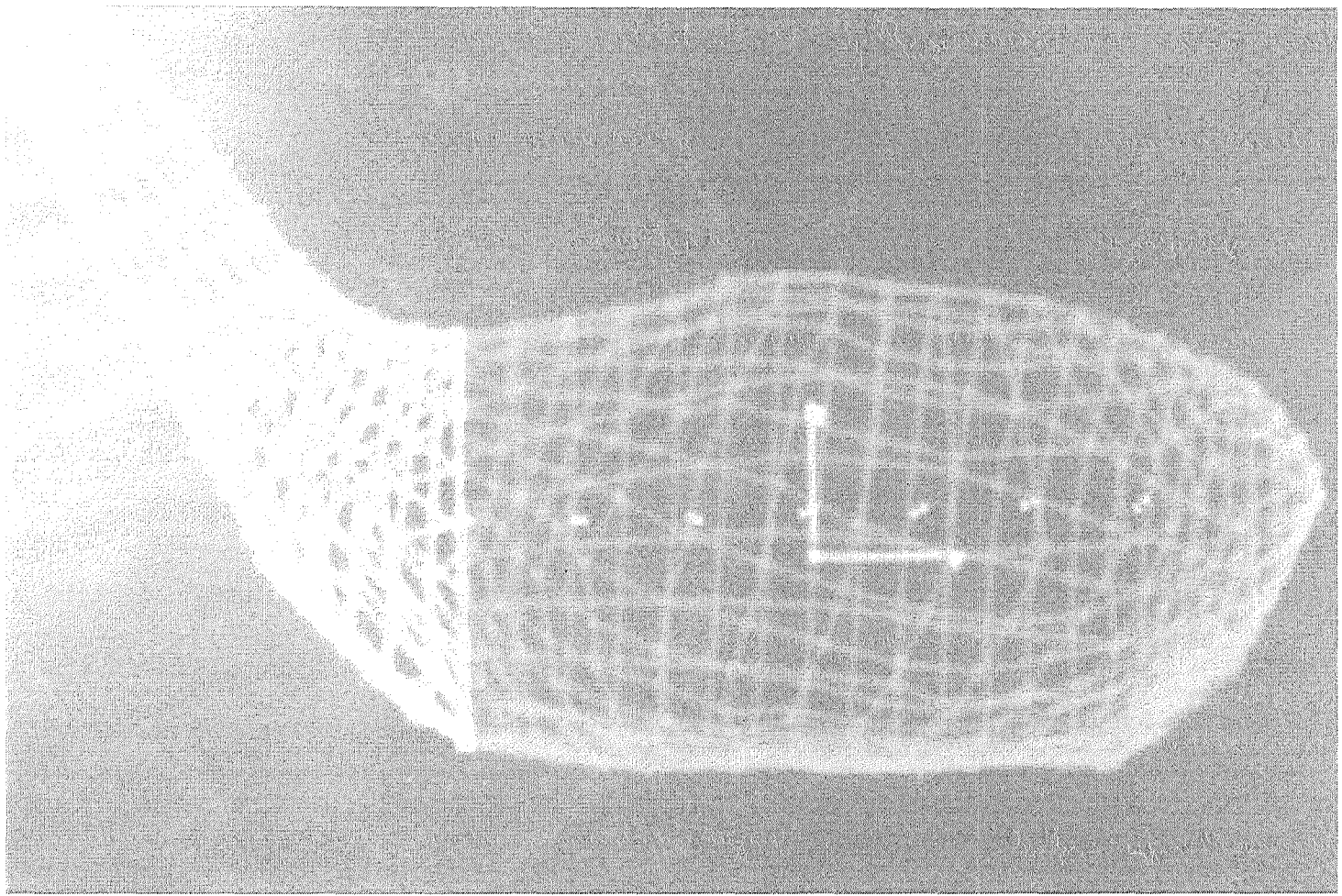


Figure 3.3 Catia CAD solid model of clubhead.

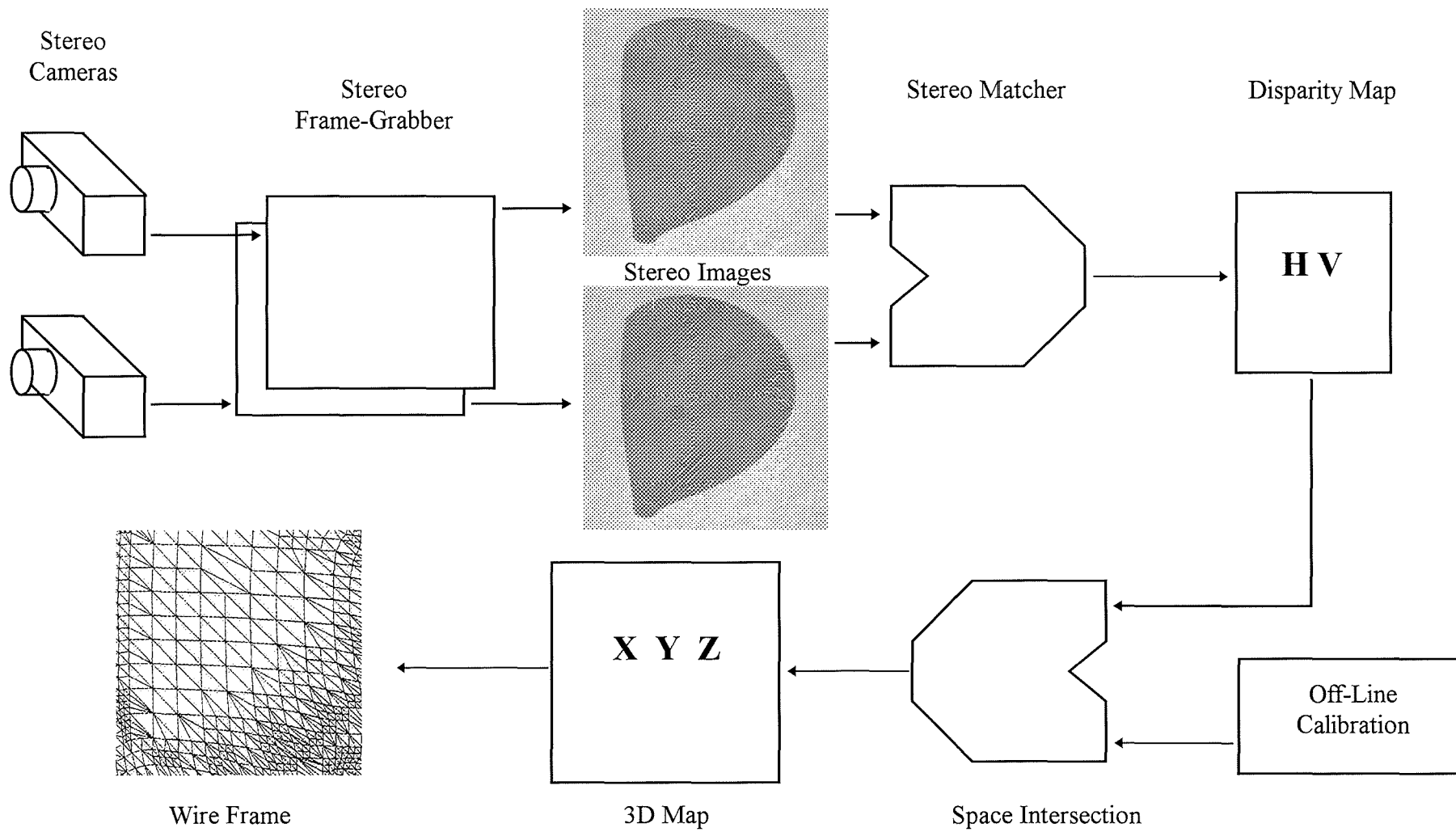


Figure 3.4 Complete C3D processing chain.



Figure 3.5 Metal driver used in C3D stereo photography process.

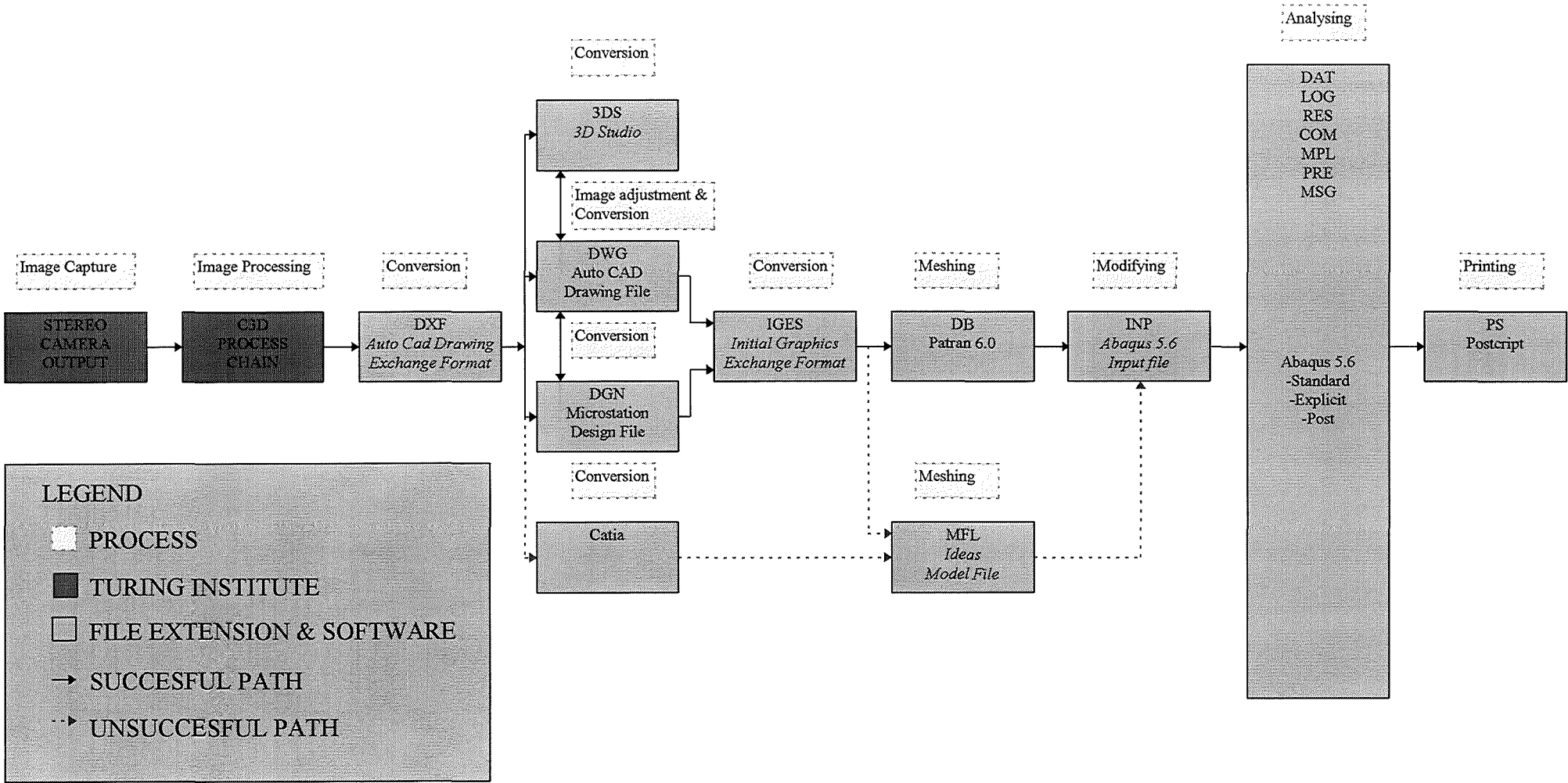
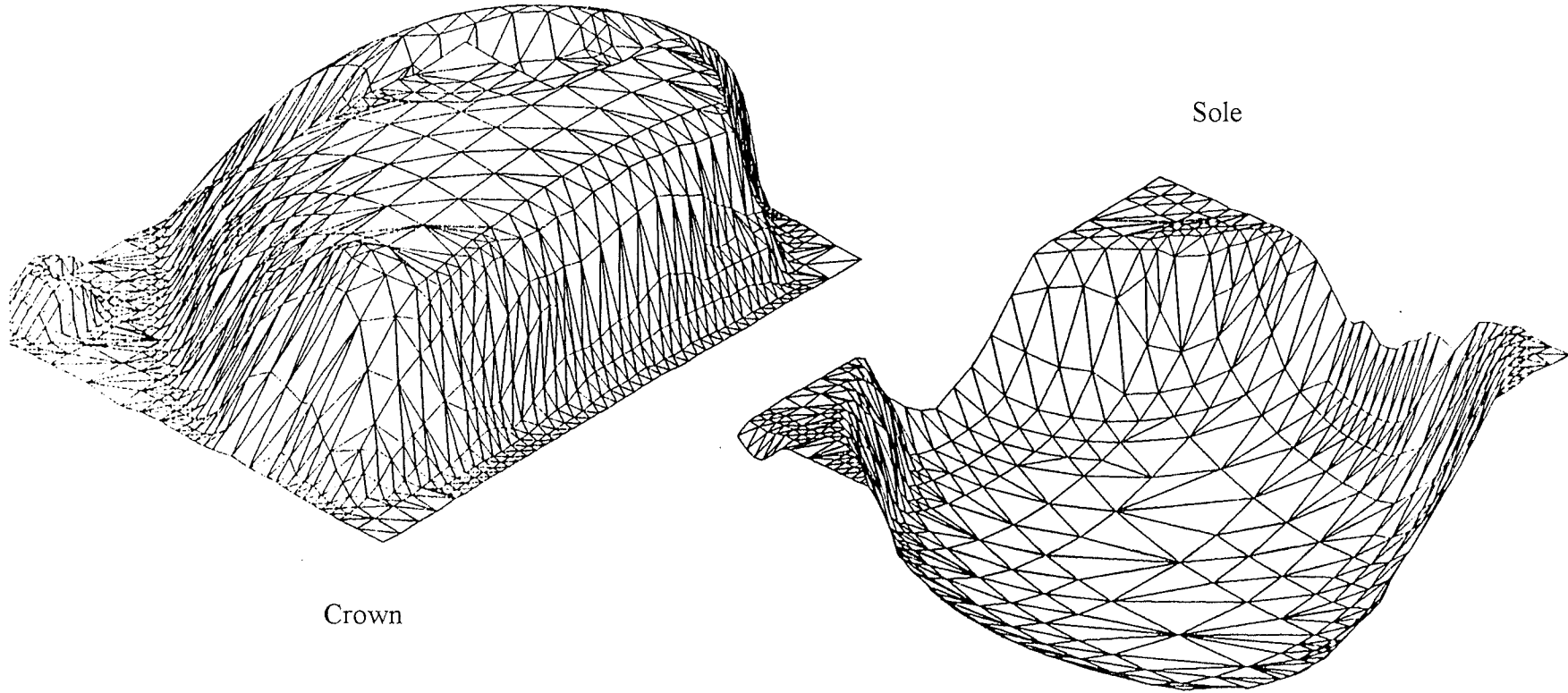


Figure 3.6 Flow chart of routes investigated.



Crown

Sole

Figure 3.7 AutoCAD representation of crown and sole surfaces.

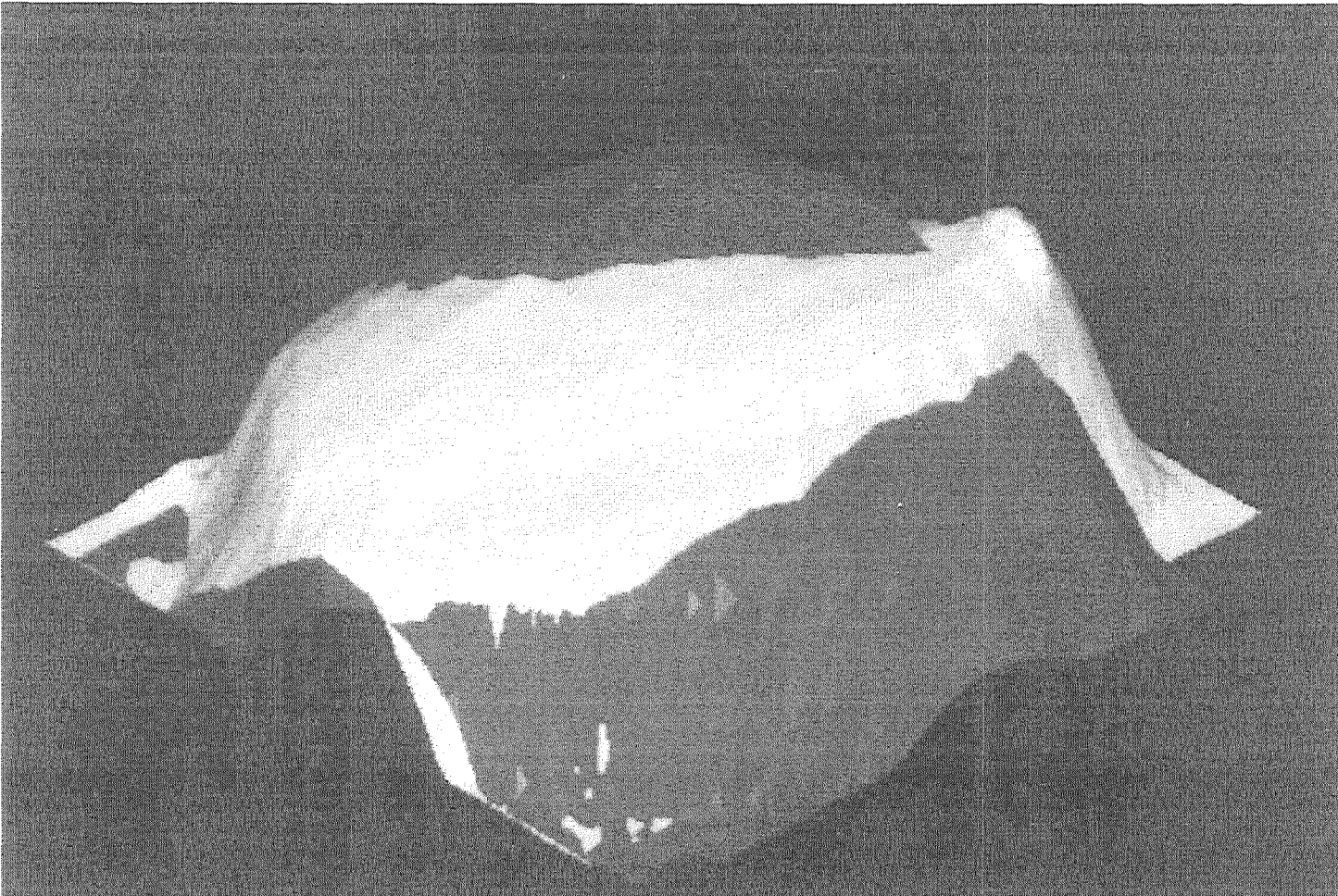


Figure 3.8 Microstation representation of crown surface.

4.0 The finite element impact model

4.1 Construction of model

To analyse the impact between clubhead and ball it is obviously important to have a model that mimics the behaviour of a real golf club. However, as noted in chapter 3, automated reverse engineering from an existing product through to computational stress analysis is not yet a practical option. This is inconvenient but not serious in the current work since fine geometric details, such as the fillet radius at the hosel, are less important than parameters such as loft angle which undoubtedly have a significant influence on performance and which must be open to systematic change if their quantitative effect is to be studied (indeed it is a common fault of inexperienced finite element analysts to concentrate too much on fine geometric details while giving insufficient attention to such matters as material models and boundary conditions). For the current work it is then appropriate to analyse a geometrically simplified clubhead.

4.1.1 The clubhead

Finite element meshes were partly created using Patran 3, an industry-standard commercial pre-processor package. Such pre-processors are capable of automatically generating a complete input file for the analysis package, in this case Abaqus 5.7, but this is really only practical for straightforward “production” runs. Here, as in much research work, it was found to be more efficient to generate only a partial analysis file containing nodal positions and element connectivity and to manually edit in such data as material properties and initial conditions.

Solid element model

Following Cochran and Stobbs (1968), it is assumed that the clubhead behaves as a free body during impact. A solid model of a clubhead was therefore generated as in figure 4.1. This contains 385 nodes and 240 8-noded linear solid elements, giving a total of 1155 degrees of freedom. The model was analysed using Abaqus/Explicit with C3D8R reduced-integration elements (Hibbitt, Karlsson and Sorensen 1997). Only linear elements are currently available in Abaqus/Explicit, that part of the Abaqus suite which is

specifically tailored for the analysis of impact and contact problems. The club face was planar and smooth, with no grooves, but with the option to include friction. The loft angle was initially chosen as 30° . The back of the club was also flat, ie. with no cavity-back, and so the model represents a mid-range blade such as a 5 or 6 iron. The position of the centre of mass of such a clubhead is within the material and this, together with the moments of inertia, can be ascertained at the pre-processing stage of an Abaqus static analysis. These inertias are given in figure 4.2 along with a schematic of the clubhead and dimensions.

Rigid element model

Dynamic analyses of full solid models are computationally expensive and, since one of the objectives of the current work is to point towards an economic tool for club designers, an alternative mesh was constructed from rigid elements. By definition, such a mesh does not allow any deformation, in particular at the clubface, but it reduces the analysis time and, when assigned appropriate masses and inertias, allows the effect of different loft and rotational inertias to be quickly and cheaply evaluated.

The rigid clubhead model is shown in figure 4.3. This uses a single Abaqus/Explicit R3D4 rigid element, (Hibbitt, Karlsson and Sorensen 1997) which requires a “reference node” at which mass and rotational inertias are located. This can be seen behind the hitting face. The reference node remains in a fixed position relative to the rigid surface element and, while the mass and rotational inertia may be freely assigned by the analyst, values equal to those of the whole solid-element model were initially used.

4.1.2 The ball

As with the clubhead, it is less important that the finite element model should mimic any particular ball than that it should be representative of a typical modern ball. One such type is the popular ‘two-piece’ variety, which comprises a resilient, reasonably stiff, solid core covered by a wear-resistant, dimpled, cover of a different material.

A finite element mesh was again generated with Patran, version 3, using 8-noded solid elements (Abaqus type - C3D8R). The whole model was generated by replicating an

1/8 octant, to give a model which was almost spherically symmetrical. A cut away drawing (figure 4.4) shows the separate core and cover elements, and the steps taken to avoid the undesirable effects of a focused mesh at the ball centre.

The core, which is expected to undergo large strains during the impact, is given the properties of a hyperelastic material. Such a material is nonlinear, perfectly elastic and is characterised by a strain energy function Φ . The Cauchy stress σ is obtained as the derivative of Φ with respect to the deformation gradient ∇x , thus:

$$\sigma = \partial\Phi/\partial(\nabla x).$$

The strain energy function for such materials is a function of the principal stretches and cannot be inferred from a single set of tests such as uniaxial tensile or compression tests. Data for such materials are therefore difficult to obtain and test data for vulcanised rubber, which is similar in composition to a typical two-piece ball core material, was taken initially from the Abaqus/Explicit example problems manual (Hibbitt, Karlsson and Sorensen 1997). This was entered as test results into the input file, from which Abaqus calculates the constant coefficients which best fit a polynomial model of a strain energy function defined as

$$U = \sum_{i+j=1}^N C_{ij} \left(\bar{I}_1 - 3 \right)^i \left(\bar{I}_2 - 3 \right)^j + \sum_{i=1}^N \frac{1}{D_i} \left(J^{el} - 1 \right)^{2i}$$

where

- U is the strain energy per unit reference volume.
- N is a material parameter.
- C_{ij} and D_i are temperature dependent material parameters.
- \bar{I}_1 and \bar{I}_2 are 1st and 2nd deviatoric strain invariants defined as

$$\bar{I}_1 = \bar{\lambda}_1^2 + \bar{\lambda}_2^2 + \bar{\lambda}_3^2$$

and

$$\bar{I}_2 = \bar{\lambda}_1^{(-2)} + \bar{\lambda}_2^{(-2)} + \bar{\lambda}_3^{(-2)}$$

where the deviatoric stretches $\bar{\lambda}_i = J^{-\frac{1}{3}} \lambda_i$

- J is the total volume ratio.
- J^{el} is the elastic volume ratio for thermal expansion.
- λ_i are the principal stretches.

The **Initial shear modulus** is given by

$$\mu_o = 2(C_{10} + C_{01})$$

The **Initial bulk modulus** is given by

$$k_o = \frac{2}{D_1}$$

The constants calculated by Abaqus to best fit this model are given in table 4.1.

Hyperelastic material coefficients						
D_1	D_2	C_{01}	C_{10}	C_{11}	C_{02}	C_{20}
9.92×10^{-9}	-4.43×10^{-8}	3.48×10^4	1.16×10^5	-1779.0	2269.0	85.0

Table 4.1 Hyperelastic material coefficients calculated for test data by Abaqus/Explicit.

This core material gave a ball which was rather too compliant in compression compared to modern balls (Mather and Immohr 1996) and is discussed in more detail in section 4.5. However it allowed the effects of changing the constants in the material model to be observed in a computational experiment and this suggested possible changes in core material properties which could be achieved without deviating from the hyperelastic shape of the stress/strain curve, shown in figure 4.5, for the original test data of vulcanised rubber. Material density was taken as 1100 kgm^{-3} , consistent with actual ball core materials measured.

The cover material, although undergoing large displacements (rotational and translational) was not expected to undergo large strains. A linear elastic material response was therefore assumed to be reasonable and properties appropriate to DuPont 'Surlyn', a popular thermoplastic cover material manufactured by DuPont was used.

Statz (1990) gives an elastic modulus of such material at 0.34 GPa and this value was confirmed by experiments on tensile specimens made from reconstituted granules of the material, as supplied by the manufacturer. Material density was measured and taken as 950 kgm^{-3} .

4.1.3 Computing facilities

As noted in section 4.1 the FE analyses were performed using Abaqus, an industry-standard commercial package from Hibbitt, Karlsson and Sorensen, Inc. Particular use was made of the Abaqus/Explicit module, which is designed specifically for the analysis of non-linear, large-displacement, contact problems. The present work spans some three years and several upgrades of the software were used, from version 5.4 through to 5.7. Abaqus operates in batch mode, reading from an input file which contains the 'model' and 'history' data, the latter describing the loading history. Appendix B-1 gives the input file for a typical analysis. The input file may reference other user-defined files for specific blocks of data, such as the mesh definition or material properties, thus allowing clearer structuring of whole input and allowing such files to be shared by different analyses. The analysis module generates a number of output files, such as tables of numerical results some of which are suitable for inspection by the user. Other results files are in binary format and require additional post-processing, by Abaqus/Post for example, which allows generation of graphical output such as undeformed and deformed plots, animation sequences, contour plots, hard-copy output and graphs.

Over the three years of the current work, the analysis was carried out on a variety of workstations from IBM RS6000s to a Sun sparystation-20. Analysis times vary depending on the machine, the time to be simulated and the complexity of the model but a typical clubhead/ball impact analysis on the Sun took 1 hour of processing time for a 5 millisecond dynamic simulation.

4.1.4 Additional input data

The initial position of the solid clubhead relative to the ball is shown in figure 4.6. For most analyses the clubhead was given an initial velocity in the global 3-direction, ie directly towards the ball, and the mechanical properties of steel (Ashby 1996).

Particular attention is drawn to the coordinate system the model is constructed in as reference is made to this throughout the text. The 2-direction is vertical and the 3-direction is horizontal along the intended direction for a straight hit. The 1-axis is perpendicular to the target line such that for a right-handed golfer the positive 1-direction goes left of target, a hook. A negative 1-direction goes right, a sliced shot.

In Abaqus the interface between impacting surfaces may be assigned a coefficient of friction (μ). A coulomb friction model is used, with no distinction made between limiting static friction and dynamic friction. The initial separation of club and ball was such that impact occurs after 0.035 milliseconds, when the clubhead was given an initial velocity of 50ms^{-1} . The analysis was set to record the behaviour of the model for 5 milliseconds. The clubhead did not have any constraints or boundary conditions except its initial velocity and is free to move in any degree of freedom on impact with the ball.

		Elastic clubhead	Ball
Mass (kg)		0.322	0.039
Centre of Mass (metres from origin of coordinate system)	X	-7.542×10^{-3}	-2.391×10^{-10}
	Y	-5.708×10^{-3}	-8.551×10^{-10}
	Z	-3.060×10^{-2}	-2.117×10^{-10}
Moments of Inertia (kgm about centre of mass)	XX	7.496×10^{-5}	6.972×10^{-6}
	YY	1.526×10^{-4}	6.972×10^{-6}
	ZZ	1.897×10^{-4}	6.973×10^{-6}

Table 4.2 Initial centres of mass and inertias of the clubhead and the ball.

The mass of the head and ball, the initial positions of the centre of mass and the rotational inertia are given in table 4.2 which indicates that the vector joining the ball and

clubhead centres of mass does not point in the direction of motion. It is thus expected that a rotation of the clubhead during impact will occur with a hooking effect on the ball. This model with minor amendments was used for all the solid clubhead analyses; the input file is given in appendix B-1. The rigid clubhead analyses uses a simplified input file (appendix B-2) which calls separate files containing the ball node and element definitions. The rigid clubhead loft can be modified by a rotation of the nodes about a given axis, followed by a translation such that the clubhead and ball have the same initial separation. However, the contact position on the ball depends on the loft of the head and the initial conditions for each loft are given in appendix B-3.

4.2 Impact results

The following sections describe, in detail, features which are common to most of the impact analyses performed. Results are for a 30° lofted solid clubhead, with the properties of steel (Ashby 1996), initially traveling at 50ms⁻¹ along a vector coincident with the positive 3 axis. The analysis simulates 5 ms of real time and a coefficient of friction 0.6 is used.

4.2.1 Deformed plots

Figure 4.7 shows an Abaqus/Post plot of the model clubhead and ball 0.150 ms into the analysis and 0.110 ms after initial contact. These times differ as the clubhead travels a small but finite distance before impact. For brevity, timings given hereafter are analysis times; the time from initial impact is 0.040 ms less. Hidden lines have been removed to give a clearer view of the ball deformation. From figure 4.7, it can be seen that the ball has started to deform on the impact side while the free surface has not yet moved. This in itself illustrates the need for a full 3-D mesh of the ball, rather than a cheaper axisymmetric model, if the impact is to be properly simulated.

Figure 4.8 shows the ball near its maximum deformation at 0.270 ms. The clubhead has slowed to 44.4 ms⁻¹ and twisted 1.2° about the 2-axis. At 0.470 ms, separation occurs and elastic recovery of the ball causes an increase in velocity. The ball leaves the clubhead as a deformed sphere (figure 4.9) with backspin induced by the oblique impact

of the lofted club on the spherical underside of the ball. The clubhead velocity has been reduced further by the impact and the head has rotated about its centre of mass, as a result of the off-centre impact, the cover of the ball being slightly obscured by the head. Rotation of the clubhead about a horizontal axis also results from the position at which it strikes the ball.

At the end of the analysis, at 5 ms, the ball is 0.347 m away from its initial starting position and 0.204 m away from the clubhead which, being unconstrained by a shaft, continues with a rather unrealistic constant velocity after impact. The ball has recovered its spherical shape but, since material damping was not specified (some damping is assigned by Abaqus for numerical stability), this must be due to multiple reflections of the stress waves within the core.

This sequence of post-processed results can be run as an animation file (clearly not reproducible here) and rotated by the user to give a clearer view of the impact. Figure 4.10 shows nine snapshots of the impact from time = 0.0 ms to time = 0.8 ms.

4.2.2 Stress and strain plots

Figure 4.11 is a sectional view of the core, showing ϵ_{33} , the direct logarithmic strain in the 3-direction, near the time of greatest deformation of the ball. The maximum strain appears in an element close to the face and has a (compressive) value of -0.258 . This is quite reasonable for the hyperelastic rubber core and produces an increased stiffness which would not be shown by a linear elastic material.

Figure 4.12 shows ϵ_{33} at the end of the analysis, at 5 ms, when the ball has nearly recovered its spherical shape. The maximum compressive strain within the core material has reduced to -2.75×10^{-3} , while the cover shows a tensile strain of 3.02×10^{-3} .

Figure 4.13 shows σ_{33} in the clubhead at 0.270 ms. The maximum stress value is 35.9 MPa, well below the yield stress of steel (Ashby 1996). This is reassuring as permanent deformation of the clubface on impact is neither a desired or observed phenomenon. It

also, incidentally, means that engineering 'hardness' is not an appropriate parameter with which to describe golf clubs.

4.2.3 Variable-variable graphs

Abaqus/Post allows the analyst to produce, both on-screen and in hard copy, a wide variety of variable-variable graphs, such as stress-strain plots, to aid interpretation of the results. These can also be expressed in tabular form suitable for manipulation by other third-party software such as Microsoft Excel.

Figure 4.14 plots the development of speed of the clubhead and ball. These were measured as the speed of nodes 433 and 1661 respectively, which are closest to the centres of mass of the ball and the clubhead. The graph shows the clubhead traveling at 50 ms^{-1} prior to impact during the course of which it falls to 42.0 ms^{-1} . The ball is initially static and its central node (433) begins to move slightly after initial impact. After separation the ball attains a maximum velocity of 77 ms^{-1} . Fluctuations in the velocity of the ball after impact are due to multiple reflections of the stress waves and the non-spherical shape of the ball leading to corresponding small variations in the instantaneous velocity of node 433. The clubhead speed after impact is slightly higher than would be experienced in an actual golf shot as the head mass was 322 grams, somewhat greater than 255 grams which is typical of a 5-iron (and confirmed by measuring a number of heads).

4.2.4 Post processing of numerical output

Abaqus/Post is also capable of producing user-readable files for further post-processing. This method is used in the next sections to obtain further information on the behaviour of the ball after impact. The large number of restarts generated by Abaqus/Explicit can make direct manipulation of the output within the Abaqus/Post environment, a tedious business. Performance can then be improved by the use of macros contained in journal files (with extension .jnl).

4.2.5 Derivation of ball flight predictors

The critical performance indicator in golf is the flight of the ball and a method is required to admit the calculation of the initial ball flight descriptors. Only by a comparison of these dynamic variables can the effect of differing clubhead or impact conditions be evaluated. The key variables are the initial translational velocity of the ball, ie both speed and trajectory, and its spin rate about some principal axis. Various methods were developed to determine these from Abaqus output and amendments were continually made to improve the accuracy of the results obtained. The following sections give the final procedures used, with the occasional note as to problems encountered with previous methods.

4.2.5.1 Speed

The speed of the ball is best estimated from the behavior of the node closest to its centre of mass and, from figure 4.14, it is seen that this fluctuates after impact. An 'average' speed is then of more practical use. From a knowledge of the position of the centre of mass at various instants after the ball has left the clubhead, the average speed could be obtained within any particular time interval. Figure 4.15 shows the average speeds returned for the ball after impact. The clubhead is the solid 30° loft model and the friction coefficient of the interface was varied from 0.0 to 1.0. The effect of the coefficient of friction is discussed later and here it is the integrating period which is to be considered. The legend indicates the period over which the displacement of node 433 is averaged and the intervals are chosen from 1 ms after the start of the analysis so as not to include the acceleration phase of the ball as this will vary for different impact conditions. An average taken over a 1 ms interval starting 1ms after initial impact was originally used since the analysis was originally only run for a (simulated) time of 2 ms. However, later experience with longer runs showed that the calculated speed was too high. This arises because the instantaneous centre of mass of the deformed ball is not coincident with the (initially) central node shortly after impact and the backspin causes the central node to translate more than the instantaneous centre of mass. A velocity estimate averaged over a longer period, such as the 4 ms period starting 1 ms after initial impact, should give a more reliable result but this includes the 1-to-2 ms interval and so

was rejected. A later period, say a 1 ms interval starting 4 ms after impact allows for the ball to recover an almost spherical shape but the shorter duration of this period leads to less reliable results. After much trial and error, the period from 2-5 ms was adopted. Although this technique is open to discussion and may be improved it is superior to the method of Iwatsubo et al (1998), who calculated post-impact ball velocities by taking an average of all the instantaneous nodal velocities within the ball, a method also originally used in the current work. After impact node velocities can be shown to fluctuate widely between computational iterations and a less noisy solution is obtained from nodal displacements over many iterations.

4.2.5.2 Direction

To admit comparison of different ball flights, it is appropriate to resolve the trajectory vector into two angular components, viz launch angle and dispersion. Launch angle is defined as the angle the trajectory vector makes with the ground while dispersion is defined as the angle away from the intended target line (the 3-axis in most of the analyses).

The launch angle of the ball is best calculated from its displacement during a period after the ball has left the clubhead, and may be expressed as a vector. However each impact condition results in a different position at which the ball and clubhead separate and the vectors for different impacts can not be compared directly. This problem is demonstrated in Figure 4.16 which shows the initial position of the ball, and two exaggerated, different ball position vectors **a** and **b**, recording their trajectories for a 5 ms analysis. An approximation uses the initial position of the ball, in this way the vectors caused by different impact conditions can be compared.

The displacement vector is best estimated at an instant as far away from impact as possible such that the error in approximating this by the vector from the original starting position is minimised. Figure 4.17 shows how the error is diminished for an instant further away from impact, for the ball trajectory **b**. The origin vectors to the 2 and 5 ms instant are shown as dashed lines. Using the central node of the ball in calculating the

coordinates of the ball, figure 4.18 shows the launch angle calculated for the steel clubhead, with varying coefficients of friction.

The legend gives the instant from which the launch angle is calculated. Showing that at 2 ms the launch angle is underestimated whereas by 4 or 5 ms the calculation converges to a constant value. The position of the ball at 5 ms after the analysis is therefore used to describe the launch conditions. Mishit shots, which exhibit greater dispersion, suffer from the same approximation error and again the 5 ms position is used to describe the dispersion angle.

4.2.5.3 Spin rate

Spin on the ball is a key performance variable and its measurement needs to include not only backspin but also sidespin. Initial backspin rates were calculated by measuring the angle through which the ball rotates over a given time period, based on measurements from plots of the displaced mesh. This method was both manually intensive and was prone to human error. A numerical method was then devised, using the velocities of antipodal nodes on the surface of the ball, perpendicular to the axis of backspin. This method shows large fluctuations due to the stress waves traveling within the ball. Averaging the spin estimates over time gave a reasonably constant value but the method does not allow for the spin calculation other than backspin. To overcome this problem, a method was developed based on mapping a visible hemispherical surface of the ball onto a plane grid. In this method all the instantaneous nodal coordinates on one hemisphere of the ball are noted and vectors from the instantaneous centre of the ball to these nodes are calculated. The angle through which these vectors turned in a fixed period was then calculated. Figure 4.19 shows a view of one side of the ball with node numbering and figure 4.20 a 2 dimensional mapping of these nodes onto a plane grid.

The vector which rotates the least is closest to the axis of spin, and the rotation of the vectors perpendicular to this vector gives the spin rate about this axis. These can be averaged to remove the fluctuations due to the stress waves. Figure 4.21 shows the spin rates generated for a steel clubhead, with varying friction. The legend shows the period over which the vectors are calculated. The spin rates nearly agree, with the exceptions

of the estimates between 1-5 ms, 1-4 ms and 2-5 ms. This is due to the integrating period being too great and the vector rotating through an angle $\theta > 180^\circ$. The angle between the vectors was then taken as $360 - \theta$ by the automatic solution algorithm and inversion of the graph occurs. This is common in the analysis of highly lofted clubs which produce higher spin rates. Corrections for this error are included in subsequent calculations. Amongst the other curves, closer examination revealed the 1-2 ms interval to overestimate the spin rate, due to the deformation of the ball. With an increasing fraction of the later period of the analysis, convergence is seen towards the values of the spin calculated between 4-5 ms. A larger period however is beneficial in smoothing out any fluctuations and the period 2-5 milliseconds is used in the current work.

4.3 Clubhead properties, straight hit

For an investigation of clubhead effects on impact it is first necessary to precisely categorise the shots possible in golf. This is best done in the current work by separation into two distinct categories using the terms, *straight hit* and *mishit*. These terms familiar in golfing phraseology are chosen to simplify an approach to the results and should not be confused with their common usage in describing ball flight. A *straight hit* is defined as a shot in which no rotation of the clubhead occurs during impact, this is an erroneous concept in a real situation as explained in section 4.4 but is an acceptable approximation for analysis. For *straight hit* impact studies the clubhead may therefore be constrained about the necessary degrees of freedom to restrict rotation of the clubhead or if this is not convenient for the analysis a clubhead rotation of less than 1° may be considered as a straight hit. This definition of a *straight hit* therefore includes shots with open and closed clubfaces, clubhead trajectories at impact up or down, in to out and out to in.

By comparison a *mishit* is a shot in which the clubhead rotates during impact, such analyses require a free body clubhead, fully unconstrained. *Mishit* shots are covered in section 4.4.

It is important to note that the term *straight hit* or *mishit* is not connected with the flight of the ball but rather the clubhead approach velocity and position. It is totally possible that a *mishit shot* hit above and to the left of the sweetspot off a closed club, of reduced loft, hit down on the ball will fly perfectly straight.

4.3.1 Material

As mentioned in chapter 1 there are many references in golf literature to the effect clubhead materials may play in a golf shot. A change in the rules in 1992 allowed for the use of insert materials in all clubs and much speculation over the relevance of insert material properties still abound. The number of material properties that can affect the mechanical study of impact are however limited. The following sections use the computational model to investigate and quantify in isolation, the role each material property plays.

4.3.1.1 Stiffness

As clubheads are durable products, with no permanent deformation occurring after impact with a golf ball (in normal use) any deformation is elastic and the elastic modulus of the clubhead is therefore a key parameter to be investigated.

A finite element analysis of impact was carried out using a range of elastic moduli, from a low value of 0.01 GPa typical of polyvinylchloride (PVC) or a foamed polymer, through 0.1 GPa representative of low density polyethylene (LDPE) to 1000.0 GPa, that of diamond. This large range was chosen to ensure that any effects over the range of materials currently or possibly used for head manufacture could be well covered by the extremes. The friction coefficient and density were held constant at 0.6 and 7800.0 kgm⁻³ respectively, the former being thought at the time to be typical of a steel clubhead, (see results on friction). The results are given in terms of the subsequent ball flight in figures 4.22 to 4.25.

Figure 4.22 shows over the whole range of modulus the dispersion of the ball is between +0.3° and +1.3° (sign convention given in section 4.1.4). This is caused by rotation of

the clubhead during impact as a result of the ball being slightly offset relative to the centre of mass of the head. To simulate an absolutely straight hit, the club nodes could be constrained in the relevant degrees of freedom or the club translated to a new position prior to impact. The former is not an option as such boundary conditions would lead to spurious deformations of the clubhead. However, it was felt that $< 1.5^\circ$ dispersion of the ball and the $< 1.0^\circ$ rotation of the clubhead was representative of a 'real' shot a player may consider straight and no change in the model was necessary. Over the range of realistic moduli possible for clubheads the dispersion changed by a negligible 0.1° and it is concluded that elastic modulus has no effect on the dispersion for an approximately straight hit.

Elastic modulus was observed to have a greater effect on ball speed (figure 4.23) and, contrary to the perceived wisdom that a stiffer clubhead produces increased speed, the results show that increasing the stiffness beyond that of current materials causes reduced ball speed. The result shows a peak of 73.2 ms^{-1} for a modulus of 10.0 GPa, typical of soft woods and epoxy, and a slightly lower 72.7 ms^{-1} for 200.0 GPa, typical of steel, indicating that decreasing the modulus from current materials would increase ball speed, although only slightly. Below 10 GPa the ball speed drops rapidly as the deformation of the clubhead leads to energy loss and less energy being stored in the more efficient ball deformation.

The spin rate (figure 4.25) also appears to follow in accord with the speed of the ball varying little over a range of modulus suitable for clubhead manufacture. The spin peaks at 181 revs/sec, at 0.1 GPa, and is relatively constant over the higher modulus values, showing less than 1 revs/sec variation between 100.0 and 1000.0 GPa. Below 1 GPa the spin behaviour of the ball becomes unpredictable due to the large clubhead deformations and the coarseness of the finite element mesh. If such modulus clubheads need to be analysed more accurately a refined mesh is advisable. Results for the launch angle (figure 4.24) are in accordance with the other results showing little variation over higher modulus values.

It is possible that the slight increase in speed with reduction in modulus results from additional force produced by elastic recovery of the clubhead as the ball leaves the face.

The deliberate use of such an effect is specifically banned under the rules of golf (R & A 1997), but they admit it will inevitably occur to a greater or lesser degree with any material chosen (Fay 1998). An examination of the stress and strain in the clubhead at the maximum deformation of the ball, gives maximum values of, -4.1×10^7 Pa / -2.2×10^{-3} for the 10.0 GPa clubhead and -4.3×10^7 Pa / -2.2×10^{-5} for 1000.0 GPa.

Another explanation for the slight increase in speed may be that stress waves from the impact are reflected around the model geometry such that they are focused at the clubface in a manner coincident with the balls recovery phase. The stress wave velocity is dependent only on the modulus and the density and this is examined in more detail using further analysis in section 4.3.1.5. Indeed if stress wave reflection is a genuine effect, the modulus results given here may be unique for this geometry of clubhead alone. Of course a deformed clubhead will also lead to a change in the pattern of reflection of the stress waves, but this is to be considered a second order effect.

Another likely cause of the observed modulus effect is the increased contact time which would be expected with a more compliant clubface. Greater deformation will lead to a longer ball/clubhead contact time and the ball being present for longer during the clubhead's elastic recovery phase. Contact times from the finite element analysis can be slightly misleading as the automatic increment time steps are chosen based on the deformation wave speed, in turn based on the material stiffness and density. Close examination of the model revealed an acceptable accuracy of ± 2.5 μ s could be achieved in studying contact times. The 10 GPa model gives an impact time of 440 μ s, and for 1000 GPa 435 μ s. The maximum energy transfer to the ball thus occurs at a modulus where the contact time and elastic recovery of clubhead face are optimised such that effects of damping are minimised. However, the exact modulus to impart maximum energy to the ball must also depend on the ball properties as they affect contact time. Results in the current work are therefore particular to the ball material properties prescribed and care must be taken in drawing firm conclusions.

Cochran & Stobbs (1968) reported the contact time of impact as being reasonably invariant for most golf shots, for the limitations of the test equipment they used. The computational model shows differences in contact time with modulus and more so with

clubhead approach velocity, (see later section). However the significance of these differences ($< 5 \mu\text{s}$) is not likely to be perceivable to human golfers.

This elastic recovery of the hitting surface during impact is more clearly demonstrated with an analogy to a tennis shot where the ball remains on the racquet strings for a longer period, approximately 5 ms (Brody 1995). A tennis ball has a much lower coefficient of restitution than a golf ball and is designed to lose energy on deformation, the specification for tournament quality is that the ball rebounds to between 53 and 58 inches when dropped from 100 inches onto a concrete floor (International Tennis Federation, (ITF) 1998). The ball is thus designed to dissipate approximately half of its energy during impact with a rigid surface, and racquets are constructed to reduce ball deformation and store the kinetic energy of the traveling ball as elastic potential energy in the strings. The recovery of this potential energy during impact imparts speed and spin to the ball. Less stiff stringed racquets allow for longer contact times and corresponding reduced ball deformation, but at the expense of greater energy loss due to friction between the elastic strings (Brody 1995) and possibly less energy return to the ball as the strings do not fully recover before the impact ceases. An optimum between the two effects is desired for maximum power. The fact that more power may be obtained from less stiff stringed racquets can appear as a revelation to the average player (Brancazio 1988). Incidentally, when a tennis shot is required to impart speed to a reasonably stationary ball, as in a serve (cf. to golf), the professional players are seen to hit of a part of the racquet known as the dead spot (Knight 1997). At this point near the tip, most of the energy of the racquet is transferred to the ball, and in an opposite experiment a ball dropped on the racquet at this point stops dead, the strings return none of the elastic energy. The same theory is applied in golf to give the axiom that stiffer clubfaces impart more energy to the ball, as less energy is lost in club deformation (though it is noted that the tennis player may use a point close to the tip of the racquet as it will be travelling faster). However, it would appear from modulus results here that, as the golf ball deforms and impact lasts a finite time, a slightly longer contact time allows for more elastic recovery of the face. The current brouhaha about the spring-back effect, and the new Enhanced Rebound Velocity Test Protocol (USGA 1998) concerns measuring any advantage the elasticity of the clubface may offer. In the test a maximum coefficient of restitution of 0.822 for ball/clubhead impact has been defined from that of a standard titanium plate. The modulus results here indicate that no significant advantage is to be

had from a change in the elastic modulus, at least for a reasonably solid clubhead such as an iron. However, the overall stiffness of the clubface can also be changed by an alteration of the geometry, for example in a modern driver a thin face may allow greater deformation. This indeed is the concern of the ruling bodies as the new test procedure applies only to metal 'woods' with loft of less than 10° .

Irrespective of the mechanism, the theory that increased performance results from stiffer clubfaces is shown to be in doubt (at least for irons) and current results predict slight improved performance by reducing the modulus. However this may lead to an infringement of the rules of golf, which prohibit the deliberate use of the elasticity of the clubface to aid the ball flight, even though it may already play a part unintentionally in club head designs. It must be remembered however that the observed effects of changing the elasticity of the club head are small, particularly over the range of materials currently used and likely to figure in future clubhead designs. Of greater interest is the relative lack of effect that stiffness has on the ball behavior. This is not in accord with practical experimentation using different real materials but there it is not possible to alter the stiffness alone. Other material properties must then be examined and a return to the elasticity question will be made later, during an examination of the role of friction.

The lack of effect of a change in modulus allows analyses to be performed with a computationally cheaper rigid clubhead model, (section 4.1.1), without great deviation from the results of using the expensive solid model. The validation for using the rigid clubhead is based on its performance against the solid clubhead, such a verification is given after the effect of friction is examined using the solid model.

4.3.1.2 Friction

Given the results of section 4.3.1.1, further FE analyses were carried out using the solid clubhead model, with all the properties of steel held constant other than friction coefficient (μ). The Abaqus version used, has a coulomb friction model that does not distinguish between the coefficient of static friction and dynamic friction. Values of μ were first varied at equal intervals from 0.0 to 1.0 but on inspection of the results, further attention was given to the lower friction range. Again no boundary conditions were

applied to the clubhead and an approximate straight hit was made. This was expected to show slight dispersion of the ball no greater than 1.3° , due to the rotation of the clubhead caused by the ball being offset from the sweetspot.

Figure 4.26 shows the effect of friction on launch angle. For $\mu = 0.0$ the ball leaves the clubhead with nearly the loft of the club i.e. almost normal to the face. This is in accord with classical rigid body theory (Gobush 1995) as no tangential force is present to reduce the trajectory below the loft angle. The ball trajectory is not quite 30° as the impact force is directed below the centre of mass of the head and rotation occurs to reduce the loft of the club during impact. This effect is considered in section 4.4 as a mishit. For $\mu = 0.0$ the deformed ball slides freely up the clubface during impact then as friction is increased to $\mu = 0.3$, sliding is reduced along with the launch angle. For $\mu > 0.3$ the ball has stopped sliding and the ball/clubhead interface remains stationary throughout impact while the launch angle is seen to increase asymptotically to 23.8° by $\mu = 1.0$.

Figure 4.27 shows how friction changes the speed in a inverse manner to that of the launch angle. As the ball slides up the face, with $\mu = 0.0$, its final velocity is reduced as ball compression is reduced. As friction is increased to 0.3 and sliding stops, the ball increases in velocity to a 72.8 ms^{-1} . At $\mu > 0.3$ the ball speed drops to approach a constant value of 72.5 ms^{-1} . Both speed and launch angle results show little effect in increasing friction above the level at which the ball/clubhead interface remains stationary. The appearance of this stationary interface contradicts the results based on rigid body theories exemplified in many work including Jorgensen (1994), that sliding and rolling initiate spin. The current results however support the experimental work by Mather and Immohr (1996), who report surprise that impact interface shapes showed only small variations from a circle.

Interestingly, figure 4.28 shows the current model also runs counter to classical spin theory in its prediction of spin rates at zero friction, indicating that $\mu = 0.0$ produces 10 rev/s and that this rate increases rapidly to 178 rev/s at $\mu = 0.3$. Beyond this, the rate decreases to 135 rev/s. Indicating that higher friction does not always play a role in increasing spin rates, this does conform to rigid body theory that once maximum spin (rolling) is achieved, further contact - or higher friction leads to a reduction in the spin

rate due to rolling friction. However this cannot be the cause here as the interface is static. This and the fact of spin at $\mu = 0.0$ leads to a re-examination of the model.

To confirm that, at zero friction, the ball was indeed sliding up the clubface, the coordinates of a ball node lying within the interface were plotted. If the club moves at constant velocity, such a node's displacement against time in the 2-direction would appear to be linear. The coordinates of the node were also recorded for $\mu = 0.2$ which, showing near maximum spin rate, should indicate no movement in the 2-direction during contact. Figure 4.29 gives the coordinates of the node during a 0.5 ms analysis, confirming that the ball is sliding up the clubface at $\mu = 0.0$ and remaining stationary for $\mu = 0.2$. The small fluctuations of the displacement of the node when sliding up the face under zero friction can be explained by the deceleration of the club, head deformation and the reflection of stress waves within the ball.

The spin induced at $\mu = 0.0$ cannot be explained by current theory, due to the absence of a tangential force. At $\mu = 0.2$, the spin rate of 178 revs/sec, cannot be attributed to rolling of the ball, nor to a tangential turning force which is less than the limiting static friction, as the ball is stationary. Other forces must account for the spin rate generated in the model. The prediction of spin at zero friction confirms one of the initiators of spin must be a turning moment about the centre of mass due to the deformed shape of the ball model. Although this may be due to the approximation of a sphere by finite elements leading to slippage of the ball during the first stages of impact (see section 4.3.2.2), it is also to be expected that a turning moment will be present at non-zero friction values due to the non-symmetrical deformation of the ball.

The normal force, rather than acting at a point in rigid body theory, is distributed over the interface such that its resultant effect is a turning moment about the centre of mass of the ball, which is no longer in a perpendicular direction from the centre of the interface. Rather than consider the normal force distribution, the resultant force can be thought to occur at the centre of the interface and is shown in figure 4.30 for $\mu = 0.0$. The turning moment is a product of the resultant normal force (\mathbf{F}_n) and its perpendicular distance from the centre of mass (\mathbf{A}). As friction is increased, the ball does not slide as much and deforms up the clubface as shown in figure 4.30 for $\mu > 0.0$. Such deformation leads to

an increase in the turning moment arm (A^1) and an increase in spin. For friction values sufficient to stop sliding the deformation is greatest and the line A^1 attains its maximum value.

The turning moment about the centre of mass is not the sole cause of spin. As impact occurs strain energy is stored in the deformed ball and, during the latter stages of impact, this elastic energy is recovered and converted into rotational kinetic energy. An onion model for the way this occurs has been proposed by Gobush (1995) as discussed in section 1.6.1.1. Using the same model it can be hypothesized that the outer layers are rotated due to the initial deformation, and energy is stored in the springs. As the contact time is very short and the deformation wave travels at a finite rate, the first period of contact causes an energy gradient across the layers, and the core layers of the ball remain relatively stationary. The outer layers have a higher moment of inertia and are held in place by the high frictional contact force, the springs thus rotate the core layers anti-clockwise, and reduce the tangential force the outer layer exerts on the clubhead. This was shown in figure 1.10, a reproduction of Gobush's results (1990). During the latter stages of impact the deformation strain energy is nearly all recovered and the core over rotates and the ball begins to exert a negative tangential force on the clubhead in the opposite direction to that at the start of impact. The ball tries to backspin as it leaves the clubhead and, with the normal force dropping to zero (at the break of contact), there must be a period when the ball slips against the face.

Figure 4.31 confirms the notations used in describing the forces applied to the clubhead by the ball. The normal force perpendicular to the face F_n and the tangential force F_t acting upwards along the plane of the face.

As the maximum frictional force at contact is given as:

$$\max F = F_n * \mu$$

movement will occur if

$$F_t > F_n * \mu$$

$$\Rightarrow \left| \frac{F_t}{F_n} \right| > \mu$$

where a -ve F_t/F_n merely represents a tangential force down the face of the clubhead.

Figure 4.32 shows the variation of F_t/F_n during contact calculated from Gobush's (1990) result from an experiment with a plate at 20° . The scale is chosen for clarity of the results, the portion of the graph missing reaches a minimum of -26.6 at $450 \mu\text{s}$.

Movement of the ball on the clubface only occurs if $-\mu > F_t/F_n > \mu$. If $\mu > 0.2$ movement only occurs in this instance during the latter stages of impact when the ball is trying to backspin against the clubhead. This means that reducing the friction coefficient to 0.2 will have the effect of increasing backspin, a counter intuitive idea. While increasing friction above 0.2 will reduce the backspin. These calculations from Gobush's results and the finite element model are confirmed by Leiberman (1990) and the USGA experimental finding that lower friction can increase spin rates for certain lofts. The optimum friction coefficient is calculated computationally for other lofts in section 4.3.2.2.

The results show that for 30° loft greater values of friction only slightly decrease the spin rate, and this would be statistically difficult to observe in practical examination without sophisticated equipment such as available to Leiberman (1990) and the USGA. This explains Cochran and Stobbs (1968) early finding that reducing the friction did not affect spin rate; their manufactured smooth club may not have reduced the friction sufficiently.

Returning to the question of elastic modulus, it is apparent that less stiff material will deform and increase the effective friction, holding the ball in place and allowing more

deformation, leading to an increase in the spin rate and velocity. Modulus analyses similar to those described in section 4.3.1.1 were repeated with zero friction. The results for ball spin are shown in figure 4.33 (other ball flight properties are given in appendix B-4). The results indicate that decreasing the modulus from 5.5 GPa leads to higher spin all in the absence of frictional tangential forces. Speed however is reduced as less stiff materials deform too much, the ball compression is reduced and a longer time is needed for the elastic recovery of the face. It is unlikely therefore that deformation of the clubhead at friction values high enough to sustain a static interface will result directly in any improved ball flight, and modulus effects are again seen to be negligible.

Rigid model verification

The lack of importance of the modulus allows the use of a rigid model that can predict other clubhead effects. Such a model does not behave totally in the manner of the solid model as it does not deform to any extent and quantitative differences are to be noted. Figures 4.34 to 4.37 show the differences between the rigid and solid clubhead with varying friction. For all ball flight properties the discrepancies between the two types of clubhead model can be observed to be reasonably small. Speed varies consistently by 1.5 ms^{-1} , with the rigid clubhead generating a higher ball speed as no energy is used in clubhead deformation. Launch angles for the rigid clubhead are approximately 1° greater for all friction values sufficient to promote a static interface. Dispersion results are in accordance although the magnitude differs by 0.1° . Spin results appear similar but, due to the steep gradient of parts of the curve, the range can vary by up to 10 revs/s. Other verification models based on simplified regular geometries, with varying mesh densities and different loft angles confirmed the results given here.

4.3.1.3 Density

Changing the density of a homogenous material used in a clubhead has the direct effect of altering the mass and the moment of inertia. The mass is important in a golf shot as a higher mass imparts more velocity to the clubhead. However the relationship is nonlinear. Theory based on the conservation of momentum and the coefficient of restitution can be used to predict club and ball speeds before and after impact and is proved and discussed in section 1.6.1.2, results from a computational study of mass

effects is given in section 4.3.2.1. The rotational inertia of the club head is only important when turning moments are applied to the clubhead as in a mishit shot. These are considered in section 4.4.

Both density and elastic modulus affect the stress wave velocity through the material. As already mentioned this may affect the impact and be noticeable in the ball's flight descriptors. Stress wave velocity is examined in further detail in section 4.3.1.5.

4.3.1.4 Hardness

In engineering, 'hardness' is measured by a test, such as Vickers (Ashby 1996), in which a material such as diamond makes a permanent indentation in the test-piece. The size of this indentation is then (inversely) expressed as the 'hardness' of the test-piece.

Hardness is then a composite measure of the evolution of the yield stress in a material, from its initial value, as plastic deformation occurs. Hardness has been mentioned in some golf literature (Cochran 1995) as being an important material property in the construction of both the ball and the clubhead but if engineering hardness is important, it can only be indirectly. It is most likely that such reports have confused hardness with stiffness. The maximum stresses in the head that the FE model predict (4.3×10^7 Pa) show that plastic strains are unlikely to occur and hardness is not a parameter concerning clubhead/ball impact.

Although hardness may be an issue in club design and manufacture, it is not a desirable property for golfers to consider unless they wish to permanently deform their clubheads !

4.3.1.5 Stress waves

The modulus results indicate that the velocity of the stress waves in the model may play a role in the ball flight. It may be possible that increased ball speed occurs when the clubface is on the outward phase of a stress pulse. The degree to which they can have an effect is investigated here.

A finite element analysis was carried out varying the density of the clubhead such that the model mass was varied from 0.025 to 0.5 kg. Using this range of mass it is to be expected that the subsequent ball velocity will be affected to a large enough extent to be noticeable. This led to densities with a range from 0.6 to 12.1 Mgm^{-3} (low density plastics and heavy metals respectively), increasing the density further will not lead to higher ball speeds, as the mass fraction is approaching unity (see section 4.3.2.1). The clubhead stiffness was held constant at 200.0 GPa to give a range of stress wave velocities from 4,000 to 18,000 ms^{-1} . Although only one of these combinations of density and stiffness exists, ie in steel, it allows for stress wave velocity effects to be evaluated. To indicate the magnitude of the wave speed, 5000 ms^{-1} (typical of steel) would take 1.0 μsec to move through 0.5cm of steel, approximately $1/400^{\text{th}}$ of the time of impact. The results of the analysis are shown in figure 4.38 along with the analytical solution, where the coefficient of restitution was calculated from the 0.300 kg clubhead computational result. Figure 4.38 does imply speed is dependent on stress wave velocity, but this is only as stress wave velocity is dependent on the density and in turn this affects the clubhead mass.

The velocity of the ball from the finite element analysis is close to the analytical solution, the curves appear to diverge to a small degree as the wave speed is increased. This is due to the coefficient of restitution not being held constant within the computational analysis as it is with the analytical solution. But the small difference remains constant and is not of consequence. The results indicate that altering the wave velocity does not have any significant effect on the final velocity of the ball.

The analysis used the solid 5-iron clubhead shown in figure 4.1. From contour plots, the stress at impact is seen to focus on the base of the club, figure 4.39, and it may be that this geometry of clubhead does not reflect stress waves back to the impact area but rather concentrates them at the base of the club. To elucidate to what extent geometry may increase any stress wave effect, 3 different clubhead meshes were used, each with a different geometry but identical, volume, density and centre of mass (except in the 3-direction). Each clubhead had the same shape, except for the rear, behind the hitting face and had zero loft. Figures 4.40 to 4.42 show the design of each clubhead back, A-flat, B-raised cross, C-indented cross.

The results of the analyses are compared in table 4.3, and show little effect between clubheads. Differences are most likely due to the mesh designs and the increment stepping used in the Abaqus/Explicit procedure. Higher quality mesh designs including angled geometry clubheads are needed to examine further to what degree stress waves may affect the ball flight. While better material models of the ball could also be used to examine the effect of stress waves within the ball.

	Clubhead		
	A-blade	B-raised	C-indent
Speed (ms⁻¹)	89.03	88.87	88.93
Spin (rev/s)	3.23	2.37	1.92
Launch (°)	0.09	-0.05	-0.06
Dispersion (°)	-0.12	0.02	-0.05
Coefficient. of restitution	0.905	0.901	0.903

Table 4.3 Behaviour of different clubhead designs.

4.3.2 Geometry

4.3.2.1 Mass

One of the simplest physical differences between clubhead designs is the total mass of the head. It has already been stated that the head mass currently used in golf clubs has been found by evolution and, as the loft increases and the club length gets shorter, a swing weight matched set of clubs requires that the heads become heavier. The effect of the clubhead mass on the impact, when the ball and head are considered as separate bodies has typically utilised the analytical solution:

$$V_b^1 = \frac{M_c V_c^0 (1 + e)}{M_c + M_b}$$

A computational analysis was carried out using a rigid body clubhead of 30° loft, as verified in section 4.3.1.2. The clubhead mass was varied from 0.025 kg to 0.5 kg with an initial velocity towards the ball at 50 ms⁻¹ and friction coefficient of 0.6. The

clubhead had the same inertia properties as the solid model, although the centre of mass was moved horizontally to be in line with the ball such that the clubhead would rotate a negligible amount during contact and minimal ball dispersion would occur. The computational model allows the total mass of the clubhead to be changed without a corresponding change in the rotational inertia, clearly not a practical achievement. However to simplify and speed up the computational time needed for analysis, constraints were applied to the clubhead to prevent translation in any direction other than that of its initial motion. These boundary conditions were observed to have a minimal effect on the results, as the centre of mass was in line with the ball at impact.

Figure 4.43 shows how clubhead mass affects the initial ball velocity, and confirms the relationship shown in the analytical solution that as the clubhead mass is increased it has a diminishing effect on the ball velocity. In the extreme, with a clubhead of 0.5 kg the ball velocity was 78.8 ms^{-1} , an increase of 6.5 % over 74.0 ms^{-1} at 0.25 kg, and it must be remembered that a heavier clubhead could not be swung by a golfer at the same velocity. The launch angle for the ball at varying clubhead masses (figure 4.44) is below the loft of the club, due to friction and ball compression. At low mass the launch is reduced further as the compression of the ball is reduced and the ball moves away with less spin. The relationship between the spin and the club mass is comparable with the launch results and is not included for conciseness. Nor is the dispersion of the ball which, due to the clubhead boundary conditions shows dispersion no greater than $\pm 0.02^\circ$. From the results for ball velocity and launch it is possible to calculate the velocity component for the ball in the 30° direction, that initially normal to the clubhead. Figure 4.45 gives the normalised ball velocity and that for the analytical solution, where the coefficient of restitution was 0.971 and was calculated from the Abaqus result at clubhead mass of 0.2 kg. The clubhead velocity used in the analytical solution is the normal component of velocity. The two curves are in close agreement, with the only differences being attributable to the changing coefficient of restitution used in the computational model, an estimate of this value may be obtained using:

$$e = \left(\frac{V_b^1}{\frac{M_c}{M_c + M_b} * V_c^0} \right) - 1$$

Where V_b^1 represent the Abaqus calculated ball velocity in the normalised direction, and V_c^0 the initial club velocity in the normalised direction.

Figure 4.46 shows this estimate for the value of e used in the Abaqus computation, and indicates that e decreases at higher mass. The values, although only estimates due to the boundary conditions, are close to unity indicating that the collision is near perfectly elastic. This is to be expected as there is no specified damping present within the ball other than by default for numerical stability. Actual values of e for the ball/clubhead impact have been rarely published. Cochran and Stobbs (1968) quote values of 0.68 - 0.70 for top class balls, although this is expected to have changed over the last 20 years. The rules of golf have indirectly specified the maximum coefficient via the initial velocity test (Rules - Appendix III). The possible amendment to the rules of golf (Rules - Appendix II, Enhanced Rebound Velocity) specifies a maximum value from a standardised titanium plate of 0.8222. The computation model does not calculate the coefficient but rather relies on a specification of the damping within the material models, in this case the ball. If the model is to accurately represent any ball construction it would be important that these properties were accurately represented. Unfortunately knowledge on such engineering properties of materials is scant.

4.3.2.2 Loft

Another of the most striking geometrical differences between clubhead designs is the loft angle of the club and typical values were given in section 1.3.1. Computational analyses were carried out on lofts on a greater range, from 0° to 80° at intervals of 10° . This larger range was chosen to ensure that any effects over the normal range would be well covered by the extremes. In reality the shorter shafts used for higher lofts mean clubhead speed at impact is an indirect function of loft. However a constant initial velocity of 50 ms^{-1} for all loft analyses was chosen to simplify an examination of the results. The importance of friction has already been discussed and it was considered

necessary that a full range of coefficients of friction be considered for each loft. A rigid element model was used to keep construction of the clubhead as simple as possible and remove the need to create separate mesh designs. To achieve the desired loft the rigid element was rotated about a specific axis and then translated such that the distance to impact was the same in all analyses. The distance to impact is a function of the loft and the circumference of the ball. Appendix B-3 gives the values calculated to rotate and translate a 00° loft clubhead to a starting position 14.23 mm horizontally from the ball. As only loft was being examined the clubhead was constrained for translation in all directions other than that with which it is initially traveling. The error in using this boundary condition over a non-constrained clubhead was examined and found to be minimal in the context of the results presented here.

00° Loft

Figure 4.47 shows the ball speed after impact with a 00° loft clubhead, extremes of value range from 85.00 ms⁻¹ at $\mu=0.00$ to 84.67 ms⁻¹ at $\mu = 0.14$. The first downward trend of the graph confirms expectation that as friction is increased, less compression of the ball is allowed, the material in contact with the face would be under tension and resistance to elongation would reduce overall ball compression. This phenomenon would be a negligible effect in terms of a golf shot and a variation in value less than 0.5 ms⁻¹ confirms this. The graph shows abrupt changes and this is due to the mesh design, the sensitivity of the mesh is also shown in figures 4.48 and 4.49 for launch and spin. The launch angle variation is less than $\pm 0.000025^\circ$ and the spin less than ± 0.5 revs⁻¹. No negative values of spin (or forward spin) are recorded as the automatic method calculated the absolute value of rotation and not the direction. This is not a problem as in all analysis the direction of spin is clearly seen from post-processing unless the spin rate is negligible. Dispersion of the ball is not shown as the club is constrained not to rotate and only minimal dispersion was seen, values for dispersion are comparable to those of launch. The values given here for 00° loft are important as they indicate the computational errors to be considered in other analyses.

10° Loft

Results for speed, launch, and spin are given in figures 4.50 to 4.52. Over the range of friction speed varied by less than 1 ms^{-1} and can not be considered significant in view of the previous results for 00° loft. This in itself is significant as it implies that speed is independent of friction for low loft clubheads. The launch of the ball drops from the loft of the club at $\mu = 0.0$ to a minimum of 7.5° around $\mu = 0.1$ before slowly rising to 8° . At $\mu = 0.0$ the 10° launch is due to the absence of any tangential forces from the clubhead, as the friction and tangential force increases the ball launch is reduced to a minimum at which the spin would also be expected to be a maximum. This is confirmed by the spin curve showing a maximum spin rate of 55 revs^{-1} at $\mu = 0.1$. Increasing friction beyond this value causes an increase in launch and reduction in spin as the clubhead is able to resist rotation of the ball and apply an upward tangential force for longer during the last $\frac{1}{3}$ of impact (see section 4.3.1.2).

20° Loft

At 20° of loft, results (figures 4.53 to 4.55) for speed, launch and spin follow the same pattern for 10° with different absolute values. Speed has reduced 3 to 4 ms^{-1} over the previous loft due to a reduction in the velocity component normal to the clubface. The range of speed values for the varying friction is below 1 ms^{-1} and ball speed can still be considered independent of friction. Launch of the ball is reduced from the loft of the club at $\mu = 0.0$ to 15.9° at $\mu = 0.14$ before slowly rising to 17.5° at high friction. Again the trend of the spin curve is an inversion of the launch, with a maximum spin of 122 revs^{-1} at $\mu = 0.14$ and 77 revs^{-1} at higher friction. The initiation of spin, 24 revs^{-1} , at $\mu = 0.0$ is clearly shown in the results.

30° Loft

The results of the analysis for a 30° lofted clubhead have already been given in section 4.3.1.2, where a solid model of a clubhead was used and a rigid model verified. Those results differ from the results presented here as the previous clubheads had no translational or rotational constraints. In the loft analysis here, such constraints are used and results for a 30° lofted clubhead are given in figures 4.56 to 4.58. Speed is still shown to be independent of friction with a range of values less than 0.5 ms^{-1} . Launch and spin curves are inversions of each other, showing minimum launch and maximum

spin at $\mu = 0.2$, with respective values of 22.1° and 163 revs^{-1} . The initiation of spin at $\mu = 0.0$ is lower than the previous loft at 5 revs^{-1} , this is examined later after a presentation of results for all loft angles.

40° Loft

Results for speed, launch, and spin are given in figures 4.59 to 4.61. Speed is still independent of friction, with a range of values less than 1 ms^{-1} . Launch and spin results are in accordance with each other, respective minimum and maximum occurring at $\mu = 0.3$.

50° Loft, 60° Loft, 70° Loft and 80° Loft

For conciseness the results for the remaining loft angles are included on the same graphs. Figure 4.62 gives the speed of the ball for each loft angle at varying friction. For 50° the speed is independent of μ , but at increased loft the speed is seen to increase slightly with an increase in μ . This is of little significance in golf, as lofts greater than 60° are not common. It is thus concluded that for shots positioned on the clubface that cause no rotation of the head during contact, the initial speed of the ball is independent of friction. Figure 4.63 shows the result for launch. All launch angles are identical to the specific loft at $\mu = 0.0$. As μ increases the launch angles decrease to approximately 40° for all clubhead lofts but at differing values of friction. For 50° of loft the launch approaches 36° at $\mu = 0.3$, at 60° of loft launch approaches 40° at $\mu = 0.4$ and at 70° of loft launch reaches 41° at $\mu = 0.6$. For 80° the relationship between friction coefficient and launch appears approximately linear, with a launch value of 36° at $\mu = 1.0$. Figure 4.64 shows the complex relationship between the spin on the ball, the loft and the coefficient of friction. For example at $\mu = 0.3$, the lower the loft the higher the spin rate, with 50° loft - 250 revs^{-1} , 60° loft - 238 revs^{-1} , 70° loft - 163 revs^{-1} and 80° loft - 90 revs^{-1} . While for all lofts (other than 80°) an optimum friction coefficient is shown, about which increasing or decreasing the friction leads to a reduction in spin.

It is possible to present the results for loft and friction effect with loft on the abscissa, with each curve representing a friction coefficient. This is done in figures 4.65 - 4.67 for speed, launch and spin.

It is clear that the relationship between the loft, friction, launch and spin is not trivial. The results in the previous analyses use a clubhead with specific boundary conditions such that the clubhead can only translate in the direction of its original motion. For truly free body clubheads, lower friction causes the ball to slide up the clubface and rotation of the head is likely to occur to increase the loft. This may or may not increase backspin, depending on the friction coefficient. While the turning of the clubhead - gear effect - during impact will also have a gear effect promoting forward spin, or at least reducing the increase in backspin. Computational models that allow the clubhead to rotate on impact are considered under the term mishits in the current work and are considered in section 4.4 where a 30° free body clubhead is compared to the results from here.

The results for loft given above, all show how spin is induced at $\mu = 0.0$. This has been explained in section 4.3.1.2 as being due to the deformation shape of the model ball and the presence of a turning moment. However figure 4.67 shows the relationship between spin and loft is unpredictable at low values of μ . Further computational analyses over the range of lofts was made at 2° loft increments. From graphical post processing it was noted that at certain lofts, notably 28° and 62° for $\mu = 0.0$ the ball model exhibited forward spin (topspin). Recalculation of the results to include the direction of spin, with positive spin representing backspin and negative spin topspin yields figure 4.68 and implies that the mesh density of the ball at low friction has an effect on the direction of spin. At $\mu = 0.0$ spin direction is dependent upon the position on the ball contact is first made, for example below 10°, the node first in contact with the clubface slips up the face and causes local elastic deformation. When recovered this energy creates forward spin on the ball. At other loft angles and as other nodes are involved in first contact backspin may be enhanced for example at 16°. This variation in spin due to the finite element mesh is unfortunate but as friction increases it is less noticeable. For $\mu = 0.1$ node slippage reduces spin at 30° but for other loft angles if increments of 10° are considered the specific wave form of the ball spin prediction leads to minimal error. Improved results could be achieved by the use of a more dense mesh for the ball model (indeed this would be advisable for further analysis beyond the current work). This would lead to more expensive computation and it was felt that the current mesh design could still provide useful predictions if only care is taken in comparing spin between lofts of $\mu <$

0.1. In addition as ball mesh slippage is consistent for any specific loft angle the trend of the results presented earlier in this section is not affected.

4.3.2.3 Mass distribution

The mass distribution of the clubhead is characterised by the moment of inertia of the head as a free body and the position of the centre of mass. In the instance of a 'straight hit' where the impact is such as to cause minimal rotation to the head, the centre of mass of the head must be in line with the reaction force of impact and moments of inertia must be insignificant as rotation does not occur. Obviously this is not the case in a 'mishit' shot where clubhead rotation by definition does occur. Results for the effect of mass distribution only on clubhead performance are therefore covered in section 4.4.

4.3.2.4 Grooves

The effect of grooves on head performance has not been analysed computationally in the current work. This is most partly due to the constraints of time both in terms of man and computer-hours. A consideration of the performance of the grooves would require a different finite element model to the one used in the current work. A highly refined, intense and expensive mesh would be required to model ball deformation into the grooves. In addition any third party material taking part in impact, such as water, grass or grease would also need to be considered. This would add significant complexity to the finite element mesh and possibly put the analysis beyond currently available computer hardware.

However, the analysis of the effect of groove geometry is not essential in the current work. The model predicts the behaviour between the clubhead and ball and does not include any third party material. It is a reasonable assumption and has been shown by experiment (Woods and Mase 1990) that the ball deforms into the grooves proportionally to the applied normal force. The effect of grooves is thus comparable to increased friction. Thus in the current work grooves are considered to increase effective friction above that present due to the material of the head and the ball.

4.3.2.5 Curvature

It was mentioned in section 1.6.1.2 that clubheads with the centre of mass a significant distance behind the face have a curved face to reduce the gear effect and reduce the error on a mishit shot. The gear effect is only noticeable when the clubhead rotates during impact and is thus considered in greater detail in section 4.4 as a 'mishit'.

Analyses were carried out using analytical curved surfaces (available only in Abaqus versions 5.7 onwards) constrained to prevent rotation and permit translation only in the initial direction of travel. All of the surface models had the mass properties of the rigid clubhead used in loft analyses. The roll or vertical curvature was varied from a radius of 50 mm to 450 mm, values chosen about the typical roll radius of curvature 279 mm (Maltbie 1986). Initial clubhead positions were such that the point of impact occurred in each analysis at the same point on the ball and the tangent to the curved surface was 30°. This is shown in figure 4.69. For a clubhead with a radius of curvature of 279 mm a 30° tangent indicates a mishit 140 mm above the position of tangent 0°, obviously such a point does not occur in a normal clubhead but this extreme value is taken to facilitate an examination of the effect of curvature. The face was positioned such that the distance to impact was the same in each analysis, 14.23 mm and the head given an initial velocity of 50 ms⁻¹.

Figures 4.70 to 4.72 give the results for speed, launch and spin for a varying radius of curvature at two different friction values, $\mu = 0.06$ and $\mu = 0.6$ and include the results for the rigid planar loft analyses at 30°. As expected ball flight predictors approach the planar results as the radius of curvature is increased. Deviations from the planar results are increased by a reduction in friction, as the ball slides further around the curved face and effective loft is increased. This is seen most clearly at a radius of 50 mm, where the spin rate was increased 5.5% at $\mu = 0.6$ and 34% at $\mu = 0.06$.

The results show that for a radius of curvature greater than 250 mm, there is only little deviation from the results predicted by the tangent to the surface. At this radius using the worst case scenario of low friction ($\mu = 0.06$), speed is reduced by 0.7% (76.3 to 75.8 ms⁻¹), launch increased 3.8% (26.6° to 27.6°) and spin increased 3.7% (67.7 to 70.2

revs⁻¹). This indicates for surface tangents of less than 30° and radius of curvature greater than 250 mm (ie all current clubhead designs), for impact causing negligible clubhead rotation the effective loft is approximate to the tangent at the point of initial contact.

4.3.2.6 Geometrical stiffness

The effect of the stiffness of the clubhead material as a solid mass, as in an iron clubhead, has already been covered in section 4.3.1.1. During the latter stages of the current work a large amount of discussion arose, within the golf community, about the merits of a 'spring-back' effect from driver clubheads with thin faces. The discussions reached a peak in November 1998 with the formal adoption of a new clubhead test for 'Enhanced Rebound Velocity' by the USGA executive committee (USGA 1998). The finite element procedures used in the current work are ideal for a thorough examination of the effect. Unfortunately the restrictions of time have prevented the inclusion of any such investigations. Hopefully such further work will be published separately.

4.3.2.7 Open/Closed

In all previous analyses the clubface leading edge has been perpendicular to the line of travel, which in turn has been coincident with a vector along the 3-axis (the target line). If the leading edge of the clubhead is not perpendicular to the line of motion the clubhead is known as open or closed, depending on which part of the head is closest to the ball pre-impact, heel closest - open, toe closest - closed. Such misalignment causes initial ball flight away from the target line towards the perpendicular of the face at impact and with sidespin. Due to spin the ball continues to deviate sideways during flight caused by the forces associated with spin. These forces have been discussed previously in connection with backspin, however sidespin on the ball can create a more dramatic flight as the spin is not counteracted by another force. For conciseness the term open is used to refer to both open and closed situations as their effects are symmetric about the line of clubhead travel.

The results for open faces can be gleaned from the loft results (section 4.3.2.2) via a rotation of the model coordinate system. In this way backspin represents sidespin and launch the dispersion angle, for a zero lofted clubhead. Finite element clubheads can be created to represent lofted open or closed situations, but the presentation of data from such impacts is difficult and not covered in the current work.

The degree to which the face may be open at impact is expected to be smaller than the loft angles examined, and possibly no greater than 20° . While results over this range can be inferred from the loft data presented, a closer examination of the spin yields a highly interesting effect. Figure 4.73 gives a more detailed examination of spin generated from open clubheads between 0° and 20° for varying friction. Analyses used a clubhead constrained to prevent rotation and translation about any direction other than initial travel. It is clearly shown for all angles, that for friction coefficients greater than 0.2, higher friction leads to reduced spin. This counter intuitive fact occurs at 20° , as the friction to create maximum spin is 0.14 (see section 4.3.2.2) and increasing friction above this value inhibits the spin of the ball as it leaves the clubface. This indicates that if the friction coefficient between the ball and clubhead is at least 0.14, creating higher effective friction (by the use of vertical grooves maybe) will reduce sidespin. This value of 0.14 is for a 20° open face, for less open faces the critical friction is less and increased friction above this value more effective in reducing sidespin.

It is worth noting that these results use a clubhead that can not translate during contact (other than the direction of travel), and this reduces the predicted value of the spin compared to a free body clubhead, with which analyses were also carried out to confirm the trend of the result.

4.3.3 Dynamics

4.3.3.1 Speed

The analytical solution (see section 4.3.2.1) predicts a linear relationship between clubhead velocity and initial ball velocity but does not make predictions about the effect on spin or launch. Finite element models were created varying the clubhead velocity

from 5 ms^{-1} to 70 ms^{-1} , a 30° rigid clubhead ($\mu=0.6$) was used, constrained not to rotate and translate only in the initial direction of travel. Figure 4.74 shows model results for initial ball speed, confirming the analytical solution of a linear relationship. Figures 4.75 and 4.76 give the launch and spin. Over a range of typical clubhead speeds (25 to 50 ms^{-1}) launch appears to decrease by only 1° as the tangential velocity of the clubhead increases. Spin shows a clear linear relationship and between 25 and 50 ms^{-1} nearly doubles from 71 revs^{-1} to 134 revs^{-1} .

Making use of the analytical solution, the effective coefficient of restitution (e) used in the finite element model can be calculated. Velocities used for the clubhead and ball are normalised to a vector perpendicular to the clubface. Figure 4.77 shows estimates for e , decreasing at higher velocity. Values are close to unity (the perfect elastic collision) as there is no specified damping within the ball, other than that present by default to aid computation. Typical values for e in the golf impact were discussed in section 4.3.2.1.

4.3.3.2 Trajectory

The trajectory of the clubhead in all previous analyses has been along a vector coincident with the 3-axis. A term often used in golf is 'hitting down on the ball', in this manner the clubhead elevation is inclined below the horizontal and the known effect of which is increased backspin. Figure 4.78 shows diagrammatically how a 30° lofted clubhead with a swing elevation -10° (ie inclined below the horizontal) can be considered as motion along a vector Z^1 in a coordinate system Y^1Z^1 . Results for a 40° lofted clubhead moving along Z^1 can be calculated from the loft data (see section 4.3.2.2). Launch results are transformed to the YZ coordinate system via the subtraction of 10° , while speed and spin remain the same. This is demonstrated in table 4.4, which gives the ball flight predictors for horizontal hits at 30° and 40° , and those predicted by the transformation method for 10° below the horizontal for a 30° lofted clubhead. A computational analysis with the clubhead velocity initially 10° below the horizontal shows close correlation to the predicted values. Also included is the predicted and Abaqus value for a 20° lofted clubhead hit down at 10° .

One of the problems for the non expert golfer attempting to hit down on the ball is the likelihood that they will reduce the loft of the clubhead at impact. In the worst expected case hitting down at 10° with a 30° lofted clubhead may lead to the dynamic loft at impact being reduced to 20° . Table 4.4 shows that such a shot leads to the same speed and spin being achieved to a normal 30° clubhead shot but at much reduced launch. The effects of which would cause a reduced angle of incidence for the ball landing and an increased run after pitch. (These results explained why the authors attempts at applying extra spin to a golf ball by hitting down normally only end in extra run !)

The same transformation method may be used for open or closed clubfaces that are swung 'in to out', or 'out to in'. A finite element model can be constructed to show all these dynamic clubhead elements concurrently in a single analysis, and the ball flight predictors can be calculated including the spin rate about a specific axis. A structured presentation of such results is difficult to achieve and thus the current work has studied each clubhead property in isolation.

4.4 Mishits

Mishits are described in the current work as impacts that cause clubhead rotation. It has already been mentioned in a previous section that due to loft all impacts between clubhead and ball lead to rotation of the clubhead. This is examined later in section 4.4.2. Firstly the most obvious type of mishit giving rise to clubhead rotation, that of hitting to the left, right, above or below the sweetspot is considered.

4.4.1 Off-sweetspot impacts

The sweetspot is a ubiquitous ball sports term used in the marketing of equipment. Manufacturers often make claims about improved size of sweetspot for various equipment designs. There are two definitions for the term sweetspot. It may be the contact position that leads to minimum discomfort to the player from the sudden deceleration of impact (otherwise known as the centre of percussion), or the contact position that leads to minimal equipment rotation and the preferred ball flight trajectory.

The current work uses the latter definition for the term sweetspot. Section 1.6.1.2 described how off-sweetspot impact positions lead to clubhead rotation and that increased clubhead rotational inertia (achieved by peripheral weighting) has been shown to reduce rotation leading to less deleterious effects from mishits.

To investigate mishits a series of computational analyses were carried out. These utilised the rigid clubhead model set at a loft angle of zero degrees, $\mu = 0.6$, initial velocity of 50ms^{-1} and no boundary conditions. Vertical mishits above the clubhead centre of mass were made at 2 mm increments from zero to 40 mm. From theory discussed in section 1.6.1.2 it is to be expected that such mishits will lead to increased launch and backspin for iron clubs where the centre of mass is close to the face. Again, as in a previous section involving open or closed clubfaces, via looking at the model from a different perspective the mishits could be considered horizontal with the spin representing sidespin and launch representing dispersion. Results presented here will consistently use the terms launch and spin. The mass and inertia of the rigid clubhead was the same as the solid model described earlier in this chapter. Rotation of the clubhead model occurs about the global 1-axis and, when studying improved inertia, the rotational inertia about the 1-axis was doubled in accordance with Whittaker et al (1990). It was expected that the positioning of the centre of mass behind the face would have an effect on the results, so firstly a series of analyses are presented where the centre of mass of the head was in plane with the face, ie at 0 mm behind. The mass was then placed at 5 mm behind the face and finally 30 mm behind, typical of a modern wood.

Centre of mass 0 mm behind face

Figure 4.79 shows how the initial speed of the ball reduces with the severity of mishit, an approximately linear decrease in the ball speed is seen from 15 to 40 mm. Speed reduction is due to clubhead rotation and reduced compression on the ball. For the double inertia clubhead (di-head) less rotation occurs and speed is less reduced. The advantage of the double inertia is increasingly significant for mishits greater than 5 mm and as the degree of mishit increases, the di-head approximately halves the reduction in speed caused by clubhead rotation. For example; a mishit at 20 mm causes a reduction in speed of 13.6ms^{-1} (from 84.9ms^{-1} to 71.3ms^{-1}) for the normal clubhead and only 7.5ms^{-1} for the di-head. Figure 4.80 shows the launch of the ball and the interesting fact

that the model predicts for mishits greater than 20 mm the launch angle decreases. This is explained by the fact that as the face rotates the tangential component of the clubhead velocity applies a force on the ball of sufficient magnitude to reduce the ball launch below that due to the normal force. The model predicts a maximum error in initial ball flight trajectory of less than 1° , indicating that the large error in the trajectory of the ball flight, to be expected from a mishit, must come from the sidespin induced. For the di-head, rotation is less and, as the point at which maximum launch occurs corresponds to a mishit of 26 mm, the relationship between the two head inertias is clearly non trivial. Indeed at very large mishits, greater than 34 mm, the normal head shows smaller launch angles. The mishit which causes maximum launch is dependent on the friction coefficient, with a reduction in friction shifting the peak to greater mishits. It is to be noted that a 20 mm mishit is significant and for most clubheads would lead to the ball wrapping around the edge of the club, a situation not considered in the current work. For reduced inertia clubheads however the peak will occur below 20 mm and the strange fact that increased mishits may lead to less of an error in launch. These facts are not likely to have a significant effect on clubhead design since, as already mentioned, the main error in ball flight trajectory must be caused by spin. Figure 4.81 shows how spin is induced on the ball and predicts an approximately linear relationship. The di-head shows clear reductions in spin over the normal head and closer examination of the data reveals the di-head to approximately halve the spin generated. There appears to be nothing significant at 20 mm, where a peak in the launch data was noted.

Centre of mass 5 mm behind face

With the centre of mass of the clubhead 5 mm behind the face the effect of mishits on speed reduction is identical to that at 0 mm behind the face and is shown in figure 4.82. However major differences in launch and spin from previous results are to be noted and these are shown in figures 4.83 and 4.84. The launch of the ball is greater than the previous results and still tends to imply a maximum launch at a specific mishit. For this clubhead design the mishit would need to be in excess of 40 mm before the launch reduces and in a real golf shot this size of error would most certainly lead to the ball wrapping around the side of the club, if not the ball being missed altogether ! The di-head shows clear improvements in reducing the launch, approximately halving the launch of the normal head. For the range of mishits the ball spin is no greater than 7 revs^{-1} and

shows clearly the gear effect negating any spin the ball would acquire from the oblique blow. Indeed below 15 mm mishits the spin rate is negative, indicating topspin, and the gear effect must be predominant. The value is however less than 1 revs^{-1} and must be considered negligible, considering the spin prediction method. For greater mishits the di-head approximately halves the spin generated.

The results show clearly the advantage in mishit shots of having the centre of mass behind the clubface. However as the mass is moved further behind the face the gear effect becomes predominant and the spin on the ball can be over-correcting (see section 1.6.1.2). To investigate this effect mishits were carried out with the centre of mass 30 mm behind the face, as might be the case with a 'wood' clubhead.

Centre of mass 30 mm behind face

Figure 4.85 shows the speed diminishes for increased mishits, as predicted with the centre of mass in other positions. The actual reduction in speed is approximately 2 ms^{-1} less than at the other positions (0 and 5 mm) and can thus be considered as one of the benefits of using a 'wood' clubhead to achieve longer distances. Again the di-head approximately halves the speed reduction. The launch results given in figure 4.86 are of more than with the other clubhead designs, while the di-head confirms the inertia relationship emerging by halving the launch. Figure 4.87 gives the spin results, which are all negative (ie topspin) and caused by the predominant gear effect. The spin is of such magnitude that it would be over correcting during ball flight, as shown in figure 1.13. With the centre of mass so far behind the face it is clearly necessary to use a curved surface to reduce the gear effect and send the ball off with an increased launch and reduced corrective spin.

Curved surface model

A curved analytical surface clubhead model with the same mass and normal inertia properties was analysed. The radius of curvature was taken as 279 mm (11 inches), a typical value (Maltbie 1986). Figures 4.88 to 4.90 show the results for the curved and planar models with various centres of mass. All models have the normal inertia values. Figure 4.88 shows that for mishits, the reduction in ball speed decreases as the centre of mass is further behind the face and decreases even further when a curved clubface is

used. In figure 4.88 the 0 mm results are not clearly shown as they are almost coincident with the 5 mm results. The launch of the ball is increased by moving the centre of mass behind the face and, as anticipated, is increased by a curved surface. This increased launch helps reduce the over-correction caused by spin generated by the gear-effect. Figure 4.90 shows how the spin on the ball moves from +ve (backspin) to -ve (topspin) as the centre of mass moves further behind the clubface. The 5 mm result would appear as the clear ideal as the two spin inducers cancel each other out. The curved surface reduces the spin generated for a centre of mass at 30 mm. This can be explained in two ways by the surface tangent promoting backspin, or the curved effect reducing the gear-effect.

The computational methods used here would be of significant advantage in prototype clubhead design. If the centre of mass, inertias and clubface geometry are known, direct comparisons for different severity of mishits can be compared. The results presented here are also dependent on friction, the effects of which can be inferred from the results presented in section 4.3.1.2.

4.4.2 Clubhead rotation due to loft.

From a lofted clubhead there is no position of impact that does not cause clubhead rotation. This was the reason that previous results on loft used a constrained clubhead. It is not that a constrained clubhead gives different ball flight to an unconstrained head but rather a time consuming process is necessary to predict the position of the centre of mass such that minimum rotation occurs.

Analyses were carried out using a 30° rigid clubhead, $\mu = 0.6$, initial velocity 50 ms⁻¹ and fully unconstrained. Mass and inertia properties were taken from the solid clubhead model. The centre of mass was positioned on the face and the rotational displacement of the rigid body reference node noted at time = 0.5 ms, just after the break of contact. An iterative procedure, linearly interpolating between results, was used to predict the centre of mass position that gave a negligible rotational displacement (less than 1.0×10^{-3} radians ($57.3^\circ \times 10^{-3}$)). The positions of the centre of mass on the face were calculated for varying values of friction and are shown in table 4.5.

The vertical positions are higher for lower friction, as the ball slides up the face and the centre of mass needs to be higher up the face to be in a position at which the average reaction force acts. At higher friction, $0.5 < \mu < 1.0$, the difference between the position of the desired centre of mass is almost constant. Remaining small differences could be calculated if a higher tolerance on clubhead rotation is required.

Friction	Global coordinates (m)	
	Y	Z
0.0	-0.00669	-0.02191
0.1	-0.00702	-0.02172
0.2	-0.00742	-0.02149
0.3	-0.00764	-0.02136
0.4	-0.00779	-0.02128
0.5	-0.00800	-0.02115
1.0	-0.00800	-0.02115

Table 4.5 Coordinates for minimal clubhead rotation.

Using the same procedure, the position of the centre of mass behind the face can be found to give minimal rotation and this was done for $\mu = 0.1$ and $\mu = 0.6$. At each friction coefficient the desired positions form a line which represents the average reaction force vector (Rf_A). Figure 4.91 shows the two vectors, separated by 1 mm vertically on the face and intersecting approximately 10 mm behind. The reaction force vectors are 5.7° and 10.4° from the normal to the clubface for $\mu = 0.1$ and $\mu = 0.6$ respectively, and show a similar trend to the launch of the ball (given in section 4.3.2.2), 24.7° and 23.8° for each friction coefficient.

Examining the $\mu = 0.6$ impact further, the rotation can be plotted for the clubhead that shows minimal rotation after impact. Figure 4.92 shows the rotation of the rigid body clubhead's reference node during 500 μ s. Positive rotation is clockwise for the clubhead shown in figure 4.91. During impact the rotation of the clubhead is positive and then negative indicating that the ball at first applies a force on the clubhead below the Rf_A and then towards the end of impact a force above the Rf_A . This is due to the

ball applying a distributed force on the clubhead, that not only changes magnitude during impact but also its distribution. This is ideal, as positive rotation increases the speed of the top of the clubhead where the shaft tip is attached. At impact, as the clubhead decelerates, the shaft tip is deflected and vibrational modes are set up in the shaft. These are felt by the player as the 'shot'. The excitation of the shaft can be reduced if the shaft tip deceleration is reduced by a positive rotating clubhead. As the centre of mass is moved further behind the face, the rotation of the clubhead during impact changes and becomes initially negative and then positive. This is shown in figure 4.93 which gives the rotation during contact for the centre of mass at varying positions behind the face from 0 mm to 30 mm. The results indicate the early and late reaction forces intersect between 5 and 10 mm behind the face and that moving the centre of mass forward promotes an increased initial positive clubhead rotation. This may be the reason for the popularity of off-set iron clubheads. These are typically for beginners and have the leading edge significantly behind the hosel of the head. The hosel brings the centre of mass forward and may even bring it in front of the face. To further demonstrate the possible effect of clubhead rotation on shaft tip velocity figure 4.94 gives the velocity of nodes at the top of the rigid clubhead, which was remodeled to have the face size of a more typical iron (ie vertical height - 60 mm). For clubhead designs with the centre of mass further behind the face, the initial deceleration of impact is greater and would lead to greater shaft tip deflection. Different designs end up at various speeds as the clubhead continues to rotate after impact, and the rotational speed and direction affects the nodal velocity.

The phenomenon that the clubhead rotates positive and then negative for a shot off the sweetspot, confirms the results of Masuda and Kojima (1994). Their work, utilising high frequency strain gauging, showed that the clubhead could rotate as given by the finite element model. However they believed that the cause of such an effect was shaft vibration. This can obviously not be the case in the current work, as the clubhead is a separate body. The results presented here, imply that what they measured was not due to shaft vibration but due to ball clubhead impact.

The results also imply that reduced shaft excitation may be achieved by moving the centre of mass forward in the clubhead. However the mishit performance for such clubs

have been shown in the previous section to be poorer, than when the centre of mass is 5 mm behind the face. Hedrick and Twigg (1995) attempted analysis of how the complex shaft vibrations excited by impact transfer into feel of the shot. They concluded that the shaft vibrations are too complex to make practical analysis near impossible. The results presented here on how the clubhead may rotate during impact is imperative if attempting to predict the post impact shaft behavior.

The patterns of clubhead rotation previously shown are for hits off the face, where minimal clubhead rotation occurs during impact. For hits only slightly offset from this position the clubhead rotates as predicted in section 4.4.1. Analyses were carried out with the impact above and below the sweetspot by 1 mm, for the 30° lofted clubhead with $\mu = 0.6$. While no difference was discernible in the ball flight predictors, the clubhead rotation is shown in figure 4.95 for a shot off the sweetspot and 1 mm above and below. Also included are shots of a clubhead with double rotational inertia (post script - di). For such a small error in mishit the clubhead rotations are large compared to the rotations experienced from the sweetspot and cast doubt on the advantage to be had from positive head rotation from shots from the sweetspot. As anticipated the double inertia clubheads reduced the nodal rotation. This indicates the benefit for experienced players of playing reduced inertia clubheads (such as blades) if they are to receive feedback on the accuracy of their shots. As the ± 1 mm mishit showed no change in ball flight prediction the procedure was repeated for ± 5 mm. Table 4.6 shows the ball flight predictors for the mishits. The clubhead rotation pattern was similar to the 1 mm mishits with maximum rotation reaching 8° at 500 μ s. Figure 4.96 shows the predicted shaft tip velocity through impact, with the 5 mm mishit below greatly reducing the tip deceleration. While such reductions in the deceleration are noticeable, the difference between the ball flight predictors is still only small. These results imply that the preferred hitting position on the clubhead would therefore be below the sweetspot, where ball flight remains near ideal and shaft excitation is minimised.

	Speed (ms ⁻¹)	Launch (degrees)	Spin (revs ⁻¹)
above	73.3	23.1	154
sweetspot	74.9	22.9	150
below	74.3	22.3	150

Table 4.6 Ball flight predictors for mishits ± 5 mm from sweetspot, 30° loft clubhead.

4.5 Ball properties

A large number of different types of golf ball are allowed under the rules of golf, each with a different construction and offering different playing characteristics. The constructions of the various balls has been discussed in chapter 1 but there is little published work, with the exception of patents, on how the performance of balls is affected by their design (Statz 1990). Most of the small number of published articles have been written by chemists, who are more interested in producing new ball cover materials that have high durability and other beneficial non-mechanical properties rather than engineering properties such as stiffness. In the current work, the finite element model of the ball was not primarily designed to show the behaviour of balls of different constructions but rather to elicit the effect of the impact of different club designs on a 'typical' ball. As the work progressed however, it became apparent that it was necessary to investigate the role of ball construction on performance, currently based on largely untested beliefs about the merits of the cover and the core.

Sullivan & Melvin (1995) report the relationship between the 'hardness' of the cover material and the spin rate of the ball. Their experiment used balls with the same core material but different cover 'hardness'. They observed a decreasing spin rate with increasing cover 'hardness'. However, as with clubheads, plastic deformation of the ball is undesirable and engineering hardness can not be a property which directly affects spin rate. It is of course possible that hardness was chosen as a ball parameter simply because it is easily measured and clarification as to whether the cover material has other constant properties, such as elastic modulus or surface friction, is not given. Sullivan & Melvin (1994) report on the effect which compression of the ball has on spin rate, which decreases with a more compressive ball, but they state that the covers used have the

same 'hardness'. Again there is no mention of whether other material properties remain constant. In their work, the compression on the ball is measured as the displacement when subjected to a compressive load of 200 lbf and expressed in hundredths of an inch, ie as a Reihle compression value, so named after the device used to squeeze the ball. They give an approximate conversion to the standard PGA compression test, for balls with the standard diameter as:

$$160 - \text{Reihle compression} = \text{PGA compression.}$$

Unfortunately, the measured Reihle compression is of little practical use as it does not admit the large displacements experienced by the ball during impact. Indeed these compression values were only introduced as a quality control measure to sort out as-manufactured wound balls resulting from inconsistent production methods. Modern methods of manufacture do not require such sorting of the balls but Reihle compression values are still used to indicate their stiffness. Sullivan & Melvin (1995) state that such compression values have little effect on the ball flight, only influencing the sound of the shot and the players perception of feel.

4.5.1 Compression tests

In accordance with the compression tests of Sullivan and Melvin (1995), a finite element half-model was constructed with a flat rigid element to make contact with the ball (figure 4.97). A half model was used as it is computationally cheaper and can be constrained so that the ball does not slip under compression. It is necessary to apply the correct symmetry boundary conditions to the planar cut through the ball so that it represents a whole ball under compression. The middle of the ball is pinned while all other nodes on the midplane are constrained in only the vertical direction, in the line of action of the force. Practical compression tests on half ball models as carried out by other researchers are not representative of the behaviour of a whole ball, as the cut edge is subject to friction and the material can not move horizontally as in a real whole ball.

A static analysis was carried out using Abaqus/ Standard, initially ignoring dynamic effects. A Reihle value of 17.3 was calculated, giving a 'PGA compression' of 142, much higher than the values found in existing golf balls (PGA 60 - 120).

Given the reservations about the Reihle compression of the golf ball, it is more important to model the compression of the ball under higher loading. Mather and Immohr (1996) carried out tests in which a 10 mm compression was applied to golf balls at rates of 10 mm min⁻¹ and 50 mm min⁻¹. Force-displacement curves at different strain rates were thus obtained. Comparison with the initial finite element results showed the FE ball, based on the hyperelastic material data for vulcanised rubber, to be too compliant. Compression tests alone are not sufficient to generate hyperelastic material constants (this is discussed more fully in 4.4.3) but, given the original experimental data, Abaqus returned values for these constants and these were adjusted and input directly in order to match Mather and Immohr's compression test data. A good fit was obtained when the C10 constant in the polynomial equation describing the core material was multiplied to 120 times its original value.

Figure 4.98 shows the force-displacement of the model along with those of Mather and Immohr, who tested two typical two-piece balls and a wound ball. The finite element model shows good agreement, with a 10 mm compression of the ball requiring 8 kN force. The current finite element model does not include strain rate effects, which were regarded by Mather and Immohr as significant under the loading in a golf shot.

4.5.2 Cover stiffness

The cover stiffness of the FE ball model was normally chosen as 0.34 GPa, to mimic the DuPont Surlyn material mentioned in section 4.1.2. Other cover materials such as Balata have a reduced stiffness of 0.23 GPa and give a lower PGA compression value and higher spin rates (Statz 1990). Analysis was carried out using covers with a range of stiffness from 0.12 to 0.45 GPa, while the core material was held constant at 120 x C10 and friction = 0.6. These four types of ball give different Reihle/PGA compression values (table 4.7) and different 10 mm compression curves (figure 4.99). Figures 4.100

to 4.102 show the effect of the cover stiffness on the ball flight when different lofts are used.

Figure 4.100 shows the speed of the ball is not greatly affected by the stiffness of the cover. The largest discrepancy between covers is at 60° loft, where the speed increases from 49.9 to 51.4 ms⁻¹ as the cover stiffness is decreased. This inverse relationship remains at all lofts but the absolute difference in speed is reduced. For example at 20° loft, the difference in speed is only 0.2 ms⁻¹. It is to be noted that although increases in speed are possible, the low-stiffness covered ball would be less durable. It is also to be noted that damping in the FE ball is only present by default and the observation of increased speed may not be applicable to real materials.

The effect of cover stiffness on launch angle is greater, as shown in figure 4.101, with a higher launch angle for an increased modulus of elasticity cover. The maximum difference in launch angle increases with loft, to 3.5° at 60° loft. The difference between the Surlyn and balata covers is approximately 1/3 of this and the effects of the cover stiffness in current balls can be considered negligible in terms of speed and launch. The same is not true for the spin rate differences as shown in figure 4.102, where a lower stiffness cover is observed to generate more backspin. This is in accord with prevalent golf knowledge that balata covered balls spin more than those with Surlyn. The relationship between the stiffness and the spin rate is linear at any given loft and the magnitude of the difference is likely to be significant in a golf shot. At 10° loft the change is from 28 to 57 revs⁻¹, and at 50° from 240 to 300 revs⁻¹. Although the variation between balata and Surlyn are approximately only 1/3 of these values, such differences would still be demonstrable in a golf shot.

4.5.3 Core stiffness for a two-piece ball

It was regarded as essential for the current work that the elastic properties of the core are accurately described within the finite element analysis by a suitable constitutive model. Such a model is that of a hyperelastic material, for which there exists a strain energy function by which the stresses may be obtained as the derivatives of the strains. The material constants appear in a polynomial equation of the strain energy function, as

described in 4.1.2. However obtaining these constants is not trivial and typically requires a combination of uniaxial tension, compression and biaxial shear tests before sufficient data are available. The simple uniaxial compression test used by Mather and Immohr (1996) is not sufficient to generate the strain energy function but more sophisticated tests were beyond the capabilities of the available test equipment. The core material was therefore initially modelled using test data for vulcanised rubber, taken from the Abaqus/Explicit Example problems manual (Hibbitt, Karlsson and Sorensen 1997). The effects of changing the constants in the material model were observed in a computational experiment and this suggested possible changes in core material properties which would match Mather and Immohr (1996) while retaining the generic shape of the hyperelastic stress/strain curve. Figure 4.103 shows the effect of changing the constant C_{10} in the polynomial form of the hyperelastic strain energy function to 90, 120 and 150 times its initial value. These three different material models were used to examine ball core effects. Figure 4.104 gives corresponding results for the 10 mm compression test of the half ball model while the Reihle/PGA compression values are given in table 4.7. The results of using these three different stiffness properties for the core are given in figures 4.105 to 4.107, which show the final effects of core stiffness on the flight properties of the ball.

Figure 4.105, shows how the initial speed of the ball varies for a “standard” impact with the clubhead traveling at 50 ms^{-1} . Over the total range of lofts the difference in core stiffness has only a small effect and the largest difference is observed at low loft angles. At 10° loft the ball speed varies from 83.2 ms^{-1} with the flexible ball to 84.6 ms^{-1} for the stiffer core. This slight difference in speed is likely due to the greater deformation of the ball with the less stiff core and to the numerical damping present within the material model.

The launch angle is affected to a similar degree, with only a slight variation occurring over the range of loft angles.

The spin of the ball is affected to a greater extent by the core stiffness as shown in figure 4.107, and is observable over the full range of loft with the stiffer ball showing a 30% increase in spin at 10° loft, from 30 to 40 revs^{-1} . This variation is reduced to 17% by

30° of loft and to 13.5% by 50°. This difference in spin is not negligible and would have a discernible effect on a golf shot. The results here confirm the experimental evidence of Sullivan and Melvin (1995), that more flexible cores give lower spin rates when balls of the same cover thickness and 'hardness' are used.

Of great interest is the clear distinction between the effects of cover and core, with the cover stiffness having an inverse effect on spin while the stiffer core results in increased spin. This implies that the overall stiffness (or compression) of the ball cannot be used as a property in predicting behavior. The relative properties of the core and cover are important, as suggested by Sullivan & Melvin (1995), and the properties of concern must be density and stiffness. These are examined in further detail in the next sections.

4.5.4 Stiffness distribution

Three-piece wound balls have a dual stiffness to their core, the inner core being stiffer than the stretched elastomer windings. Also available in the current market are solid core balls that boast dual stiffness properties (see advertisements in Golf World (Various 1997)), either by having dual core materials or double covers. The FE model was therefore changed to examine the effects of dual stiffness, keeping the mass distribution constant (not a simple matter in a physical test). The inner core and the outer core material properties were amended to be both stiffer (C10x150) and less stiff (C10x90) than normal, by varying the polynomial coefficient described in section 4.5.3. The models are compared to the 'normal' two-piece ball with a homogenous core. Figure 4.108 shows the three types of ball analysed and figure 4.109 gives the 10 mm ball compression confirming (as expected) that the balls differ less in compression to the core stiffness models of section 4.5.3. PGA and Reihle values are given in table 4.7.

Figures 4.110 and 4.111 shows how the stiffness configuration affect speed and launch respectively. The trend is similar to the findings in section 4.5.3 that less stiff cores (higher compressibility) give lower speeds and higher launch angles. The low inner ball having a reduced speed and a greater compressibility.

Figure 4.112 shows how the spin is affected by the stiffness distribution. Initial findings are that the overall compressibility of the balls affects the spin rate as in section 4.5.3, with the stiffer balls giving increased spin. However, the variation in spin rates is greater at all lofts than when a single core effect alone were studied, even though the variation in ball compressibility is less. This confirms that the spin is not solely a result of compression of the core. The high inner dual stiffness ball exhibits higher spin rates than the stiffer single core ball even though the overall compression is less. This indicates the predominant mode of spin generation in the ball and is discussed more in the next section.

4.5.5 Mass distribution

In constructing a model of the ball it is also important to represent the mass distribution correctly. For two-piece, homogeneous core balls this is not difficult as the maximum weight of the ball under the rules of golf dictate the inertia of the ball. For more complex designs of ball, such as a three-piece or wound ball, the inertia of the ball can be varied by using different densities of material in the inner and outer core. The finite element model of the ball was amended to allow for density variation without an accompanying variation in stiffness (again not a simple practical achievement). The inertia models are shown in figure 4.113. The density of the inner core in the low inertia ball was chosen as 1700 kgm^{-3} , as given by Mather and Immohr (1996) for a wound ball core. The outer core was given a density of 762 kgm^{-3} to maintain the overall mass of the ball at the legal value. A ball of increased inertia was then created by reducing the density of the inner core to 500 kgm^{-3} , with a suitable change in the outer core density. The results for impact with the rigid clubhead, with $\mu=0.6$ and at varying lofts, are compared to the normal two-piece ball, with a homogenous density of 1100 kgm^{-3} in figures 4.114 to 4.116

Figure 4.114 shows the effect of the inertia on the speed of the ball to be minimal, with the greatest variation occurring at 60° loft but still less than 1 ms^{-1} . These variations are due to differences in the deformation of the ball and in the damping in the material model. Greater variations in launch angle are seen in figure 4.115 which indicate that a decrease in the inertia results in a higher angle.

Interestingly the results for spin generation, shown in figure 4.116 indicate that an increase in the inertia leads to an increase in the spin rate. This runs counter to the idea that a turning moment arm is the predominant spin generator, as suggested in section 4.3.1.2. Indeed, a cross-over point is observed at 50° loft, after which lower inertia balls achieve higher spin. Further investigation with other finite element ball models, shows that the cross-over point is not particularly dependent on clubhead velocity or ball stiffness, but is most dependent on friction. This indicates that the predominant cause of spin below the cross-over is the shear stiffness of the ball and the strain energy stored within the ball during deformation. The onion layered model of spin generation, discussed by Gobush (1995), predicts that a lower inertia core will spin more, when the strain energy from impact is recovered. Such a model will also spin more as the inner core is stiffened to reduce its deformation from a sphere which would lead to increases in rotational inertia. It would therefore appear that the wound ball properties with a denser and stiffer core, partly cancel each other out. The stiffer core leads to higher spin but the denser core reduces the spin. This however only refers to the impact of the ball and does not include effects which appear as the ball flight continues.

During flight the balls spin rate will reduce due to air resistance. A “spin rate decay constant” resulting from the properties of the ball (Winfield and Tan 1996) describes the rate of spin reduction. The decay constant is increased by a reduction in the inertia of the ball and a balls spin reduces at a greater rate. A wound ball construction therefore would lose its spin quicker than a “normal” ball but not significantly during the time of a short iron shot.

The results indicate that it would be possible by a combination of stiffness and density to produce a ball with reduced spin on impact and increased spin rate decay. Such a ball would have advantages for particular golfers and it is difficult to imagine why manufacturers have not already constructed a ball with such properties, especially considering the number of combinations of ball properties which have been tried empirically. The role and importance of FE analysis in the rational design of balls is clear but more accurate material properties, including strain rate and energy dissipation characteristics are needed to advance the model. These areas are currently being researched.

The results here use a clubhead that is constrained for rotation about all three axes and translation in all direction other than that with which the clubhead originally moves. This leads to erroneous results and analyses using unconstrained clubheads were examined and showed little change from the results presented here. For example as the ball inertia is increased the spin will not continue increasing as a point will be reached where the clubhead twists during impact. This is only a minor effect here as the clubhead inertia is very much greater than that of the ball.

Loft	30°	40°	30°	30°	20°	20°
Trajectory	horizontal	horizontal	-10°	-10	-10°	-10°
Method	computation	computation	predicted	computation	predicted	computation
Speed (ms⁻¹)	74.9	67.6	67.6	67.1	74.9	74.3
Launch (°)	22.9	29.1	19.1	19.2	12.9	13.5
Spin (revs⁻¹)	150	208	208	217	150	153

Table 4.4 Effects of trajectory on ball flight predictors.

Ball construction		Reihle	PGA
cover	120 MPa	74.7	85.3
	230 MPa	72.1	87.9
	340 MPa	71.2	88.8
	450 MPa	70.9	89.1
core	C10 x 90	78.0	82.0
	C10 x 120	71.2	88.8
	C10 x 150	66.7	93.3
dual stiffness	low inner	71.0	89.0
	normal	71.2	88.8
	high inner	72.9	87.1

Table 4.7 Static compression values based on 200 lbf compression test (Sullivan and Melvin 1990).

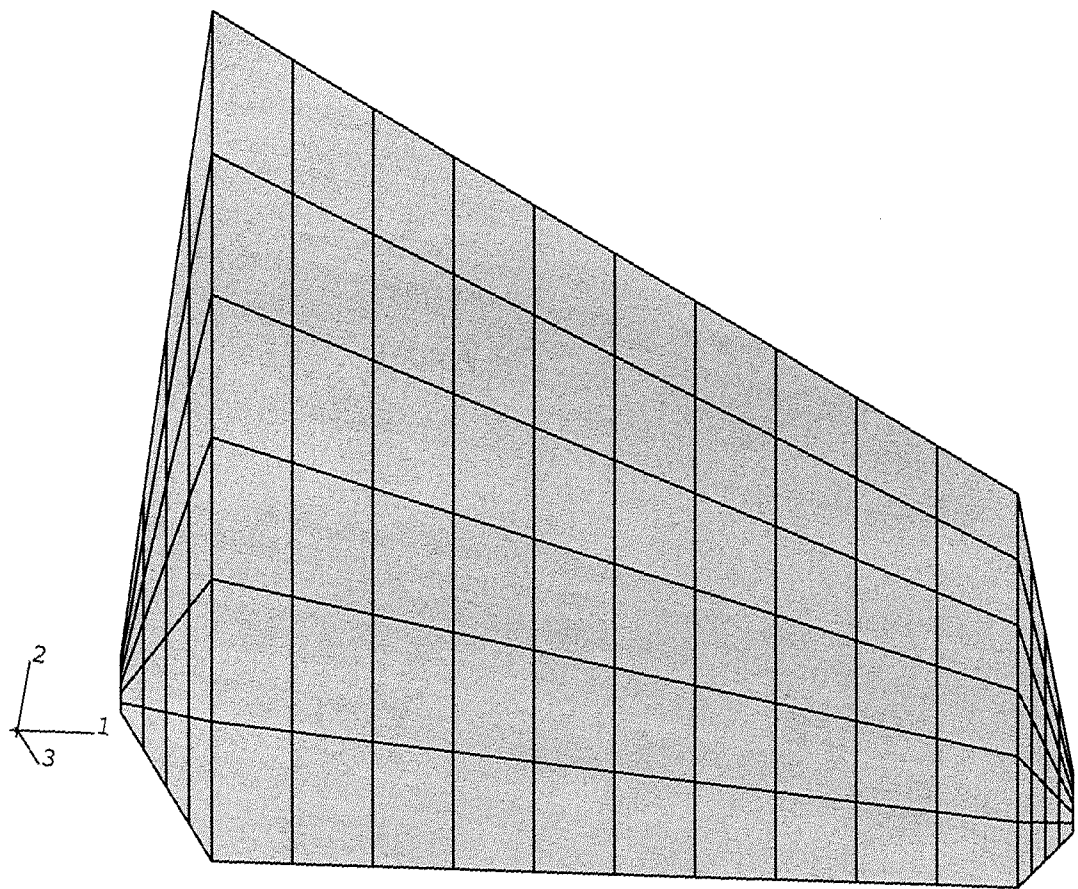


Figure 4.1 Solid model of clubhead.

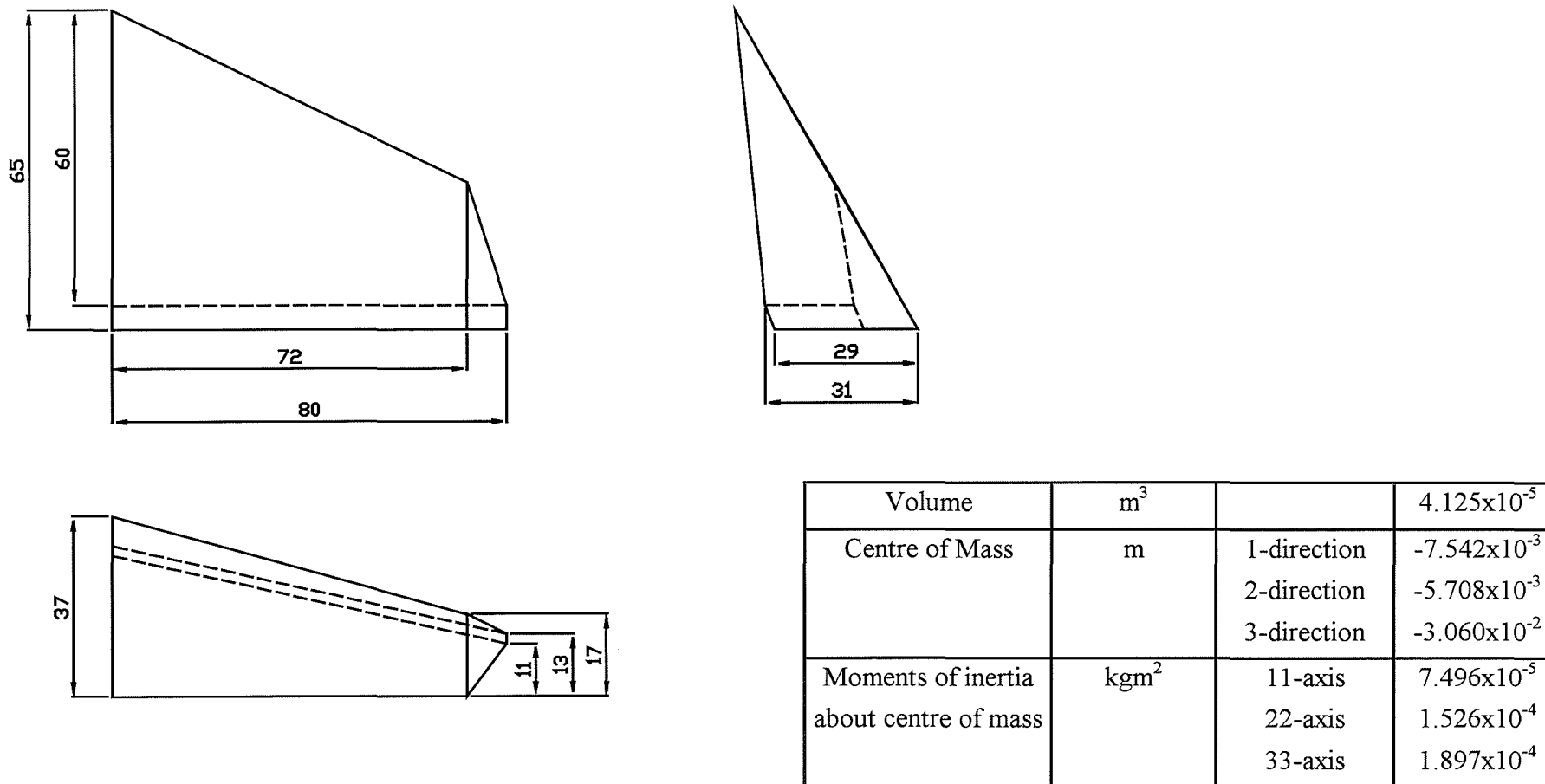


Figure 4.2 Drawing of solid model clubhead (dimensions in mm). Rotational inertias about centre of mass (density = 7800 kgm^{-3}).

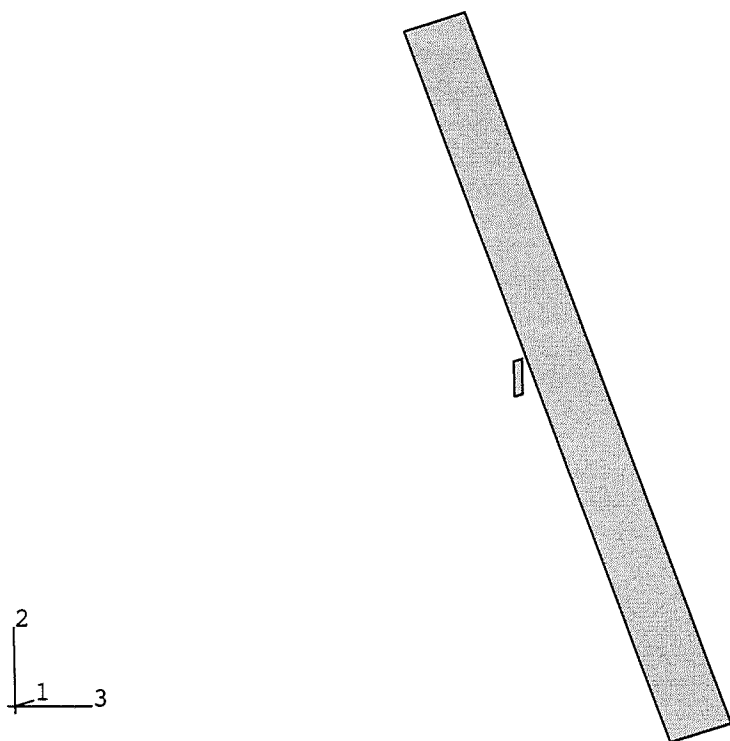


Figure 4.3 Rigid element model of clubhead, rotated to show reference node behind hitting face.

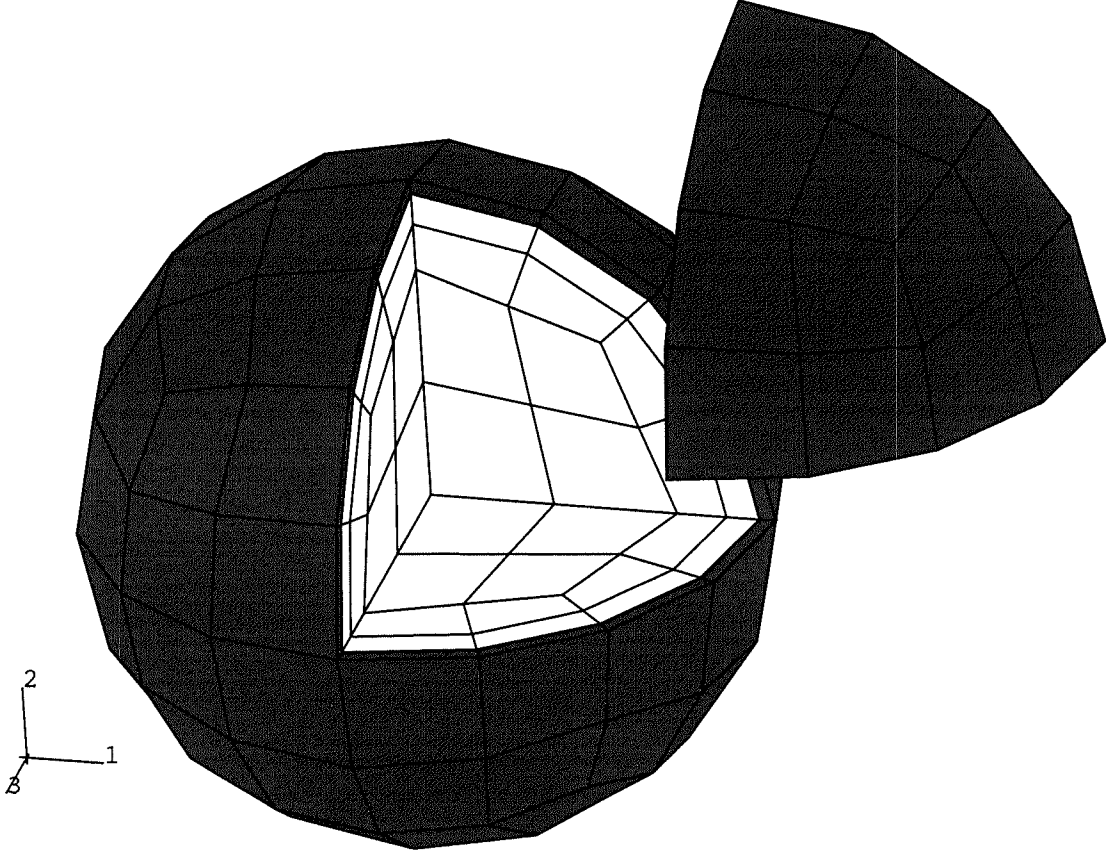


Figure 4.4 Mesh of ball model, with cut away to show inner elements of core and cover.

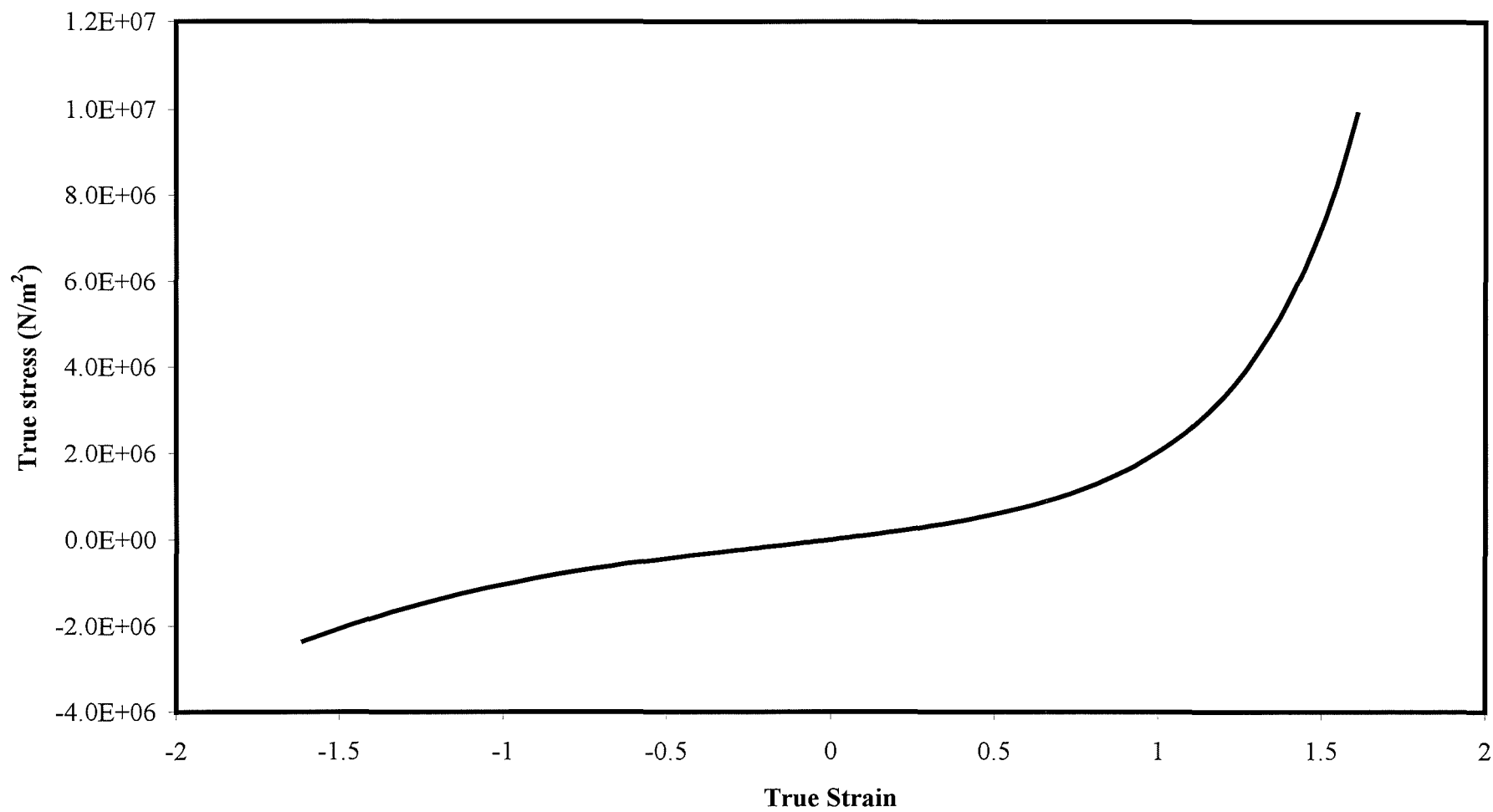


Figure 4.5 Stress/Strain relationship for a hyperelastic material (vulcanised rubber).

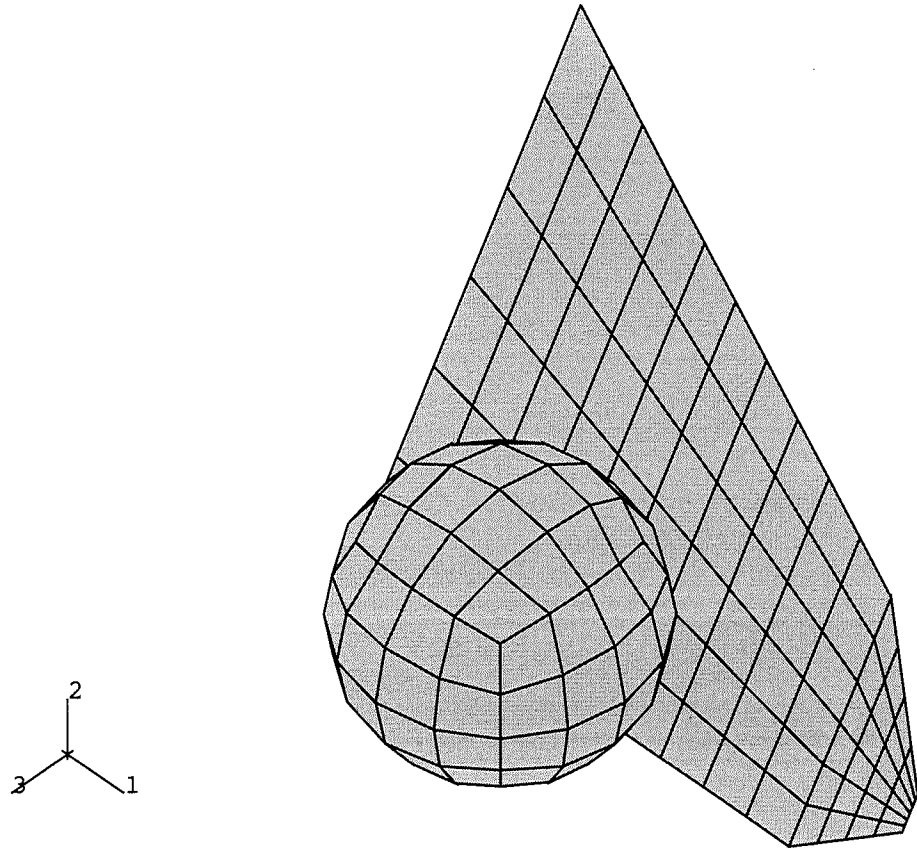


Figure 4.6 Clubhead and ball initial positions, illustrating the coordinate system.

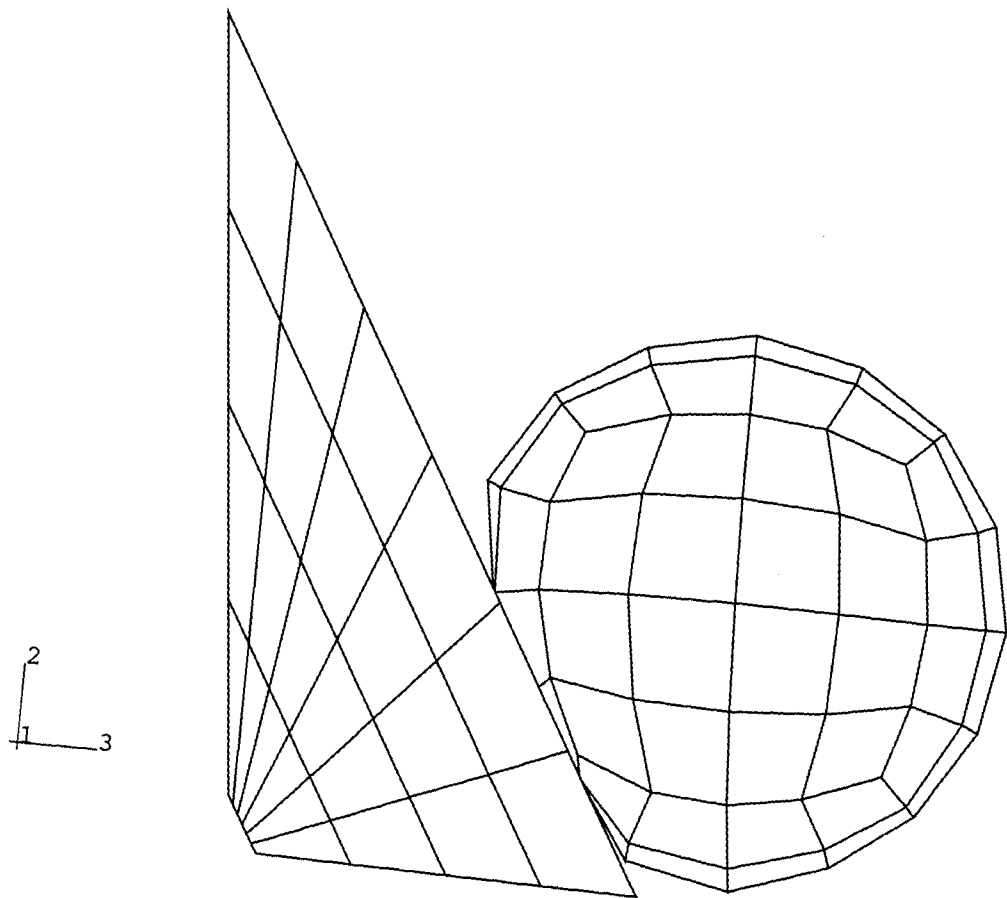


Figure 4.7 Deformed plot of the model, at 0.150 ms.

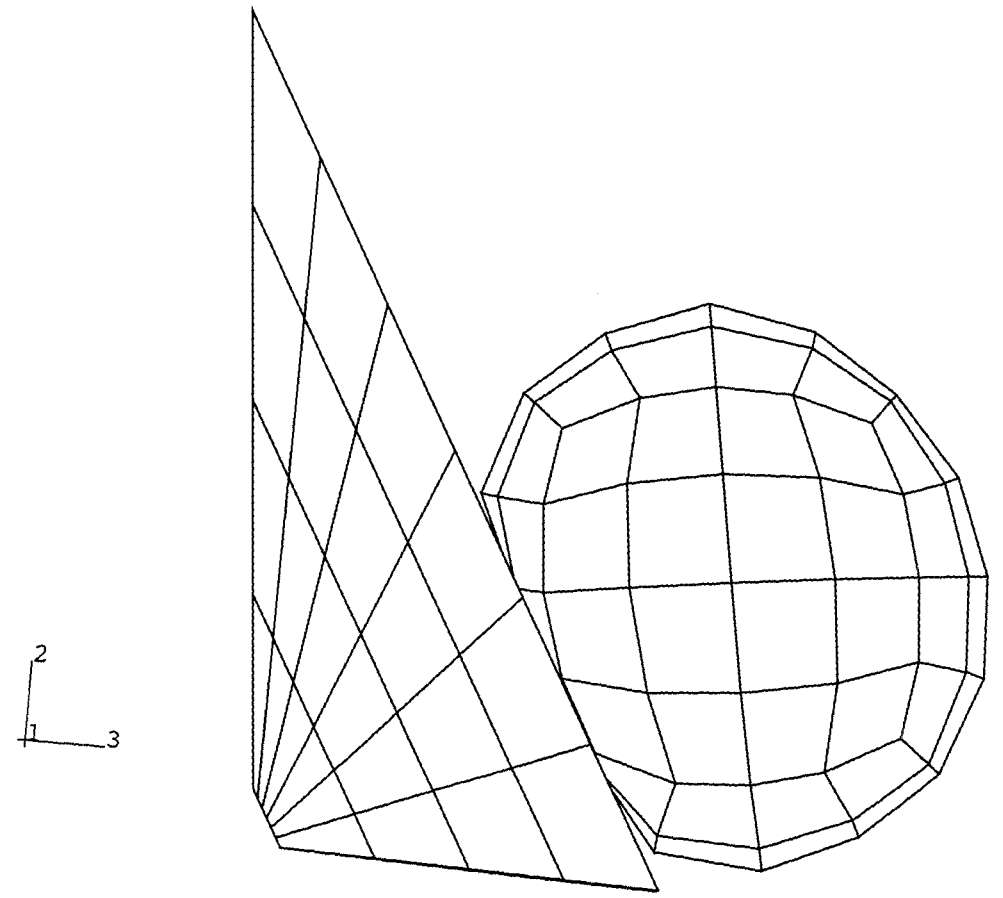


Figure 4.8 Deformed plot of the model, at 0.270 ms.

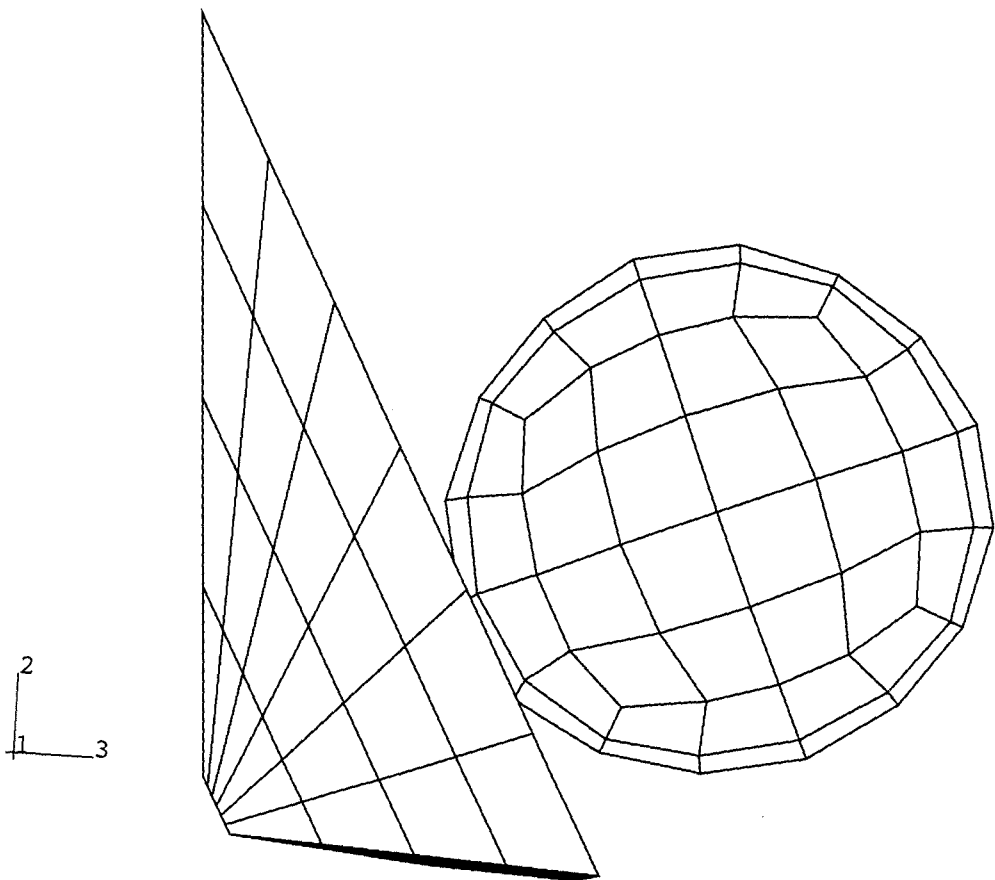


Figure 4.9 Deformed plot of the model, at 0.470 ms.

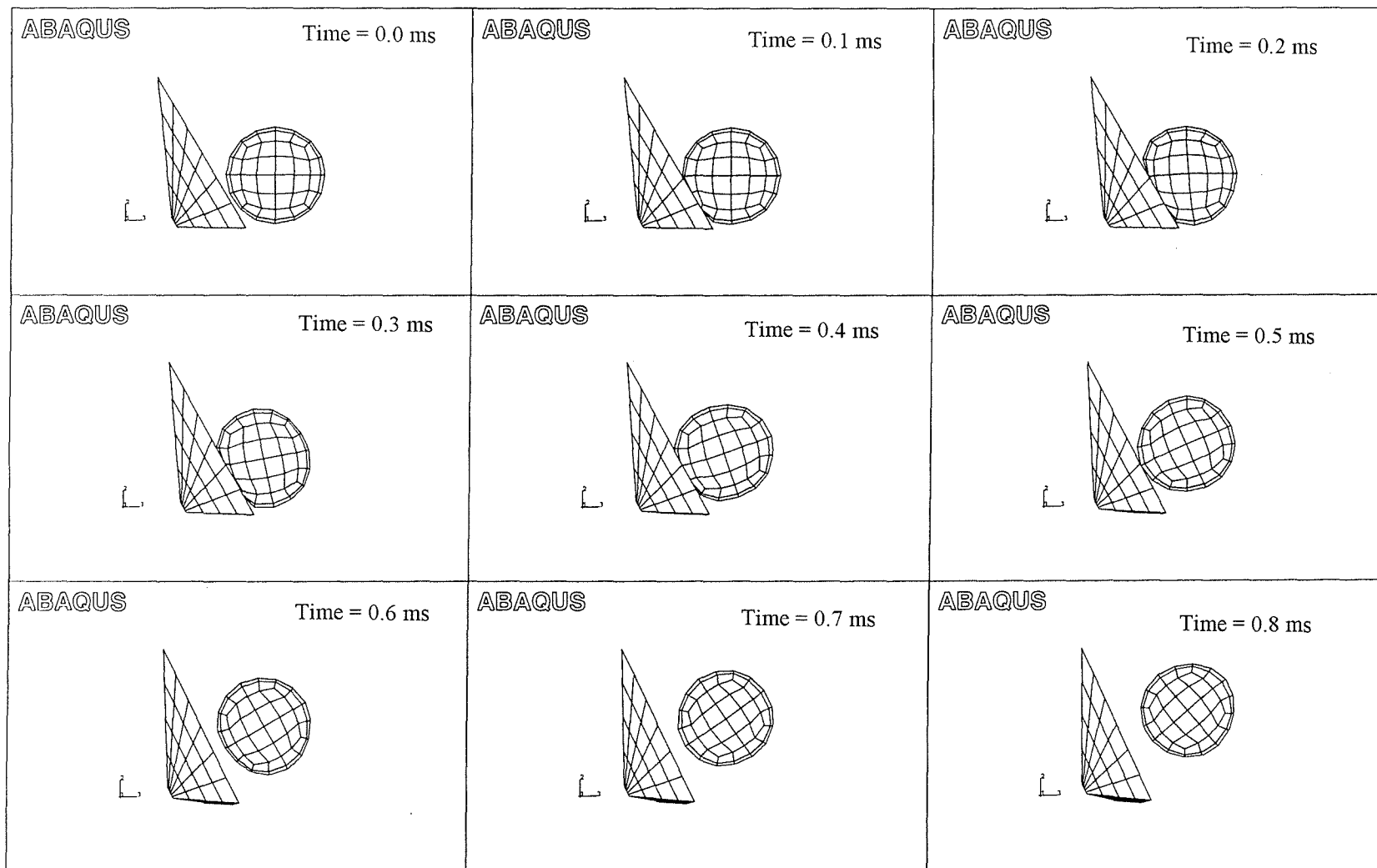


Figure 4.10 Snapshots of clubhead/ball impact.

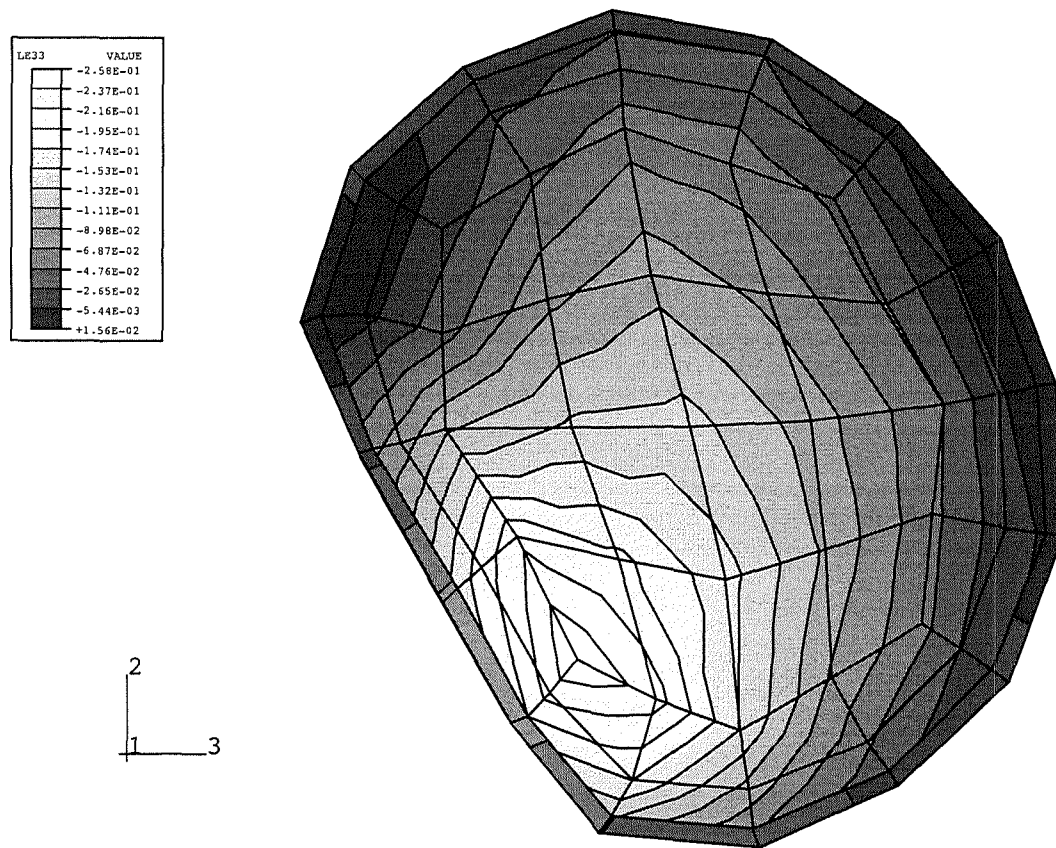


Figure 4.11 ϵ_{33} contour plot for a section of ball, 0.150 ms after impact.

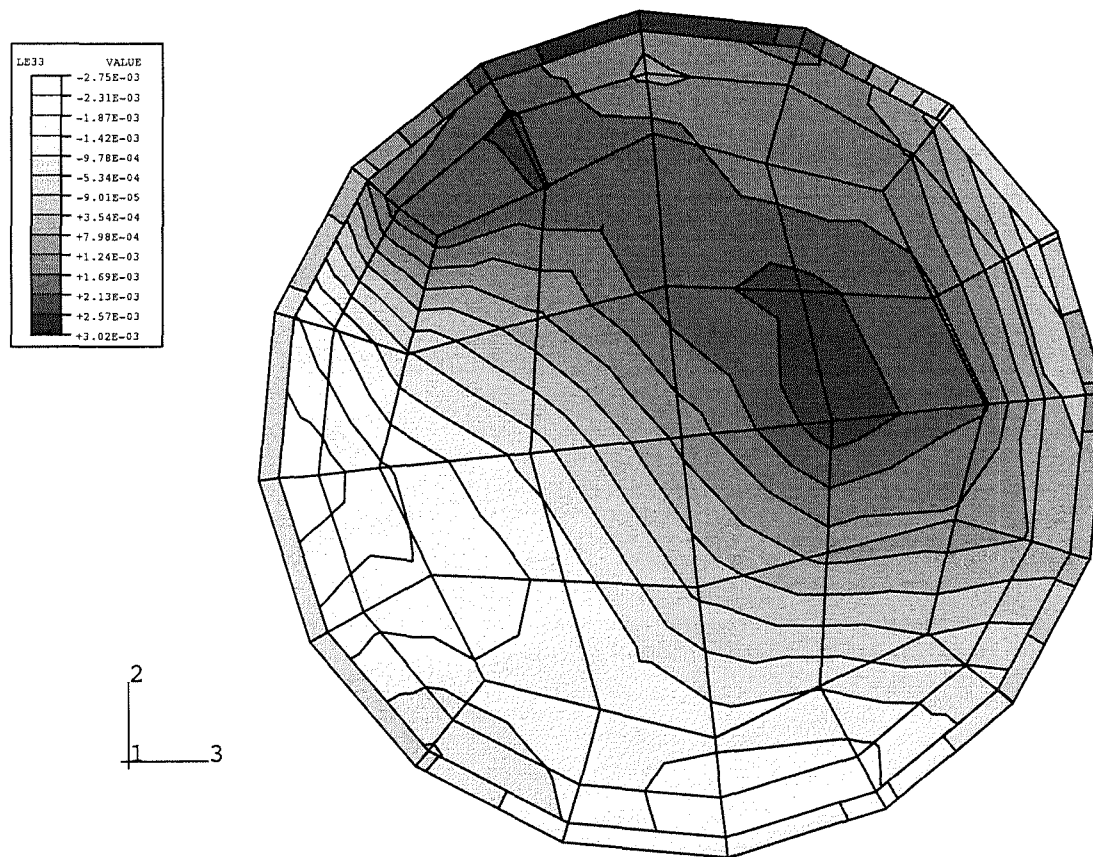


Figure 4.12 ϵ_{33} contour plot for a section of ball, 5.0 ms after impact.

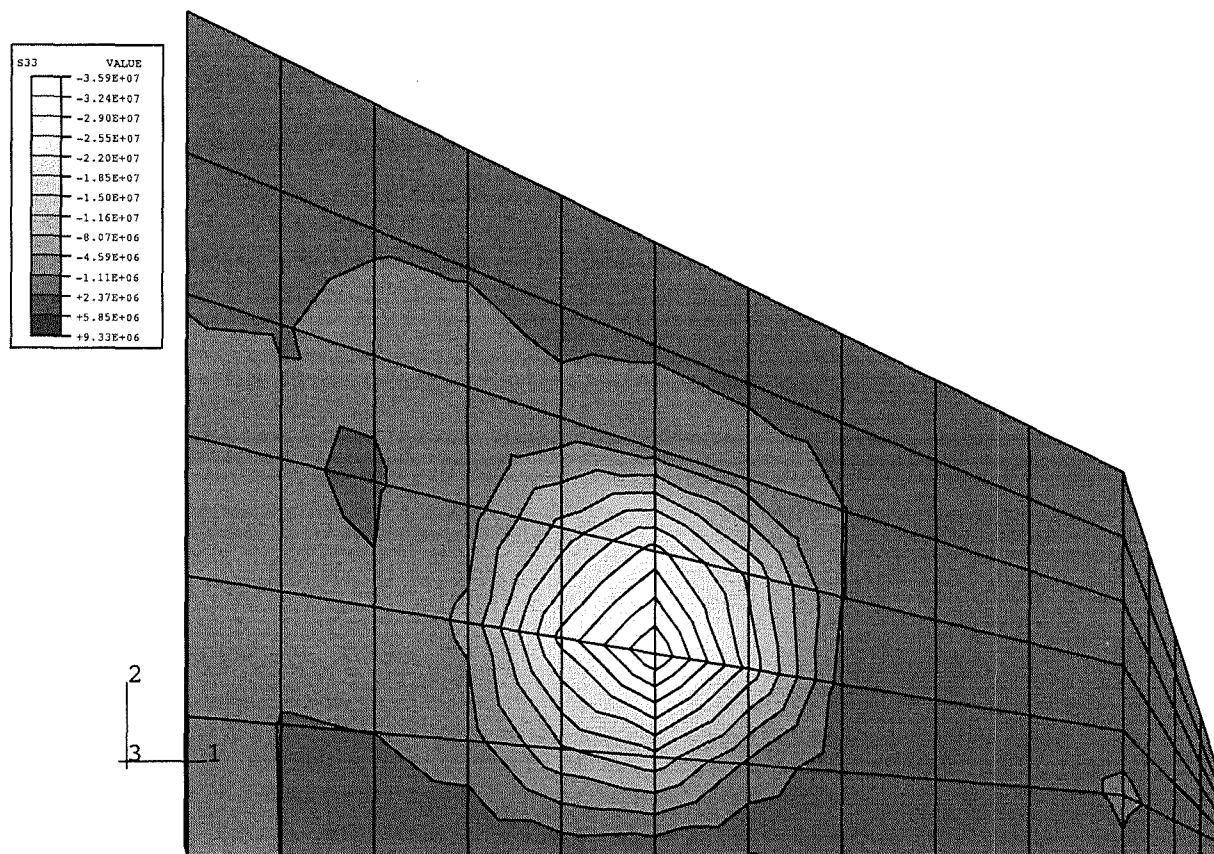


Figure 4.13 σ_{33} contour plot for clubhead face, 0.150 ms after impact.

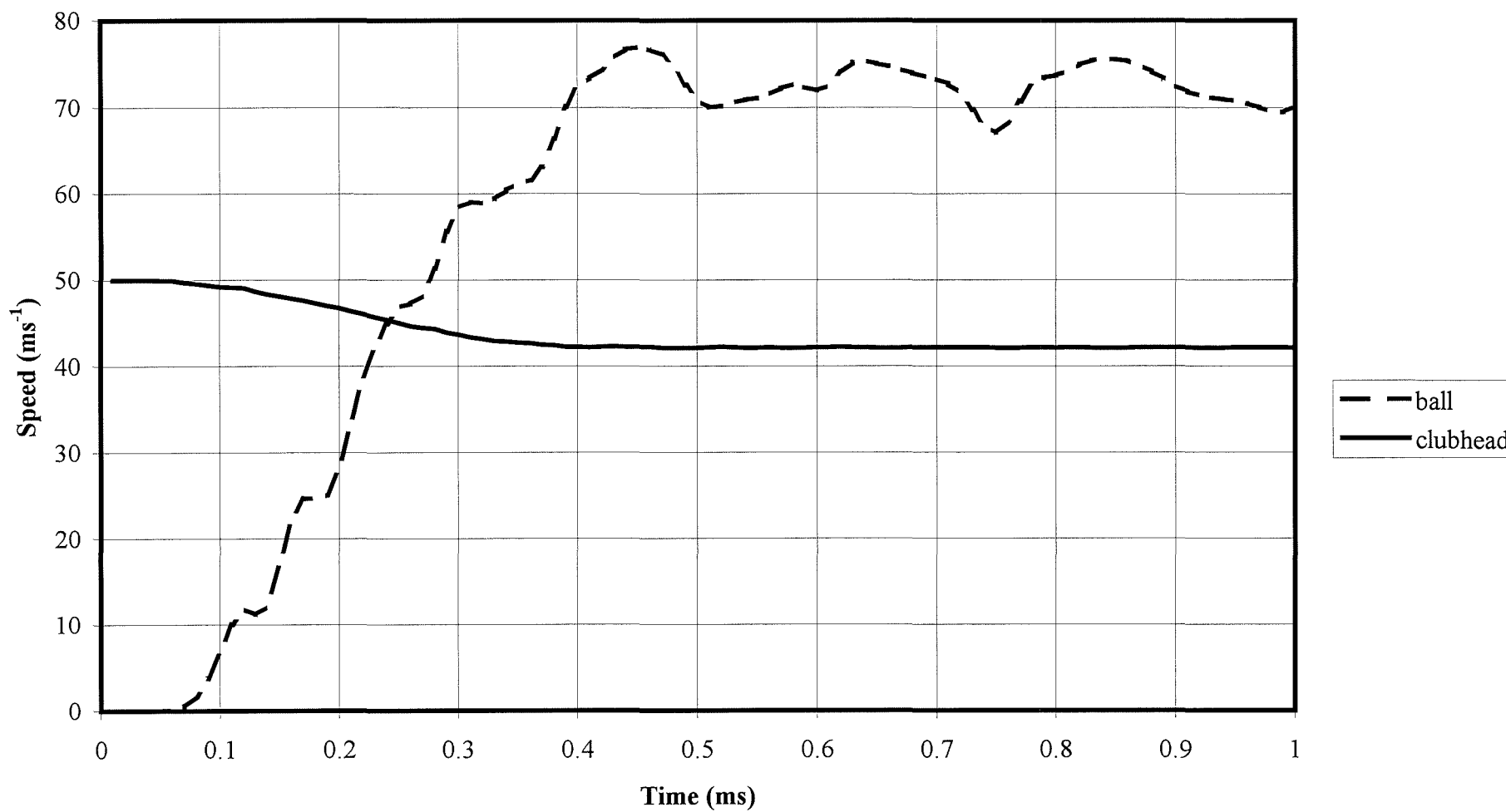


Figure 4.14 Ball and clubhead speed over a period of 1 ms analysis.

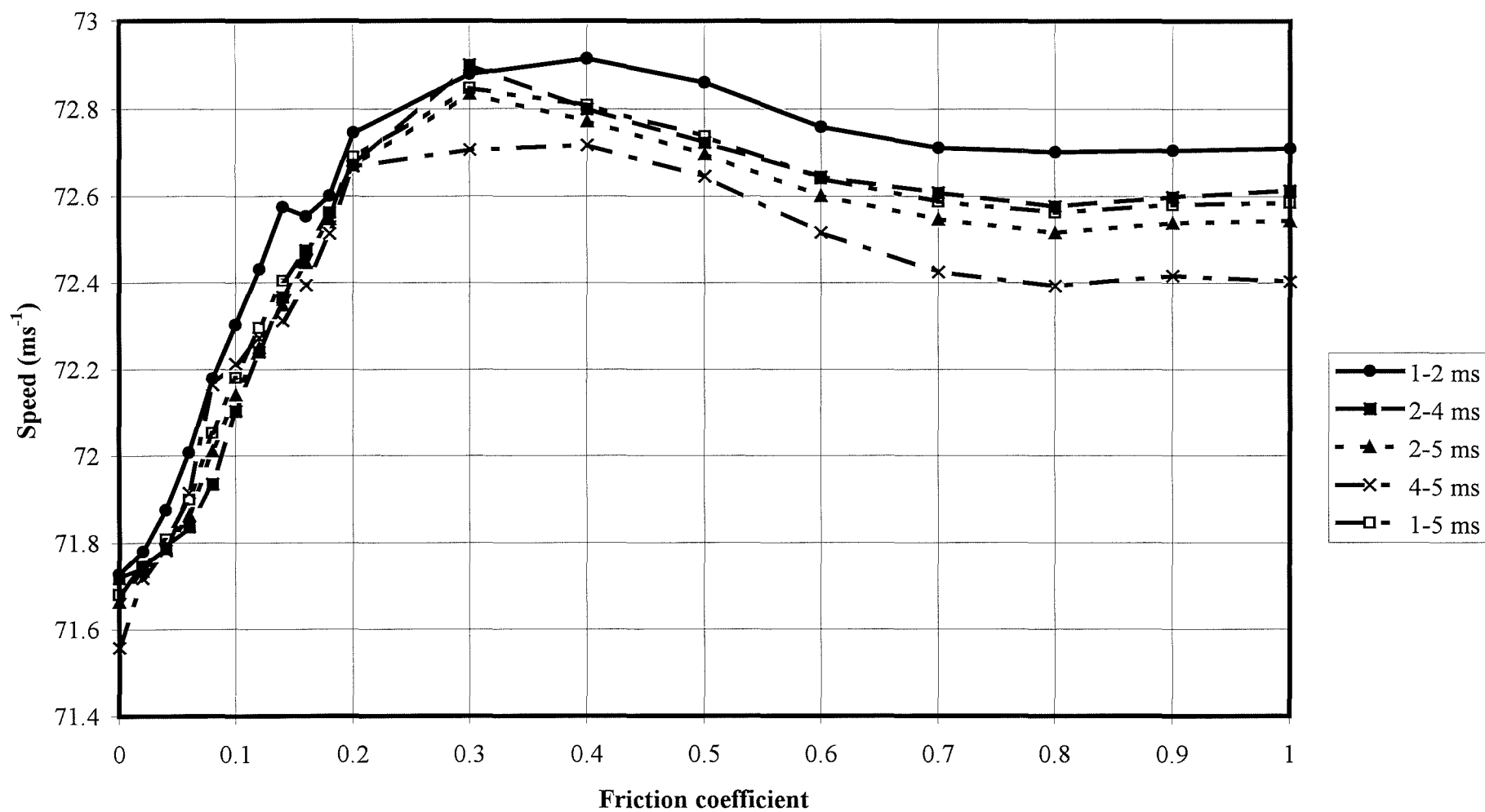


Figure 4.15 Effect of friction on ball speed, averaged over various integrating periods.

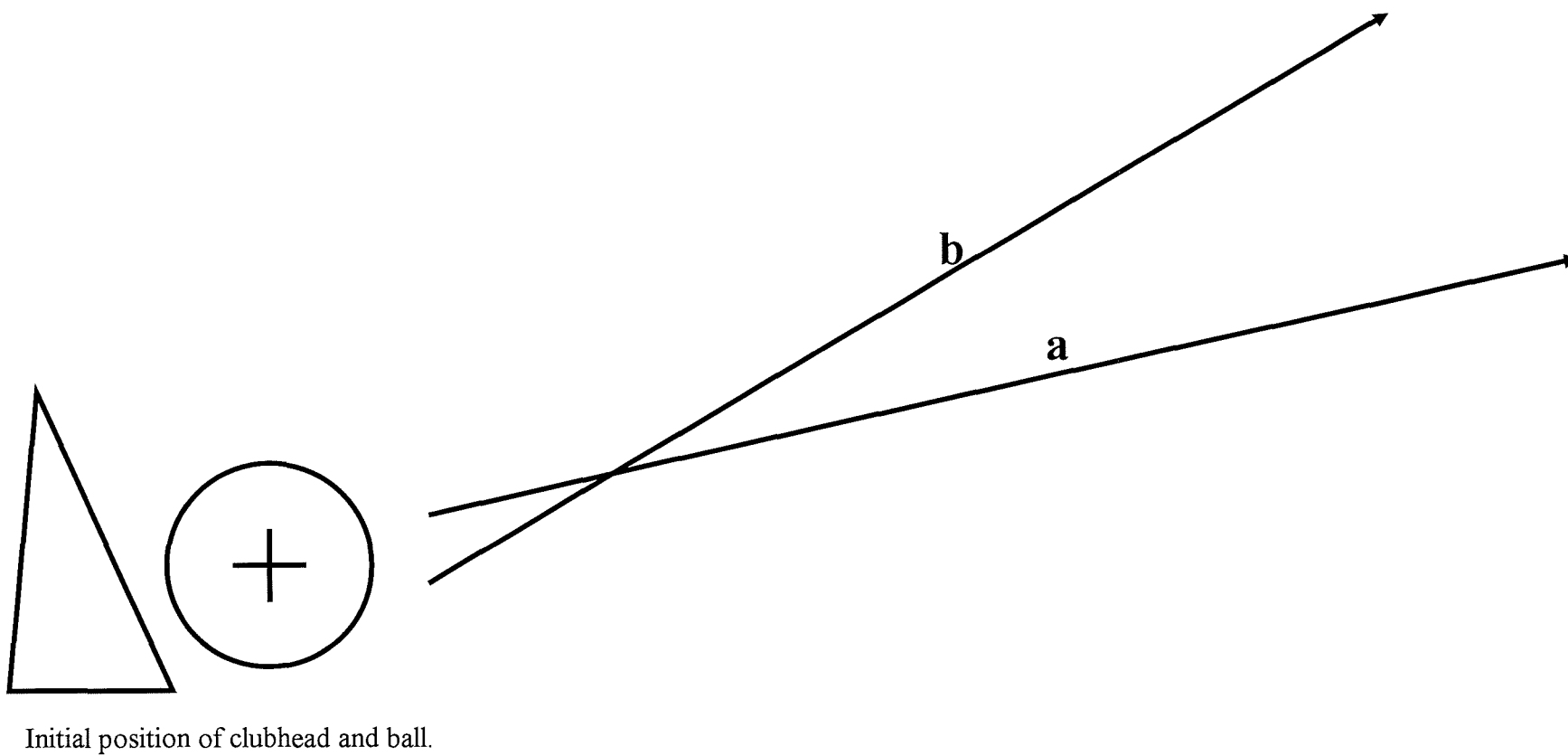


Figure 4.16 Two exaggerated ball trajectories for varying impact conditions.

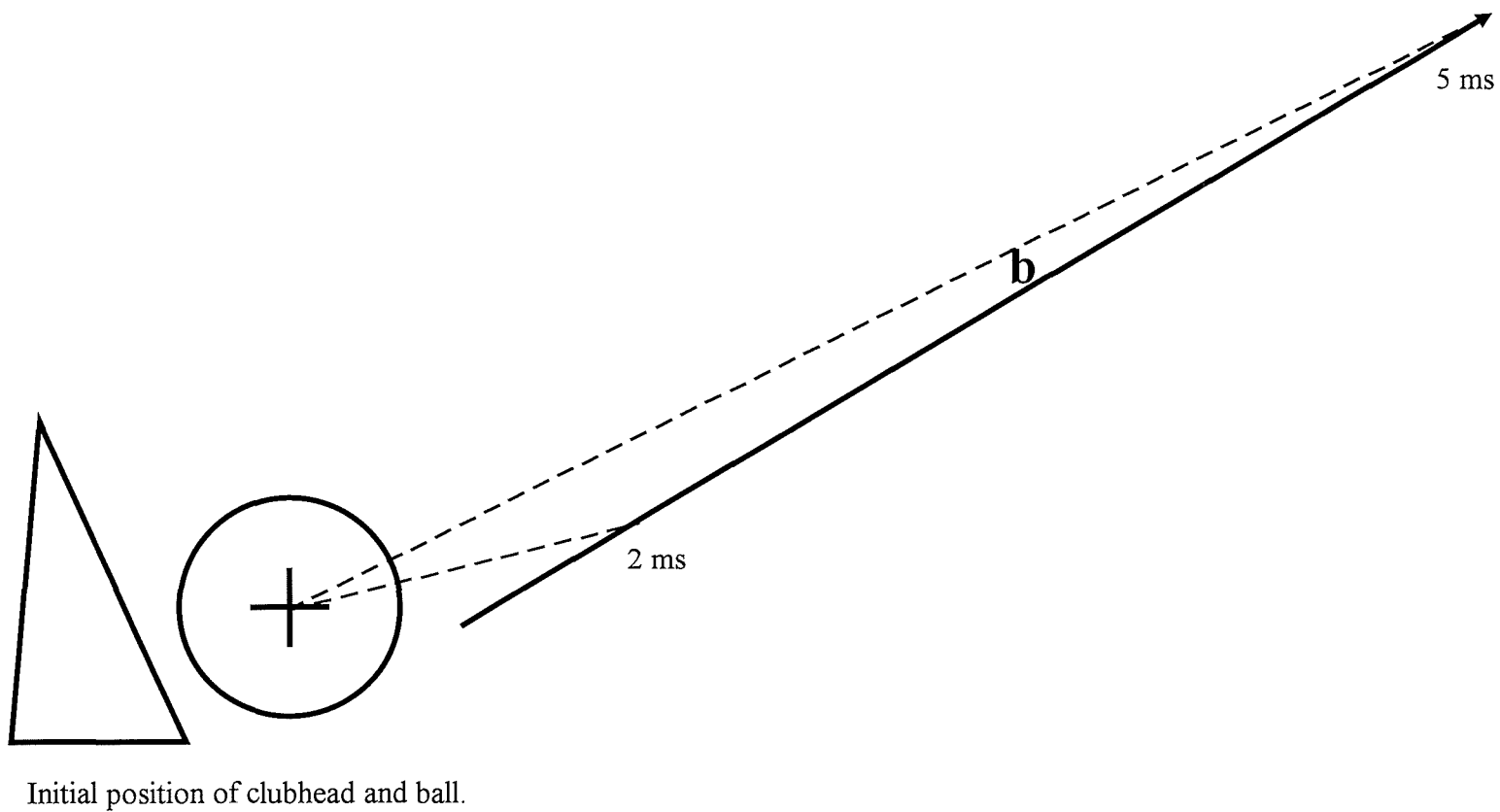


Figure 4.17 Approximating the position vector to the origin vector.

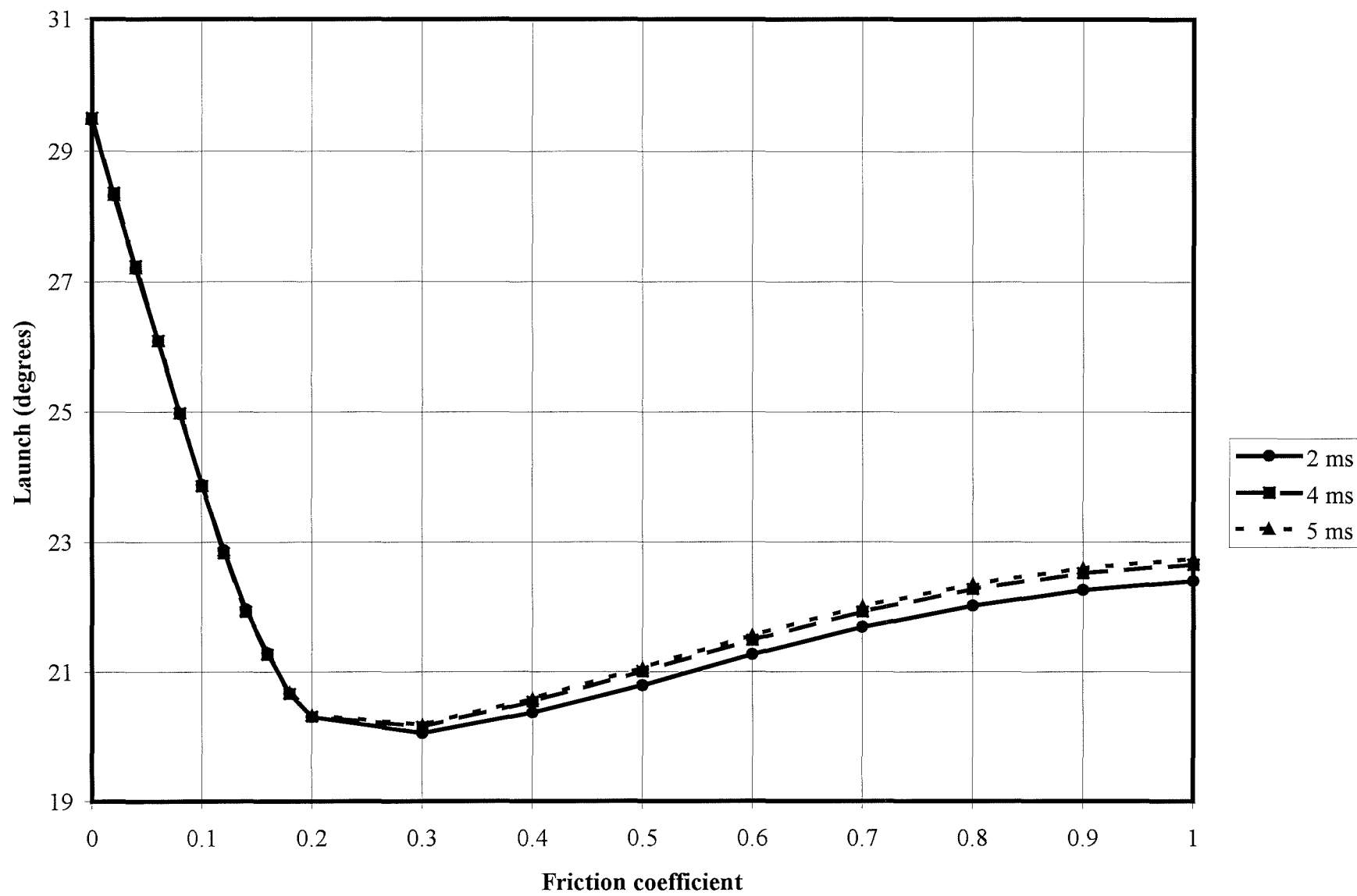


Figure 4.18 Effect of friction on launch angle. Calculated at various instants.

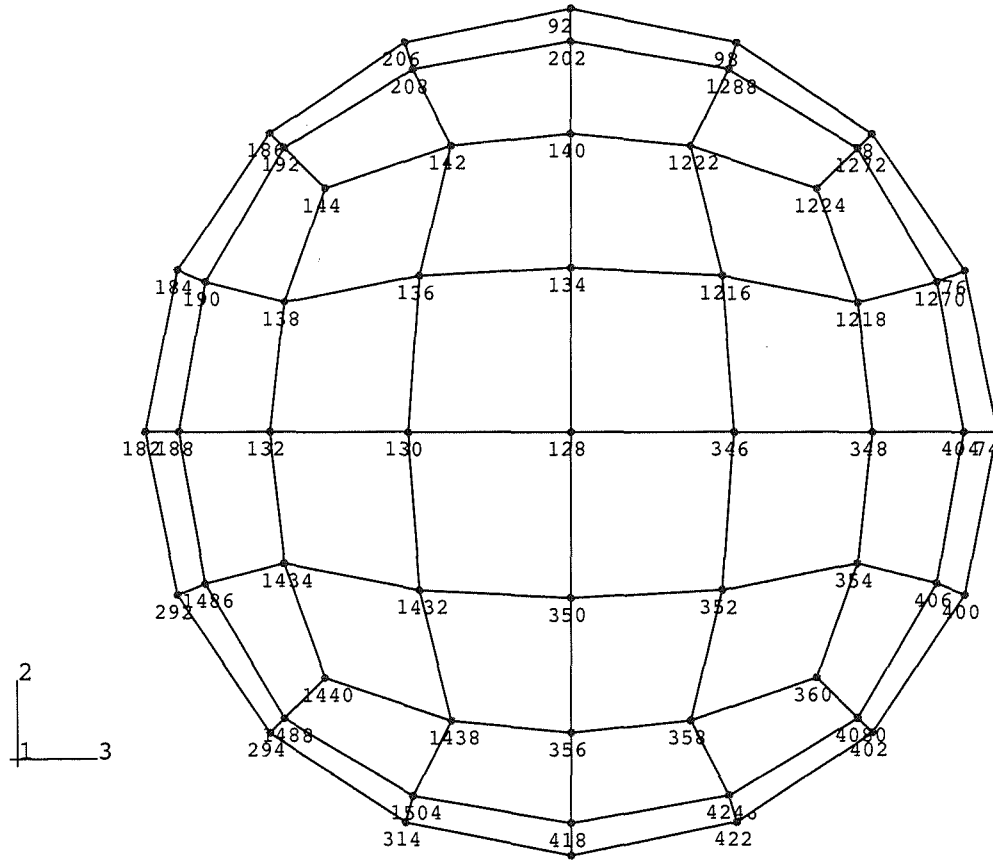


Figure 4.19 3-dimensional mesh of ball showing node numbers.

	186								78	
		192		206	92	98		1272		
				208	202	1288				
			144	142	140	1222	1224			
	184	190	138	136	134	1216	1218	1270	76	
	182	188	132	130	128	346	348	404	74	
	292	1486	1434	1432	350	352	354	406	400	
			1440	1438	356	358	360			
				1504	418	424				
		1488		314	308	422		408		
	294								402	

Figure 4.20 2-dimensional mapping of ball showing node numbers.

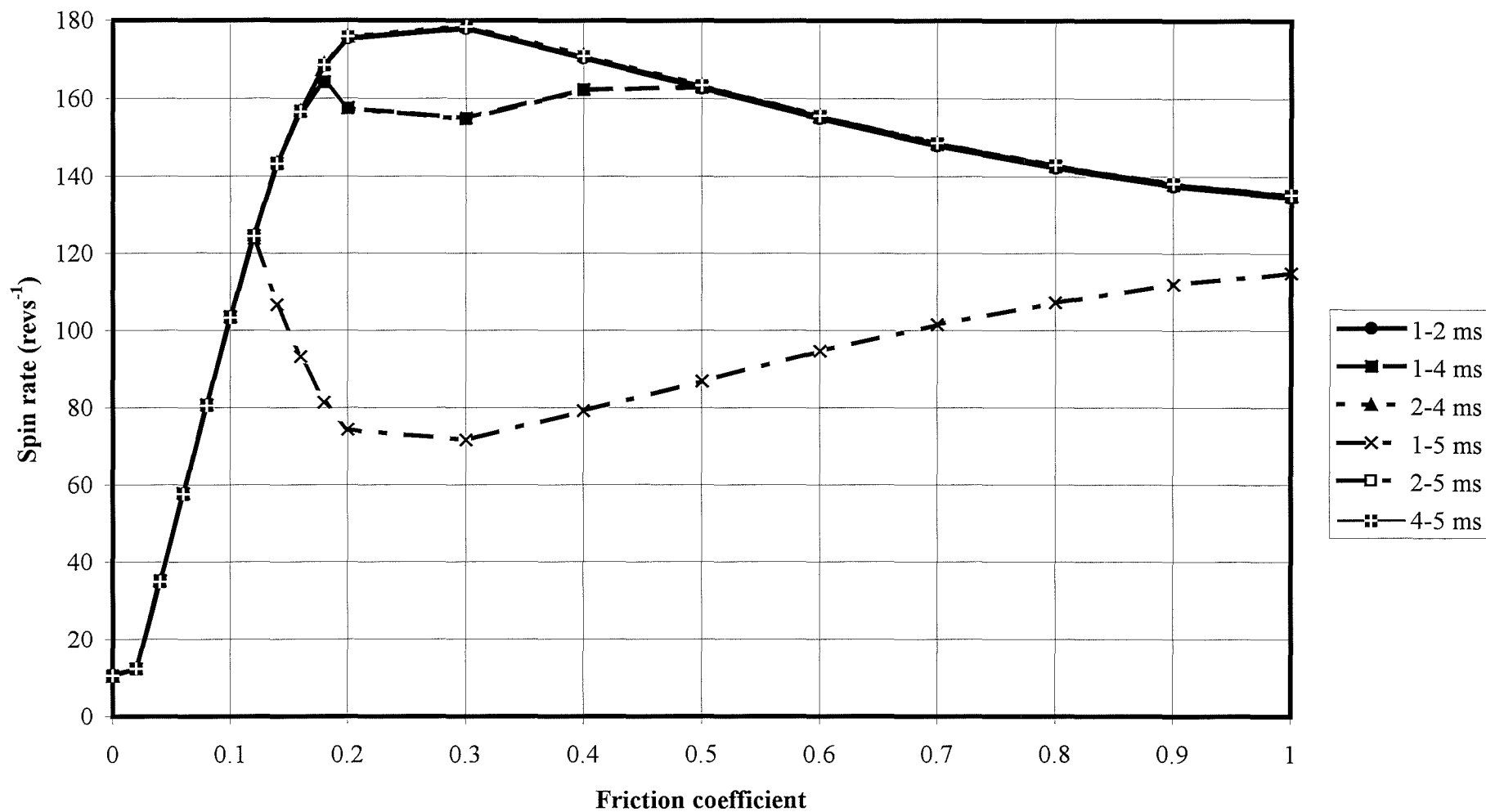


Figure 4.21 Effect of friction on ball spin, averaged over various integrating periods.

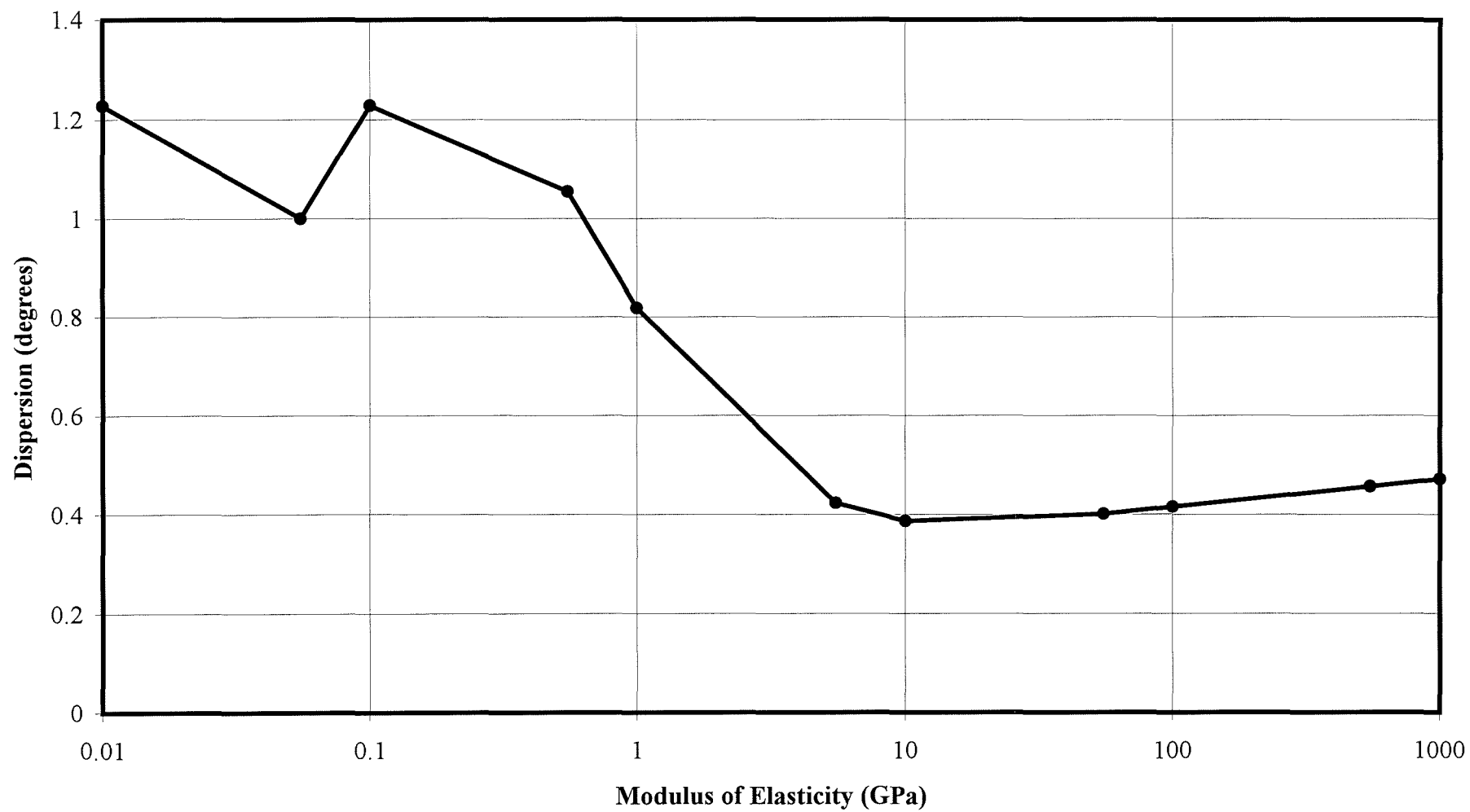


Figure 4.22 Effect of modulus on ball dispersion.

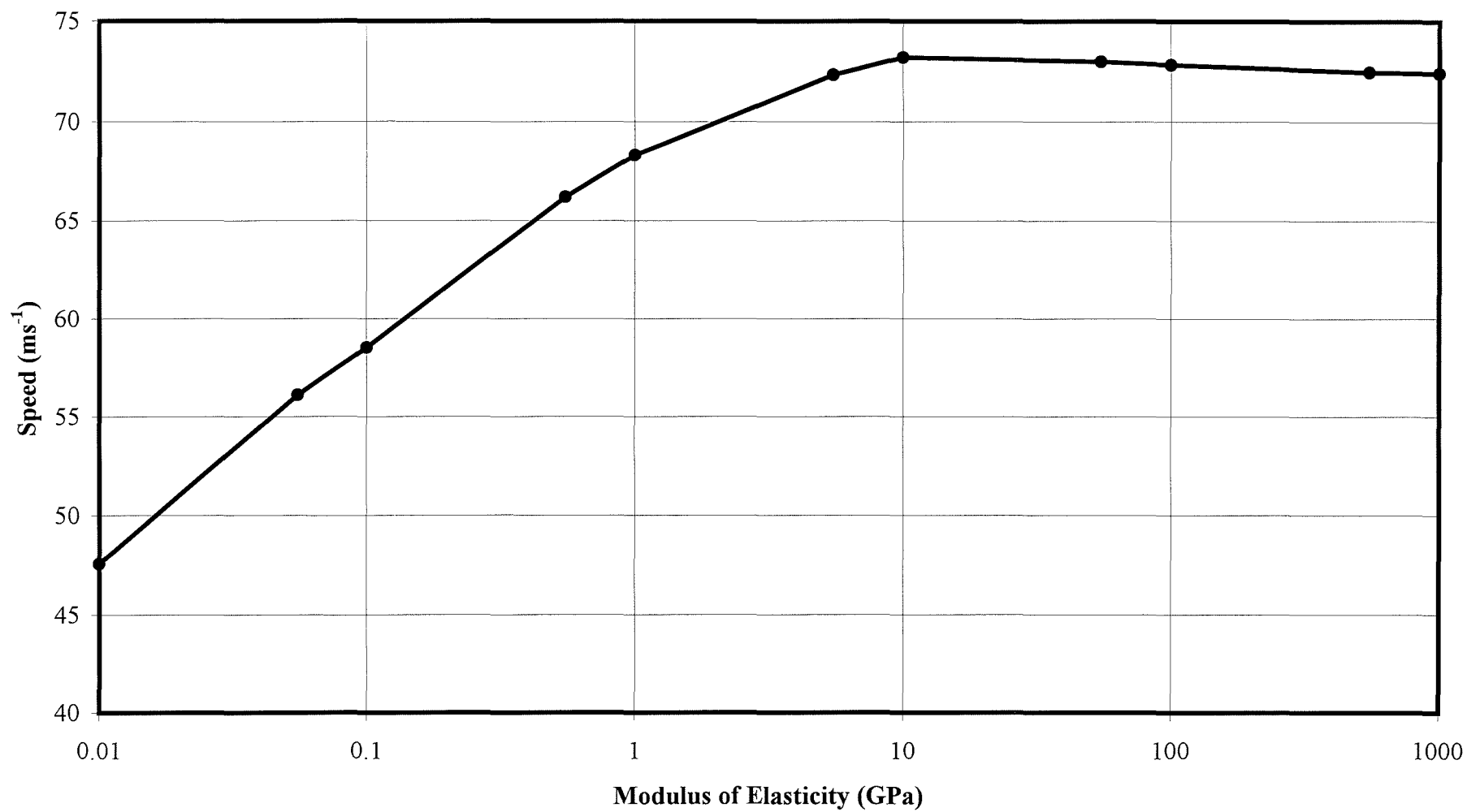


Figure 4.23 Effect of modulus on ball speed.

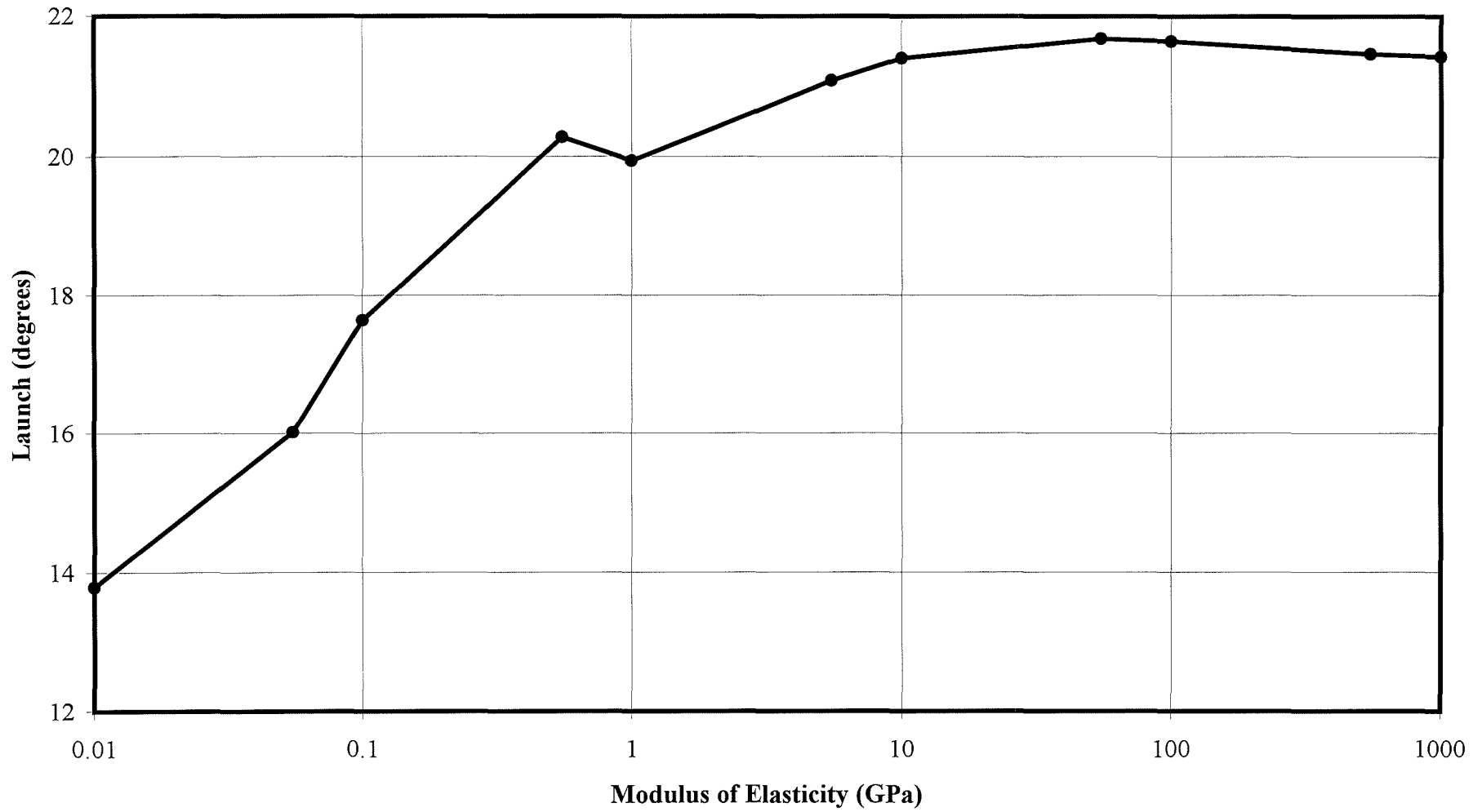


Figure 4.24 Effect of modulus on ball launch.

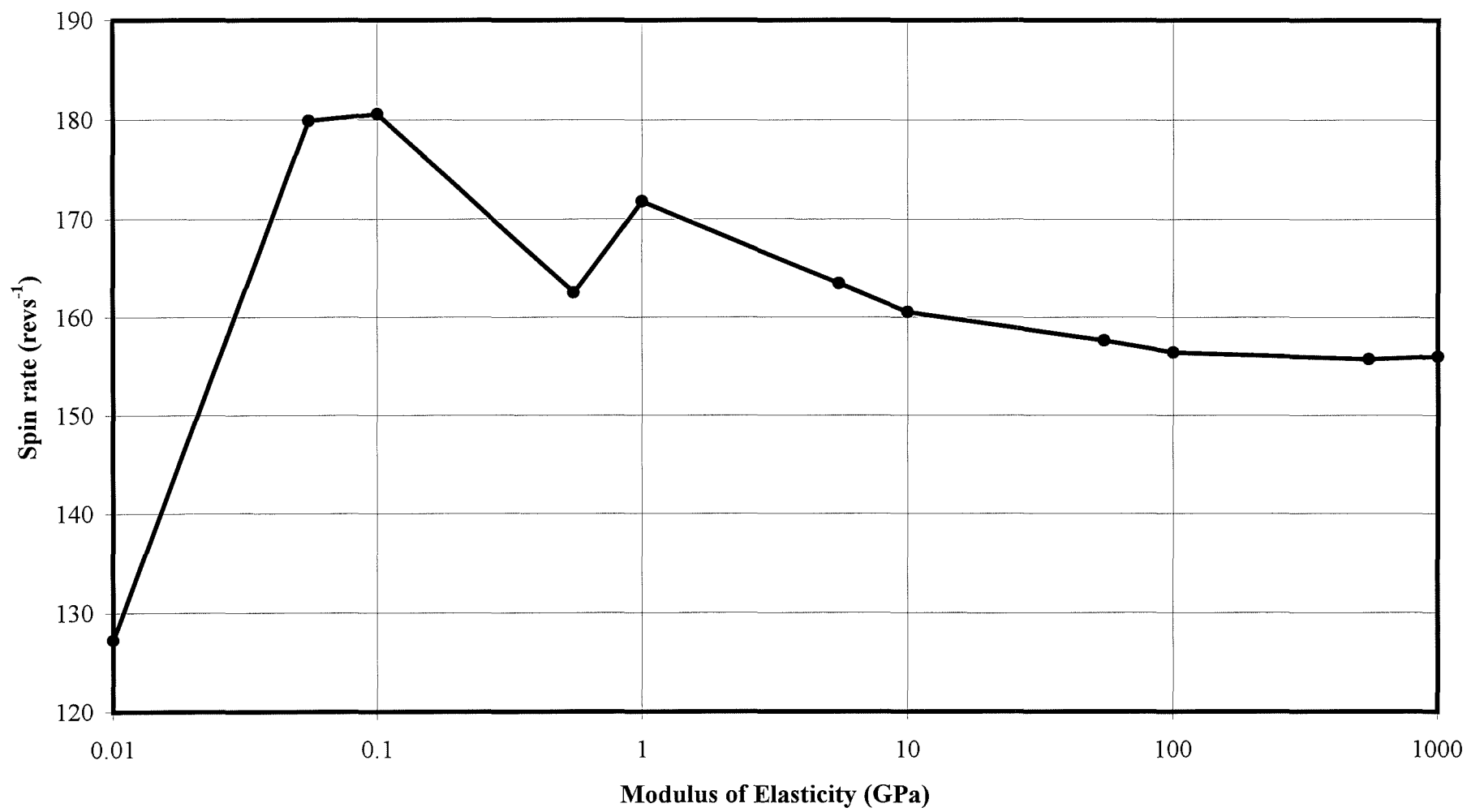


Figure 4.25 Effect of modulus on ball spin.

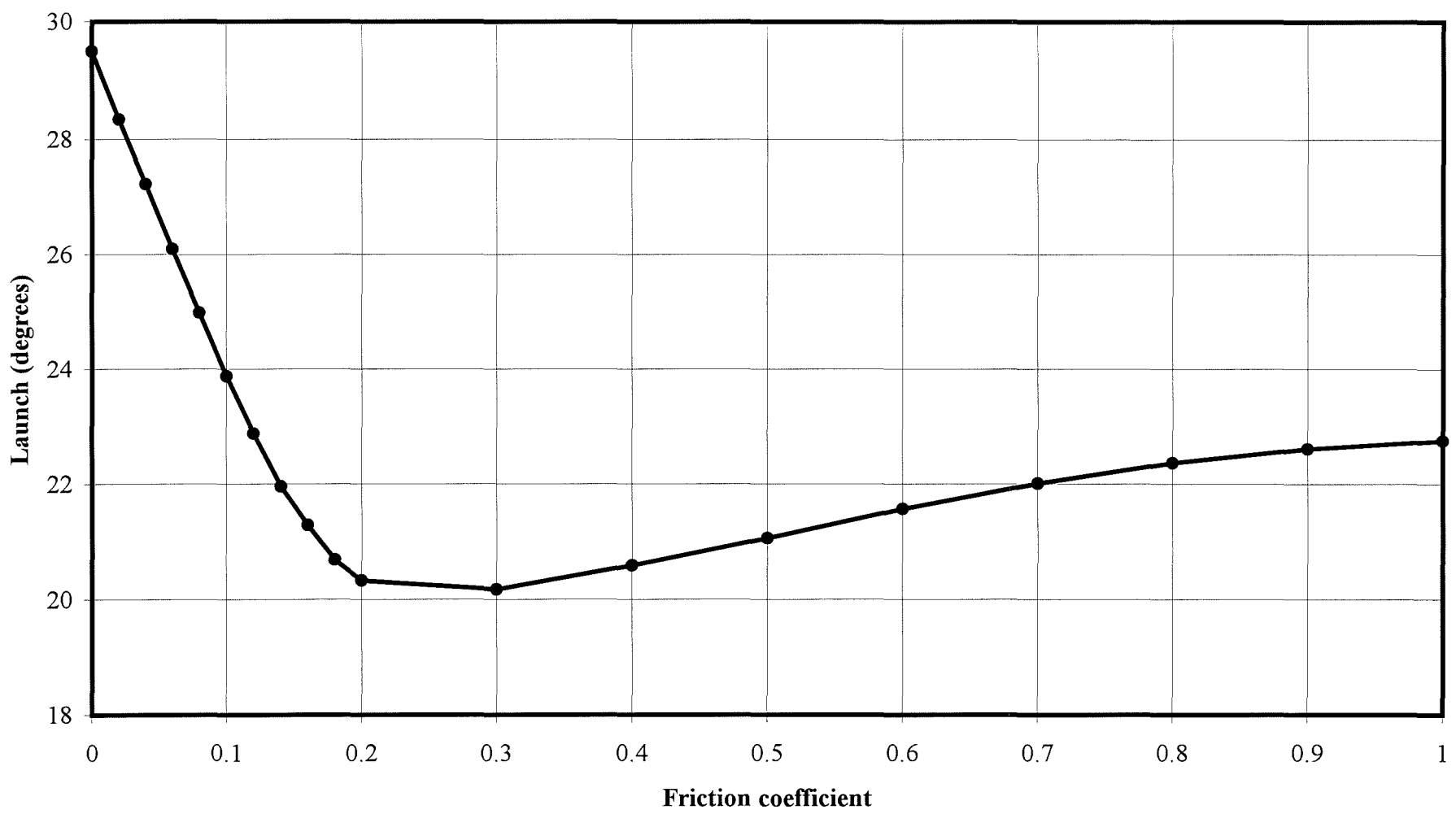


Figure 4.26 Effect of friction on ball launch.

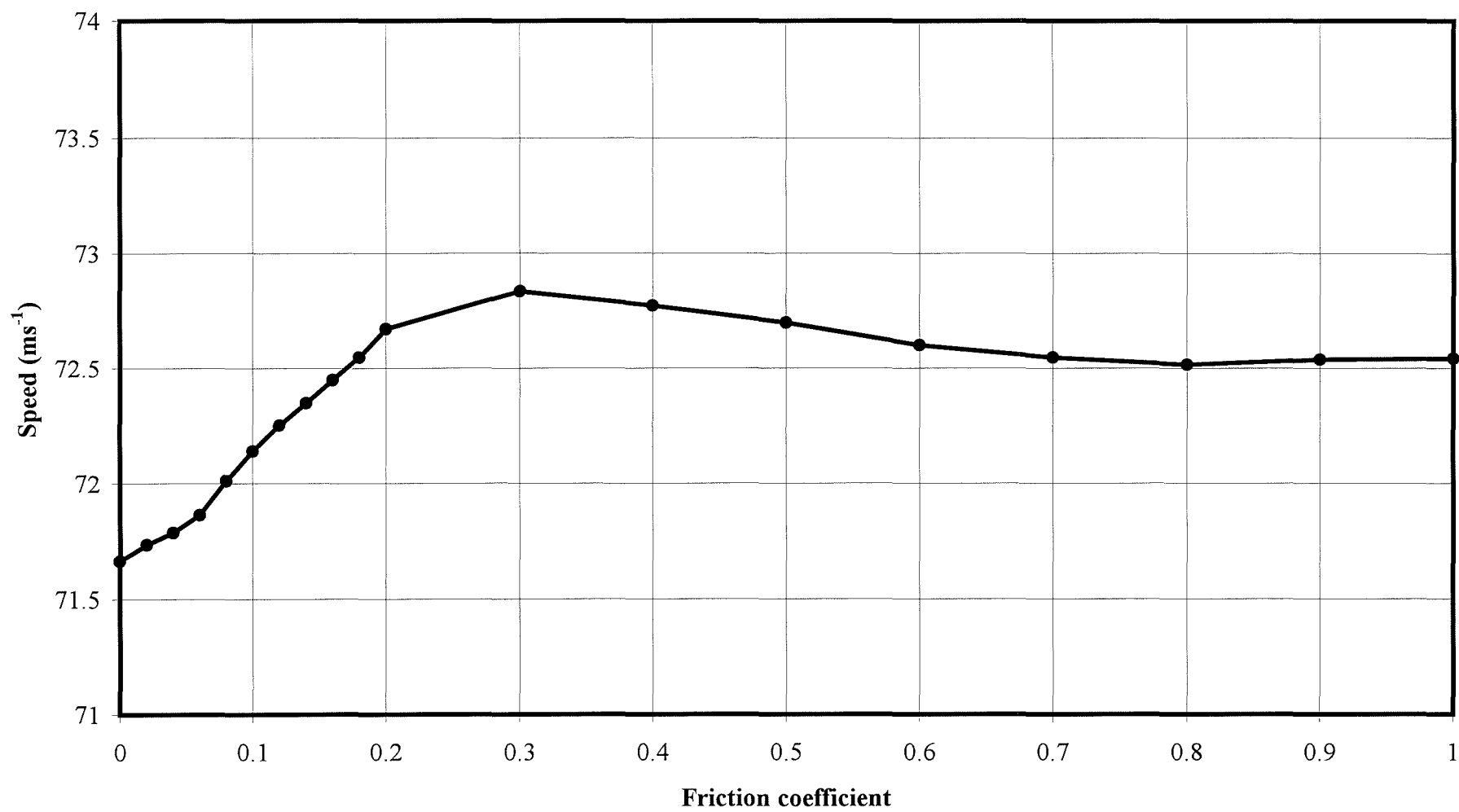


Figure 4.27 Effect of friction on ball speed.

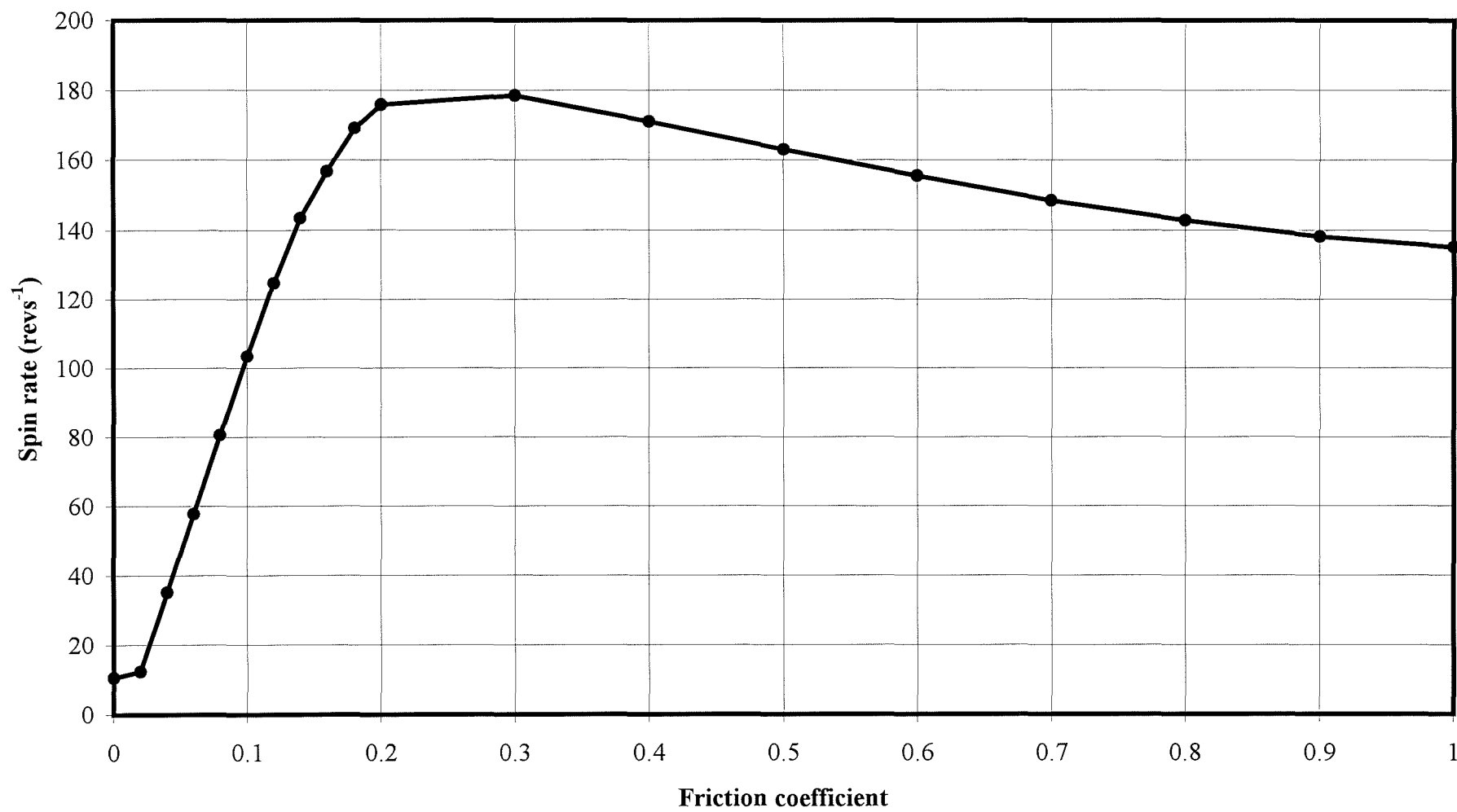


Figure 4.28 Effect of friction on ball spin.

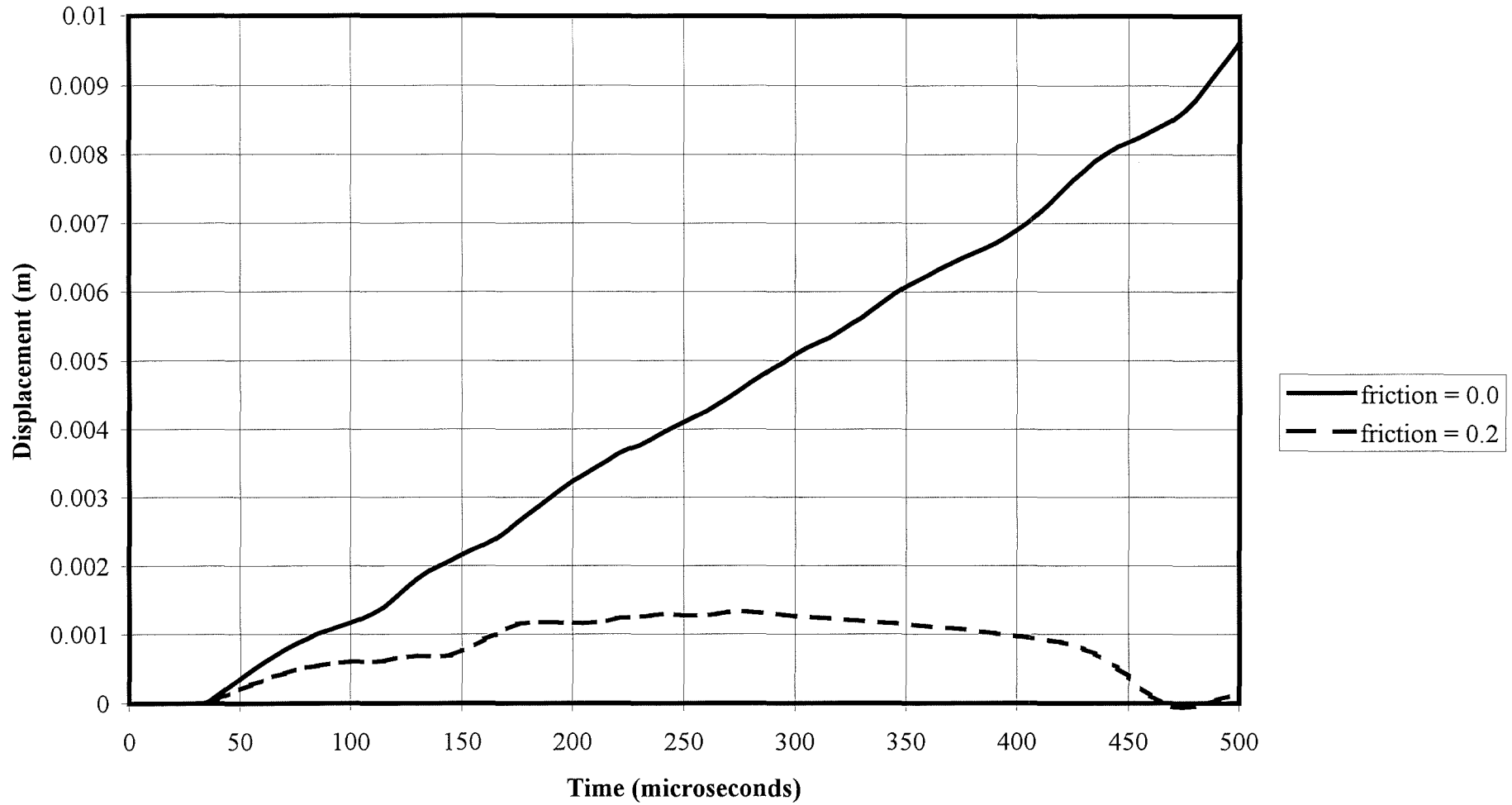


Figure 4.29 Sliding of ball on clubhead.

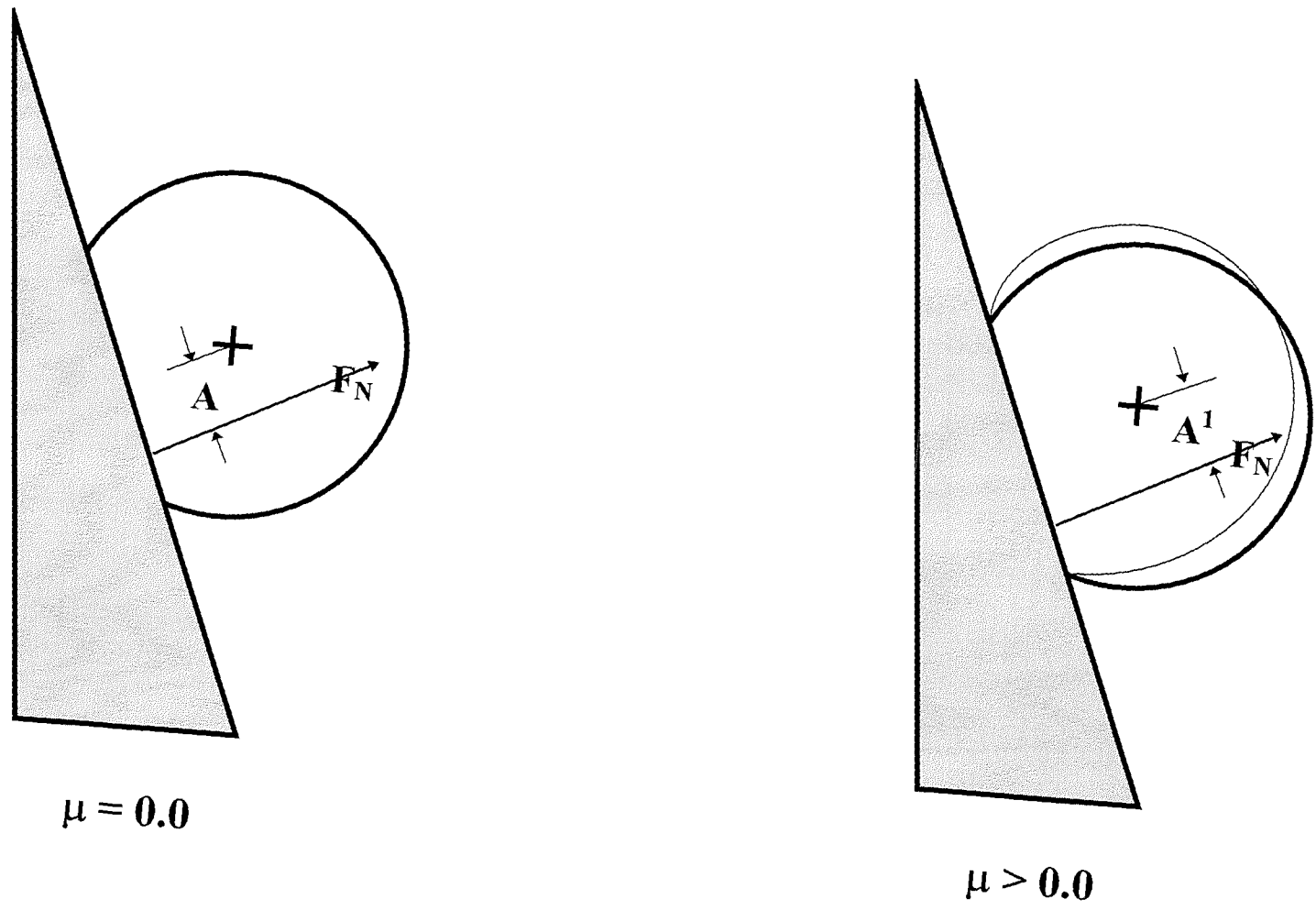


Figure 4.30 Turning moment arm about centre of mass.

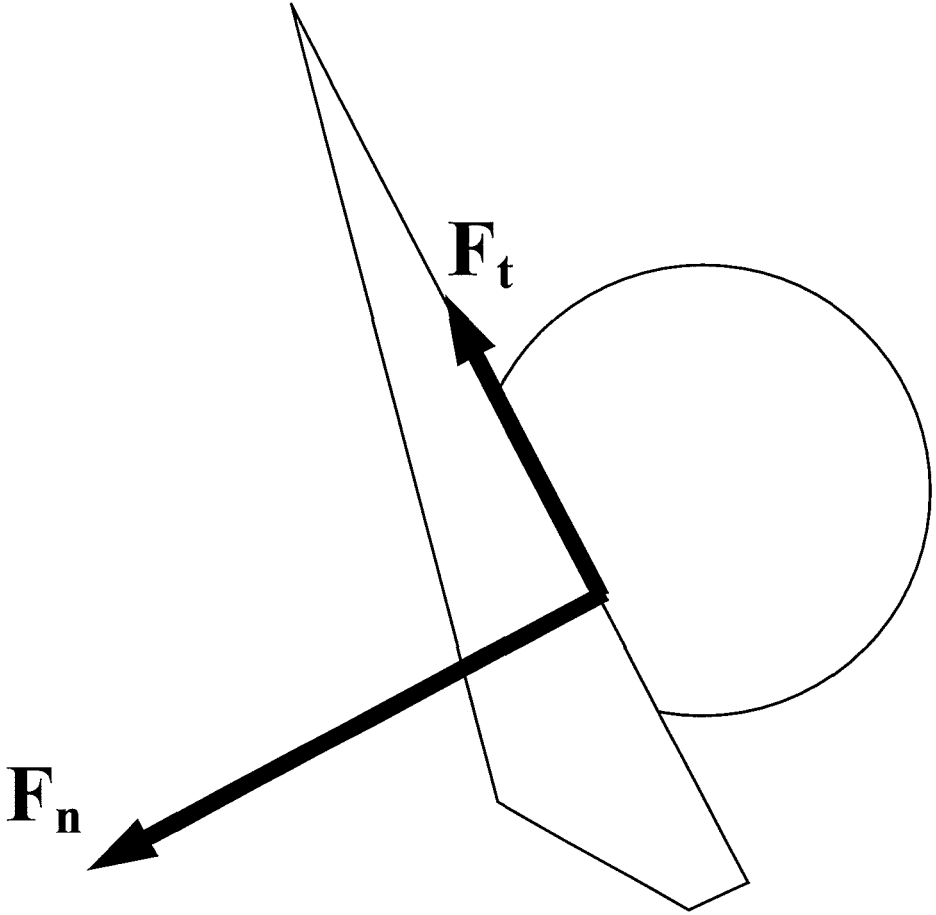


Figure 4.31 Positive tangential (F_t) and normal (F_n) force components on clubhead.

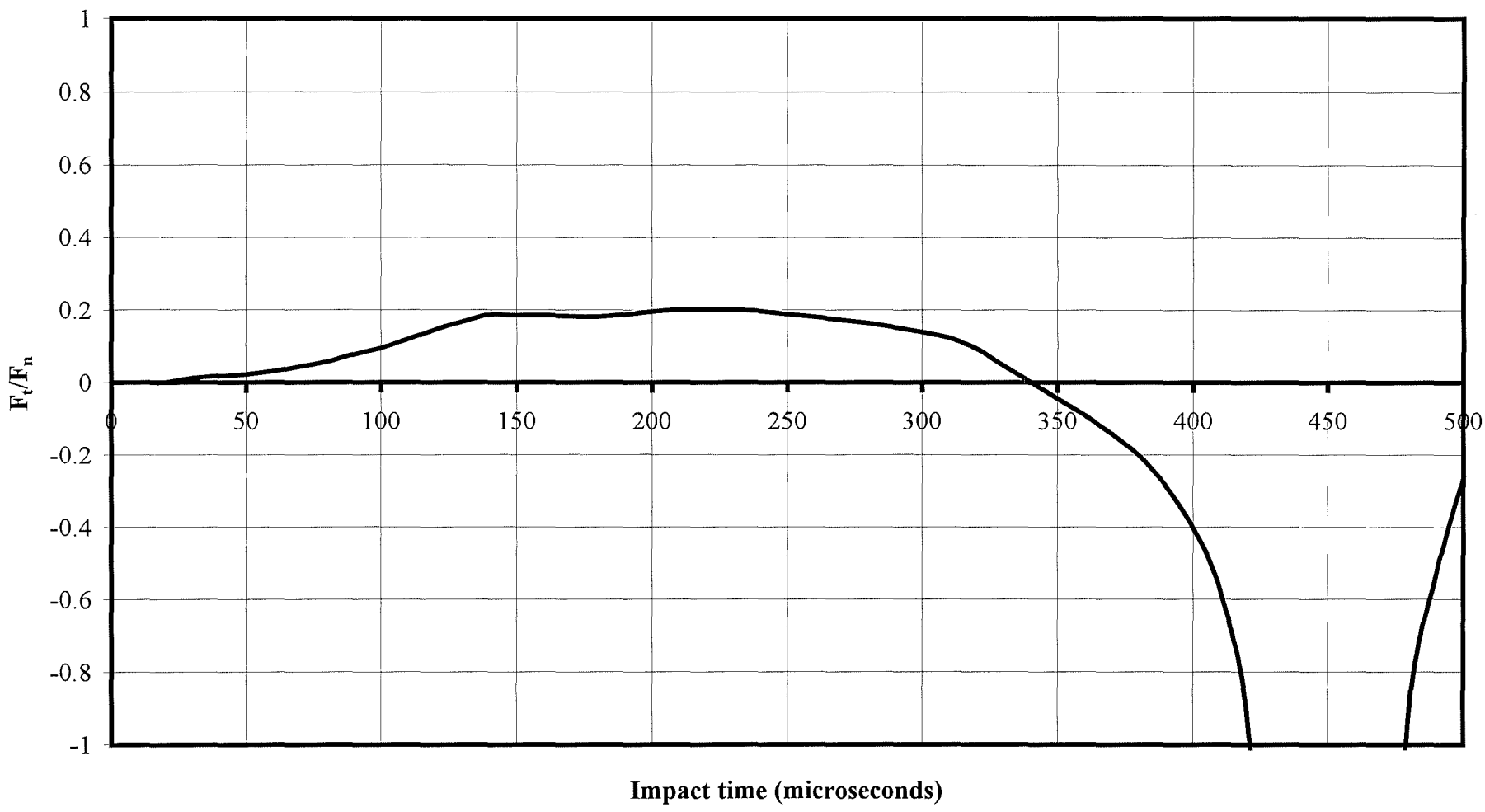


Figure 4.32 Calculation of F_t/F_n from Gobush (1990) results.

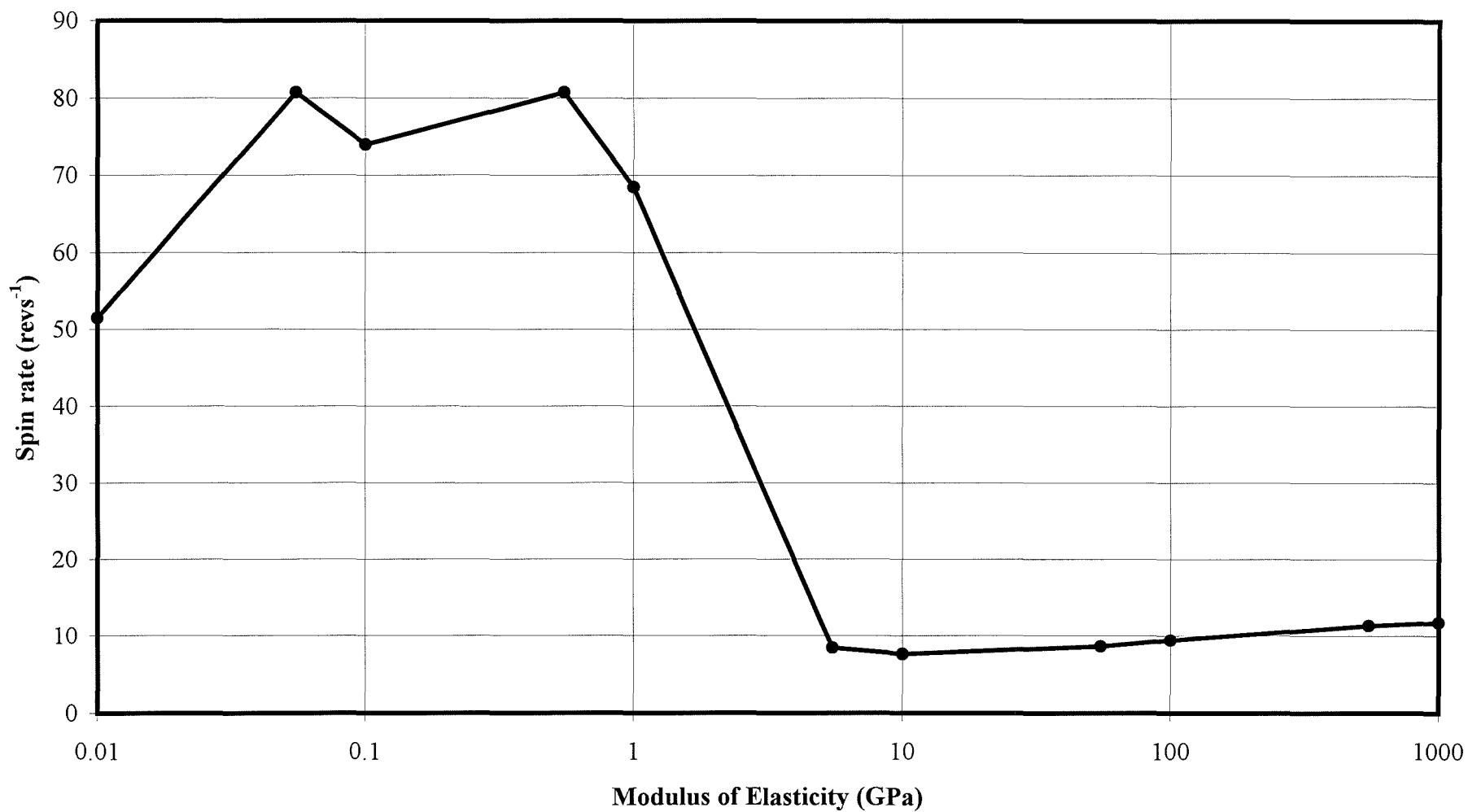


Figure 4.33 Effect of modulus on ball spin, zero friction.

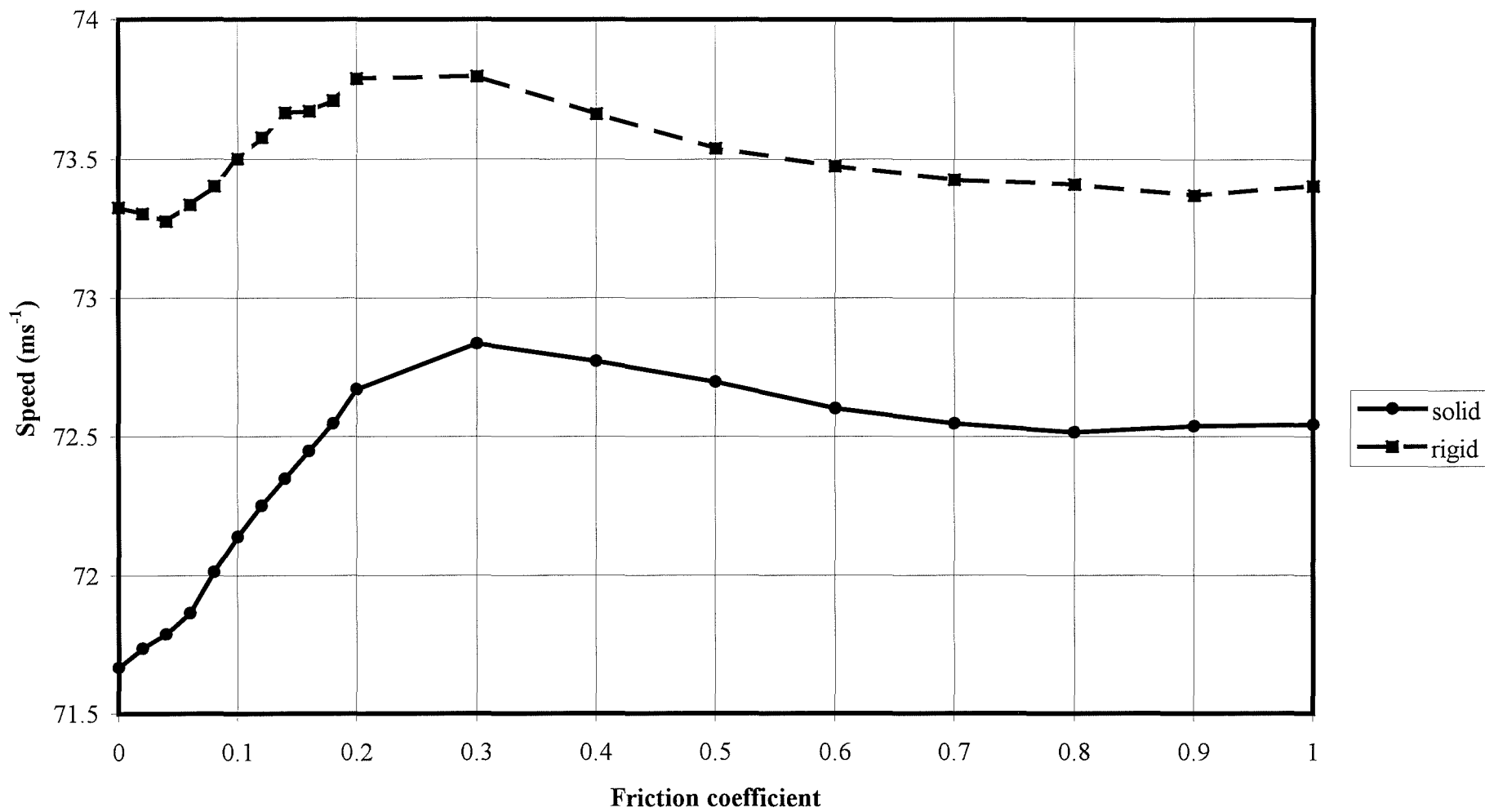


Figure 4.34 Effect of friction on ball speed, rigid and solid.

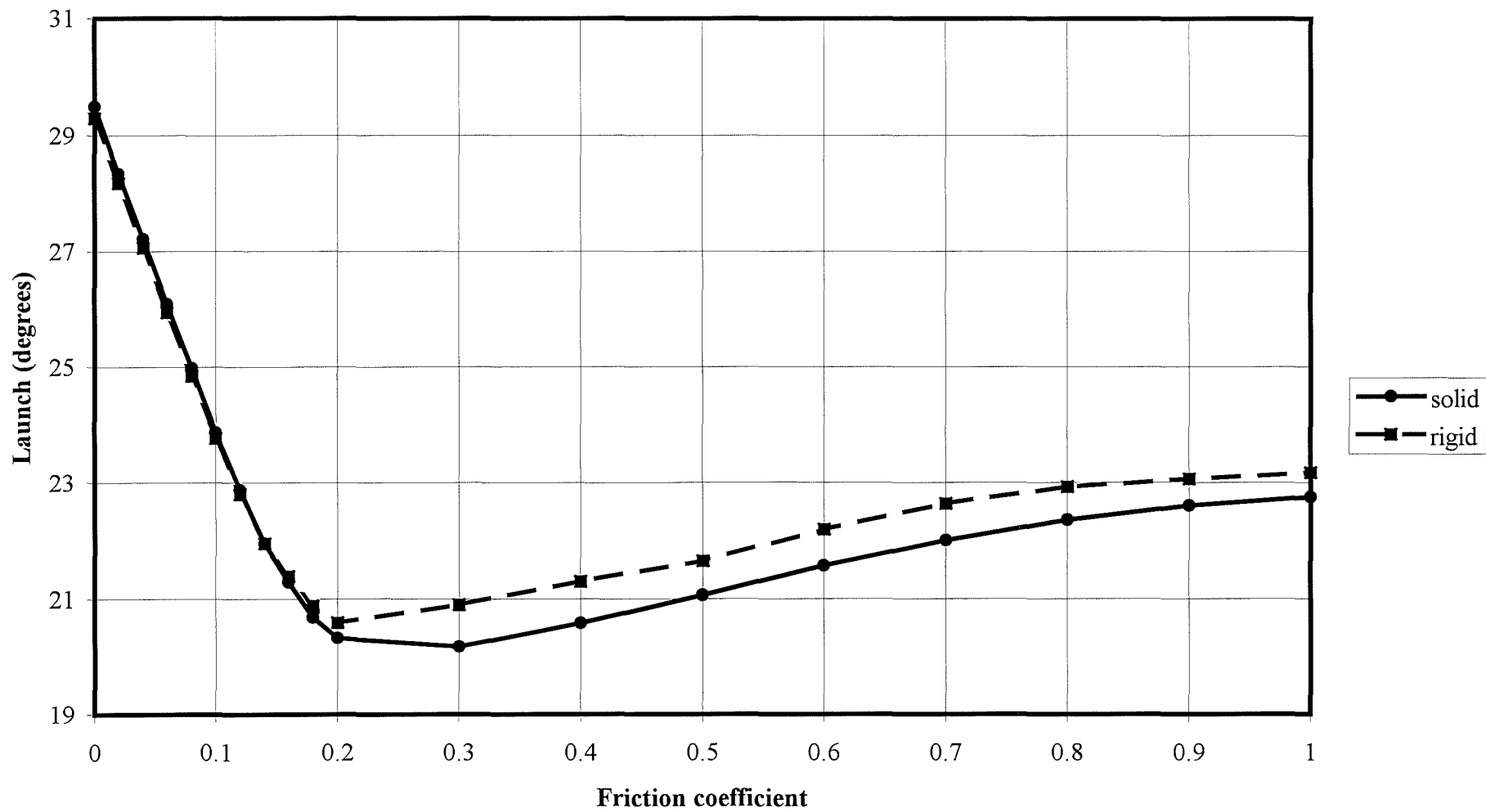


Figure 4.35 Effect of friction on ball launch, rigid and solid.

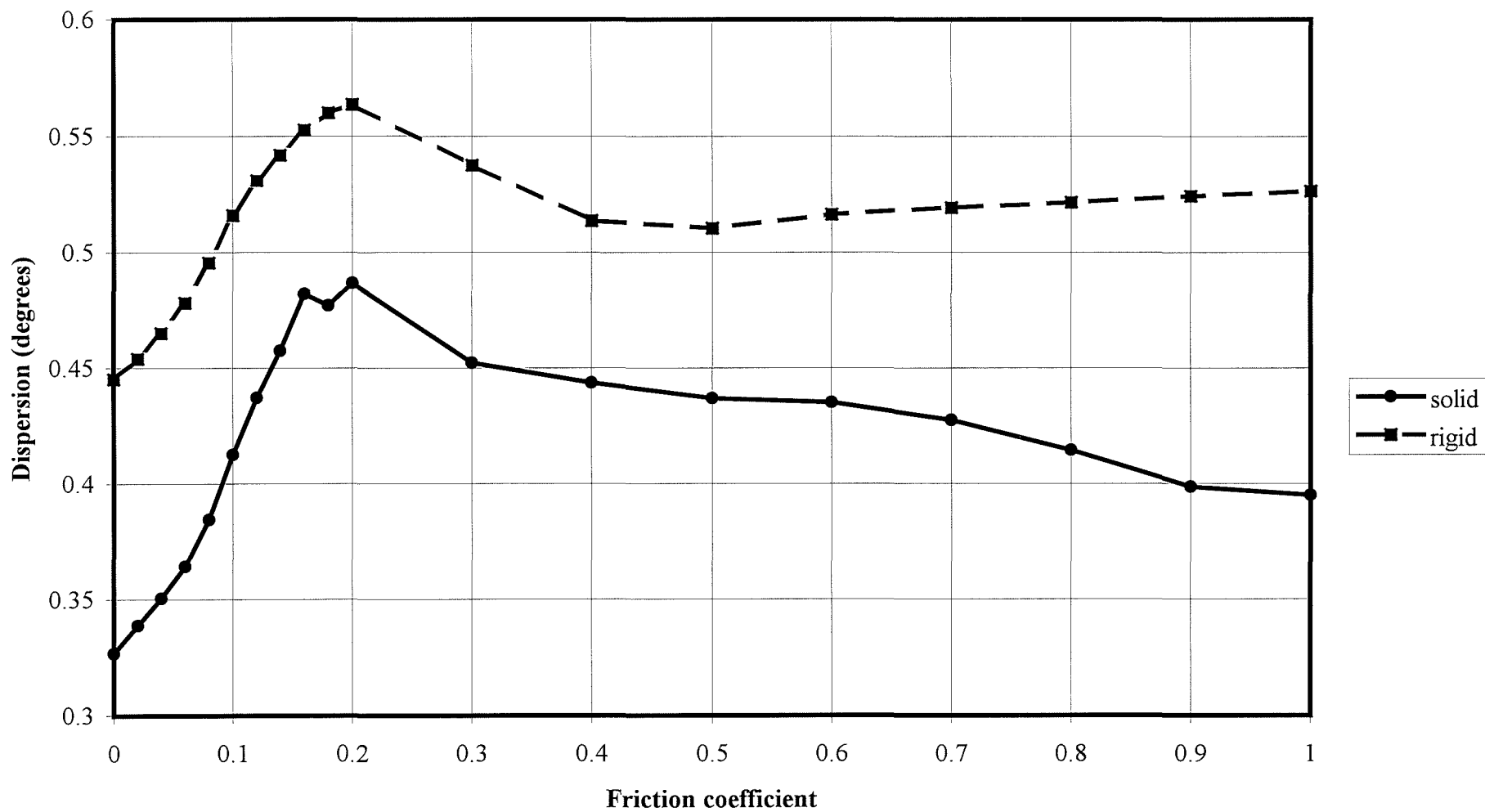


Figure 4.36 Effect of friction on ball dispersion, rigid and solid.

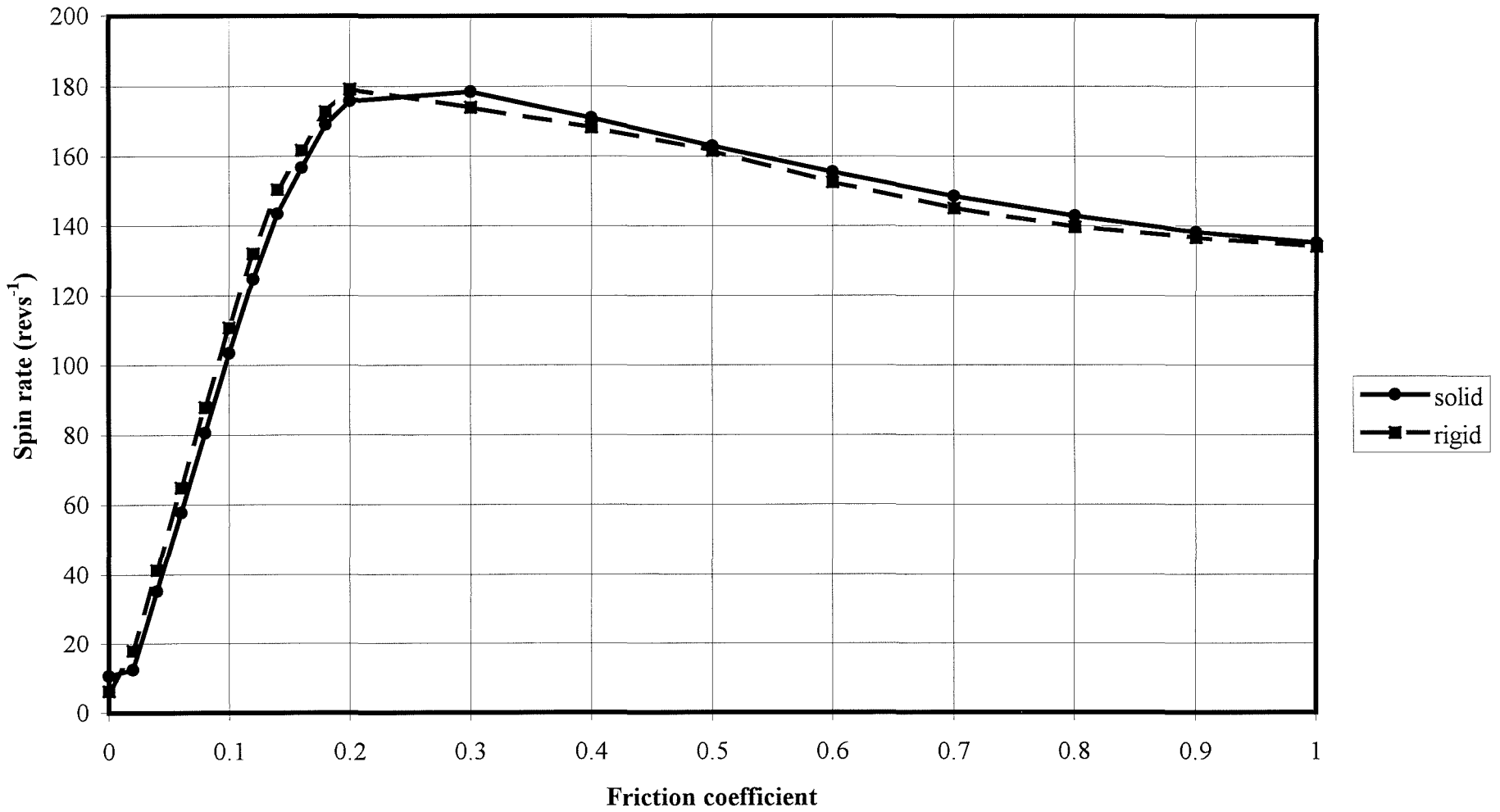


Figure 4.37 Effect of friction on ball spin, rigid and solid.

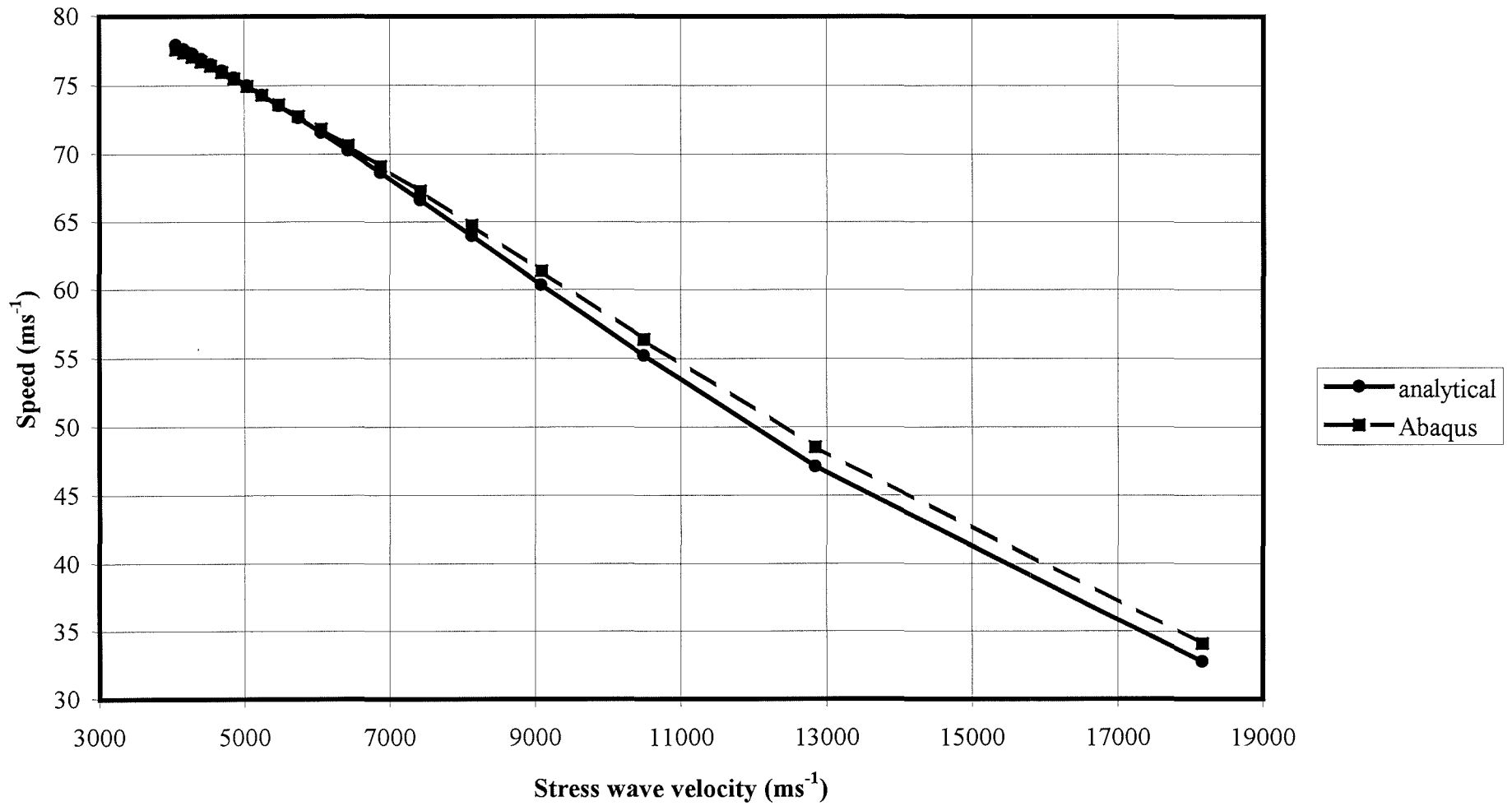


Figure 4.38 Effect of stress wave velocity on ball speed.

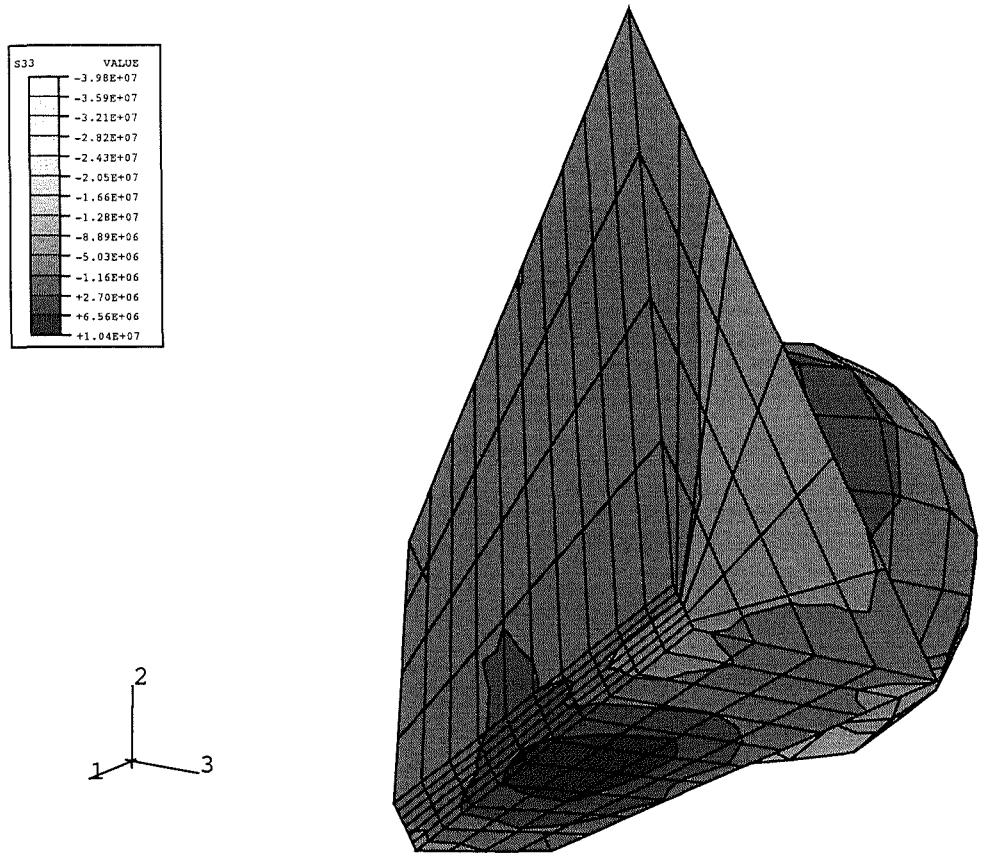


Figure 4.39 σ_{33} contour plot of underneath of solid clubhead, at 0.210 ms.

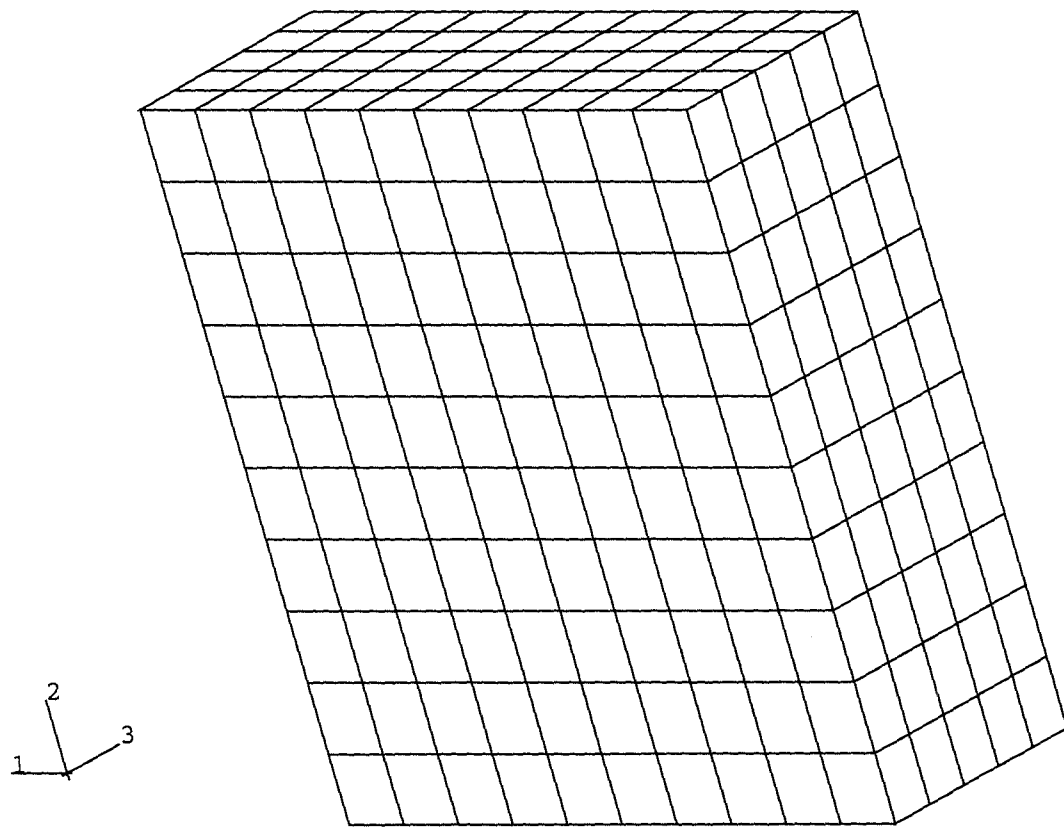


Figure 4.40 Clubhead back design, A-flat.

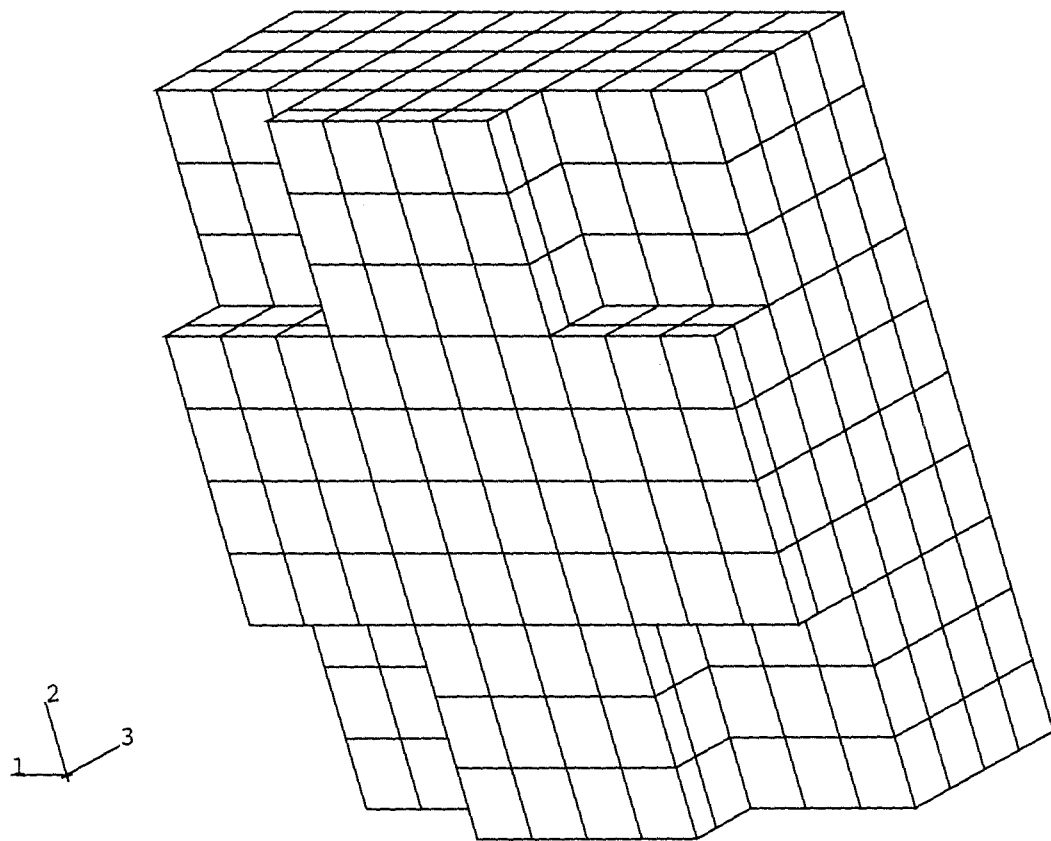


Figure 4.41 Clubhead back design, B-raised cross.

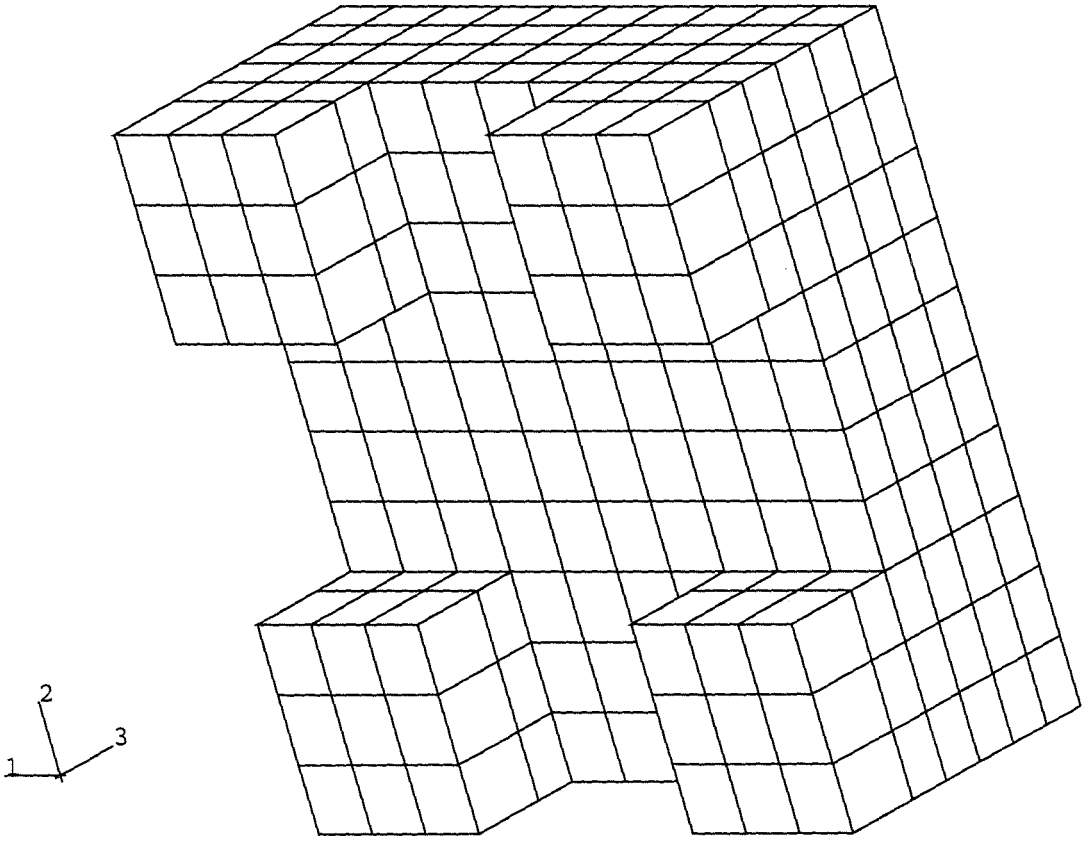


Figure 4.42 Clubhead back design, C-indented cross.

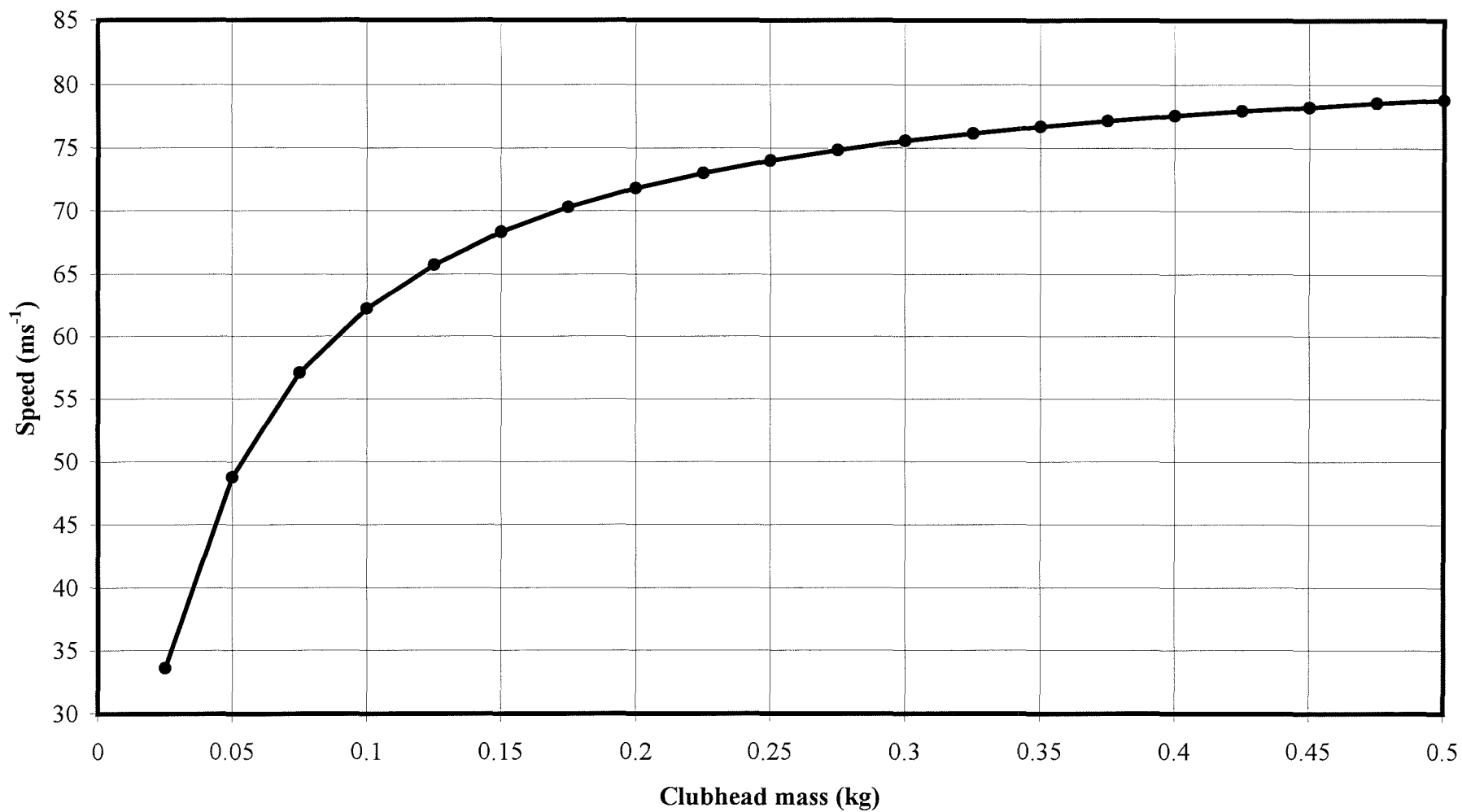


Figure 4.43 Effect of clubhead mass on ball speed.

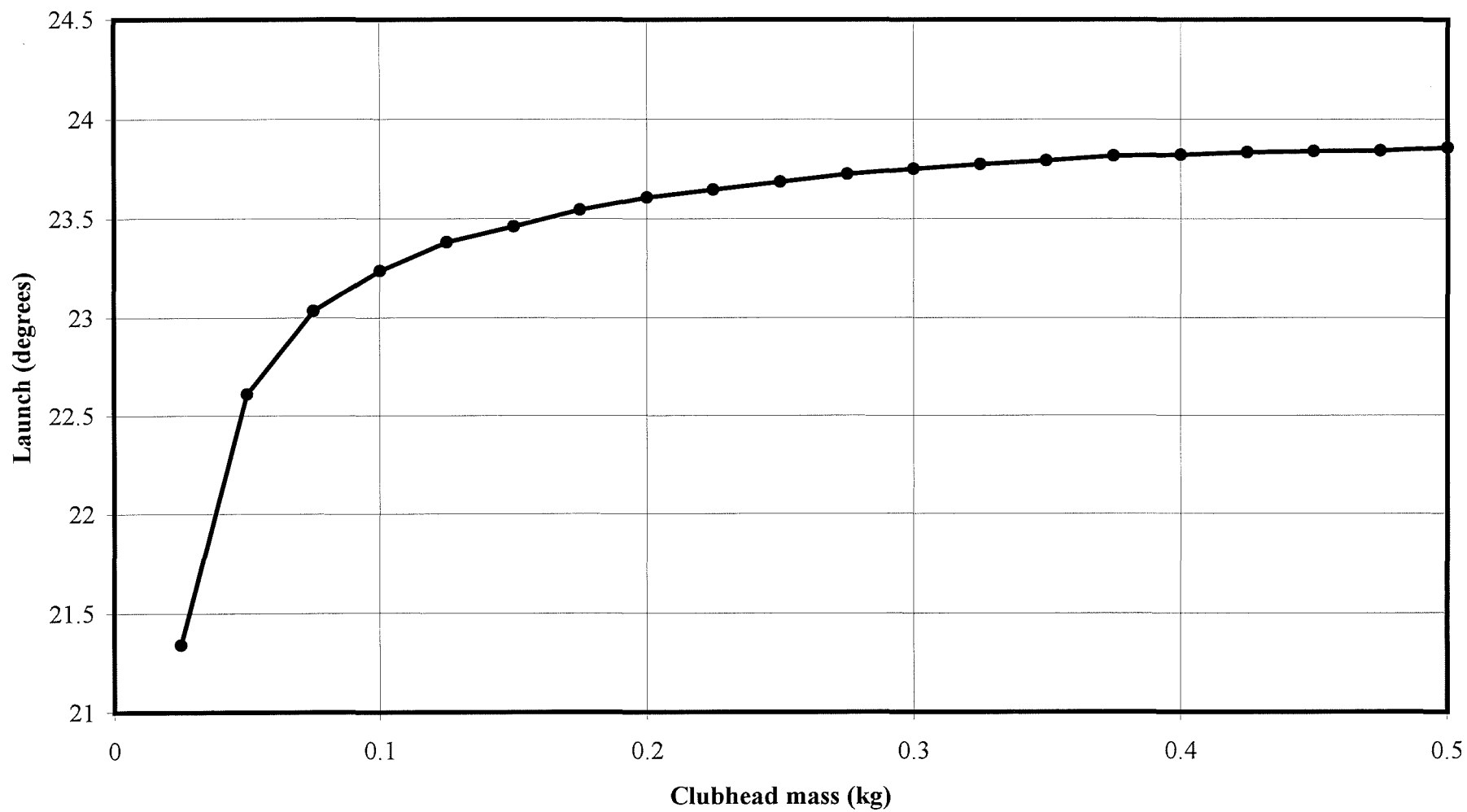


Figure 4.44 Effect of clubhead mass on ball launch.

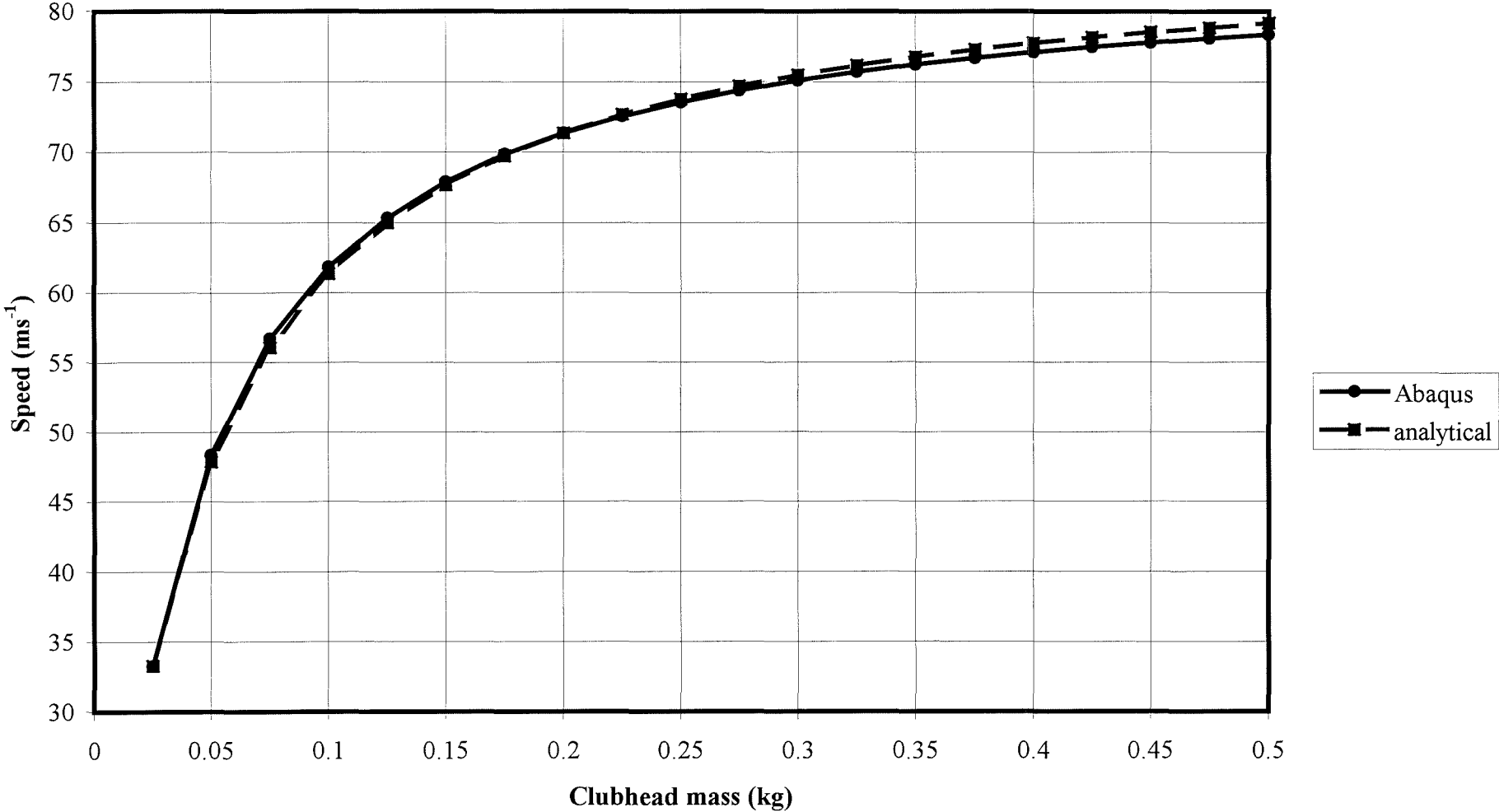


Figure 4.45 Effect of clubhead mass on ball normalised velocity. Abaqus and analytical.

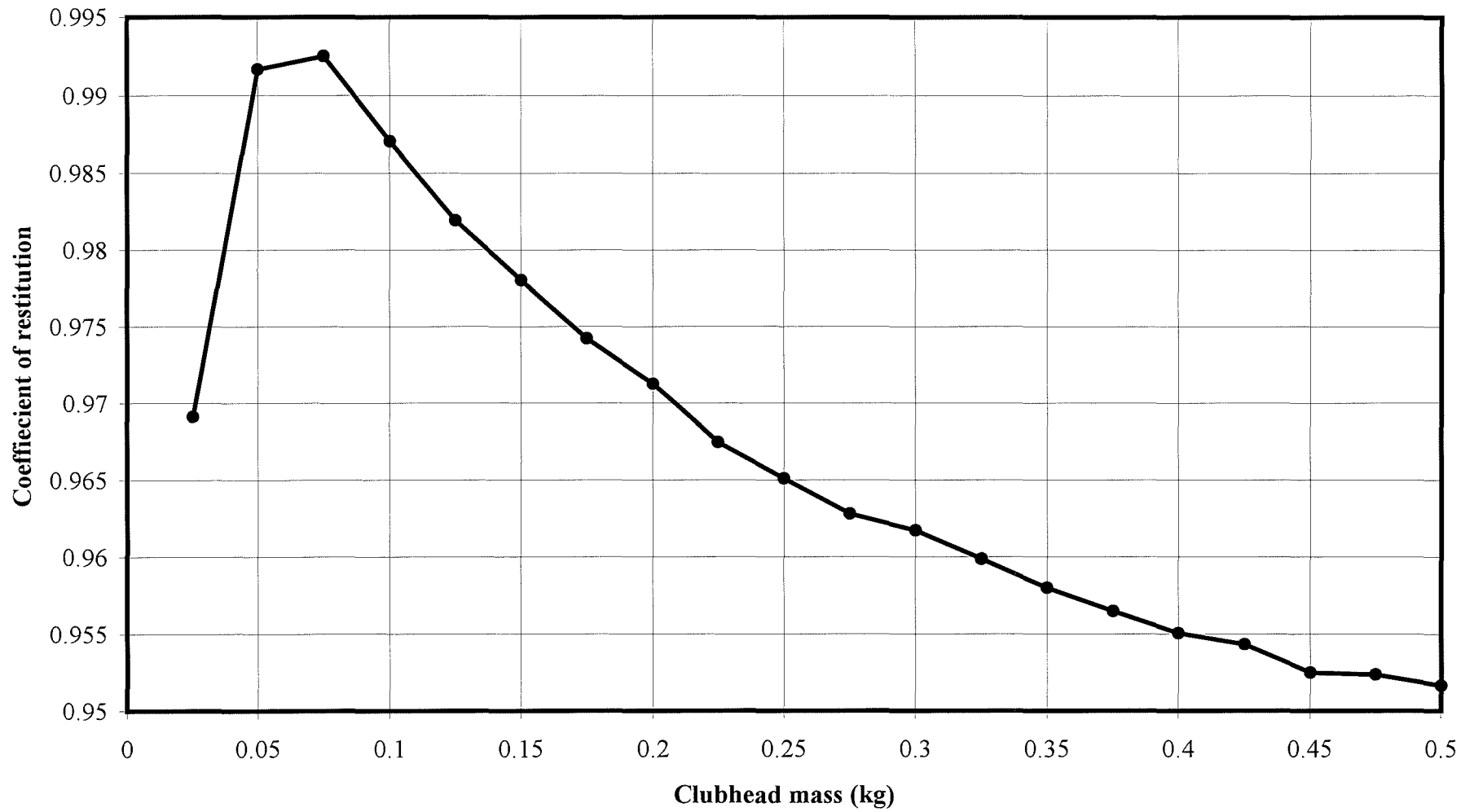


Figure 4.46 Effect of clubhead mass on effective coefficient of restitution for Abaqus.

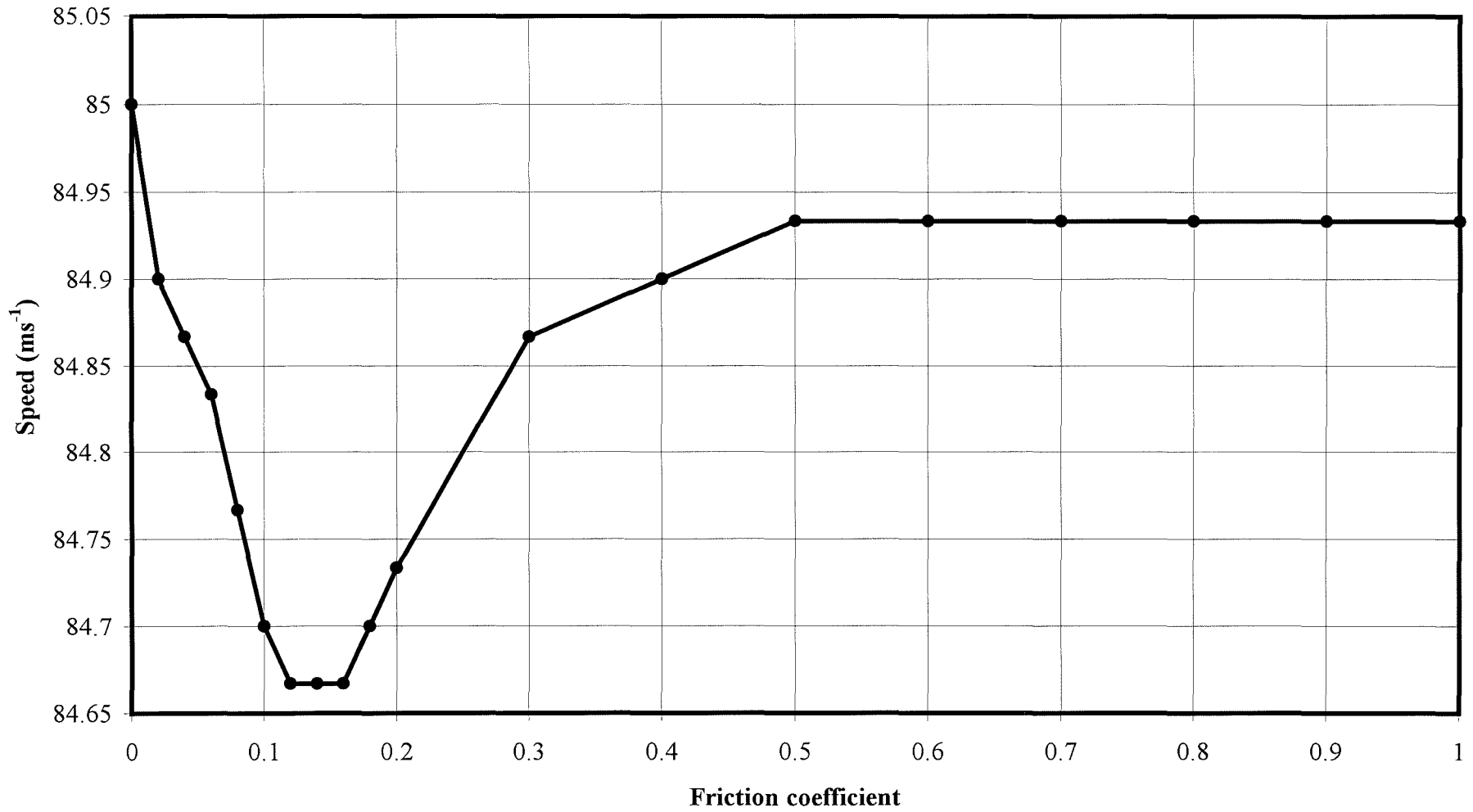


Figure 4.47 Effect of friction on ball speed, 00° loft.

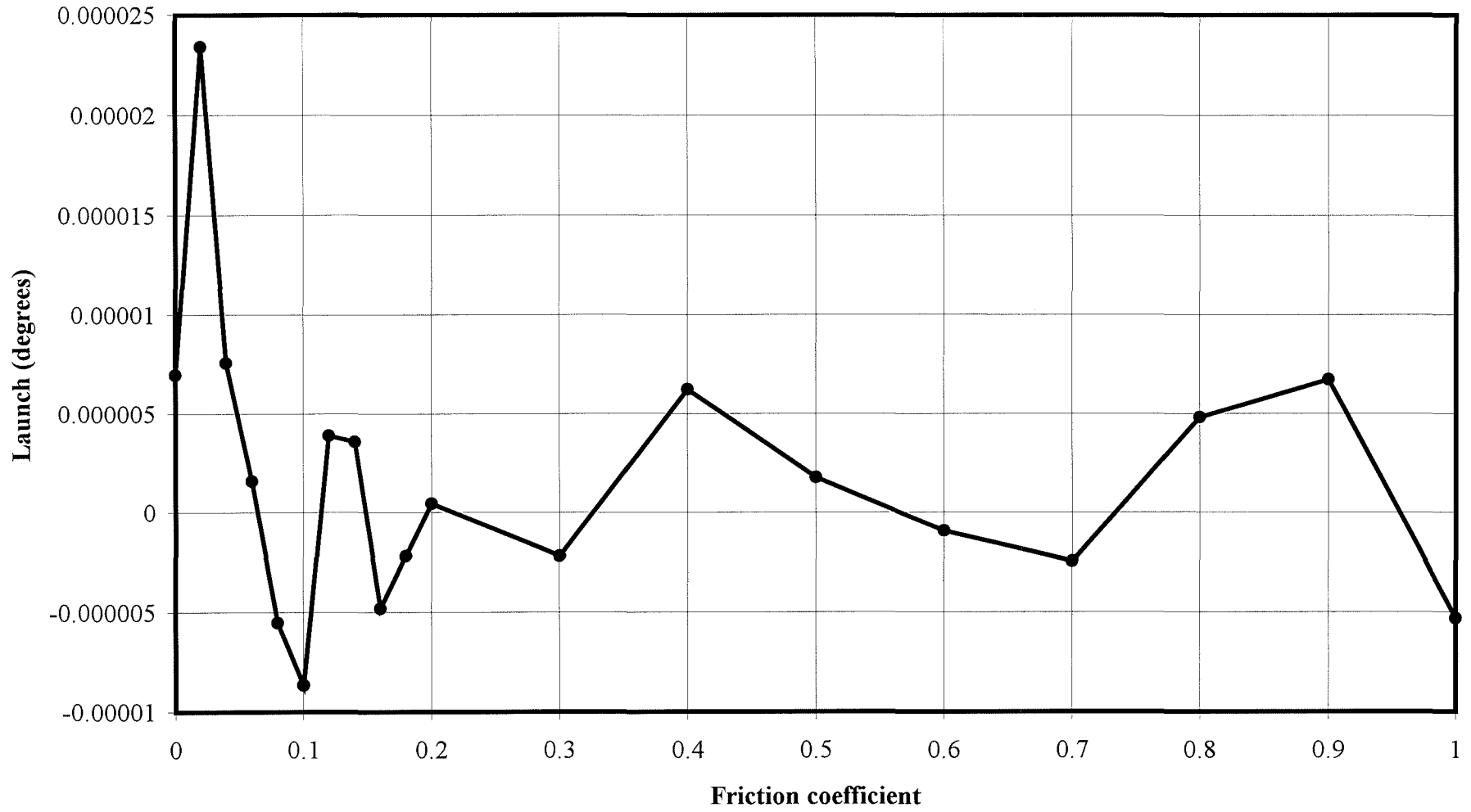


Figure 4.48 Effect of friction on ball launch, 00° loft.

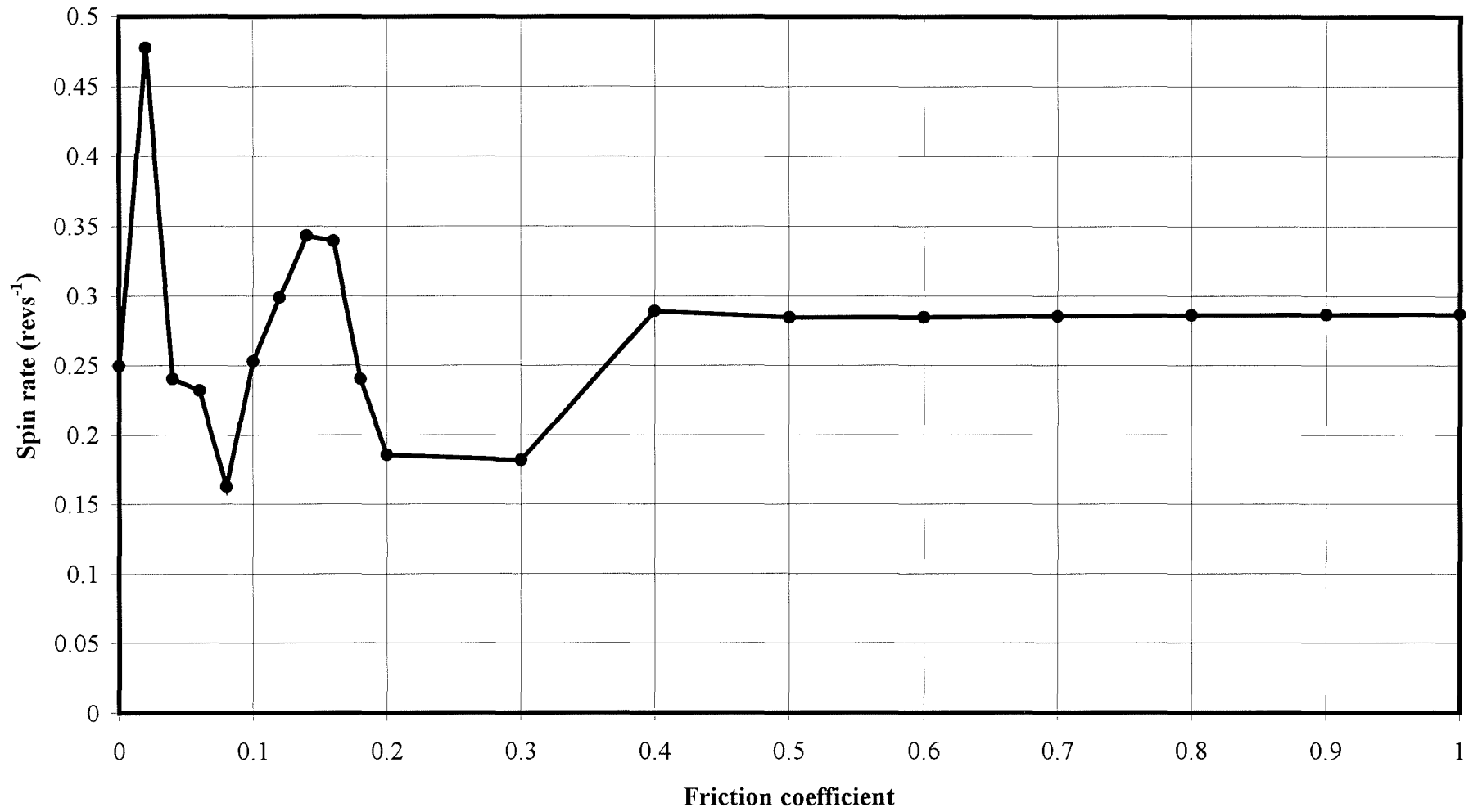


Figure 4.49 Effect of friction on ball spin, 00° loft.

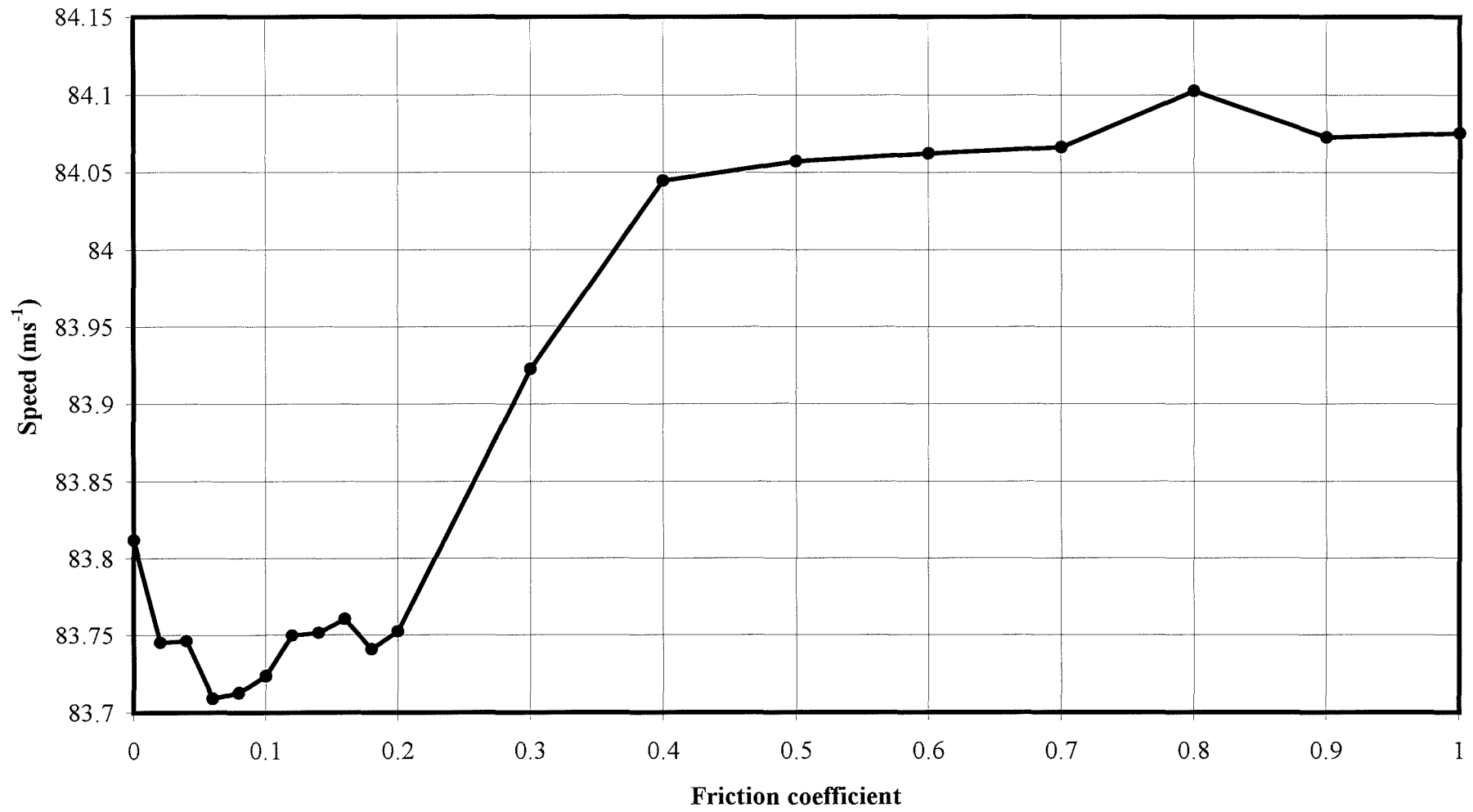


Figure 4.50 Effect of friction on ball speed, 10° loft.

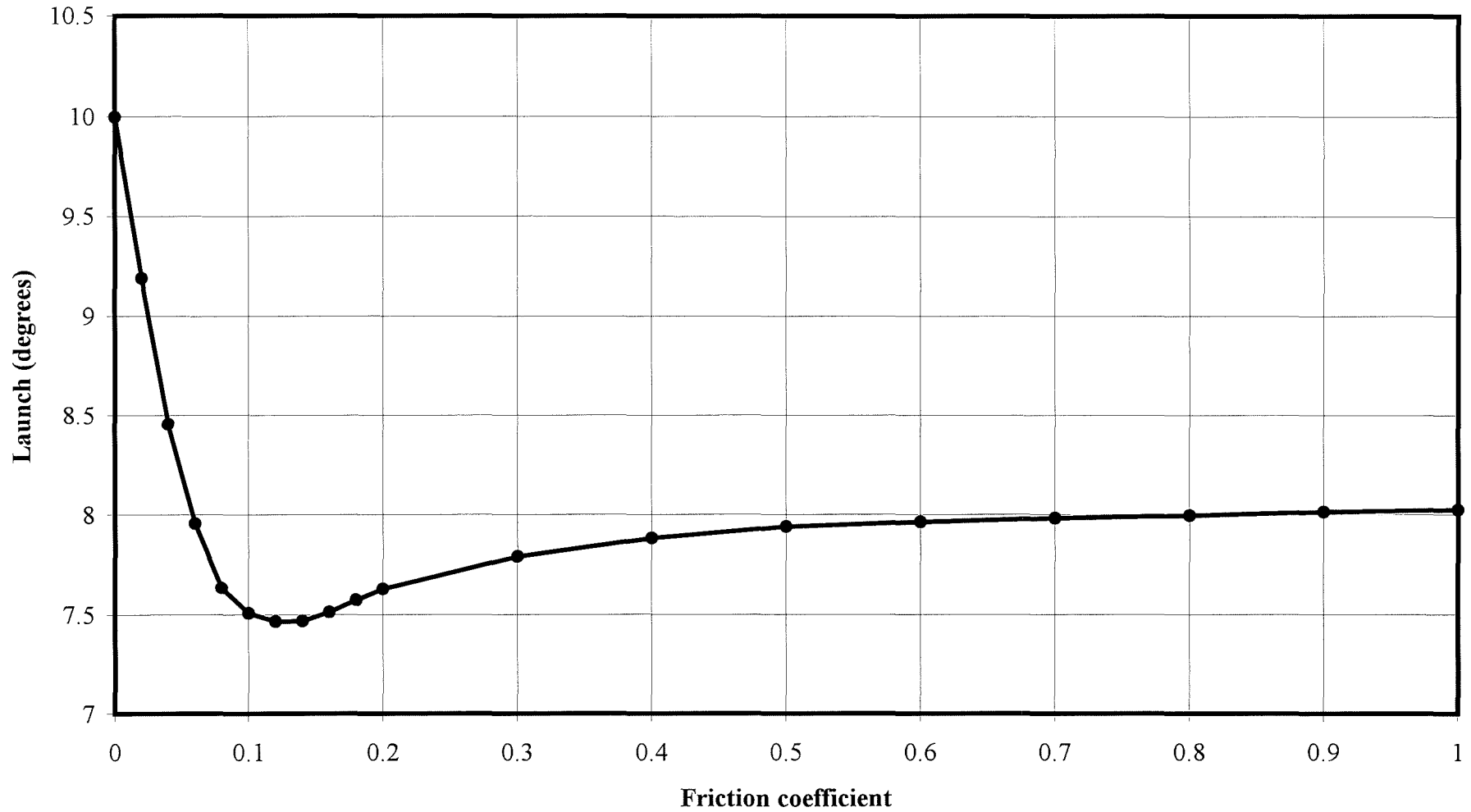


Figure 4.51 Effect of friction on ball launch, 10° loft.

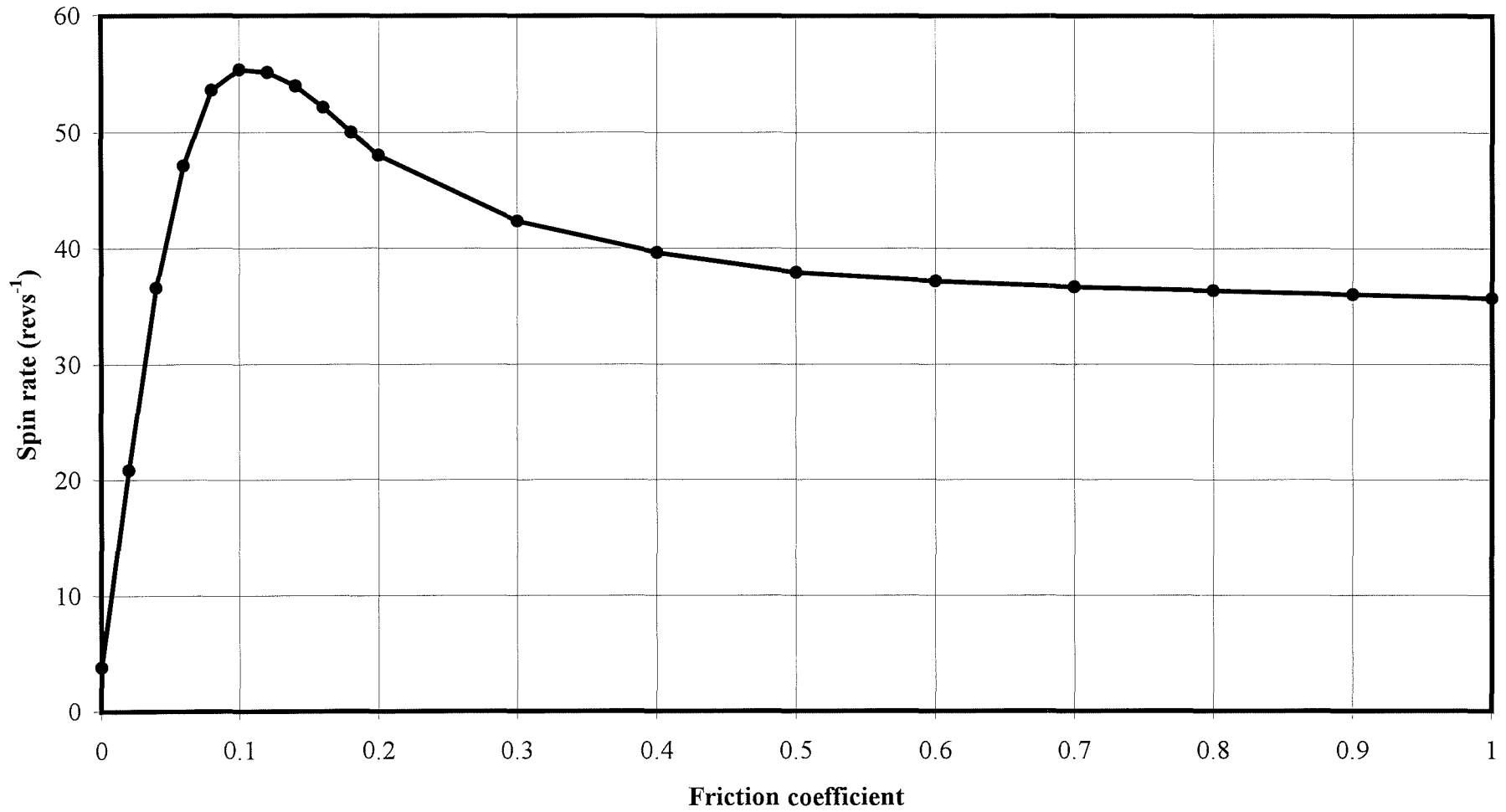


Figure 4.52 Effect of friction on ball spin, 10° loft.

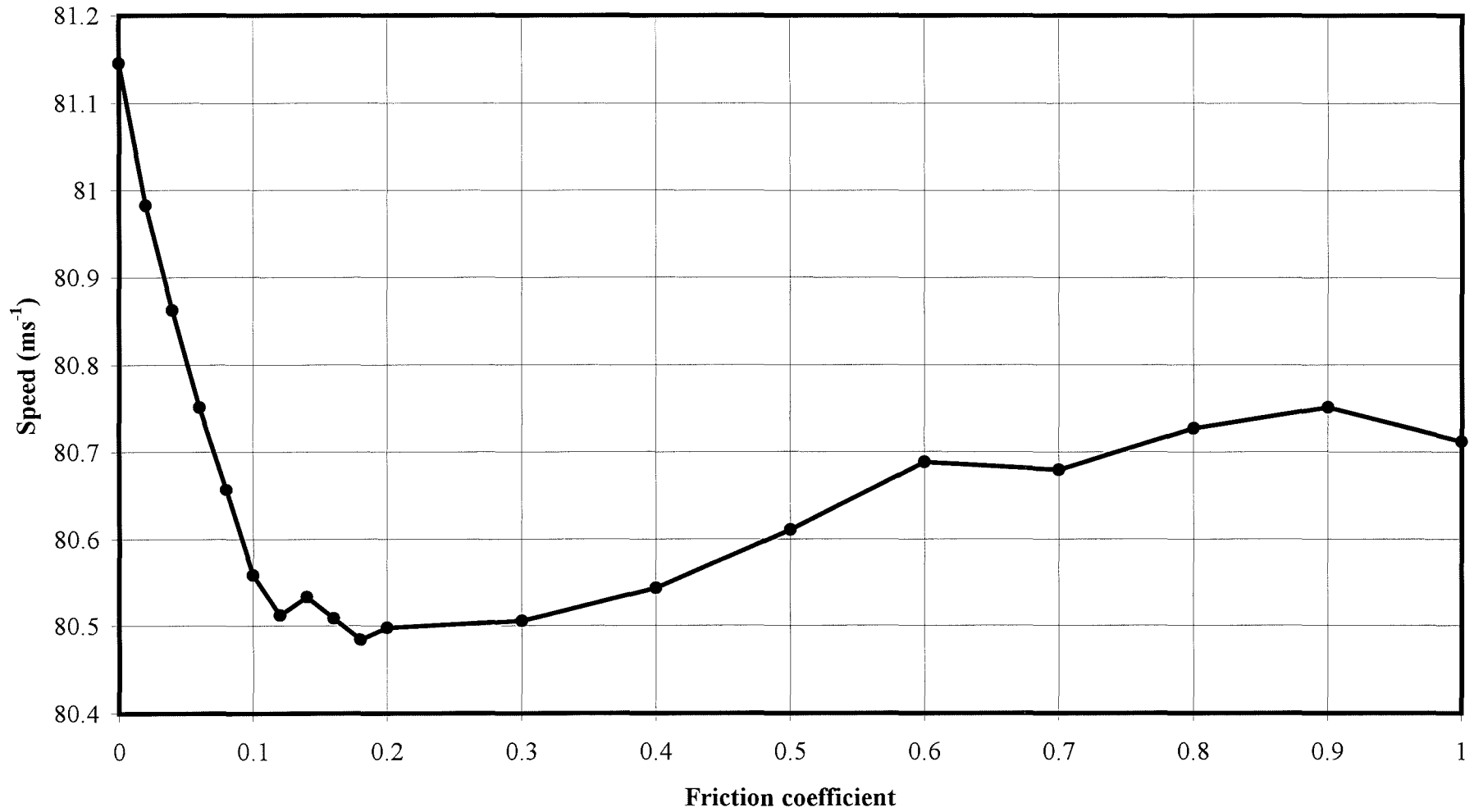


Figure 4.53 Effect of friction on ball speed, 20° loft.

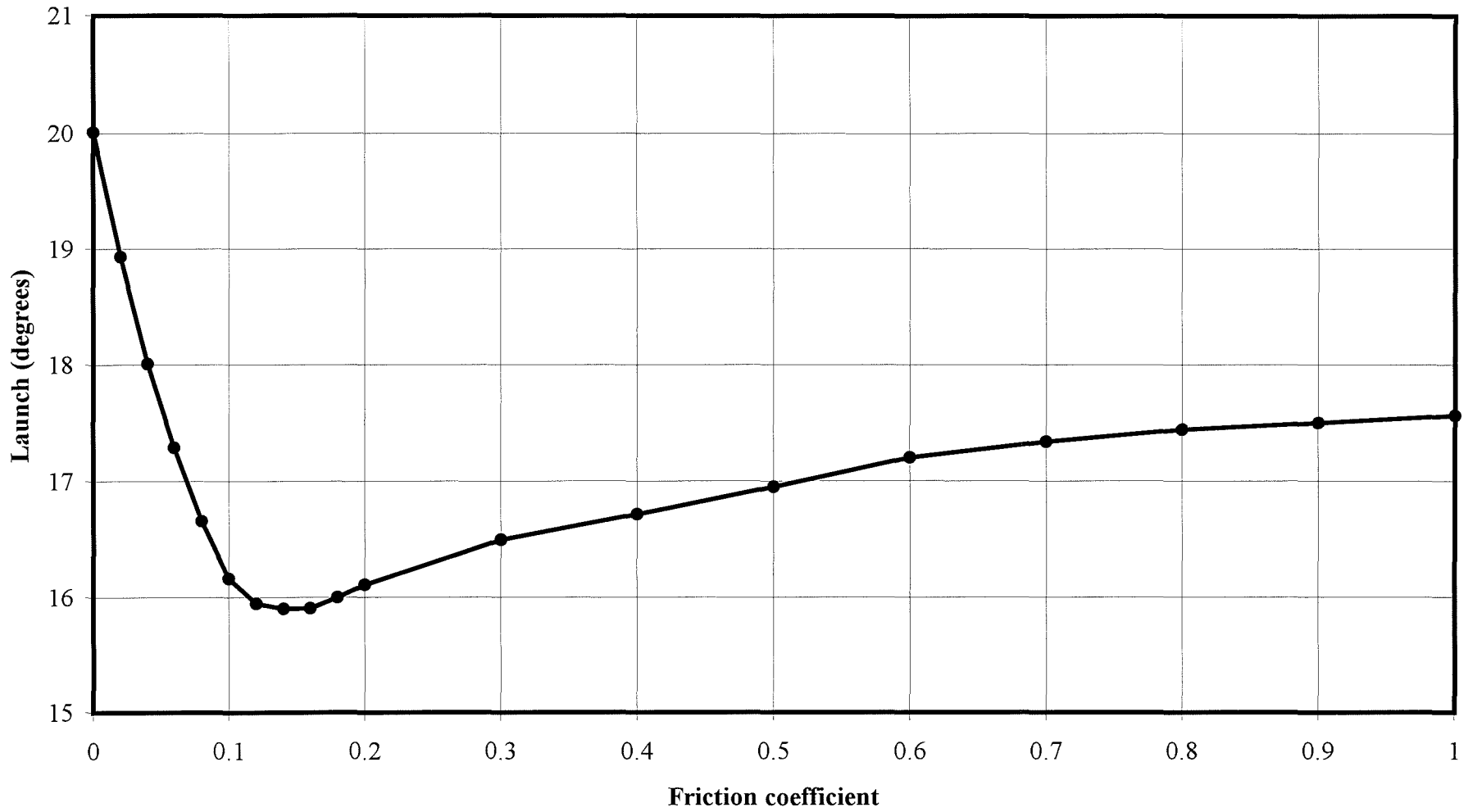


Figure 4.54 Effect of friction on ball launch, 20° loft.

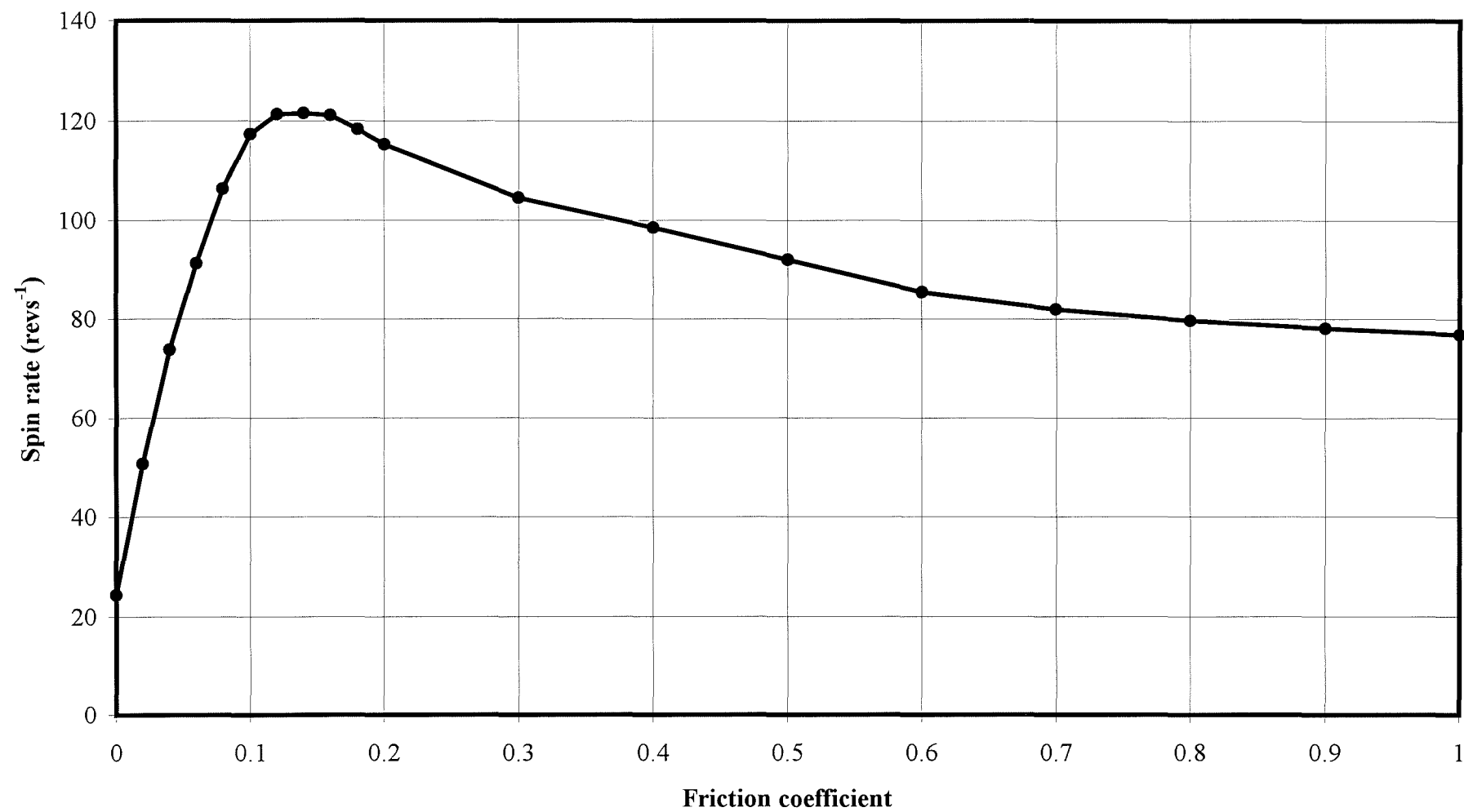


Figure 4.55 Effect of friction on ball spin, 20° loft.

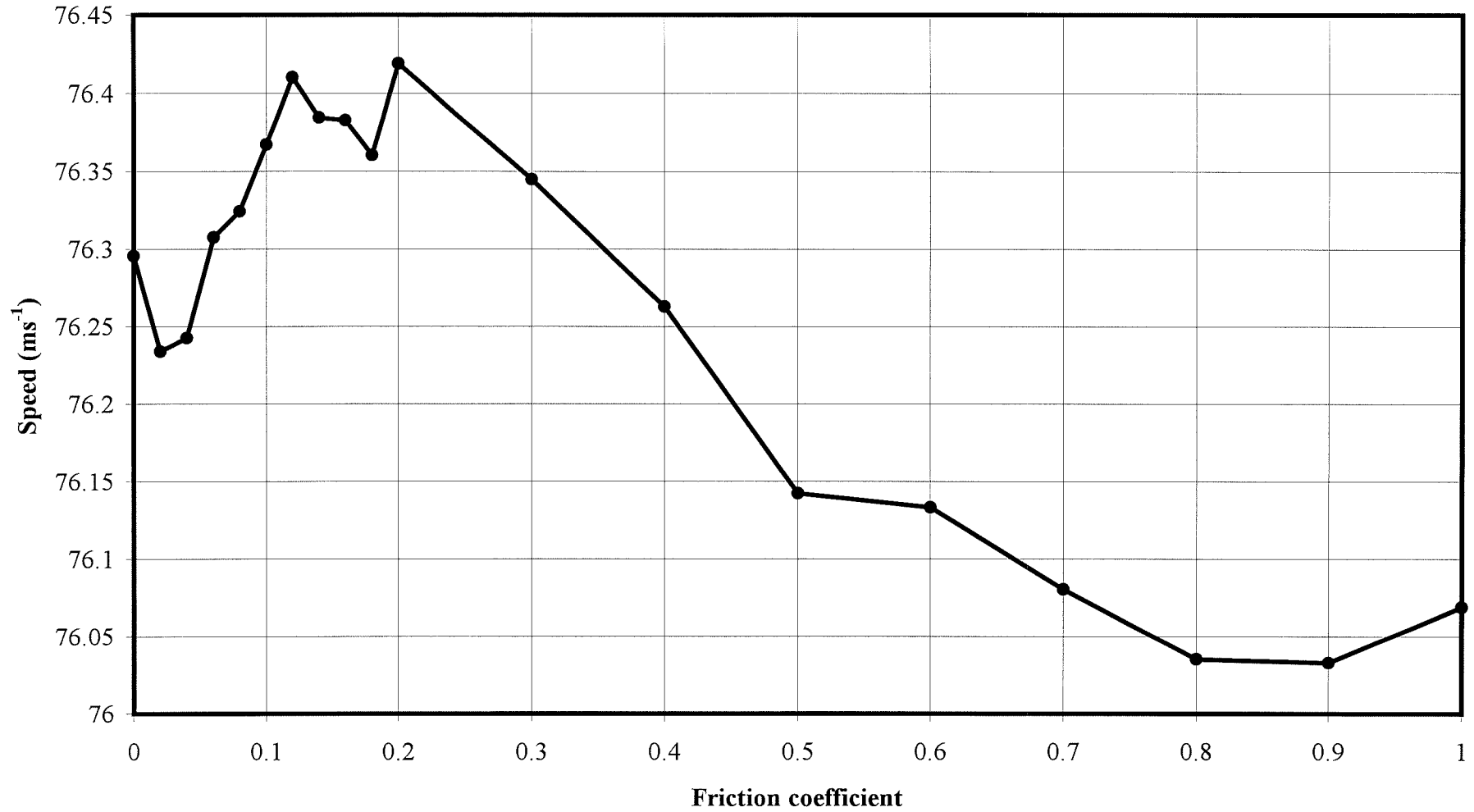


Figure 4.56 Effect of friction on ball speed, 30° loft.

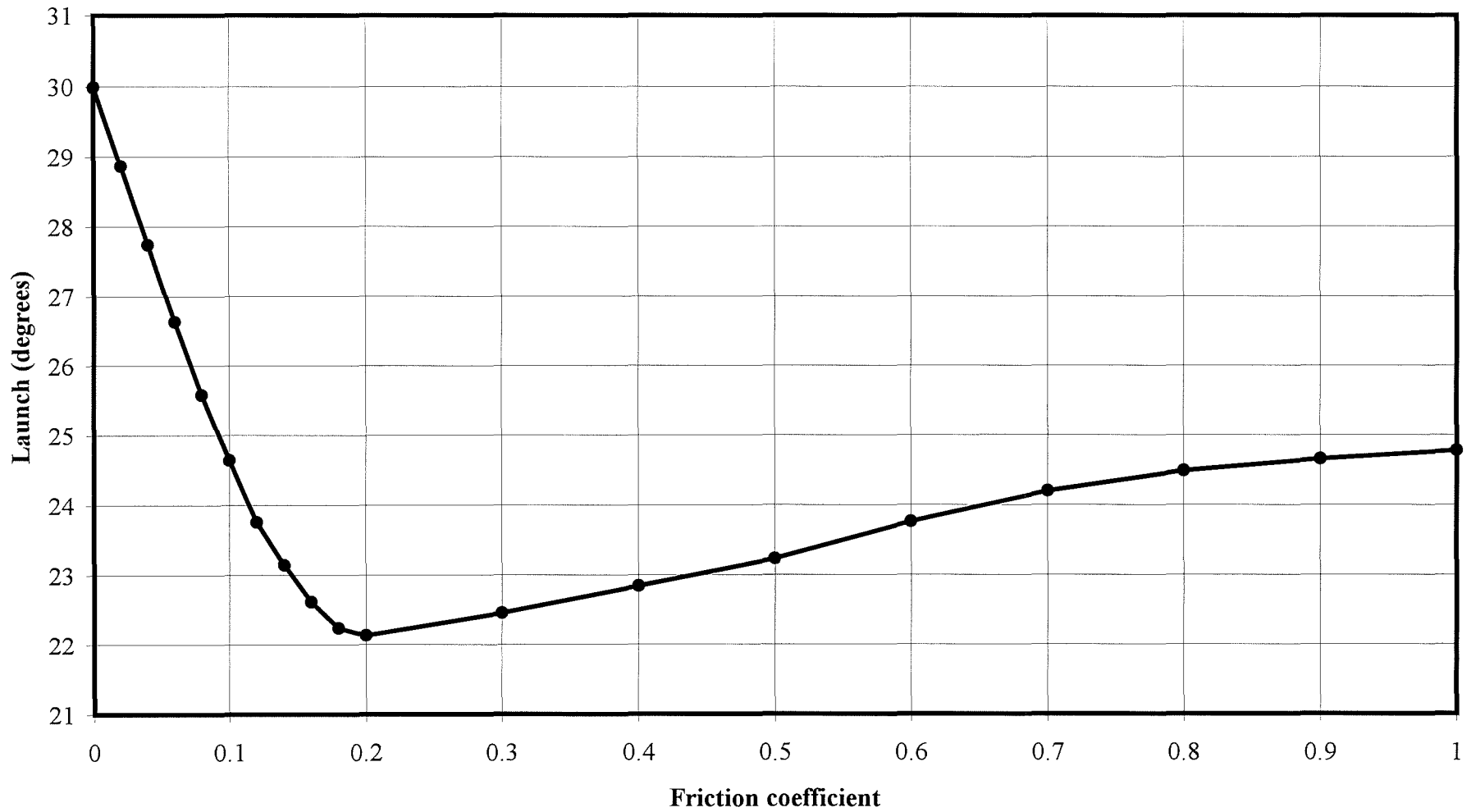


Figure 4.57 Effect of friction on ball launch, 30° loft.

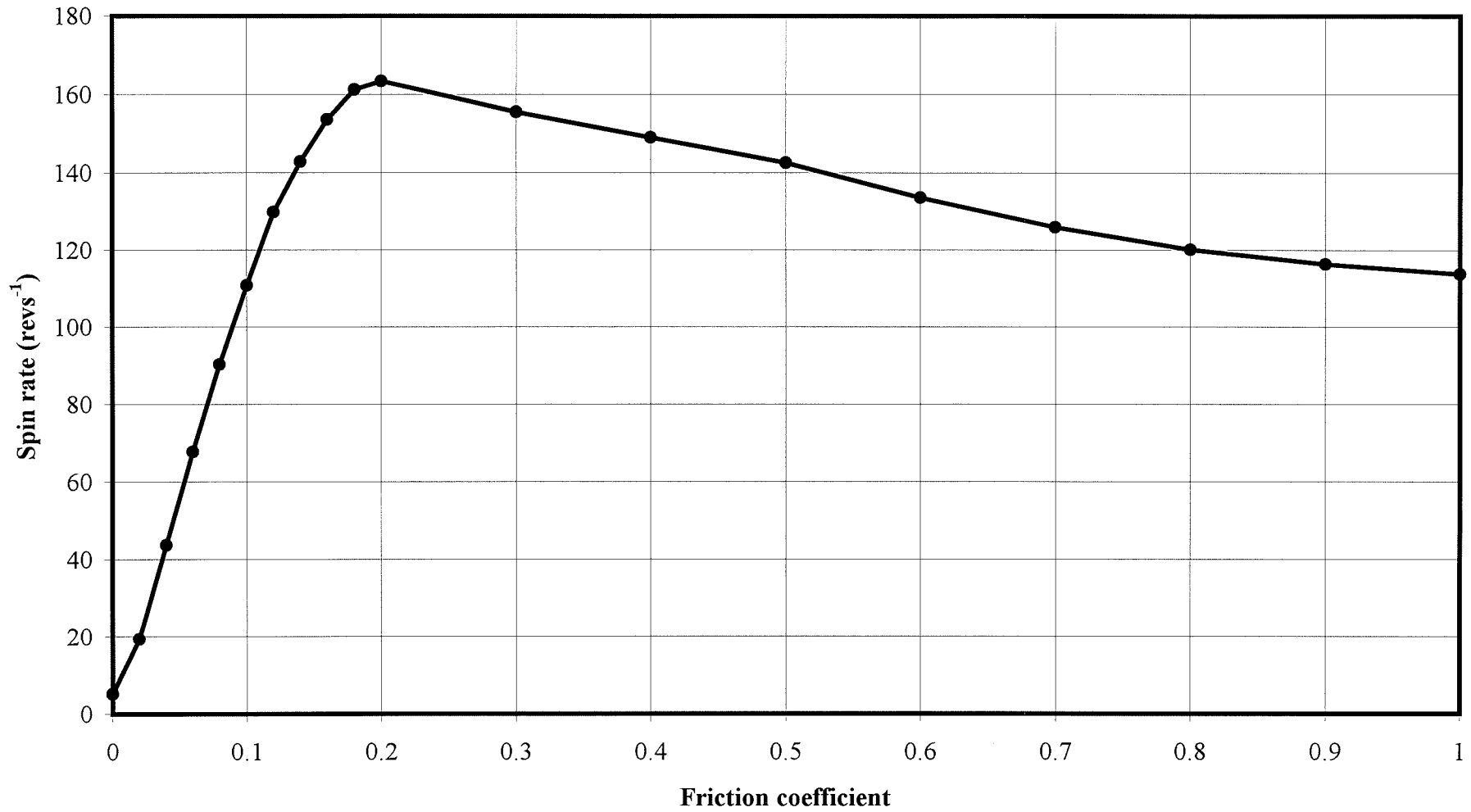


Figure 4.58 Effect of friction on ball spin, 30° loft.

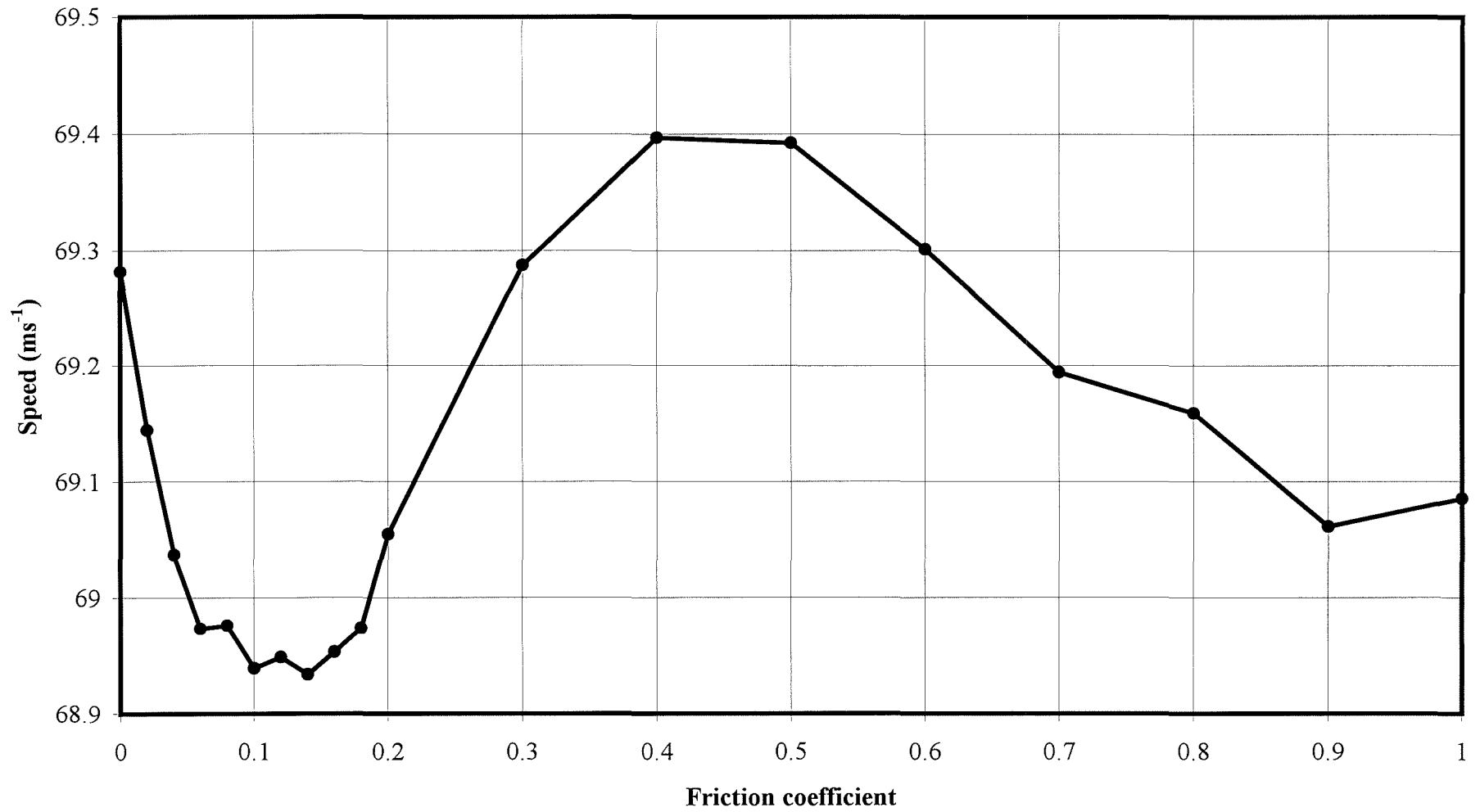


Figure 4.59 Effect of friction on ball speed, 40° loft.

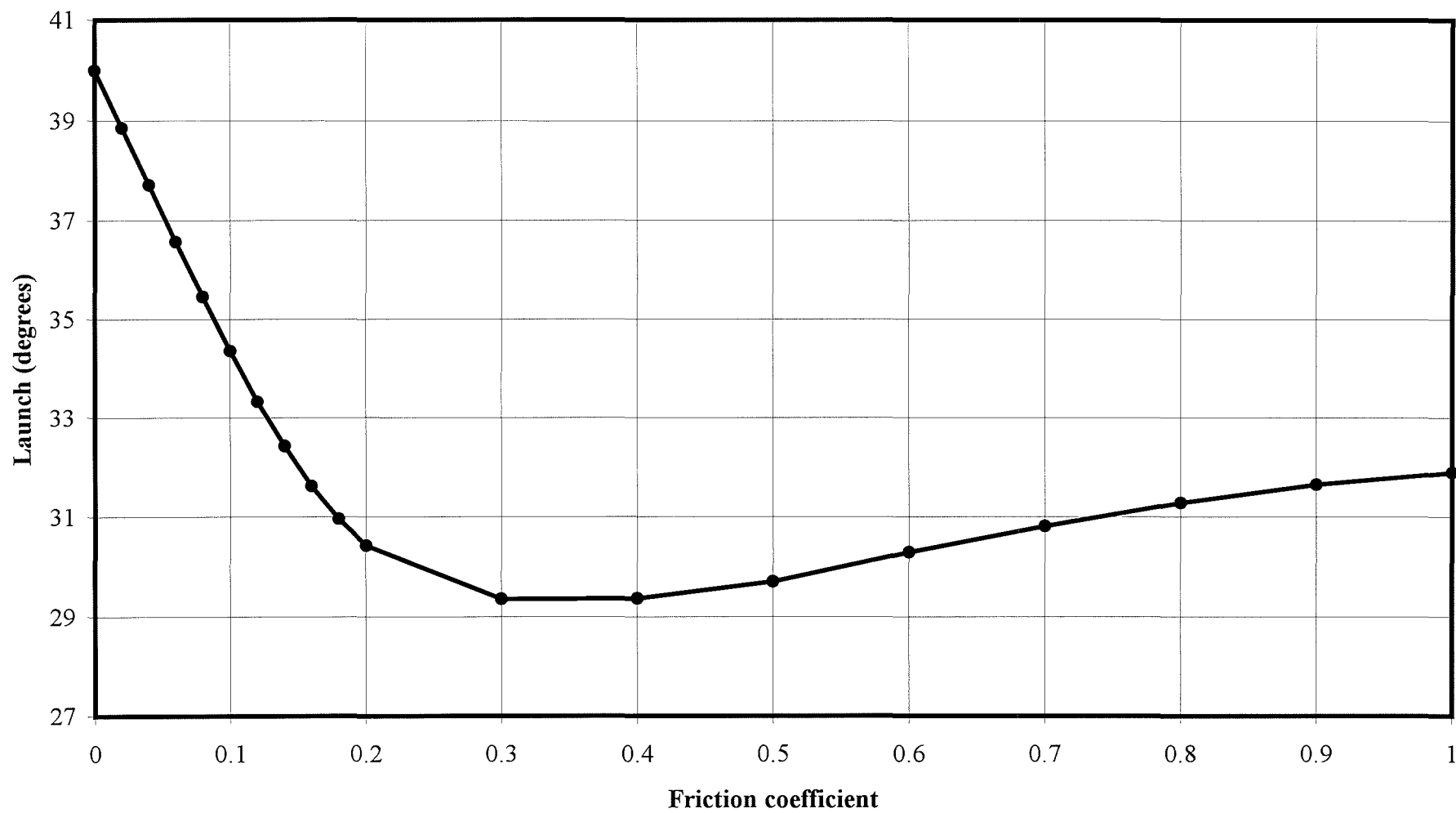


Figure 4.60 Effect of friction on ball launch, 40° loft.

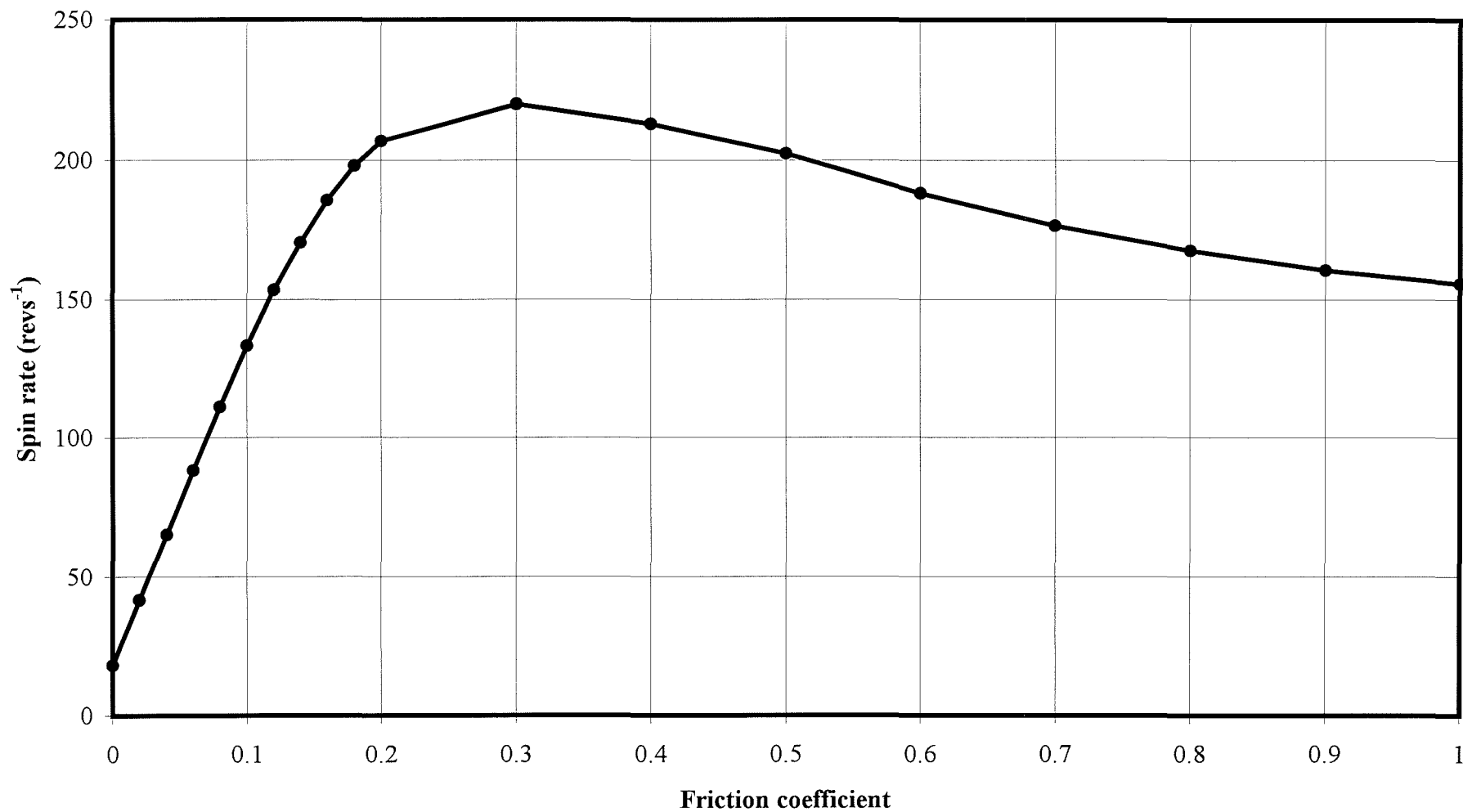


Figure 4.61 Effect of friction on ball spin, 40° loft.

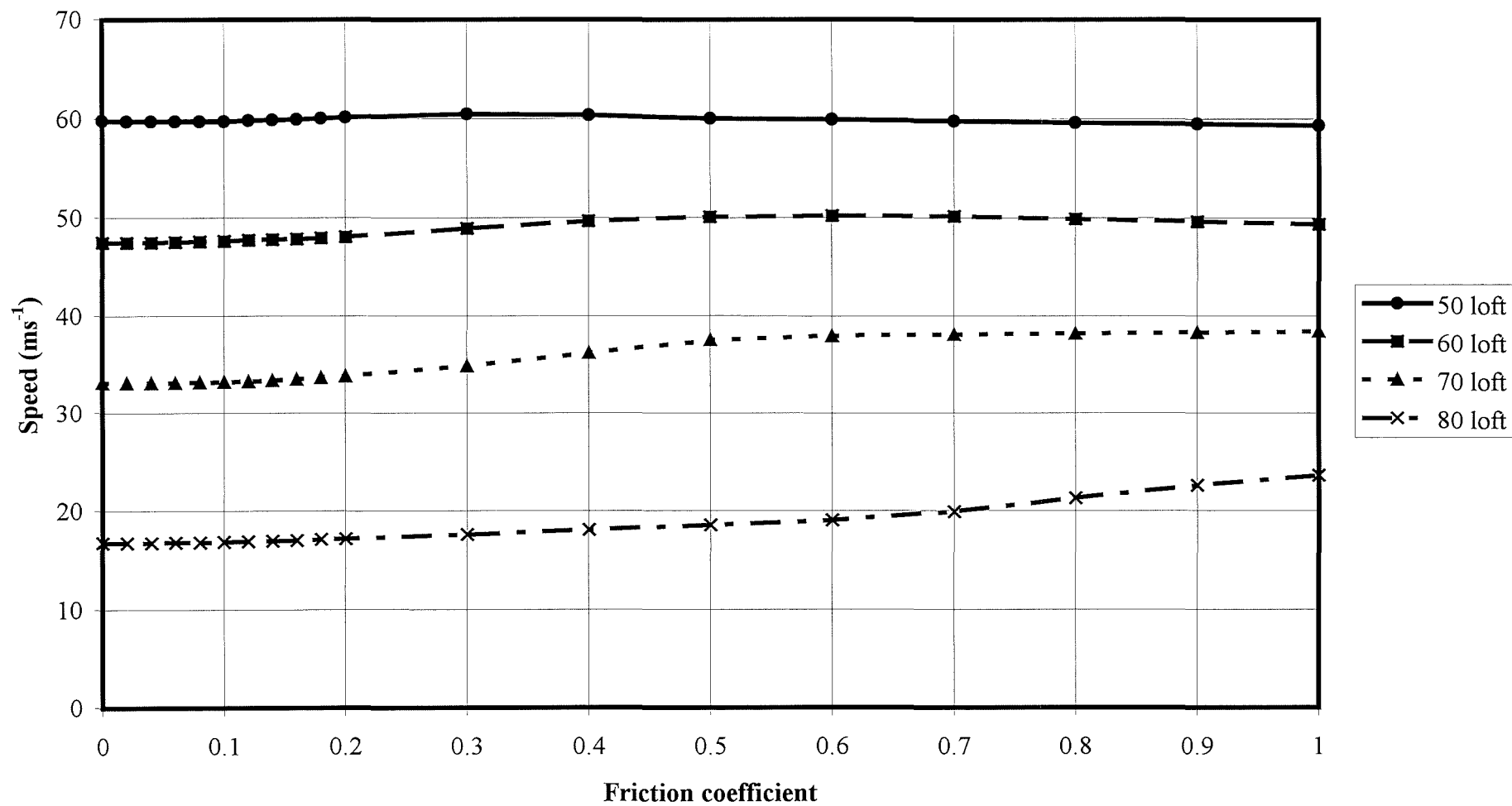


Figure 4.62 Effect of friction on ball speed, 50, 60, 70 and 80° loft.

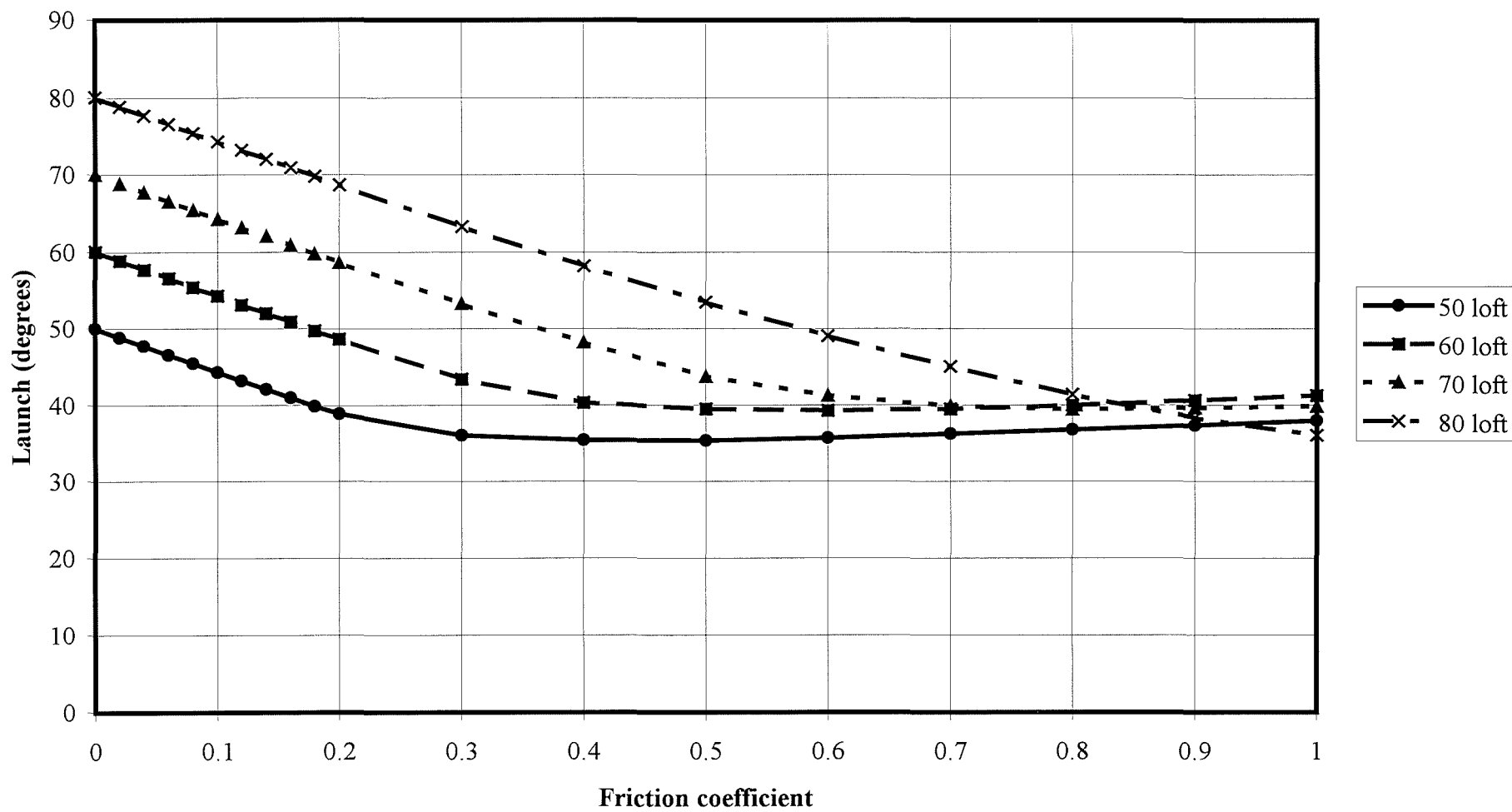


Figure 4.63 Effect of friction on ball launch, 50, 60, 70 and 80° loft.

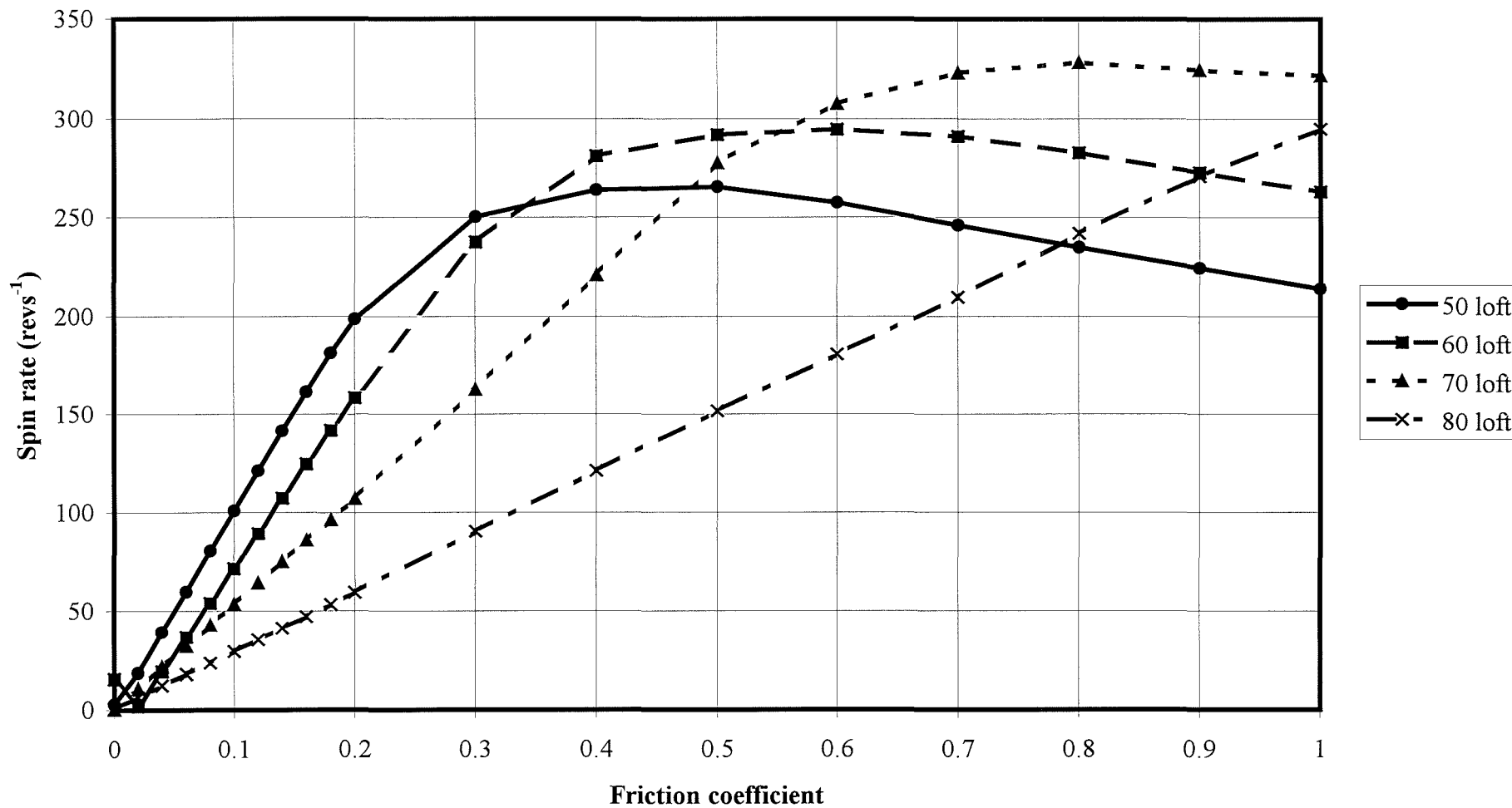


Figure 4.64 Effect of friction on ball spin, 50, 60, 70 and 80° loft.

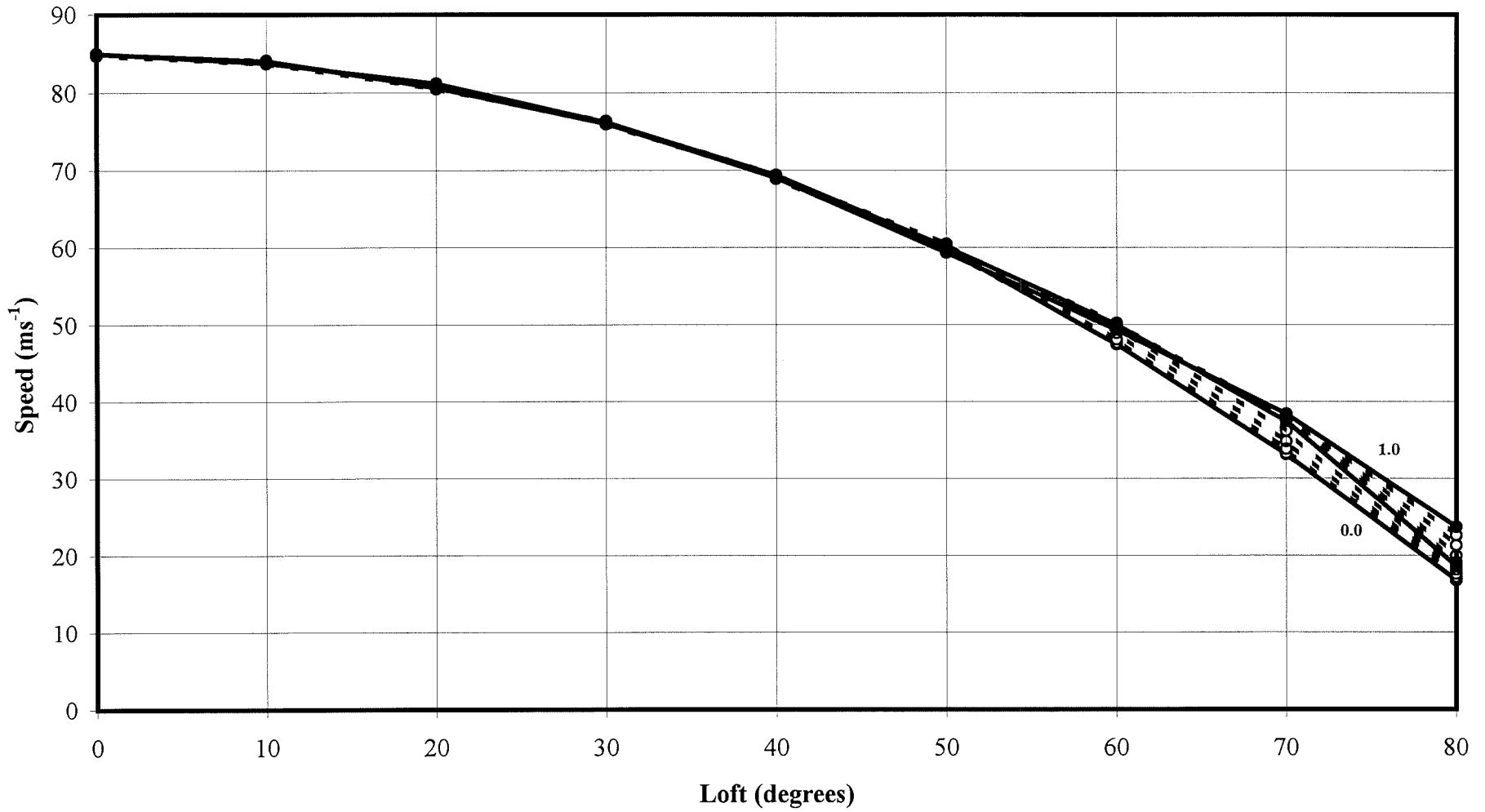


Figure 4.65 Effect of loft on ball speed.

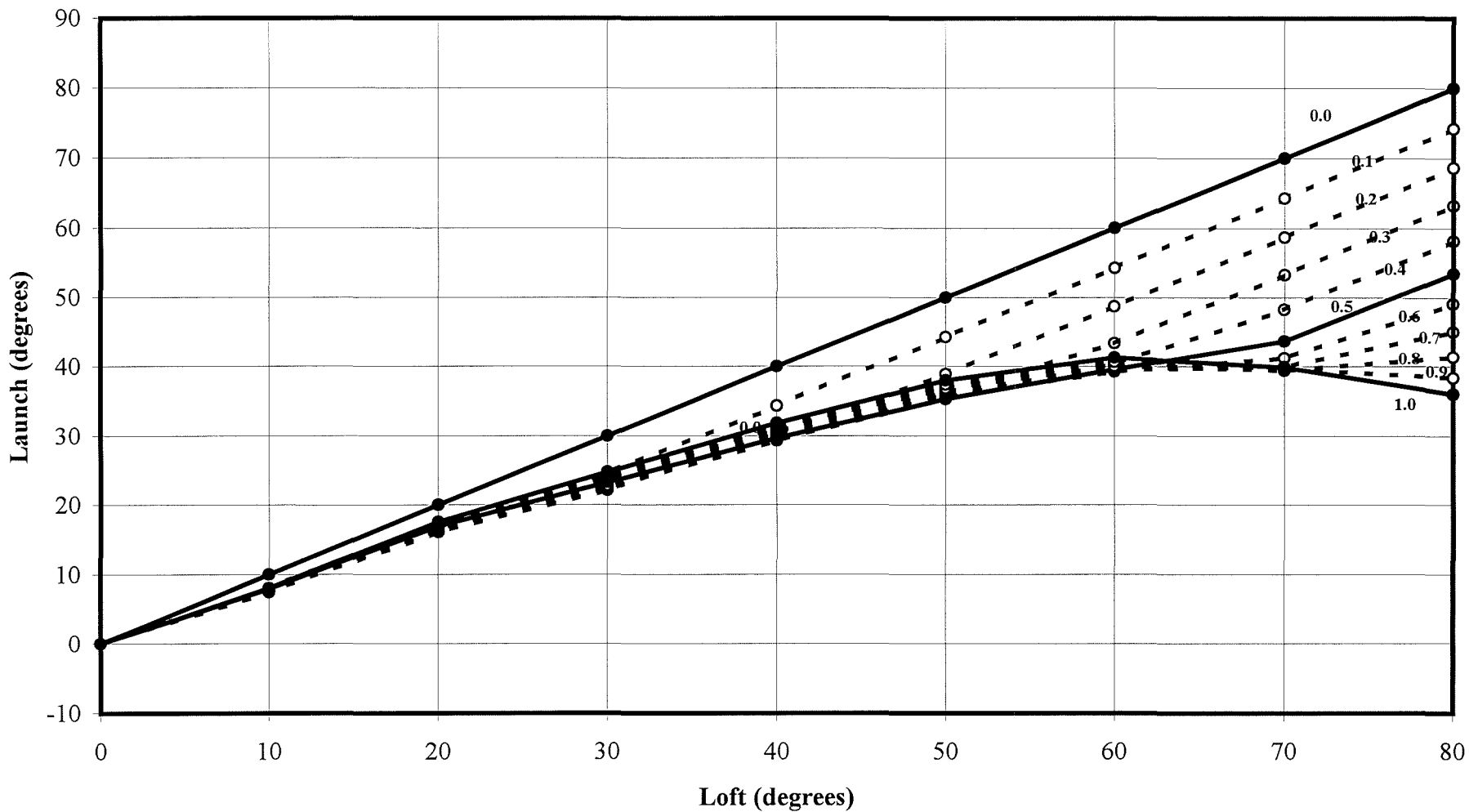


Figure 4.66 Effect of loft on ball launch.

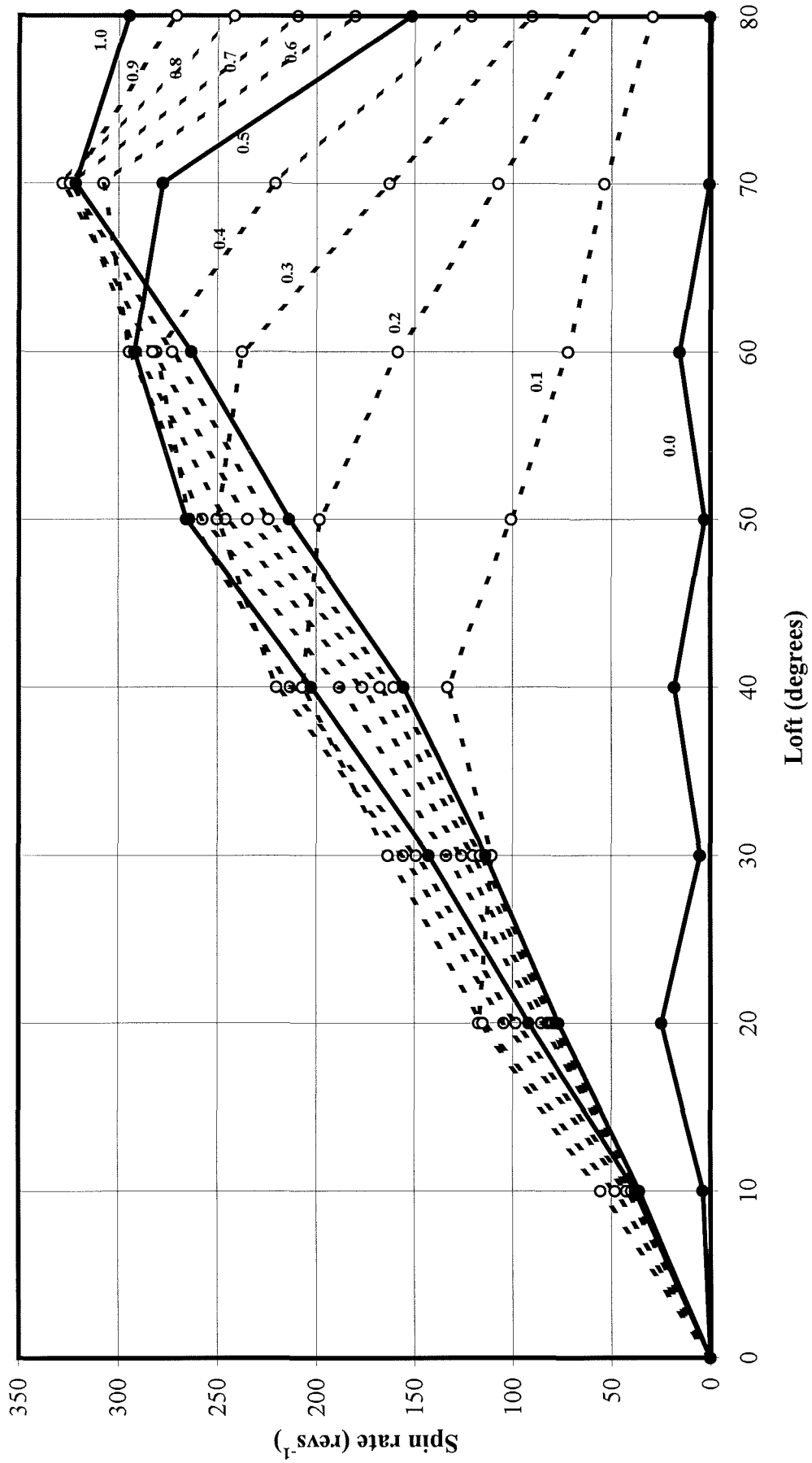


Figure 4.67 Effect of loft on ball spin.

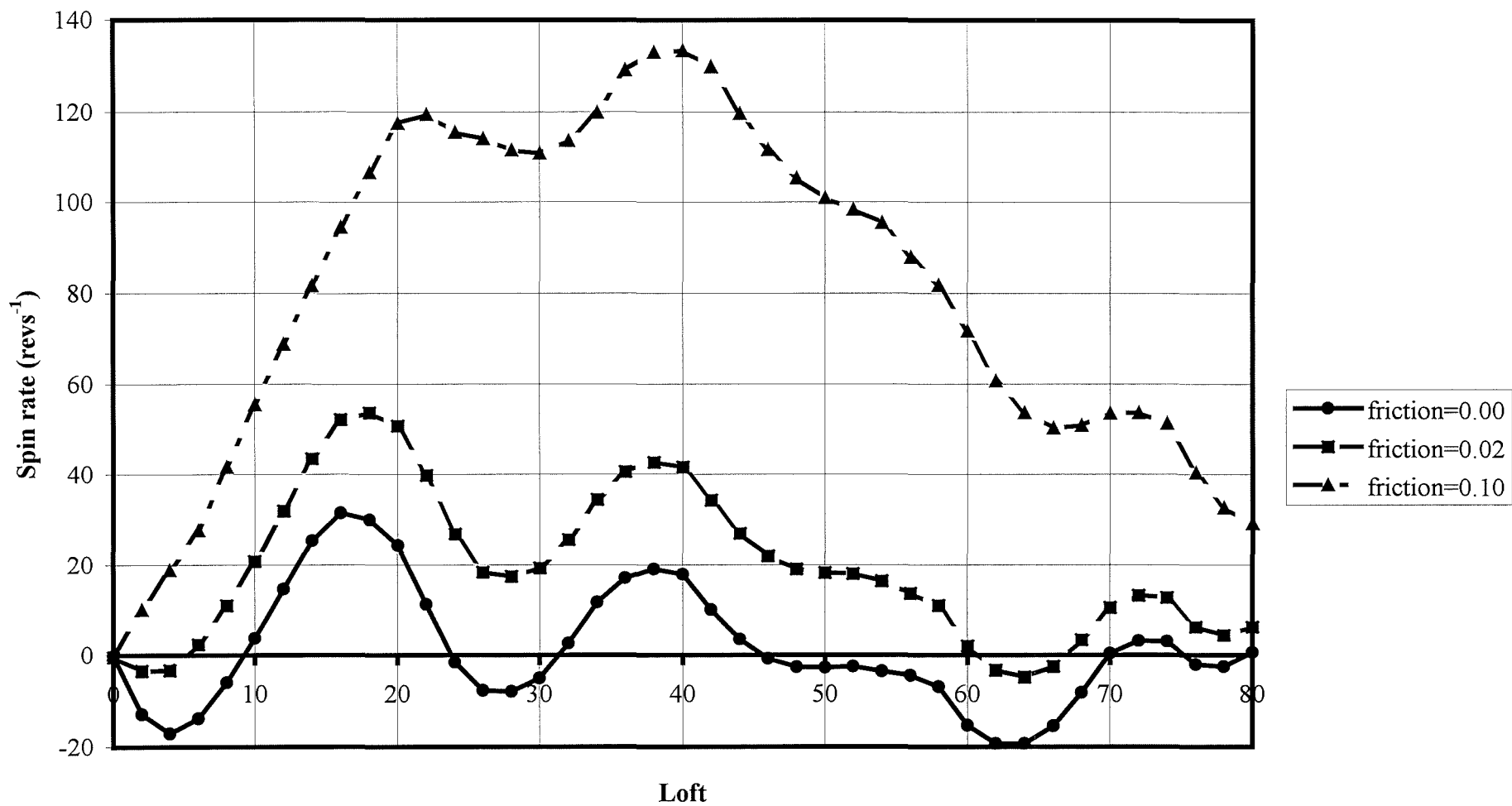


Figure 4.68 Error in spin prediction for low friction.

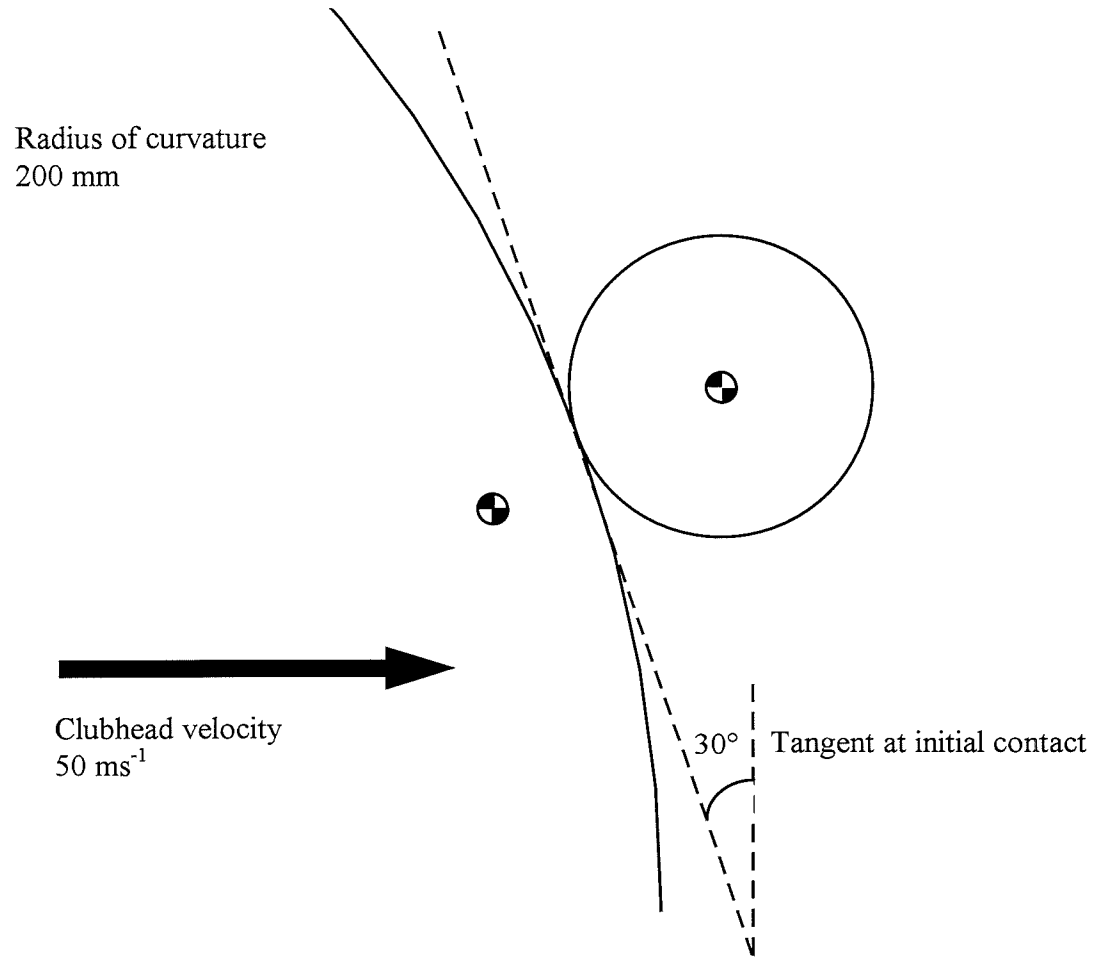


Figure 4.69 Curved clubface, 30° tangent at initial point of contact.

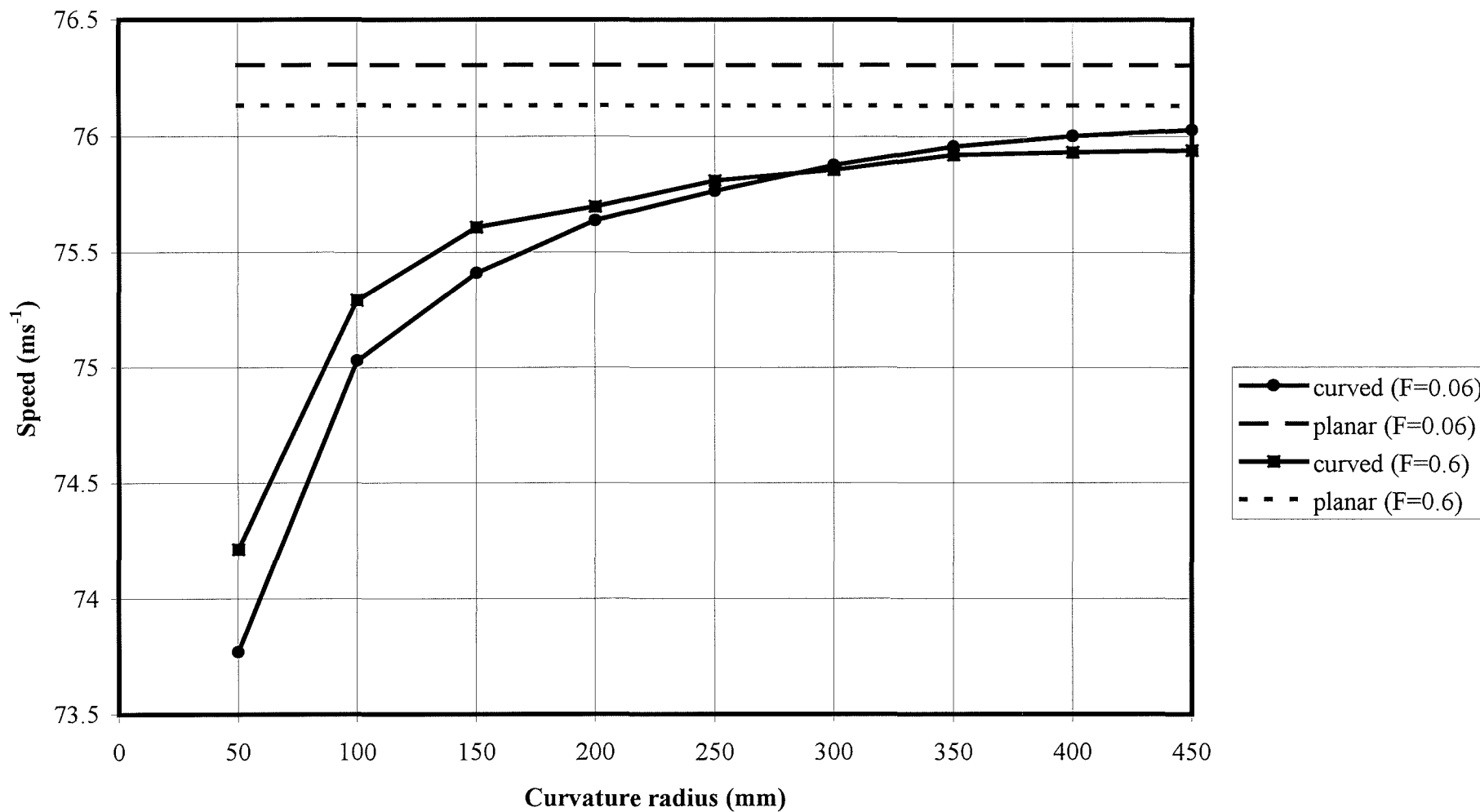


Figure 4.70 Ball speed from curved surface, tangent = 30°.

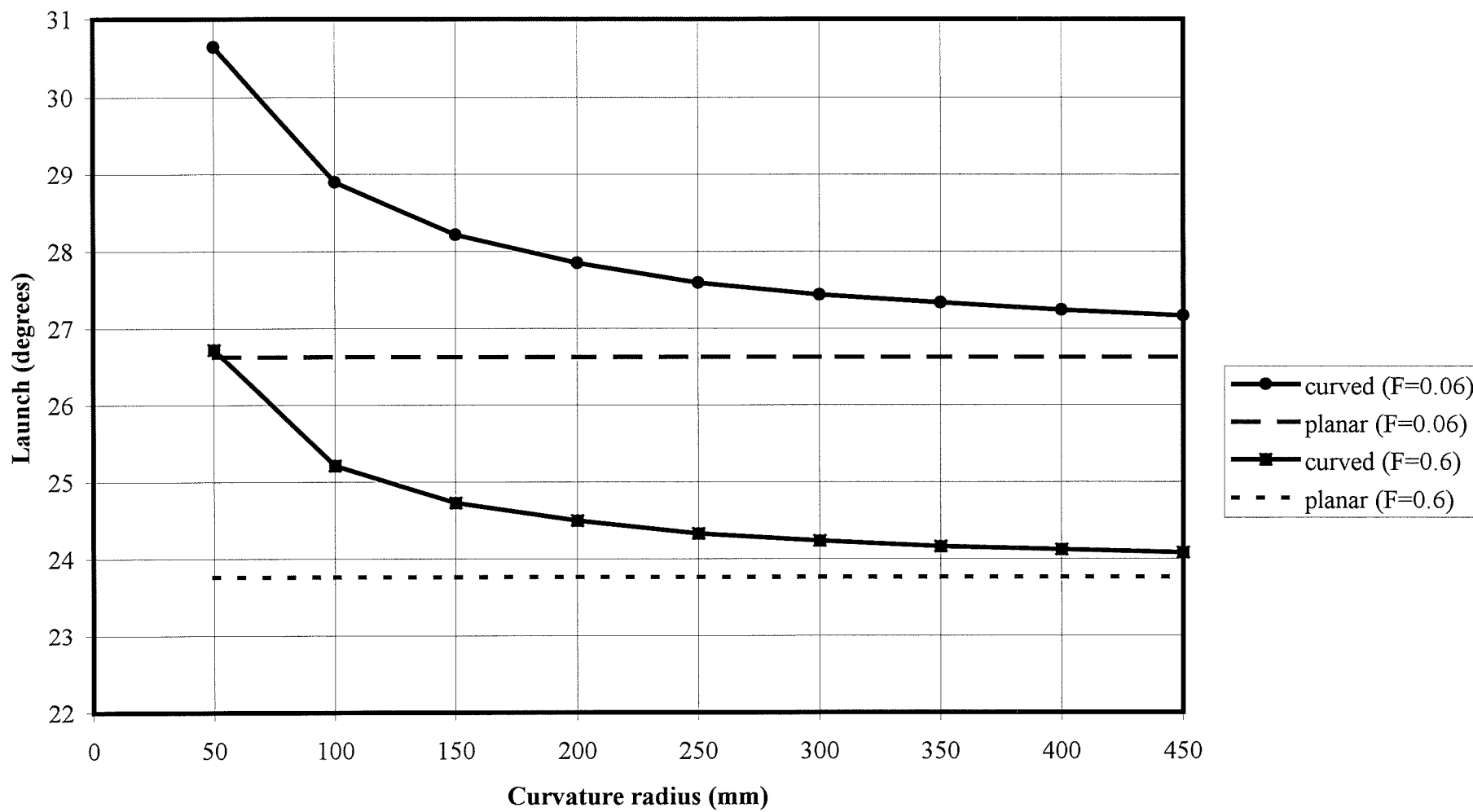


Figure 4.71 Ball launch from curved surface, tangent = 30°.

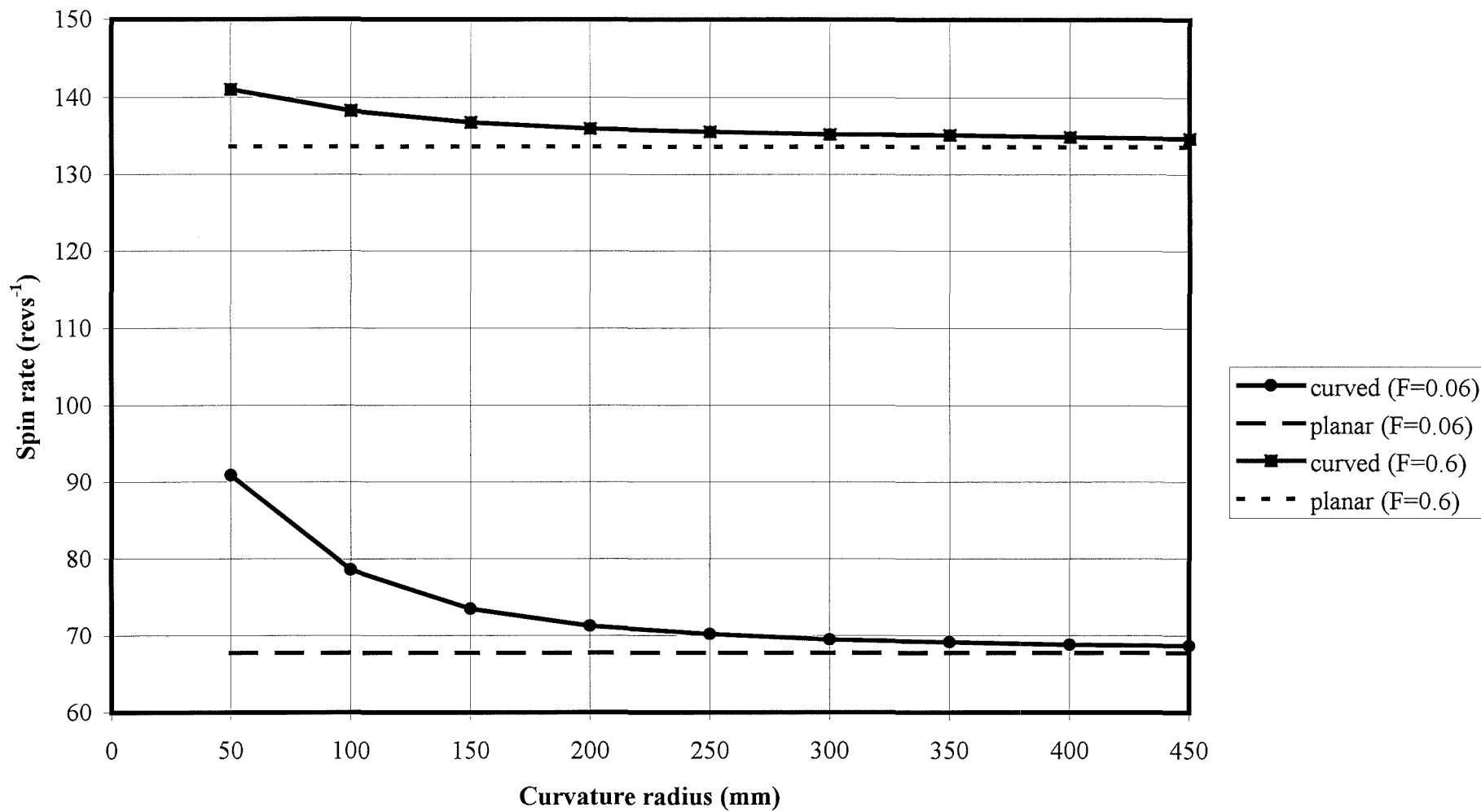


Figure 4.72 Ball spin from curved surface, tangent = 30°.

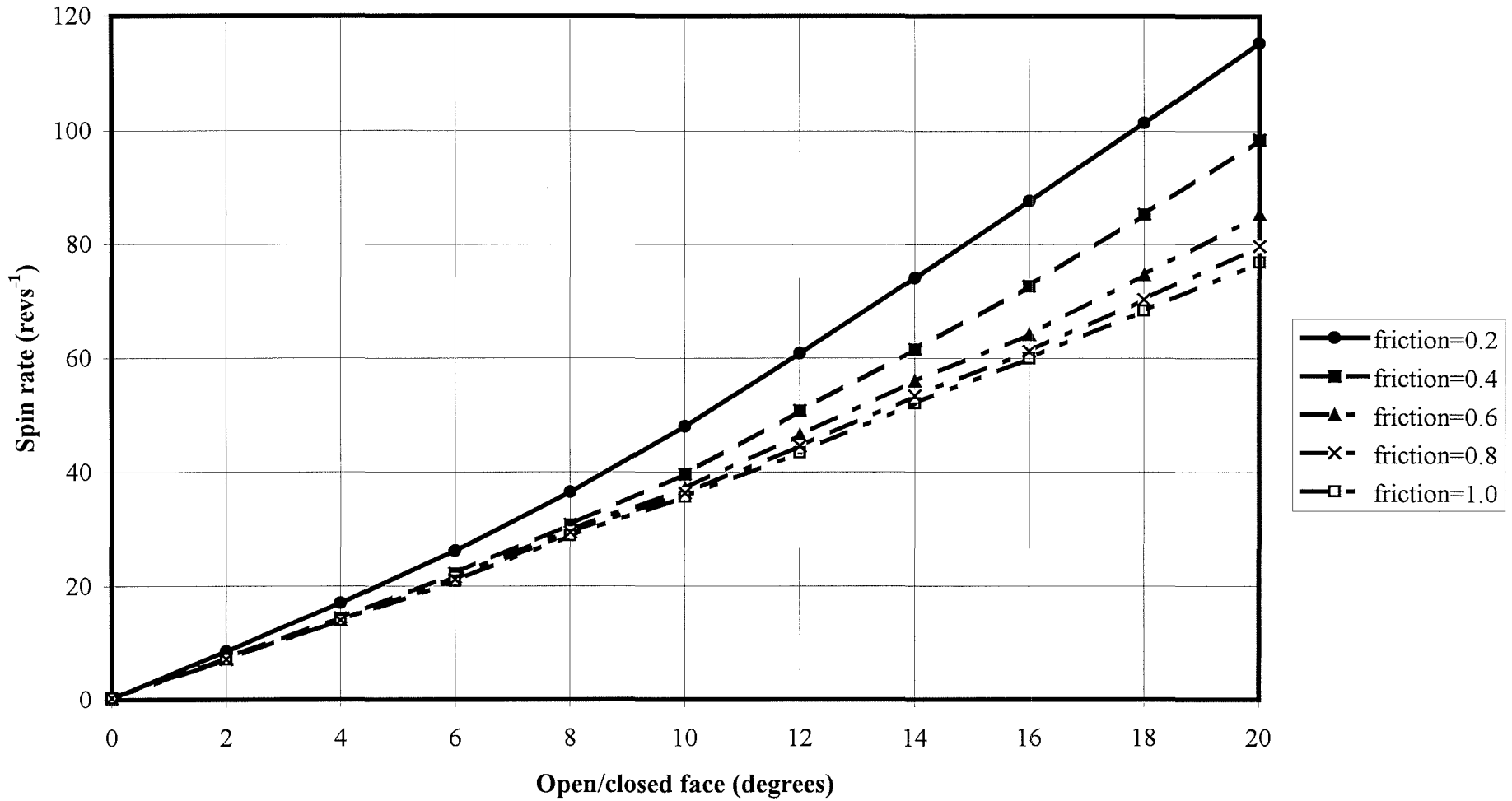


Figure 4.73 Sidespin generated by open clubface.

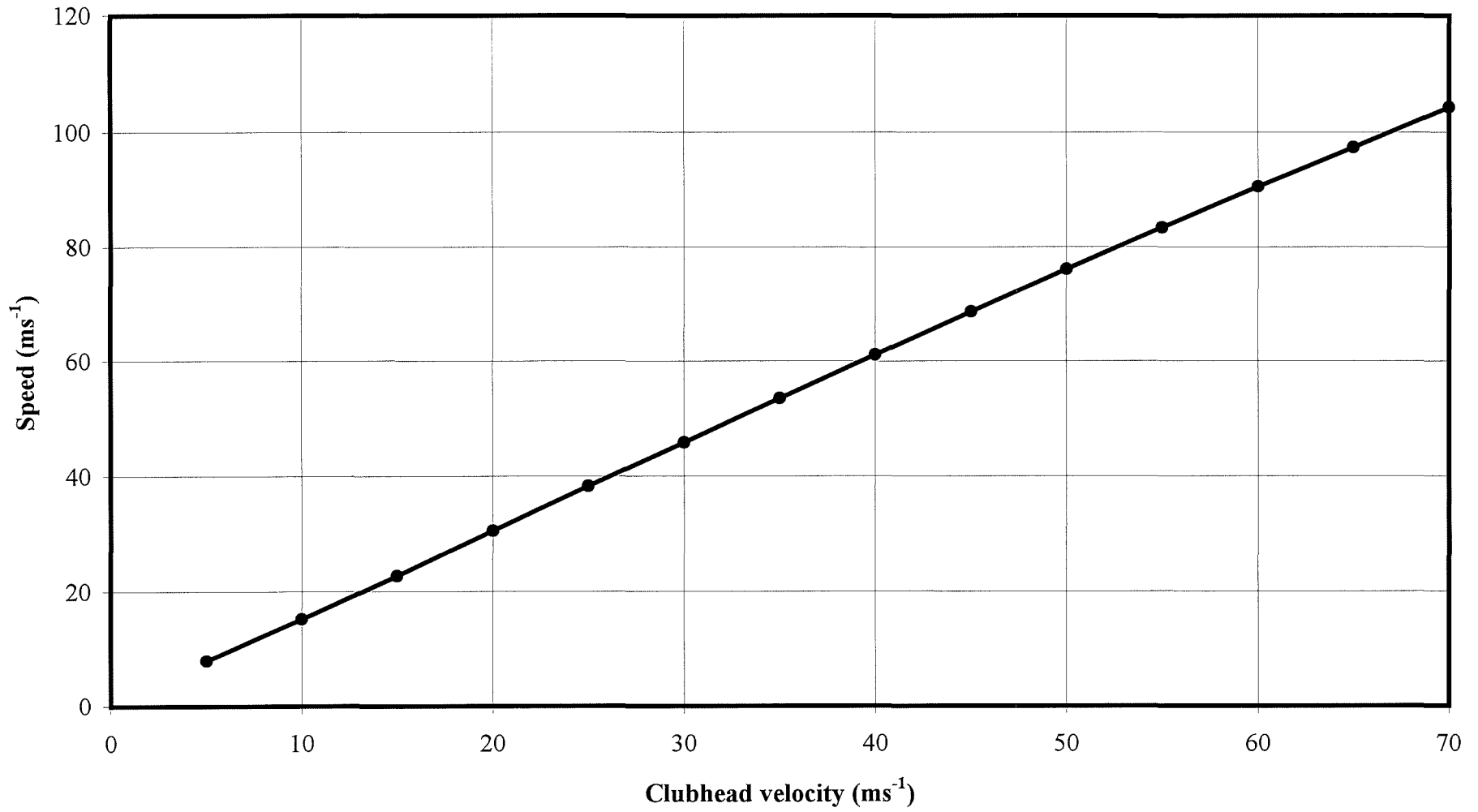


Figure 4.74 Effect of clubhead velocity on ball speed.

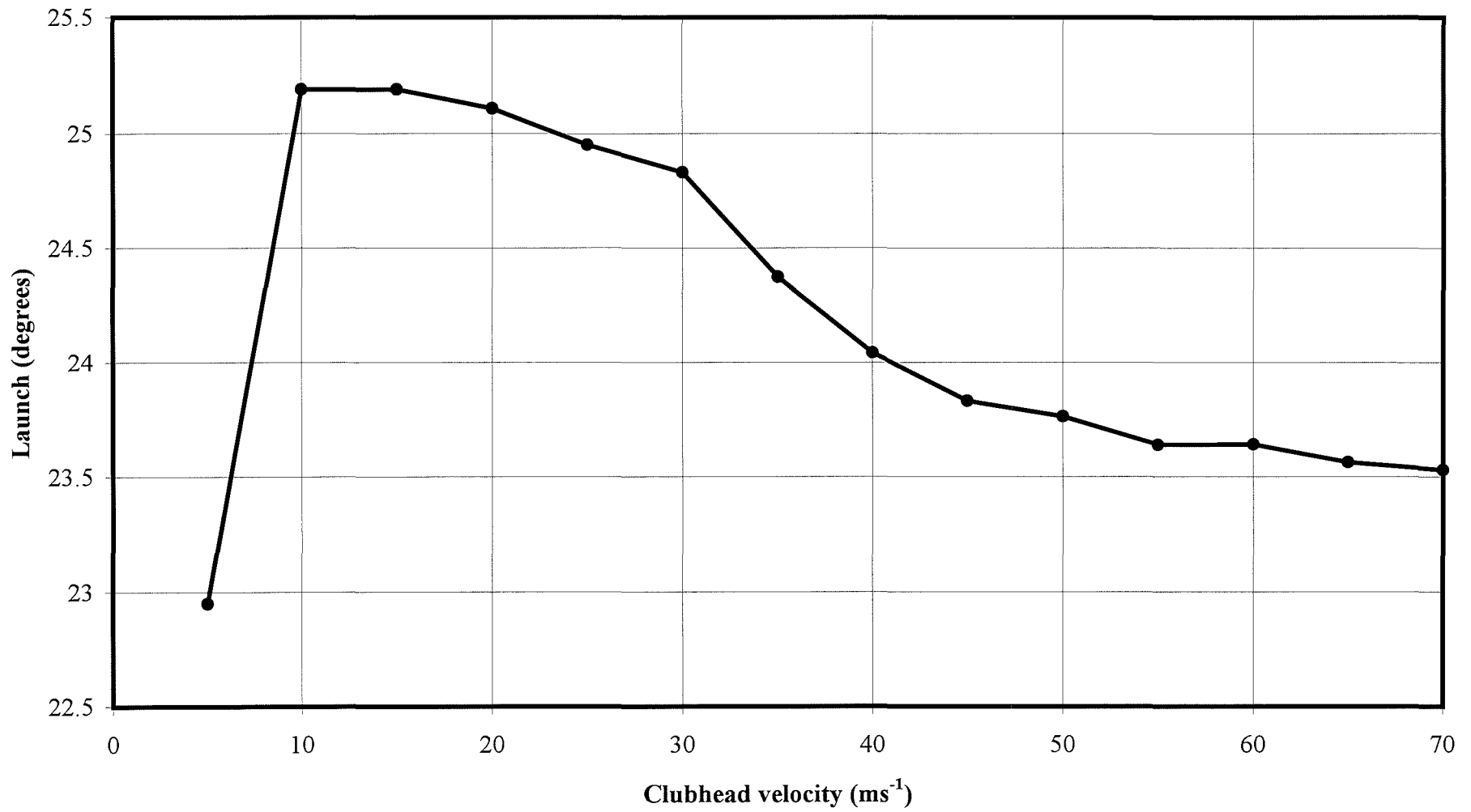


Figure 4.75 Effect of clubhead velocity on ball launch.

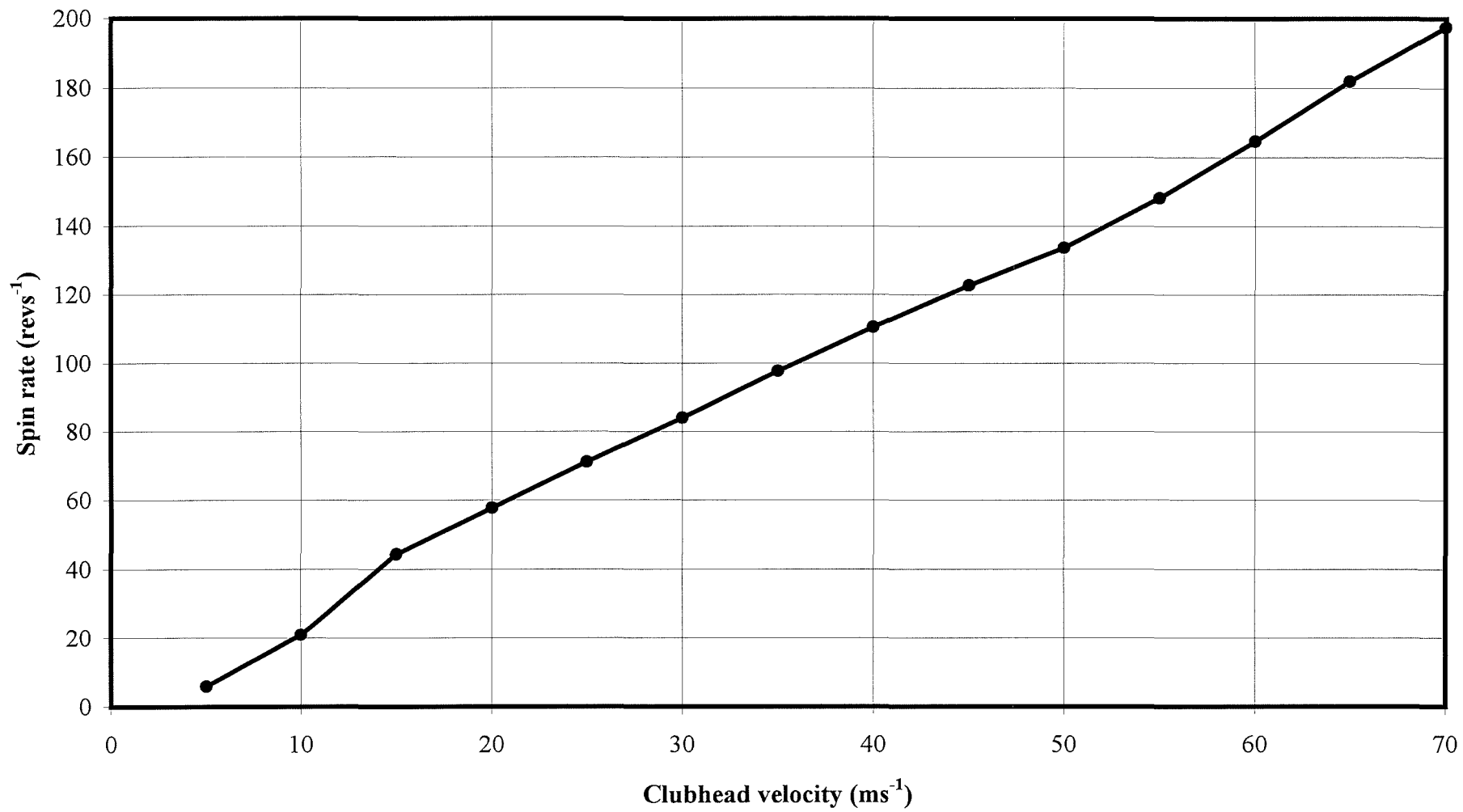


Figure 4.76 Effect of clubhead velocity on ball spin.

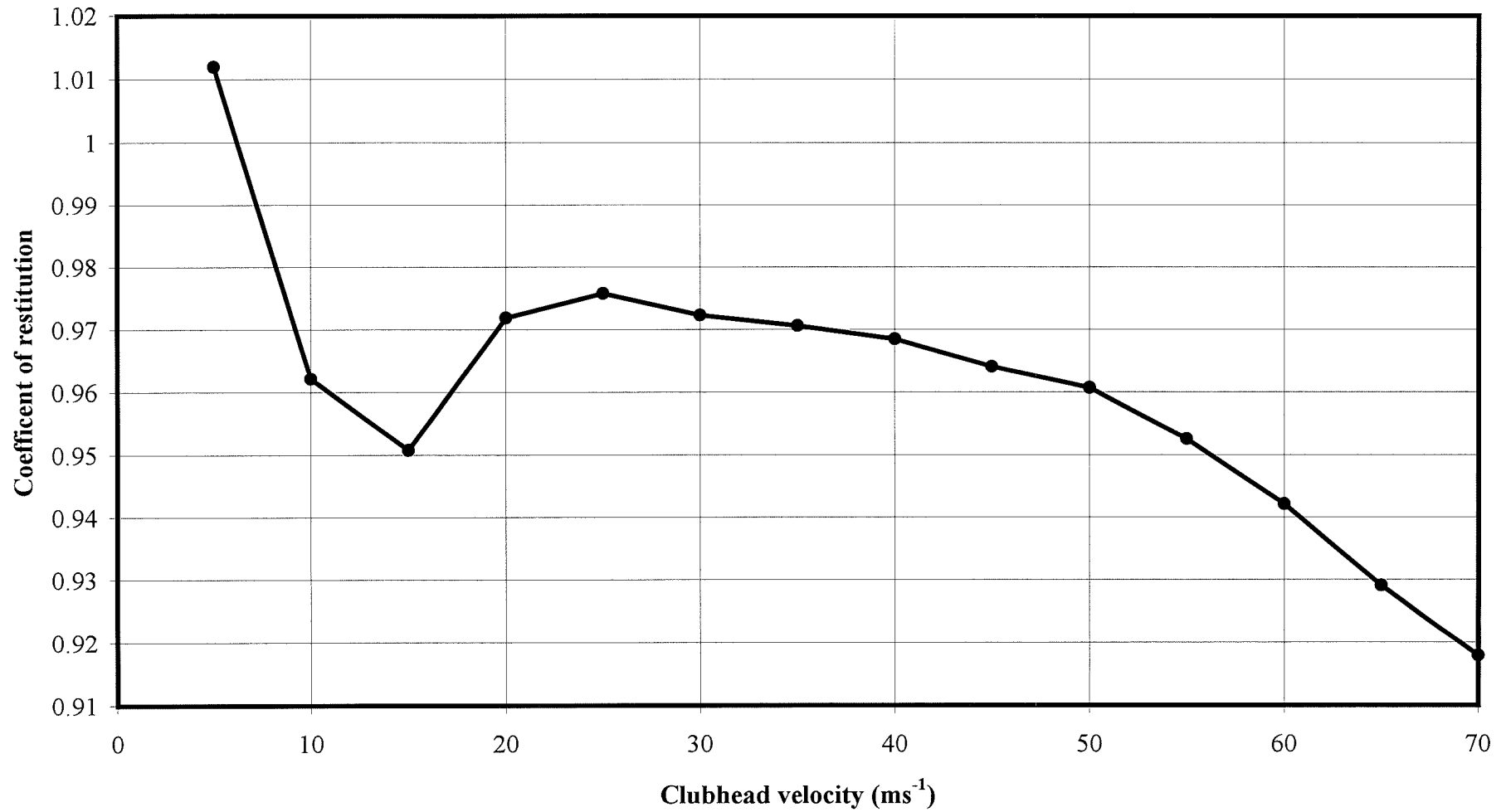


Figure 4.77 Effect of clubhead velocity on effective coefficient of restitution for Abaqus.

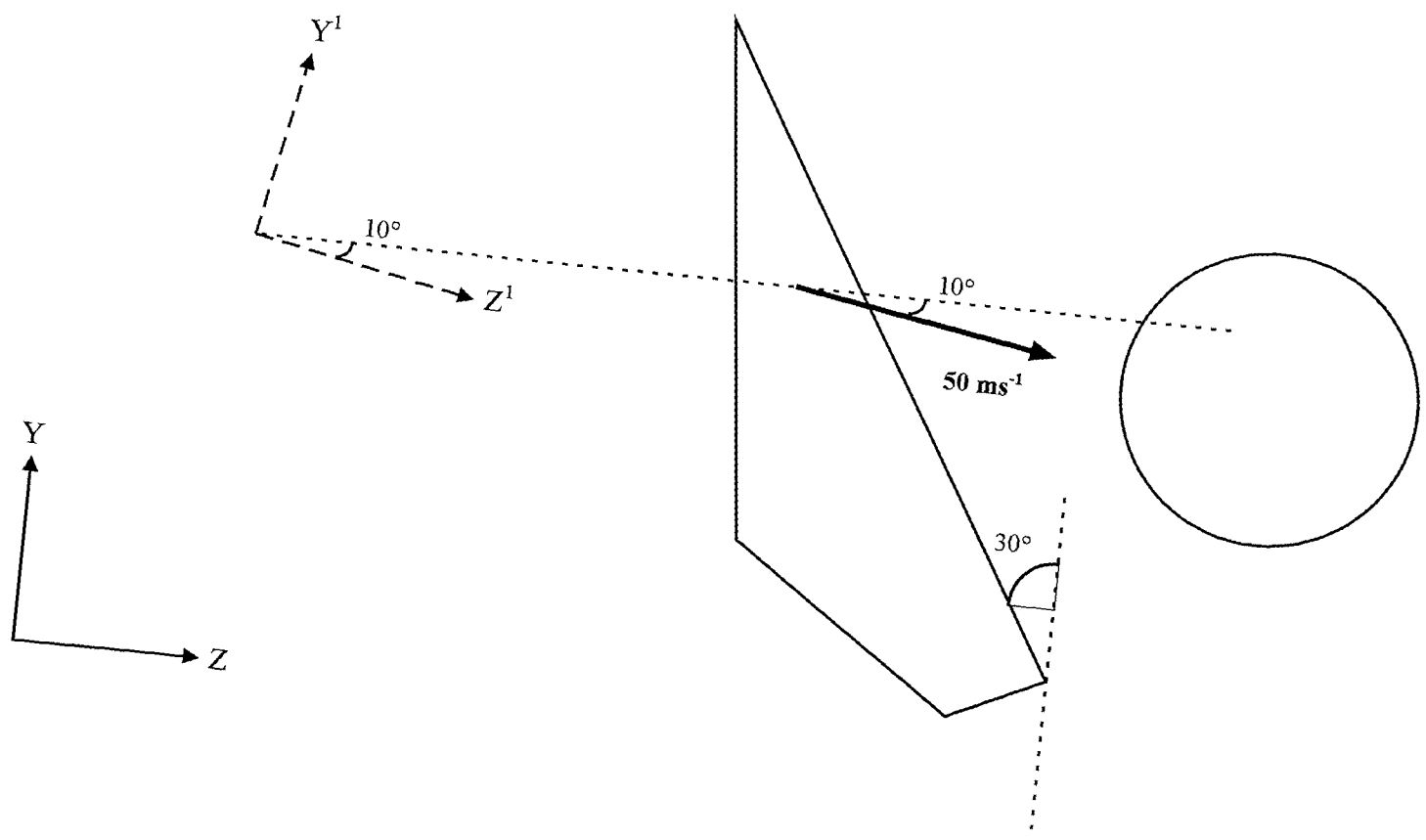


Figure 4.78 Clubhead trajectory 10° below horizontal.

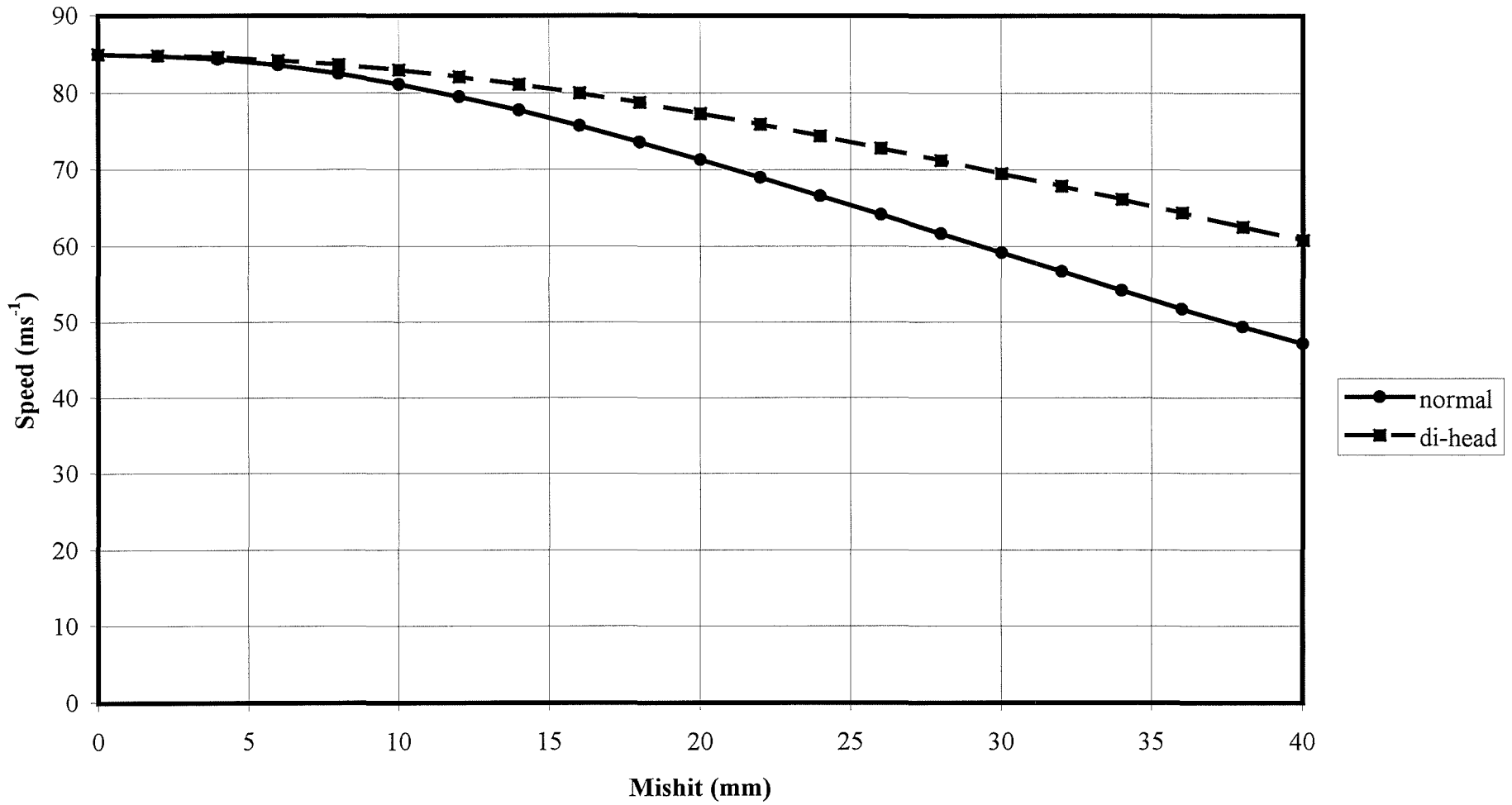


Figure 4.79 Effect of mishit on speed, centre of mass 0 mm behind face.

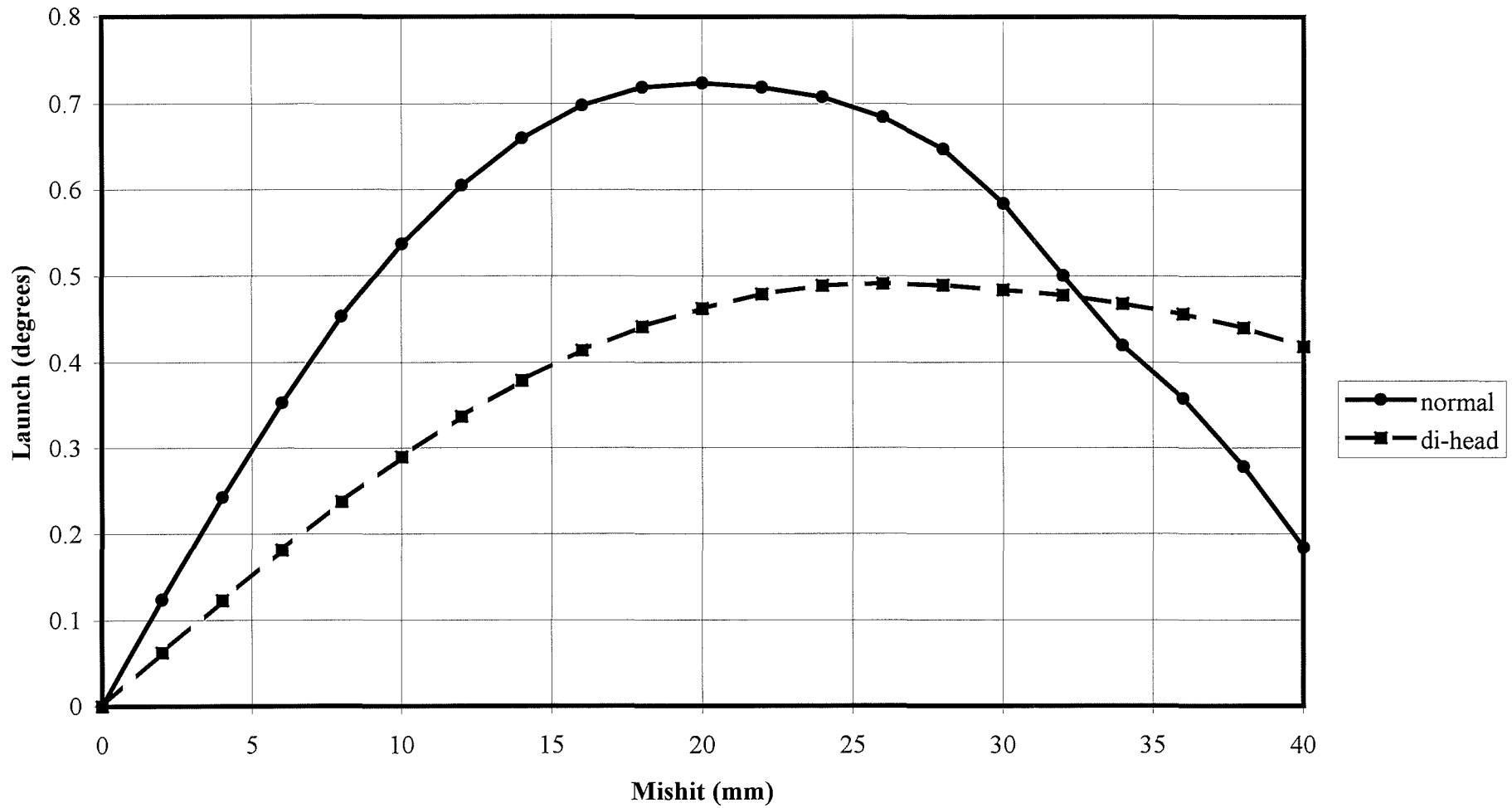


Figure 4.80 Effect of mishit on launch, centre of mass 0 mm behind face.

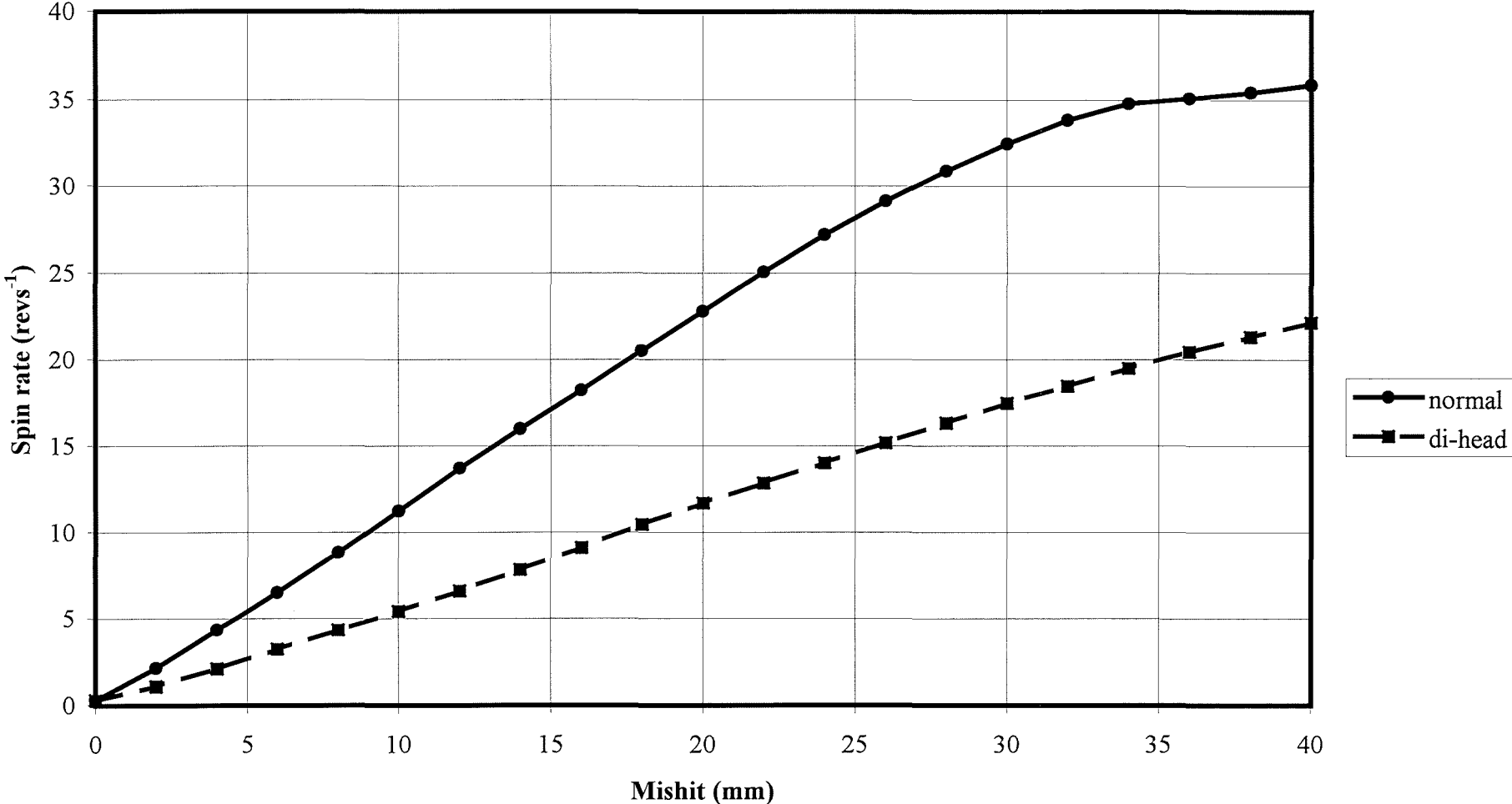


Figure 4.81 Effect of mishit on spin, centre of mass 0 mm behind face.

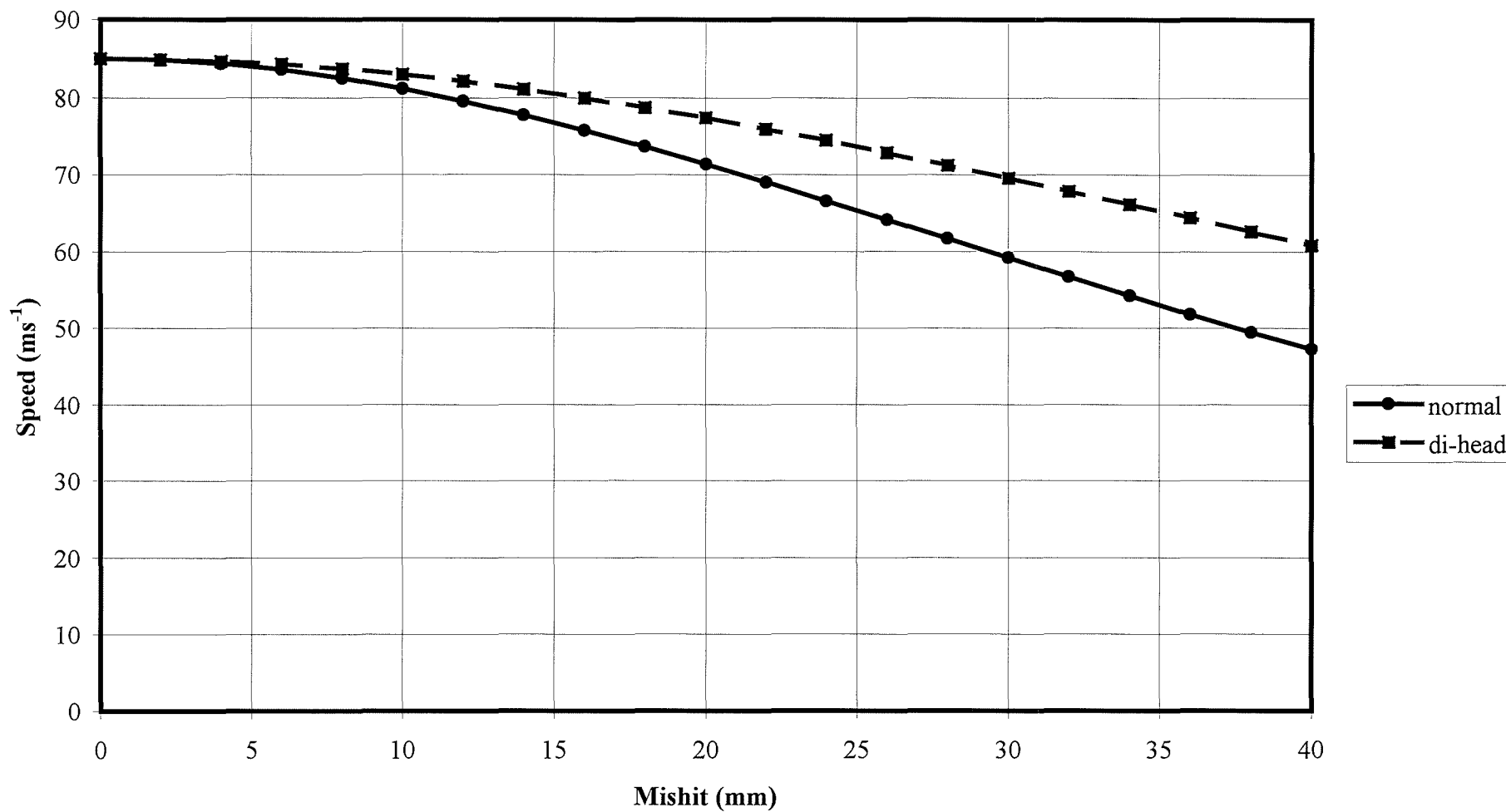


Figure 4.82 Effect of mishit on speed, centre of mass 5 mm behind face.

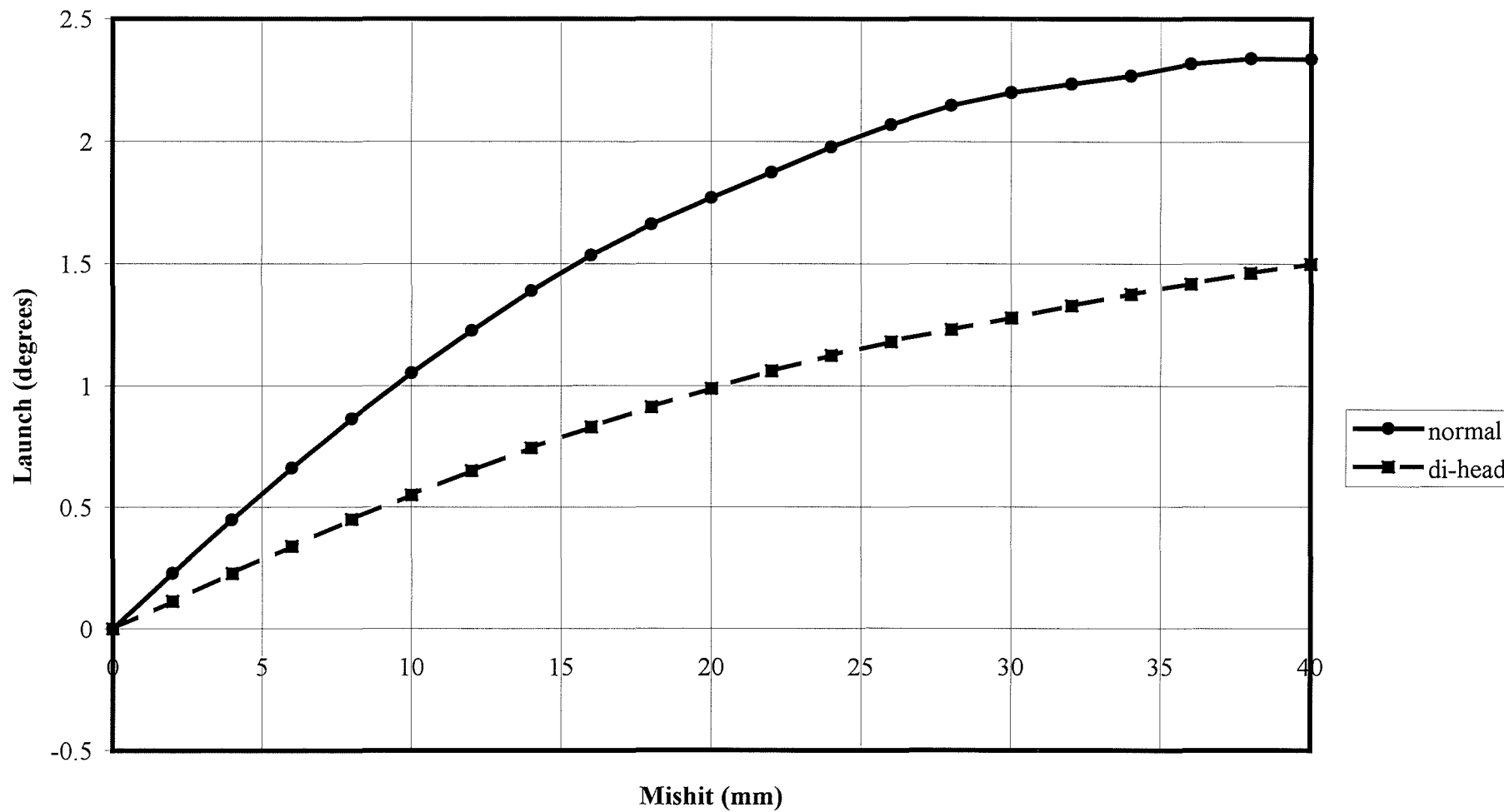


Figure 4.83 Effect of mishit on launch, centre of mass 5 mm behind face.

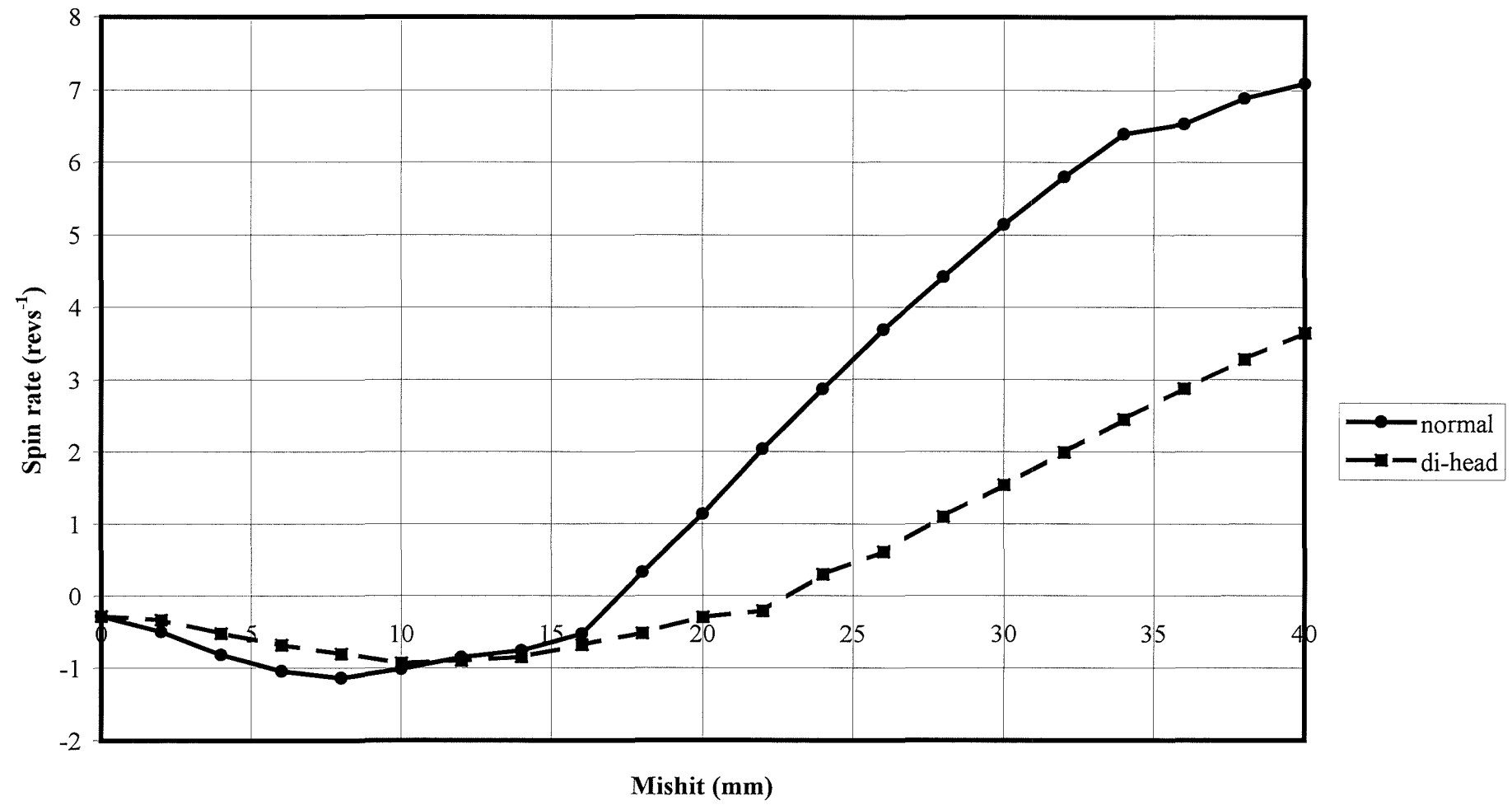


Figure 4.84 Effect of mishit on spin, centre of mass 5 mm behind face.

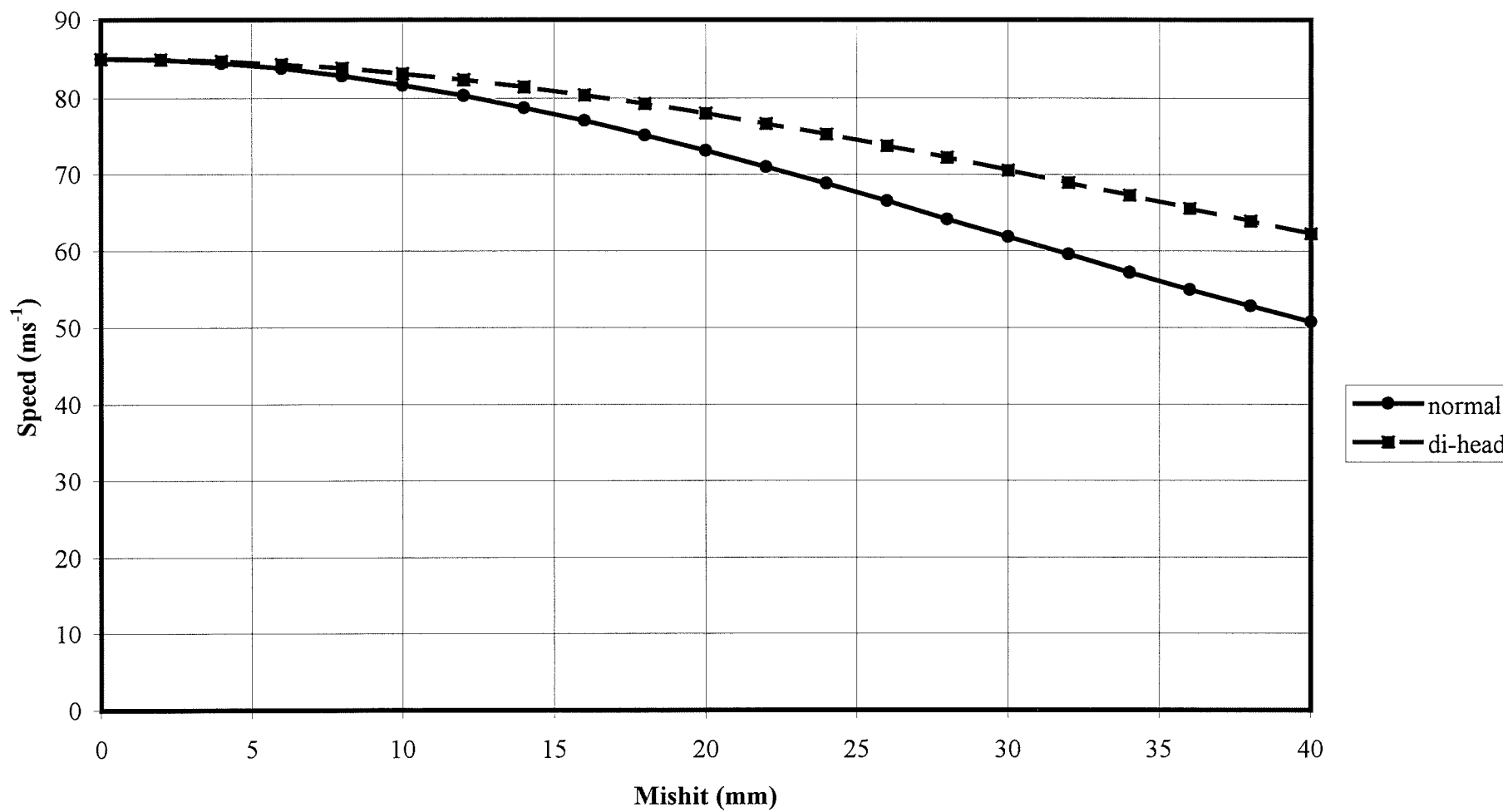


Figure 4.85 Effect of mishit on speed, centre of mass 30 mm behind face.

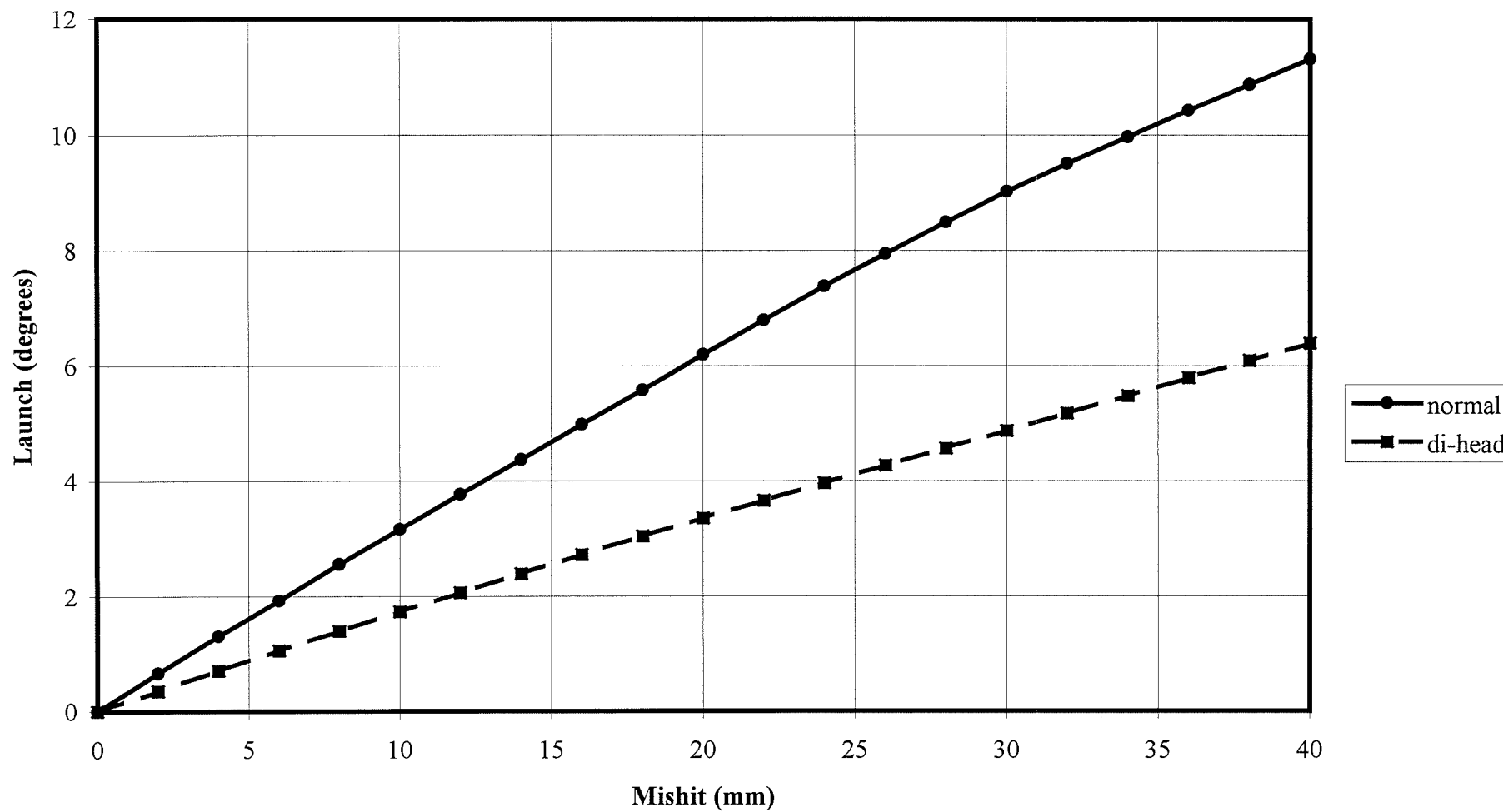


Figure 4.86 Effect of mishit on launch, centre of mass 30 mm behind face.

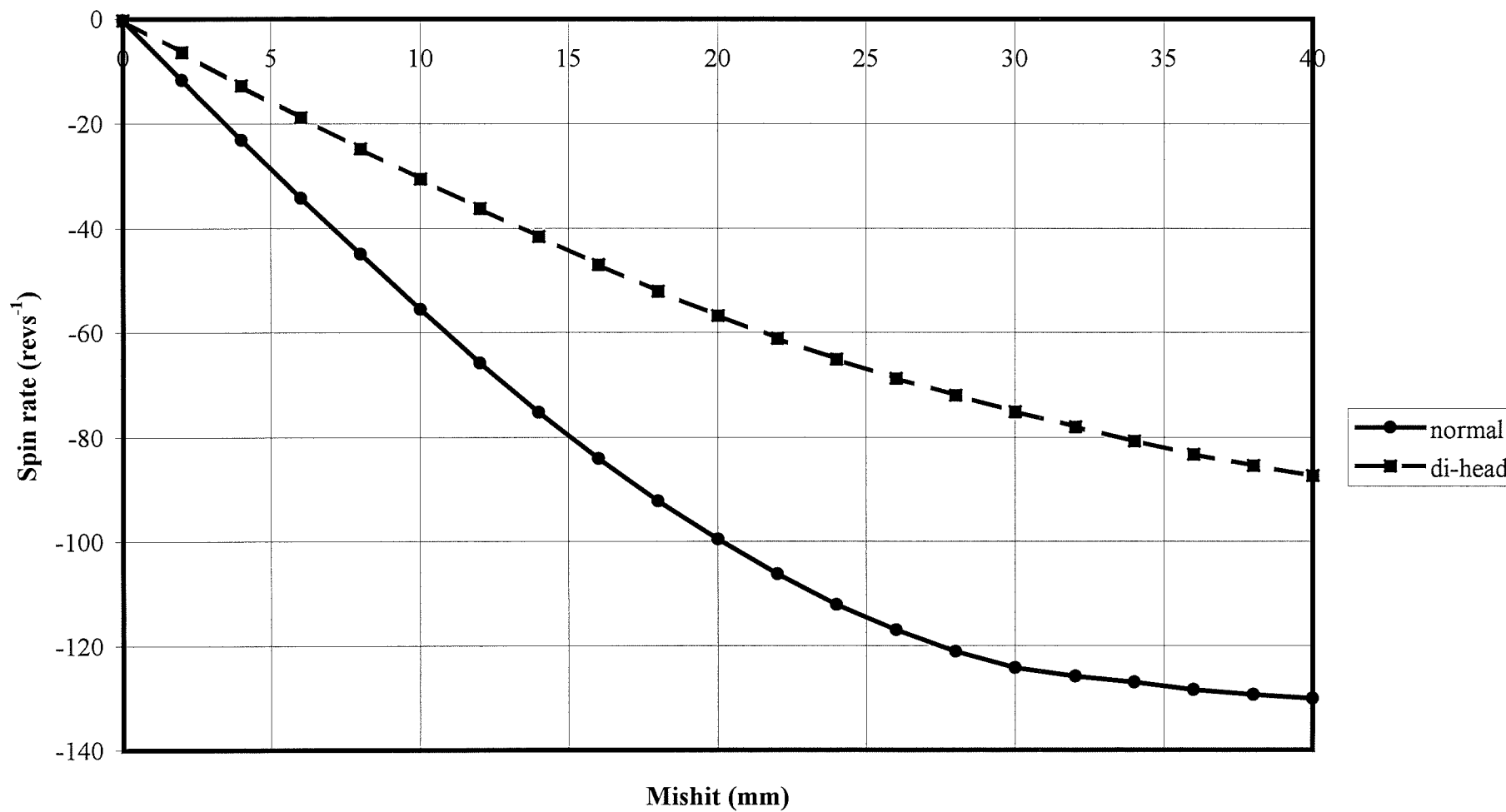


Figure 4.87 Effect of mishit on spin, centre of mass 30 mm behind face.

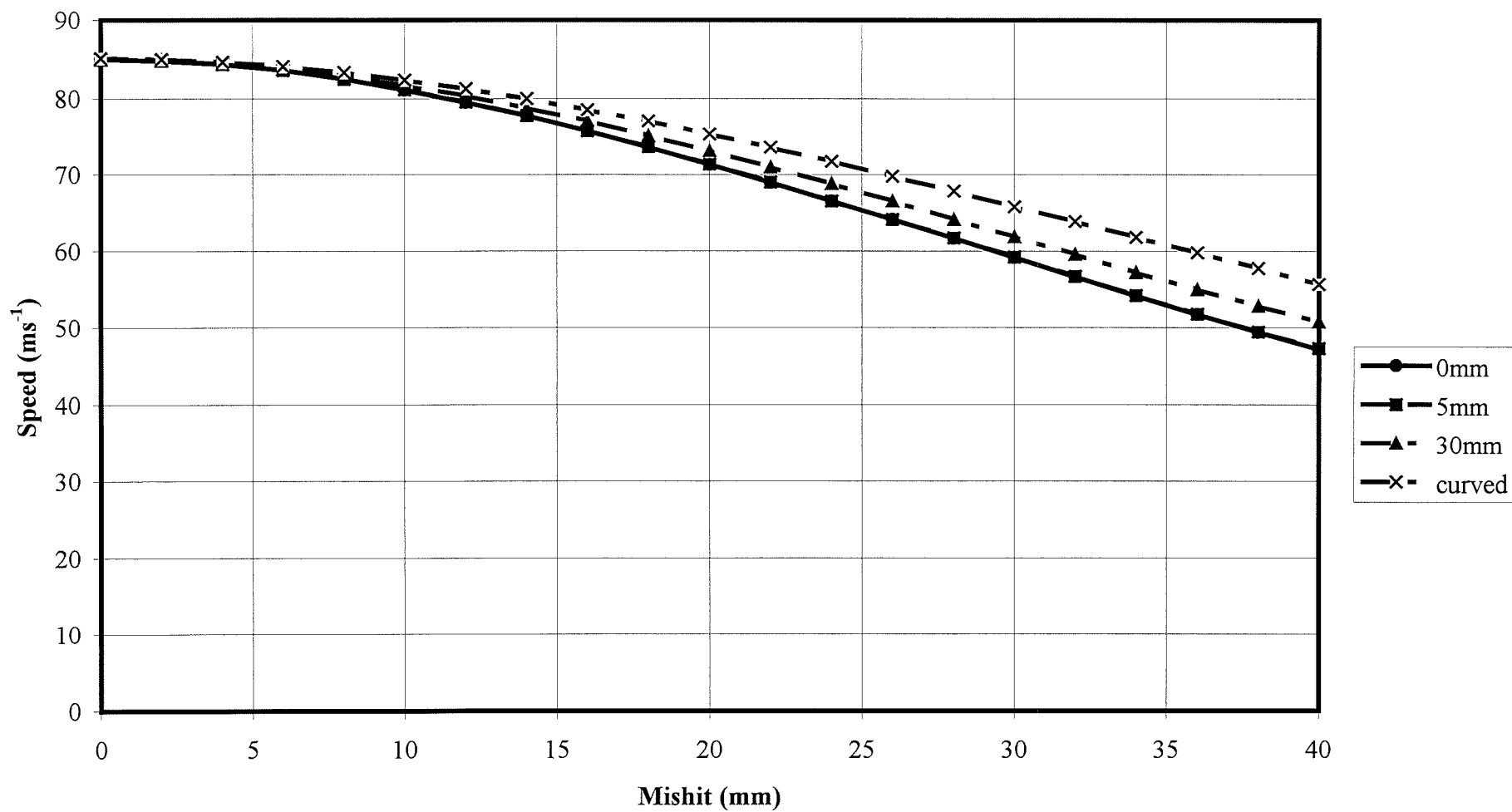


Figure 4.88 Effect of mishit on speed.

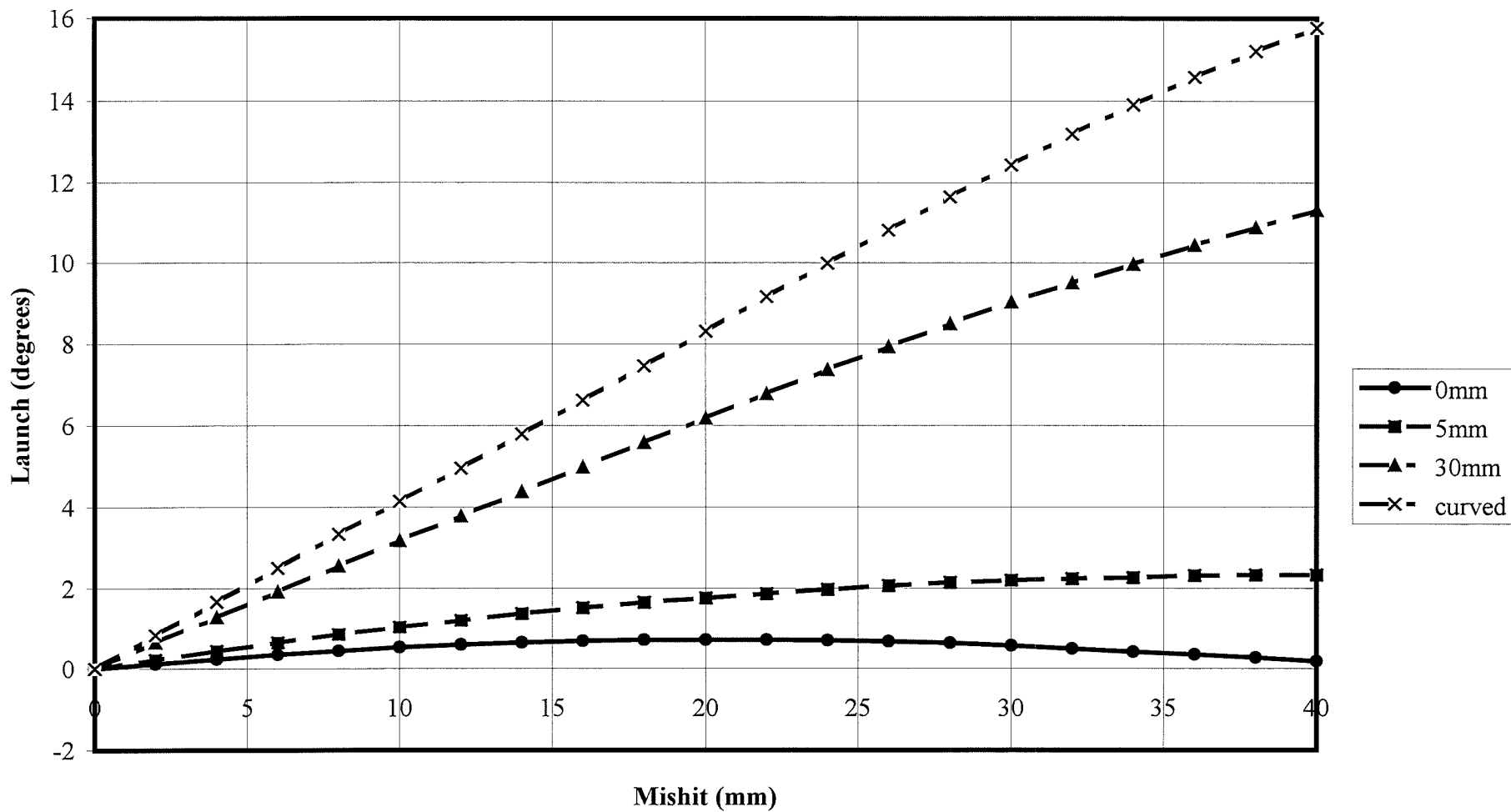


Figure 4.89 Effect of mishit on launch.

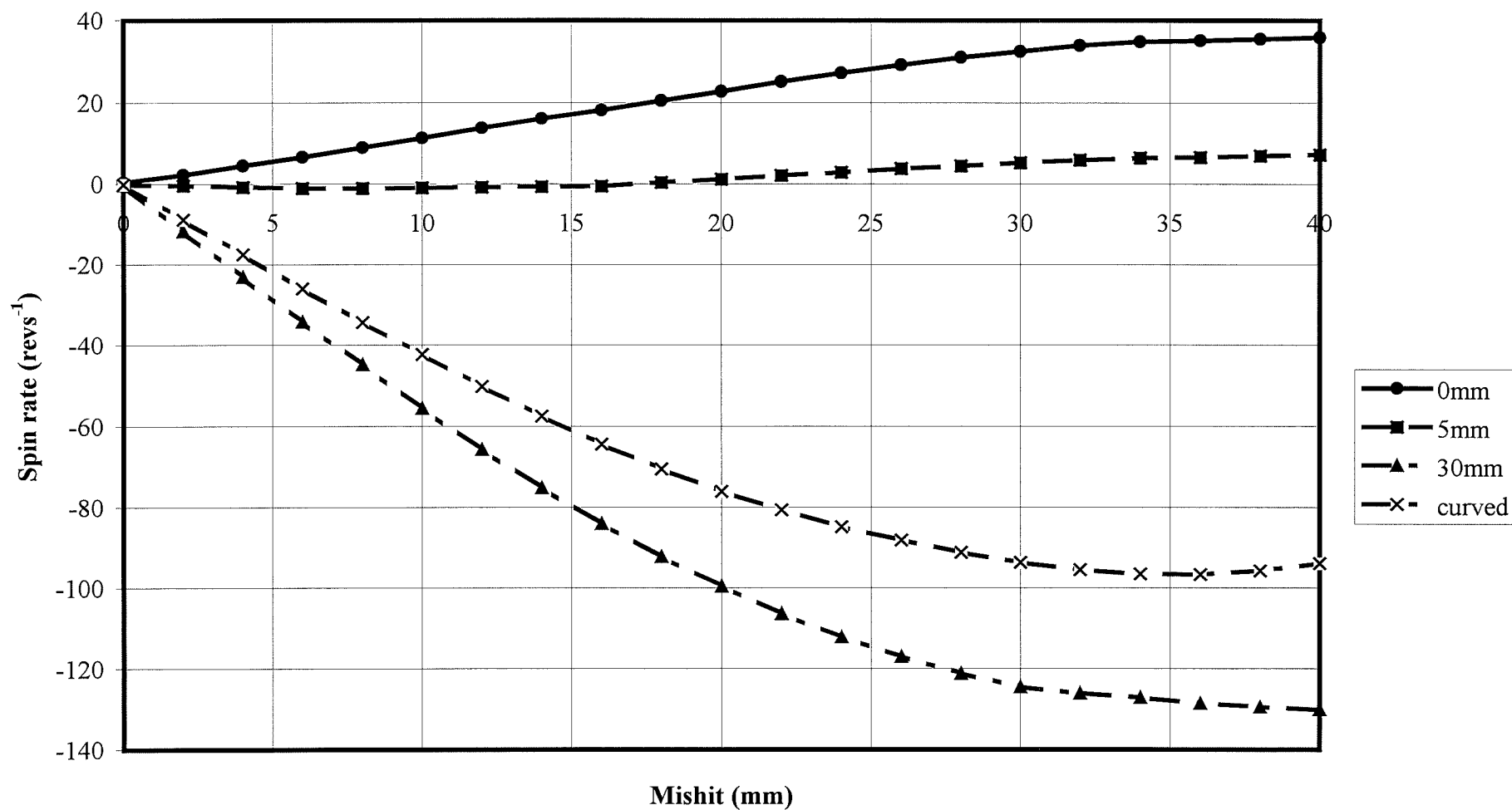


Figure 4.90 Effect of mishit on spin.

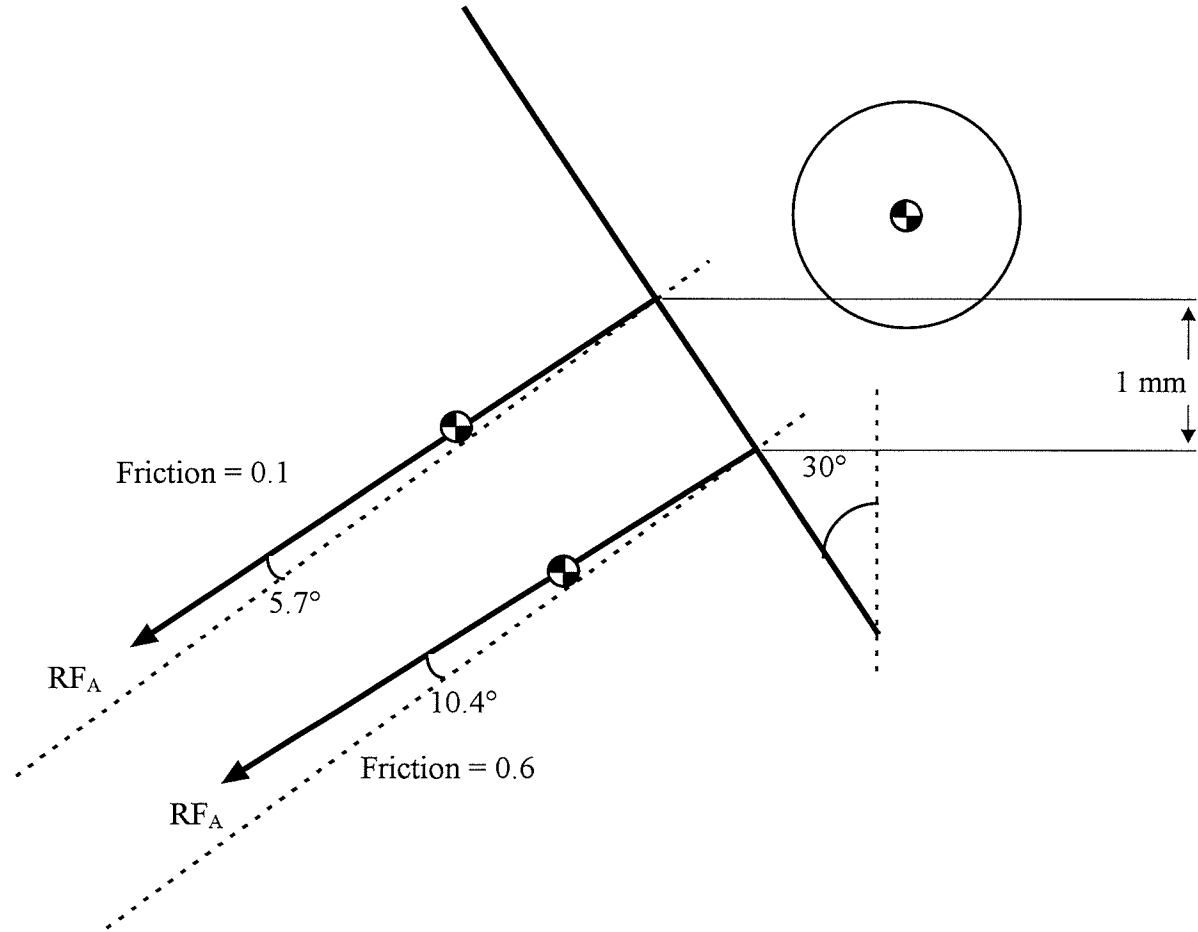


Figure 4.91 Average reaction force vectors (not to scale).

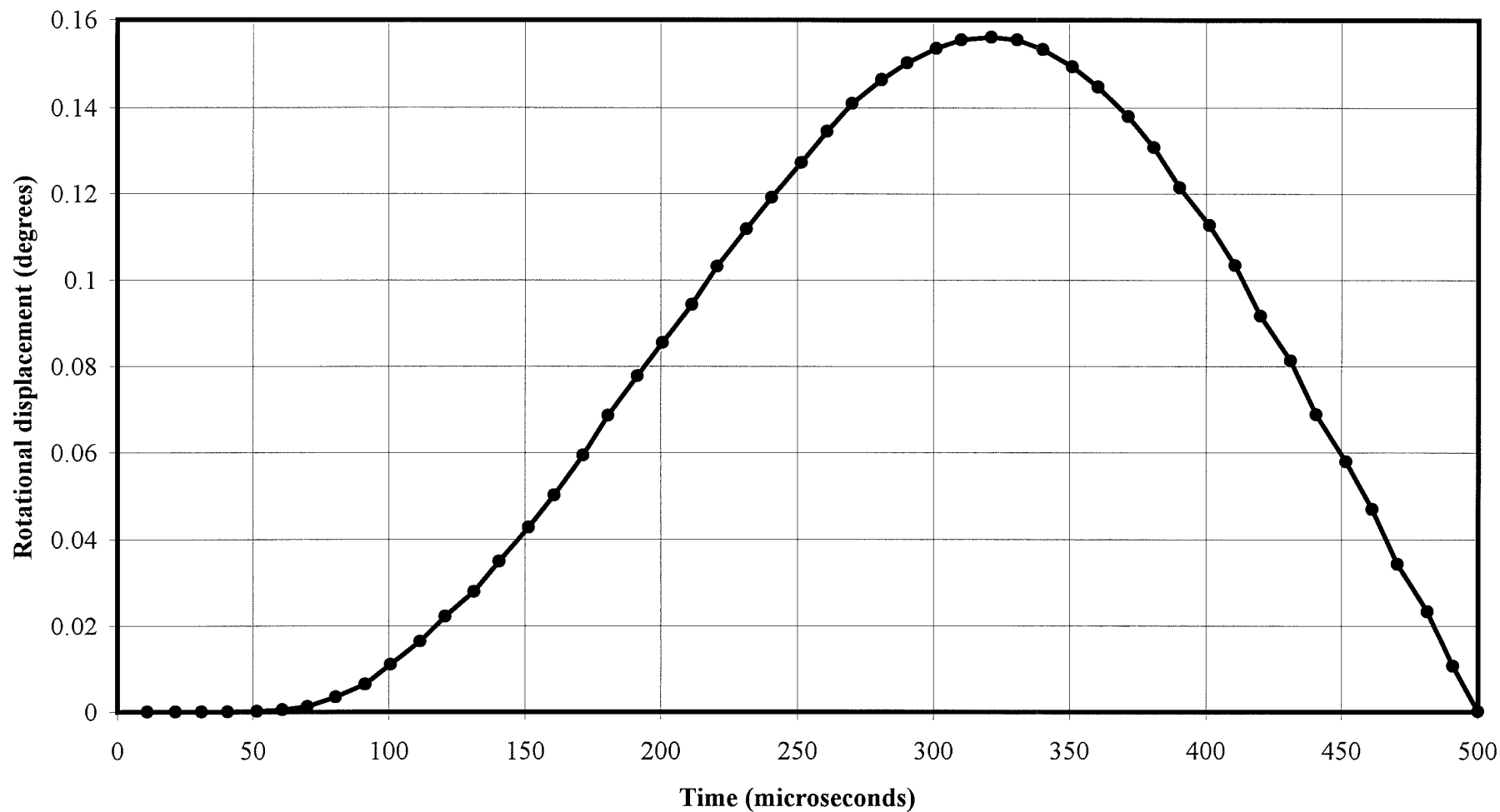


Figure 4.92 Rotational displacement of clubhead during impact, centre of mass 0 mm behind face.

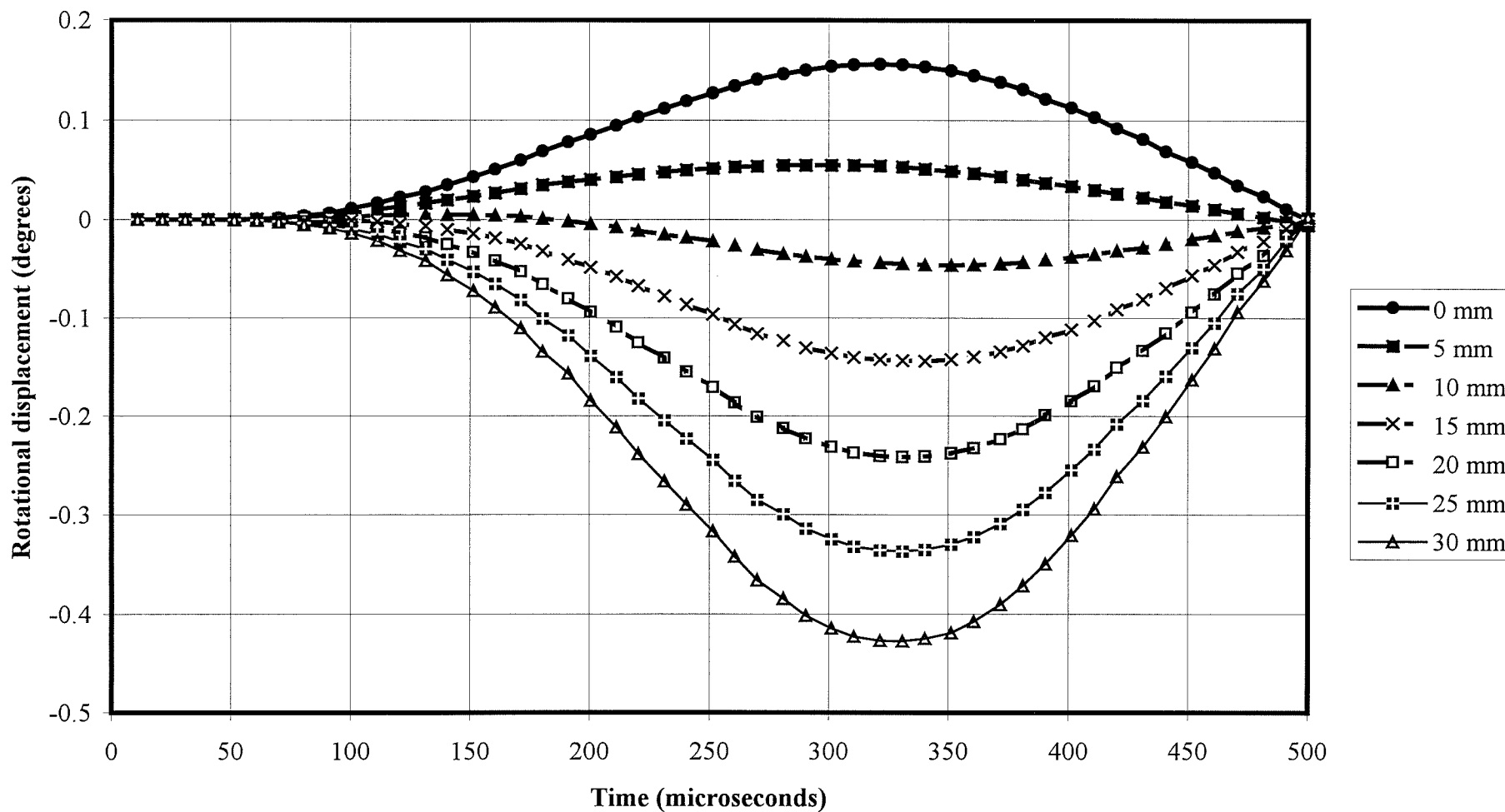


Figure 4.93 Rotational displacement of clubhead during impact, centre of mass at various distance behind face.

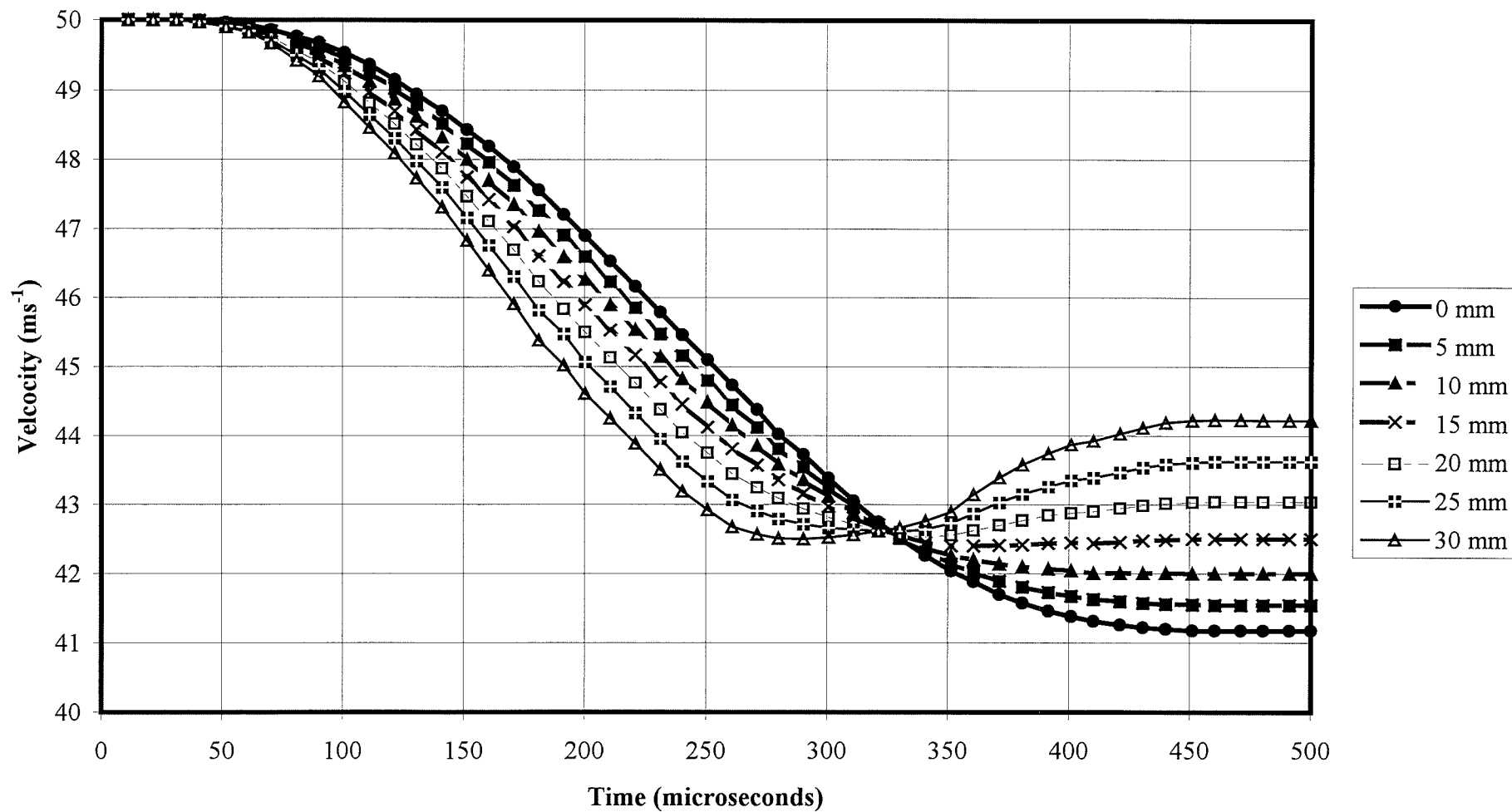


Figure 4.94 Shaft tip velocity, centre of mass at various distance behind face.

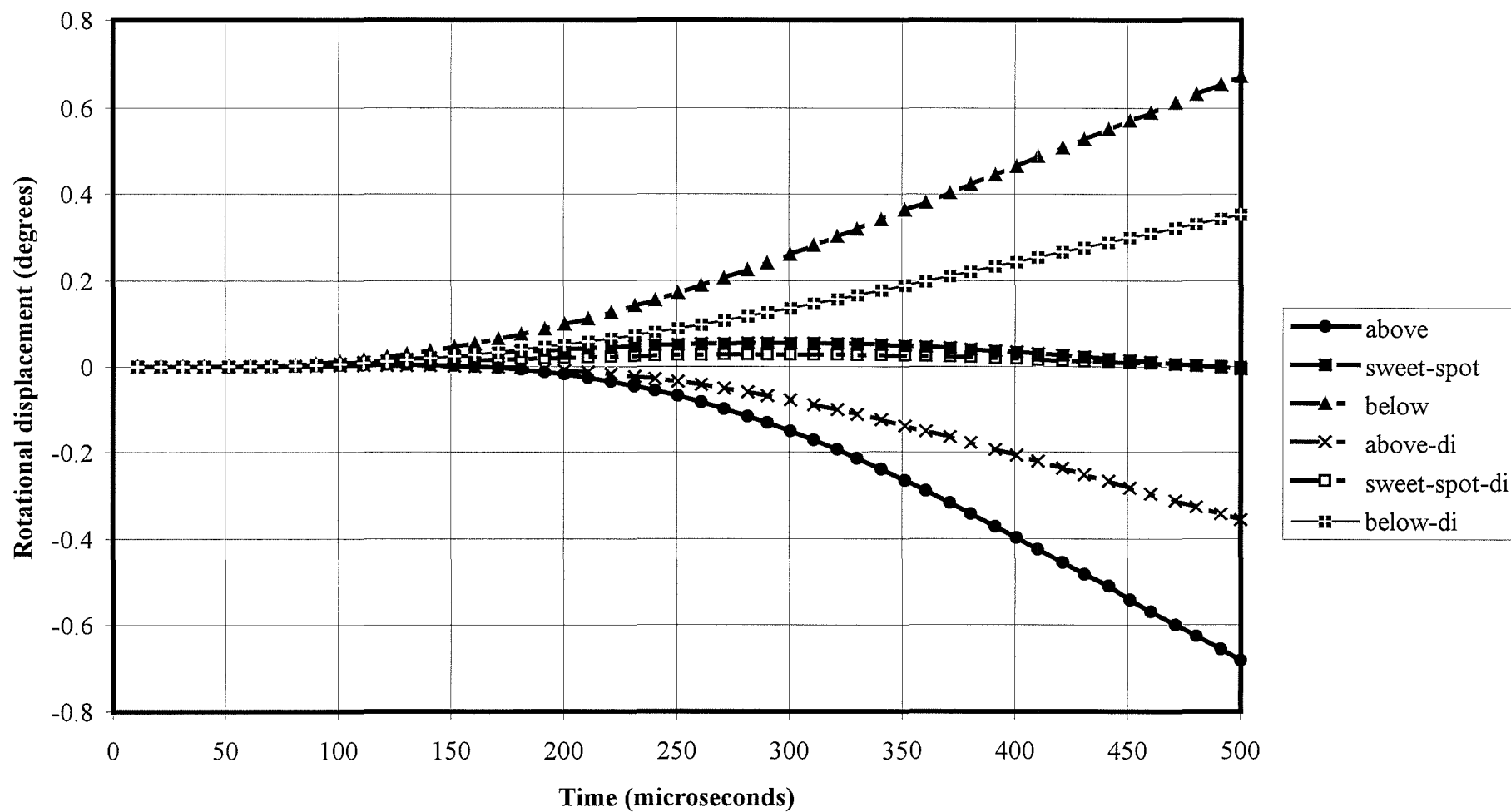


Figure 4.95 Rotational displacement for shots off the sweet spot, above and below 1 mm.

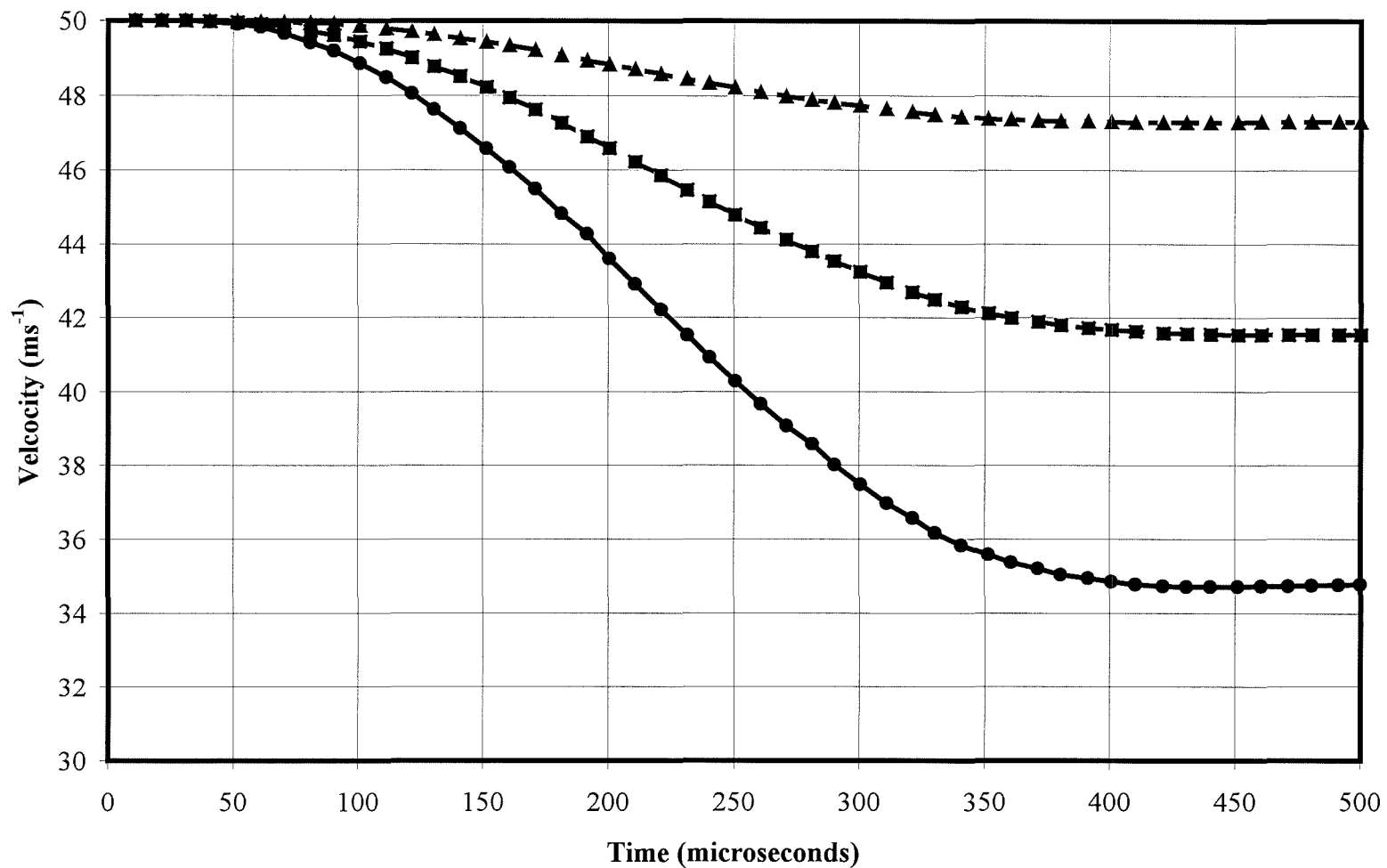


Figure 4.96 Shaft tip velocity for shots off the sweet-spot, above and below 5 mm.

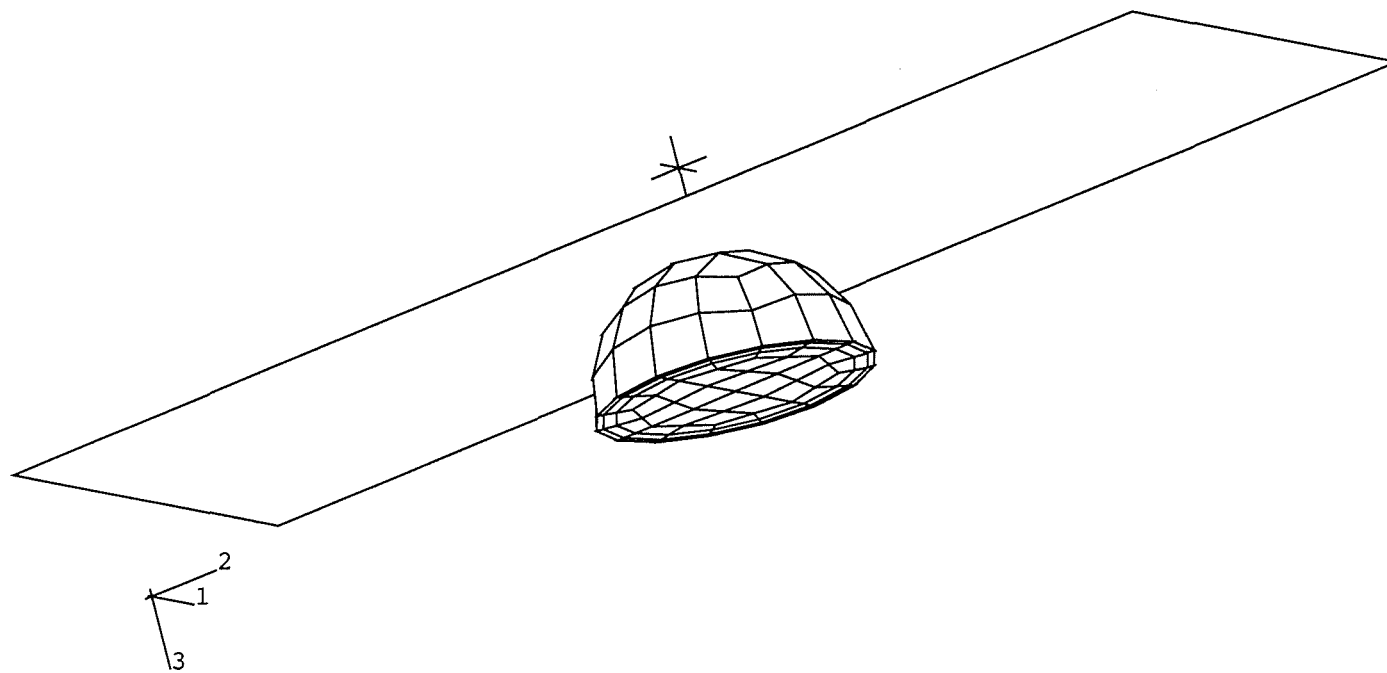


Figure 4.97 Half ball model used in compression tests.

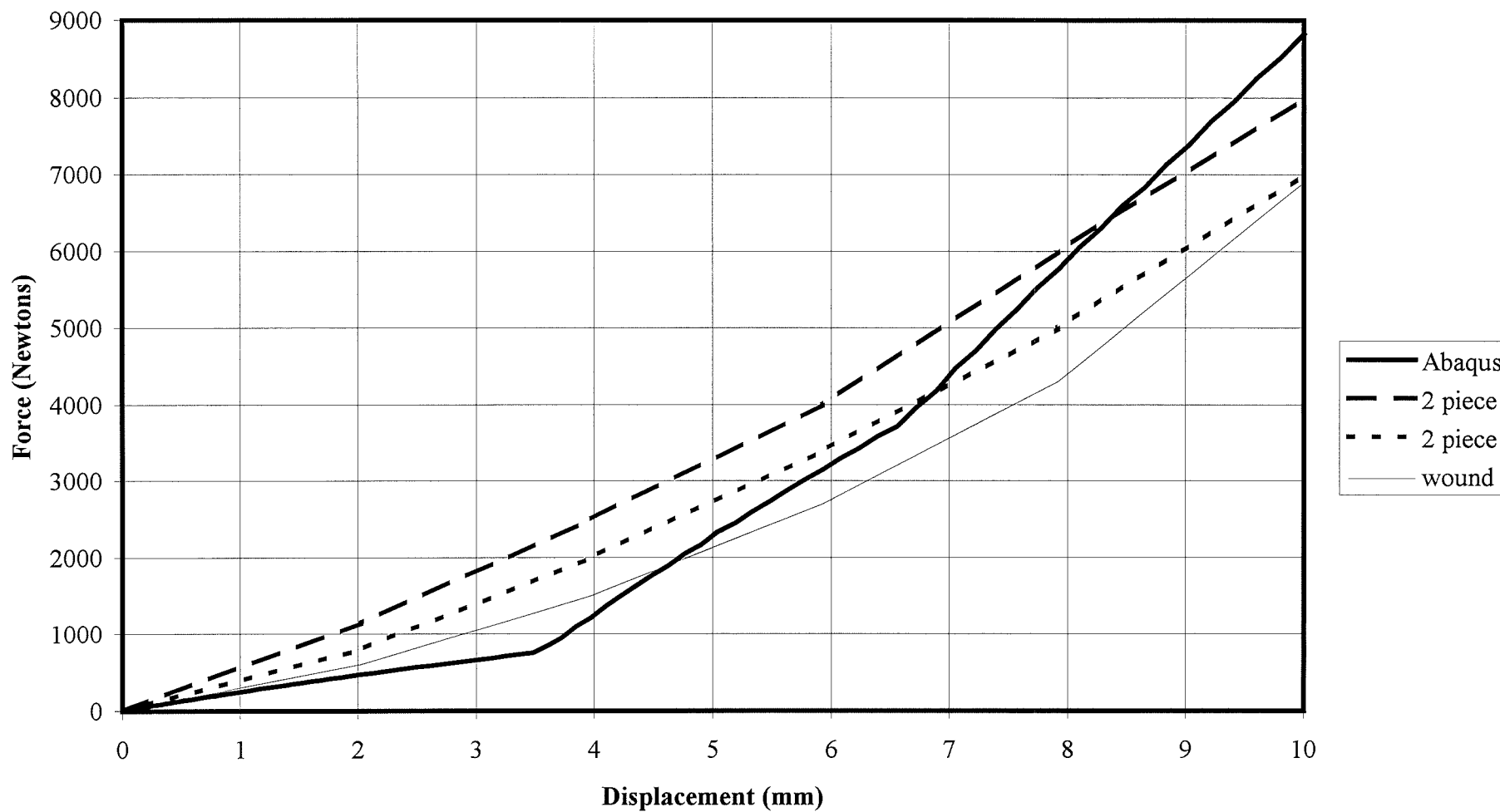


Figure 4.98 10 mm compression of model and existing golf balls (Mather and Immohr 1996).

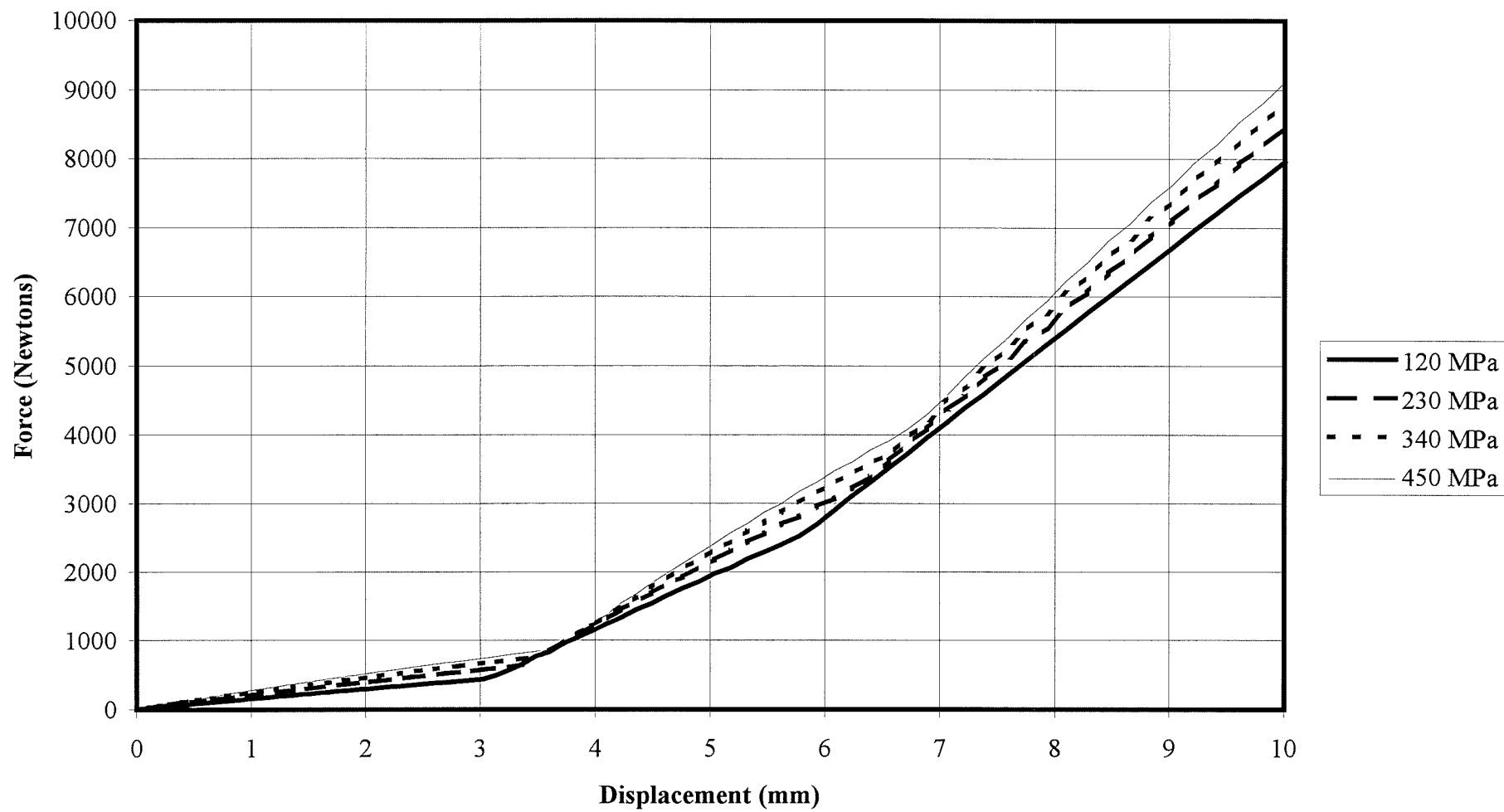


Figure 4.99 10 mm compression of varying cover stiffness models.

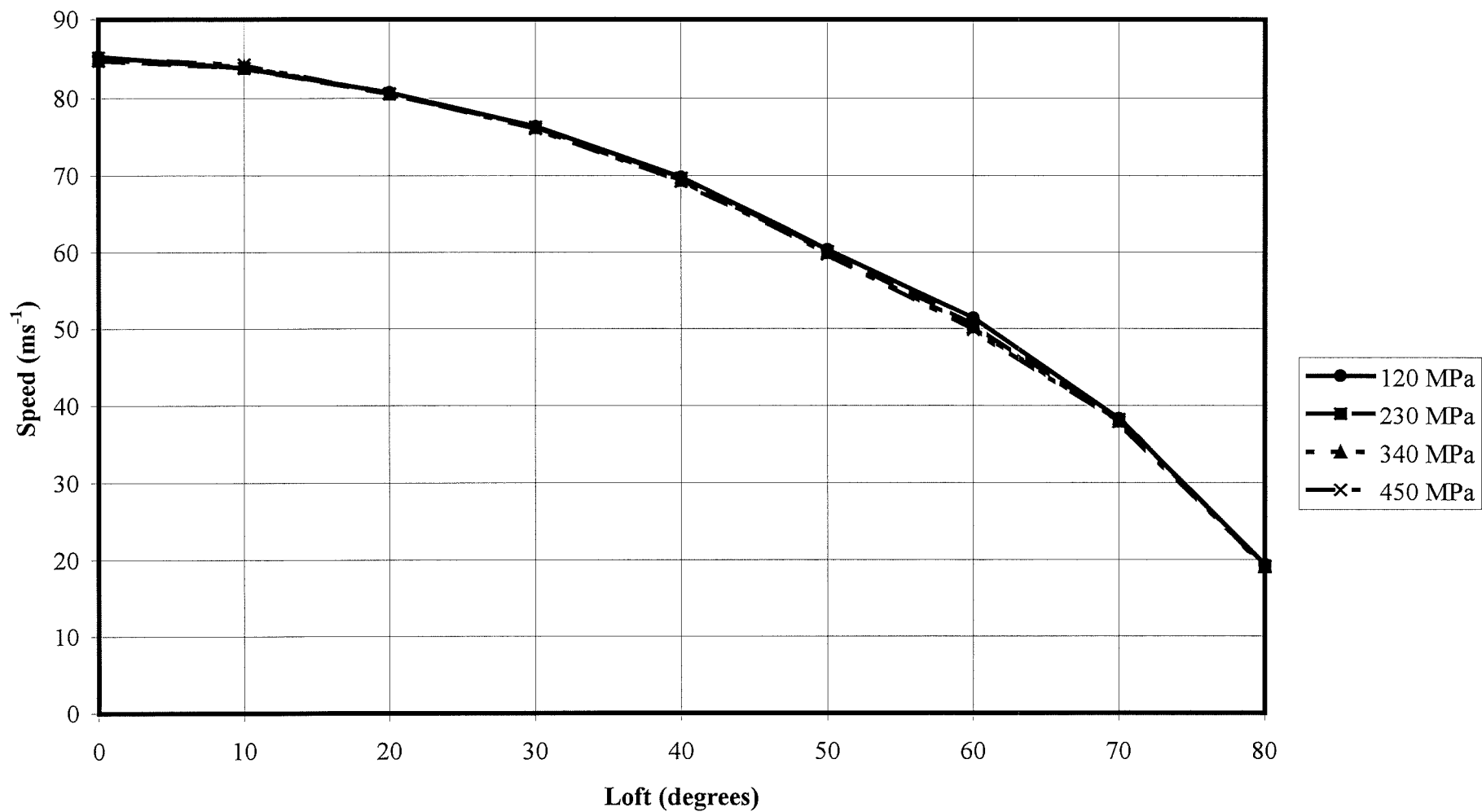


Figure 4.100 Effect of cover stiffness on ball speed.

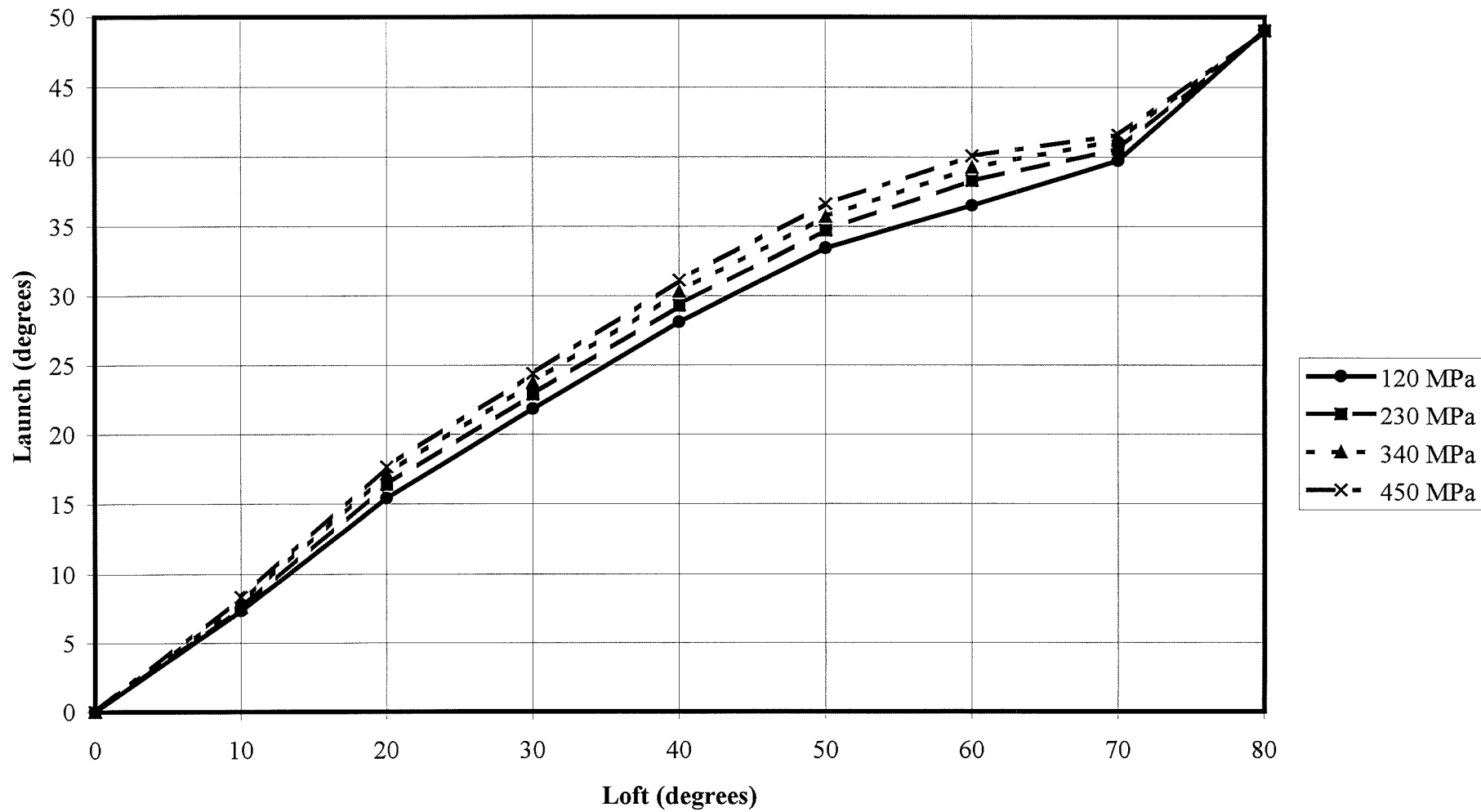


Figure 4.101 Effect of cover stiffness on ball launch.

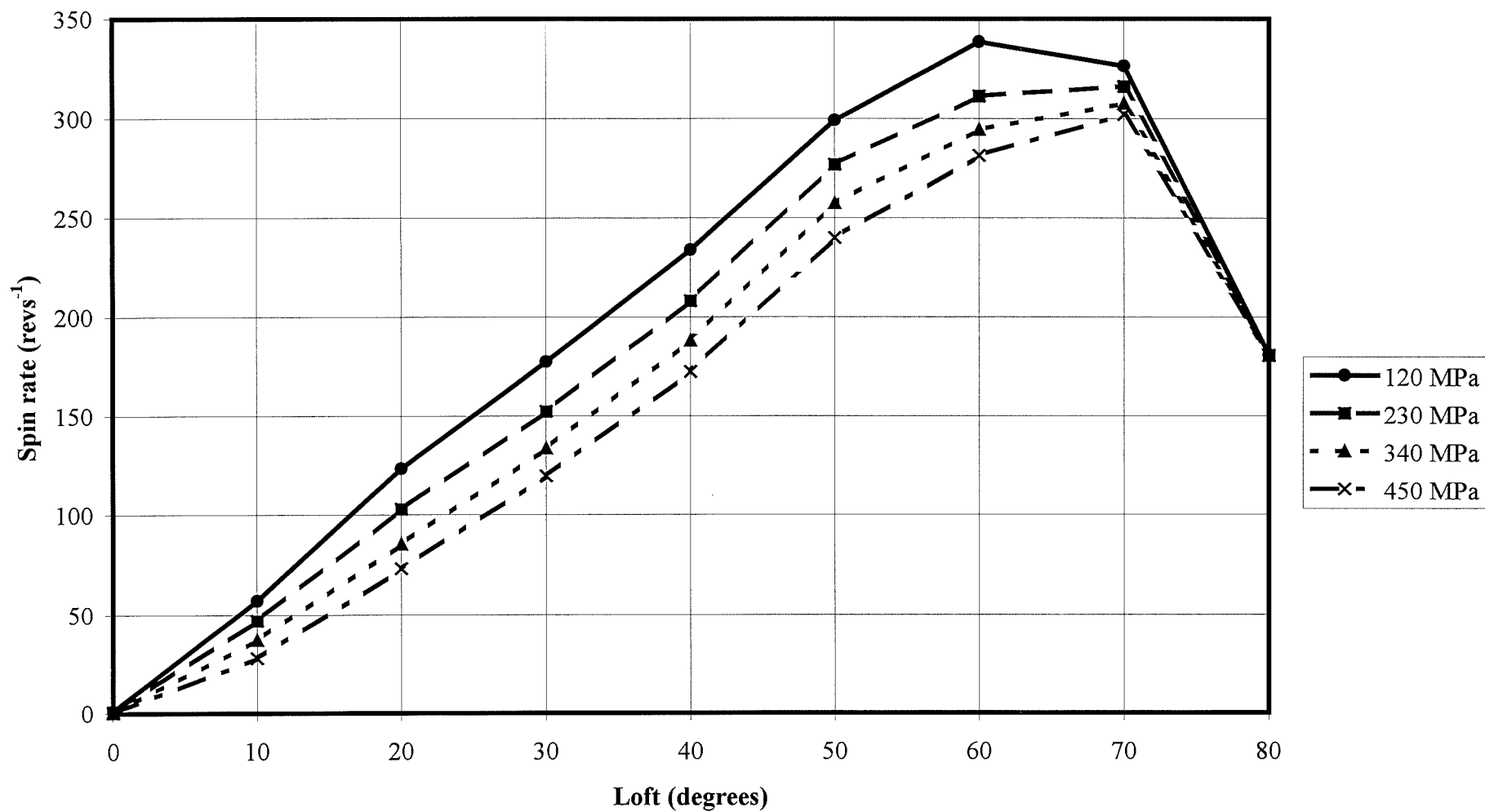


Figure 4.102 Effect of cover stiffness on ball spin.

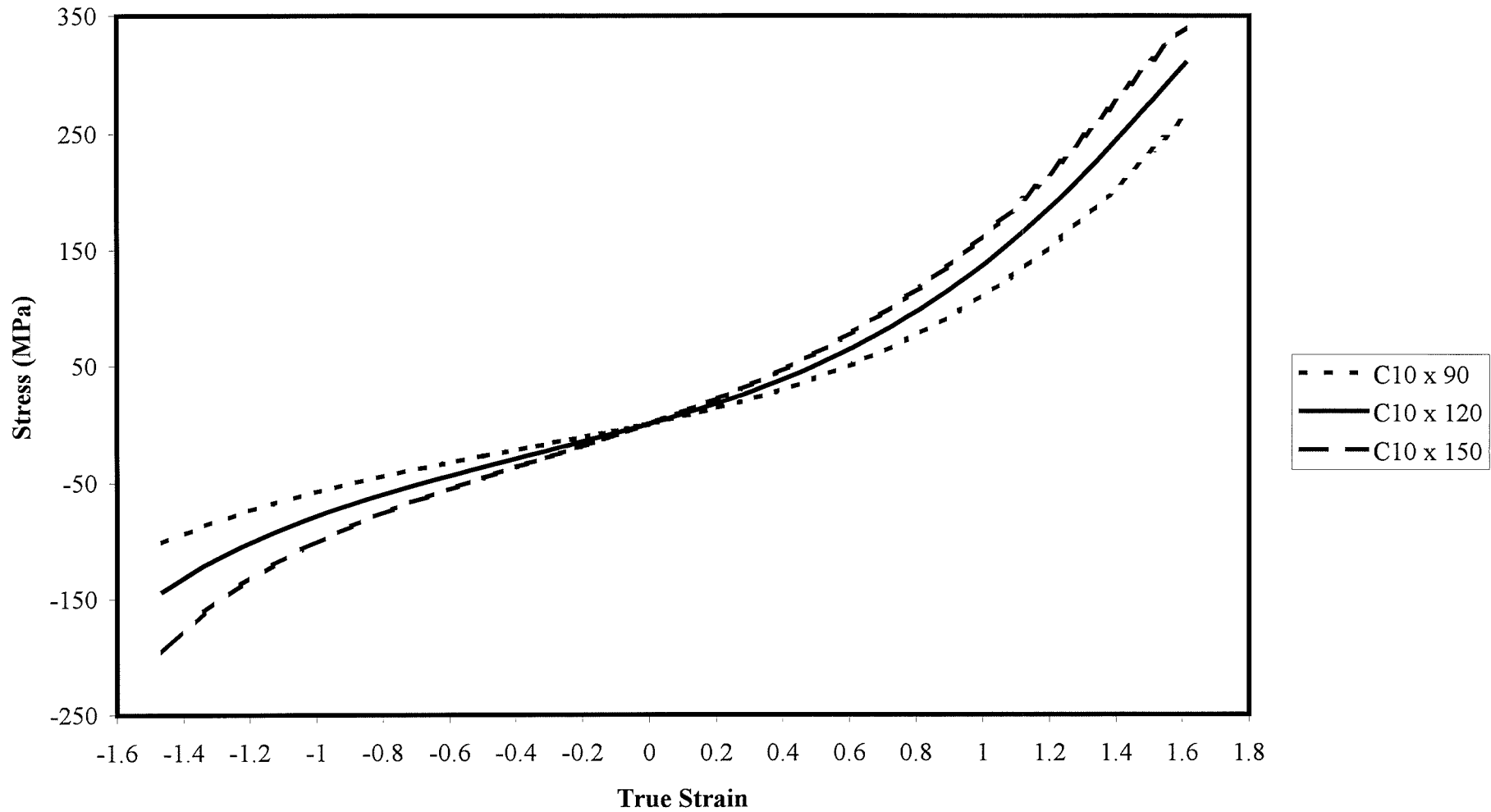


Figure 4.103 Stress/strain behaviour of various hyperelastic core stiffnesses.

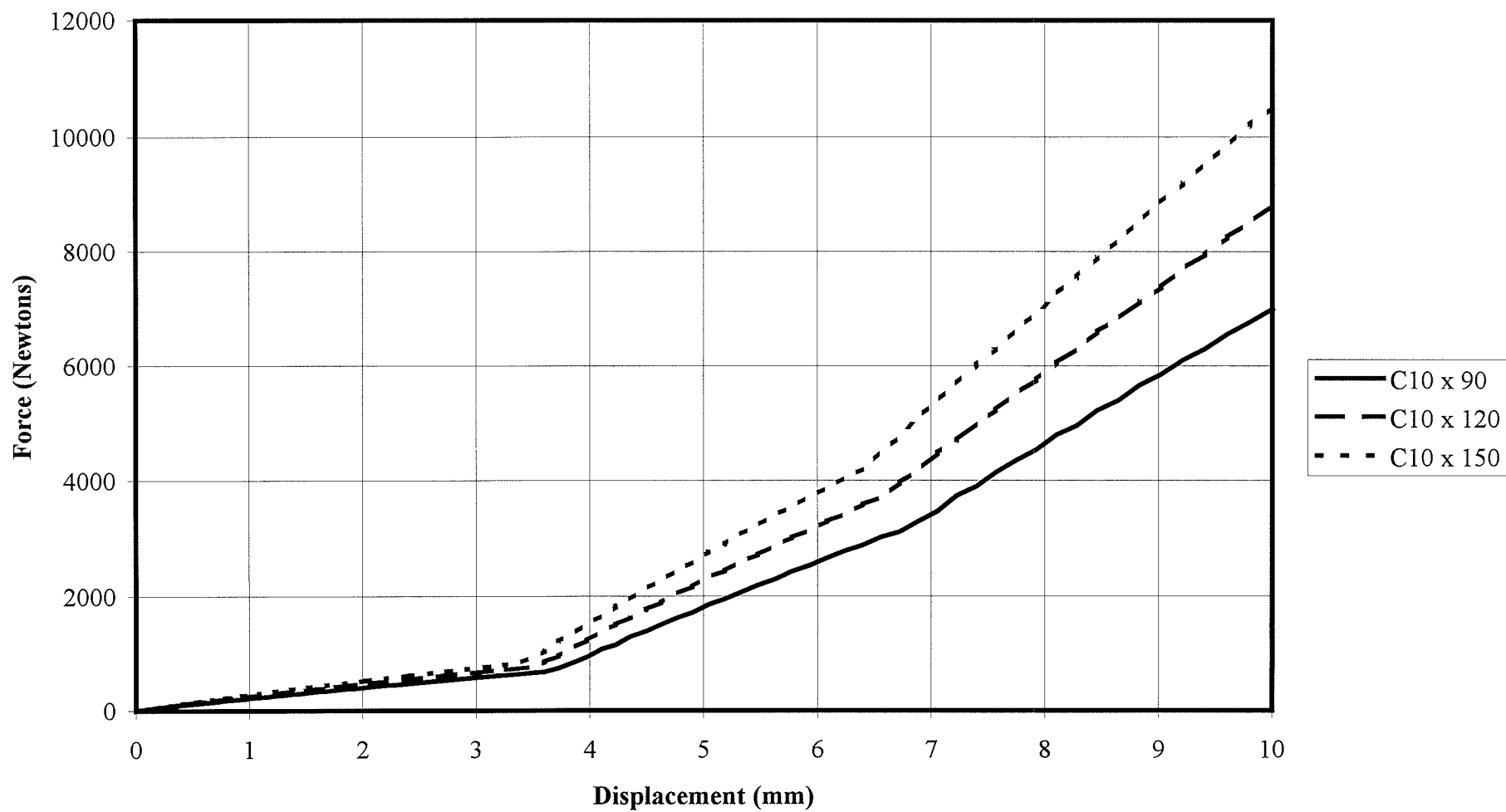


Figure 4.104 10 mm compression of varying core stiffness models.

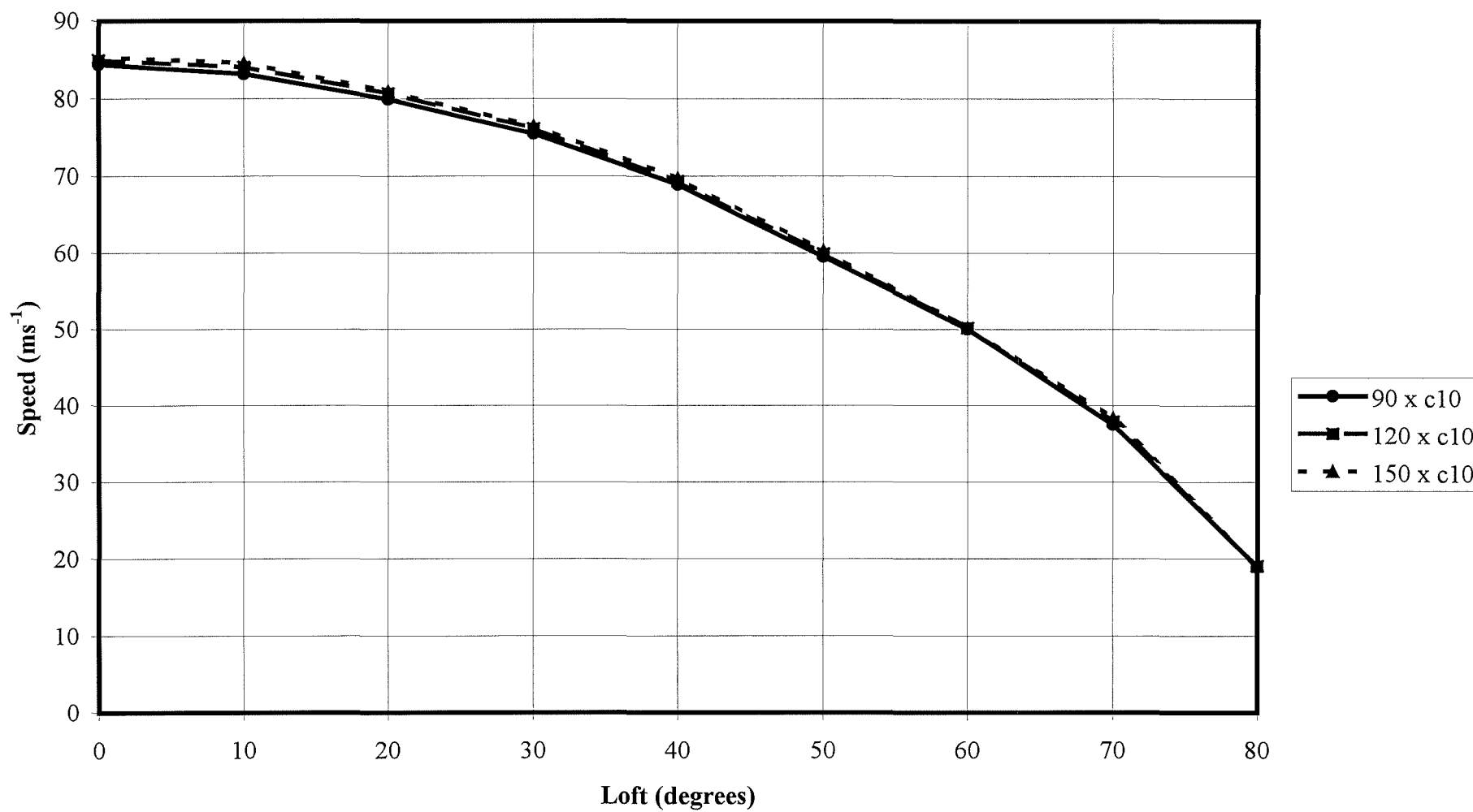


Figure 4.105 Effect of core stiffness on ball speed.

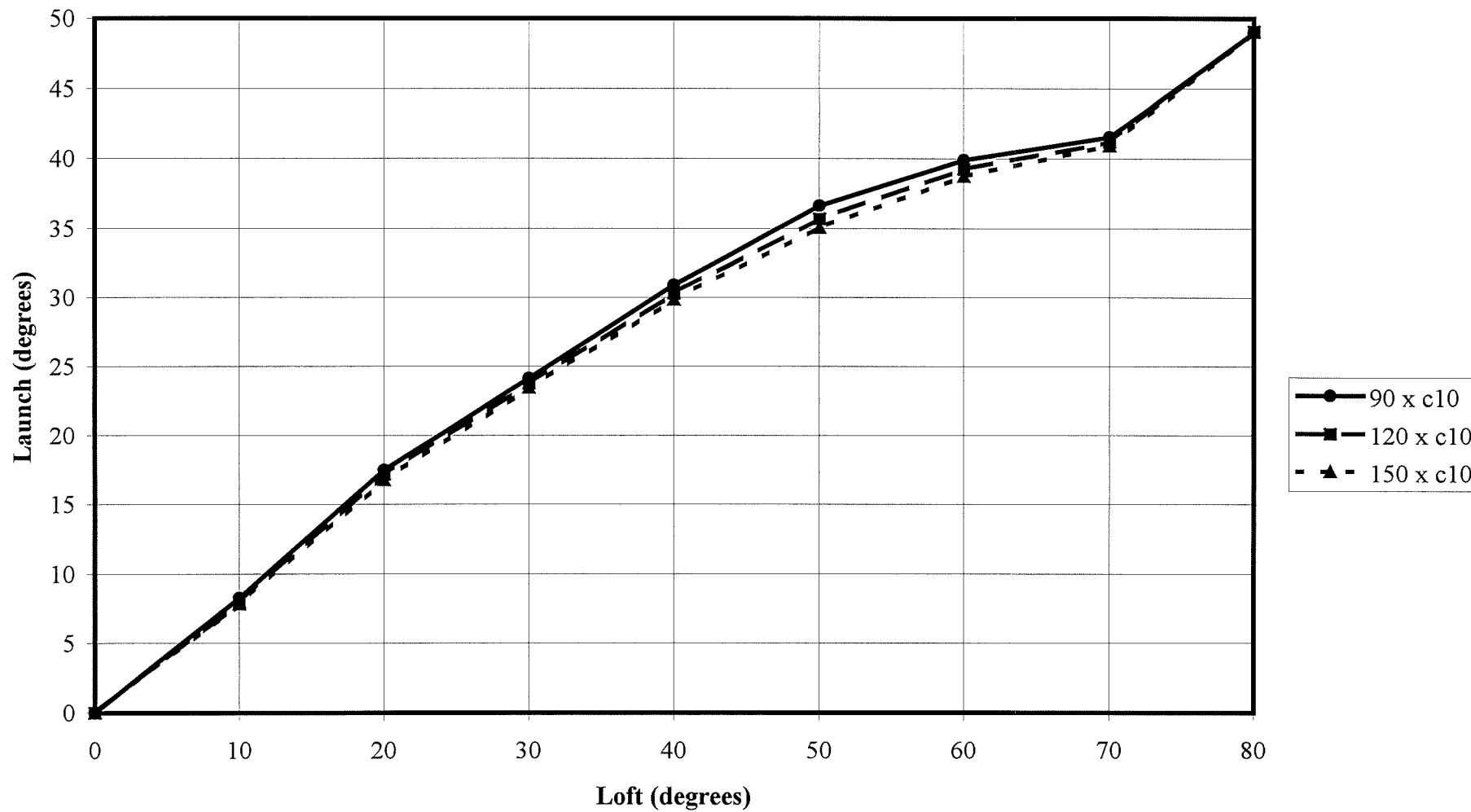


Figure 4.106 Effect of core stiffness on ball launch.

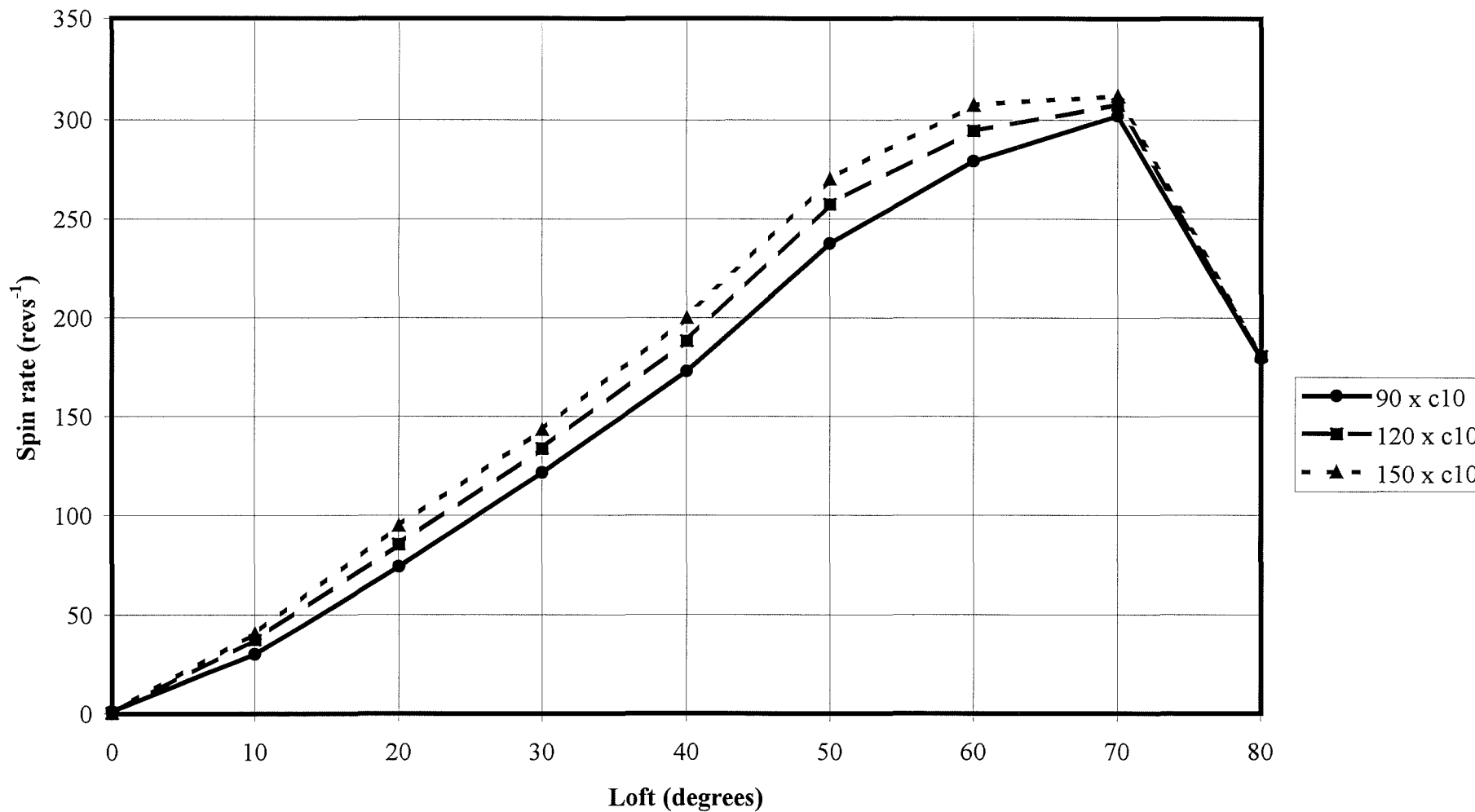


Figure 4.107 Effect of core stiffness on ball spin.

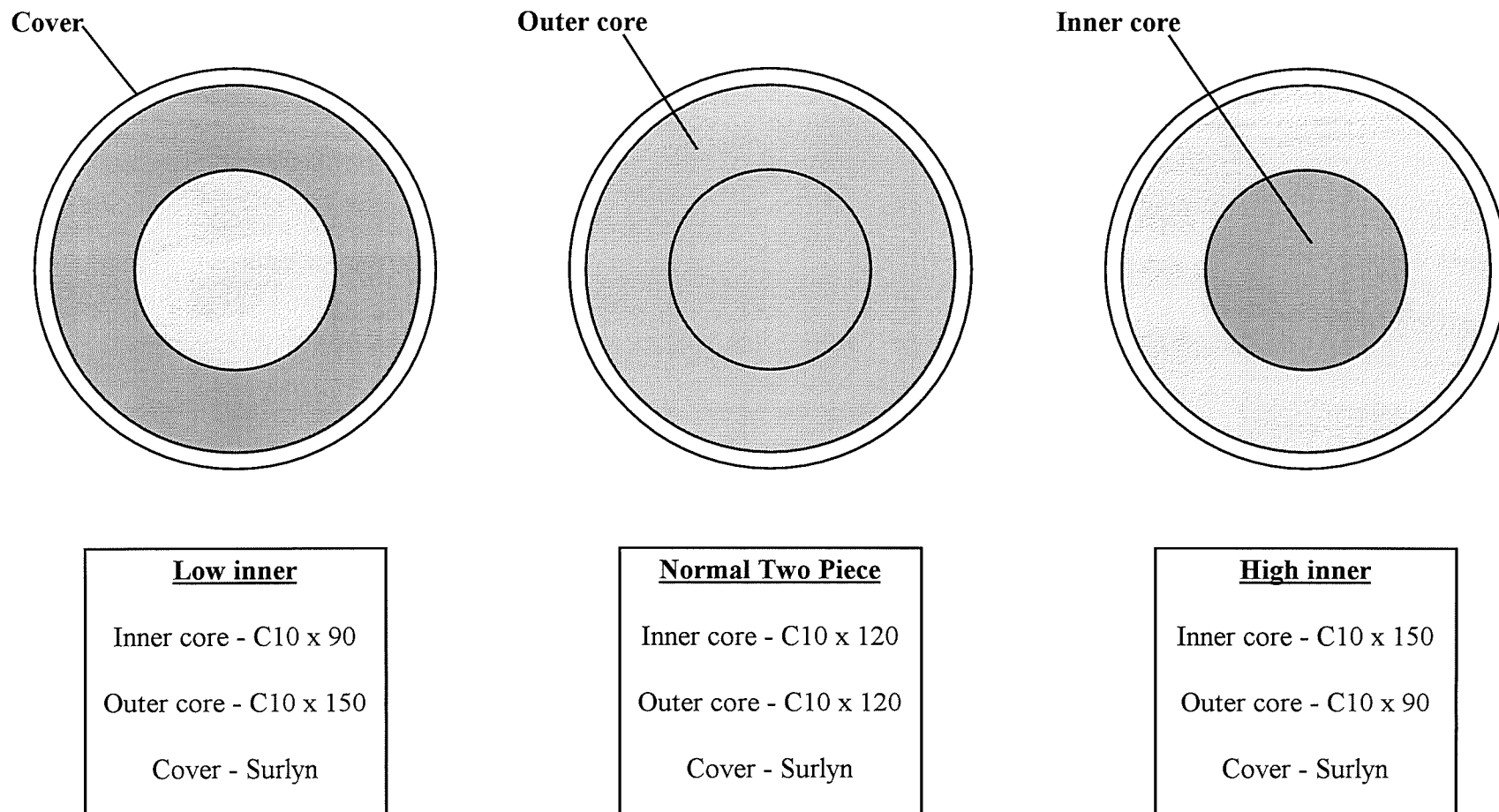


Figure 4.108 Ball constructions used to analyse dual stiffness effects.

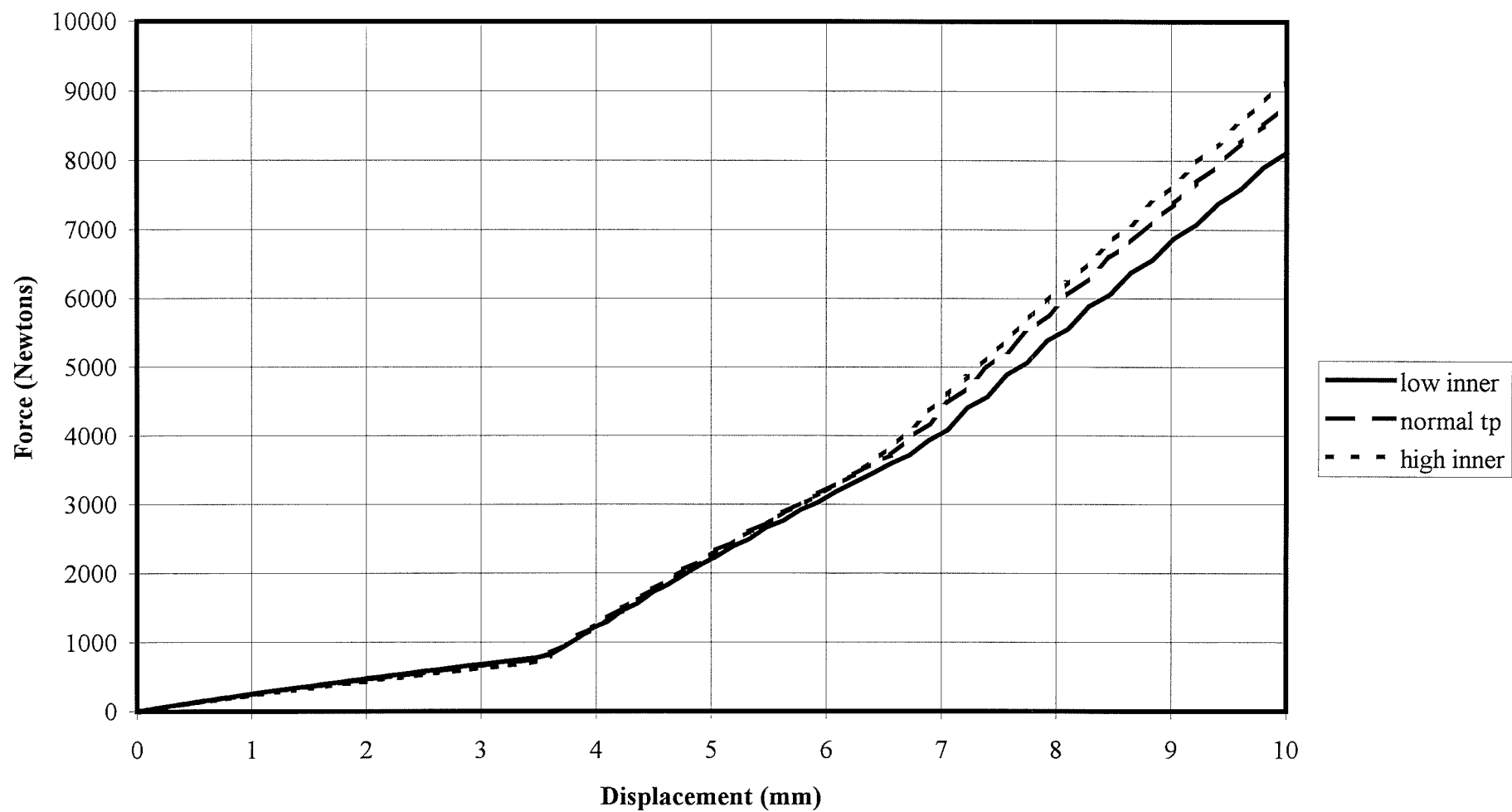


Figure 4.109 10 mm compression of varying dual core stiffness models.

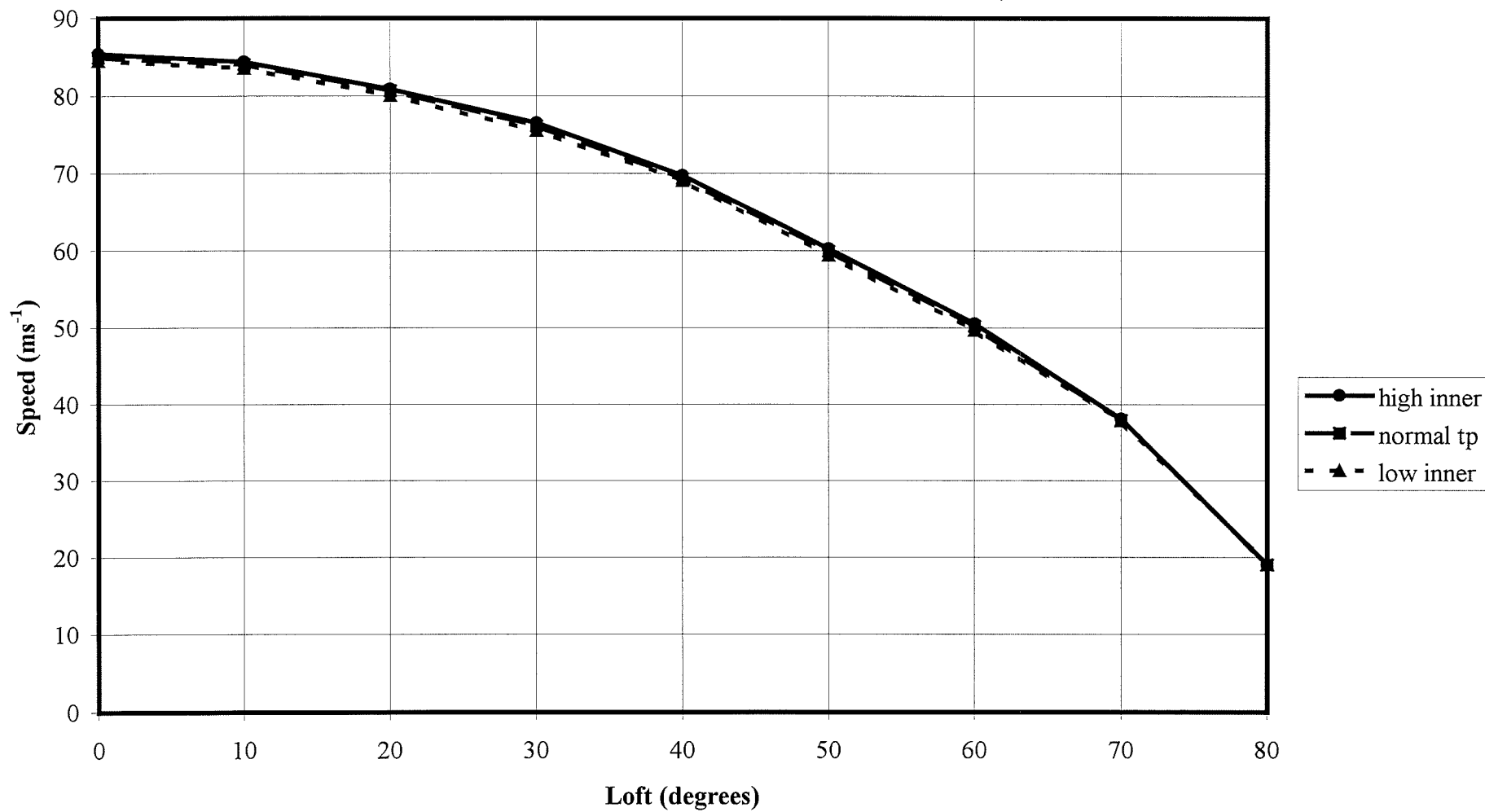


Figure 4.110 Effect of dual core stiffness on ball speed.

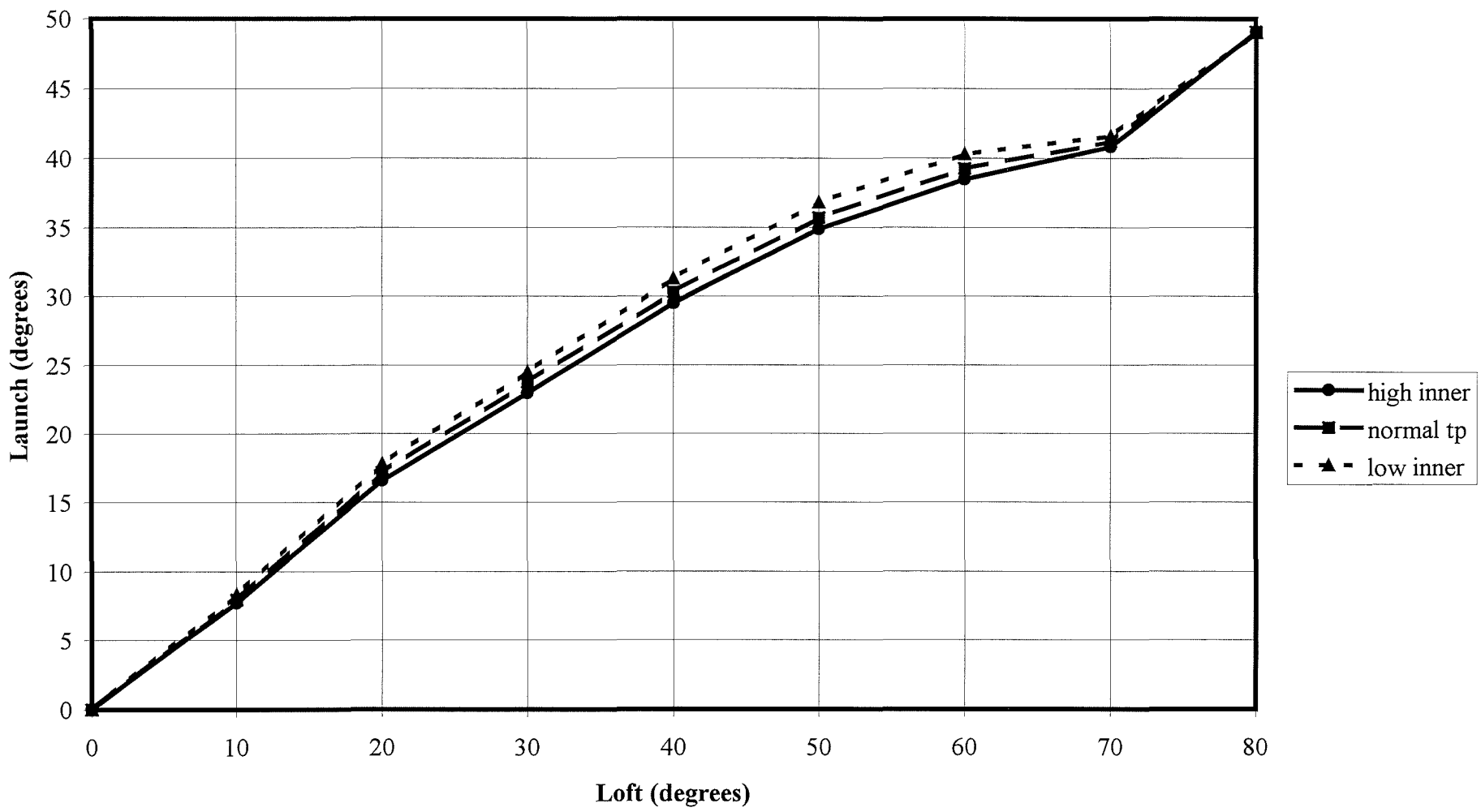


Figure 4.111 Effect of dual core stiffness on ball launch.

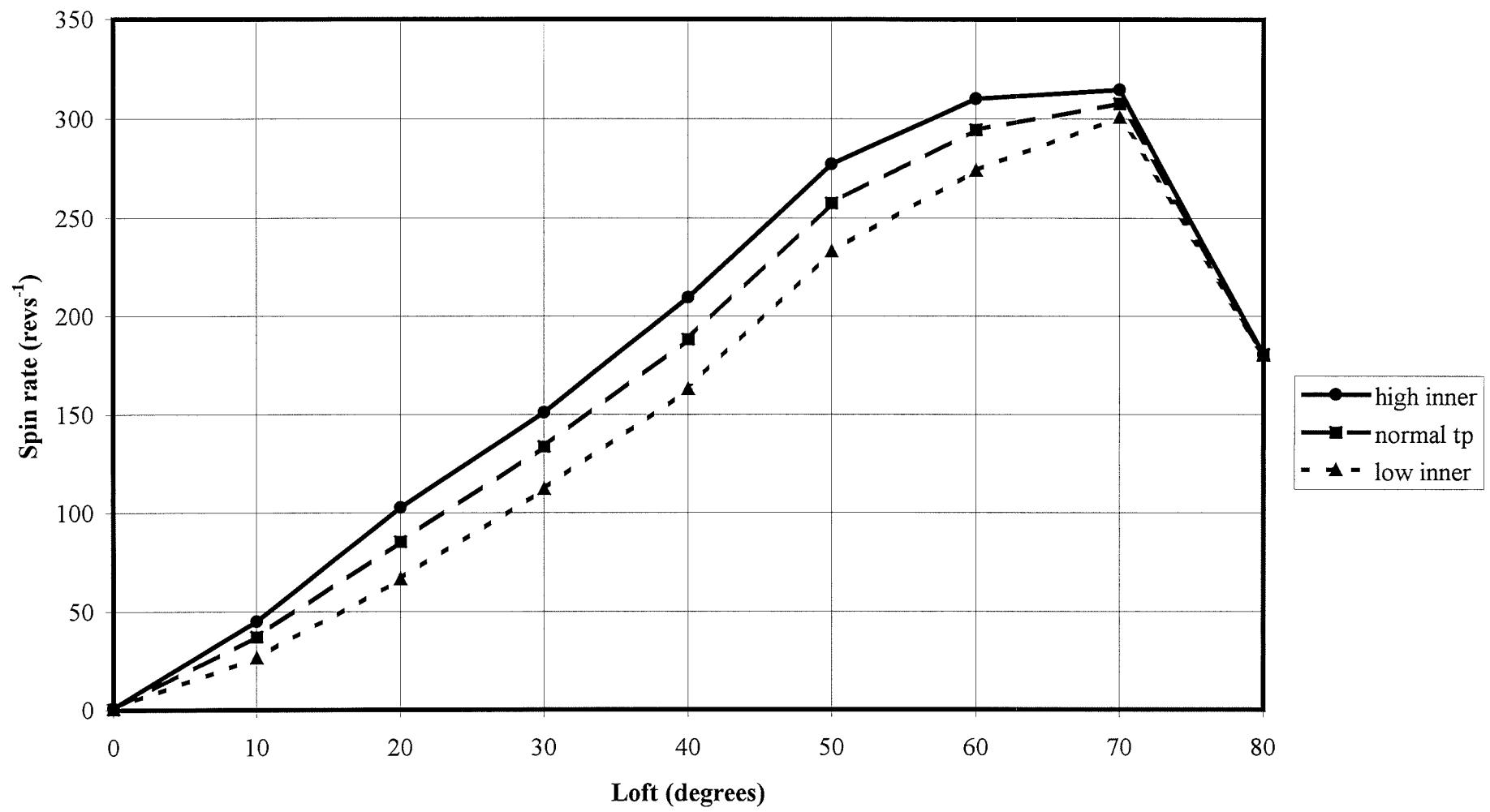


Figure 4.112 Effect of dual core stiffness on ball spin.

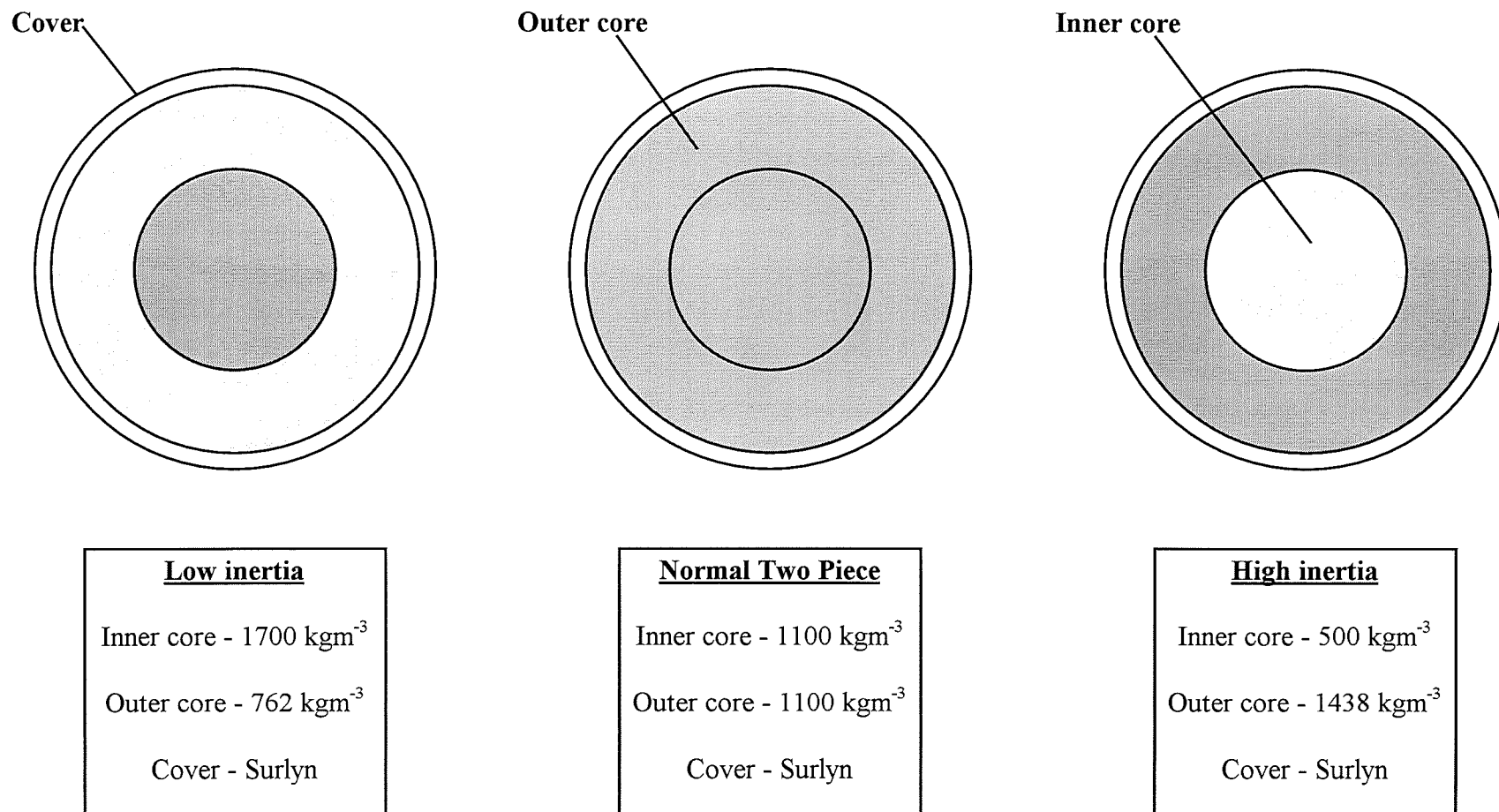


Figure 4.113 Ball constructions used to analyse inertia effects.

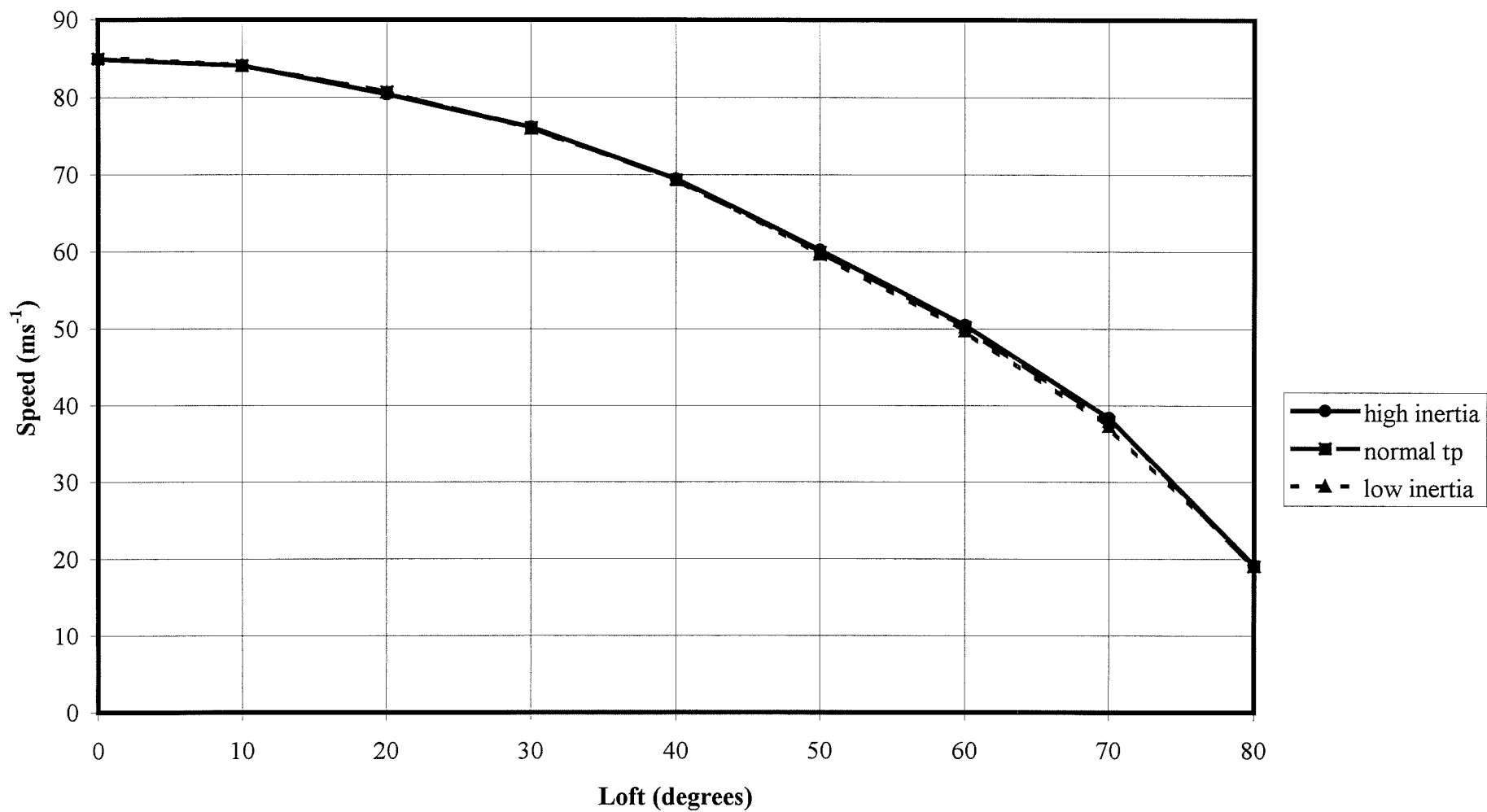


Figure 4.114 Effect of ball inertia on ball speed.

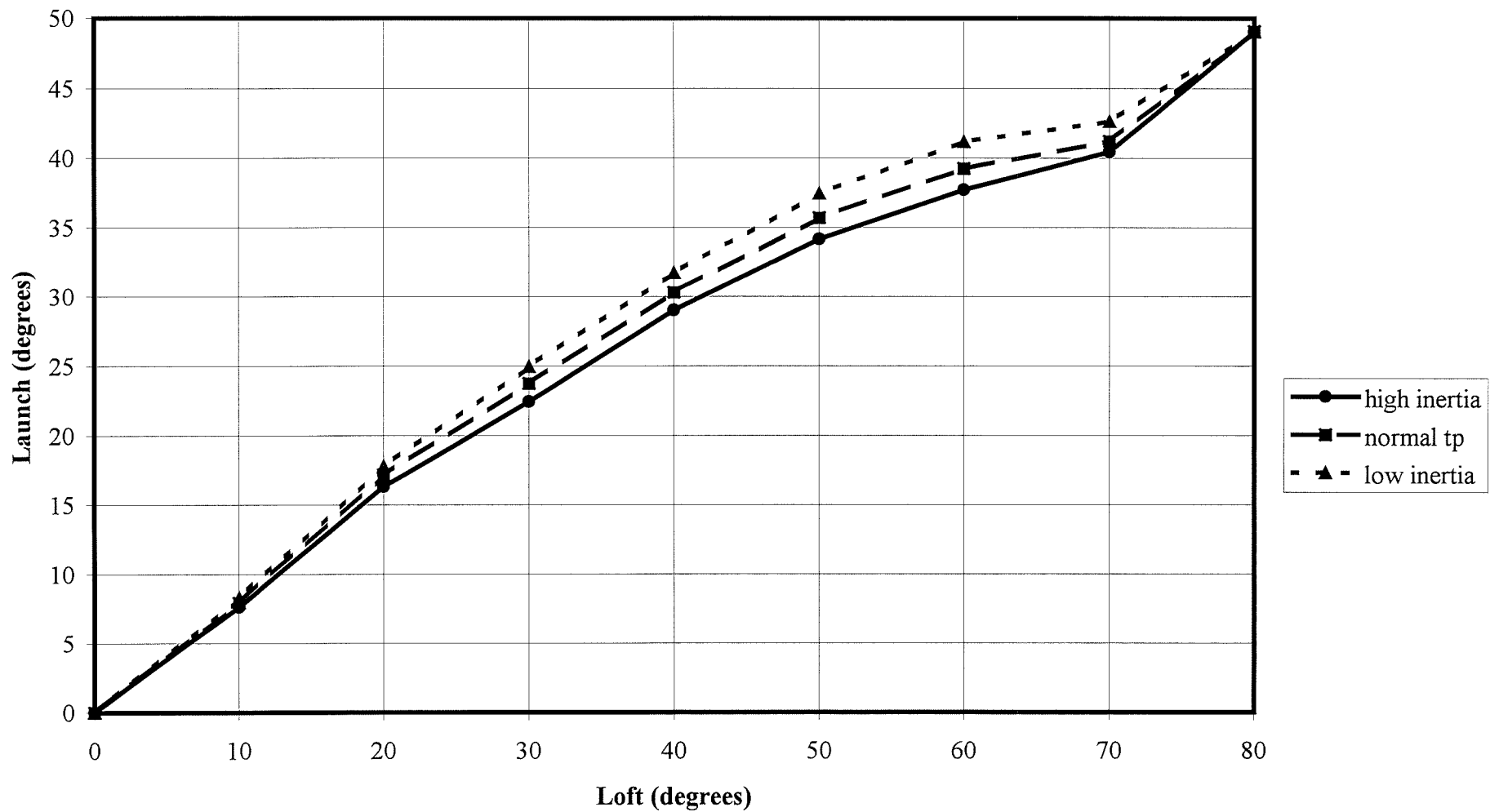


Figure 4.115 Effect of ball inertia on ball launch.

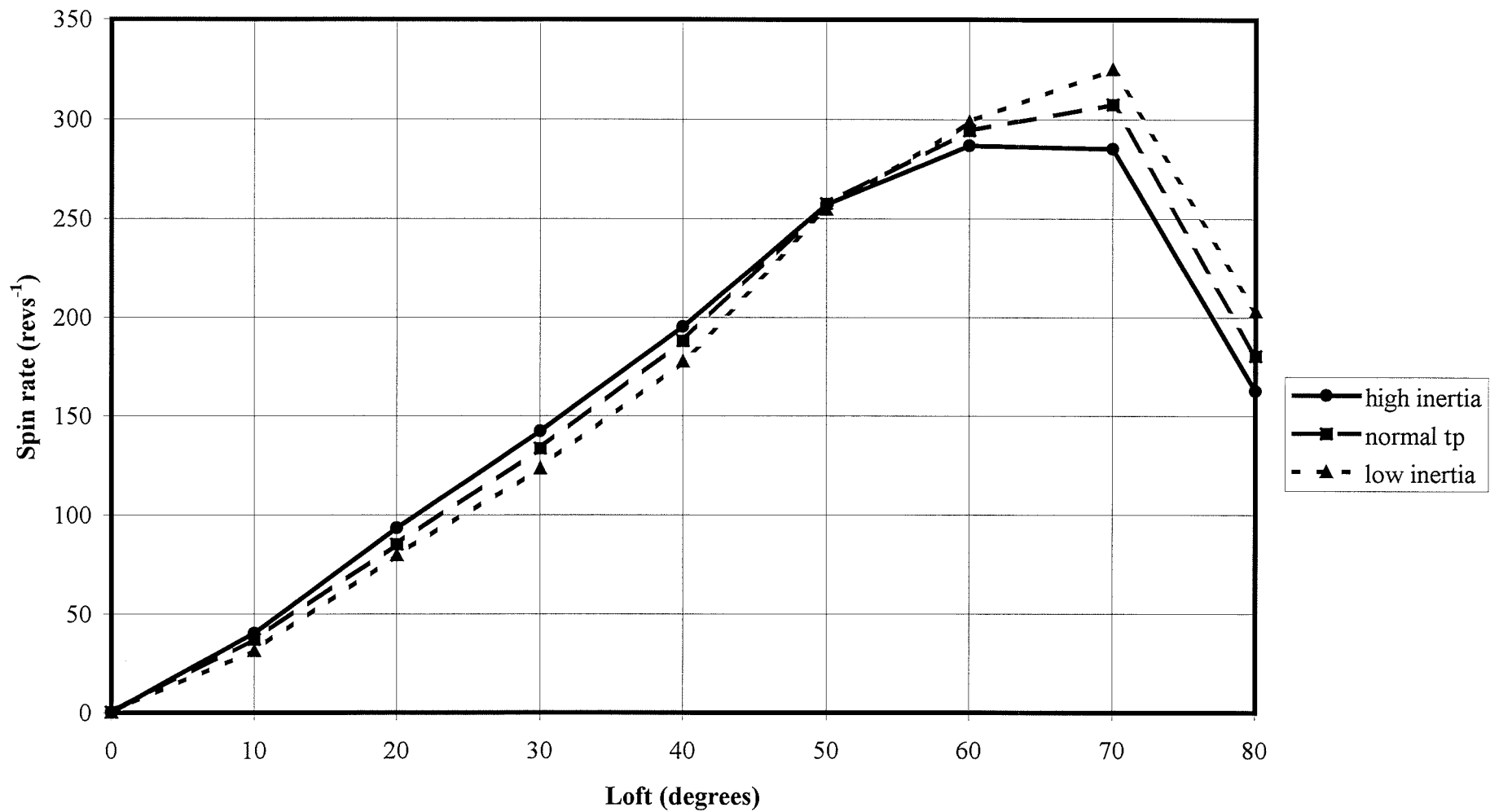


Figure 4.116 Effect of ball inertia on ball spin.

5.0 Reverse engineering of a golf shaft

There is currently a plethora of shafts available to golfers, with each shaft purporting to offer advantages for different swings. One of the aims of the current work was to model the shaft during a golf swing and quantify the mechanical properties that affect performance. It is first appropriate therefore to examine current golf shafts.

5.1 Existing shafts

A number of shafts, all composite graphite reinforced were obtained courtesy of Unifiber Europe. The geometric details of the shafts, their mass, length, internal and external diameters at the butt and tip, were recorded. The wall thickness at the ends was calculated from the diameters. The volume and density were calculated by assuming a linear variation of geometry along the shaft length and the shaft modelled using ten finite elements, each of constant cross section but with a variation from element to element. Data for the shafts is given in appendix C-1. Obtaining more esoteric properties of the shafts was attempted via procedures similar to those described in section 1.6.2.1. Difficulties were encountered in reproducing the tests but, as with clubhead modelling (chapter 3), it was felt that a generic model of a golf shaft open to systematic change was more relevant than attempting to model any individual shaft. A knife edge bending test was carried out on a randomly selected shaft to obtain a ballpark figure for the material stiffness.

5.1.2 Knife edge tests

A Unifiber T30 Senior was selected at random. The shaft was placed horizontally on two knife edges (figure 5.1) protruding 89.2 mm at each end and a mass of 2.72 kg was placed on another knife edge centrally. Deflections of the shaft were recorded at 89.2 mm intervals between the supports, these positions on the shaft were marked prior to any deformation. Table 5.1 gives the deflections for four orientations of the shaft about its longitudinal axis. A repetition of the test procedure involving a complete re-setup of the equipment and using a different operator to take deflection readings yielded the same results. Variation of the shaft displacement with rotation is in contravention of the rules

of golf (Rules - Section 4-1b). These state that the shaft shall be straight with the same bending properties in any direction. A manufacturing tolerance must be included but is not stated explicitly in the published rules. A recent ruling by the USGA Implements and ball committee (February 1999) has allowed for the conformance of clubs where the shaft has been inserted specifically to reduce any effect due to shaft spine (Achenbach 1999). They however also stated that orientating to make use of the spine remains a contravention of rule 4-1b.

A similar procedure was carried out on a further variety of shafts. Results indicated the range between deflections at specific points through rotations varied between shaft manufacturers. The range given in table 5.1 was the lowest observed. Products from another major shaft manufacturer showed ranges four times greater while a shaft manufactured using a modern processing technique, gas injection moulding, had an even higher range of asymmetry.

5.2 Shaft model

A finite element model of the Unifiber T30 shaft was constructed using 2 noded linear beams (Abaqus type B21, Hibbitt, Karlsson and Sorensen 1997) and analysed using Abaqus/Standard (Hibbitt, Karlsson and Sorensen 1997). The model was discretised as thirteen elements so that nodes would occur at the knife edges and the deflection measurement positions. It was not felt necessary to cut the shaft and measure each section, as was done by Friswell et al (1998), and a linear variation of the geometric properties was assumed along the length of the shaft. The density of the shaft was taken from the approximation method mentioned in section 5.1 as 1300 kgm^{-3} . The material was modelled as homogenous linear elastic. The model shaft was loaded at the node closest to the centre and the deflections recorded. The stiffness of the material was altered to obtain the closest match, this occurred at a stiffness of $50 \times 10^9 \text{ Pa}$. The model geometry data is given in appendix C-2. The deflections along with the mean deflection results from the practical experiment are given in table 5.1.

5.3 Discussion

Technical difficulties were encountered in reproducing the industrial test procedures used in measuring shaft properties. While overcoming the problems by the construction of appropriate equipment was possible it was felt that a more general approach to shaft modelling was of more immediate importance. It was also foreseen that difficulties would be encountered in attempting to model composite shafts with complex anisotropic stiffnesses (by virtue of the reinforcement fibre lay-up) and this idea was discounted in favour of modelling a steel shaft, where its bending and torsional stiffness is a product of only the geometric shape and homogenous material. Ballpark figures were obtained for the stiffness of a shaft taken at random. It is to be noted the shaft measured was the least stiff of all samples. It was concluded that the shaft modelling should continue using finite element beam elements as used by Friswell et al (1998) and with each beam of specific wall thickness and radius so as to approximate the shaft geometry. A fuller discussion of the model and its validation is given more appropriately in chapter 7.

<u>Displacement (mm) at position given</u>										
<u>Orientation</u>	a	b	c	d	e	f	g	h	i	j
0°	3.6	7.1	10.1	12.6	14.4	15.0	14.2	12.1	8.9	4.8
90°	3.6	7.1	10.0	12.5	14.1	14.8	14.1	12.0	8.9	4.8
180°	3.7	7.1	10.1	12.7	14.3	14.9	14.1	12.2	9.0	4.8
270°	3.6	7.1	10.0	12.4	14.1	14.8	14.1	12.1	8.9	4.8

<u>Displacement (mm) at position given</u>										
	a	b	c	d	e	f	g	h	i	j
Model	3.6	7.0	10.1	12.6	14.2	14.6	13.8	11.7	8.6	4.5
Experiment (mean)	3.6	7.1	10.1	12.6	14.2	14.9	14.1	12.1	8.9	4.8
Percentage difference	0.0	1.4	0.0	0.0	0.0	2.0	2.1	3.3	3.4	6.3

Table 5.1 Knife edge experiment and model results.

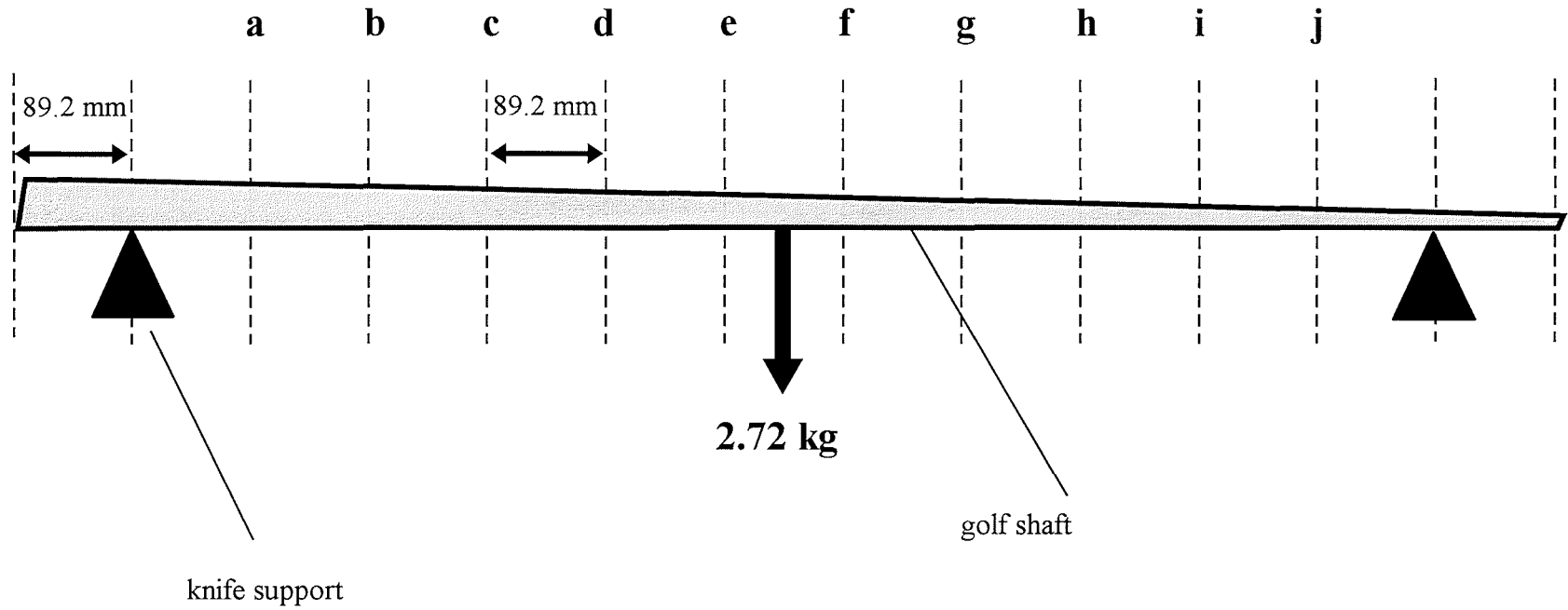


Figure 5.1 Knife edge shaft test.

6.0 Reverse engineering of a golf swing

Williams (1968) in his seminal paper on the mechanics of the swing, starts by stating

“To investigate the dynamics of the golf swing is to tackle a problem that is rather different from the run of dynamical problems. What is usually required in such problems is to determine the motion of a system under applied forces that are specified. In the golf swing on the contrary, it is the motion of the club as photographically observed, that is specified and the problem is to find out what forces must have been applied to it to produce that motion.”

Various researchers have continued investigating motion of the swing and made various attempts to estimate the forces involved (see section 1.6.2). Early on in the current work it was felt that a study of the swing in practical terms was necessary for the basis of building a model. This chapter describes, in brief, attempts to examine the golf swing.

6.1 Mechanical golfer

Golf machines capable of swinging a golf club have been around since Iron Byron's conception in 1965 (see section 1.6.2.3). On a smaller budget the Department of Mechanical Engineering, University of Glasgow created a swing machine in the late 1980's based on a double pendulum nicknamed 'Dai Laughing' (figure 6.1). The hub of the upper lever is powered by two springs, of adjustable tension, such that the force profile can be considered ramped linearly to zero as the arms return to their 'at rest' position. The lower lever is free to pivot about the upper lever with a stop included to prevent jackknifing. Design of the rig was based on double pendulum simulations and was discussed more fully by Whittaker et al (1990).

6.1.1 Practical tests

The mechanical golfer was fired 10 times with a cardboard target placed a known distance away. Figure 6.2. gives the relevant distances from the tee to a reference point on the target (marked X). The golfclub used was a John Letter's Forged Master Model

MKV 5-iron, Apollo steel stepped shaft and a Golf Pride grip. A two piece professional golf ball, 1 Pinnacle Gold, was placed on a small rubber washer which in turn was placed upon a grid attached to the leg of the 'Dai Laughing', this allowed for ease of replacing the ball in the same position for each shot. As the rig vibrates and moves after each shot it was necessary to mark the floor with respect to the position of the legs such that it could be returned to its previous position for a repeat shot. Before releasing the downswing it was important to remove small club vibrations. Also, after each shot the target underwent disturbance and it was important to be repositioned, this was easily achieved by allowing the target to swing freely before replacing the safety netting.

From the ten shots fired all ten struck the target. The first shot was slightly below and to the left of the others, this may have been due to the release mechanism which was human controlled, and a certain amount of unease was felt on the first shot as to where the ball would end up! The following 3 shots ended up in the same position with such accuracy and force to eventually punch a hole in the cardboard. The remaining 6 shots passed through the hole and ended up the other side of the target. Damage to the target had a thick black line drawn around it, photocopied and shown in figure 6.3.

6.1.2 Discussion

The vertical ball dispersion was greater than horizontal. This was most likely caused by the angle at which the ball hit the target, calculated as 26° . If it was necessary to achieve more accurate ball dispersion results then a more durable surface may have been used such as high density foam, whilst deformed the position of impact could be recorded. Another suggested method was to use carbon paper such that the impact leaves a mark on a recorder sheet. This may be possible with foam but is not advisable with a target more rigid than cardboard due to the danger of the rebounding ball.

A high degree of repeatability of 'Dai Laughing' was noted when proper precautions were made in repeating each trial shot. These included; repositioning the legs of the rig, minimal club vibration at the top of the downswing, accurate ball repositioning and a similar operator manner in releasing the downswing. Assuming impact needed to be within half a ball diameter of each other to pass through the hole, a maximum flight

dispersion of 0.7° was calculated. This compares well with the USGA test protocol for Iron Byron of 0.8° , calculated from figures given by Levin (1998). Various safety concerns were raised during testing including the possibility of a mishit and the rebounding of the ball within the small laboratory which contained a significant amount of glass. Further practical tests were put on hold until safety issues were met.

6.2 Human golfers

It was also possible for human golfers to take part in swing studies, however the same safety issues were raised when real golf balls were used. Lindsay's (1995) finding that swings without a ball present were very different from actual shots, notably the clubhead was typically open, meant practice balls must be used in any further swing studies.

6.3 High speed video

The purchase of a high speed video camera in 1997 meant that the swing studies could be taken further by analysing the swings of Dai Laughing and human golfers. The Kodak MotionCorder Analyzer, Model 1000 (Kodak Eastman) has a maximum possible frame rate of 600 frames per second (fps) and stores the images digitally in a continuous loop, overwriting previous images when the memory is full. Triggering the camera stops recording and allows access to all stored images. Via a frame grabber the images can be converted and stored as computer files. Image analyse software was available to calibrate the images and track moving objects providing coordinates and velocities.

6.3.1 Mechanical golfer

High speed video analysis of the mechanical golfer was carried out. Figure 6.4 shows a snapshot of the recording for a point in the downswing where the upper lever was approximately horizontal. While calibration of the image was possible to allow for lens distortion only a linear calibration was initially carried out. A lens with a wider field of view to include the clubhead motion would have been beneficial but was not easily obtainable and only the position of the wrist hinge during the downswing was recorded. With the camera running at 240 fps (a suitable speed to obtain full size images) the

downswing lasted 0.32 seconds and 76 images were available for analysis. A wider range of images were taken though to include the bounds. Figure 6.5 shows the velocity of the wrist hinge during the swing as calculated using the image analysis software. Five repeats of the swing were taken and results did not differ significantly. By repositioning the camera and running at 600 fps, in the impact zone, it was possible to establish the clubhead speed at impact. Five runs gave the mean speed at impact of 19.10 ms^{-1} , the range of values was 0.23 ms^{-1} .

6.3.2 Human golfers

A number of golfers were recorded with the high speed video. Figure 6.6 shows a 'rabbit' golfer (who requested anonymity) midway through the downswing. The camera was approximately perpendicular to the swing plane, calculated from prior observations behind the golfer. The downswing took 69 frames and lasted 0.29 seconds. Figure 6.7 shows the hinge velocity during the downswing. The deceleration phase of the wrist (Miura and Naruo 1998) is not noted. This should be caused by momentum transfer, however the golfer's poor timing does not allow for this swing attribute.

6.4 Discussion of results

While the results from the analysis with the high speed digital video were useful they were not in any greater detail than from other researchers for example Mather and Cooper (1994), Mather (1995) and Mather and Jowett (1998) using the method of photogrammetry. In addition further expense would be needed to build the system into 3-dimensions and accepting the view of Horwood (1994) that

"It appears that the computer technology now available to record and measure the swing is far in advance of the ability to analyse and deduce from this information what characteristics of the club best suit an individual golfer"

and with others still continuing in the field of motion analysis, such as the USGA (Logan 1997), it was felt more appropriate to pursue swing modelling and accept standard force input profiles for the upper lever of the double pendulum. An approach was taken to

model the swing incorporating 3-dimensions, variable force-acceleration profiles and wrist modelling such that when further information comes to light, from other sources, it could be included.

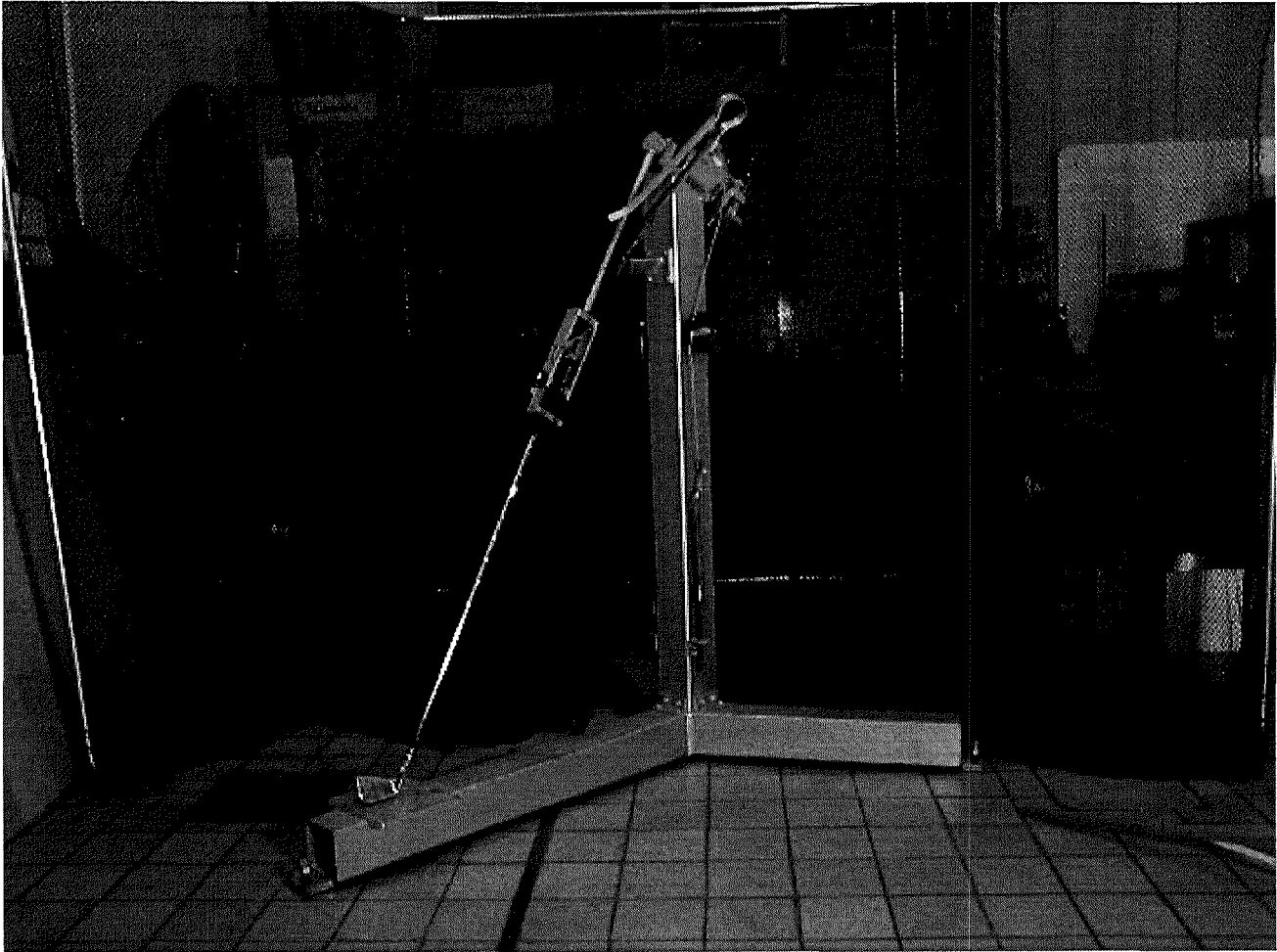


Figure 6.1 University of Glasgow’s mechanical golfer, ‘Dai Laughing’.

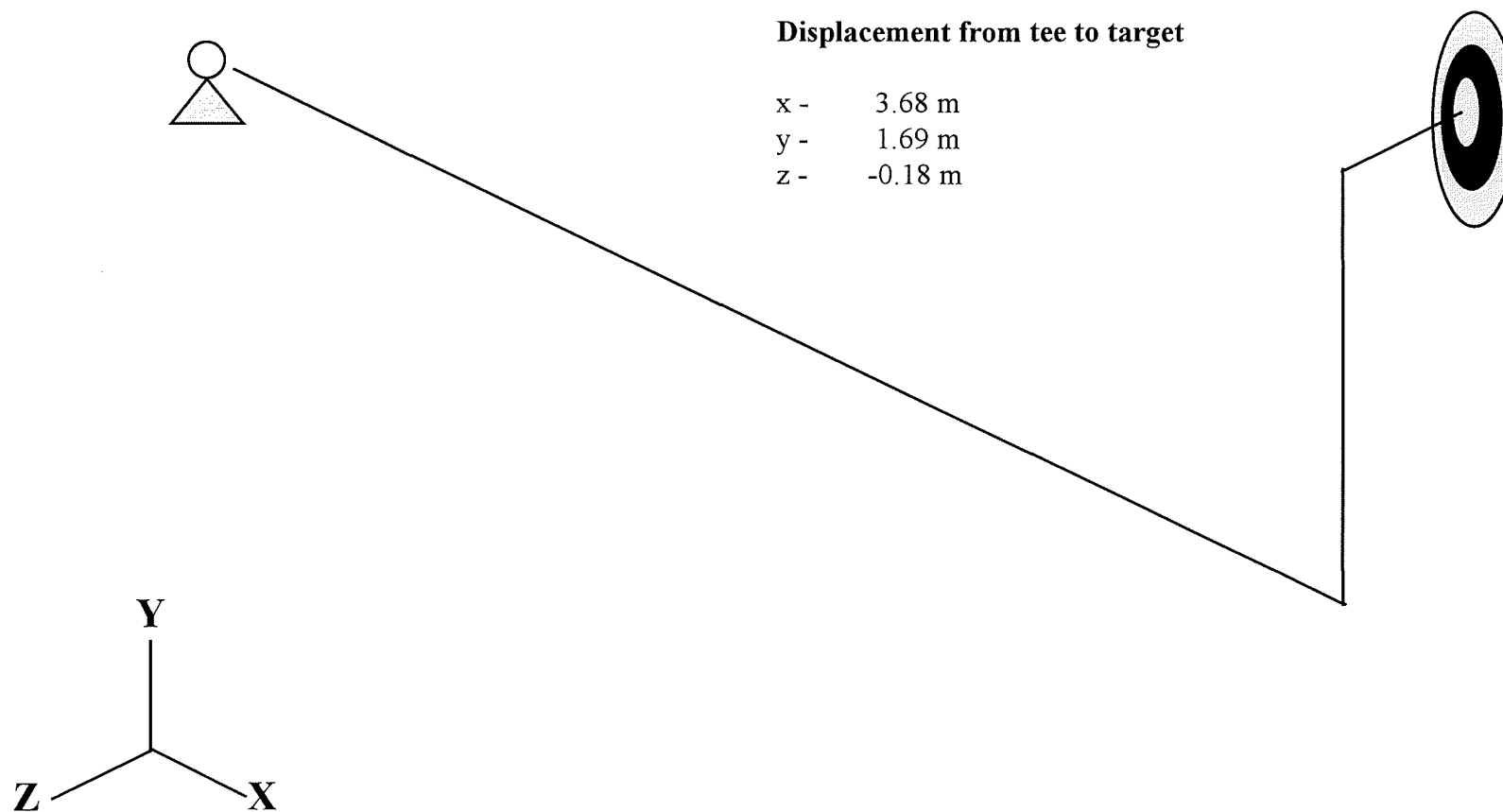


Figure 6.2 Position of target and tee in mechanical golfers tests.

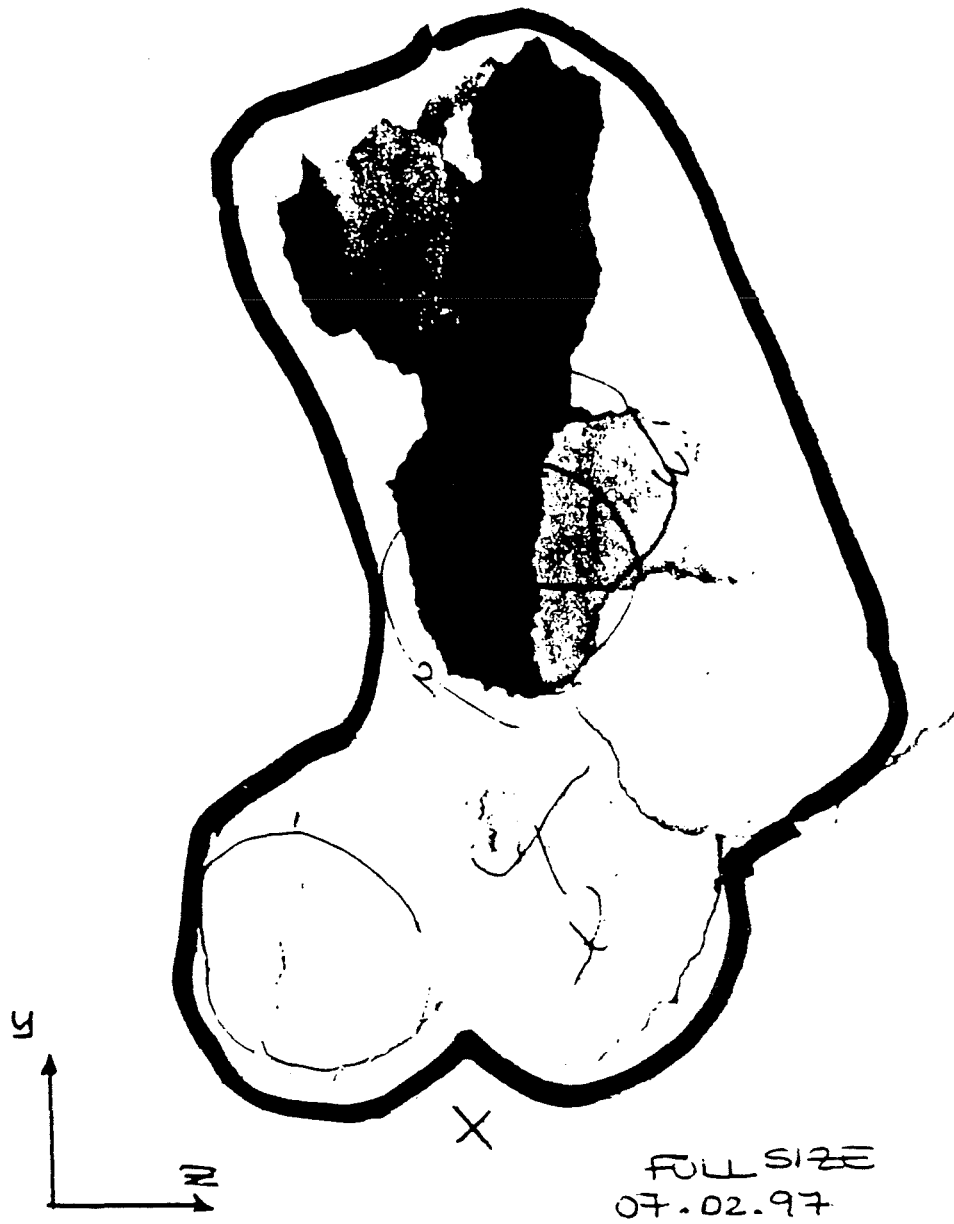


Figure 6.3 Target, thick black line shows limit of damage.



Figure 6.4 Snapshot from high speed recording of 'Dai Laughing'.

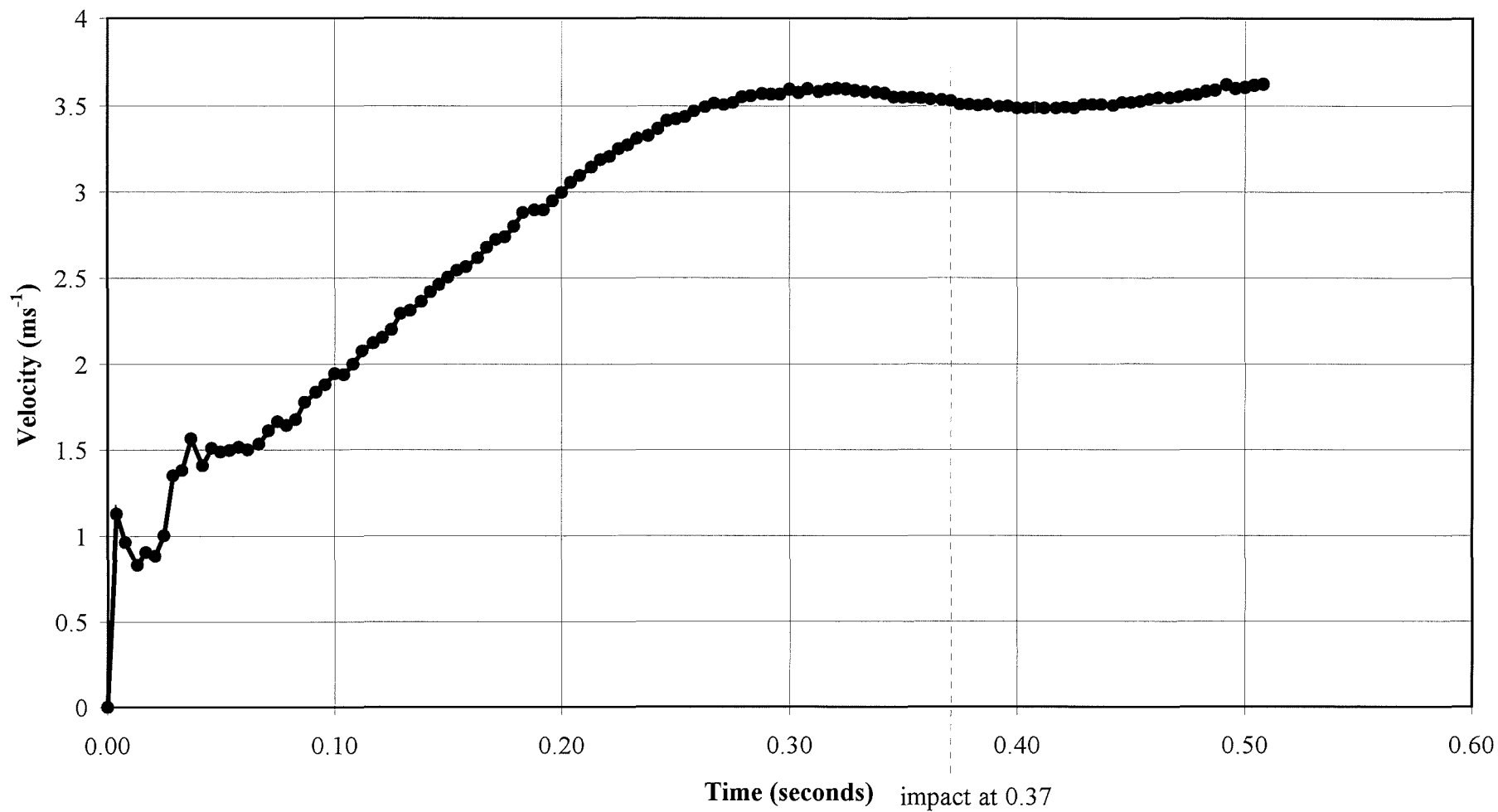


Figure 6.5 Velocity of wrist hinge of 'Dai Laughing'.



Figure 6.6 Snapshot from high speed recording of an amateur golfer.

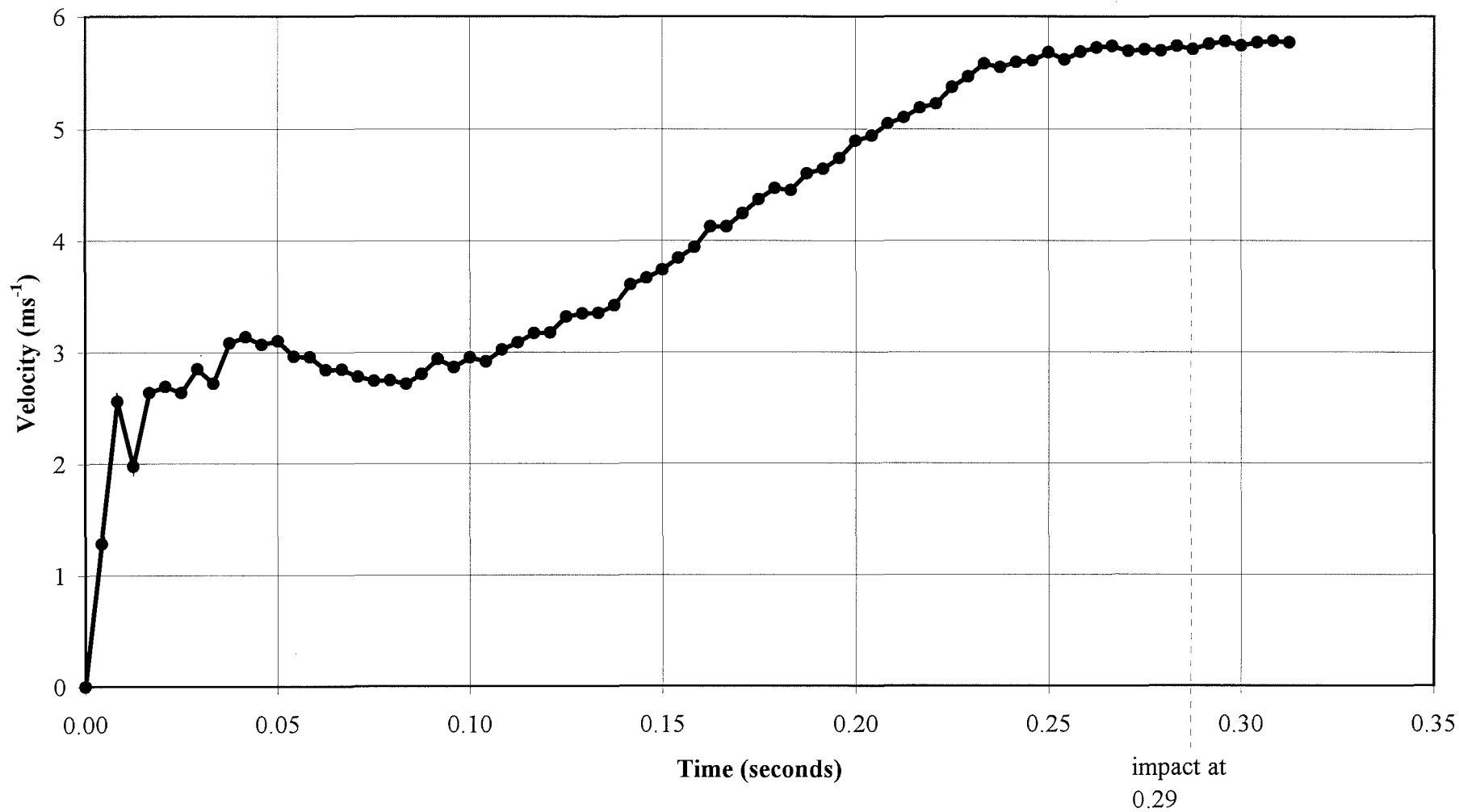


Figure 6.7 Velocity of wrist hinge of an amateur golfer.

7.0 The finite element swing and shaft model

7.1 Construction of model

Great emphasis is placed on the role the shaft plays in the golf swing. If shaft parameters are to be investigated it is desirable that a finite element model of the swing should include a shaft, subject to forces and undergoing translations similar to those in a real golf swing. Producing such a realistic swing model is a gradual process, and more sophisticated features can be added as research filters through to software upgrades. However any project must have a definite cutoff and, for the current work, this was Abaqus/Explicit, Version 5.7 (Hibbitt, Karlsson and Sorensen 1997). Further information on the finite element analysis software and hardware is given in section 4.1.3. This section describes the construction of the finite element model. This was designed to facilitate extension to full 3-dimensional analyses, beyond the scope of the current work, in which a less numerically-intensive 2-dimensional analysis is used to evaluate performance parameters for the golf shaft.

7.1.1 The swing

The finite element model of the swing was based on the double pendulum, as described in section 1.6.2.3. The upper lever (or arm) was pinned, with the lower lever (or shaft) connected to the arm by a 'multi-point constraint' (MPC). This constrains the coincident nodes of arm and shaft to have the same translations but admits independent rotations and so provides a pin joint at the hinge (or wrist), even when beam elements (as opposed to trusses) are used. To reduce computational costs further, the upper lever could be modeled as a rigid element with the appropriate mass and inertia. However, rigid elements were not available for use in 3-dimensions and, more importantly, an MPC could not be applied at their nodes. The upper lever was therefore modelled as a system of beam elements. To allow for the correct slowing of the upper lever due to momentum transfer during wrist uncocking, the mass and inertia of the upper body of the human golfer was approximated by the use of three circular-section beam elements. Their construction and dimensions are shown in figure 7.1. The mass density and dimensions of the beams are estimates based on a 'typical' human body. As in much of

the current work, the precise values of such data are less important than the ability of the model to simulate the golf swing in general. These values may be changed to allow simulation of particular cases. Deformation of the upper lever is not relevant to the current swing studies and an artificially high stiffness of 100 GPa was chosen for the beam elements. The pivot point was adjusted within the upper lever structure until it was near the hub position of a human golfer's swing, which lies within the body frame. A drawback of using such stiff beam elements for the upper lever is that the automatic incrementation procedure used by the explicit integration scheme in Abaqus/Explicit then selects very small steps, and hence a very large number of them, during analysis. This is because the deformation wave speed, which cannot be allowed to exceed a particular tolerance, is proportional to $\sqrt{E/\rho}$. (E = stiffness, ρ = density). A common method used to increase the increment size and so reduce the analysis cost is to alter the density. However this would alter the inertia within what is an essentially dynamic model and so, in this instance, the small time steps and large processing time was unavoidable.

7.1.1.2 Force-time profiles

The model was driven by applying a follower force, whose angle to the lever remains constant as the lever rotates, concentrated at a node within the upper lever structure (see figure 7.1). This was considered acceptable since the high stiffness of the elements here prevents significant bending. The magnitude of the force was varied throughout the swing, following an amplitude/time profile defined by the analyst as a sequence of points, between which the software performs a linear interpolation. The imposition of a non-linear, time varying torque is thought to be a novel feature of the current model but no actual data is yet available for typical real golf swings. A variety of force-time profiles (FTPs) were therefore generated, as shown in figure 7.2. These are denoted:

- Constant
- Stepped
- Ramped
- Non-linear1
- Non-linear2

The non-linear profiles were designed to include some of the complexities that may occur in a typical golfer's swing. They contain the same area underneath the curves. All graphs were normalised to have a maximum force value of 1 unit. The absolute value is fixed by a scale factor.

7.1.1.3 The wrist

The importance of the wrist during the golf-swing has been emphasized by many researchers (section 1.6.2). In the current work, the wrist was modeled by the MPC. To prevent jackknifing at the top of the swing, a stop must be included. This was achieved by adding a spring between the upper lever and a suitable node on the golf shaft. Like the FTP, nonlinear spring stiffness may be defined using a curve of internal spring force versus relative displacement. The simplest of these is similar to a rigid stop, in which the spring does not compress but offers no resistance to expansion. A problem with such a spring is that any external compressive impulse leads immediately to a high internal spring force and subsequent premature opening out of the wrist on the rebound. A more controlled compression is needed, such that any external forces can be matched by the internal spring force. An exponential curve, shown in figure 7.3 satisfies this and keeps compressive strain to a minimum. This wrist behaviour is known as the **passive wrist** and was used in most of the swing analyses.

Other wrist behaviours can be modelled by the non-linear spring. The prevention of 'early opening out' of the wrist under centrifugal force has been shown to be important in first class golf swings (section 1.6.2) and is achieved by a pull with the right hand (for a right handed golfer). This behaviour can be included by a hump in the positive spring displacement and is shown as the **restrictive wrist** in figure 7.3. This restricts compression whilst offering resistance to extension until a specific force is reached, after which the wrist opens out freely.

Researchers have also laid claim to the importance of applying another torque to the wrist to assist, this time, in 'opening out' during the final parts of the downswing. This most probably occurs from a push with the right hand. The non-linear spring can also include this, via an addition to the curve of a dip just prior to the particular spring

displacement at which the shaft is fully opened out. This is shown as the **active wrist** in figure 7.3. Other functions can obviously be included via the non-linear spring. In the current work however, the primary aim was to produce a model to investigate shaft performance and a full investigation of how these three wrist functions affect the swing is for future work.

7.1.1.4 Topswing positions

To cater for different ‘top of swing’ positions the finite element mesh was initially set-up in the address position. Two rotational transformations are then applied, on sets of nodes about specific axes, repositioning the undeformed mesh to give any desired starting position for the downswing. This start position is known as the ‘topswing’ and figure 7.4 shows the transformation sequence for a 90°–135° topswing:

- the address position
- transformation 1-90° wrist cock
- transformation 2-135° arm rotation about pivot point.

The wrist spring is included in the final transformation. To obtain the forces needed for each FTP and each start position was a non-trivial matter. A lengthy trial and error method was used to arrive at values that gave similarity to a real golf swing. Those chosen are given in table 7.1.

	constant	stepped	Ramped	Non-linear1	Non-linear2
90°-135° topswing	707 N	1768 N zero@0.15s	2121 N zero@0.30s	2616 N	2616 N
90°-180° topswing	1200 N	2250 N zero@0.20s	2500 N zero@0.30s	4500 N	4500 N

Table 7.1 Forces and times for FTPs and topswings.

7.1.2 The shaft model

The shaft model was constructed from a number of beam elements, each of pipe cross-section which varies from element to element as described in section 5.2. For the current 2-dimensional study, it was sufficient to use 2-noded linear elements, Abaqus type B21 (Hibbitt, Karlsson and Sorensen 1997), which allow axial and bending strain. B31 elements are available for 3-dimensions, allowing out of swing plane bending and torsion. The finite element code calculates a bending stiffness based on the initial geometry. No elbowing or change in bending stiffness, such as might occur if the cross-section ovals, is admitted.

7.1.2.1 Clubhead mass

The clubhead mass was modelled as a point mass of 0.2 kg connected to the shaft by two rigid elements. These can be changed to stiff beam elements of negligible weight if 3-dimensional model analysis is to be performed. If the mass is at the tip of the shaft and not offset its initial distance from the butt is the length of the undeformed shaft. The two rigid elements were connected from the point mass, one to a node at the shaft tip and the second to a node approximately 140 mm above. In this way the offset of the mass from the shaft can be altered. In the current work, two arrangements were frequently used, viz an offset of zero, representing a mass on the shaft tip, and an offset of 40 mm, typical of a driver. Figure 7.5 is a 90°-135° topswing plot of the finite element model. The force vectors which drive the arm are shown as hollow headed arrows while the two solid triangles below and to the right indicate the pivot point. The wrist spring is clearly shown as are the rigid links. The offset clubhead mass is shown as a square.

7.1.2.2 Frequency verification

Shaft models with 2, 4, 8, 16, 32 and 64 elements were analysed for their natural frequencies. Nodes were equally spaced along the length of the shaft and, for each shaft, the end elements had the properties of the tip and butt, as appropriate, of the Unifiber T30 shaft, investigated in chapter 5. Geometric properties of the intervening

elements were linearly interpolated between these values. Homogenous isotropic material properties were assigned, the density being 1300 kgm^{-3} and the elastic stiffness 50 GPa. Both a tip mass and 40 mm offset mass were analysed. Each shaft was constrained at the butt node against both rotation and translation. This differs from the frequency test most commonly carried out in practice (section 1.6.2.1), in which a finite length of butt is clamped. This was not done in the model since the location of the nodes, at which the clamping force must be applied, varied according to the number of elements in the model. In any case, the aim here was simply to identify the number of elements needed for convergence. Results for the frequencies and mode shapes for the offset mass are given in table 7.2.

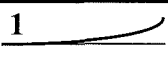
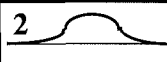
Number of Elements	Mode (Hz)			
	1 	2 	3 	4 
2	3.31	38.5	X	X
4	3.69	41.9	122.	259.
8	3.7	42.5	115.	237.
16	3.68	42.4	106.	210.
32	3.67	42.2	101.	196.
64	3.66	42.2	98.	191.

Table 7.2 Results of frequency verification, offset mass 40mm.

For the low order mode shapes, that are expected to predominate during the downswing (Whittaker (1996), (Friswell et al (1998)) satisfactory convergence is achieved with 8 elements. The frequency of the first mode (3.70 Hz) is lower than the Friswell's prediction of 4.53 Hz but this is due to the longer length of the shaft used here. The analysis gave a frequency of 4.20 Hz when the 8-element model was constrained at the first two nodes at the butt, similar to the practical test. This is still somewhat lower than Friswell et al, but confirms that the stiffness of the shaft model in the current work is approximately correct. Further verification of the shaft using models of varying degrees of mesh refinement is given in section 7.2, where the behaviour of the shaft during the swing is first considered.

7.1.3 Analysis procedure

The downswing analysis was carried out for a simulated time interval sufficient to include the passage of the head mass (hereafter called the clubhead) through the impact zone. Impact is considered to occur when the clubhead passed a vertical line passing through the upper lever pivot point, this time interval is about 0.3 s. During the analysis, model data was written to a file at a frequency of 500 Hz (analysis time). It was found that sufficient details on the dynamic behaviour of the tip at impact could not be obtained at this frequency. After the full downswing analysis was performed, the analysis was therefore restarted from the last available checkpoint before impact. This second stage analysis wrote model data at 50,000 Hz, over a time interval sufficient to include the clubhead's passage through impact. This was a lengthy technique for each swing since a change in any parameter, for example, shaft stiffness, leads to different time to impact. However it was necessary to produce consistent results and to minimise errors. Appendix D-1 gives the Abaqus input file for a typical analysis which is discussed in the next section.

7.2 Swing results

The following sections describe, in some detail, features common to most of the swing analyses performed. Detailed information on post-processing is given in section 4.2 and here results are presented for an 8-element shaft with a material stiffness of 50 GPa. The topswing was a 90°-135° transformation, ie 90° wrist cock and 135° arm turn and the FTP was ramped from 2121 N, at the start of the downswing, to zero, after 0.30 s. The analysis was continued for a simulated time of 0.40 s and the clubhead was observed passing through impact just after 0.302 s. The more accurate, second stage analysis was set to run from 0.302 to 0.304 s and showed the clubhead passing through the impact zone between 0.30376 and 0.30378 s.

7.2.1 Deformed plots

Figure 7.6 shows 9 Abaqus/Post plots of the deformed model, from the start position to just after impact. The time between frames is 0.04 s. Of course, the model club

continues through the impact zone with the no abrupt change in speed, as there is no ball impact in this case. A higher-frequency sequence of post-processed results can be run as an animation file (clearly not reproducible here) to give the user a clearer view of the swing.

Nodal coordinates can be obtained for the shaft at any instant and the relative displacements magnified to show the deformed shape more clearly as an x-y plot. Figure 7.7 shows such a plot of the shaft at impact. Any tendency of the shaft to be bent forward is masked by the butt being ahead of the tip by 110 mm overall. The coordinate basis could of course be transformed to give one axis coincident with most of the shaft but this is awkward to automate as each analysis requires a different local basis. An approach taken by Mather (1998) in practical experiments was to record the radius of curvature over the length of the shaft. In the current work, this may be done for each element and is shown in table 7.3 and figure 7.8. The shaft element at the tip is not included as it is held straight by the rigid structure forming the offset mass.

	Element number	radius of curvature (m)
butt	4	+ 12464.48
	5	- 28316.6
	6	- 428.78
	7	- 81.116
	8	- 25.604
	9	- 10.322
	10	- 4.5025
tip	RIGID	RIGID

Table 7.3 Radius of curvature in each element at impact, offset 40mm.

Negative values for the radius of curvature correspond to forward bending of the shaft. The large positive value towards the butt implies that the shaft is bent backward but only slightly. This 8-element model does not yield the detailed deformed shape and, when shaft shapes were to be compared, 32 element models were used (in fact, the difference between the 8 and 32 element model predictions was minimal, as discussed in section 7.2.5.)

7.2.2 Stress and strain plots

Contour plots over the model were available for most element variables. Figure 7.9 shows a contour plot of curvature (the inverse of the radius of curvature) for the elements. The original colour contours do not reproduce in monochrome and so tickmarks are attached. The largest changes can be seen to occur towards the tip of the shaft.

7.2.3 Variable-variable graphs

Figure 7.10 shows the speed of the wrist and clubhead during the downswing. The clubhead reaches a speed of 33.8 ms^{-1} at impact, 1% less than the maximum speed, which occurs 0.026 s later. The wrist speed is 6.37 ms^{-1} at impact, 9 % less than its speed 0.082 s earlier. This is due to momentum transfer during wrist uncocking.

Figure 7.11 shows how bending moments develop in the shaft during the downswing. The two elements chosen were the penultimate elements at each end of the shaft, to minimise distortions caused by the rigid structure at the tip and by the spring attached to the butt. These elements are just below the grip and just above the clubhead, and are labelled as such. The corresponding strain diagram, shown as change in curvature, is given in figure 7.12. The largest bending moments occur at the butt during the first part of the downswing, as the club inertia attempts to cause jackknifing but is resisted by the wrist spring. The positive moment confirms the forces cause backwards bending. As the wrist opens, the shaft boundary condition changes to only a pivot and accordingly the frequency of vibration rises. This is shown from halfway through the downswing on both the moment and curvature plots. The natural frequency of vibration of the shaft is also raised by centrifugal stiffening that increases both as the speed increases and as the moment-arm from clubhead to shoulder-pivot increases, due to wrist uncocking. The effect of such vibrations make the actual clubhead trajectory and its phase-plane diagram (ie velocity v position) almost chaotic, highly sensitive to small changes in timing or address position. It is then almost impossible to exactly reproduce a particular trajectory in detail, even computationally. Of course, such small changes are inevitable in practice.

Clubs with increased structural damping (the analysis only includes a small amount of damping for numerical stability) would benefit the golfer by reducing the amplitude of vibration but for the mere seven cycles as shown, the effect of material damping would be negligible compared to the damping from the golfer's hands and grip. No attempt has been made to model such damping here but it would be an important feature of further work.

The shaft bending moments and the curvature at the clubhead become negative after wrist uncocking, indicating that the shaft is bent forward. Golfing lore says that this is caused by the recovery of the shaft but most backwards bending during the early part of the downswing occurred near the grip and forward bending occurs near the clubhead. The main cause of the forward bending is more likely to be the offset mass and the resultant centrifugal force. This is confirmed by a similar analysis with a mass located at the tip, which shows the bending moment and curvature near the clubhead vibrating about a mean value of zero. The bending moment and curvature change plots for a tip mass model are given in appendix D-2.

7.2.4 Derivation of shaft performance predictors

The critical performance indicators of the shaft derive from the dynamic behaviour of the clubhead through the impact zone. Only by a comparison of the dynamic variables can the effect of differing shafts or swings be evaluated. The key variables are the translational velocity of the tip, both speed and direction (given as elevation), and the dynamic loft of the tip section. Various methods were developed to determine these from Abaqus output and these methods were continually improved to increase the accuracy of the results. The following sections give the final procedures used, with the occasional note as to the problems encountered with earlier methods.

7.2.4.1 Speed

The speed of the tip can be calculated from the displacement of the end node over a time period in the second stage analysis. This however gives an underestimate of the speed as it approximates the arc of travel by a straight chord. An alternative method was to

take the average of the speeds for the tip node for two instances in the second stage analysis, ie pre- and post-impact. The magnitude of the difference between the averaged values was never greater than 0.01 ms^{-1} .

7.2.4.2 Elevation

Like speed, the elevation was best calculated as the average from the pre- and post-impact velocities in the second stage analysis. Again the small time increment gave reasonable accuracy and differences were never greater than 0.05° .

7.2.4.3 Loft

The actual loft at impact is the summation of the static head loft and the shaft attitude at impact, the latter being a dynamic function of shaft bending and the position of the grip in relation to the clubhead (grip ahead of the clubhead leads to a reduction in loft). By default, the term 'loft' in the current chapter is taken as 'dynamic loft increment', a value indicating any change over the static loft. Loft was measured as the angle that a line, joining the shaft nodes attached to the rigid body at the head, made with the vertical. The average of the attitude before and after impact was calculated and differences were not greater than 0.05° .

7.2.5 Mesh density convergence

Validation of the shaft element mesh density has already been done for the vibration study in section 7.1.2.2 but it is prudent to also examine the convergence for a typical swing analysis, were the FTP or wrist spring may have an additional effect. Shafts of 2,4,8,16,32 elements were analysed for a 90° - 135° topswing, ramped profile. Table 7.4 shows the effect of the element numbers on the shaft performance predictors; speed, elevation and loft.

Number of elements	Speed (ms ⁻¹)	Elevation (°)	Loft (°)
2	32.51	-2.37	-5.42
4	32.76	-2.25	-5.08
8	34.31	-2.83	-5.81
16	34.34	-2.82	-5.81
32	34.38	-2.80	-5.81

Table 7.4 Shaft performance indicators for varying mesh densities.

For each predictor the 8-element model is satisfactorily close to the 16-element model and so the former was used in most analysis.

7.3 Shaft properties

It is believed that five key properties affect shaft performance (section 1.6.2). The finite element model allowed a quantitative examination of how these properties affect the dynamic behaviour of the shaft and thus the attitude of the clubhead at impact. Of course, the 8-element (unless otherwise stated), 2-dimensional model used here simplifies the real golf swing. However it may be readily extended to 3-dimensional and will facilitate benchmarking, beyond the scope of the current work, of the overall computational approach against practical experiments, whether using real or mechanical golfers.

7.3.1 Flex

Flex is a measure of the shaft bending stiffness and was discussed in section 1.6.2.1. A 50-flex shaft is taken here to mean that it is made of material with a modulus of 50 GPa. This value, obtained from simply-supported bending tests (section 5.1.2) on a randomly chosen shaft, was used in the current work. One of the aims of the current work is to elucidate any flex effect and a range of stiffness is needed to cover the extremes of current shaft designs. This range of stiffness was initially estimated and adjusted by comparing the frequency response to known results.

7.3.1.1 Frequency analysis

Frequency analyses in the range 40–60-flex was carried out by constraining the shaft at the butt over a distance of 138 mm, similar to the constraint used in practical tests, and calculating the low mode frequencies. Figure 7.13 shows a linear relationship between the stiffness and frequency for mode 1. Results for modes 1, 2 and 3 (shapes given in table 7.2) are given in table 7.5. The range of calculated frequencies was similar to clubs of the model length, given by Sato (1995) and Tutleman (1998). Tutleman's results for nominal flex grades are given in table 7.6, in which frequencies have been converted from cycles per minute. The range of flex chosen adequately encompasses the typical values and was used in 2 GPa increments for swing analysis. For the 50-flex model the shaft frequency was 4.2 Hz and is a typical R (regular). The shaft measured in section 5.1.2 was a low stiffness version of the manufacturer's range and, assuming Tutleman's values to be typical, the shaft range examined in chapter 5 can therefore be considered stiffer than other manufacturers'.

Flex	Mode 1	Mode 2	Mode 3
40	3.75	45.4	124
42	3.85	46.5	127
44	3.94	47.6	130
46	4.03	48.7	133
48	4.11	49.7	135
50	4.2	50.8	138
52	4.28	51.8	141
54	4.36	52.7	144
56	4.44	53.7	146
58	4.52	54.7	149
60	4.6	55.6	151

Table 7.5 Effect of shaft stiffness on modal frequencies.

Nominal Grade	Frequency (Hz)
L	3.92
A	4.08
R	4.25
S	4.42
X	4.58

Table 7.6 Graded shaft frequencies for a typical driver (Tutleman 1998).

7.3.1.2 Swing analyses

An extensive list of analyses was performed for the full range of flexes, all FTPs, topswings 90°-135° and 90°-180° and for both clubs with zero and 40 mm mass offset. Only the passive wrist was modelled. Clearly the reproduction of results for all configurations is not a practical option and a very condensed summary is necessary.

A common effect of altering the shaft flex is shown in Figure 7.14. This shows the speed of the wrist and clubhead for both extremes of flex during the swing. The analysis used the ramped FTP, 90°-135° topswing and offset mass 40 mm. Impact occurred after approximately 0.304 seconds. At impact the 40-flex head speed was 33.92 ms⁻¹ and the 60-flex was 33.31 ms⁻¹, a difference of 0.61 ms⁻¹. The speeds achieved with a 90°-180° topswing and ramped FTP were larger and the difference was correspondingly so, at 39.84ms⁻¹ for 40-flex and 38.69ms⁻¹ for 60-flex. These increases in speed can be compared to the advantages claimed by Butler and Winfield (1995) and Thomas (Tutleman 1998) for lighter shafts, as given in section 1.6.2.1. This speed increase would give 3-6 yards extra distance. The reason for the difference due to flex is that, at the start of the downswing, 40-flex bends back more than the 60-flex, the rotational inertia of the whole system is less and the angular acceleration is greater. During opening out of the wrists, the 40-flex catches up with the 60-flex and overtakes it. This is confirmed by figure 7.15, which is a bending strain plot, taken as change in curvature, for elements near the grip and clubhead. It shows that the 40-flex bends further and remains bent back longer, due to its lower natural frequency, giving a greater angular velocity of the whole structure before opening out of the wrist. The curvature change plot also shows shaft vibration during the second part of the downswing, after wrist

uncocking. This causes fluctuations in the clubhead speed but is not seen in the speed plot as the variation is very much smaller than the absolute magnitude. A change of scale allows the vibration to be observed. It affects the speed by $\pm 0.1 \text{ ms}^{-1}$. Figure 7.16 shows the clubhead speed at impact as a function of the flex. The general tendency for lower flex shafts to have higher impact speed is shown but the relationship is non-linear, due to shaft vibration.

The effect of the stiffness on the change in dynamic loft is not constant for each FTP. Figure 7.17 shows the relationship for the ramped profile, with 90° - 135° topswing. The shaft vibrations cause fluctuations of the loft within a range of 2.5° and the loft continually changes as the shaft moves through the impact zone. The values are negative, indicating a reduction in loft. This is a result of the summation of two opposing swing and shaft parameters. First, the grip is ahead of the clubhead and this reduces loft. Second, the offset mass leads to bending forward of the shaft, which increases loft. Examination of all other swings confirmed that the unpredictability due to vibration was never more 2.5° . For a more 'gentle' FTP such as the 'constant', the range was smaller, within 1.5° . The effect of the loft change due solely to the offset mass could be estimated from a comparison between zero and 40 mm offset clubs, using the same FTP and topswing. This showed that shaft bending due to the offset mass caused an increase in dynamic loft of about 2.5° , found by comparing the range in loft change due to vibration for a variety of flexes for each FTP. In summary the 40 mm offset mass leads to increased dynamic loft of 2.5° . This increase would be expected to change with flex, as is confirmed by comparing the radius of curvature in the penultimate element of the shaft for the extremes of flex. For 40-flex the radius of curvature was 3.48 m and for 60-flex was 5.94 m. However the radius of curvature for other flex (table 7.7) does not change linearly between these bounds, again due to vibration of the shaft. The change in loft of 2.5° is not as great as would be expected by such a large inertial force on the offset head and this can only be explained by the centrifugal force adding to the stiffness of the shaft.

Flex	Radius of curvature (m)
40	-3.48
42	-4.05
44	-4.85
46	-6.37
48	-5.82
50	-4.50
52	-4.51
54	-4.07
56	-4.30
58	-4.88
60	-5.94

Table 7.7 Radius of curvature for shaft tip for various flex.

Figure 7.18 shows another common result from all analyses, viz the effect of the shaft flex on the elevation of the head at impact. A clear relationship exists with lower flex reducing the elevation angle further below the horizontal. The negative value is due to the wrist being ahead of the clubhead and the shaft motion being mainly a rotation about the wrist. The clubhead travels in an arc and, at impact, its elevation is inclined below the horizon. Lower flex prolongs wrist cock and reduces rotational inertia, with the result the hands are further ahead of the clubhead at impact, pushing the elevation further below the horizontal.

7.3.1.3 Offset mass

The effect of the offset mass merits further investigation. Analyses used a 32 element shaft to give a clearer view of the shape and a 90°-135° ramped FTP. Offsets of 0, 10, 20, 30 and 40 mm were used. Figure 7.19 shows the speed of the clubhead varied by only 0.1 ms⁻¹. The nonlinear variation is due to the effect of the offset on vibration frequency but the trend is that more offset increases the speed - albeit slightly. Clubhead elevation (figure 7.20) showed similar fluctuations within a range of 0.1°. Again there is a slight trend, that more offset reduces the elevation. Both speed and elevation relationships are due to the offset club being bent more, club inertia reduced, a greater angular velocity achieved and the wrists being further ahead of the clubhead at impact.

Figure 7.21 shows the clear relationship of the effect of offset on the loft of the club at impact. More offset increases the loft, from -7.5° at zero offset to -4.5° at 30 mm, due to the effect of centrifugal force on the head causing shaft bending. The true increase in loft due to offset would be slightly greater but the effect of the reducing elevation (noted above) counteracts this. Again, the loft relationship shows evidence of shaft vibration but in this instance it is less clear as the loft difference due to offset is greater than that due to vibration. Figure 7.22 demonstrates the shaft shapes, showing the radius of curvature of elements towards the tip, before the rigid structure is attached. More offset promotes a smaller radius of curvature. The mass offset of 10 mm gave strange results, possibly as a result of excitation of a mode shape but possibly a user error such as a particularly stiff element in the shaft. No error was however found. For zero offset, the radius of curvature of any element over the whole length of the shaft was not less than 28 m and was positive, indicating that the shaft was bent back. This confirms that forward bending of the shaft at impact is not due to shaft loading during the swing but to the centrifugal force on the offset mass.

The effect of shaft stiffness on the swing can be predicted by the model and confirms much of the previous research, detailed in section 1.6.2. The relationships are complex and depend on the vibration of the shaft about the pivot point during the latter part of the swing and, to a lesser degree, the more constrained situation earlier in the swing. Imposing the correct boundary conditions for the club is therefore essential, especially in any future work modelling a real, 3-dimensional, golf swing. Rotation of the shaft about the wrist causes centrifugal force that changes flex and frequency throughout. These effects are real and are included in the model. It appears that the relationships between flex and dynamic shaft parameters at impact remain the same for very different FTPs. The effect of the flex on the loft of the club at impact, when the mass is offset, is as predicted by Milne (1992). However the difference over a typical range of flexes is very small and due, no doubt, to the centrifugal stiffening effect discussed by Mather (1994, 1995 and 1998). An improvement in clubhead speed can be achieved by lower flex, since the bending of the shaft reduces the rotational inertia of the system during the early part of the swing and the lower frequency prolongs wrist cock. However such improvements are small. The use of stiffer shafts reduces the amplitude of vibrations and makes for more repeatable shots. Vibration may have a harmful effect in shot

quality with, for example, professionals to whom accuracy is more important than distance. Then stiffer shafts may hold the balance in lowering scores. For golfers who have a poor repeatability in their swing, much greater than the variation due to vibration, the use of low flex shafts may be beneficial in promoting distance.

7.3.2 Torque

As the model was only used in 2-dimensions in the current work no attempt was made at investigations involving torque.

7.3.3 Bend point

Analyses were carried out using 32 element shaft models for three different bend profiles. The stiffness of the individual elements was altered such that the shafts gave the same static deflection in a flex test when the butt was clamped and a concentrated force of 27 N applied at the tip. Figure 7.23 shows the three shaft shapes in deflection. The mid-bend point shaft had a constant material stiffness for elements along the shaft length of 50 GPa. The low bend-point was stiffer in the butt and weaker in the tip, the high bend point the converse. Actual values for each element are tabulated in appendix D-3. The shafts were analysed using seven out the possible ten selections of FTPs and topswings.

Table 7.8 gives the clubhead dynamic properties for each swing. The highest value in each column is highlighted, to indicate any trend, along with the maximum difference between the three shafts given. The bend point has little effect on speed, except for topswings 90°-180° ramped and 90°-180° nonlinear¹. These accelerations are more 'aggressive' and promote larger shaft vibrations. No clear relationship is seen and the 'fastest' shaft appears to vary randomly. With the exception of the two swings mentioned, little difference is found in the change in elevation angle. While the results indicate that a high bend-point gives increased elevation, the effect is insignificant. The loft results are more conclusive. The low bend-point shaft gives the greatest loft in all cases and the high bend-point the smallest loft in most and for the one exception a negligible difference between the mid and high. These results confirm the predictions based on theory presented in section 1.6.2.1. The results for speed and elevation

highlight the unpredictability of the model due to shaft vibration and emphasize the need for correct damping if it is to be used in future work.

7.3.4 Damping

Abaqus includes a small amount of damping for numerical stability but this has a negligible structural effect. Significant material damping would have the effect of reducing the amplitude of vibration over a number of cycles. However, the frequency of the vibration modes that dominate the golf swing are low and only about 7 cycles occur in the swing. Material damping is not then expected to be a significant parameter in shaft design, particularly when compared to the much greater structural damping provided by the golfer's hands and grip. The claim that improved material damping reduces inaccuracies due to vibration is valid in theory but further work is needed in this area to determine the degree to which shaft damping would have a discernible effect.

7.3.5 Weight

That shaft weight is a performance parameter is clear, with lighter shafts leading to higher clubhead speeds. This is the basis for modern composite shafts. The effect of weight, over the range found in real shafts, is desired. This range is about 50 to 150 g and was studied in 10 g increments. The model swing was repeated with only the shaft density altered between runs. The material stiffness was kept at 50 GPa. Only the ramped FTP, from a 90°-135° topswing with the passive wrist was used.

Figure 7.24 shows the speed of the clubhead and wrist during the downswing for the extremes of the weight range. The lighter shaft attains a higher speed at impact, 33.88 ms⁻¹, compared to 33.31 ms⁻¹ for the 150 g shaft. The difference, 0.57 ms⁻¹, is smaller than stated by Butler and Winfield (1995) and Thomas (Tuttleman 1998) but the values are for a 90°-135° topswing. A bigger topswing (ie 90°-180°) would attain a higher clubhead speed and would be expected to show comparable values. For the 50 g shaft the reduced inertia of the system means greater acceleration during the FTP and consequently higher final clubhead speeds. The lighter shaft also has higher vibrational frequency and this might be expected to cause wrist uncocking sooner. However the

greater acceleration compensates and uncocking occurs at approximately the same time for both shafts. The effect of speed over the range of weights is shown in figure 7.25 and the general trend is confirmed, although vibration produces an anomaly at 80 g. The curve appears asymptotic above 120 g. Future work might confirm this.

Figures 7.26 and 7.27 show the effect of the shaft weight on the change in dynamic loft and clubhead elevation respectively. Previous results have shown these two effects to be related. The change in loft is susceptible to shaft vibration but a general trend can be seen, with heavier shafts producing greater dynamic loft. This is due to the wrist not being as far ahead of the clubhead at impact, for the heavier shafts. Indeed a linear relationship appears between the position of the wrist ahead of the clubhead and the shaft weight. The wrist is 117 and 91 mm ahead of the clubhead for the 50 and 150 g shafts respectively. This occurs because the time to impact is also linearly related to the shaft weight, heavier shafts taking longer. Figure 7.28 shows the position of the two swings (not to scale) at impact, along with the downswing times, the change in loft and the effect of shaft weight on elevation. The further that the wrist is ahead of the clubhead at impact, the lower is the elevation below the horizontal.

7.4 Wrist modelling

The model has been designed so that different FTPs and wrist functions could be modelled. It was found that with wrist functions other than the passive model large shaft vibrations during the swing were created. These caused results to be unpredictable and confirmed the importance of correct damping if the model is to replicate a real golf swing. Further work on wrist modelling was therefore abandoned until suitable damping was included in the model. This has not yet been attempted.

SPEED	135	135	135	180	180	180	180
	constant	ramped	nonlinear1	constant	stepped	ramped	nonlinear1
low	26.688	34.322	25.690	39.347	50.850	40.722	42.742
mid	26.707	34.412	25.740	39.564	50.950	40.247	42.812
high	26.667	34.427	25.580	39.400	51.010	40.282	43.120
MAX DIFF	0.040	0.105	0.160	0.217	0.160	0.476	0.378

ELEVATION	135	135	135	180	180	180	180
	constant	ramped	nonlinear1	constant	stepped	ramped	nonlinear1
low	-4.090	-3.453	-0.084	-1.697	0.092	-2.713	2.540
mid	-4.073	-3.446	-0.041	-1.516	0.091	1.642	2.527
high	-4.073	-3.302	-0.031	-1.582	0.191	2.282	-1.470
MAX DIFF	0.017	0.151	0.052	0.181	0.100	4.995	4.010

LOFT	135	135	135	180	180	180	180
	constant	ramped	nonlinear1	constant	stepped	ramped	nonlinear1
low	-9.917	-2.181	3.136	-0.375	7.556	9.163	9.195
mid	-10.776	-4.238	1.860	-1.318	4.894	7.583	8.938
high	-11.485	-4.140	1.479	-2.162	3.562	6.035	8.405
MAX DIFF	1.568	2.057	1.657	1.787	3.993	3.128	0.790

Table 7.8 Dynamic impact parameters for bend point swing analysis.

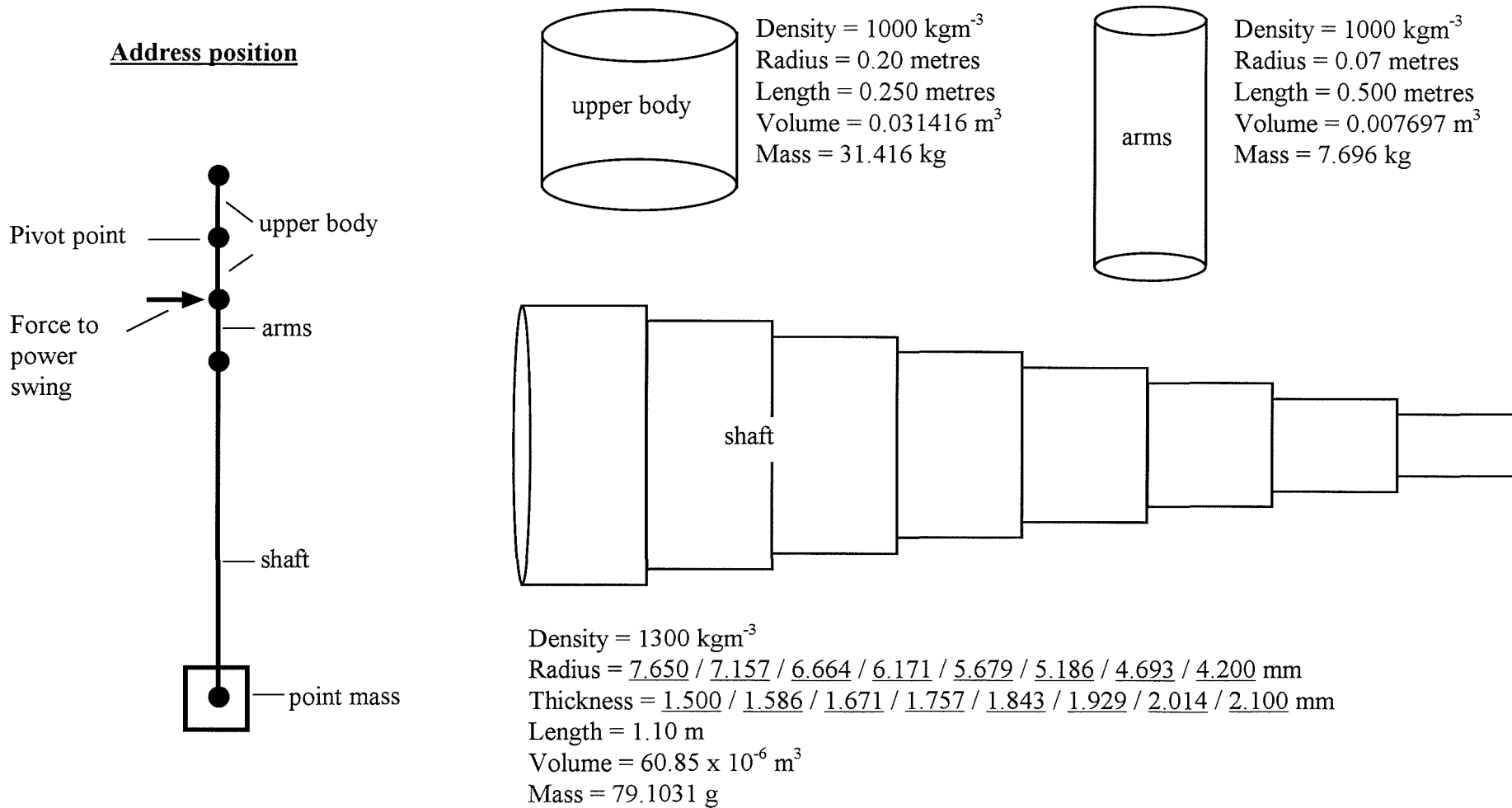


Figure 7.1 Swing model dimensions and 8 element shaft model.

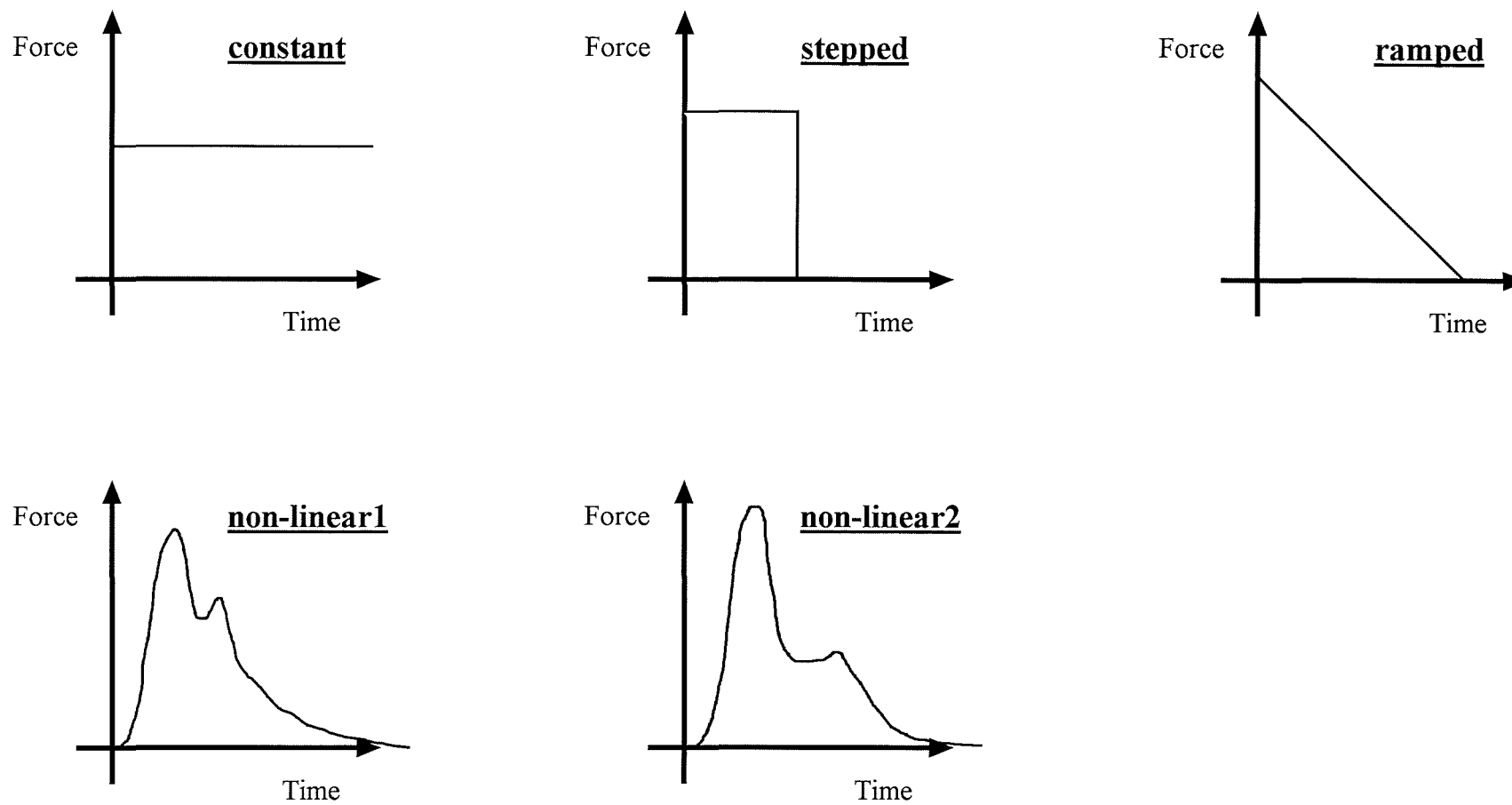


Figure 7.2 Force-time profiles (FTP).

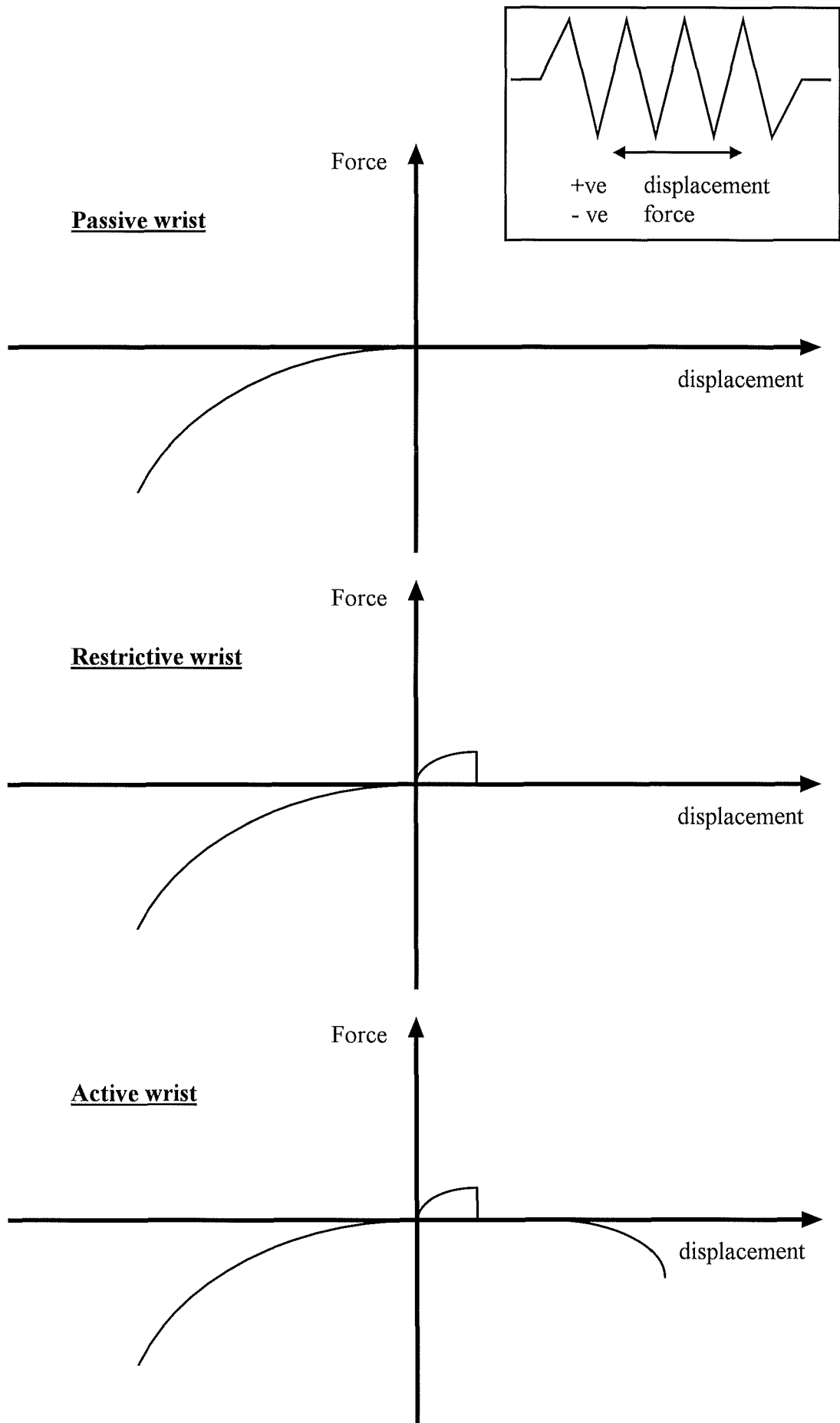
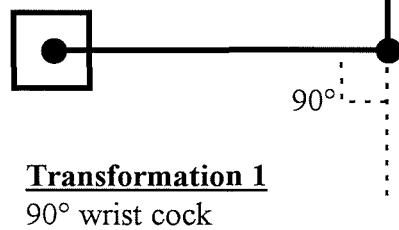
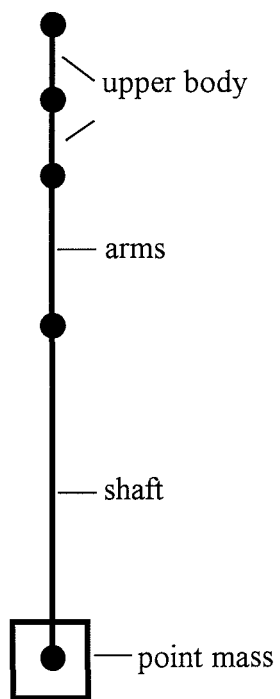
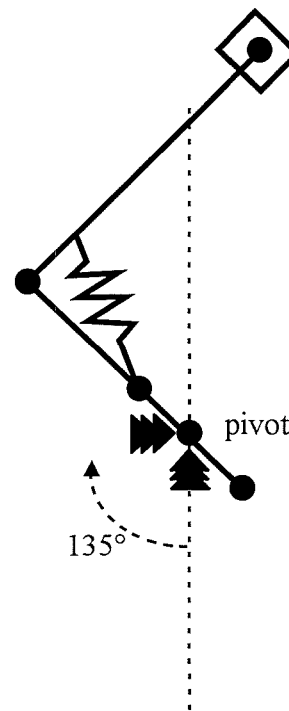


Figure 7.3 Wrist spring 'force-displacement' characteristics.

The address position



Transformation 1
90° wrist cock



Transformation 2
135° arm rotation about pivot point

Figure 7.4 Transformation from address to 90°-135° topswing.

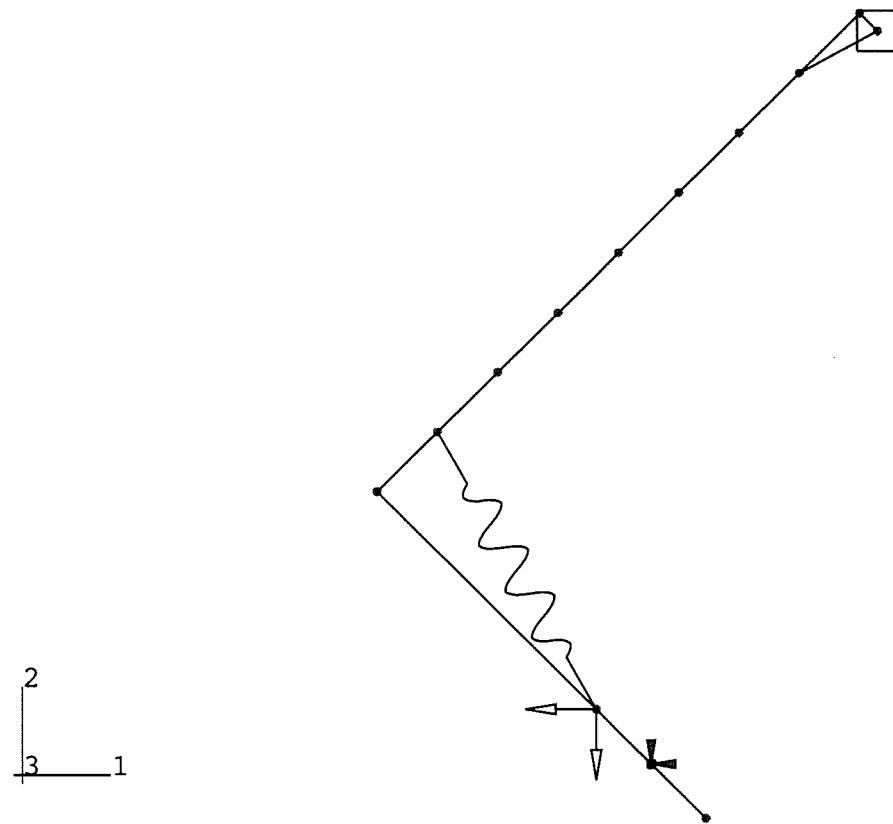


Figure 7.5 Finite element model of 90°-135° topswing.

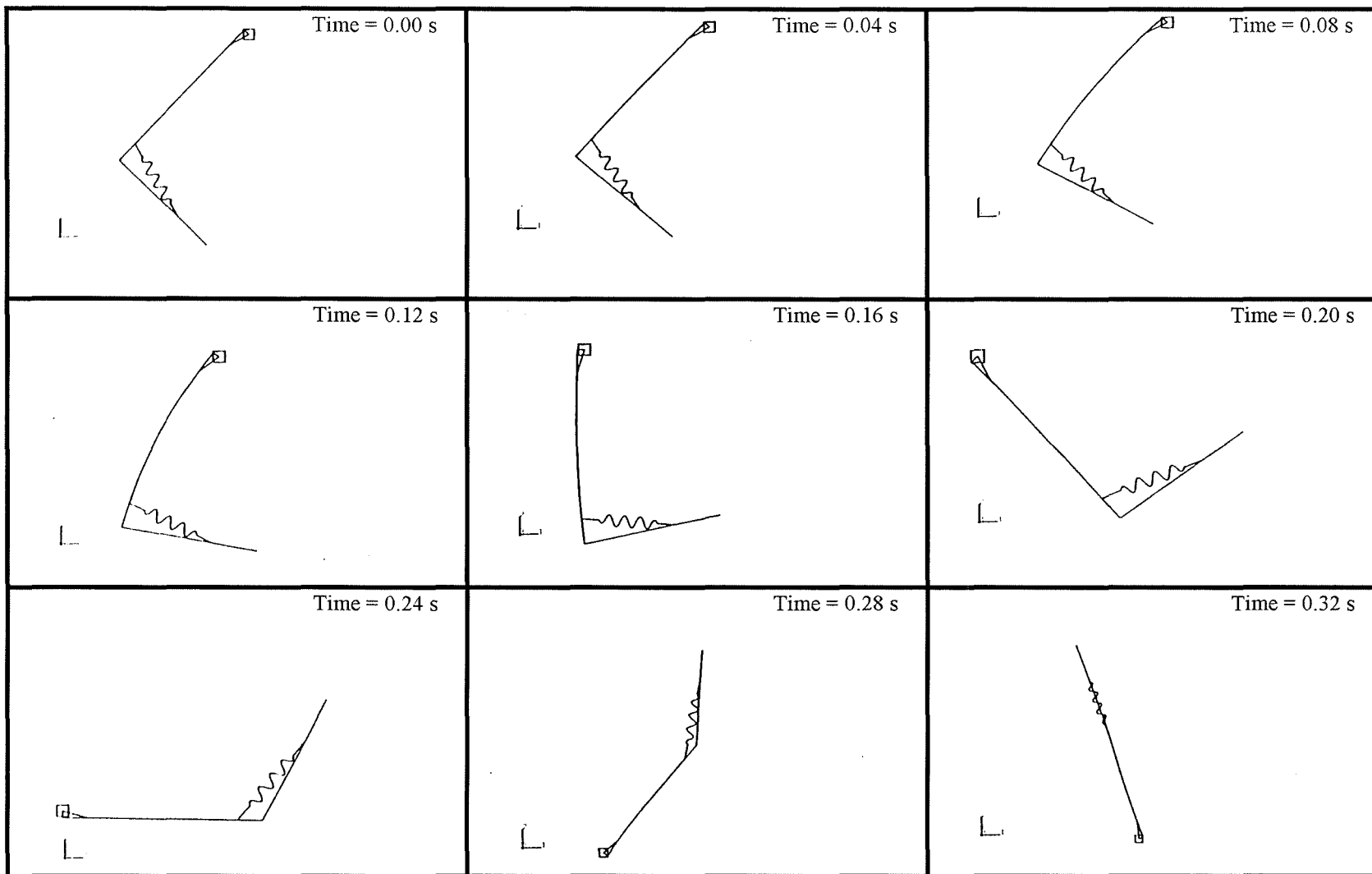


Figure 7.6 Snapshots of model downswing.

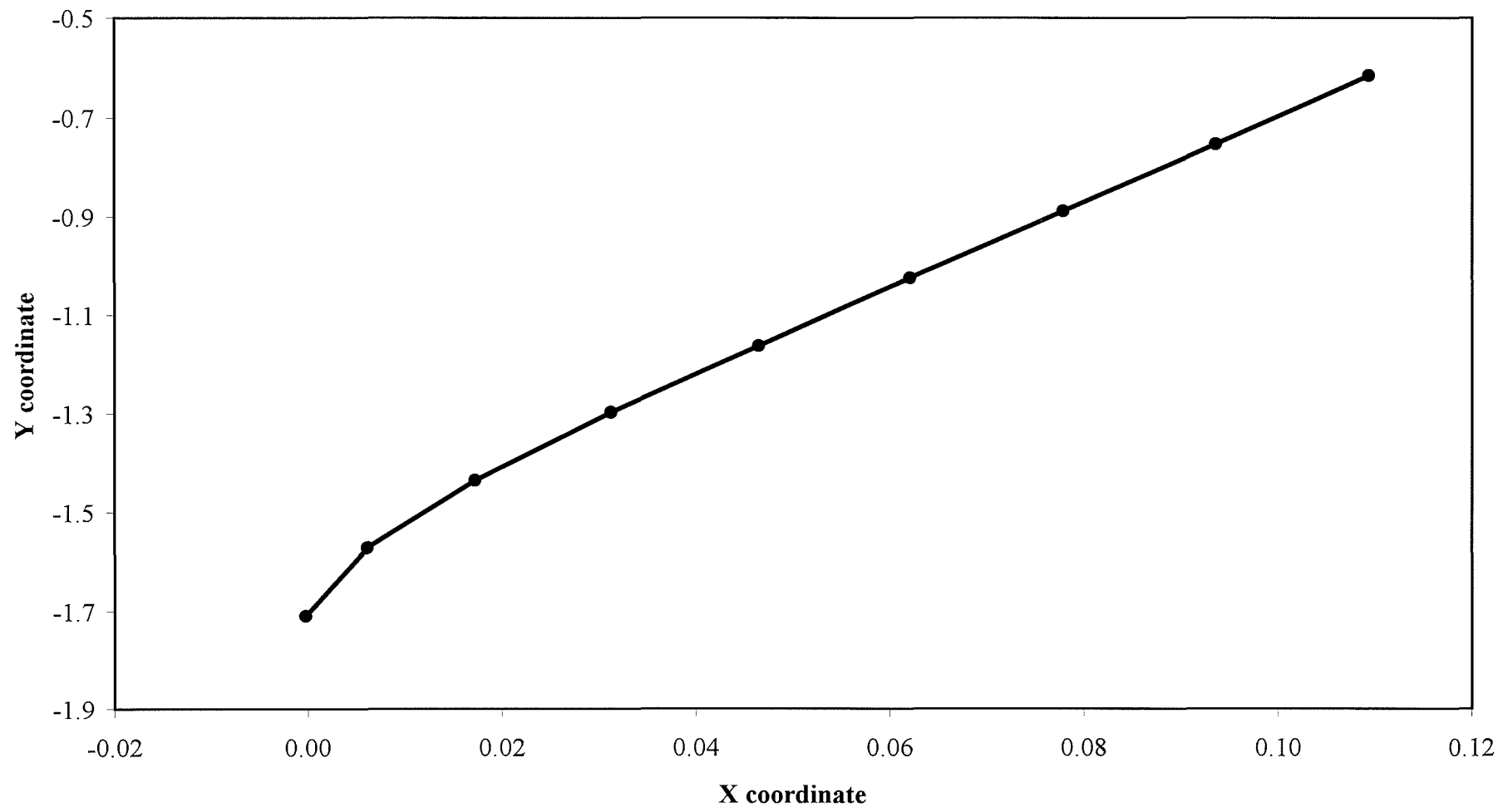


Figure 7.7 Shaft shape at impact, X-Y plot.

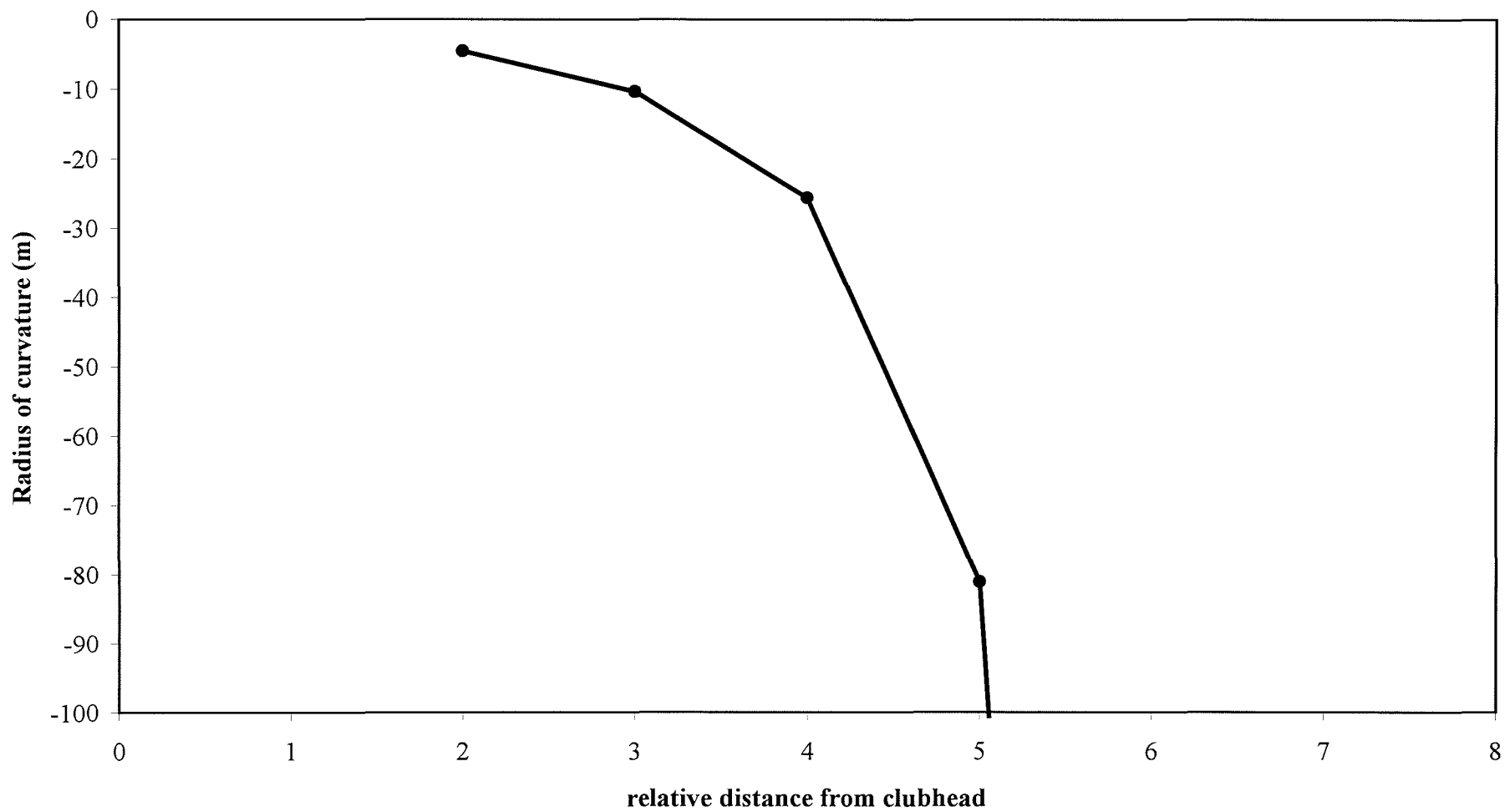


Figure 7.8 Shaft shape at impact, radius of curvature.

SK1	VALUE
1	-1.69E-01
2	-1.55E-01
3	-1.40E-01
4	-1.26E-01
5	-1.11E-01
6	-9.69E-02
7	-8.24E-02
8	-6.79E-02
9	-5.34E-02
10	-3.89E-02
11	-2.44E-02
12	-9.86E-03

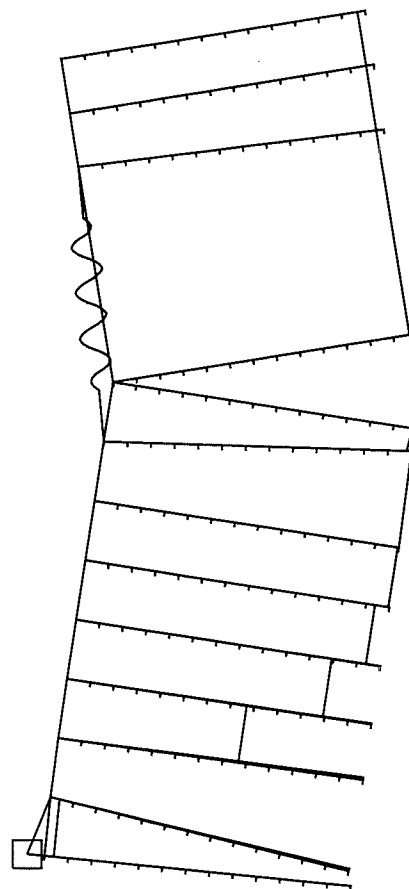
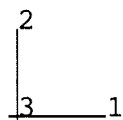


Figure 7.9 Curvature contour plot for swing model at impact.

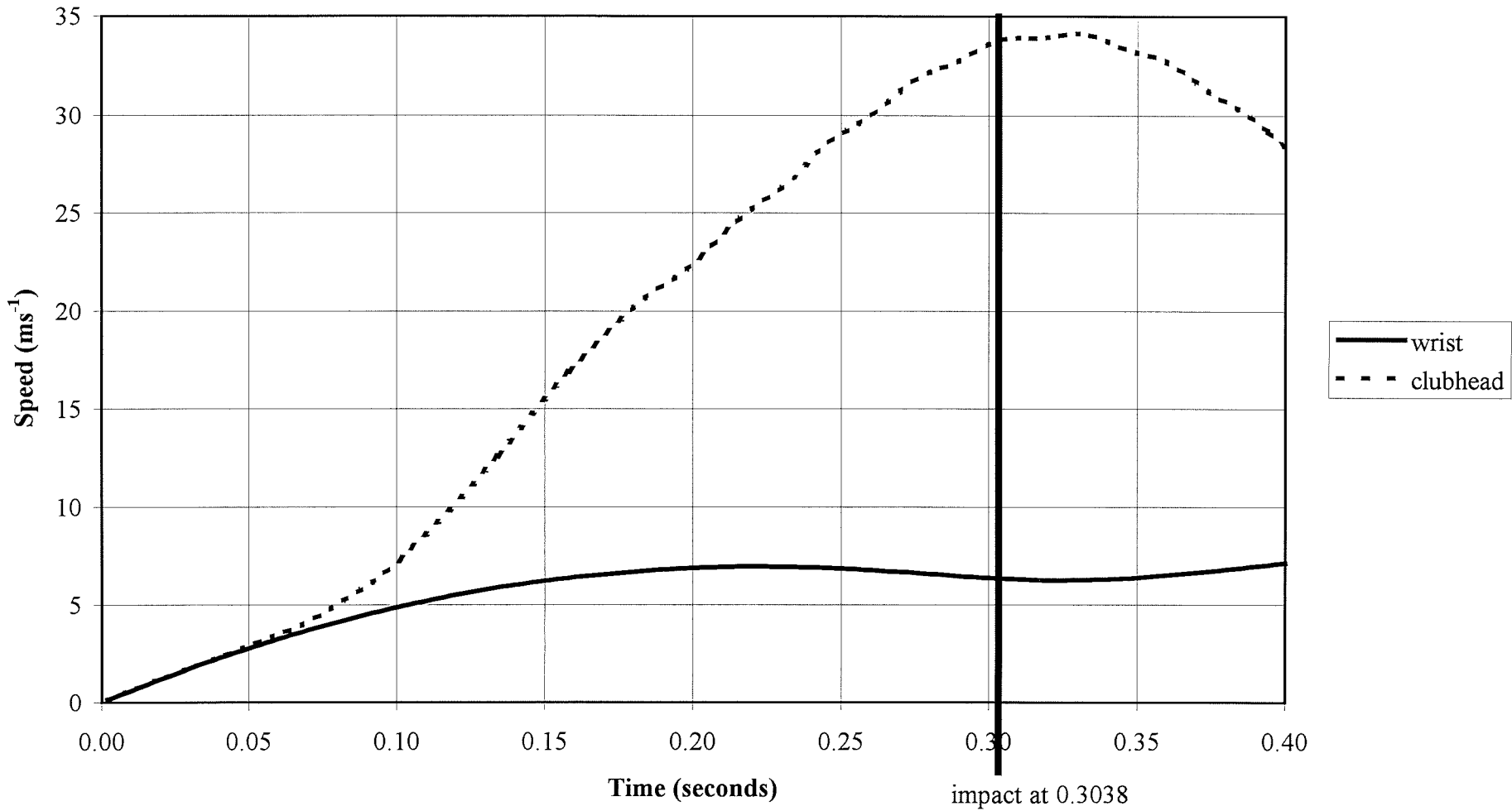


Figure 7.10 Wrist and clubhead speed during the downswing analysis.

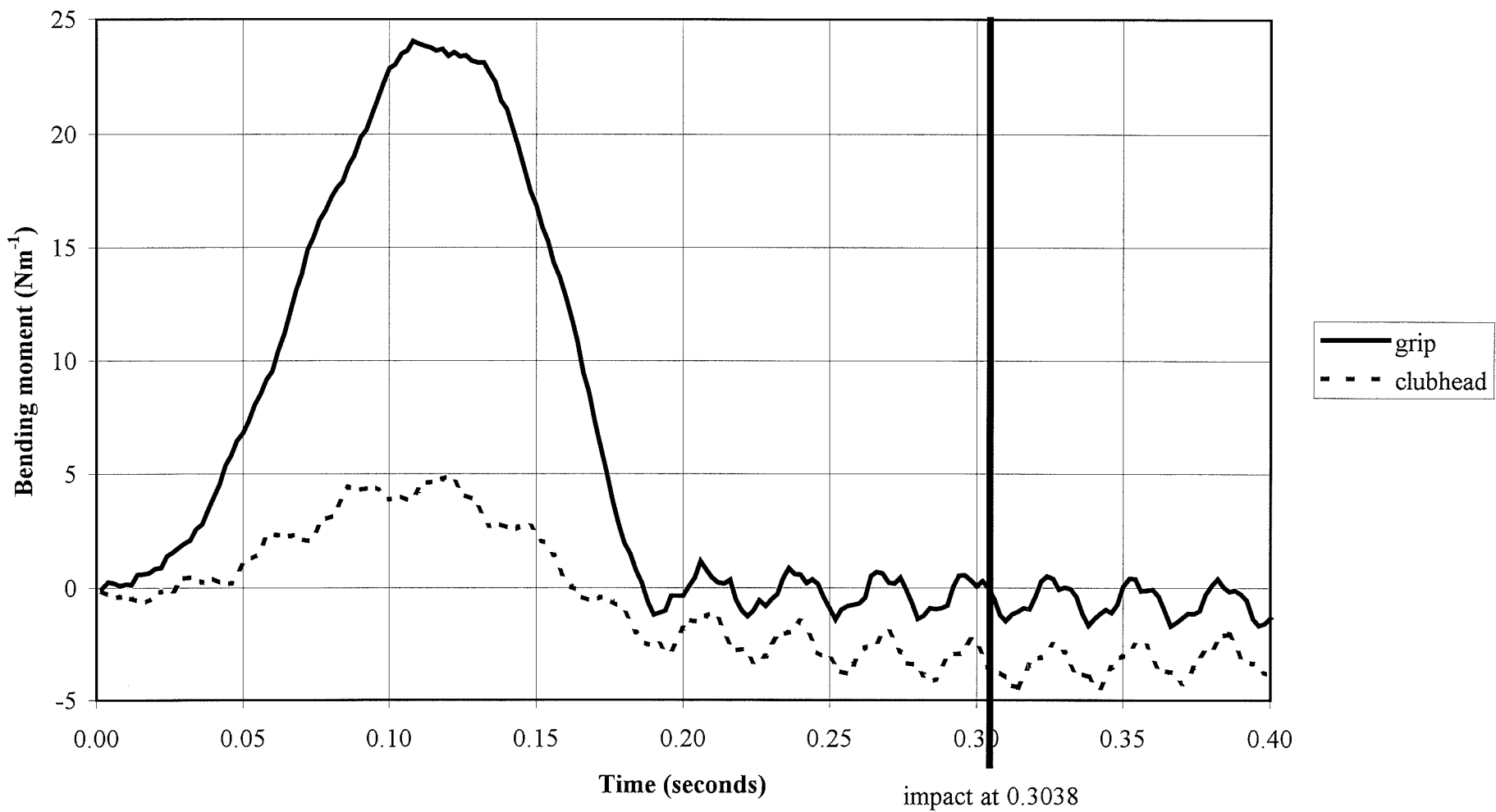


Figure 7.11 Bending moments in shaft during downswing analysis.

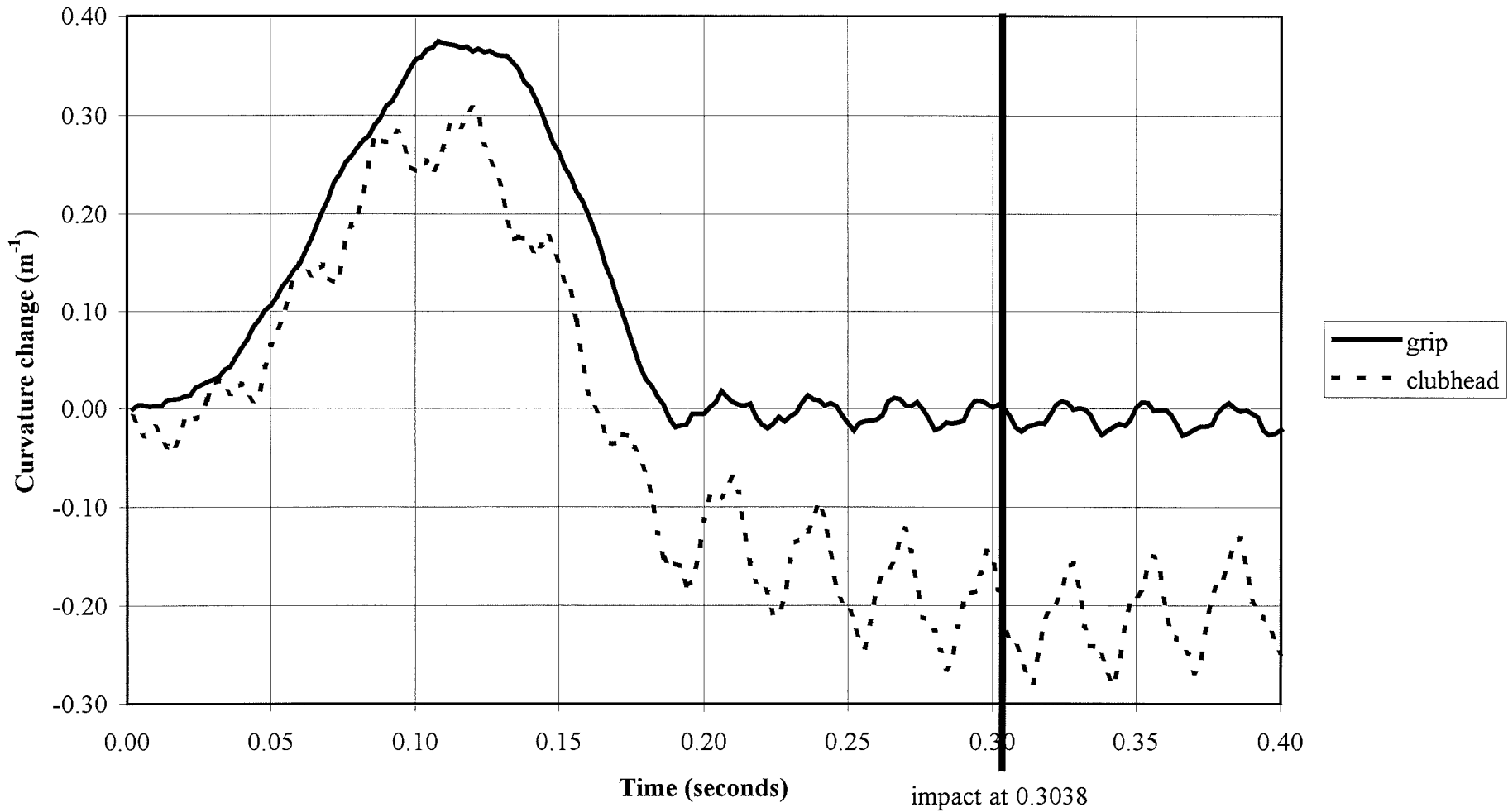


Figure 7.12 Curvature change in shaft during downswing analysis.

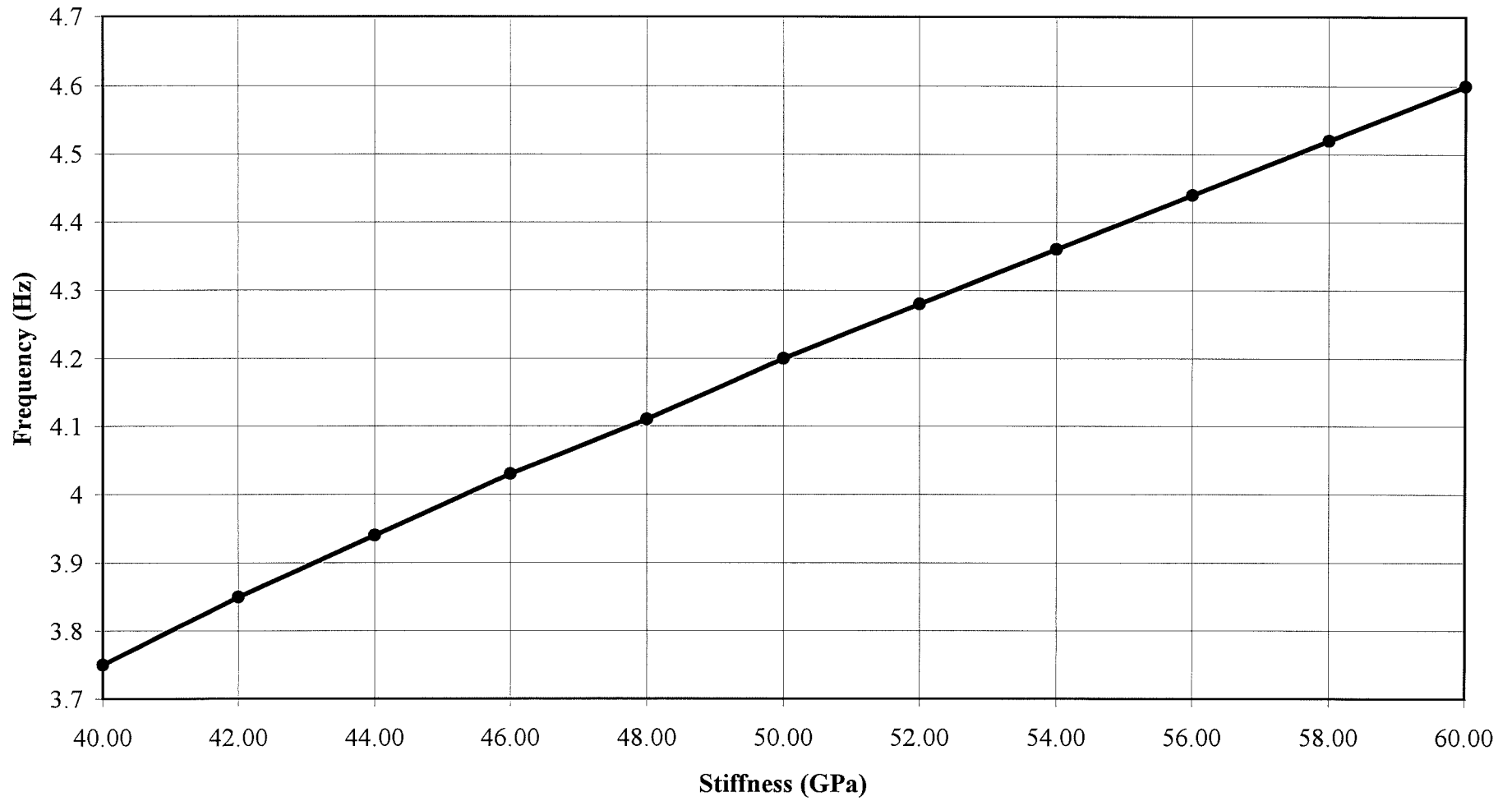


Figure 7.13 Effect of shaft stiffness on mode 1 frequency.

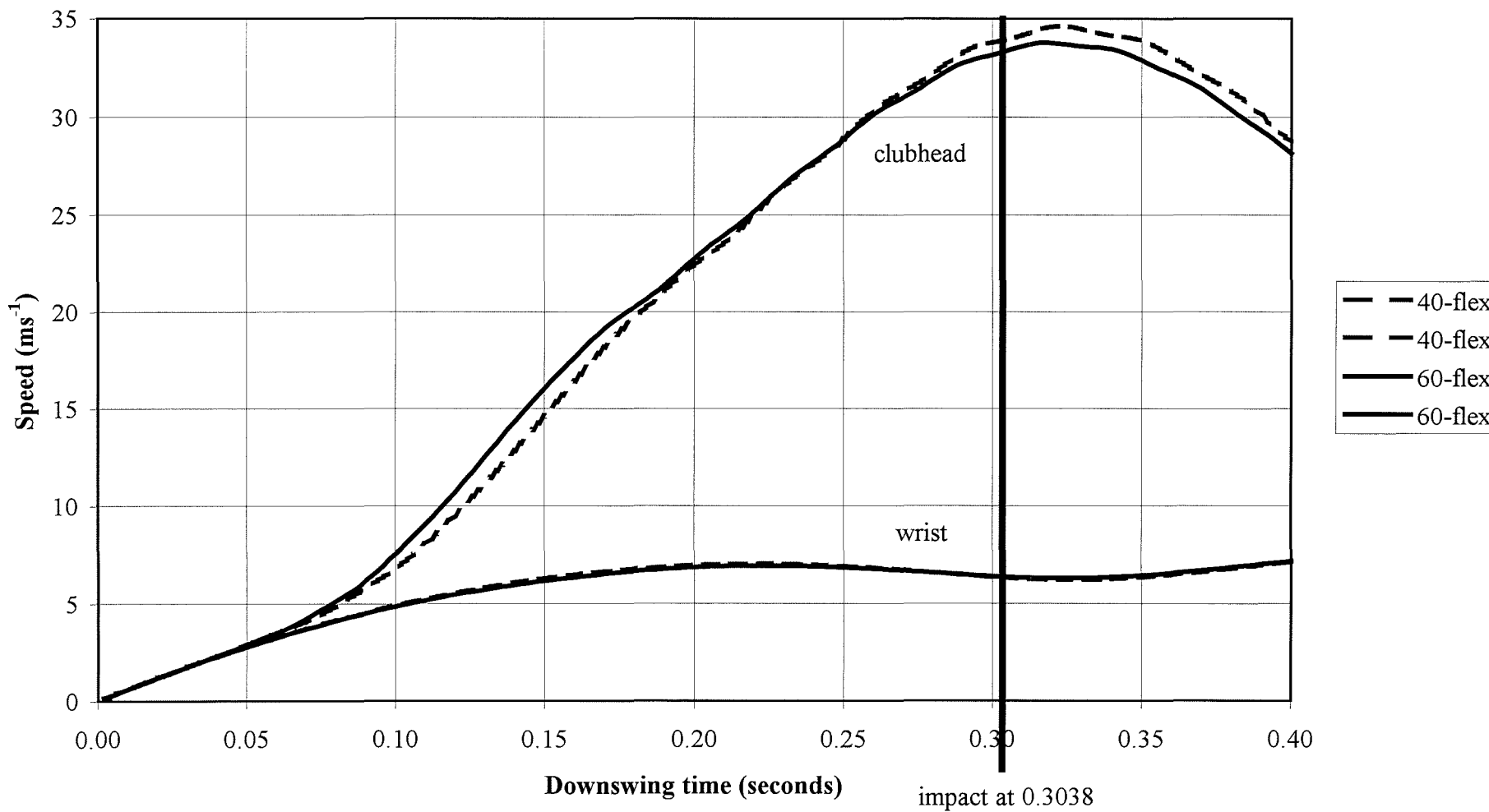


Figure 7.14 Wrist and clubhead speed during downswing, 40 and 60-flex.

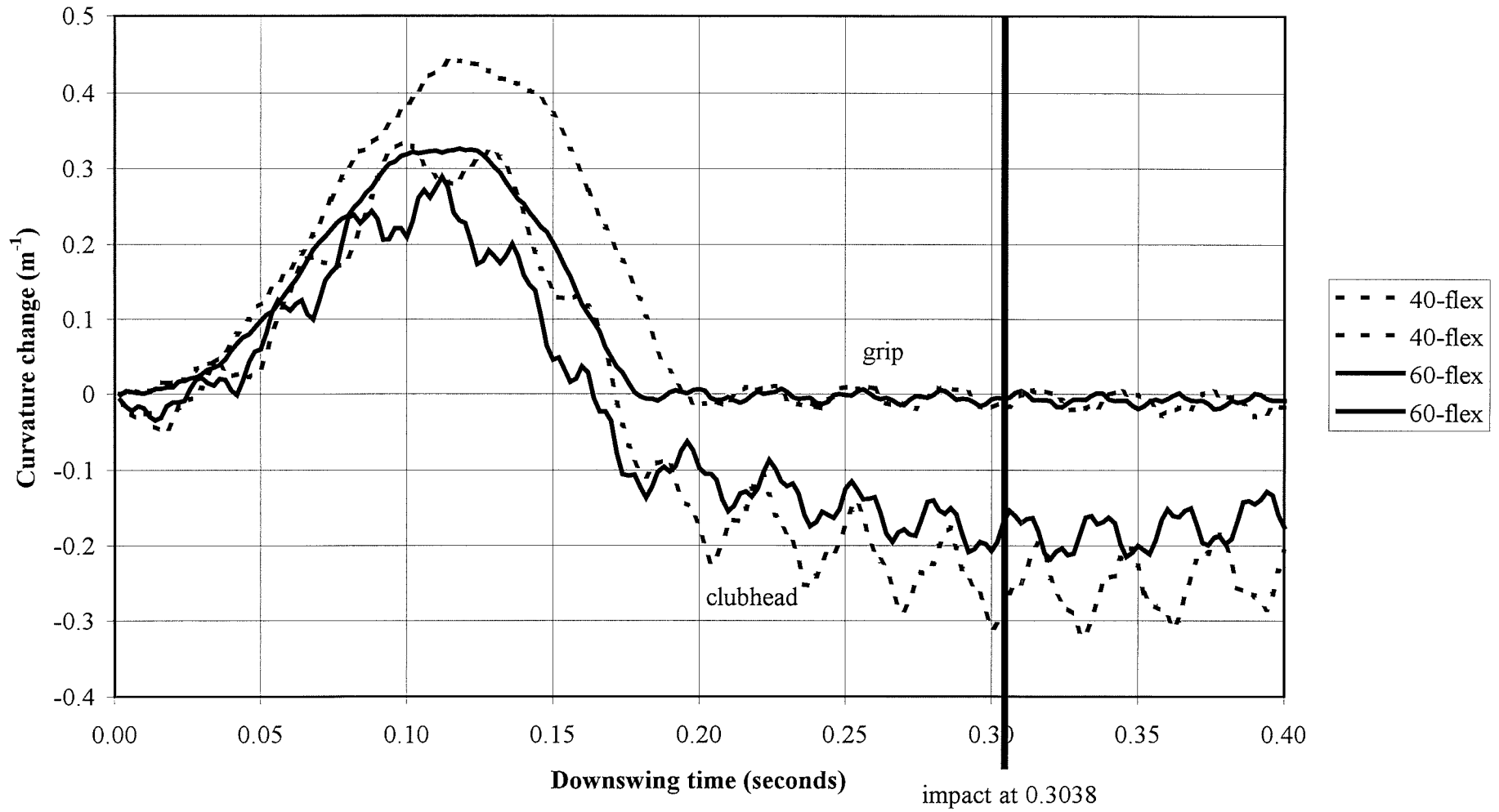


Figure 7.15 Curvature change in shaft during downswing 40 and 60-flex.

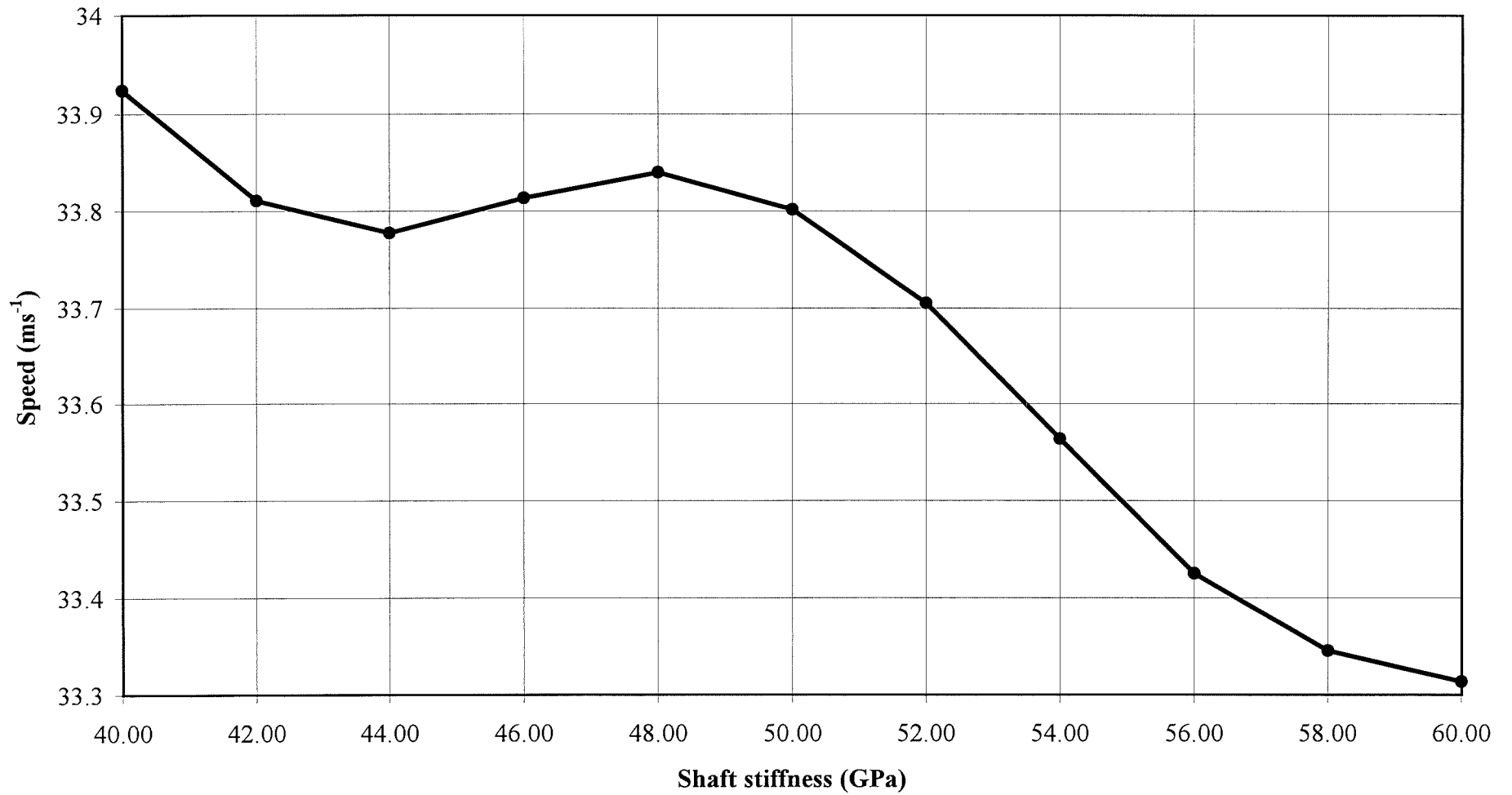


Figure 7.16 Effect of shaft stiffness on clubhead speed.

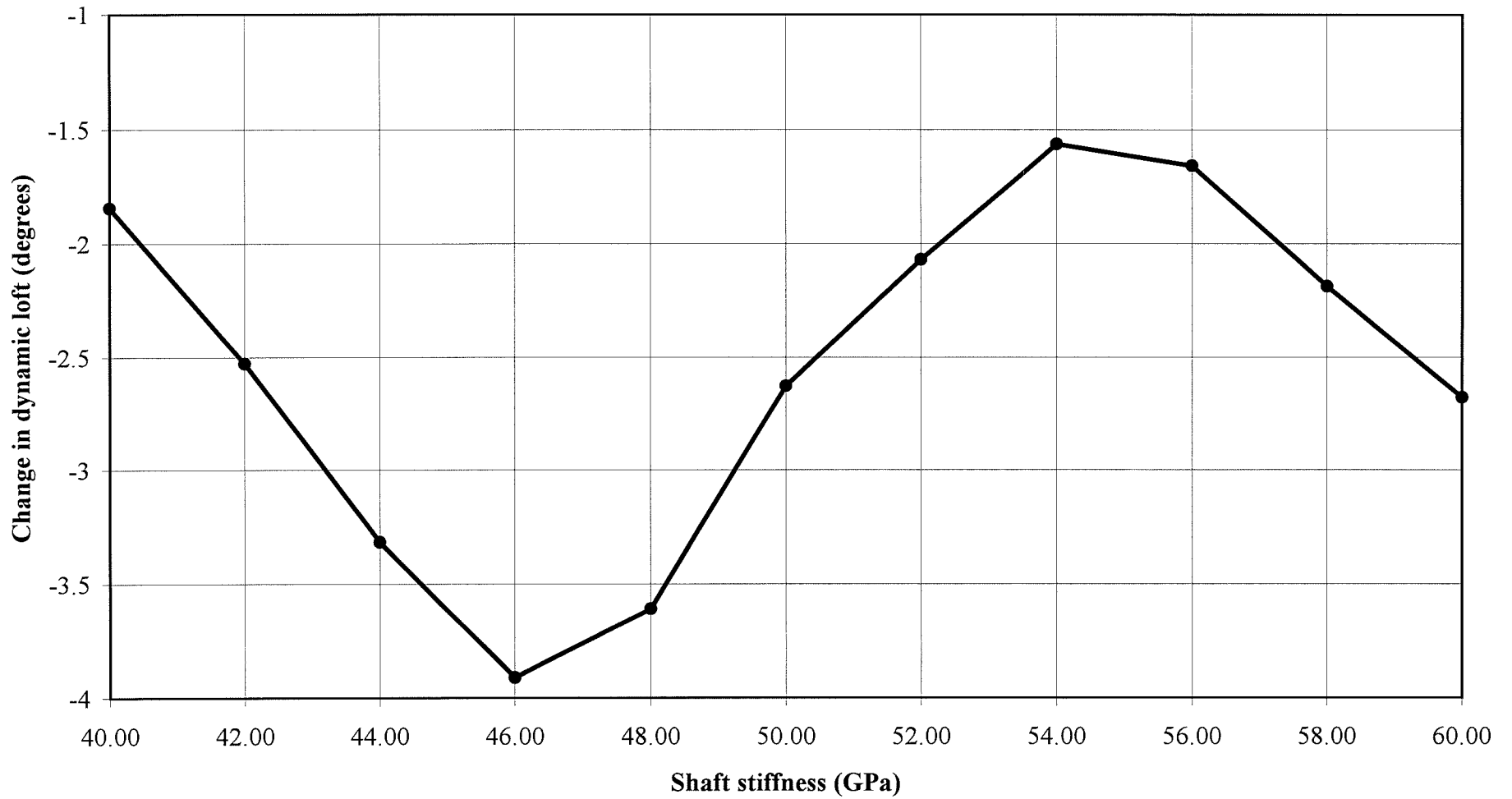


Figure 7.17 Effect of shaft stiffness on change in dynamic loft.

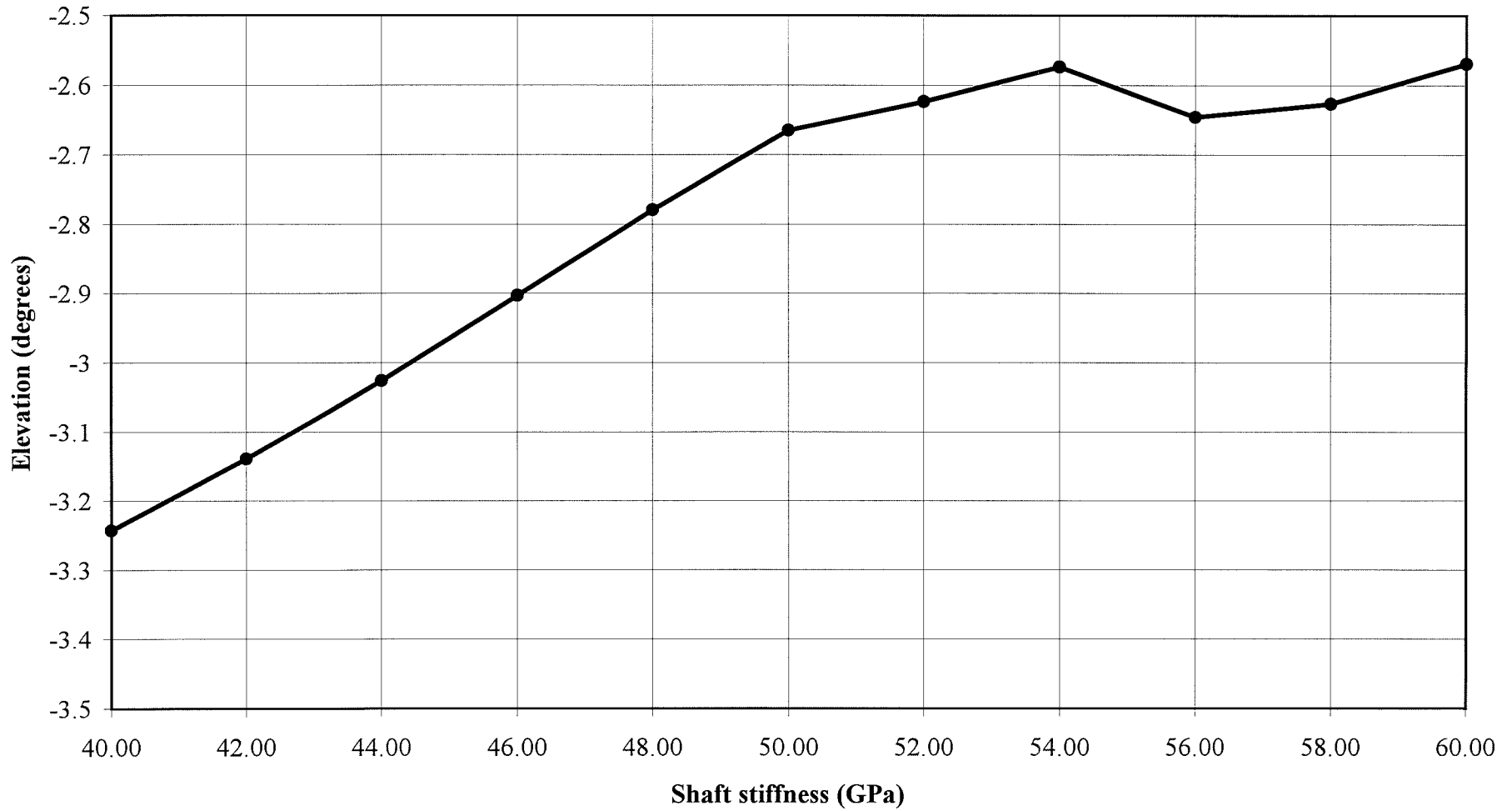


Figure 7.18 Effect of shaft stiffness on clubhead elevation.

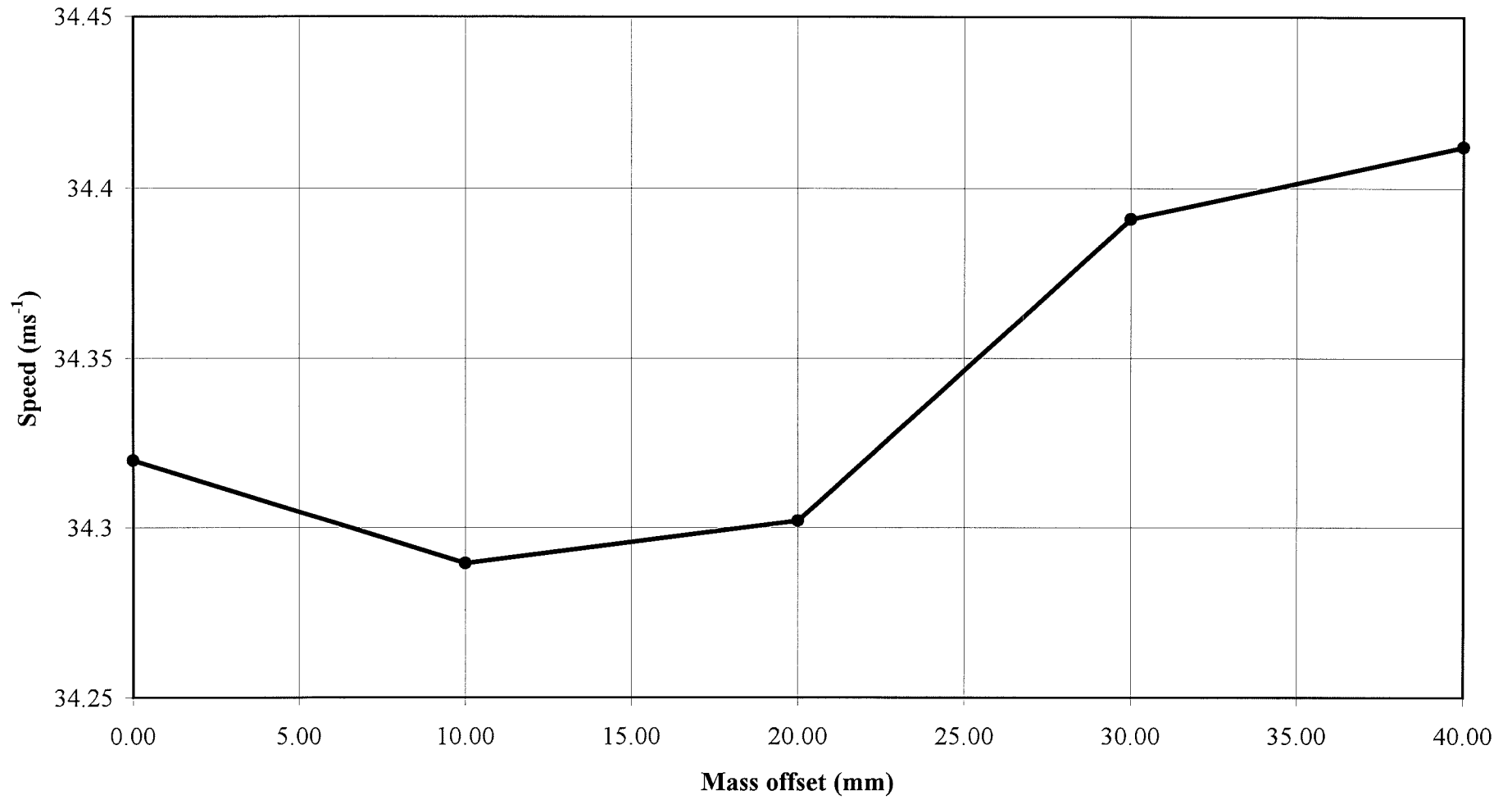


Figure 7.19 Effect of offset mass on clubhead speed.

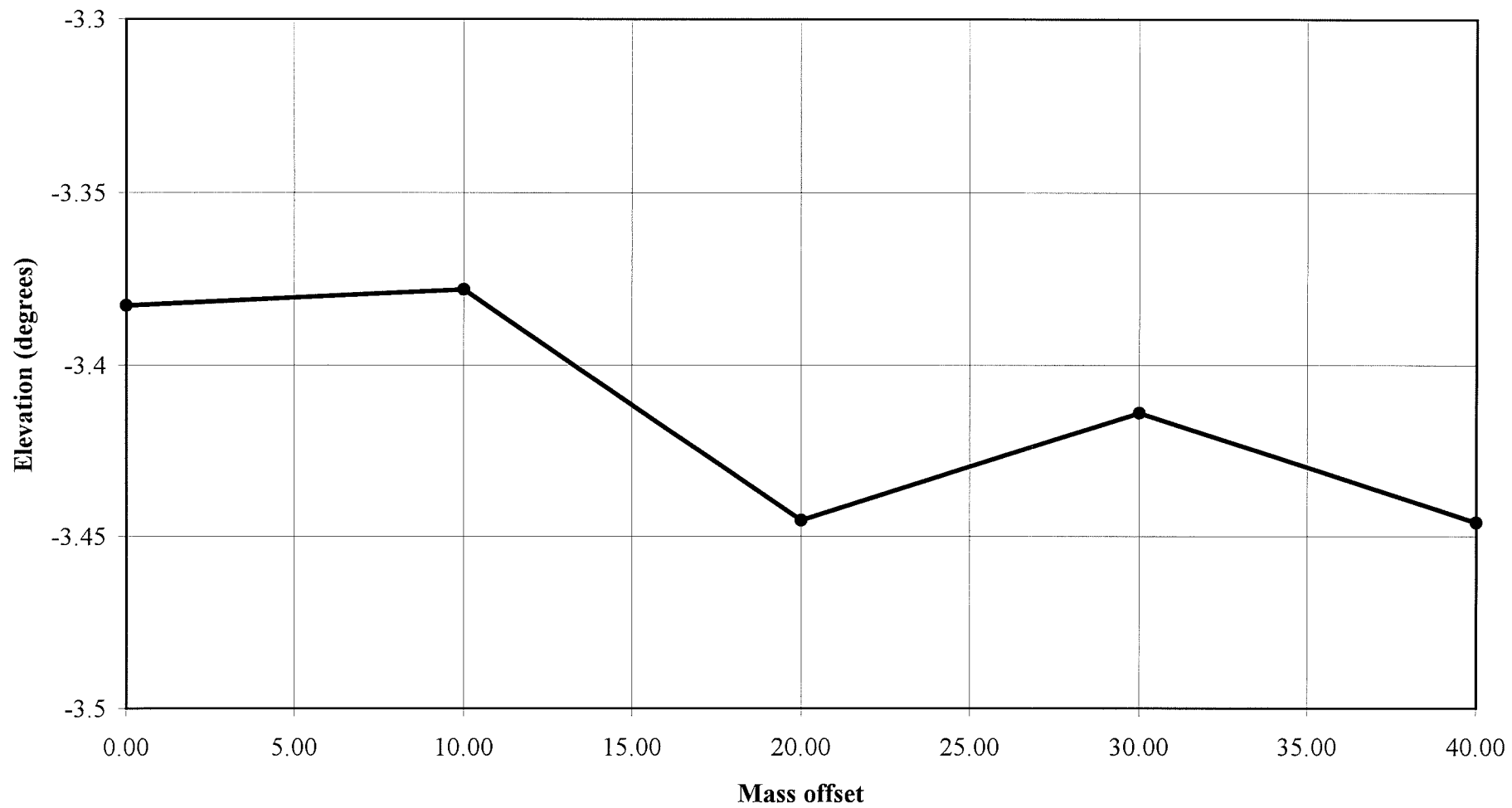


Figure 7.20 Effect of offset mass on clubhead elevation.

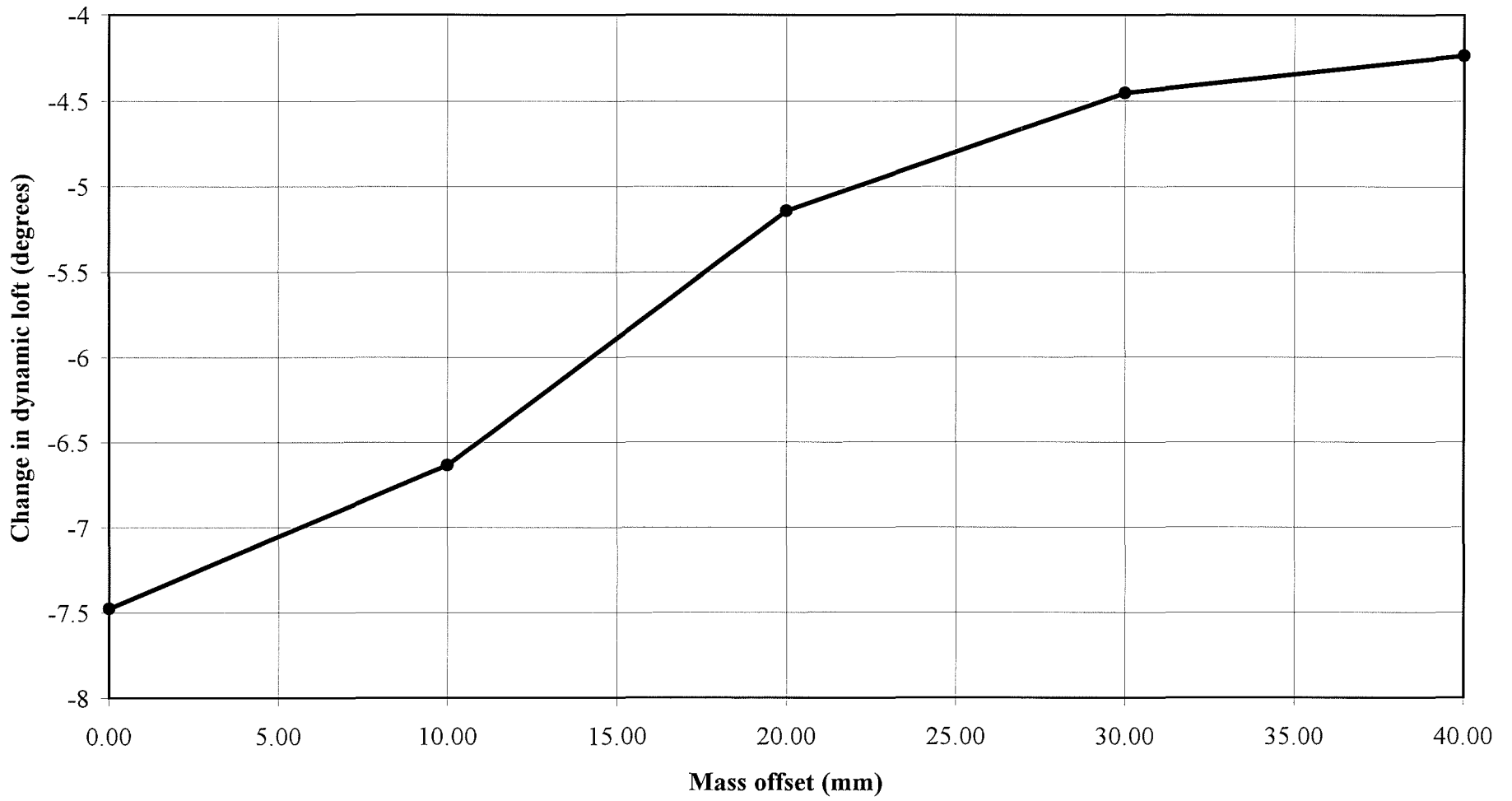


Figure 7.21 Effect of offset mass on change in dynamic loft.

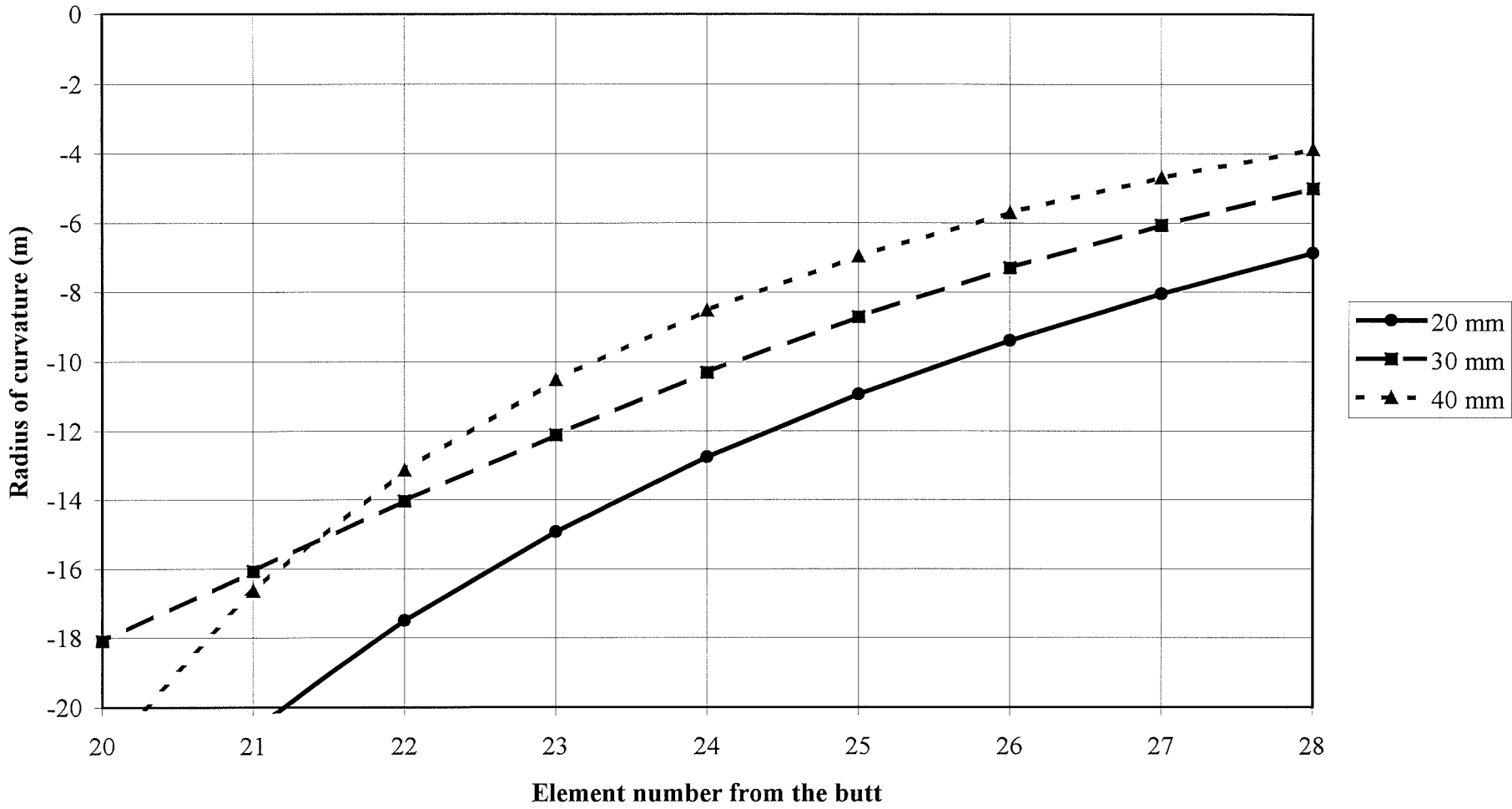


Figure 7.22 Radius of curvature near the clubhead for various offset models.

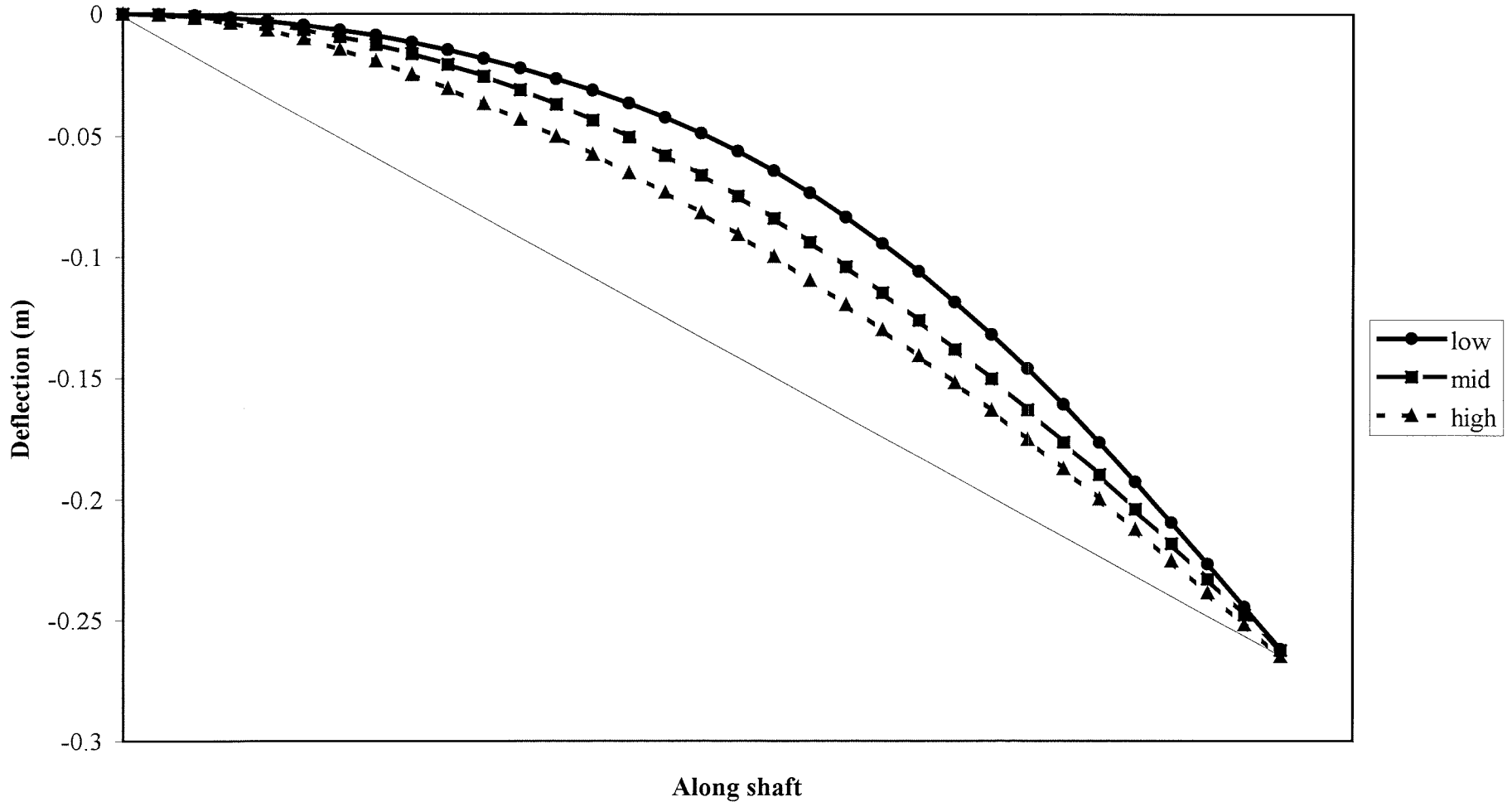


Figure 7.23 Shaft deflection plots showing bend profiles.

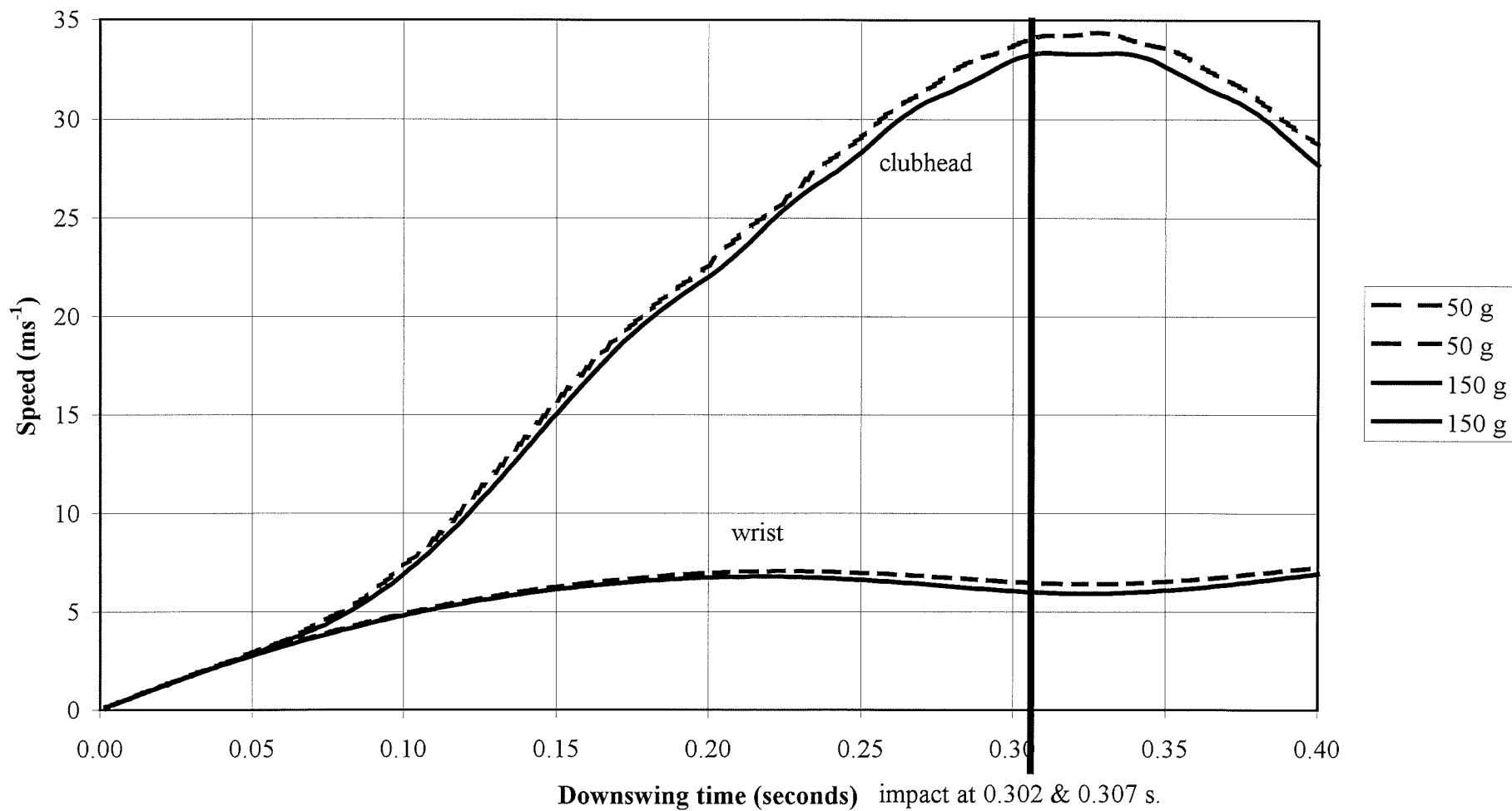


Figure 7.24 Wrist and clubhead speed during downswing, 50 and 150 g.

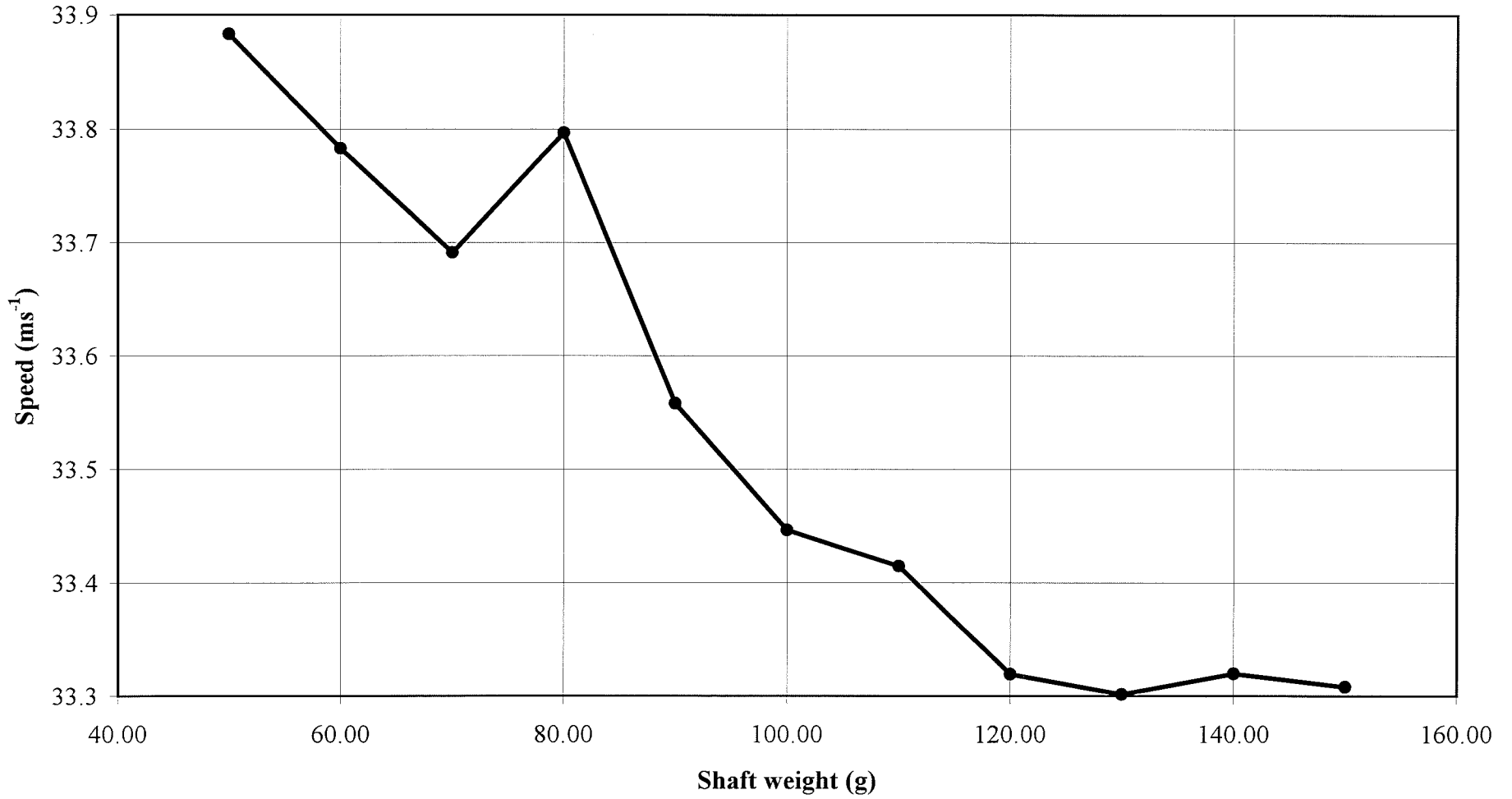


Figure 7.25 Effect of shaft weight on clubhead speed.

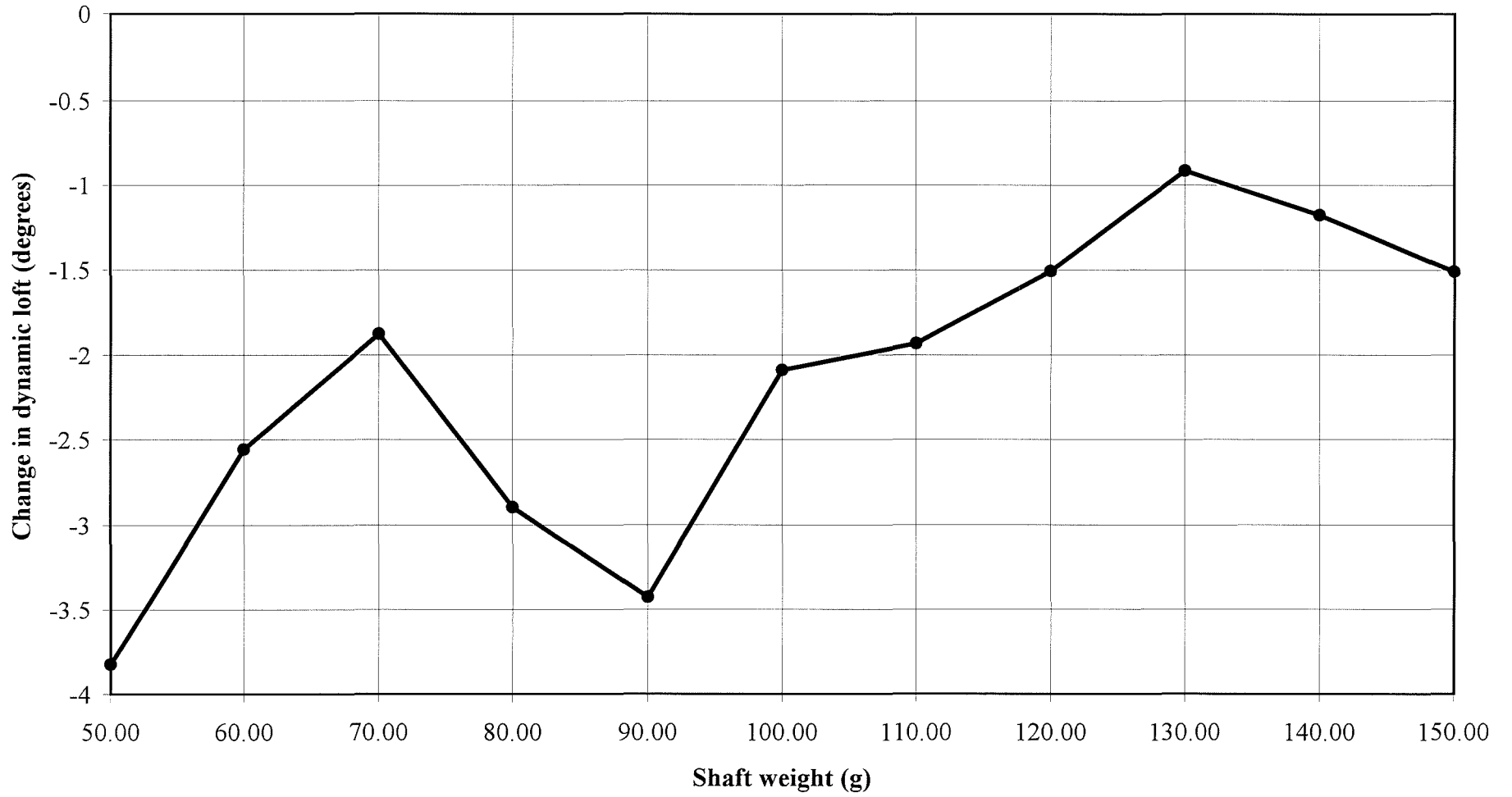


Figure 7.26 Effect of shaft weight on change in dynamic loft.

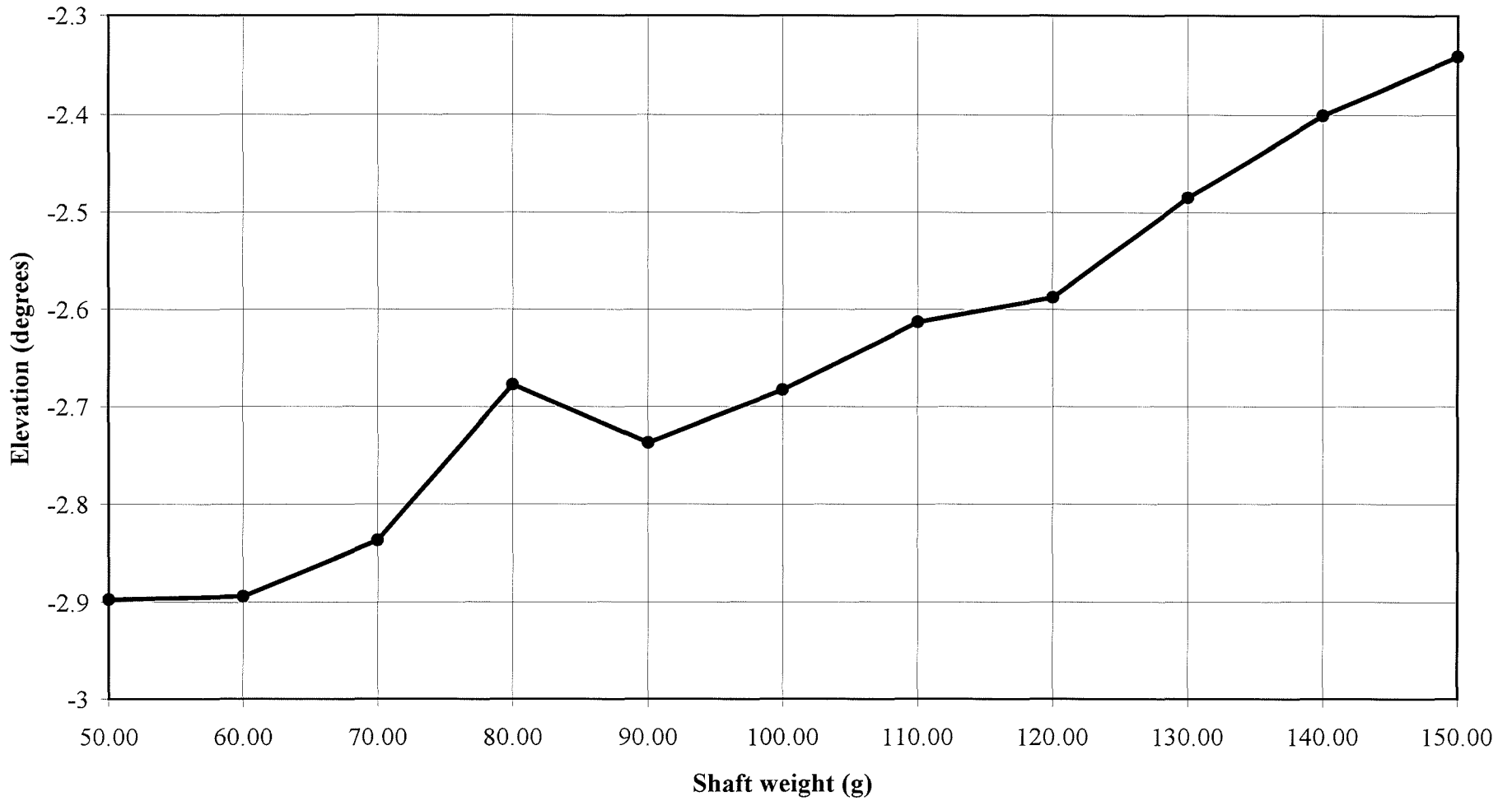


Figure 7.27 Effect of shaft weight on clubhead elevation.

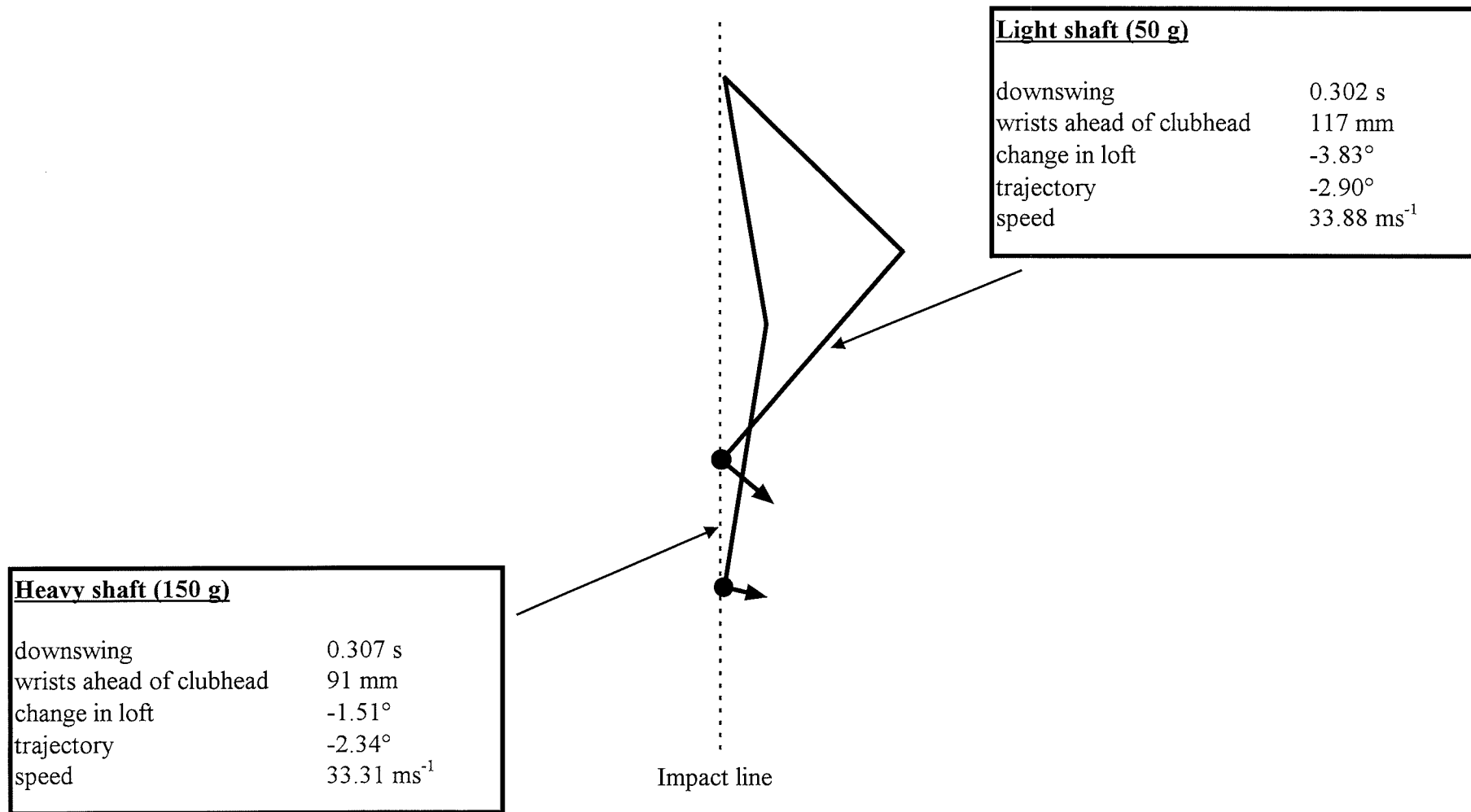


Figure 7.28 Swing impact positions for 50 and 150 g shafts (not to scale).

8.0 Conclusions and recommendations

Computational modelling of the golf stroke was successful with results comparing well with previous practical research.

8.1 Impact modelling

The clubhead was modelled as a free body impacting another free body, the ball. The effect of the shaft was ignored as it has been in much other previous research. While this is not the true practical case of a golf stroke it provided a means for verification of the model with other published studies. It is hoped that future computational modelling will include the shaft effect but this would be only prudent after further verification of the results presented in the current work.

While the specific impact results presented in the current work are particular to the ball and clubhead properties modelled, general conclusions can be drawn on clubhead and ball performance parameters.

The clubhead was first modelled as elastic and capable of undergoing deformations. The clubhead modulus at which maximum initial ball speed occurred was dependent on the ball material and construction. Clubheads with higher modulus do not necessarily produce higher ball speeds. For 'thick walled' clubheads showing only small strains during impact, and over the range of materials currently used in clubhead design, the effect of modulus on ball speed, launch and spin was negligible. For such clubheads adequate models of impact can be constructed from rigid elements if the correct mass and rotational inertia about the centre of mass are specified. A recent feature of rigid models is the creation of analytical curved surfaces. These are not susceptible to the discontinuities present in modelling curved surfaces with discrete elements. Such finite element models have been shown to be of use in evaluating the effect of bulge and roll curvatures on ball spin generation.

Geometric data on competing clubhead designs can be obtained from existing clubheads via reverse engineering techniques but these are difficult and costly. For clubheads created using computer aided design (CAD) such data would be easily obtainable.

Impact causes stress waves within the clubhead and these can be studied by the finite element technique using solid elements. Stress pulses timed to coincide with impact may increase ball speed leaving the face but preliminary tests have shown the effect may only be small.

For thin face clubheads such as a driver, where the face may be expected to deform appreciably during impact, rigid surfaces cannot suffice. Solid models with high mesh density to approximate the curved surfaces can be created but these are computationally expensive. However such models could be used to study further the existence of 'spring-back' effect.

The friction of the impact interface was shown to have a large effect on ball flight, affecting ball speed, launch and spin. The current work used a Coulomb friction model with no distinction between static and sliding friction. For any given loft a specific minimum friction coefficient exists that prevents sliding of the ball during impact. Maximum ball spin occurs at this value. Above this value the impact interface remains stationary and the spin rate decreases, contrary to popular theoretical ideas. Also running contrary is the relationship between friction and spin at low loft angles.

For the ball a non-linear elastic material model was utilised. While impact predictions compared well with previous practical published research the model showed discrepancies against classical mechanical studies of impact based on rigid bodies. In particular the model refutes the popular idea that increasing ball inertia leads to decreased initial spin rates. The model also shows the initiation of spin on the ball from a lofted impact interface with zero friction. This was caused by a pressure distribution on the interface not acting through the centre of mass of the ball, which deforms to a large extent during impact. Also, increasing the ball cover stiffness decreases ball spin whereas increasing the core stiffness increases ball spin. These effects are not included in classical mathematical models of impact and could be investigated further by the finite

element model. These results, that both the stiffness and mass density distribution throughout the ball affect performance, prove the need to model the ball as an elastic structure capable of large deformations if impact studies are to have relevance to the practical golf shot.

Finite element modelling could be improved further if additional engineering material data is available. Currently, little is known of the engineering properties of hyperelastic compounds. Practical experiments need to be devised to obtain such properties. It is to be expected that this area of material modelling will grow in future years.

More accurate results could be achieved by finer meshing of the clubhead, as would be needed in thin face drivers, but the improvement would be minimal compared to the advantages of finer meshing of the ball. However both increase the analysis time and cost and require larger amounts of computer and disk space. Considering the current growth rate in computer power, these problems are likely to disappear in the near future.

Finally, the hardness test often used to describe the materials used in golf equipment is concerned with permanent deformation. Whilst hardness is thus of issue to clubhead designer and manufacturers, it is not an appropriate parameter related to golf equipment performance, where permanent deformation is not desired.

8.2 Swing modelling

A swing model was created that allows shaft performance to be examined for various styles of golf swing. The model has only been used in 2-dimensions but can be readily expanded to 3-dimensions to include, for example torsion effects and out-of-plane bending and vibration. The model allows for a non-linear input torque as its main power source and non-linear variability of wrist torque with displacement. While the current work demonstrates the former, only a single simplified wrist torque function was used. It is to be expected that other researchers studying the human golf swing will be able to supply data, relevant to the model input variables, in the near future. The model analysis has remained in 2-dimensions, simulating the golf swing of the University of Glasgow

mechanical golfer, 'Dai-Laughing', so as to allow verification of the model. This is seen as the essential next step before the model is used in 3-dimensions.

The model causes the shaft to vibrate during the swing but the lack of structural damping in the model makes some of the results unrealistic. Shaft material damping can be included but this would be negligible compared to the damping provided by the golfer's grip and hands. Comparison of the model with practical experiments is necessary to establish how damping is best included and again the importance of verification is emphasised as the next step in continuing the current work.

References

Achenbach, J., 1997, "Fairway woods aren't for wimps anymore." [online], Golfweb - a sportslineUSA company, (sine loco), 18th July 1997, [cited 12th July 1998], available from internet - <http://www.golfweb.com/library/achenbach/achenbach970718.html>

Achenbach, J., 1999, "Revolution benefits golfers, shaft whiz." [online], Golfonline, a division of Times Mirror Magazines, (sine loco), 27th February 1999, [cited 27th February 1999], available from internet - <http://www.golfonline.com/news/golfweek/1999/february/achenbach0227.html>

Aldridge, J., 1995, "Grip technology." *Golf the Scientific Way*, Ed Cochran, Aston Publishing Group, Hertfordshire.

Anon, 1989, "Feedback." *New Scientist - 28th October*, IPC Magazine Ltd., London.

Aoyama, S., 1995, "How much longer and straighter is today's golf ball?" *Golf the Scientific Way*, Ed Cochran, Aston Publishing Group, Hertfordshire.

Ashby, M.F., 1996, *Engineering Materials*, Pergamon, Oxford.

Associated Press, 1998, "Big titanium clubs to get ok." [online], Golfweb - a sportslineUSA company, (sine loco), 17th June 1998, [cited 19th June 1998], available from internet - <http://www.golfweb.com/news/usga980617.html>

Bahill, T. and Karnavas, W., 1991, "The ideal baseball bat." *New Scientist - 6th April*, IPC Magazines Ltd., London.

Brancazio, P.J., 1988, "Tennis science for tennis players." *American Journal of Physics*, Vol. 56, No. 4, April.

Brody, H., 1995, "How would a physicist design a tennis racket?" *Physics Today*, March.

Brylawski, A.M., 1994, "An investigation of three dimensional deformation of a golf club during the downswing." *Science and Golf II*, Ed Cochran and Farrally, E. & F.N. Spon, London.

Budney, D.R. and Bellow, D.G., 1990, "Evaluation of golf club control by grip pressure measurement." *Science and Golf*, Ed Cochran, E. & F.N. Spon, London.

Burden, A.M., Grimshaw, P.N. and Wallace, E.S., 1998, "Hip and shoulder rotations during the golf swing of sub-10 handicap players." *Journal of Sports Sciences*, 16, 165-176.

Butler, J.H. and Winfield, D.C., 1994, "The dynamic performance of the golf shaft during the downswing." *Science and Golf II*, Ed Cochran and Farrally, E. & F.N. Spon, London.

Butler, H. and Winfield, D., 1995, "What shaft is best for you?" *Golf the Scientific Way*, Ed Cochran, Aston Publishing Group, Hertfordshire.

Chou, A. and Roberts, O.C., 1994, "Golf shaft flex point - an analysis of measurement techniques." *Science and Golf II*, Ed Cochran and Farrally, E. & F.N. Spon, London.

Chou, A., Gilbet, P. and Olsavsky, T., 1995, "Clubhead designs: how they affect ball flight." *Golf the Scientific Way*, Ed Cochran, Aston Publishing Group, Hertfordshire.

Cochran, A.J. and Stobbs, J., 1968, *The Search for the Perfect Swing*, Heinemann, London.

Cochran, A.J., 1990, "Science, equipment and standards." *Science and Golf*, Ed Cochran, E. & F.N. Spon, London.

Cochran, A.J., 1995, "Editorial." *Golf the Scientific Way*, Ed Cochran, Aston Publishing Group, Hertfordshire.

Cooper, M.A.J. and Mather, J.S.B., 1994, "Categorisation of golf swings." *Science and Golf II*, Ed Cochran and Farrally, E. & F.N. Spon, London.

Cubic Balance, 1998, "Grooveless super megasize titanium drivers." [online], Cubic Balance Golf Technology Inc., California, 19th September 1998, [cited 12th November 1998], available from internet - http://www.cubicbalance.com/sup_mega_drivers.html

Daish, C.B., 1972, *The Physics of Ball Games*, English Universities Press, London.

Dillman, C.J. and Lange, G.W., 1994, "How has biomechanics contributed to the understanding of the golf swing." *Science and Golf II*, Ed Cochran and Farrally, E. & F.N. Spon, London.

Dorling Kindersley, 1998, *Visual Encyclopedia*, Dorling Kindersley, London.

Easterling, K.E., 1993, *Advanced Materials for Sports Equipment*, Chapman & Hall, London.

Farrally, M.R., 1990, "Foreword." *Science and Golf*, Ed Cochran, E. & F.N. Spon, London.

Fay, D., 1998, "A USGA press conference with:" [online], United States Golf Association, New Jersey, June 1998, [cited 12th July 1998], available from internet - http://www.usga.com/test_center/fay_buzz_conference.html

Friswell, M.I., Mottershead, J.E. and Smart, M.G., 1998, "Dynamic models of golf clubs." *Sports Engineering*, No. 1, p41-50.

Gobush, W., 1990, "Impact force measurements on golf balls." *Science and Golf*, Ed Cochran, E. & F.N. Spon, London.

Gobush, W., 1995 "Spin and the inner workings of a golf ball." *Golf the Scientific Way*, Ed Cochran, Aston Publishing Group, Hertfordshire.

Gobush, W., 1996, "Friction coefficient of golf balls." *The Engineering of Sport*, Ed Haake, Blackwell Science, Oxford.

Haake, S.J., 1989, *Apparatus and Test Methods for Measuring Impact of Golf Balls on turf and Their Application in the Field*, Ph.D. Thesis, The University of Aston, Birmingham.

Hale, T., Bunyan, P. and Sewell, I, 1994, "Does it matter what ball you play?" *Science and Golf II*, Ed Cochran and Farrally, E. & F.N. Spon, London.

Hale, T., 1995, "Analysing Play." *Golf the Scientific Way*, Ed Cochran, Aston Publishing Group, Hertfordshire.

Hartzell, T.A. and Nesbit, S.M., 1996, "Analytical design of Iron golf club heads." *Journal of Sports Sciences*, 14, 311.

Hedrick, M., and Twigg, M., 1995 "The feel of a golf shot: can we measure it?" *Golf the Scientific Way*, Ed Cochran, Aston Publishing Group, Hertfordshire.

Hibbitt, Karlsson and Sorensen, 1997, Abaqus manuals, vers. 5.4-5.8, Hibbitt, Karlsson and Sorensen, Inc., Rhode Island.

Horwood, G.P., 1994, "Golf-shafts - a technical perspective." *Science and Golf II*, Ed Cochran and Farrally, E. & F.N. Spon, London.

Horwood, G., 1995, "Flexes, bend points and torques." *Golf the Scientific Way*, Ed Cochran, Aston Publishing Group, Hertfordshire.

ITF, 1998, "Rules and regulations." [online], International Tennis Federation, London, 1998, [cited 4th Demcember 1998], available from internet - <http://www.itftennis.com>

Iwatsubo, T., Kawamura, S., Miyamoto, K. and Yamaguchi, Y., 1998, "Numerical Analysis of golf club head at various restitution conditions." *The Engineering of Sport II*, Ed Haake, Blackwell Science, Oxford.

Johnson, S.H., 1994, "Experimental determination of inertia ellipsoids." *Science and Golf II*, Ed Cochran and Farrally, E. & F.N. Spon, London.

Johnson, S.H. and Lieberman, B.B., 1996, "Normal impact models for golf balls." *The Engineering of Sport*, Ed Haake, Blackwell Science, Oxford.

Johnson, T., 1997, "Don't blame it on the clubs." [online], Golfweb - a sportslineUSA company, (sine loco), 22nd August 1997, [cited 04th August 1998], available from internet - <http://www.golfweb.com/library/johnson/johnson970822.html>

Johnson, T., 1999, "New balls debut at PGA show." [online], Golfweb - a sportslineUSA company, (sine loco), 29th January 1999, [cited 29th January 1999], available from internet - <http://www.golfweb.com/library/johnson/balls990129.html>

Jordan Golf, 1998, Various articles, [online], The Jordan Group of Companies, (sine loco), dated unknown, [cited 15th October], available from internet - <http://www.jordangolf.com>

Jorgensen, T.P., 1994, *The Physics of Golf*, AIP Press, London.

Karsten, 1998, "The first ping putter." [online], Karsten Manufacturing Corporation, Phoenix, 1998, [cited 12th September 1998], available from internet - <http://www.pinggolf.com/history.html>

Knight, J., 1997, "Game, set and match." *New Scientist* - 6th September, IPC Magazines Ltd., London.

Knott, C.G., 1911, *Life and scientific work of Peter Guthrie Tate*, Cambridge University Press, London.

Lampsa, M. A., 1975, "Maximizing distance of the golf drive an optimal control study." *Journal of Dynamic Systems, Measurement, and Control*, December 1975, p362-367.

Lancaster, J., 1995, "Grip selection." *Golf the Scientific Way*, Ed Cochran, Aston Publishing Group, Hertfordshire.

Levin, E., 1998, "Death of a swinger.", [online], American Express Company, (sine loco), May 1998, [cited 15th October 1998], available from internet - <http://www.pathfinder.com/travel/TL/golf/mayjune/ironbyron.html>

Lewis, P., 1995, "The history of the golf ball in Britain." *Golf the Scientific Way*, Ed Cochran, Aston Publishing Group, Hertfordshire.

Lieberman, B.B., 1990, "The effect of impact conditions on golf ball spin rate." *Science and Golf*, Ed Cochran, E. & F.N. Spon, London.

Lindsay, N., 1995, "The practice swing." *Golf the Scientific Way*, Ed Cochran, Aston Publishing Group, Hertfordshire.

Lockwood, C., 1992, "Testing time for sport." *New Scientist - 25th July*, IPC Magazines Ltd., London.

Logan J., 1997, "Project is getting into the swing.", [online], Philadelphia Newspapers Inc. , Philadelphia, 1997, [cited 15th October 1998], available from internet - <http://sports.phillynews.com/golf/library/97/stroke.asp>

Macaulay, M., 1987, *Introduction to Impact Engineering*, Chapman & Hall, London.

Mahaffey, S. and Melvin, T., 1995, "Metal woods or wooden woods?" *Golf the Scientific Way*, Ed Cochran, Aston Publishing Group, Hertfordshire.

Maltbie, R., 1986, *The Professional Golf Club Fitting Program*, Ralph Maltbie Enterprises.

- Masuda, M. and Kojima, S., 1994, "Kick back effect of club-head at impact." *Science and Golf II*, Ed Cochran and Farrally, E. & F.N. Spon, London.
- Mather, J.S.B. and Cooper, M.A.J., 1994, "The attitude of the shaft during the swing of golfers of different ability." *Science and Golf II*, Ed Cochran and Farrally, E. & F.N. Spon, London.
- Mather, S., 1995, "Golf club dynamics." *Golf the Scientific Way*, Ed Cochran, Aston Publishing Group, Hertfordshire.
- Mather, J.S.B. and Immohr 1996, "The dynamic response of a golf club head." *The Engineering of Sport*, Ed Haake, Blackwell Science, Oxford.
- Mather, J.S.B. and Jowett, S., 1998, "The effect of centrifugal stiffening on the bending stiffness of a golf shaft." *The Engineering of Sport II*, Ed Haake, Blackwell Science, Oxford.
- Maw, N., Barber, J.R. and Fawcett, J.N., 1975, "The oblique impact of elastic spheres." *Wear*, Elsevier Sequoia S A., Lausanne
- McKirby, A.S., 1990, "Professor P.G. Tait and the physics of golf." *Science and Golf*, Ed Cochran, E. & F.N. Spon, London.
- McLaughlin, P.A. and Best, R.J., 1994, "Three-dimensional kinematic analysis of the golf swing." *Science and Golf II*, Ed Cochran and Farrally, E. & F.N. Spon, London.
- McTeige, M. and Lamb, S.R., 1995, "Hip and spine motion during the swing." *Golf the Scientific Way*, Ed Cochran, Aston Publishing Group, Hertfordshire.
- Milne, R.D. and Davis, J.P., 1992, "The role of the shaft in the golf swing." *Journal of Biomechanics*, Vol. 25, No. 9, pp 975—983.

Mitchell, S.R., 1996, *A Feature based approach to computer aided design of sculptured products*, Ph.D. Thesis, Loughborough University, Loughborough.

Miura, K. and Naruo, T., 1998, "Accelerating and decelerating phases of the wrist motion of the golf swing." *The Engineering of Sport II*, Ed Haake, Blackwell Science, Oxford.

Nesbit, S.M., Cole, J.S., Hartzell, T.A., Oglesby, K.A. and Radich, A.F., 1994, "Dynamic model and computer simulation of a golf swing." *Science and Golf II*, Ed Cochran and Farrally, E. & F.N. Spon, London.

Olsavsky, T., 1994, "The effects of driver head size on performance." *Science and Golf II*, Ed Cochran and Farrally, E. & F.N. Spon, London.

Pedler, D., 1997, "Equipment:Inserts." *Golf World - September*, Vol.38, No.9, EMAP, London.

Pelz, D., 1990, "A simple, scientific, shaft test: steel versus graphite." *Science and Golf*, Ed Cochran, E. & F.N. Spon, London.

Pickering, W., 1998, "A computational study of the double pendulum model of the golf swing." *The Engineering of Sport II*, Ed Haake, Blackwell Science, Oxford.

Proctor, S., 1995, "The golf equipment market 1984-1994." *Golf the Scientific Way*, Ed Cochran, Aston Publishing Group, Hertfordshire.

R & A, 1997, *Rules of golf* [online], Royal and Ancient golf club, St. Andrews, 1997, [cited 15th June 1998], available from internet - <http://www.randa.org/menu2/rules.uk/rules.htm>

Robinson, R.L., 1994, "A study of the correlation between the swing characteristics and clubhead velocity." *Science and Golf II*, Ed Cochran and Farrally, E. & F.N. Spon, London.

- Sato, F., 1994, "Choosing golf clubs." *Golf the Scientific Way*, Ed Cochran, Aston Publishing Group, Hertfordshire.
- Scheie, C.E., 1990, "The golf club-ball collision-50,000 g's." *Science and Golf*, Ed Cochran, E & F.N. Spon, London.
- Shames, I.H., 1989, *Introduction to solid mechanics*, Prentice Hall, New Jersey.
- Shaw, M., 1995, "Aerodynamics of golf balls." *Golf the Scientific Way*, Ed Cochran, Aston Publishing Group, Hertfordshire.
- Statz, R.J., 1990, "Surlyn' ionomers for golf ball covers." *Science and Golf*, Ed Cochran, E. & F.N. Spon, London.
- Sullivan M.J. and Melvin T., 1994, "The relationship between golf ball construction and performance." *Science and Golf II*, Ed Cochran and Farrally, E. & F.N. Spon, London.
- Sullivan M.J. and Melvin T., 1995, "Golf ball construction and performance." *Golf the Scientific Way*, Ed Cochran, Aston Publishing Group, Hertfordshire.
- Suzuki, S. and Inooka, H., 1998, "A new golf-swing robot model utilizing shaft elasticity." *Journal of Sound and Vibration*, 217(1), 17-13, Article No. sv981733.
- Swider, P. and Ferraris, G., 1994, "Theoretical and experimental dynamic behavior of a golf club made of a composite material." *Modal Analysis*, v 9 n1, Jan, p57-69.
- Take, S., 1995, "Club face inserts." *Golf the Scientific Way*, Ed Cochran, Aston Publishing Group, Hertfordshire.
- Taylor, P., 1998, "The economics of the sports products industry." *The Engineering of Sport II*, Ed Haake, Blackwell Science, Oxford.

Thomas, F.W., 1994, "The state of the game, equipment and science." *Science and Golf II*, Ed Cochran and Farrally, E. & F.N. Spon, London.

Tomita, S. and Chikaraishi, T., 1995, "Effect of different dimple patterns on flight." *Golf the Scientific Way*, Ed Cochran, Aston Publishing Group, Hertfordshire.

Tutleman, D., 1994, "Square grooves are legal." [online], University of Princeton, Princeton, 1994, [cited 2nd November 1998], available from internet - <http://dunkin.Princeton.edu/golf/clubmaking/square.groovs.html>

Tutleman, D., 1998, Various golf articles, [online], University of Princeton, Princeton, 1998, [cited 2nd November 1998], available from internet - <http://dunkin.Princeton.edu/golf/>

Uihlein, W., 1998, "Presentation by Acushnet." [online], United States Golf Association, New Jersey, 6th October 1998, [cited 08th October 1998], available from internet - http://www.usga.com/test_center/transcript/acushnet.html

USGA, 1998, "Testing for conformity : An inside job." [online], United States Golf Association, *Golf Journal*, New Jersey, May 1998, [cited 12th July 1998], available from internet - http://www.golfjournal.com/features/98/may/test_for_conformity.html

USGA, 1998, "A new test pattern." [online], United States Golf Association, Far Hills, New Jersey, May 1998, [cited 15th October 1998], available from internet - http://www.golfjournal.com/features/98/may/new_test_pattern.html

USGA, 1998, "Enhanced rebound velocity test protocol." [online], United States Golf Association, New Jersey, 14th July 1998, [cited 20th July 1998], available from internet - http://www.usga.com/test_center/test_protocol.html

Van Gheluwe, B., Deporte, E. and Ballegeer, K., 1990, "The influence of the use of graphite shafts on golf performance and swing kinematics." *Science and Golf*, Ed Cochran, E. & F.N. Spon, London.

Various, 1997, advertisements in *Golf World - September*, Vol.38, No.9, EMAP, London.

Whittaker, A., Thomson, R., McKeown, D. and McCafferty, J., 1990, "The application of computer-aided engineering techniques in advanced clubhead design." *Science and Golf*, Ed Cochran, E & F.N. Spon, London.

Whittaker, A., 1996, "Modelling and simulation of the golf stroke." *Computer Modeling and Simulation in Engineering*, 1: 31—45.

Williams, D., 1967, "The dynamics of the golf swing." *Quarterly Journal Mech. and Applied Math.*, Vol. XX, Pt. 2.

Winfield, D.C. and Tan, T.E., 1994, "Optimization of the clubhead loft and swing elevation angles for maximum distance of a golf drive." *Computers & Structures*, 53(1), 19.

Winfield, D.C. and Tan, T.E., 1996, "Optimization of the clubface shape of a golf driver to minimise dispersion of off-center shots." *Computers & Structures*, 58(6), 1217.

Wishon, T.W., 1995, "Modern shaft fitting - combining flex and torque." *Golf the Scientific Way*, Ed Cochran, Aston Publishing Group, Hertfordshire.

Wood, D. and Wood, C., 1995, "Modern persimmon clubheads." *Golf the Scientific Way*, Ed Cochran, Aston Publishing Group, Hertfordshire.

Woods, J.B. and Mase, G.T., 1990, "A review of motion analysis systems and the use of high speed cinematography and laser fiber optics for golf research." *Science and Golf*, Ed Cochran, E. & F.N. Spon, London.

Yamada, M., 1995, "Effect of temperature on ball performance." *Golf the Scientific Way*, Ed Cochran, Aston Publishing Group, Hertfordshire.

Yasuda, 1999, "Rookies heat up ball war." [online], Golfonline, a division of Times Mirror Magazines, (sine loco), 23rd January 1999, [cited 23rd January 1999], available from internet -

<http://www.golfonline.com/news/golfweek/1999/january/ballwar0123.html>.

Appendices

- A-1** Calibration plate used for calibration of C3D process. Plate constructed from 10mm perspex and posts from aluminum. Middle section replaceable with mounted clubhead.
- A-2** Dimensions and coordinates of posts. Tolerances on posts ± 0.001 mm.
- A-3** Original design of mount for clubhead, not constructed due to current limitations of the C3D process.
- B-1** Abaqus input file for solid clubhead analysis.
- B-2** Abaqus input file for rigid clubhead analysis.
- B-3** Rotation and translation for rigid lofted clubheads.
- B-4** Ball flight properties, varying modulus and zero friction.
- C-1** Measured properties of selection of graphite composite shafts.
- C-2** Finite element shaft model data, used in knife edge tests.
- D-1** Abaqus input file for swing and shaft analysis.
- D-2** Bending moment and curvature plots during downswing for zero offset mass.
- D-3** Element stiffness values for bend point analysis.

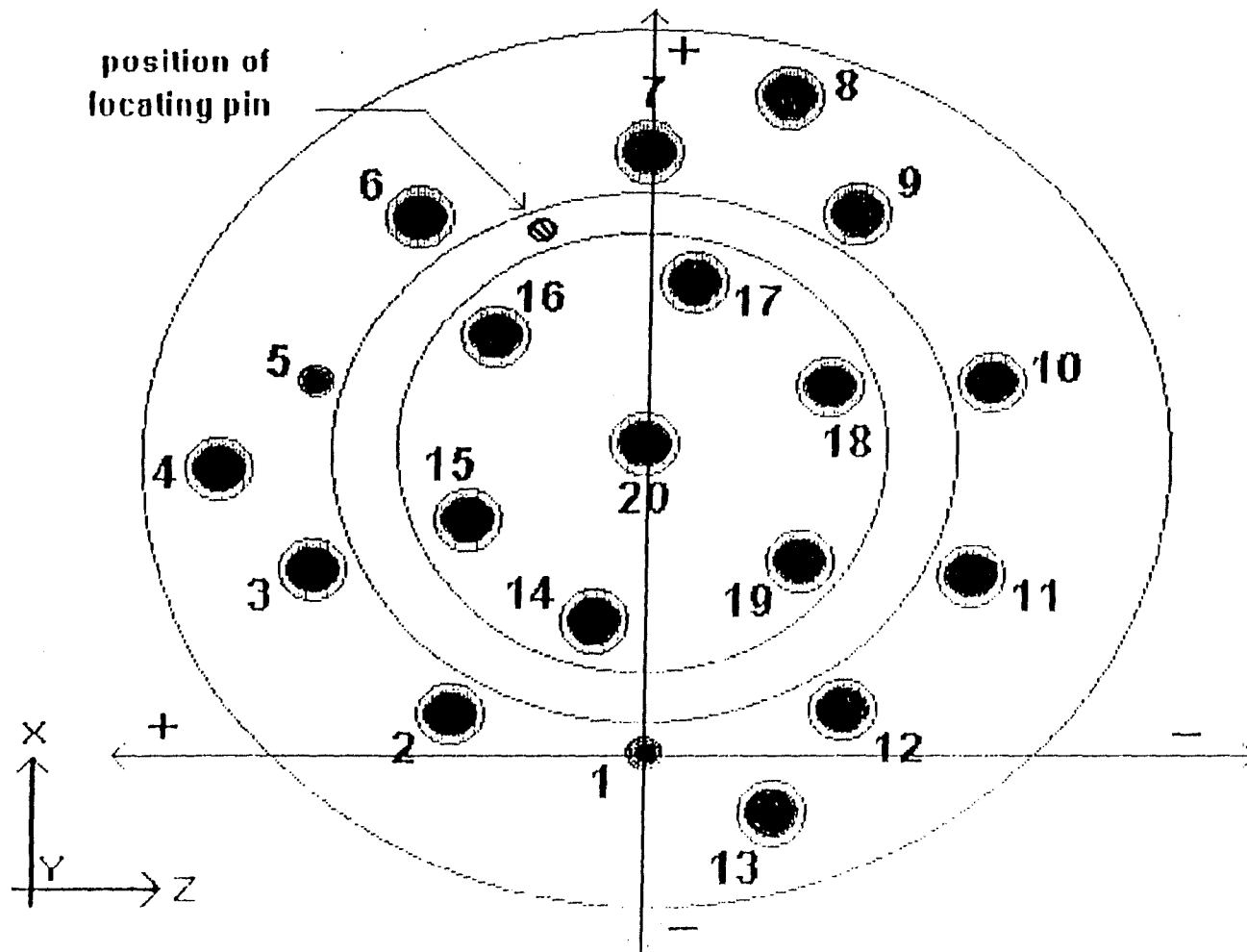


Figure A-1(1) Calibration plate used for C3D process.

Post number	X (mm)	Y (mm)	Height (mm)	Diameter (mm)
1	0.000	0.000	30.074	8.052
2	13.970	42.545	30.074	12.802
3	51.689	69.672	15.037	12.802
4	76.581	99.949	15.164	12.802
5	96.774	69.240	29.845	8.026
6	133.401	41.910	20.142	12.802
7	145.720	-2.032	25.019	12.802
8	167.386	-32.766	15.138	12.802
9	130.988	-44.323	10.287	12.802
10	94.818	-69.596	40.183	12.802
11	49.987	-69.672	35.179	12.802
12	13.513	-35.052	5.207	12.802
13	-22.606	-28.626	15.614	12.802
14	29.210	11.728	10.185	12.802
15	61.189	43.688	20.244	12.827
16	103.937	33.147	35.179	12.802
17	116.992	-10.744	25.044	12.802
18	85.522	-43.180	30.099	12.827
19	40.818	-31.902	15.138	12.827
20	72.822	0.000	5.080	12.802

Table A-2(1) Dimensions and coordinates of posts. Tolerances on posts ± 0.001 mm.

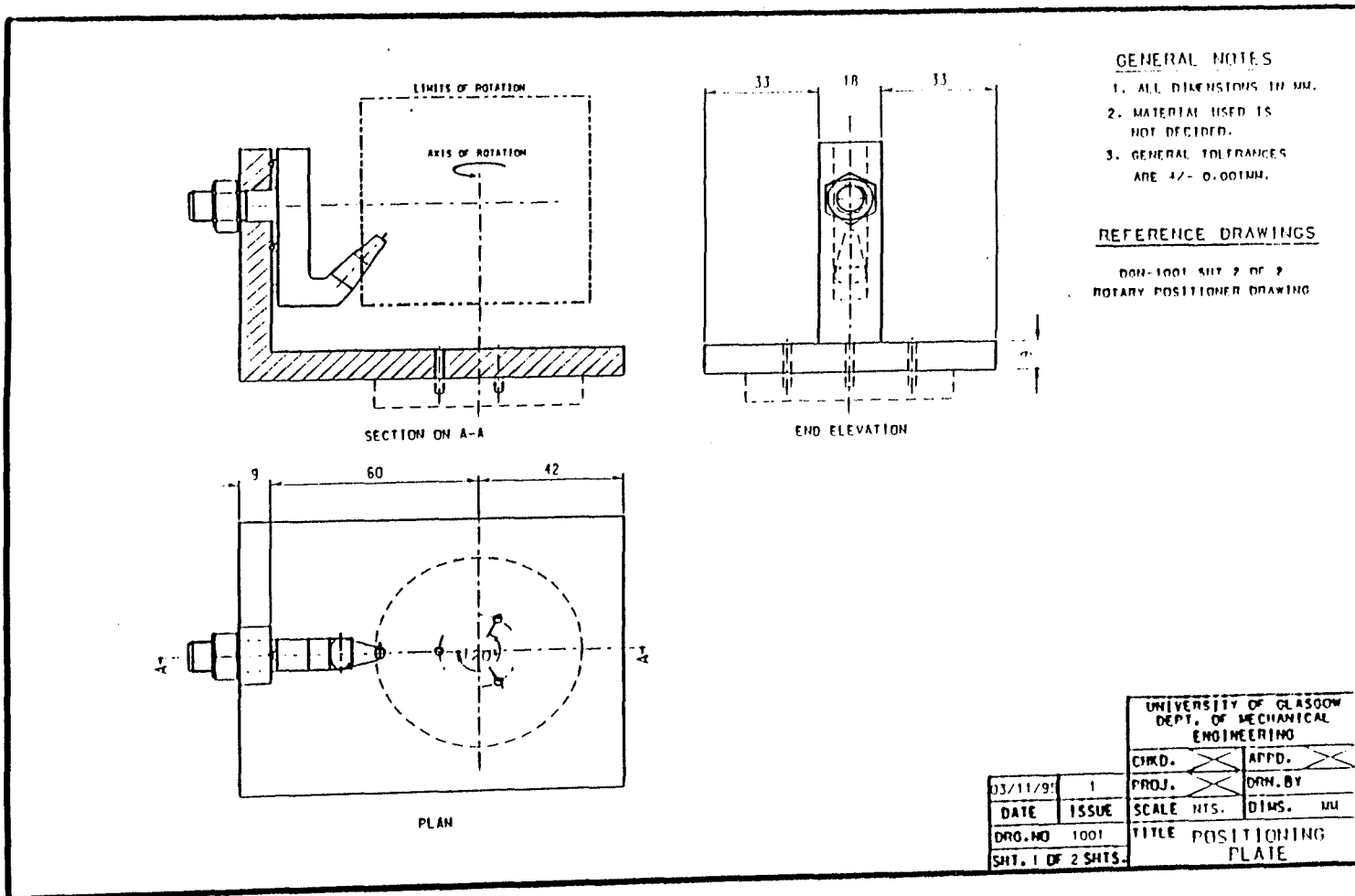


Figure A-3(1) Original design of mount for clubhead, not constructed due to limitations of the C3D process, sheet 1.

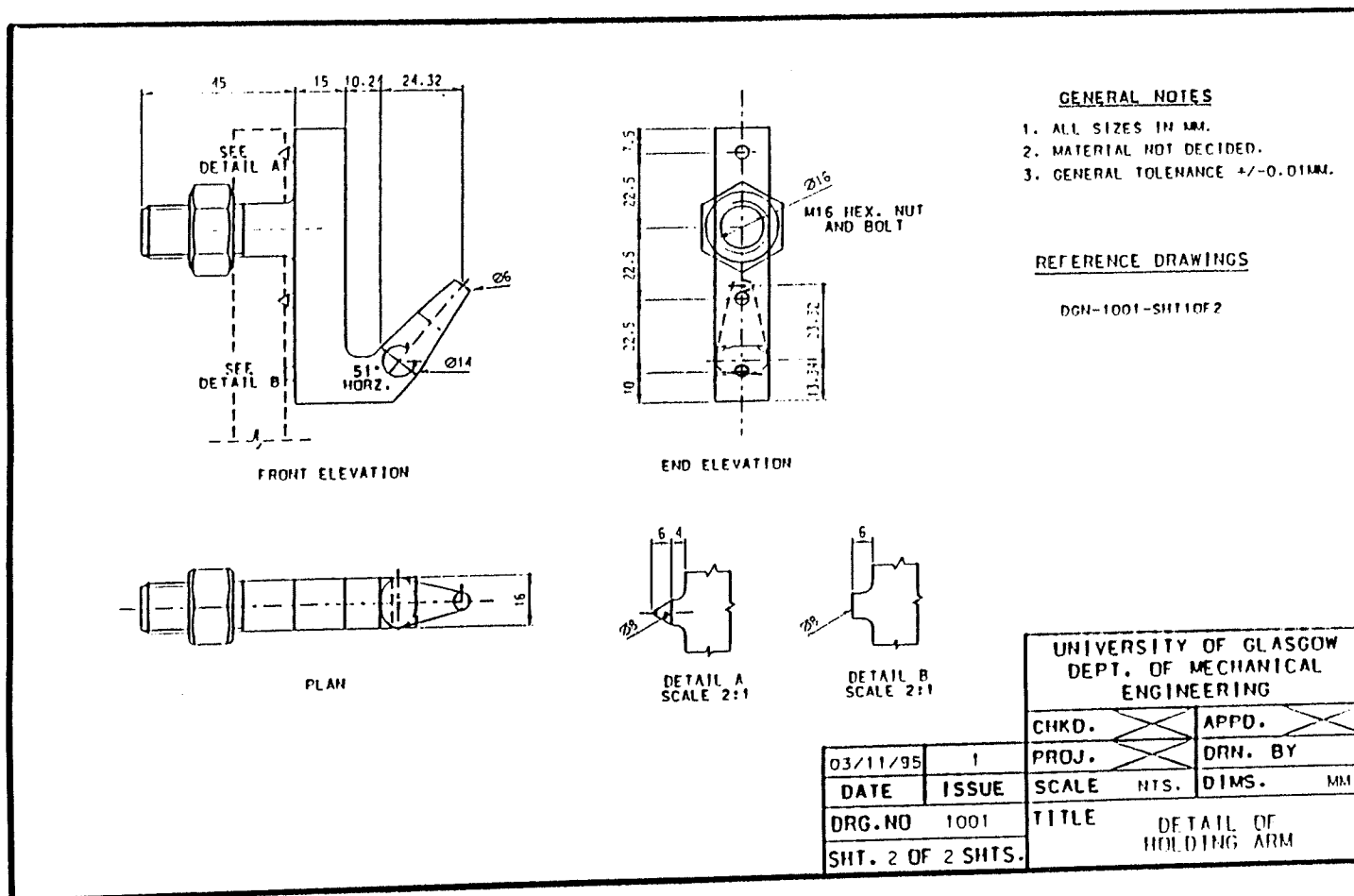


Figure A-3(2) Original design of mount for clubhead, not constructed due to limitations of the C3D process, sheet 2.

*****START OF DATA

**

*HEADING, UNSYMM

3-D HYPERELASTIC GOLF BALL IMPACTING LINEAR ELASTIC CLUBHEAD

*PREPRINT, ECHO=YES, MODEL=YES, HISTORY=YES

**

***** BALL NODES

**

*NODE, NSET=BALLN

1, 0.179999992E-01, 0.000000000E+00, 0.000000000E+00
 2, 0.199999996E-01, 0.000000000E+00, 0.000000000E+00
 3, 0.166298300E-01, 0.000000000E+00, 0.688830297E-02
 4, 0.184775908E-01, 0.000000000E+00, 0.765366852E-02
 5, 0.127279200E-01, 0.000000000E+00, 0.127279228E-01



Data omitted for conciseness

1486, -0.778589863E-02, -0.746710366E-02, -0.180262309E-01
 1488, -0.647215964E-02, -0.141306296E-01, -0.141306240E-01
 1504, -0.746710086E-02, -0.180262309E-01, -0.778589677E-02

**

***** CLUB NODES

**

*NODE, NSET=CLUBN

1505, -0.359999985E-01, -0.229903813E-01, -0.125000002E-01
 1506, -0.359999985E-01, -0.228677858E-01, -0.197876580E-01
 1507, -0.359999985E-01, -0.227451902E-01, -0.270753186E-01
 1508, -0.359999985E-01, -0.226225965E-01, -0.343629755E-01
 1509, -0.359999985E-01, -0.225000009E-01, -0.416506343E-01



Data omitted for conciseness

1887, 0.399999991E-01, -0.558576547E-02, -0.280143376E-01
 1888, 0.419999957E-01, -0.118916808E-01, -0.271065030E-01
 1889, 0.439999998E-01, -0.181975979E-01, -0.261986684E-01

**

***** BALL ELEMENTS

**

*ELEMENT, TYPE=C3D8R, ELSET=BALLE

1, 1, 3, 4, 2, 7, 9, 10, 8
 2, 3, 5, 6, 4, 9, 11, 12, 10
 3, 7, 9, 10, 8, 13, 15, 16, 14
 4, 9, 11, 12, 10, 15, 17, 18, 16
 5, 2, 4, 22, 20, 8, 10, 28, 26



Data omitted for conciseness

350, 575, 576, 639, 636, 255, 257, 1060, 1072
 351, 529, 636, 645, 538, 151, 1072, 1038, 113
 352, 636, 639, 648, 645, 1072, 1060, 1044, 1038

**
 ***** CLUB ELEMENTS
 **

*ELEMENT, TYPE=C3D8R, ELSET=CLUBE
 353, 1505, 1506, 1511, 1510, 1540, 1541, 1546, 1545
 354, 1506, 1507, 1512, 1511, 1541, 1542, 1547, 1546
 355, 1507, 1508, 1513, 1512, 1542, 1543, 1548, 1547
 356, 1508, 1509, 1514, 1513, 1543, 1544, 1549, 1548
 357, 1510, 1511, 1516, 1515, 1545, 1546, 1551, 1550
 587, 1842, 1843, 1848, 1847, 1877, 1878, 1883, 1882



Data omitted for conciseness

590, 1846, 1847, 1852, 1851, 1881, 1882, 1887, 1886
 591, 1847, 1848, 1853, 1852, 1882, 1883, 1888, 1887
 592, 1848, 1849, 1854, 1853, 1883, 1884, 1889, 1888

**
 ***** CLUB PROPERTIES
 **

*SOLID SECTION, ELSET=CLUBE, MATERIAL=STEEL
 *MATERIAL, NAME=STEEL
 *ELASTIC
 210.E9, 0.3
 *DENSITY
 7800.
 *MATERIAL, NAME=AL
 *ELASTIC
 80.E9, 0.3
 ** ONLY THE MODULUS IS CHANGED FROM THAT OF STEEL, TO ALLOW
 ** INVESTIGATION OF THE EFFECT OF ELASTICITY ON BALL FLIGHT
 *DENSITY
 7800.
 *MATERIAL, NAME=NYLON
 *ELASTIC
 3.E9, 0.3
 ** ONLY THE MODULUS IS CHANGED FROM THAT OF STEEL, TO ALLOW
 ** INVESTIGATION OF THE EFFECT OF ELASTICITY ON BALL FLIGHT
 *DENSITY
 7800.
 *MATERIAL, NAME=LDPE
 *ELASTIC
 0.2E9, 0.3
 ** ONLY THE MODULUS IS CHANGED FROM THAT OF STEEL, TO ALLOW
 ** INVESTIGATION OF THE EFFECT OF ELASTICITY ON BALL FLIGHT
 *DENSITY
 7800.

**
 ***** BALL PROPERTIES
 **

*ELSET, ELSET=COVERE, GENERATE

5, 8
 17, 24
 49, 52
 61, 68
 93, 96



Data omitted for conciseness



281, 288
 313, 316
 325, 332
 *ELSET, ELSET=COREE, GENERATE
 1, 4
 9, 16
 25, 48
 53, 60
 69, 92



Data omitted for conciseness



289, 312
 317, 324
 333, 352
 *SOLID SECTION, ELSET=COVERE, MATERIAL=SURLYN
 *MATERIAL, NAME=SURLYN
 *ELASTIC
 750.E6, 0.25
 *DENSITY
 950.
 *SOLID SECTION, ELSET=COREE, MATERIAL=RUBBER
 ** THE CORE SHOULD REALLY BE HD FOAM BUT DATA IS SCARCE
 ** THE FOLLOWING DATA IS FOR A VULCANISED RUBBER MATERIAL
 ** THE SOURCE IS THE NOTES FROM THE EXPLICIT SAMPLE PROBLEMS
 *MATERIAL, NAME=RUBBER
 *HYPERELASTIC, N=2, TEST DATA INPUT
 *UNIAXIAL TEST DATA
 1.5506E5, 0.1338
 2.4367E5, 0.2675
 3.1013E5, 0.3567
 4.2089E5, 0.6242
 5.3165E5, 0.8917



Data omitted for conciseness



53.1646E5, 6.4650
 56.9304E5, 6.5541
 64.2405E5, 6.6433
 *BIAXIAL TEST DATA
 0.9384E5, 0.0200
 1.5900E5, 0.0600

2.4087E5, 0.1100
 2.6220E5, 0.1400
 3.3240E5, 0.2000



Data omitted for conciseness

20.1058E5, 3.0700
 22.4502E5, 3.2600
 24.6530E5, 3.4500
 *PLANAR TEST DATA
 0.6000E5, 0.0690
 1.6000E5, 0.1034
 2.4000E5, 0.1724
 3.3600E5, 0.2828
 4.2000E5, 0.4276



Data omitted for conciseness

14.8800E5, 3.4483
 16.5800E5, 3.7793
 18.2000E5, 4.0621
 *VOLUMETRIC TEST DATA
 60.E5, 0.9703
 118.2E5, 0.9412
 175.2E5, 0.9127
 231.1E5, 0.8847
 *DENSITY
 1100.
 **
 ***** DEFINE FIXED BOUNDARY CONDITIONS
 **
 *INITIAL CONDITIONS, TYPE=VELOCITY
 CLUBN, 3, 50.
 *RESTART, WRITE, NUMBER INTERVAL=10
 *STEP
 *DYNAMIC, EXPLICIT
 , 0.002
 *ELSET, ELSET=BALLS1
 49, 50, 51, 52, 61, 62, 63, 64, 65, 66, 67, 68,
 313, 314, 315, 316, 325, 326, 327, 328, 329, 330, 331, 332
 *ELSET, ELSET=BALLS2
 137, 138, 139, 140, 149, 150, 151, 152, 153, 154, 155, 156,
 225, 226, 227, 228, 237, 238, 239, 240, 241, 242, 243, 244,
 *SURFACE DEFINITION, NAME=BALLS
 BALLS1, S4
 BALLS2, S5
 *ELSET, ELSET=CLUBS
 353, 357, 361, 365, 369, 373, 377, 381, 385, 389, 393, 397,
 401, 405, 409, 413, 417, 421, 425, 429, 433, 437, 441, 445,
 449, 453, 457, 461, 465, 469, 473, 477, 481, 485, 489, 493,

497, 501, 505, 509, 513, 517, 521, 525, 529, 533, 537, 541,
545, 549, 553, 557, 561, 565, 569, 573, 577, 581, 585, 589

*SURFACE DEFINITION, NAME=CLUBS

CLUBS, S6

*CONTACT PAIR, INTERACTION=CLUBF

BALLS, CLUBS

*SURFACE INTERACTION, NAME=CLUBF

*FRICTION

0.6

*END STEP

**

***** END OF DATA

```

*****START OF DATA
**
*HEADING
RIGID
*PREPRINT,ECHO=YES, HISTORY=YES, MODEL=YES
*RESTART, WRITE, NUMBER INTERVAL=10
**
***** BALL NODES
**
*NODE, NSET=BALLN, INPUT=BALLN
**
***** CLUB NODES
**
*NODE, NSET=CLUBN
2001, -3.6000E-02, 0.13094, -3.0000E-02
2002, 3.6000E-02, 0.13094, -3.0000E-02
2003, 3.6000E-02, -1.0000E-01, -3.0000E-02
2004, -3.6000E-02, -1.0000E-01, -3.0000E-02
*NODE, NSET=MASSN
2005, 0000000000, 0.00000000, -0.04
*NCOPY, CHANGE NUMBER=1000, OLDSET=CLUBN, SHIFT, NEWSET=ROTN

4.00E-02, -1.00E-01, -3.00E-02, -4.00E-02, -1.00E-01, -3.00E-02, 30.0
*NCOPY, CHANGE NUMBER=1000, OLDSET=ROTN, SHIFT, NEWSET=TRANN
0.000, 0.000, 0.061965

**
***** BALL ELEMENTS
**
*ELEMENT, TYPE=C3D8R, ELSET=BALLE, INPUT=BALLE
**
***** CLUB ELEMENTS
**
*ELEMENT, TYPE=R3D4, ELSET=CLUBE
2001, 4001, 4002, 4003, 4004
*RIGID BODY, ELSET=CLUBE, REF NODE=2005
*ELEMENT, TYPE=ROTARYI, ELSET=ROTA
2002, 2005
*ROTARY INERTIA, ELSET=ROTA
7.496E-05,1.526E-04,1.897E-04
*ELEMENT, TYPE=MASS, ELSET=MASS
2003, 2005
*MASS, ELSET=MASS
0.32179
**
***** BALL PROPERTIES
**
*ELSET, ELSET=COVERE, GENERATE
5, 8
17, 24

```

49, 52
61, 68
93, 96



Data omitted for conciseness

281, 288
313, 316
325, 332
*ELSET, ELSET=LAYER3, GENERATE
1, 4
9, 16
45, 48
53, 60
89, 92



Data omitted for conciseness

273, 280
309, 312
317, 324
*ELSET, ELSET=LAYER2, GENERATE
33, 44
77, 88
121, 132
165, 176
209, 220
253, 264
297, 308
341, 352
*ELSET, ELSET=LAYER1, GENERATE
26, 32
70, 76
114, 120
158, 164
202, 208
246, 252
290, 296
334, 340
*ELSET, ELSET=COREE
25
69
113
157
201
245
289
333
*SOLID SECTION, ELSET=COVERE, MATERIAL=SURLYN
*SOLID SECTION, ELSET=LAYER3, MATERIAL=NORMAL

```

*SOLID SECTION, ELSET=LAYER2, MATERIAL=NORMAL
*SOLID SECTION, ELSET=LAYER1, MATERIAL=NORMAL
*SOLID SECTION, ELSET=COREE, MATERIAL=NORMAL
*MATERIAL, NAME=SURLYN
*ELASTIC
340.E6, 0.25
*DENSITY
950.
*MATERIAL, NAME=NORMAL
*HYPERELASTIC, N=2
13.896E6, 0.3475E5, 2269.0, -1779.0, 85.25, 0.9923E-8, -0.4433E-7
*DENSITY
1100.0
*MATERIAL, NAME=OTHER
*HYPERELASTIC, N=2
13.896E6, 0.3475E5, 2269.0, -1779.0, 85.25, 0.9923E-8, -0.4433E-7
*DENSITY
1700.
**
***** DEFINE FIXED BOUNDARY CONDITIONS
**
*INITIAL CONDITIONS, TYPE=VELOCITY
2005, 3, 50.0
*BOUNDARY
2005, 1, 2
2005, 4, 6
*STEP
*DYNAMIC, EXPLICIT
, 0.005
*ELSET, ELSET=BALLS1
49, 50, 51, 52, 61, 62, 63, 64, 65, 66, 67, 68,
313, 314, 315, 316, 325, 326, 327, 328, 329, 330, 331, 332
*ELSET, ELSET=BALLS2
137, 138, 139, 140, 149, 150, 151, 152, 153, 154, 155, 156,
225, 226, 227, 228, 237, 238, 239, 240, 241, 242, 243, 244,
*SURFACE DEFINITION, NAME=BALLS
BALLS1, S4
BALLS2, S5
*ELSET, ELSET=CLUBS1
2001
*SURFACE DEFINITION, NAME=CLUBS
CLUBS1, SNEG
*CONTACT PAIR, INTERACTION=CLUBF
BALLS, CLUBS
*SURFACE INTERACTION, NAME=CLUBF
*FRICTION
0.6
*END STEP
**
***** END OF DATA

```

loft	ball contact point		top coord	club contact point		seperation	translation	centre of face position		pos. of mass element	
	x	y		x	y			x	y	z	y
0	-0.021000	0	0.100000	-0.030000	0	0.009000	0.007479	-0.022521	0	-0.036751	0
5	-0.020920	-0.001830	0.100764	-0.038589	-0.001830	0.017669	0.016148	-0.022601	0	-0.036831	0
10	-0.020681	-0.003647	0.103085	-0.046990	-0.003647	0.026309	0.024788	-0.022845	0	-0.037075	0
15	-0.020284	-0.005435	0.107055	-0.055339	-0.005435	0.035054	0.033533	-0.023262	0	-0.037492	0
20	-0.019734	-0.007182	0.112836	-0.063783	-0.007182	0.044049	0.042528	-0.023869	0	-0.038099	0
25	-0.019032	-0.008875	0.120676	-0.072492	-0.008875	0.053460	0.051939	-0.024692	0	-0.038922	0
30	-0.018187	-0.010500	0.130940	-0.081673	-0.010500	0.063486	0.061965	-0.025770	0	-0.040000	0
35	-0.017202	-0.012045	0.144155	-0.091587	-0.012045	0.074384	0.072863	-0.027157	0	-0.041387	0
40	-0.016087	-0.013499	0.161081	-0.102583	-0.013499	0.086496	0.084975	-0.028935	0	-0.043165	0
45	-0.014849	-0.014849	0.182843	-0.115151	-0.014849	0.100302	0.098780	-0.031220	0	-0.045450	0
50	-0.013499	-0.016087	0.211145	-0.130004	-0.016087	0.116505	0.114984	-0.034191	0	-0.048421	0
55	-0.012045	-0.017202	0.248689	-0.148248	-0.017202	0.136202	0.134681	-0.038133	0	-0.052363	0
60	-0.010500	-0.018187	0.300000	-0.171705	-0.018187	0.161205	0.159684	-0.043521	0	-0.057751	0
65	-0.008875	-0.019032	0.373240	-0.203635	-0.019032	0.194760	0.193239	-0.051211	0	-0.065441	0
70	-0.007182	-0.019734	0.484761	-0.250530	-0.019734	0.243348	0.241827	-0.062921	0	-0.077151	0
75	-0.005435	-0.020284	0.672741	-0.327503	-0.020284	0.322067	0.320546	-0.082659	0	-0.096889	0
80	-0.003647	-0.020681	1.051754	-0.479841	-0.020681	0.476194	0.474673	-0.122455	0	-0.136685	0
85	-0.001830	-0.020920	2.194743	-0.933888	-0.020920	0.932057	0.930536	-0.242469	0	-0.256699	0
89	-0.000367	-0.020997	11.359738	-4.556090	-0.020997	4.555724	4.554203	-1.204794	0	-1.219024	0

Notes

Mass element lies 0.01423 metres horizontally behind clubface, at same vertical height as centre of mass of ball.

Clubhead is translated after rotation such that distance to impact is 1.52E-03 metres. Based on a analytical spherical ball.

The upper coordinate of the clubhead is calculated so that the clubhead appears 0.1m above and the centre of the ball.

Table B-3(1) Rotation and translation for rigid body lofted clubheads.

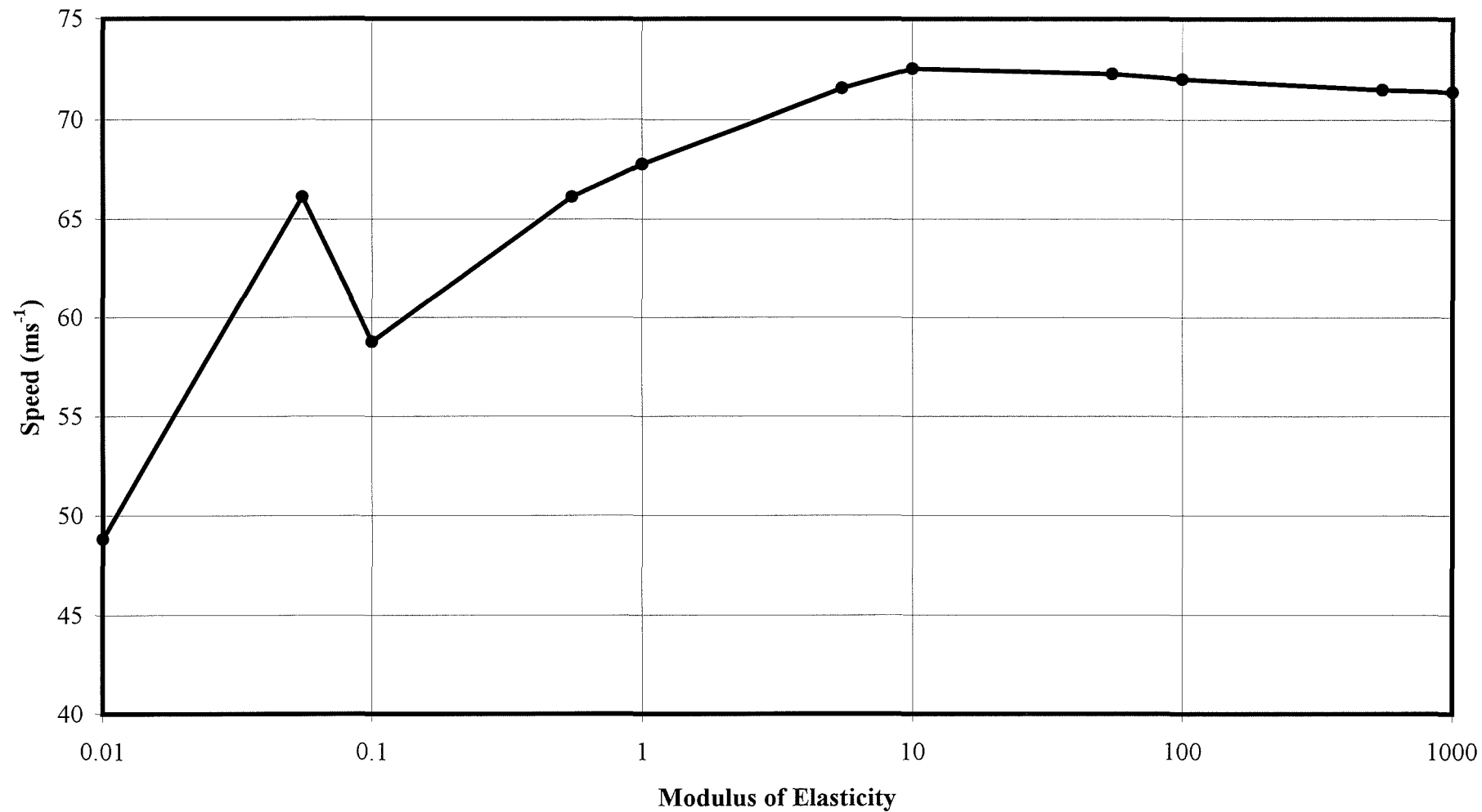


Figure B-4(1) Effect of clubhead modulus on ball speed, zero friction.

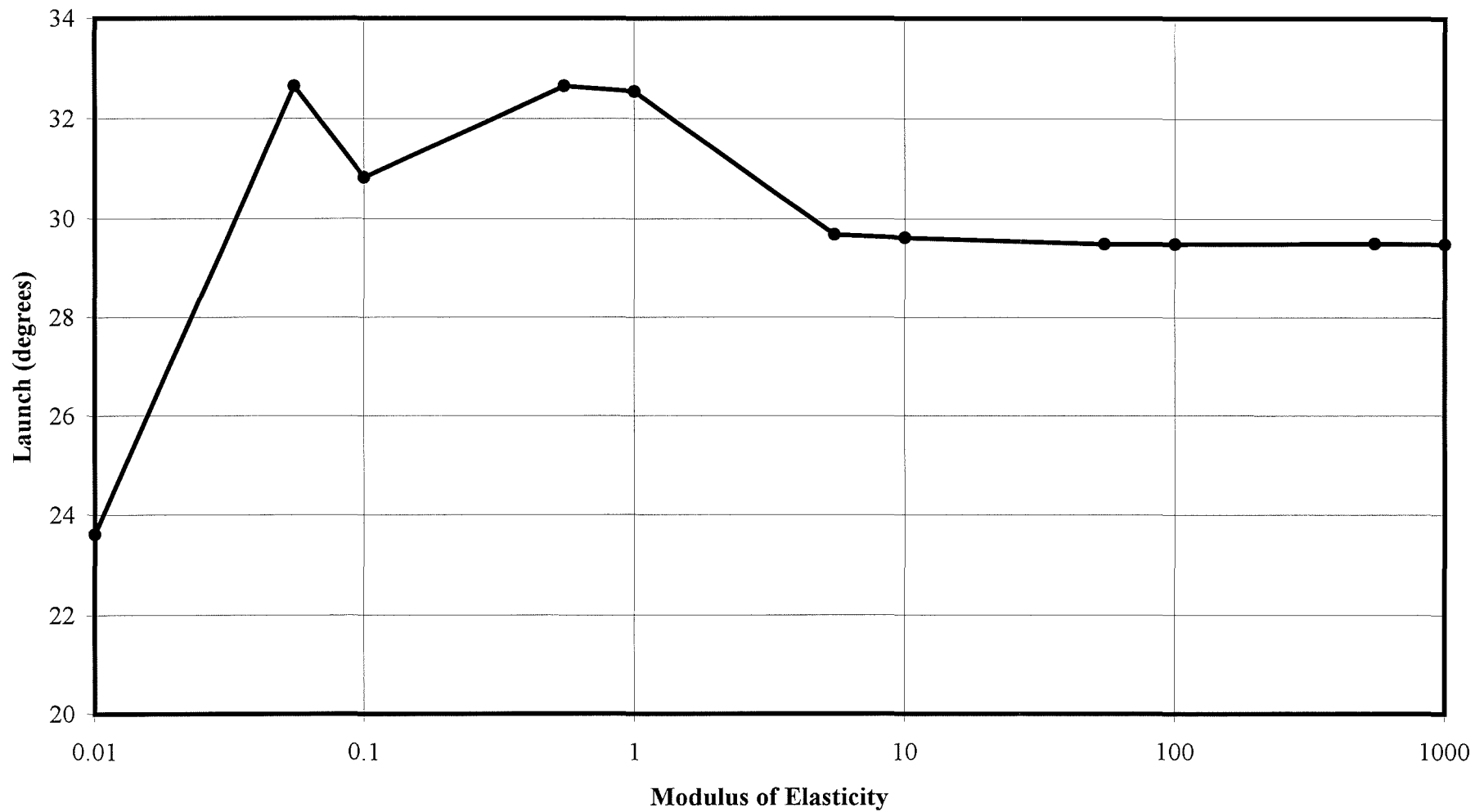


Figure B-4(2) Effect of clubhead modulus on ball launch, zero friction.

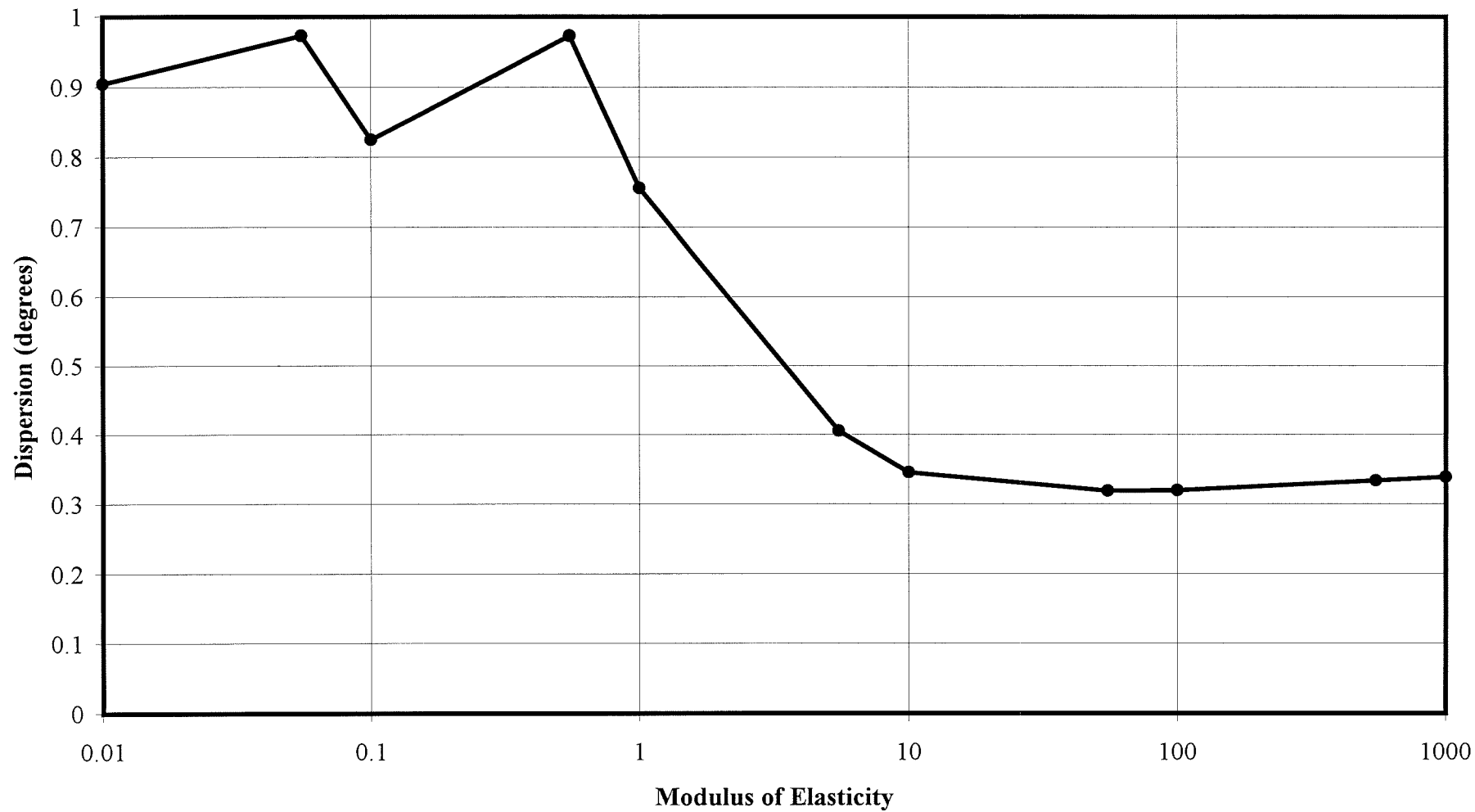


Figure B-4(3) Effect of clubhead modulus on ball dispersion, zero friction.

Model of shaft	Length (mm)	mass (g)	butt		tip		volume (m ³)	density (kgm ⁻³)
			external diameter (mm)	wall thickness (mm)	external diameter (mm)	wall thickness (mm)		
GIM	1120.	113.	15.3	2.8	8.4	2.5	8.60x10 ⁻³	1314.
X, 2.5, high	1120.	96.	14.4	1.0	8.4	2.1	5.09x10 ⁻³	1885.
R, 3.0, low	990.	82.	15.2	1.5	9.3	2.5	6.03x10 ⁻³	1360.
S, 3.0, low	1120.	82.	15.2	1.5	9.3	2.3	6.64x10 ⁻³	1235.
R, 3.5, mid	1141.	86.	15.4	1.7	8.5	2.2	6.85x10 ⁻³	1247.
S, 3.5, high	1145.	90.	15.2	1.5	8.5	2.1	6.26x10 ⁻³	1438.
R, 3.7, low	990.	85.	15.1	1.4	9.3	2.6	6.00x10 ⁻³	1416.
L, 5.0, low	1160.	84.	15.3	1.5	8.4	2.1	6.43x10 ⁻³	1307.
X	1142.	121.	15.1	1.6	8.5	2.6	6.89x10 ⁻³	1755.

Notes: Model of shaft refers to manufacturer specifications of flex rating, torque and bend point, where given.
GIM refers to gas injection moulded shaft.

Table C-1(1) Measured properties of selection of graphite composite shafts.

Node	X coordinate (mm)
1	0.0
2	89.2
3	178.5
4	267.7
5	356.9
6	446.2
7	353.4
8	624.6
9	713.8
10	803.1
11	892.3
12	981.5
13	1070.8
14	1160.0

Element	External radius (mm)	thickness (mm)
1	7.65	1.50
2	7.36	1.55
3	7.08	1.60
4	6.79	1.65
5	6.50	1.70
6	6.21	1.75
7	5.93	1.80
8	5.64	1.85
9	5.35	1.90
10	5.06	1.95
11	4.78	2.00
12	4.49	2.05
13	4.20	2.10

Notes Nodes 2, 13 are pinned in the Finite Element model.
External radius and thickness are assumed to vary linearly between the bounds.

Table C-2(1) Finite element shaft model data, used in knife edge tests.

```

*****START OF DATA
**START OF PROGRAM
*HEADING
EIGHT ELEMENT SHAFT MODEL 50-FLEX
*****NODE DEFINITION
*NODE
  1, 0.000, 0.125, 0.000
  2, 0.000, 0.000, 0.000
  3, 0.000, -0.125, 0.000
  4, 0.000, -0.625, 0.000
  5, 0.000, -0.625, 0.000
 13, 0.000, -1.725, 0.000
 14,-0.040, -1.725, 0.000
 15,-0.040, -1.725, 0.000
*NGEN
  5, 13, 1
*****TRANSFORMATION 1
*NSET, NSET=OLDSHAFT, GENERATE
  6, 15, 1
*NCOPY, CHANGE NUMBER=100, OLDSET=OLDSHAFT,
NEWSSET=NEWSHAFT, SHIFT

0.0,-0.625,1.0,0.0,-0.625, -1.0,90.0
*****TRANSFORMATION 2
*NSET, NSET=OLDALL
  1,3,4,5,NEWSHAFT
*NCOPY, CHANGENUMBER=100, OLDSET=OLDALL, NEWSSET=NEWALL,
SHIFT

0.0,0.0,1.0,0.0,0.0,-1.0,135.0
*****ELEMENT DEFINITION
*ELEMENT, TYPE=B21, ELSET=CHEST
  1, 101, 2
  2, 2, 103
*ELEMENT, TYPE=B21, ELSET=ARM
  3, 103, 104
*ELEMENT, TYPE=B21, ELSET=SHAFT1
  4, 105, 206
*ELEMENT, TYPE=B21, ELSET=SHAFT2
  5, 206, 207
*ELEMENT, TYPE=B21, ELSET=SHAFT3
  6, 207, 208
*ELEMENT, TYPE=B21, ELSET=SHAFT4
  7, 208, 209
*ELEMENT, TYPE=B21, ELSET=SHAFT5
  8, 209, 210
*ELEMENT, TYPE=B21, ELSET=SHAFT6
  9, 210, 211
*ELEMENT, TYPE=B21, ELSET=SHAFT7
 10, 211, 212

```

```
*ELEMENT, TYPE=B21, ELSET=SHAFT8
11, 212, 213
*ELEMENT, TYPE=MASS, ELSET=CLUBMASS
12, 214
*ELEMENT, TYPE=SPRINGA, ELSET=WRIST
13, 103, 206
*ELEMENT, TYPE=R2D2, ELSET=HEAD
14, 213, 214
15, 212, 214
*BEAMSECTION, SECTION=CIRC, ELSET=CHEST, MATERIAL=HUMAN
0.20
*BEAMSECTION, SECTION=CIRC, ELSET=ARM, MATERIAL=HUMAN
0.07
*BEAMSECTION, ELSET=SHAFT1, SECTION=PIPE, MATERIAL=SHAFTM
7.650E-03, 1.500E-03
*BEAMSECTION, ELSET=SHAFT2, SECTION=PIPE, MATERIAL=SHAFTM
7.157E-03, 1.586E-03
*BEAMSECTION, ELSET=SHAFT3, SECTION=PIPE, MATERIAL=SHAFTM
6.664E-03, 1.671E-03
*BEAMSECTION, ELSET=SHAFT4, SECTION=PIPE, MATERIAL=SHAFTM
6.171E-03, 1.757E-03
*BEAMSECTION, ELSET=SHAFT5, SECTION=PIPE, MATERIAL=SHAFTM
5.679E-03, 1.843E-03
*BEAMSECTION, ELSET=SHAFT6, SECTION=PIPE, MATERIAL=SHAFTM
5.186E-03, 1.929E-03
*BEAMSECTION, ELSET=SHAFT7, SECTION=PIPE, MATERIAL=SHAFTM
4.693E-03, 2.014E-03
*BEAMSECTION, ELSET=SHAFT8, SECTION=PIPE, MATERIAL=SHAFTM
4.200E-03, 2.100E-03
*RIGID BODY, ELSET=HEAD, REF NODE=215
*****WRIST SPRING
*SPRING, NONLINEAR, ELSET=WRIST

-1600, -0.040
-1225, -0.035
-900., -0.030
-625., -0.025
-400., -0.020
-225., -0.015
-100., -0.010
-25.0, -0.005
0.00, 0.000
0.00, 0.005
0.00, 0.010
0.00, 0.015
0.00, 0.020
0.00, 0.025
0.00, 0.030
0.00, 0.035
0.00, 0.040
```

```
*****MULTI POINT CONSTRAINT
*MPC
PIN, 104, 105
*MASS, ELSET=CLUBMASS
0.200
*****MATERIAL DEFINITION
*MATERIAL, NAME=HUMAN
*ELASTIC
100.0E9, 0.25
*DENSITY
1000.0
*MATERIAL, NAME=SHAFTM
*ELASTIC
50.0E9, 0.25
*DENSITY
1300.0
*BOUNDARY
2, PINNED
*****FORCE ACCELERATION PROFILE
*AMPLITUDE, NAME=NLINEAR, INPUT=ramped.pro
*****DOWNSWING ANALYSIS
*STEP
*DYNAMIC, EXPLICIT
,0.40
*RESTART, WRITE, NUMBERINTERVAL=200, TIMEMARKS=YES
*CLOAD, FOLLOWER, AMPLITUDE=NLINEAR
103, 1, -1500.0
103, 2, -1500.0
*END STEP
**END OF PROGRAM
```

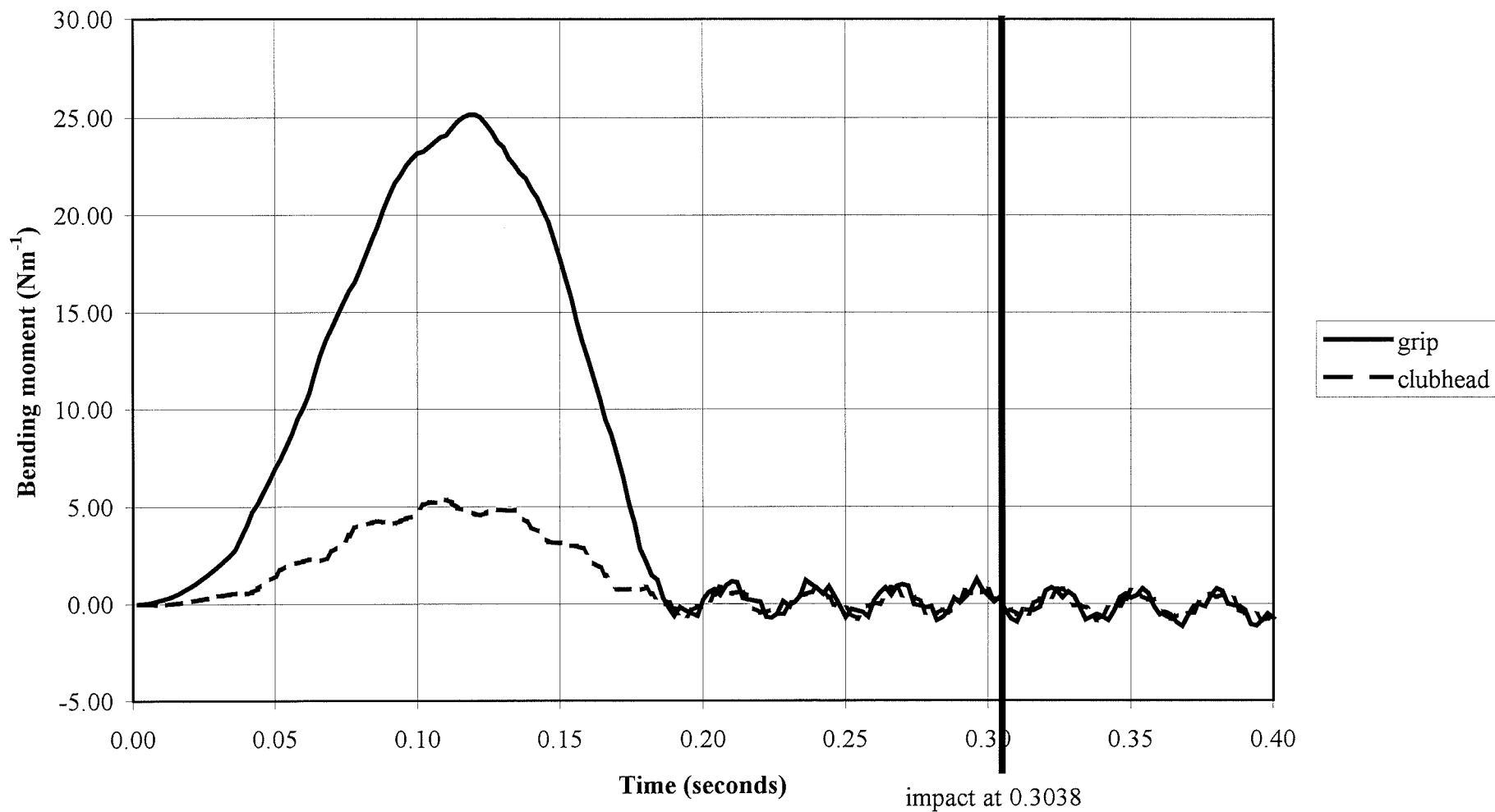


Figure D-2(1) Bending moments in shaft during downswing, zero offset mass.

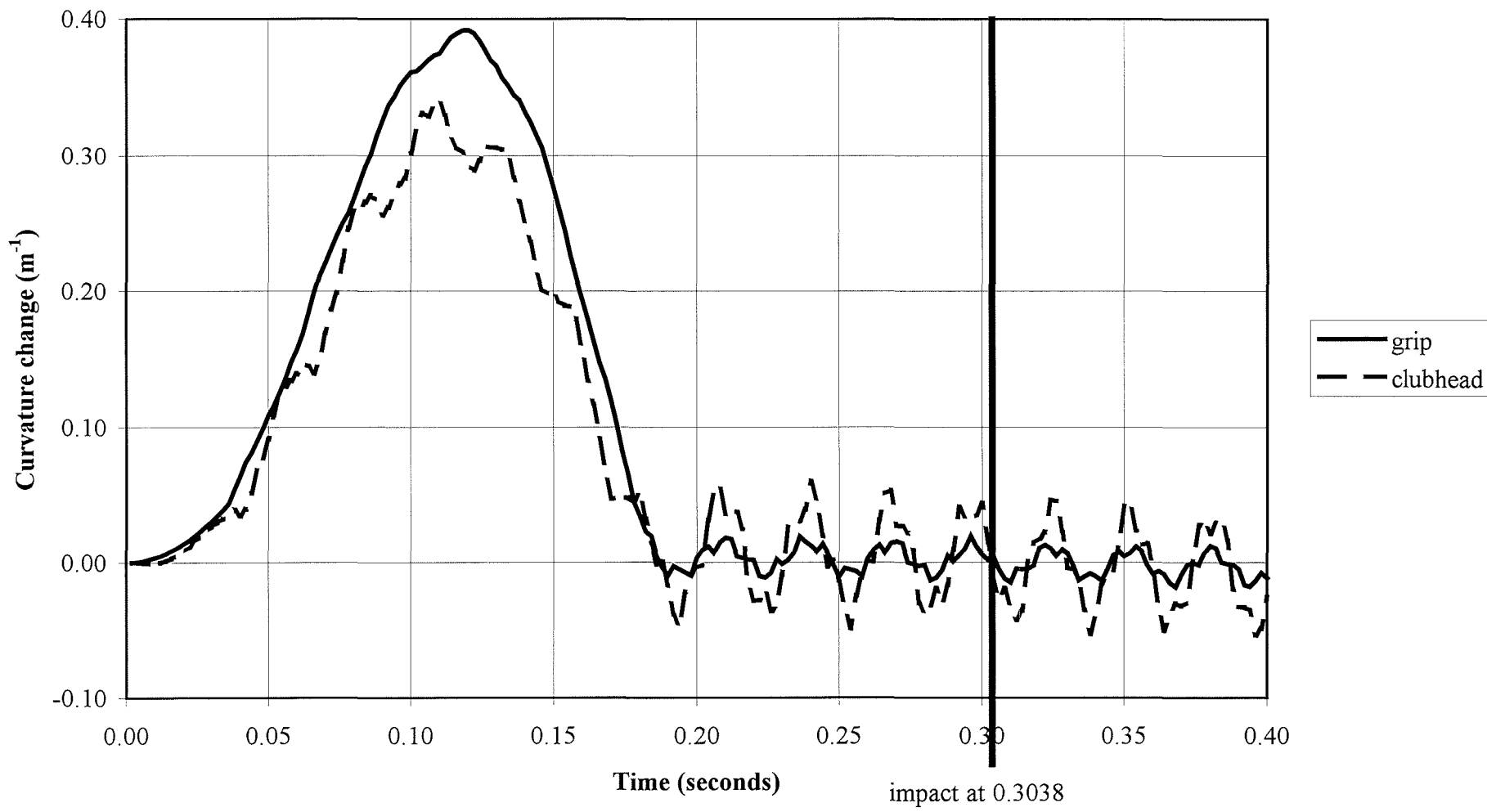


Figure D-2(2) Curvature in shaft during downswing, zero offset mass.

Element No.	Low BP	Mid BP	High BP
1	70.00	70.00	30.31
2	70.00	70.00	30.63
3	70.00	70.00	31.25
4	69.98	69.98	32.50
5	69.96	69.96	35.00
6	69.92	69.92	40.00
7	69.84	69.84	50.00
8	69.69	69.69	60.00
9	69.38	69.38	65.00
10	68.75	68.75	67.50
11	67.50	67.50	68.75
12	65.00	65.00	69.38
13	60.00	60.00	69.69
14	50.00	50.00	69.84
15	40.00	40.00	69.92
16	35.00	35.00	69.96
17	32.50	32.50	69.98
18	31.25	31.25	70.00
19	30.63	30.63	70.00
20	30.31	30.31	70.00
21	30.16	30.16	70.00
22	30.08	30.08	70.00
23	30.04	30.04	70.00
24	30.02	30.02	70.00
25	30.00	30.00	70.00
26	30.00	30.00	70.00
27	30.00	30.00	70.00
28	30.00	30.00	70.00
29	30.00	30.00	70.00
30	30.00	30.00	70.00
31	30.00	30.00	70.00
32	30.00	30.00	70.00



Table D-3(1) Element stiffness values for bend point analysis.